

Seal movements in tidal stream environments:
New methods and ecological insights for the
tidal stream turbine industry



Swansea University
Prifysgol Abertawe

Submitted to Swansea University in fulfilment of the requirements for the
Degree of Doctor of Philosophy (PhD)

Presented by

William Penry Kay

October 2021

Supervisory Committee:

Swansea University:	Dr James C. Bull
	Professor Luca Börger
	Professor Rory P. Wilson
Natural Resources Wales:	Dr Thomas B. Stringell

Examining Committee:

External Examiner: Dr James Waggitt, Bangor University

Internal Examiner: Professor Carlos Garcia De Leaniz, Swansea University

I fy nheulu

Araf deg mae mynd ymhell

“Be curious, and try to make sense of what you see.”

— Stephen William Hawking

Seal movements in tidal stream environments: New methods and ecological insights for the tidal stream turbine industry

William Penry Kay

Abstract

With the increasing threats of climate change, there is an ever-pressing need to reduce fossil fuel emissions. Thus, recent years have seen a dramatic increase in the development of marine renewable energy (MRE) devices – in particular tidal stream turbines (TSTs) – to exploit tidal stream environments (TSEs) for green electricity generation. However, TSTs may pose threats to marine megafauna and relatively little is known about how animals operate in the environments targeted by these devices, and how they may be affected by them. This information is crucial for informing appropriate management strategies to mitigate the risk of conflict between animals and TST developments. Here, using grey seals (*Halichoerus grypus*) and harbour seals (*Phoca vitulina*) as my study species, with data collected from around the UK and neighbouring waters, including the Celtic and the North Sea, I aim to understand and quantify how seals move in TSEs and the implications of this for the TST industry. To achieve this, I quantify the broad-scale movement patterns of seals in coastal waters and their overlap with TSTs, examine the fine-scale movement and behaviour of seals in response to tidal conditions, derive recommendations on sample size and recording duration for animal tracking studies, and design new tags to track seals in TSEs at very fine-scales whilst minimising tag impact. My results suggest that the movements and behaviour of seals are driven by a combination of measurable (and in some cases predictable) demographic and environmental factors, and that the conservation strategies developed to manage the interaction between individuals and populations with TST devices must consider site-specific differences and account for individual variation, with consequences regarding data requirements. Further investigation is required to fully elucidate the extent of variability of seal movements in TSEs and the threats of TST developments, however the research presented herein provides new tools and ecological insights to support this need for both researchers and practitioners.

Keywords: climate change, marine renewable energy (MRE), tidal stream turbine (TST), tidal stream environment (TSE), marine megafauna, movement, behaviour, overlap, tags, tracking, grey seal, *Halichoerus grypus*, harbour seal, *Phoca vitulina*, site-specific differences, individual variation, conservation, management.

Author's declaration

Statement 1

This work has not previously been accepted in substance for any degree and is not being concurrently submitted in candidature for any degree.

Signed [REDACTED]

Date 05/10/2021.....

Statement 2

This thesis is the result of my own investigations, except where otherwise stated. Where correction services have been used, the extent and nature of the correction is clearly marked in a footnote(s). Other sources are acknowledged by footnotes giving explicit references. A bibliography is appended.

Signed [REDACTED]

Date 05/10/2021.....

Statement 3

I hereby give consent for this thesis, if accepted, to be made available online in the University's Open Access Repository and for inter-library loan, and for the title and summary to be made available to outside organisations (unless a bar is in place).

Signed [REDACTED]

Date 05/10/2021.....

Statement 4

In the preparation of this thesis, Swansea University's ethical procedures have been followed and, where appropriate, that ethical approval has been granted.

Signed [REDACTED]

Date 05/10/2021.....

Contents

Abstract	1
Author's declaration	2
Contents	3
Acknowledgements	6
List of figures and tables	10
List of definitions, abbreviations, and key words	13
Chapter 1: Introduction	15
1.1 Marine megafauna – The threat of anthropogenic environmental change and the emergence of tidal stream turbines (TSTs)	16
1.2 Marine megafauna in tidal stream environments (TSEs) – the threat of TSTs and information needs	18
1.3 Studying marine megafauna in TSEs and their interactions with TSTs	29
1.4 Applied movement ecology – studying animal movement responses to anthropogenic change	34
1.5 Study species	38
1.6 Thesis aim and objectives	42
1.7 Collaborator contributions	47
Chapter 2: Predicting the spatio-temporal overlap risk of dispersing grey seal pups with a tidal stream turbine site	49
2.1 Abstract	50
2.2 Introduction	51
2.3 Methods	56
2.4 Results	65
2.5 Discussion	76

Chapter 3: Grey seal pup dispersal: Data and sample size requirements	85
3.1 Abstract	86
3.2 Introduction	87
3.3 Methods	91
3.4 Results	99
3.5 Discussion	115
Chapter 4: Moving in a moving medium: Tidal drivers of harbour seal (<i>Phoca vitulina</i>) fine-scale movement and behaviour	123
4.1 Abstract	124
4.2 Introduction	125
4.3 Methods	130
4.4 Results	136
4.5 Discussion	153
Chapter 5: Development of a remote-release biologging tag for tracking the high-resolution movements of wild seals	158
5.1 Abstract	159
5.2 Introduction	160
5.3 Tag details	164
5.4 Evaluation	177
5.5 Discussion	188
5.6 Perspectives	191
Chapter 6: Minimising the impact of biologging devices: Using Computational Fluid Dynamics for optimising tag design and positioning	193
6.1 Abstract	194

6.2 Introduction	195
6.3 Methods	198
6.4 Results	205
6.5 Discussion	211
Chapter 7: Conclusions	216
7.1 Context and rationale	217
7.2 Broad-scale overlap with TSEs	220
7.4 Fine-scale movements in TSEs	223
7.4 Tag developments for tracking animals in TSEs	225
7.5 Final conclusions	228
References	229
Appendix I: Supplementary material for Chapter 1	267
Appendix II: Supplementary material for Chapter 2	270
Appendix III: Supplementary material for Chapter 3	279
Appendix IV: Supplementary material for Chapter 4	297
Appendix V: Supplementary material for Chapter 5	327
Appendix VI: Supplementary material for Chapter 6	400
Appendix VII: Supplementary material: Other	434

Acknowledgements

This work was supported by a Knowledge Economy Skills Scholarship funded by the European Social Fund through the Welsh Government's Convergence Programme, with additional funds provided by NRW and SEACAMS2.

I had wondered if after so much writing whether I would struggle to find the words. On the contrary, and perhaps as usual, I have plenty to say. And so, as another chapter comes to a close, all that remains is for me to look back on this journey and acknowledge all those who have supported me along the way.

First, to my supervisors, to whom I am so grateful: Dr James Bull, Professor Luca Börger, Professor Rory Wilson, and Dr Thomas Stringell.

Jim, thank you for your unwavering support, patience and understanding. I have truly appreciated your door always being open for me. Thank you for the many stimulating conversations we have had regarding my work, which have honed my ideas and helped me to shape the way I think about research. Your knowledge, ideas, and constructive criticism have always been appreciated. Thank you for your enormous efforts in administrative duties and for keeping me focused on crucial targets and timelines. Thank you for the swift turnaround on so many supporting statements, often at rather short notice, which have led to successful grants, conference attendances, and more. Thank you also for your support in my many extracurricular activities, especially in teaching for which you have provided direct opportunities and helpful feedback. And of course, thank you for the two wonderful seagrass diving expeditions to the Isles of Scilly – I will not forget the dives with seals, nor the gin!

Luca, you have given me so much in the form of both pastoral support and research guidance. Thank you for your ceaseless energy and enthusiasm, which have been a constant source of motivation and encouragement, and have inspired in me both a deep-rooted passion for my subject and the confidence to tackle it. Thank you for your continuous reassurance and belief in me. Thank you for introducing me to so many new methods, and for your close support in helping me to develop the skills to utilise them. In particular, thank you for imparting your knowledge and passion for statistics on to me. At the beginning of this journey I could have never imagined developing such a passion for statistics, let alone it now being one of the things that I look forward to teaching the most. Thanks to you too for your support in my extracurricular activities and your crucial feedback on so many applications, which have opened the door to incredible opportunities for me: an internship at the Royal Society, mentoring for the BES, hosting an international conference, and countless training workshops with world experts. And of course, thank you for joining me on so many exhilarating fieldwork efforts both at home and abroad. I hope you look back on our ventures as fondly as I do, especially the occasions where the seals got the better of us!

To **Rory**, the wisest of owls, you have always been there when I have needed you – even in times where life has challenged you the most. Your strength and character are unquestionable. Thank you for your humour and good

judgement, and for remaining such a close friend to me all these years. Thank you for being the force of positive energy which drives the research team that has been such a joy and privilege to be a part of.

Tom, thank you for the great part you have played in making this project a reality. From your immense efforts in administrative duties on behalf of Natural Resources Wales, to your comprehensive and constructive feedback on my work and ideas which has always been outstanding. Your perspective and expertise on policy and wider issues have been extremely complementary to the other guidance I have received, and your wisdom and approach has ignited in me my own passion for policymaking. Above all, thank you for your warmth on this journey – working with you has been a pleasure.

Finally to my supervisors, thank you all for so much of your most precious resource – your time.

I am thankful for the support of the **Department of Biosciences at Swansea University** which I have been a part of for the last decade. Thank you for shaping me into the person and professional that I am today. In particular I would like to thank the outstanding efforts of members of the administrative and finance teams for their assistance over many years: **Liz Cozens, Rosemary Muxworthy, Lindis Glover, Sara Fenn, Alison Caughlin, Helena Sainsbury, Alayne Harris, Andrew Gregory, Alan Davies, Pauline Jones, Susan Davies** and **Mark Pritchard**. And to the staff at the KESS office who have provided ongoing administrative support with my funding agency: **Cassy Froment, Jane Kelly, Jane Phipps** and **Mike McMahon**. Further colleagues have contributed great individual support: **Emily Shepard**, thank you for countless stimulating conversations over the years regarding my research and for providing such useful feedback as a member of my Progression Panel; **Carlos Garcia de Leaniz**, thank you also for your helpful feedback on my Progression Panel, and for always stopping in the department corridor to check in with me and express words of encouragement; **Kam Tang**, you also provided extremely helpful feedback at my final Progression Panel meeting. **Laura Roberts, Gethin Thomas** and **Ed Pope**, for your fantastic support in furthering my abilities as a teacher. **Dan Forman**, for your friendship, and your encouragement and generous comments on my work and extracurricular activities. To **Mark Holton**, there are few who share such reassuring calm as you – thank you for the hours of your time spent discussing and testing tag equipment with me, and for your tremendous soldering expertise. **Nicole Esteban**, you also provided extremely useful advice on the choice of tag technologies. **Steve Shaw**, thank you for all of the IT support over the years which has been absolutely fundamental to my progress. **Phil Hopkins**, so much of what I have undertaken in this thesis has been underpinned by your hard work and skill in the workshop – you truly are a wizard. I am forever grateful for the warmth of your welcome every time I came to you with yet another problem to solve. You are one of the most patient and diligent men I know. You also took a genuine interest in my personal and professional development and I am grateful for the friendship we built. **Julian Kivell**, you too gave me so much of your time, ideas, words of encouragement, and assistance in the workshop – thank you.

To my labmates, whom I have shared so much of this journey with and who have provided great moral support: **Baptiste Garde, Manos Lempidakis, Alexis Malagnino, Lloyd Hopkins, James Redcliffe, Hannah Williams, Richard Gunner, Dania Albin, Daniel Strömbom, Lottie Rodders, Rhian Ricketts, Holly English, Angharad James, Richard Lewis, Alex Arkwright, Gwen Wilson, Charlotte Davies, Nahaa Al-Otaibi, Pedro Roberts, Becky Phillips, Tom Fairchild**. Thank you all for making the office such a wonderful place to work and thrive. In particular, thank you Baptiste for our R problem solving sessions, it has been so great to work together with you to tackle coding challenges; Manos, thank you for being such a good and sincere friend; Alexis, for such hilarity in the office – you are dab-ulous; James and Lloyd, thank you both for your infectious humour and for your great assistance in building tags; Lottie, for your warmth and friendship, and for the dog walks; Hannah, for being such an excellent role model and an all-round wonderful human being; Angharad, for being a member of the dream team and sharing such great times together; Holly, thank you for your loyalty and close friendship, for all the times you supported me on a personal level, and for the fun we had building tags together (thanks for your help with that too, by the way!). I will never forget our frog-face emoji in-jokes. Stay schwifty. And to Nahaa, one of the kindest and most fearless people I know. Thank you for being such a supportive friend and role model, for introducing me to your culture, for your supply of Arabian tea and other indulgences, and for your thoughtful messages which lifted my spirits.

Vielen Dank an meine deutschen Kollegen bei ITAW: **Dominik Nachtsheim, Abbo van Neer, Bianca Unger, Stephanie Groß, Steffen Mumme, Tobias Schaffeld, Miriam Hillman, and Ursula Siebert**. Without a doubt, my fondest PhD memories are of the times I spent in Germany. Thank you for welcoming me into your research team at ITAW with such warmth and open arms. Dom and Abbo, you in particular made me feel at home. You were also always so generous with your time and advice, especially with regards to tagging techniques and tag design. You provided me with some of the most stimulating research discussions that I can recall. I will never forget my trips to Büsum, especially the celebratory beers and games after a successful seal catch. I cannot thank you both enough for your immense efforts in recovering the tags that we deployed. Ursula, thank you also for your kindness and your valuable time.

To my collaborators and others who assisted me – a huge thanks to **Euan Mortlock** for his assistance digitising the historical ringing records, and thanks to **Kate Lock, Richard Lewis, Michael Alexander** and **Mark Jessopp** for helping to georeference the locations in this dataset; to **David Naumann, Benjamin Evans, Hannah Bowen** and **Simon Withers** for their excellent work in helping me to design biologging devices and model their impact – I am extremely proud of our collaborative paper and thoroughly enjoyed working with you all in this interdisciplinary capacity. Thank you for all of the time and effort you put in to this work. Thank you also to **Roy Mayer** for providing the CAD files of the seal and tag A geometry used in this study. To **Simon Moss, Matthew Bivins, Matt Carter, Joe Onoufriou, Gordon Hastie, Debbie Russell, Dave Thompson**, and many others from the Sea Mammal Research Unit that have shared their valuable expertise, time and assistance with me,

including allowing me to join them for seal captures. Thank you for the most exhilarating fieldwork I have ever experienced, and for incorporating me into your team as a valued member. Thank you to Simon in particular for your words of wisdom and constructive criticism over the years, to Matt for ongoing support and friendship, and to Debbie for providing the data for Chapter 3. Thanks also to **Kimberley Bennett, Clare Embling, and Paul Thompson** for stimulating research conversations and fieldwork opportunities.

To so many other companions that I have made along the way who have offered such great friendships (as well as sofas to sleep on for attending various international conferences!) – the UKIRSC and ECS crowd: **Tom Bean, Cynthia Barile, María Pérez Tadeo, Claudia Allen, Heather Vance, Katherine Whyte, Izzy Langley, Natalie Sinclair, Tilen Genov, Aude Benhemma, Kayleigh Jones, Laura Oller López, Lucía Merino, Nicola Piesinger, Sara Niksic, Virginia Iorio, Tom Grove, Cristina Otero Sabio, James Waggitt, Ceri Morris, Rod Penrose, Rob Deaville;** and others: **Chaïm de Mulder, Søs Gerster Engbo, Adam Mulkern, Mike Burgum, Karen Devine, Amy Padfield.**

To colleagues who I had the pleasure of working with alongside this PhD: **Richard Unsworth, Sam Rees, Evie Furness, Chiara Bertelli, Keith Naylor, Max Robinson, Hanna Nuuttila, David Clarke, Georgina Blow, Mike Gwilliam, Anouska Mendzil, Emma Butterworth, David Tonge.** Thank you all for the opportunities you have given me, the fun we have had, and for being fantastic friends.

To close friends: **Michael François, Kris Page, Benjamin Jones, Joseph Peters, Eleanor Hatton, Dom Fisk, Will Denny, Poppy Disney, Sam Petts, Eve Uncles, Mike Cahill, Kate Clark.** Thank you all for the part you have all played in my journey, from assisting me with recovering tags, to recreational SCUBA diving, and to putting me up when I needed a place to stay. I'm so grateful to be able to call you my friends.

To the crew of the **Mumbles Lifeboat RNLI.** What a truly fantastic experience it has been volunteering with you for the last few years. Thank you for welcoming me so warmly into the team, and believing in my ability. Thanks to all of the crew for your interest in my work on seals and the friendships you have given me. Thank you in particular to **Ben Billingham** for being such a good friend these last few years.

To my family, **Mum, Dad, Alex, and Nan.** Thank you for your enduring support in my work, for never failing to believe in me, for making every moment spent at home and visits to The Mumbles a blessing, and simply for always being there. To **Dave and Carole,** thank you for your support these last few years; for welcoming me into your family and to the farm with such generosity, and for the exceptional Sunday dinners!

Finally, to **Leah.** It is difficult to know how I would have made it to the end without you. You have been my light in the dark. Thank you for your never ending support and extraordinary patience, and for all of the wonderful times we have had together. May we have many more. I love you and cannot wait to start our next chapter.

List of figures and tables

Chapter 1

Figure 1.1	<i>Distribution of grey and harbour seals in the Celtic and North Sea, and locations of example TSTs</i>	39
Figure 1.2	<i>Mind map of thesis objectives</i>	46

Chapter 2

Figure 2.1	<i>Output from least-cost path function to calculate biological distance of seal movements</i>	58
Figure 2.2	<i>Schematic diagram of typical displacement curves</i>	60
Figure 2.3	<i>Schematic diagram of spatio-temporal overlap with a buffer zone at the Ramsey Sound TST site</i>	62
Figure 2.4	<i>Map of grey seal pup mark and resight locations and summary movement metrics</i>	67
Figure 2.5	<i>Displacement distance as a function of time</i>	70
Figure 2.6	<i>Displacement distance as a function of sex</i>	70
Figure 2.7	<i>Displacement distance as a function of colony</i>	71
Figure 2.8	<i>Sex-dependent effect of NAO on displacement distance</i>	71
Figure 2.9	<i>Displacement predictions over time for seals from Pembrokeshire</i>	74
Figure 2.10	<i>Number of pups predicted to overlap with a TST site</i>	75
Table 2.1	<i>Details of the models fitted to derive time-dependent displacement curves</i>	63
Table 2.2	<i>Summary details of individual seal dispersal</i>	66
Table 2.3	<i>Model comparisons of different NAO interpretations</i>	69
Table 2.4	<i>Output table for model of displacement distance drivers</i>	69
Table 2.5	<i>Concordance correlation values for each fitted model</i>	73
Table 2.6	<i>Predictions for the timing of overlap between seal pups and a nearby TST</i>	74

Chapter 3

Figure 3.1	<i>Pup tagging sites in Wales</i>	93
Figure 3.2	<i>Schematic diagram of typical displacement curves</i>	96

Figure 3.3	<i>Example pup trajectories</i>	100
Figure 3.4	<i>Example pup trajectories with NSD patterns</i>	104
Figure 3.5	<i>Distribution of recording durations for movement modes</i>	106
Figure 3.6	<i>Fitted individual-level movement models and population-level ringing models</i>	108
Figure 3.7	<i>Fitted individual-level movement models and population-level ringing models for the first 90 days</i>	109
Figure 3.8	<i>Predicted displacement distance from models fitted to individual- and population-level data</i>	110
Figure 3.9	<i>Predicted time elapsed when key movement events occurred for individual- and population-level data</i>	111
Figure 3.10	<i>Bootstrapped estimates of displacement distance</i>	113
Table 3.1	<i>Deployment summary information</i>	91
Table 3.2	<i>Details of the models fitted to derive time-dependent displacement curves</i>	95
Table 3.3	<i>Estimates from fitted displacement over time models</i>	103
Table 3.4	<i>The scale of displacement of pups at 3 months old</i>	105
Table 3.5	<i>Sample size required to estimate summary statistics of displacement distance</i>	114
Chapter 4		
Figure 4.1	<i>Schematic diagram of HMM dependence structure</i>	134
Figure 4.2	<i>State-dependent parameter distributions for final HMM</i>	139
Figure 4.3	<i>Example trajectory with behavioural state assignments</i>	140
Figure 4.4	<i>Covariate effects on state dependent step length mean parameter</i>	142
Figure 4.5	<i>Covariate effects on state dependent directional persistence parameter</i>	144
Figure 4.6	<i>Estimated stationary state probabilities</i>	147
Figure 4.7	<i>Estimated transition probabilities</i>	150
Figure 4.8	<i>Estimated behavioural state persistence probabilities</i>	151
Figure 4.9	<i>Number of BCs utilised as a function of the number of trips</i>	152

Table 4.1	<i>Details of the 24 harbour seals investigated in this study</i>	138
Chapter 5		
Figure 5.1	<i>Tag design in CAD software</i>	168
Figure 5.2	<i>The final tag design</i>	169
Figure 5.3	<i>The final baseplate design</i>	171
Figure 5.4	<i>Attachment of the tag to the baseplate</i>	172
Figure 5.5	<i>Seal tagging sites</i>	175
Figure 5.6	<i>Example deployment of tag on harbour seal</i>	176
Figure 5.7	<i>Recovery condition of tags</i>	179
Figure 5.8	<i>Example of a fastloc-GPS trajectory</i>	185
Figure 5.9	<i>Example of raw data from a Daily Diary</i>	186
Table 5.1	<i>Details of components used in the tags developed</i>	166
Table 5.2	<i>Tag deployment and summary information</i>	181
Table 5.3	<i>Details of search efforts and tag recoveries</i>	182
Table 5.4	<i>Recording durations of data acquired from tag deployments</i>	184
Chapter 6		
Figure 6.1	<i>Example of CFD mesh</i>	200
Figure 6.2	<i>Summary of CFD methodology used for simulations</i>	201
Figure 6.3	<i>The tag positions studied in the CFD modelling</i>	204
Figure 6.4	<i>Turbulence and pressure differentials of the two tags</i>	206
Figure 6.5	<i>Drag coefficient of the two tag designs</i>	210
Figure 6.6	<i>Two methods for reducing the drag impact of tags</i>	212
Table 6.1	<i>Summary dimension and drag values of the two tags</i>	207
Table 6.2	<i>Drag details as a function of position of the two tags</i>	208

List of definitions, abbreviations, and keywords

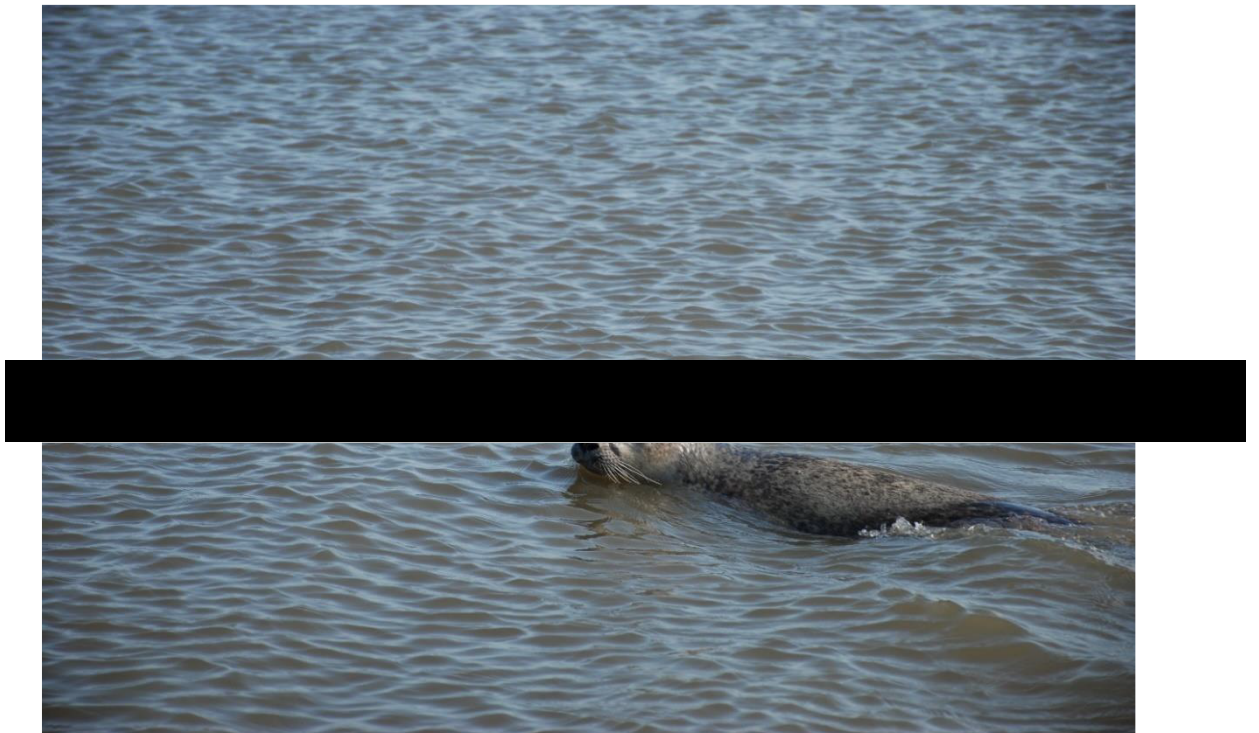
2D	Two-dimensional
3D	Three-dimensional
AAS	Active acoustic sonar
ACF	Autocorrelation function
AIC	Akaike information criterion
ARGOS	Advanced Research and Global Observation Satellite
ARS	Area-restricted search
CAD	Computer-aided design
CC	Concordance correlation
C_d	Drag coefficient
CFD	Computational fluid dynamics
CI	Confidence interval
CLS	Collecte Localisation Satellites
COT	Cost of transport
CPF	Central-place forager
DD	Daily Diary
dsb	Days since birth
EIA	Environmental Impact Assessment
EMEC	European Marine Energy Centre
GOF	Goodness of fit
GLS	Global location sensors (geolocators)
GPS	Global positioning system
GSM	Global System for Mobile Communications
HMM	Hidden Markov model
HRA	Habitat Regulations Assessment
Hz	Hertz; number of cycles per second
IMASEN	Inter-mandibular angle sensor
IMU	Inertial movement unit
IQR	Interquartile range
ITAW	Institute for Terrestrial and Aquatic Wildlife
L	Likelihood
Lat	Latitude
Lon	Longitude
mAh	milliamp hour
MCZ	Marine Conservation Zone
MINOS	Marine warm-blooded animals in North and Baltic Seas
MNR	Marine Nature Reserve
MRE	Marine renewable energy
MSD	Mean-squared displacement
MSP	Marine spatial planning
MW	Megawatt

NAO	North Atlantic Oscillation
ND	Net-displacement
nmi	Nautical mile
NNR	National Nature Reserve
NRW	Natural Resources Wales
NSD	Net-squared displacement
OFT	Optimal foraging theory
PAM	Passive acoustic monitoring
PBR	Potential biological removal
PCoD	Population consequences of disturbance
PID	Photo-identification
PTT	Platform transmitter terminal
RSPB	The Royal Society for the Protection of Birds
SAC	Special Area of Conservation
Sampling frequency	The frequency at which data are recorded
SD	Standard deviation
SEACAMS	The Sustainable Expansion of the Applied and Coastal Marine Sector
SMRU	Sea Mammal Research Unit
SPOT	Smart Position Only Tag
SSSI	Site of Special Scientific Interest
SSE	Sea surface elevation
SST	Sea surface temperature
Tag	An animal-attached tracking device; either a transmitting biotelemetry device or an archival biologging unit
TDR	Time-depth recorder
TSE	Tidal stream environment
TST	Tidal stream turbine
UAV	Unmanned aerial vehicle (drone)
UHF	Ultra-high frequency
VHF	Very-high frequency

Chapter 1

Introduction

“For all animals both impart movement and are moved for the sake of something, so that this is the limit to all their movement:
the thing for-the-sake-of-which.”
(Aristotle, *De Motu Animalium*, 384-322 BC)



Moving away from its captors: A harbour seal departs the beach following release
(Photograph by Abbo van Neer).

1.1 Marine megafauna – The threat of anthropogenic environmental change and the emergence of tidal stream turbines (TSTs)

Marine megafauna, a group comprising seabirds and marine mammals (Hazen et al., 2019), play a crucial role in the functioning of marine ecosystems (Heithaus et al., 2008; Maxwell et al., 2013; Hobday et al., 2015), for example through the top-down control of prey (Hobday et al., 2015). They also serve as indicator species (Zacharias & Roff, 2001; Hazen et al., 2019) by responding to environmental change or major disturbance (Sergio et al., 2008; Sydeman, Poloczanska, Reed, & Thompson, 2015) and indicating the presence of other species, or the condition of habitats (Zacharias & Roff, 2001; Estes, Heithaus, McCauley, Rasher, & Worm, 2016), making them important for conservation.

Threats to marine megafauna, especially those of anthropogenic environmental change, are numerous and substantial (Halpern et al., 2015). Marine megafauna are at high risk (Maxwell et al., 2013), with many globally endangered (e.g. 33 % of marine mammal species; Avila, Kaschner, & Dormann, 2018). This risk stems from the fact that they share similar scales of habitat and resource use as humans (Young et al., 2015; Machovsky-Capuska & Raubenheimer, 2020) e.g. frequently occurring in coastal environments (Maxwell et al., 2013). As a result, marine megafauna are disproportionately affected by both direct and indirect detrimental interaction with humans and anthropogenic developments (Rivalan et al., 2010; Madin et al., 2016; Lotze et al., 2019). Further, marine megafauna can also be far-ranging (Block et al., 2011) which may expose them to a wide range of threats (Halpern et al., 2008; Maxwell et al., 2013; Harrison et al., 2018). Key threats to marine megafauna, and their impacts, include: waste pollution (Avila et al., 2018) causing lethal effects (e.g. Senko et al., 2020); noise pollution (Hückstädt et al., 2020) causing behavioural disruption (e.g. disruption to foraging; Wisniewska et al., 2018); habitat loss (Runge et al., 2014) leading to relocation (Kavelaars et al., 2020); by-catch (Luck et al., 2020) and entanglement (Van Der Hoop et al., 2013) resulting in mortality; interactions with fisheries causing resource

depletion (e.g. Wildermann et al., 2020) and competition (DeMaster, Fowler, Perry, & Richlen, 2001); and ship strikes causing injury or death (Abrahms et al., 2019), amongst others (Maxwell et al., 2013; Avila et al., 2018). Impacts are not limited to the short term; anthropogenic environmental change may incur lifetime negative effects on the fitness of marine megafauna (Pirodda et al., 2019).

Climate stress – ocean warming, acidification and deoxygenation – poses the greatest potential impact to marine megafauna (Maxwell et al., 2013; Sampaio & Rosa, 2020). Climate change is predicted to cause global ocean biomass decline (Lotze et al., 2019), stripping ecosystems of lower trophic level prey sources that directly support marine megafauna (Young et al., 2015). The loss of marine megafauna has widespread consequences for marine ecosystems, such as trophic downgrading (Myers, Baum, Shepherd, Powers, & Peterson, 2007; Estes et al., 2011) or variation in carbon flux (Wilmers et al., 2012). Mitigating the impacts of anthropogenic environmental change on marine megafauna is therefore crucial and, given its widespread impact, there is a global urgency to tackle climate change (Gills & Morgan, 2020).

In recent years, a key component of the worldwide effort to tackle climate change has been the development of marine renewable energy (MRE) devices, especially tidal stream turbines (TSTs). TSTs can come in many forms (Wade, 2015), including open-centre turbines with enclosed blades, and kites tethered to the seabed, however I focus here on traditional horizontal-axis turbines which represent the most advanced device designs to date (Chowdhury et al., 2020). These TSTs exploit the fast flowing movement of water through tidal channels for energy generation, analogous to wind turbines generating energy from the movement of wind. Whilst there has been considerable progress made in recent years in the development and testing of TSTs, the industry remains in its nascent stage (Chowdhury et al., 2020). The UK sector, for example, is positioned to be a global leader in the development of TSTs (Ocean Energy Systems, 2020) with access to some of the fastest tidal currents in the world (e.g. exceeding 3 ms^{-1} in the Ramsey Sound; Malinka et al., 2018; and 5 ms^{-1} in the Pentland Firth; Adcock et al., 2013). Indeed, the UK was responsible for the world's first TST – the “SeaGen” installed in 2008

– and currently maintains a total of 1,287 MW of leased tidal stream sites (Carter et al., 2020). However, despite this potential, widespread commercialisation of TSTs in the UK has not yet been achieved. This is because, amongst other challenges, TST devices are expected to pose risks to marine megafauna, and this hence represents a key consenting hurdle for the industry (Copping & Hemery, 2020). Indeed, the need to meet stringent Environmental Impact Assessment (EIA) and Habitats Regulations Assessments (HRA) consenting requirements has contributed to a stagnation in the growth of the industry (Chowdhury et al., 2020); for example, the need to collect substantial baseline and post-installation monitoring data for proposed TST developments. Hence while there is great potential, to date the UK has only 6 out of 20 proposed tidal energy development sites in operation, and boasts just 10 MW of operational TST capacity (Marine Energy Council, 2019; Carter et al., 2020; Ocean Energy Systems, 2020).

1.2 Marine megafauna in tidal stream environments (TSEs) –

The threat of TSTs and information needs

In the marine environment, resources for marine megafauna (i.e. prey) are patchily distributed in space and time (Embling et al., 2012). However, this patchiness is often predictable, being driven by physical processes such as eddies or fronts (Cox, Scott, & Camphuysen, 2013) which drive productivity and influence the distribution of zooplankton and fish (Uda & Ishino, 1958; Riley, 1976; Wolanski & Hamner, 1988; Zamon, 2001, 2003; Genin, 2004), generating highly predictable aggregations of prey. This is particularly the case in tidal stream environments (TSEs), where the flow of water during flood and ebb tides (i.e. tidal currents) is accentuated by topography (e.g. being constrained through straits, around headlands, or over banks). TSEs are characterised as sites where tidal current velocities exceed 1 ms^{-1} (Benjamins et al., 2015) and which typically exhibit a high degree of structure in their physical oceanographic processes (e.g. eddies or fronts). In TSEs, tidal currents are primarily responsible for driving aggregations of prey, making these sites particularly profitable for foraging marine megafauna (Cox, Scott,

& Camphuysen, 2013), and thus giving rise to “hotspots” (Embling et al., 2012). For example, harbour seals in Netarts Bay, Oregon, were observed to aggregate around the mouth of Whiskey Creek 2.5 hours either side of high tide to exploit the influx of chum salmon entering the creek (Brown & Mate, 1983). Braune & Gaskin (1982) observed that larids foraging off Deer Island in New Brunswick were concentrated in highest numbers during tidal floods, when water moves over topographical rises in the Letete Passage. Cairns & Schneider (1990) observed that Thick-billed murre aggregated to forage at the Nuvuk Islands during times when tidal currents generated a predictable abundance of nekton. These findings, amongst numerous others (see Hunt et al., 1999 for a review), encouraged the general term “tidal-coupling hypothesis” to be coined by Jeannette Zamon in the early 2000s, to describe how tidal phase drives predictable energy flow to higher trophic levels (such as marine megafauna) in TSEs (Zamon, 2001, 2003).

In the last two decades, a plethora of research has been undertaken examining the behaviour, movements, and distribution of marine megafauna in TSEs (reviewed in Benjamins et al., 2015). This research has shown that there is substantial variation in the use of TSEs and specific tidal features (i.e. eddies, boils, fronts, etc.) by marine megafauna, and that this is likely to vary by taxa, sex, age class, and as a result of individual variation (Benjamins et al., 2015). Briefly, in seabirds, penguins, auks, and cormorants have been well observed to exploit tidal features in TSEs (such as currents or boils) for foraging or travelling, or both (Slater, 1976; Hunt Jr et al., 1998; Holm & Burger, 2002; Zamon, 2003; Ladd et al., 2005; Watanuki et al., 2008; Rey et al., 2010; Wade et al., 2012); likewise gulls, terns, boobies, and gannets have also been observed aggregating in and foraging in TSEs, including targeting various specific tidal features common to these environments (boils, eddies, and upwellings) (Braune & Gaskin, 1982; Vermeer, Szabo, & Greisman, 1987; Zamon, 2003; Elliott, 2004; Scott et al., 2013). Contrastingly, for procellariiformes there is little evidence of use of TSEs, except for Northern Fulmar (*Fulmaris glacialis*) that have been shown to exploit eddies for foraging (Ladd et al., 2005). Toothed whales are frequently associated with tidal currents (both fast and slow) and other dynamic features of TSEs (especially

porpoises, belugas, bottlenose, humpback dolphin, risso's dolphin, and orca) (Lydersen et al., 2001; Mendes et al., 2002; Bordino, 2002; Hobbs et al., 2005; Pierpoint, 2008; Embling et al., 2010; Li et al., 2010; Barrett-Lennard et al., 2011; Rayment et al., 2011; Isojunno, et al., 2012; Wilson et al., 2013; Stafford, et al., 2013; de Boer et al., 2014; Benjamins et al., 2016; 2017), but uncertainty remains as to how consistent these associations are and thus whether TSEs are fundamental habitats for these taxa or whether they are used opportunistically (Benjamins et al., 2015); for baleen whales relatively limited information exists for most species and it is unclear how important TSEs are (Benjamins et al., 2015), but grey, minke and fin whales have demonstrated preferences for tidal currents (Gill, Jr. & Hall, 1983; Johnston et al., 2005; Ingram et al., 2007; Chenoweth et al., 2011; Anderwald et al., 2012) and it is possible that the foraging strategies of baleen whales are assisted by the tidal movements of their prey (Benjamins et al., 2015). In pinnipeds, otariids (fur seals and sea lions) have been recorded to make use of frontal features (such as migrating through tidal flows and foraging on prey that aggregate in such conditions) (Ragen, Antonelis, & Kiyota, 1995; Ream, Sterling, & Loughlin, 2005; Stabeno et al., 2005) though there is insufficient evidence (including a lack of data with high enough spatial and temporal resolution) to fully assess the importance of TSEs generally (Benjamins et al., 2015). For odobenids (walrus) there is a paucity of evidence to support the use of TSEs (Benjamins et al., 2015). Greater evidence of the use of TSEs exists for phocids (true seals) with most notably grey and harbour seals regularly reported making use of high tidal flows for foraging and travelling through channels – the latter includes ice-free channels in high-latitudes which are also used by ringed and bearded seals (facilitated by tidal currents) (Mansfield, 1967; Stirling, 1980; Brown & Mate, 1983; Thompson et al., 1996; Suryan & Harvey, 1998; Cunningham et al., 2010; Hastie et al., 2016, 2017, 2019; Joy et al., 2018; Lieber et al., 2018; Onoufriou et al., 2021).

In summary, it is clear that to varying extents marine megafauna use TSEs, including for essential behaviours such as foraging, however there is a need to obtain more evidence for many taxa (Benjamins et al., 2015). This is crucial because, just as marine megafauna use TSEs, so too does the TST industry

for energy generation (Lewis et al., 2015). This presents a challenge, as there is a large degree of uncertainty regarding the consequences of any interactions between marine megafauna and TSTs (Copping & Hemery, 2020). Impacts are predicted to differ between sites due to varying physical features (Benjamins et al., 2015); between TSTs due to differences in device type and differences in installation and operational procedures (Fox et al., 2018); and between taxa due to differences in animal behaviour (Benjamins et al., 2015). The key concerns to marine megafauna include the noise levels generated by TSTs during both the installation and operation of devices (Hastie et al., 2018; Lossent et al., 2018; Copping et al., 2020), direct collisions between animals and TSTs which may result in severe or fatal injury (Band et al., 2016; Onoufriou et al., 2019; Copping et al., 2020; Horne et al., 2021), and spatial overlap of animals with TSTs which may lead to avoidance behaviour, potentially resulting in displacement from key habitats or barrier effects (Waggitt & Scott, 2014; Hastie et al., 2017; Sparling et al., 2018). Assessing the risk of these impacts requires consideration of the degree of overlap that animals may have with TSTs. Risks can be generally considered at three spatial scales (cf. Waggitt & Scott, 2014):

1.2.1 Broad-scale (1–10 km)

The potential for broad-scale impacts to occur relates to the general distribution and occupancy patterns of animals in relation to TSEs, and their far-field responses to TSTs. The locations of many sites proposed for TST developments – areas with energy resources consisting of 2–2.5 ms⁻¹ mean spring peak tidal currents over an area 1 nmi² (Fraenkel, 2006; Waggitt & Scott, 2014) – typically occur in TSEs. Such areas are expected to overlap with the distribution of key sites for marine megafauna, for example seabird nesting areas or seal haul-out sites (e.g. Hastie et al., 2016; Cole et al., 2018). This raises necessary concerns of the potential threats that TSTs may pose to animals, with potential consequences to individuals and potentially population-level implications (Copping et al., 2020). However, for many marine megafauna species, occupancy patterns in TSEs and thus the predicted

degree of overlap with TSTs remains poorly understood (ORJIP Ocean Energy, 2020). Overlap of marine megafauna with TSTs may lead to avoidance behaviour (Hastie et al., 2019; Onoufriou et al., 2021), resulting in large scale displacement of individuals or populations away from areas where TST devices are installed on account of increased noise or electromagnetic fields (EMFs), with implications for the broad-scale distribution of individuals and populations (Copping & Hemery, 2020). For example, Lossent et al., (2018) measured the noise levels generated by a TST and estimated this to be detectable by marine mammals at up to 1 km. Similarly, Hastie et al., (2018) observed that harbour seals exhibited spatial avoidance of the noise generated by a TST at range of up to 500 m. More recent research suggests that the response range may be even greater; Onoufriou et al., (2021) observed a 44% decrease in seal abundance up to 2 km away from a TST during operational periods compared to non-operational periods. Many marine megafaunal species have the capacity to detect EMFs (Kirschvink, 1997; Copping et al., 2016), however compared to noise, an understanding of their risks and impacts remains relatively uncertain (Taormina et al., 2018).

The distribution of a species varies according to life history stage or breeding cycle and can also vary seasonally (Allen, Metaxas, & Snelgrove, 2018), and thus so too can their occupancy in TSEs and hence risk of overlap with TSTs. For example, as pups, many pinnipeds undertake a far-ranging natal dispersal after weaning (Greig et al., 2018; Peschko et al., 2020) which sees them move away from their coastal birth site to new areas, including other coastal habitats. Such displacements could involve movement(s) past a TST (Malinka et al., 2018) whilst they are at their most vulnerable and naïve (Thompson, 2012). Adult pinnipeds on the other hand predominantly undertake central-place foraging (CPF) trips (≤ 50 km offshore; Thompson, Mackay, Tollit, Enderby, & Hammond, 1998; Jones et al., 2015) which may see them need to negotiate TSTs on multiple occasions during return foraging trips (Russell et al., 2015). During the breeding season, many seabirds and pinnipeds will spend extended periods inshore, restricted by the need to remain relatively close to resting sites or areas of reproductive activity (Parijs, Thompson, & Tollit, 1997; Van Parijs, Hastie, & Thompson, 1999; Waggitt & Scott, 2014). This makes them more

likely to use coastal habitats such as TSEs where TSTs are likely to be installed. Conversely, the breeding season may involve large-scale displacements for some taxa; adult grey seals have been recorded moving up to 230 km annually between breeding locations (Sayer et al., 2019). Finally, the occupancy patterns of animals in TSEs can also vary in response to annual or seasonal prey availability or quality (Waggitt & Scott, 2014). For example, Sveegaard et al., (2012) observed that the distribution of harbour porpoises in the Sound between the Kattegat and the Baltic Sea varied seasonally in response to differences in prey availability. Specifically, during summer months, the Sound supported relatively large (i.e. higher quality) and more diverse prey items, supporting larger densities of porpoise, compared to the winter months which saw a smaller diversity and poorer (i.e. smaller) prey quality, supporting lower densities of porpoise. Similarly, Wanless, Gremillet, & Harris (1998) found that between the end of May and the beginning of August the distribution of shags (*Phalacrocorax aristotelis*) foraging from the Isle of May switched from a range of 10 km from the colony to 0.8 km away, likely in response to a concurrent improvement in the availability of prey (sandeels) near to the island.

Taken together, predicting the broad-scale overlap of marine megafauna within TSEs, and thus their potential to come into contact with TSTs, requires an understanding of the distribution of animals across life and seasonal cycles, and in response to physical features of the environments they target and the associated availability of prey.

1.2.2 Fine-scale (100 m – 1 km)

If an animal occupies a TSE with an operational TST, the risk of coming into contact with a device depends on that animal's fine-scale behaviour and habitat use (including the use or avoidance of any specific tidal features) which will influence its proximity to any device present (Benjamins et al., 2015). For example, the risk of interaction with a device will vary depending on whether an animal is foraging within a TSE or merely transiting through it (e.g. Hastie et al., 2016); an animal foraging in a TSE may be subject to more opportunities

to interact with a device than an animal undertaking a single passage. Lieber et al., (2018) found that during peak tidal flows grey seals avoided areas of extreme backscatter (i.e. areas of high macro-turbulence) in the centre of a tidal channel, preferring areas at the edges of the channel, highlighting how the risk of interaction with a device can vary depending on whether an animal targets the same tidal feature within a TSE as that exploited (or indeed created; Williamson et al., 2019) by a TST; evidence has shown that the installation of TSTs can cause direct changes to hydrodynamic flow regimes (Martin-Short et al., 2015; Roche et al., 2016) and create artificial reefs (Taormina et al., 2020). This can influence the distribution and behaviour of prey in TSEs (Williamson et al., 2019) that are targeted by marine megafauna, and in so doing vary the fine-scale habitat use of predators, potentially attracting them to TSTs (as for other anthropogenic structures at sea; Russell et al., 2014).

As for broad-scale distribution patterns, the fine-scale habitat use of animals in TSEs can also vary seasonally, driven by the availability and abundance of prey. For example, Waggitt et al., (2016b) found that the use of tidal features differed by species and season, with breeding Atlantic puffins (*Fratercula arctica*) targeting fast, horizontal currents and non-breeding European shags (*Phalacrocorax aristotelis*) making use of downward vertical currents. In the Bering Sea, short-tailed shearwaters (*Puffinus tenuirostris*) forage predominantly on euphausiids during summer months due to their increased abundance associated with near-shore fronts (Jahncke et al., 2005).

TSTs are mounted on the seafloor in depths ca. 20–50 m (Lewis et al., 2015) with the turbine blades positioned ca. 10–20 m above the seabed with a minimum clearance below the sea surface of 8 m (Bir, Lawson, & Li, 2011); thus well within the depth limits achievable by many diving marine megafauna, including juveniles for many taxa (Ponganis, 2015). The risk of fine-scale overlap will thus also depend on the diving behaviour of animals relative to the position of the turbine blades in the water column (i.e. the “turbine swept area”) (Horne et al., 2021). For example, benthic foragers will be at low risk when on the surface and during the foraging proportion of their dive, but at high risk during transit to and from the seabed when their depth overlaps with that of the turbine swept area (Hastie et al., 2019); this has been observed in seals

who tend to swim at the surface or on the seabed in TSEs, rather than in the pelagic zone (Evers et al., 2017; Joy et al., 2018; but see Hastie et al., 2019). Conversely, depending on the depth that they target, pelagic foragers may be at risk from collision throughout the entire duration of their time spent underwater and those species that consistently dive to turbine-swept depths are perceived to be at greatest risk (Waggitt & Scott, 2014).

Finally, at fine-scale the risk of marine megafauna interacting with TSTs also depends on how they behave around turbines and whether they exhibit any avoidance behaviour in response to them. This area of research is in its infancy (Copping & Hemery, 2020) with only few studies having documented overt avoidance responses to TSTs (Hastie et al., 2018; Joy et al., 2018; Sparling, Lonergan, & McConnell, 2018; Onoufriou et al., 2021); though this evidence is currently restricted to just one taxa (harbour seals *Phoca vitulina*). These studies have shown that operational TSTs do not present a barrier to harbour seal movements but that seals exhibit avoidance behaviour towards them at scales of 200–500 m (Hastie et al., 2018; Joy et al., 2018; Sparling, Lonergan, & McConnell, 2018). Specifically, in the Strangford Narrows, Northern Ireland, when TSTs were not operational, seals generally transited through the centre of the tidal channel relatively close to the turbine compared to the edges of the channel when the turbine was operating (Joy et al., 2018; Sparling et al., 2018). Moreover, seals swim past TST devices under varying current conditions but preferentially during periods of slack water when the operation of turbines is minimal (Sparling et al., 2018). Hastie et al., (2018) observed that seals exhibited avoidance behaviour at distances of up to 500 m away from the sound of an operational TST, with individuals moving on average 24 m away from the source of the noise, and similarly Onoufriou et al., (2021) demonstrated that that seal abundance was significantly reduced at up to 2 km from a TST array when devices were operational. Whilst providing key insights, these studies have been limited to TSEs in Scotland and Northern Ireland, and have revealed conflicting behaviour between sites (Copping & Hemery, 2020). For example, in Kyle Rhea, seals swam predominantly with the flow (Hastie et al., 2019) whereas in the Strangford Narrows they swam against it (Joy et al., 2018). There thus remains the need to obtain further information, especially

from the many other sites that have potential for TST developments (Pelc & Fujita, 2002; Carter et al., 2020), to make generalisations about the movement and behaviours (including avoidance) that animals exhibit in response to tidal conditions and TST devices (Copping & Hemery, 2020). In addition, understanding is generally lacking with respect to the variability of marine megafauna responses between species (Wade, 2015), between age classes (Carter, 2018), and both within- and between-individuals (Waggitt et al., 2017; Johnston et al., 2018; Johnston, 2019).

1.2.3 Near-field (< 100 m)

At the finest scale, the risk of TSTs to marine megafauna relates to the evasive behaviours employed by animals to prevent a direct interaction with a device (Hastie et al., 2019). While the broad- and fine-scale impacts of TSTs are potentially substantial and thus important to understand (Langton, Davies, & Scott, 2011; Copping & Hemery, 2020), the most tangible, perceived threat to marine megafauna is that of direct collision with moving components of TSTs (Waggitt & Scott, 2014; Fox, Benjamins, Masden, & Miller, 2018; Horne et al., 2021), and this hence presents the greatest challenging to consenting (Copping & Hemery, 2020). This risk is analogous to the risk of birds colliding with wind turbines – a topic that by comparison has received substantial research (Largey et al., 2021). The risk of marine megafauna colliding with TSTs will vary depending on the ability of animals to detect devices – using sight, sound (including echolocation), or tactile cues (e.g. seals detecting wake with vibrissae; Witte et al., 2012) –, something made difficult in TSEs on account of typically poor visibility, sediment suspension, and bubbles caused by turbulence (Benjamins et al., 2015). If animals come into contact with a device that they are able to detect, then the risk of collision will depend on any evasive behaviours undertaken. Harbour porpoise generally avoid the area of water swept by turbine rotors (Gillespie et al., 2021), but empirical evidence of evasive behaviour at near-field scales (< 100 m) for other taxa of marine megafauna does not currently exist. Simulated collision risk modelling undertaken by Horne et al., (2021) found that seals had a probability of up to

21.4 % of colliding with the rotor-swept area of a TST; although greater probabilities were associated with collision between seals and the static base of the device given seals' preferential use of the benthic part of the water column (Evers et al., 2017; Joy et al., 2018; but see Hastie et al., 2019).

If a collision occurs between an animal and the rotor-swept area of a TST, the risk of injury or even mortality may be high; the rotor speed of turbine blades in some areas can be as high as 12 ms^{-1} (Onoufriou et al., 2019), exceeding three times the velocity at which ship strikes are expected to kill large cetaceans (Vanderlaan & Taggart, 2007). Indeed, in an empirical study examining the impact of collisions between seals and turbine blades, severe trauma was detected in collisions exceeding 5.5 ms^{-1} velocity (Onoufriou et al., 2019). Mortality risk from collision will vary with the size of taxa or life history stage, with smaller or juvenile conspecifics perceived at greater risk owing to their relative vulnerability (e.g. Daunt et al., 2007; Thompson, 2012). The ecological impact of collision events will depend on the number of individuals affected and the potential effect of this at a population or ecosystem level (Onoufriou, 2021). For example, the risk to population viability will be particularly high for at-risk species or populations i.e. those that are small, spatially restricted, or already in decline (Copping et al., 2020).

1.2.4 Information needs

In summary, the use of TSEs by animals and the risks that TSTs pose will vary according to a complex combination of factors, including an animal's spatio-temporal distribution in both horizontal and vertical space, their speed relative to moving parts of TSTs, their behaviour and condition, and the influence of fine-scale hydrodynamics (Wade, 2015; Thompson et al., 2016; Waggitt et al., 2017; Lieber et al., 2018; Hastie et al., 2019; Onoufriou et al., 2019; Copping et al., 2020; 2020b; Horne et al., 2021). In order to mitigate the risks that TSTs pose to marine megafauna it is crucial to understand the broad-scale distribution and fine-scale habitat use of animals in TSEs and thus their potential overlap with TSTs, as well as their near-field interactions with installed devices. Improving our understanding of these risks will support the

TST industry to develop devices towards meeting sustainable energy generation commitments by providing the industry with evidence to meet the consenting targets put in place by environmental legislators (Copping & Hemery, 2020; ORJIP Ocean Energy, 2020).

In line with the above, recent years have seen a number of articles and reports published that have reviewed the knowledge gaps pertaining to the risks that TSTs pose to marine megafauna (ORJIP Ocean Energy, 2016, 2020; Copping et al., 2020; Isaksson et al., 2020). Among the most recent of these – the ORJIP Wave and Tidal Critical Evidence Needs report (ORJIP 2020) – has outlined a number of key information needs:

- (i) Improve understanding of the spatio-temporal use of TSEs by marine megafauna i.e. understand their distribution, occupancy patterns, and fine-scale habitat use in TSEs and hence their potential for overlap with TSTs.
- (ii) Determine the frequency and consequences of far-field responses to, and near-field interactions with, TSTs (including collision) at both the individual- and population-level.
- (iii) Improve the methods and instruments used to measure (i) and (ii), and
- (iv) Refine the techniques used to assess and manage the risks of any detrimental interaction(s) between animals and devices.

While the focus of the ORJIP Wave and Tidal Critical Evidence Needs report is on the information needs in the United Kingdom, the report was written in alignment with the global State of the Science 2020 report (which largely echoes its conclusions), and thus reflects well the general information needs of the industry as a whole internationally. Addressing these information needs will help to promote the use of evidence-based marine spatial planning (MSP) to plan and develop the installation of TSTs and other MRE devices effectively (Copping & Hemery, 2020). In tandem, this will support the development of appropriate conservation management strategies to protect marine megafauna at both the individual-level, e.g. via improvements to collision-risk modelling (Horne et al., 2021) and the development of appropriate mitigation

strategies, and at the population-level e.g. by understanding population consequences of disturbance (PCoD; King et al., 2015; Keen, Beltran, Pirodda, & Costa, 2021) and informing levels of potential biological removal (PBR; Brandon et al., 2017).

1.3 Studying marine megafauna in TSEs and their interactions with TSTs

Studying marine megafauna in TSEs and their potential interaction with TSTs presents many challenges (Fox et al., 2018). Generally speaking, marine megafauna are difficult taxa to study as they spend much of their time underwater where they are not easily observed and are typically only seen fleetingly at the surface (Shillinger et al., 2012; Carter et al., 2016). They are also fast moving and can cover large distances, thus making them challenging to observe directly, especially continuously and over long periods. These challenges are compounded in TSEs which are typically harder to work in than less dynamic environments (Embling et al., 2012); logistically TSEs are problematic, with strong currents and eddies making it difficult to operate research vessels, deploy survey equipment and collect data. Given these challenges, it is essential that a broad range of methods and approaches are used – including both traditional and modern techniques. Indeed, there are several different ways that the movement and behaviour of marine megafauna in TSEs and their potential interactions with TSTs are currently studied.

Visual surveys are the most common method for surveying marine megafauna in TSEs (Benjamins et al., 2015). These surveys can be land-based (Wade, Masden, Jackson, & Furness, 2012), boat-based (Lieber et al., 2018), or aerial (Joy et al., 2018; Lieber et al., 2021), and are advantageous in that they make use of often widely available and affordable observational equipment such as binoculars or cameras. Land-based surveys can be undertaken repeatedly at low cost and with relatively few logistical constraints. In contrast, boat-based surveys and aerial surveys come at considerably greater cost and are more logistically challenging but can survey larger areas. Visual surveys in TSEs

have traditionally been used to record animal abundance and discriminate species (Waggitt & Scott, 2014), as well as monitor behaviours (such as birds sitting on the water surface or flying; Camphuysen, Fox, Leopold, & Petersen, 2004) and these methods are increasingly being used to record the movement and behaviour of individuals in TSEs, especially where more advanced, novel survey technology is used such as Ornithodolites (Cole et al., 2018), range-finder binoculars (Heal, Hoover, & Waggitt, 2021) or UAVs (Lieber et al., 2021), to complement traditional approaches. For example, Cole et al., (2018) examined the movement of great cormorants (*Phalacrocorax carbo*) in a TSE using an ornithodolite and concluded that collision risk with TSTs was low by observing that individuals avoided tidal conditions associated with operational devices.

Visual surveys however have their limitations. The survey time of aerial and boat-based surveys is limited and this can result in sparse spatial and temporal coverage (Waggitt & Scott, 2014), although datasets can be augmented by opportunistic sightings from commercial vessels and data can be pooled from multiple surveys providing the survey methods are standardised (Waggitt & Scott, 2014). Land-based surveys can monitor for prolonged durations but may not be able to cover the full spatial extent of large sites (Benjamins et al., 2015). Visual surveys also rely on good visibility and the turbulent nature of TSEs can make the detectability of animals in these environments challenging (Waggitt & Scott, 2014; Benjamins et al., 2015). Finally, while results from visual surveys can infer the movements and behaviour of animals underwater (e.g. Cole et al., 2018), they are unable to record these directly; this makes it difficult for such techniques to determine any evasive behaviours in response to TSTs.

Passive acoustic monitoring (PAM) and active acoustic sonar (AAS) methods offer alternatives to visual surveys. PAM can be used to detect, locate, and track animals underwater in 3D (Malinka et al., 2018). However, PAM is restricted to use with vocalising animals that echolocate frequently, such as porpoise and dolphins (Malinka et al., 2018). Moreover, high turbidity – a common feature of TSEs – can severely limit the detection range of PAM equipment (Nuuttila et al., 2013). Active acoustic sonar (AAS) technology can track marine mammals that cannot echolocate, such as seals, or animals that

can echolocate but choose not to (Hastie, 2012). However, AAS is limited in its ability to discriminate between species (Hastie, 2012) and can only detect objects at a range of tens of metres (Hastie et al., 2019). This restricts its application to studying only near-field interactions of animals (< 100 m) with TSTs, meaning it is not able to determine what animals do once they have moved away from a device; for example, whether animals remain within a fine-scale distance from a device (i.e. 100 m – 1 km) or displace to further afield (i.e. greater than 1 km; broad-scale). This highlights a general and significant challenge of studying marine megafauna in TSEs and their interactions with TSTs which is that methods vary in their ability to study animals at different spatial scales (Waggitt & Scott, 2014; Benjamins et al., 2015). In addition to PAM and AAS, video systems have been developed to monitor animal movements around tidal turbines (Joslin, Polagye, & Parker-Stetter, 2014), however these are also restricted to (very) near-field monitoring (~ 10 m) and are severely limited by underwater visibility.

In recent decades, the development of advanced biologging and biotelemetry devices (hereon “tags”) has provided novel approaches to research marine megafauna in TSEs by having revolutionised our ability to study animals in the wild (Williams et al., 2020). Depending on the study species, the deployment duration, and the specific technology used and its programming (see Williams et al., 2020), tags can provide opportunities to study marine megafauna over very broad to very fine spatial scales (Shimada et al., 2020), including to within near-field range of TSTs (Hastie et al., 2019). Moreover, some tags can provide the means to collect data on animals whilst underwater (Hussey et al., 2015), including in 3D and at very high resolutions. The potential to collect high resolution data is desirable as this allows researchers to determine the influence of complex physical features of TSEs on the movement and behaviour of marine megafauna, including physical features which vary over fine spatio-temporal scales, such as boils, eddies, and currents (Benjamins et al., 2015). However, the resolution of data that can be obtained from tags fundamentally depends on the technology used and how it estimates locations (Williams et al., 2020; Shimada et al., 2020), and not all tags are able to collect data at very high resolutions. Specifically, global positioning system (GPS)

tags triangulate their position from multiple radio signals received from satellites orbiting around the earth; global location sensor (GLS) loggers record light levels and, using daylight length and the midpoint between dawn and dusk, can determine latitude and longitude respectively; platform transmitter terminals (PTTs) work by transmitting sequential radio signals to the ARGOS satellite network, though there are considerably fewer satellites operating in this network (7) than there are in the GPS system (29), resulting in typically fewer satellite fixes and thus poorer accuracy of estimated locations (Thomson et al., 2017). Spatially, GPS tags collect data with an accuracy of up to tens of meters or even less, whereas the accuracy of ARGOS positions and GLS loggers is usually within the scale of hundreds to thousands of kilometres (Heylen & Nachtsheim, 2018). In order to determine an animal's depth, these tags are typically coupled with time-depth recorders (TDRs) which record the 2D vertical profile of an animal in the water column using data recorded from an on-board pressure sensor. On the other hand, multi-sensor archival tags containing accelerometers and/or magnetometers such as Daily Diaries (see Wilson, Shepard, & Liebsch, 2008), are able to record 3D animal movement data (i.e. location and depth) at extremely high spatial and temporal resolutions (e.g. > 40 Hz) via a process called dead-reckoning (Adachi et al., 2017). Here, given a known starting location of an animal, sequential positions are determined from vectorial calculations of animal speed, pitch, and heading (Wilson et al., 2007). These data are key to reconstructing the 3D movements of seals underwater, including in high enough resolution to understand near-field interactions with TSTs (Hastie et al., 2019). Tags are also able to record data over a wide range of temporal scales (Williams et al., 2020), from (sub)seconds (Del Caño et al., 2021) to entire life histories (Horning et al., 2017), with some tags offering the versatility to study animals continuously over annual, seasonal, or tidal cycles.

The use of tags for studying the movements and behaviour of marine megafauna is advantageous in that it offers the ability to track animals in potentially very high resolutions (Williams et al., 2020) and thus provides the potential to record near-field interactions with TSTs, including any avoidance or evasion behaviours (Hastie et al., 2017; Onoufriou et al., 2021), and the

miniaturization of tags means that even relatively small marine megafauna can be studied in this way (e.g. Atlantic puffins, *Fratercula arctica*; Harris et al., 2012). Moreover, advanced multi-sensor loggers are able to quantify the energetic expenditure of such behaviours, something that is key to determining the effect of interactions with TSTs on individuals (Copping & Hemery, 2020).

Tracking marine megafauna with tags is however not without difficulty. The harsh environment that marine megafauna inhabit is challenging for solid-state devices; tags must be built to withstand pressure at extreme depths and large fluctuations in temperature which affect battery performance (Ruiz-Garcia et al., 2009). When animals are underwater satellite transmission telemetry cannot function and when animals do surface there is often only a matter of seconds for tags to communicate with satellites before the animal returns underwater – and even then a successful satellite fix is only acquired if sufficient satellites are available (Carter et al., 2016). Further, transmitting tags only function correctly if the part of the animal to which they are attached is suitably exposed (Jones et al., 2011). In short, a plethora of factors must fall into place simultaneously to achieve successful data acquisition (Bidder et al., 2014).

Tracking marine megafauna using tags in TSEs specifically, including their interactions with TSTs, is even more difficult, for several additional reasons: there is no guarantee that animals tagged near the study site will necessarily use the area of interest (Waggitt & Scott, 2014) and this, combined with the fact that marine megafauna often exhibit high individual variation (Sequeira et al., 2019), necessitates the collection of large sample sizes, something that is often precluded by the high cost of tags (Waggitt & Scott, 2014); tagging animals is an invasive procedure with consequences for the individuals being tagged (Casper, 2009) such as increases in drag (Vandenabeele et al., 2015), and tag-induced drag is worsened in fast flow conditions (Kyte, Pass, Pemberton, Sharman, & McKnight, 2019); high tidal flow causes drift, making it challenging to accurately georeference locations and determine the net movement of animals through the water (Gaspar et al., 2006; Wilson et al., 2007) and; very-high-resolution 3D trajectories are required to fully elucidate the fine-scale movements that animals make in TSEs and to record near-field

interactions with TSTs (ORJIP Ocean Energy, 2020), something that only multi-sensor archival loggers are currently able to do (Hastie et al., 2019). Indeed most marine megafauna tagging studies, including those examining animals in TSEs and their interactions with TSTs, have only examined the 2D horizontal and/or vertical movements of animals independently and have not been able to reconstruct 3D movement trajectories at very fine scales (Copping & Hemery, 2020). This makes this a frontier subject for research (Abrahms et al., 2020). Fortunately, in recent years there has been substantial progress in the field of movement ecology that promises to make this possible (Goldbogen et al., 2015; Adachi et al., 2017; Bras et al., 2017; Jouma'a et al., 2017).

1.4 Applied movement ecology – studying animal movement responses to anthropogenic change

The study of animal movement, coined “Movement Ecology” (Nathan et al., 2008), is critical to ecological and evolutionary science (Hooten et al., 2017; Chapman & Reyna-hurtado, 2019) with the movement of organisms being fundamentally linked to processes that are essential to life (Nathan & Giuggioli, 2013); including searching for food, the acquisition of mates for reproduction, finding suitable places to rest, and evading predators (Nathan et al., 2008; Hooten et al., 2017). Given its importance and utility in advancing our understanding of these processes, movement ecology has seen a recent surge in popularity (Joo et al., 2020). Up until 2008, over 26,000 articles featured the subject of animal movement (reviewed in Holyoak et al., 2008) and in the last decade this number has risen by at least 8,000 new publications (30.7 %) (Joo et al., 2020). Movebank, a free online database for animal movement data, established in 2007, now holds over 2.8 billion animal location estimates from over 6,350 studies, supported by over 20,000 users (Wikelski & Kays, 2019).

In recent decades, there has been a shift in movement ecology research towards more applied aims, with an increased focus on its potential

applications to conservation science, management, and policy (Claudet et al., 2010; Dunn et al., 2019; Hays et al., 2019; Isaksson et al., 2020; Riotte-Lambert & Matthiopoulos, 2020). For example, between 1990 and 2014, publications making use of the phrase “movement ecology” together with “conservation” or “management”, amongst others, increased more than tenfold (from 4 % to 44 %). In tandem, movement ecology research has seen a shift from Eulerian to Lagrangian approaches, with an increased focus on studying the movement of individual animals (Nathan et al., 2008), especially using animal tracking tags (Hazen et al., 2012; Fraser et al., 2018; Joo et al., 2020). Movement ecology has proven itself a pivotal field of research – and animal tracking a key method within this – for advancing our knowledge of animal behaviour and ecology in the wild (Weimerskirch, 2009; Börger, 2016; 2020; Hays et al., 2019; 2021). Moreover, these approaches have been crucial for investigating the effects of anthropogenic environmental change on animals and informing appropriate species conservation management strategies (see reviews in: Runge et al., 2014; Allen & Singh, 2016; McGowan et al., 2017; Fraser et al., 2018; Hays et al., 2019; Katzner & Arlettaz, 2020). For example, tracking data collected on adult wandering albatrosses in South Georgia revealed that foraging ranges overlapped by up to as much as 74 % with areas of longline fishing activity; these findings were used to inform a no-fishing period during the key risk period of overlap, leading to a tenfold reduction in by-catch rates of albatrosses (Croxall & Prince, 1996); Copeland et al., (2014) examined migratory routes of mule deer from Wyoming using GPS data, revealing that 66–70 % of their migration corridors overlapped with areas that already existed for the conservation of sage-grouse, highlighting that direct conservation of the latter could indirectly protect the former; and through tracking the movements and diving behaviour of olive ridley sea turtles, Dawson et al., (2017) revealed that 34.1 % of turtle space use overlapped with commercial shipping, and that turtles spent 19.7 % of their time diving to the seabed where they were at risk from entanglement in bottom set gillnets – these findings contributed to the expansion of two Marine Protected Areas (MPAs) and a greater restriction of commercial fishing activities in these locations. These examples showcase how detailed data obtained on individual-level movements and behaviour using tags can be used to inform

management strategies for entire populations. Indeed, providing a sufficient number of individuals are studied, understanding individual responses can be used to estimate population-level effects (Schofield et al., 2013; Fossette et al., 2014; Allen et al., 2016; Hays et al., 2019; Sequeira et al., 2019; Ferreira et al., 2020).

Studying marine megafauna in TSEs and their potential interactions with TSTs is a key applied research need within the field of movement ecology research and ongoing developments in tags – comprising both improvements to technology, and advancements in software and methods to analyse data (Williams et al., 2020) – provide avenues to tackle this research (Fraser et al., 2018). Indeed, GPS tracking studies have already revealed that there is relatively low potential collision risk between black guillemots *Cephus grylle* and European shags (*Phalacrocorax aristotelis*) in relation to TSTs in the Pentland Firth (Johnston et al., 2018; Isaksson et al., 2021), and that harbour seals avoid TSTs (Hastie et al., 2017; Joy et al., 2018; Onoufriou et al., 2021). However, these studies have focused on the broad- and fine-scale movements of animals only, excluding near-field movements. To build on these, multi-sensor loggers need to be utilised to track the near-field movements of marine megafauna in 3D around TSTs in order to understand responses to them, including evasive behaviour (Copping & Hemery, 2020). To support this, tags are now able to store extremely large volumes of data (MicroSD cards can have up to 1 TB of storage capacity; Holton et al., 2021) which allow them to record high-resolution data over extended periods. While tags currently remain limited in their ability to transmit such very large data packets – owing to the battery power and time required, and transmission bandwidth available to do so (Cox et al., 2018; Holton et al., 2021) – recent progress has been made in the on-board processing of summary data (Cox et al., 2018; Heerah et al., 2019; Nuijten et al., 2020; Skubel et al., 2020). However, in order to recover the full, raw data from many archival tags, recovery of devices is essential (Whitmore et al., 2016). For tags deployed on marine megafauna this is challenging because most are highly mobile and wide-ranging, and remote-release mechanisms built to release tags from marine megafauna for recovery are notoriously susceptible to malfunction due to corrosion (Hill, 2011; Wilson

& Moss, *pers. comms.*). Nevertheless, in recent years remote-release tags have been recovered with marked success from several large marine predators including tuna, sharks, cetaceans and seabirds (Gleiss et al., 2009; Block et al., 2011; Chapple et al., 2015; Lear & Whitney, 2016; Whitmore et al., 2016; Arranz et al., 2019), though consistently reliable applications on pinnipeds are yet to have been demonstrated.

Finally, whilst tags have been deployed on relatively small marine megafaunal taxa (such as guillemots; Isaksson et al., 2021), tag size generally remains a limiting factor for its widespread application and this largely constrained by battery size (Holton et al., 2021). This is particularly pertinent for smaller animals as the impact of a tag generally increases with its size (Vandenabeele et al., 2015). Due to the relatively adverse effects of tagging on smaller animals (Walker et al., 2012) coupled with high mortality rates (Bjørge et al., 2002; Bowen et al., 2015; Carter et al., 2017; Afán et al., 2019), researchers preferably tag larger individuals (Hazen et al., 2012; but see Portugal & White, 2018) which has resulted in a relative paucity of data on young conspecifics (Hazen et al., 2012; Shillinger et al., 2012). Young marine megafauna are perceived to be at greatest risk of detrimental interaction with TSTs due to their relative naivety and vulnerability (Daunt et al., 2007; Thompson, 2012), and so tracking their movements around TSTs is essential (not least because juvenile marine megafauna often comprise up to half the population in long-lived species; de Grissac et al., 2016).

For the TST industry to progress with minimal anthropogenic disturbance, addressing the key technological needs outlined above to track marine megafauna in TSEs and around TSTs is essential in order to meet the information needs (1.2), especially those relating to near-field interactions. More broadly, information is required on the degree of overlap between individuals and devices, the responses of animals to TSTs, and the potential for collision. This information will assist the industry in adopting appropriate mitigation strategies to minimize the threat to individual animals and populations.

1.5 Study species

British waters boast no fewer than 20 designated tidal energy lease sites (Carter et al., 2020). However, around the UK and adjacent waters, including the Celtic and North Sea, marine megafauna are abundant (European Parliament, 2010; Waggitt et al., 2020). This creates the need to identify and mitigate threats to marine megafauna from tidal energy generating devices such as TSTs in these areas. Grey seals (*Halichoerus grypus*) and harbour seals (*Phoca vitulina*) have been identified as potentially vulnerable to impacts from TSTs because they occupy both coastal and shelf sea areas and their distribution is well known to overlap with numerous areas planned for TST development (Fig. 1.1 and see Carter et al., 2020). The UK and surrounding waters is home to a large proportion of the worldwide populations of both species; the UK hosts around 38 % of *H. grypus* globally (~ 149,700 individuals; SCOS, 2020), and 30 % of the European *P. vitulina* population (~ 80,000 individuals; Thompson et al., 2019). Both species are protected under primary legislation in the UK; by the Marine (Scotland) Act 2010, the Wildlife (Northern Ireland) Order 1985, and the Conservation of Seals Act 1970 (in England and Wales). Both species are also afforded “Favourable Conservation Status” under the European Union (EU) Habitats Directive 92/43/EEC. This means that populations must be protected from anthropogenic disturbance, such as any detrimental impact from the installation and operation of TSTs.

Grey seals are the larger and more sexually dimorphic of the two species, with adult males and females weighing between 170–310 kg and 100–190 kg respectively (Hall & Russell, 2018), whereas harbour seals display only semi-dimorphism (Wilson et al., 2015), with weights ranging from 75–104 kg and 67–83 kg for males and females, respectively (Teilmann & Galatius, 2018). Both species are large enough to bear animal tracking tags, and indeed many of the insights into their movements in TSEs to date have been made using tags (Hastie et al., 2017; Joy et al., 2018; Sparling et al., 2018; Onoufriou et al., 2021; but see Lieber et al., 2018). This highlights that there is the potential to track these animals with high-resolution multi-sensor loggers to understand more about their near-field interactions with TSTs. However, the impact of tags has been shown to manifest in as much as a 12 % increase in drag coefficient

(C_d) on adult grey seals (Hazekamp, Mayer, & Osinga, 2010); an impact that will inevitably be compounded in fast flowing environment such as TSEs (Kyte et al., 2019). Tags will also have greater impact on smaller adults, juveniles, or pups from both species, and while the empirical risks have not been studied directly *per se*, several weaned pups tagged with GPS-GSM tags have been later observed emaciated or dead (Carter et al., 2017). Indeed, there are potentially severe implications of tagging relatively small individuals in fast flowing TSEs, which may in part explain the lack of data from young individuals in these environments. For these reasons, in this thesis I target my research efforts on studying grey and harbour seals in the UK, with specific focus where possible on young individuals.



Fig. 1.1. Distribution of grey and harbour seals in the Celtic and North Seas (orange areas – also see Appendix S1.1) and locations of example TSEs. Grey seal distribution in orange; Harbour seals in brown (adapted from <http://iucnredlist.org/>). Example devices clockwise from bottom left: Deltastream™ turbine, Ramsey Sound; Minesto's DG500 kite, Holyhead Deep; Orbital O2 turbine, EMEC; MeyGen turbine, Pentland Firth; Nova M100 turbine, Shetland; Torcado turbine, Afsluitdijk; SeaCurrent TidalKite™, Kornwerderzand (Ocean Energy Systems, 2020).

At a broad-scales (1 – 10 km), adults of both grey and harbour seals overlap with areas planned for TST development (Copping et al., 2017; Carter et al., 2020). Their at-sea movements consist predominantly of central-place foraging (CPF) where individuals move ~ 50 km offshore (Thompson et al., 1998; Jones et al., 2015), potentially putting them at risk of interaction with coastal TSTs on multiple occasions during foraging trips (Russell et al., 2015). During the breeding season, both species spend extended periods inshore (Parijs, Thompson, & Tollit, 1997; Van Parijs, Hastie, & Thompson, 1999) and use coastal habitats where TSTs are likely to be installed. As pups, both species undertake far-ranging natal dispersal (Greig et al., 2018; Peschko et al., 2020) which sees them move offshore from their birth sites, potentially passing through areas of TST development. However the movement mechanisms underlying natal dispersal remain relatively poorly understood owing in part to the paucity of data for younger individuals (Carter et al., 2017). In addition to conducting CPF, some adult grey seals have also been observed making extended displacements (Sayer et al., 2019) somewhat analogous (although typically shorter in scale) to the natal dispersal observed in pups.

At fine-scales (100 m – 1 km), research from as early as the 1980s (e.g. Brown & Mate, 1983) has shown that both grey and harbour seals utilise TSEs. They also have the capacity to dive to the depths at which most TST devices are planned to be deployed at (30–40 m; Copping & Hemery, 2020), including as pups (Hicks et al., 2004; Carter et al., 2017). Both species have been shown to dive whilst within TSEs, but this is modulated by flow speed and tidal phase and there is variation between sites and between individuals (Lieber et al., 2018; Joy et al., 2018; Hastie et al., 2016; 2019). Specifically, Lieber et al., (2018) showed that seals in the Strangford Narrows were concentrated at the edge of the channel at peak flow speeds ($> 2 \text{ ms}^{-1}$), and that dives were limited to the centre of the channel when flow speeds reduced to below 1 ms^{-1} . Results from Hastie et al., (2016; 2018) contrasted this, showing that seals in a narrow tidal channel in Kyle Rhea concentrated their diving to the narrowest part of the channel during peak flow. Copping et al., (2017) examined both grey and harbour seal movements in tidal channels in Scotland and Wales, demonstrating that across sites fine-scale use of tidal channels was consistent,

with individuals from all sites swimming head-on into currents. However, individual variation and variation across the tidal cycle between sites were high, with flood tides being exploited by some individuals but not others, providing evidence of specialisation to specific tidal conditions by some individuals. Further variation has been observed in tidal current usage between sites, with Joy et al., (2018) demonstrating that seals in the Strangford Narrows predominantly swam against prevailing currents whilst Hastie et al., (2018) demonstrated that seals in Kyle Rhea swam predominantly with the current. These studies have provided key insights, but given the variation between sites and between individuals more research is needed to understand the mechanisms that drive variation in the fine-scale use of TSEs by seals and their responses to tidal conditions.

Also at fine-scales, both grey and harbour seals are also known to be attracted to anthropogenic structures at sea due to the associated artificial reefs that form aggregations of prey (Russell et al., 2014; Grecian et al., 2018; Taormina et al., 2020). This raises the risk that individuals will be attracted to and come into contact with TSTs. That said, recent evidence has shown that harbour seals generally avoid TSTs (Hastie et al., 2017; Joy et al., 2018; Onoufriou et al., 2021) however these results are limited to tidal channels in Scotland (Pentland Firth and Kyle Rhea) and, given the aforementioned variation between sites and individuals, more research is needed to determine if these behaviours are consistent in other areas and across individuals. Currently no evidence is available for avoidance behaviour of grey seals towards TSTs.

Evidence of grey and harbour seal movements in TSEs and in response to TSTs at near-field scales (< 100 m) is currently extremely limited. This evidence is critical to record any evasive behaviours undertaken by seals to avoid TSTs and thus determine potential collision risk. To date, only Hastie et al., (2019) has examined the fine-scale 3D movements of seals in a tidal channel. This study revealed that harbour seals generally swam in the direction of the current and used the central part of the water column, potentially putting them at risk of colliding with TSTs. However, this research did not explicitly examine near-field responses of harbour seals to TSTs. The findings are also limited to harbour seals; no data of this kind currently exists

for grey seals. The lack of these data exists largely on account of the lack of technology available to record the 3D movements of animals at such very fine-scales (Hastie et al., 2019), hence new technological developments or improvements to existing technologies are required.

In summary, our understanding of the use of TSEs by grey and harbour seals, and the risks of that TST devices pose, remain poorly understood, and there exists a lack of information in three key research areas:

1. The distribution and occupancy patterns of seals in TSEs at a broad-scale (1 – 10 km), including at various life history stages; In other words: “When are seals likely to occupy TSEs?”
2. The fine-scale (100 m – 1 km) movements of individuals in TSEs; “When occupying a TSE, how do seals move and behave in these environments?”, and
3. The response of individuals when they are near to TSTs (< 100 m) and thus their collision risk; “What do seals do when they encounter a TST?”

1.6 Thesis aim and objectives

In this thesis, I aimed to improve our understanding of the movement of grey and harbour seals in TSEs and their potential for interaction with TSTs. To achieve this, and in line with the information needs outlined by ORJIP (2020), I focused my research efforts on two main themes: Developing new methods to study these species in TSEs and obtaining novel ecological insights of their movements in these areas, and in relation to TSTs (Fig. 1.2). Specifically, my objectives were to:

1. Quantify the scales and patterns of displacement of seals in TSEs and their potential overlap with TSTs at broad-scales.
2. Quantify the movement responses of seals to tidal currents at fine-scales, and

3. Develop new tags for collecting data on the very-fine scale movements of seals in TSEs and their near-field responses to TSTs.

Thus, in **Chapter 2** I used an historical ringing record of grey seal pups to investigate the drivers of displacement during natal dispersal. The objective of this chapter was to quantify the displacement distances that grey seal pups reached during their first few months at sea and determine if (and if so how) variation in displacement was driven by differences in demographic and environmental drivers. I also sought to quantify the timing of dispersal for grey seal pups to predict the age at which they may reach a given distance offshore, such as the distance required to encounter a nearby TST. I combined these displacement predictions with daily pup count data to derive a population-level time window of maximum spatio-temporal overlap of dispersing grey seal pups with a nearby TST site. Results from this chapter improve our understanding of grey seal ecology and provide predictions for estimating collision risk with TST devices. This chapter is in preparation as a Research Article for *Ecological Solutions and Evidence* as:

Kay, W. P., Bull, J. C., Stringell, T. B., Lock, K. M., Börger, L. (*In Prep*) Predicting the spatio-temporal overlap risk of dispersing grey seal pups with a tidal stream turbine site.

In **Chapter 3** I analysed GPS telemetry data from grey seal pups to again quantify and model the patterns and scales of their displacement during natal dispersal but this time using high-resolution individual-level data. I compared the displacement predictions of individuals to the population-level predictions derived in **Chapter 2** with the aim of establishing what sample size and recording duration is required to reliably estimate grey seal pup displacement over time from individual tracking data. Such information is required by researchers and practitioners to determine the type and volume of data that need to be collected in order to make robust inferences of displacement and thus of spatial overlap of animals with TSTs. This chapter is in preparation as an Article for *Marine Mammal Science* as:

Kay, W. P., Bull, J. C., Stringell, T. B., Börger, L. (*In Prep*) Quantifying grey seal pup dispersal: data and sample size requirements.

In **Chapter 4** I investigated the fine-scale movement strategies of seals in TSEs by examining the effect of tidal currents on seals moving in the Wadden Sea. The objectives of this work were to model how seal movements varied in response to the strength and direction of tidal currents, and how tidal current conditions affected the probability for seals to switch between behavioural modes (travelling, foraging, and resting). I sought here to quantify within- and between-individual variation as well as variation between sites and sexes in an effort to determine if there are any general mechanisms of seal movement responses to tidal conditions. The ultimate aim of this work was to provide the TST industry with insights into how seals respond to variation in tidal currents at relatively fine-scales. This chapter is in preparation as a Research Article for the *Journal of Animal Ecology* as:

Kay, W. P., Bull, J. C., Wilson, R. P., Siebert, U., Stringell, T. B., Börger, L. (*In Prep*) Moving in a moving medium: Tidal drivers of harbour seal *Phoca vitulina* fine-scale movement and behaviour.

To understand the very fine-scale (< 100 m) movements of seals in TSEs and thus the near-field responses of seals to TSTs, researchers must utilise high-resolution archival animal tracking tags. However, devices such as these are not readily available for seals. Thus, in **Chapter 5** I aimed to develop a new archival, multi-sensor, remote-release tag that can be used to track seals in the wild to obtain high-resolution data on their 3D underwater movements. This information is urgently needed by researchers to elucidate the near-field interactions of animals around TSTs, including any evasive behaviour. This chapter hence indirectly supports the TST industry by supporting researchers and practitioners to study this. This chapter is in preparation as a Practical Tools article for *Methods in Ecology and Evolution* as:

Kay, W. P., Wilson, R. P., Holton, M. D., Hopkins, P. W., Bull, J. C., Nachtsheim, D. A., van Neer, A., Siebert, U., Stringell, T. B., Börger, L. (*In Prep*) Development and performance of a remote-release biologging tag for tracking the high-resolution movements of wild seals.

However, tagging seals has been shown to increase drag and this will be exacerbated in fast-flowing TSEs. Thus, in **Chapter 6**, I used Computational

Fluid Dynamics (CFD) to evaluate and optimise the design of tags for tracking seals in TSEs. The objectives of this chapter were to examine the factors that influence tag-induced drag impact and determine by how much streamlining tag design can potentially minimize this impact. A secondary aim of this chapter was to prepare a step-by-step guide for evaluating the drag impact of tags in order to support other researchers who intend to track wild animals in TSEs. This chapter was published as a Research Article in *Methods in Ecology and Evolution* in June 2019 as:

Kay, W. P.[†], Naumann, D. S.[†], Bowen, H. J., Withers, S., Evans, B. J., Wilson, R. P., Stringell, T. B., Bull, J. C., Hopkins, P. W., Börger, L. (2019) Minimising the impact of biologging devices: Using Computational Fluid Dynamics for optimising tag design and positioning. *Methods in Ecology and Evolution*. DOI: 10.1111/2041-210X.13216.

Finally, in **Chapter 7** I discuss the key findings of this thesis in the context of the TST industry and provide future directions for studying seal ecology in TSEs.

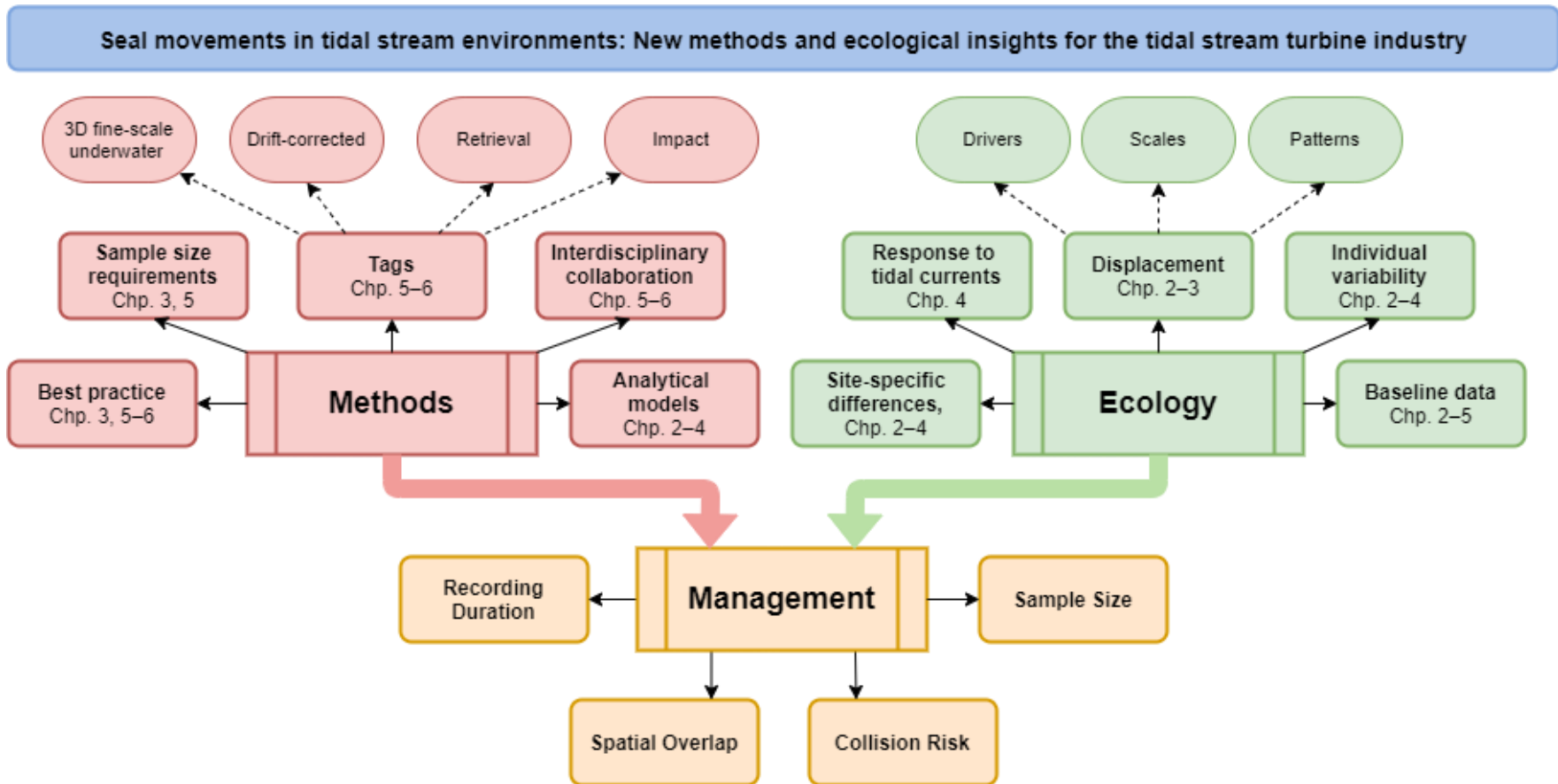


Fig. 1.2. Mind map of thesis objectives.

1.7 Collaborator contributions

Chapter 1 was prepared by me, in consultation with my supervisors: Dr James C. Bull (JCB), Professor Luca Börger (LB) and Professor Rory P. Wilson (RPW) from Swansea University; and Dr Thomas B. Stringell (TBS) from Natural Resources Wales (NRW). All supervisors provided feedback on the chapter drafts.

Chapter 2 was conceived and designed by me, in consultation with LB and with further contributions from JCB, TBS and KML. Data used for this chapter were provided by NRW. LB provided consultation in the use of the analytical methods implemented in this chapter, with further contributions by JCB and TBS. All co-authors contributed critically to chapter and associated manuscript drafts.

Chapter 3 was conceived and designed by me, in consultation with LB and with further contributions from JCB and TBS. Data used in this chapter were provided by Dr Debbie J. Russell (DJF) from the Sea Mammal Research Unit (SMRU). LB provided consultation in the use of the analytical methods implemented in this chapter, with further contributions by JCB and TBS. All co-authors contributed critically to chapter and associated manuscript drafts.

Chapter 4 was conceived and designed by me, in consultation with LB and JCB. Data used in this chapter were provided by RPW and Professor Ursula Siebert (US) from ITAW. I led the analysis, with support from LB and JCB. All co-authors contributed critically to chapter and associated manuscript drafts.

Chapter 5 was conceived and designed by me, in consultation with LB, RPW, JCB, PWH and TBS. I led the tag design and development with consultation provided by RPW, LB, JCB, PWH, Dr Mark D. Holton (MDH) from Swansea University, colleagues from the University of Hannover's Institute for Terrestrial and Aquatic Wildlife (ITAW): Dr Abbo van Neer (AN) and Mr Dominik A. Nachtsheim (DAN); and TBS. I built tag prototypes with practical support from RPW, MDH, PWH and EM. I led tag testing, with support from LB, PWH, MDH, EM, AN and DN. I led the deployments of tags in the field with support from

LB, AN, DN and colleagues from the Sea Mammal Research Unit (SMRU): Mr Simon E. W. Moss (SEWM) and Dr Matthew I. D. Carter (MIDC) (who also provided critical feedback). All co-authors contributed critically to chapter and associated manuscript drafts.

Chapter 6 was conceived and designed by me, in consultation with LB, RPW, colleagues from Swansea University's Aerospace Engineering department: Dr Benjamin J. Evans (BJE), Dr David S. Naumann (DSN), Ms Hannah J. Bowen (HJB) and Mr Simon J. Withers (SJW); and with further contributions from JCB and TBS. DSN led the implementation of the simulations required for the analyses, and was supported in this by HJB and SJW, under supervision from BJE and me. Mr Phil W. Hopkins (PWH), Swansea University, created the tag B geometry. BJE, DSN, HJB and SJW wrote the supplementary step-by-step guide in consultation with me. I led the statistical analyses, supported by LB. I led the writing of the chapter and associated publication with all authors providing critical feedback to manuscript drafts.

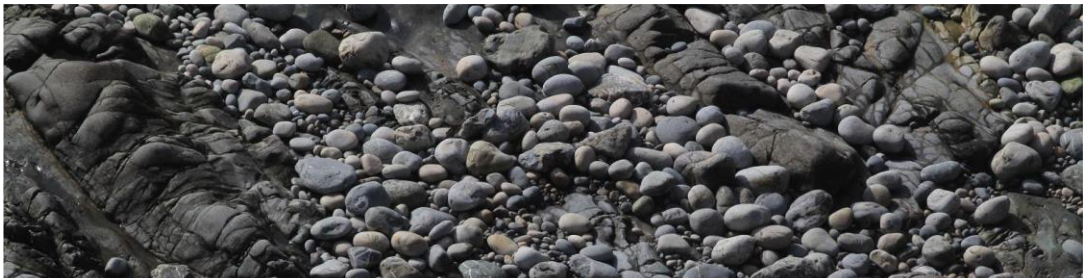
Chapter 7 was prepared by me in consultation with LB, JCB, TBS, and RPW. LB provided critical feedback on chapter drafts.

Chapter 2

Predicting the spatio-temporal overlap risk of dispersing grey seal pups with a tidal stream turbine site

“There is no very obvious reason why a seal born on Ramsey should be more likely than one born on Skomer to come into contact, later in its life, with human beings, but, if the present trend continues, someone must try and find the answer to this problem.”

(Johnson, 1956)



Pups on Skomer Island suckle from their mothers. Once weaned, they will be abandoned and will have to decide for how long to stay before dispersing
(Photograph by Kate M. Lock).

2.1 Abstract

The development of the marine renewable energy (MRE) industry requires the potential impacts on wild marine animals to be understood. One method is to quantify the spatial overlap of animals with proposed tidal stream turbine (TST) development sites. Grey seals (*Halichoerus grypus*) are an important marine predator whose distribution frequently overlaps with tidal stream environments (TSEs). Despite this, relatively little is known about their degree of overlap with TST devices. This information is particularly important for grey seal pups because they can undertake far-ranging dispersal movements in their early life which may bring them into areas proposed for TSTs. Here I analyse the early life movements of 246 grey seal pups in Wales using a net-squared displacement modelling approach to quantify displacement over time during natal dispersal, reveal drivers of displacement distance, and predict the population-level spatial overlap of pups with a proposed TST site. My results indicate that individuals cover vast ranges (up to 964.3 km) during their first few months at sea and that there are (small) site-differences in the displacement distance reached. Specifically, distances reached by seals from different sites can vary by up to 2.9 km. Further, I reveal sex-specific responses to a broad-scale climate index, the North Atlantic Oscillation (NAO), such that males increase their dispersal distance by 1.57 km in response to more positive phases of the NAO, whilst females reduce their dispersal distance by 1.51 km. I also reveal that grey seal pups can demonstrate neonatal aquatic dispersal behaviour, initiating movements offshore from as young as 16 days old. I combine predictions of displacement over time with daily pup count data to derive a time window of maximum overlap risk with a nearby TST site, demonstrating that 80 % of grey seal pups overlap during a 30-day period that occurs between 88–117 days after the start of the pupping season. These results can aid the TST industry in devising strategies that consider sex-and site-differences in grey seal pup dispersal in order to minimise the risk of overlap between individuals and TSTs, for example by limiting the operation of devices during peak-risk periods.

2.2 Introduction

The development of marine renewable energy (MRE; wind, wave, and tidal electricity generating devices) is essential to achieve net-zero emissions to mitigate climate change (IPCC, 2014). The sustainable and successful development of the MRE industry requires responsible consenting and this includes an assessment of the potential detrimental impact that MRE devices may have on the marine environment and important ecological indicators within it (e.g. sentinel species such as marine megafauna) (Copping et al., 2020; 2020b). However, the potential for detrimental impact of MRE devices remains highly uncertain and this is particularly the case for the tidal stream energy industry which is in its infancy compared to other MRE sectors (Chowdhury et al., 2020). This industry utilises tidal stream turbines (TSTs) – typically horizontal-axis turbines with rotating blades – to generate green energy, and of key interest is understanding the occupancy patterns and space-use of animals in the tidal stream environments (TSEs) in which TSTs are being installed (Waggitt & Scott, 2014). This will enable predictions of the potential degree of overlap, and hence collision risk, between individuals and devices (Isaksson et al., 2021). Given that only relatively few devices are presently operational, investigating collision risk directly remains difficult (Copping et al., 2020b). An alternative approach is to quantify the spatio-temporal overlap of animals with devices or areas targeted for installation, in order to predict the potential rates of interaction (Waggitt & Scott, 2014).

Grey seals *Halichoerus grypus* are an apex predator in the marine environment and an important biological indicator species (Kauhala et al., 2019). They are a coastal marine mammal and are known to make use of TSEs (Lieber et al., 2018), including as pups (Thompson, 2012). This puts them at risk of interaction with TSTs as their distribution and space-use overlaps with areas targeted by the tidal stream energy industry. This is particularly pertinent in the United Kingdom which is home to approximately 38 % of the world's grey seal population and where the species' distribution overlaps with all of the 20 sites currently leased for tidal energy development (Carter et al., 2020). Of particular importance are grey seal pups which make up almost half (45 %) of the total UK population (SCOS, 2020), making their survival critical to

population maintenance (Harwood & Prime, 1978), but who are perceived to be at greater risk of detrimental interaction with TSTs than their adult conspecifics (Thompson, 2012). Grey seal pup mortality is high, especially in their first year where detrimental interaction with anthropogenic threats such as fishing gear (i.e. by-catch) is responsible for up to 79 % mortality, with deaths during the first 3 months accounting for up to 25 % of this (Bjørge et al., 2002). Their vulnerability to existing threats raises concerns that further anthropogenic disturbance such as potential detrimental interaction with TSTs will pose additional risk (Thompson, 2012). Risks from TSTs are likely because pupping-grounds are typically in topographically complex and (consequently) high current habitats such as TSEs (Benjamins et al., 2015; Carter et al., 2020), putting pups in close proximity to sites of tidal energy development from birth.

Given the proximity of birth sites to TSEs, a grey seal pup's first movements into the marine environment could be into an area with an operational TST, with potentially devastating impacts (Onoufriou et al., 2019). Despite this, no study has investigated the spatial overlap of grey seal pups with these devices. Such information is crucial for determining collision risk and informing consenting processes for both new and existing TST developments. In particular, consideration is urgently needed on what risk TSTs may pose to grey seal pups immediately after weaning. This is because pups are abandoned by their mothers after weaning at just 15–21 days old (Fedak & Anderson, 1982), and must undertake their first movements at sea with no experience or guidance (Carter et al., 2017). This makes them vulnerable and naïve (Thompson, 2012). Moreover, in their first few weeks grey seals can undertake far-ranging natal dispersal which can see them move several hundreds of kilometres (Peschko et al., 2020), typically travelling close to the coastline as they disperse (Carter et al., 2017). This means their space-use could overlap with even relatively distant TSEs. In fact, Thompson (2012), demonstrated that pups can spend several weeks of their early life in TSEs (Thompson, 2012); swimming in high tidal current areas and diving to the seabed, presumably for foraging (Thompson, 2012). Such behaviour is likely to put grey seal pups at risk of encountering TSTs.

Animal-borne telemetry data has recently been used to quantify the spatial overlap of wildlife with marine renewables (Isaksson et al., 2021). Grey seal pups are large enough to bear animal tracking tags however the variation in their early life movements, including dispersal, is high (Carter et al., 2017; 2020; Peschko et al., 2020; Baylis et al., 2019). In addition, studies attempting to examine the space-use of animals in TSEs must consider variation between sites (ORJIP Ocean Energy, 2020), because differences in physical features between TSEs (such as differences in tidal currents) are well known to influence the observed patterns of animal occupancy and space use (Benjamins et al., 2015). This means that large sample sizes including individuals from different sites are required to make population-level inferences (Sequeira et al., 2019). Such large sample sizes are difficult to obtain using animal tracking tags because of the cost, ethics, and logistics associated with collecting these data (Sequeira et al., 2019). Moreover, grey seal pups are particularly challenging to work with due to their high mortality rates and low re-encounter probability (Carter et al., 2017). An alternative approach is to deploy greater numbers of relatively crude devices such as flipper ID tags, for which substantially larger sample sizes can be accrued (e.g. 204 pups; Hall et al., 2002) and with which the broad-scale movement of individuals can be investigated. For example, Bjørge et al., (2002) successfully applied this method on weaned grey seal pups to examine the natal dispersal of individuals from the Norwegian coast. Moreover, because such large sample sizes can be collected, data can be used to model and predict the population-level displacement of individuals over time, analogous to the ‘waves’ of bird population movements derived from migratory bird ringing data (e.g. Harnos, Fehérvári, & Csörgő, 2015). This would enable predictions of population-level overlap of dispersing grey seal pups with nearby TSTs.

Variability in dispersal is generally high and deriving predictive models of dispersal requires an understanding of its underlying drivers (Bowler & Benton, 2005; Clobert et al., 2009; Hawkes, 2009). Numerous factors are understood to drive the movements of grey seal pups in their early life. Sex-differences are prevalent (Bennett et al., 2010; Breed et al., 2011; Russell et al., 2015; Carter et al., 2017; 2019), such as females moving offshore during their natal

dispersal at faster speeds on average ($\sim 0.84 \text{ ms}^{-1}$) than males ($\sim 0.77 \text{ ms}^{-1}$) (Carter et al., 2019). Baylis et al., (2019) demonstrated that during dispersal males reached maximum distances offshore that were approximately 100 km greater than that reached by females. Similarly Peschko et al., (2020) observed that male pups dispersed approximately 75 km further from their birth site than their female conspecifics. Carter et al., (2017) demonstrated that sex-differences in grey seal pup movements during dispersal can also be region-specific, with males from the Celtic and Irish Seas (CIS) travelling further than females, whilst no sex-difference was observed in travel distance for pups in the North Sea (NS). Region-specific differences that are not sex-dependent can also occur, for example Carter et al., (2017) showed that the travel distances and durations recorded from CIS pups was approximately 200 km and 7 days shorter, respectively, than those recorded from NS pups.

Within regions, site-specific variation has also been observed in the movements of weaned grey seal pups (Thompson, 2012). For example, Thompson (2012) showed that at three TSE sites in Wales, the early life movements of individuals varied in their proximity to natal beaches. Specifically, seals tagged in the Skerries spent at least the first five weeks within TSEs, remaining close to shore (within 10 km); conversely seals from Ramsey Island dispersed far away from their birth site up with none remaining resident with the first five weeks; seals at Bardsey Island conducted movements up to approximately 40 km offshore before returning to their natal site (Thompson, 2012). Site-specific variation may be attributed to differing responses to variation in fine-scale biotic or abiotic features within sites (Nichols et al., 2020). Such differences between TSEs can be profound due to their unique topographies and resulting variability in physical features (Benjamins et al., 2015). Differences in dispersal between sites may also arise due to variation in the density of individuals at different sites (Le Boeuf & Briggs, 1977; Gaggiotti et al., 2002). Whilst evidence of this in grey seal pups has not been observed, density-dependence in dispersal has been shown for other juvenile pinnipeds as a means to distance themselves from adult conspecifics (Field et al., 2005; Zeppelin et al., 2019). These factors highlight

the need for studies examining grey seal pup dispersal to consider site- and regional-specific variation.

Finally, broader-scale environmental phenomena such as climatic variation and major ocean currents are known to affect the dispersal of young seals. For example, Lea et al., (2009) observed that northern fur seal pups made use of favourable wind conditions for dispersing in extreme weather events, and Baylis et al., (2019) demonstrated that the eastward dispersal of grey seal pups from Iceland may be facilitated by the eastward flowing North Icelandic Irminger Current. Such responses to broad-scale environmental drivers have also been observed in other taxa of marine megafauna; the dispersal distance of Arctic terns was positively associated with the North Atlantic Oscillation (NAO) (Møller et al., 2006) and fledgling European shags demonstrated sex-specific responses to the NAO in their dispersal distance (Barros, Álvarez, & Velando, 2013).

Understanding the underlying drivers of grey seal pup dispersal has clear implications for predicting the spatial overlap of pups with TSTs and thus providing robust predictions of collision risk. Specifically, understanding the influence of sex-differences, site-differences, and environmental drivers, can aid us in determining whether there is likely to be sex-bias in risk, whether risk is likely to vary between different regions or sites, and whether we might anticipate greater risk of overlap under certain environmental conditions, respectively.

In the study presented here, I aim to develop a model that predicts the number of grey seal pups potentially overlapping with a TST site. To achieve this, I use a large ringing record ($n = 246$ individuals) of grey seal pups to quantify natal dispersal and derive sex- and site-specific displacement kernels of individuals dispersing from three breeding sites in Pembrokeshire, Wales. These sites are in close proximity to the Ramsey Sound, a TSE that is proposed for TST development. I combine displacement predictions with recent pup count data to derive predictions over time for the number of pups overlapping with this TST development site. This predictive model provides a tool to assess the risk of spatial overlap of grey seal pups with TSTs, and thus supports the TST

industry to develop appropriate operational strategies that mitigate collision risk. This predictive model can be easily adapted for other areas and for other taxa. To generate further useful information for the industry, I also aim to understand the effect of sex, site, and environmental conditions on the displacement distance reached by individuals. This information will improve our ability to predict whether individuals have the capacity to disperse to distant sites, and thus whether individuals are at risk from overlapping with sites that are relatively far away from their place of birth.

2.3 Methods

2.3.1 Data used and processing

I analysed historical (1954–1971) ringing records of pre-weaned grey seal pups from breeding sites in Pembrokeshire, Wales, UK (Kay et al., 2020). These data represent the marking of $n = 1357$ grey seal pups using metal rings (identification tags) attached to their hind flippers (Hewer, 1955). Seals were caught by hand on land (in beaches or in caves) and were restrained in a net for marking (Johnson, 1955). The age of pups was estimated by qualitative visual assessment and is accurate to within a few days (Boyd, Lockie, & Hewer, 1962). After marking, seals were released and were resighted on subsequent return visits (approximately once per month) to the colonies; seals were resighted by identifying the metal rings which could be viewed from a distance using binoculars or a telescope (Lockley, 1958). National and international efforts were undertaken to resight individuals from a range of sites, including in neighbouring countries (Ireland, France, and Spain). These efforts were coordinated by the Zoological Society of London (Johnson, 1972).

Of the 1357 originally marked, $n = 246$ seals were resighted. Data from 7 individuals were discarded because either (i) I could not determine the location of these individuals accurately from the records ($n = 4$), (ii) they were marked outside the research areas of interest ($n = 1$) or (iii) because the records were erroneous ($n = 2$). I further subset the data by the years of main research effort

(1956-1958 and 1960-1961; see Johnson, 1972). With the exception of two individuals that were found in a very decomposed state, I did not exclude records of individuals that were found dead because – following the notion that most dead animals tend to sink (Hewer, 1974) – these individuals would likely have been near to their resighting location at the time of death and so their resighting locations are representative of their movements whilst alive (Thompson, Kovacs, & McCocConnell, 1994). This produced a final sample size of $n = 184$.

From text descriptions of their locations, I derived a georeferenced position of the mark and resighting locations for each individual seal (see Kay et al., 2020). Marking locations were grouped into the three geographical breeding colonies (hereon “sites”) for analysis: Ramsey Island (51.86 N, - 5.34 E), Skomer Island (51.74 N, - 5.29 E), and North Pembrokehire (52.03, - 5.07 E). These areas are of particular concern with respect to overlap of grey seal pups with TSTs because tidal stream energy is abundant. Between marking and resighting locations, I calculated displacement distance using a 16-grid, least-cost path function implemented in the ‘gdistance’ package in R (van Etten, 2017). This method calculated the distance between mark and resighting sites via the sea (Fig. 2.1) and so avoids biases otherwise introduced by Euclidean-distance (‘as the crow flies’) measures, as seals do not cross land to disperse. I term this the ‘biological’ distance.



Fig. 2.1 An example output from the least-cost path function implemented in the 'gdistance' package in R to calculate the biological distance between mark sites (black dots) and resighting sites (red dots) for each individual.

2.3.2 Predictive modelling of overlap with a nearby TST site

To develop a predictive model of overlap risk of seal pups with a nearby TST development site, I first developed site- and sex-specific displacement ('dispersal') kernels to model how far seal pups will have displaced at any given time after birth. I then combined these with estimates of the number of seal pups born each day during the pupping season, obtained from long-term records of daily pup counts. To obtain the displacement kernels, I used the squared displacement method of Börger & Fryxell, (2012). This method is based on measures of net and net-squared displacement, which are the cumulative straight-line distance, or squared distance, of any point along a movement trajectory from the first point of origin (in my case, the natal site). Net (squared) displacement (NSD) is a fundamental statistic in movement analysis, as different patterns of NSD over time can be predicted by theory for animals moving according to different modes, such as dispersal, migration, or

home range movements (Turchin 1998; Moorcroft & Lewis 2006; Borger & Fryxell 2012). The method of Börger & Fryxell, (2012) provides a non-linear mixed effects modelling framework with which to identify the movement mode displayed by animals (e.g. separating dispersing and stationary (within-home range) animals), and obtain continuous-time predictions of the average distance from the origin of an individual over time. This method is very popular for movement studies (Nouvellet, Bacon, & Waxman, 2009; Bastille-Rousseau et al., 2015) and has been extended to other fields such as analysis of vegetation community composition dynamics (Bagchi et al., 2017). Here, I adopt the method to model the average location of individuals from different sites (and of different sexes) over time since birth, thus enabling use of the ringing records.

Specifically, the displacement distances are the “biological” (at-sea) distances between the starting points (the mark location of each individual in their natal site) and resighting location for all individuals respectively, within each site-sex group (to allow for site- and sex-differences). I considered five general displacement types, each with underpinning biological interpretation (Fig. 2.2; Table 2.1): (1) dispersal without settlement (i.e. diffusive movement); (2) non-dispersal (i.e. ‘stationary’ individuals remaining close to the natal site); (3) 3-stage dispersal (accounting for a prolonged post-weaning fast prior to dispersal and settlement); (4) displacement and return (hereon “return”; a double-sigmoid displacement function accounting for pups returning to their natal site at a later date following an initial dispersal); and (5) dispersal with return to a nearby area i.e. “mixed-return” (Börger & Fryxell, 2012). These 5 movement modes are linked to current understanding of the patterns of early movements made by weaned grey seal pups (Thompson, 2012; Carter et al., 2017; Carter et al., 2019; Peschko et al., 2020).

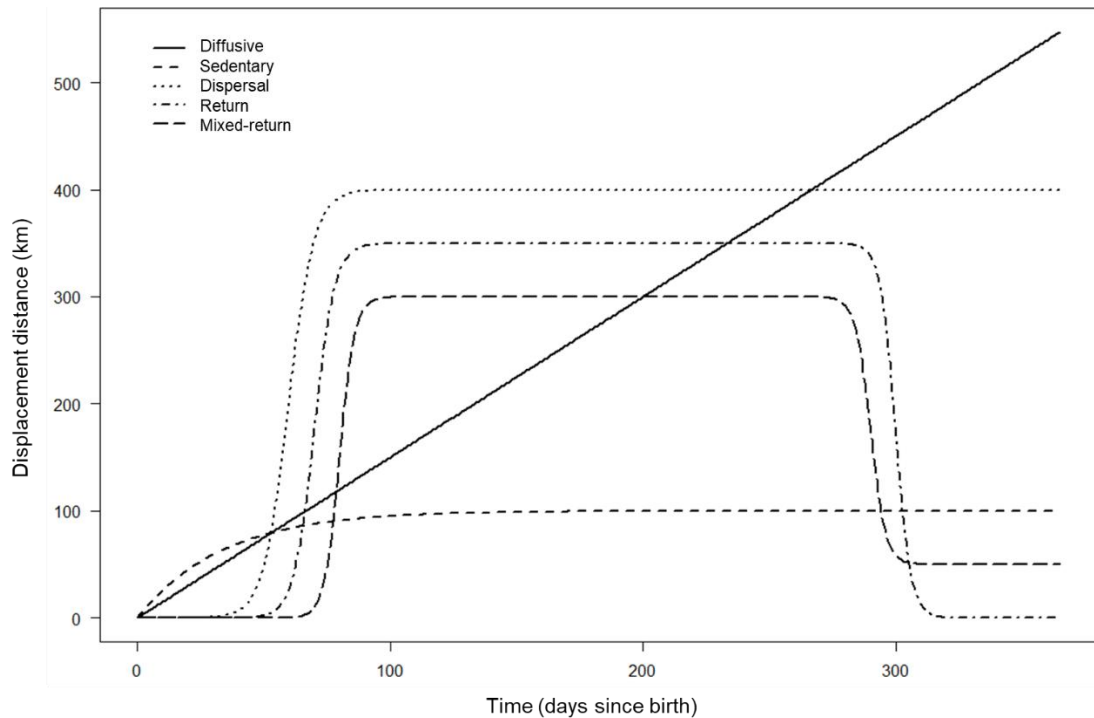


Fig. 2.2. Schematic diagram of displacement curves of the five movement modes considered (see Table 2.1 for equations).

I fitted a total of 9 non-linear displacement curves (Table 2.1) to each site-sex group using the “nls” function in the ‘stats’ package in R, using net displacement as the response variable, as model convergence was better than using net-squared displacement. Note that the patterns of displacement retain their form also when considering non-squared values of displacement (Turchin, 1998).

Model evaluation was undertaken by first examining goodness of fit (GOF) using the concordance correlation (CC) coefficient (Huang, Meng, & Yang, 2009), which provides a measure of model fit similar to the R^2 statistic (but with values of 0 to -1 indicating lack of fit, and 1 for perfect fit) and is well suited for nonlinear models (Börger & Fryxell, 2012). I also checked the displacement predictions from each model to ensure that these were biologically plausible; grey seal pups wean for an average duration of 15–21 days before leaving their natal site or undergoing a post-weaning fast (Pomeroy et al., 1996), and thus models that predicted large displacements substantially prior to this time period were less favourable, and in such cases I also considered the 2nd best-

fitting model. I thus obtained a time-dependent displacement curve for each site-sex group in units of days since birth.

Following this, I calculated the (biological) at-sea distance from the centroid of each natal site, to the TST development site in the nearby Ramsey Sound (51.878 N, -5.322 E) (Tidal Energy Limited, 2009) and, using my displacement predictions, estimated the age at which new-born pups could have displaced the distance required to reach a (500 m) buffer zone surrounding the TST site from their respective locations (Fig. 2.3). I was particularly interested in the first three months immediately following birth as this time period has been shown to be crucial in determining survival to recruitment (Lindström, 1999; Sæther et al., 2013), and is a time period in which grey seals have been shown to be most vulnerable to incidental mortality (Bjørge et al., 2002). Thus, I combined displacement estimates for the first 90 days after birth, with daily pup count survey data from the pupping season (1st August to 31st December; Bull et al., 2017a) to obtain predictions for the number of pups from each colony that could reach the TST location – in other words, obtaining population-level predictions of daily ‘waves’ of dispersing seal pups (Fig. 2.3). Pup count data for Skomer and Ramsey were obtained from a 2015 annual survey, whereas for North Pembrokeshire these data were from 2005.

All analyses were performed in R version 3.6.3 (R Core Team, 2018).

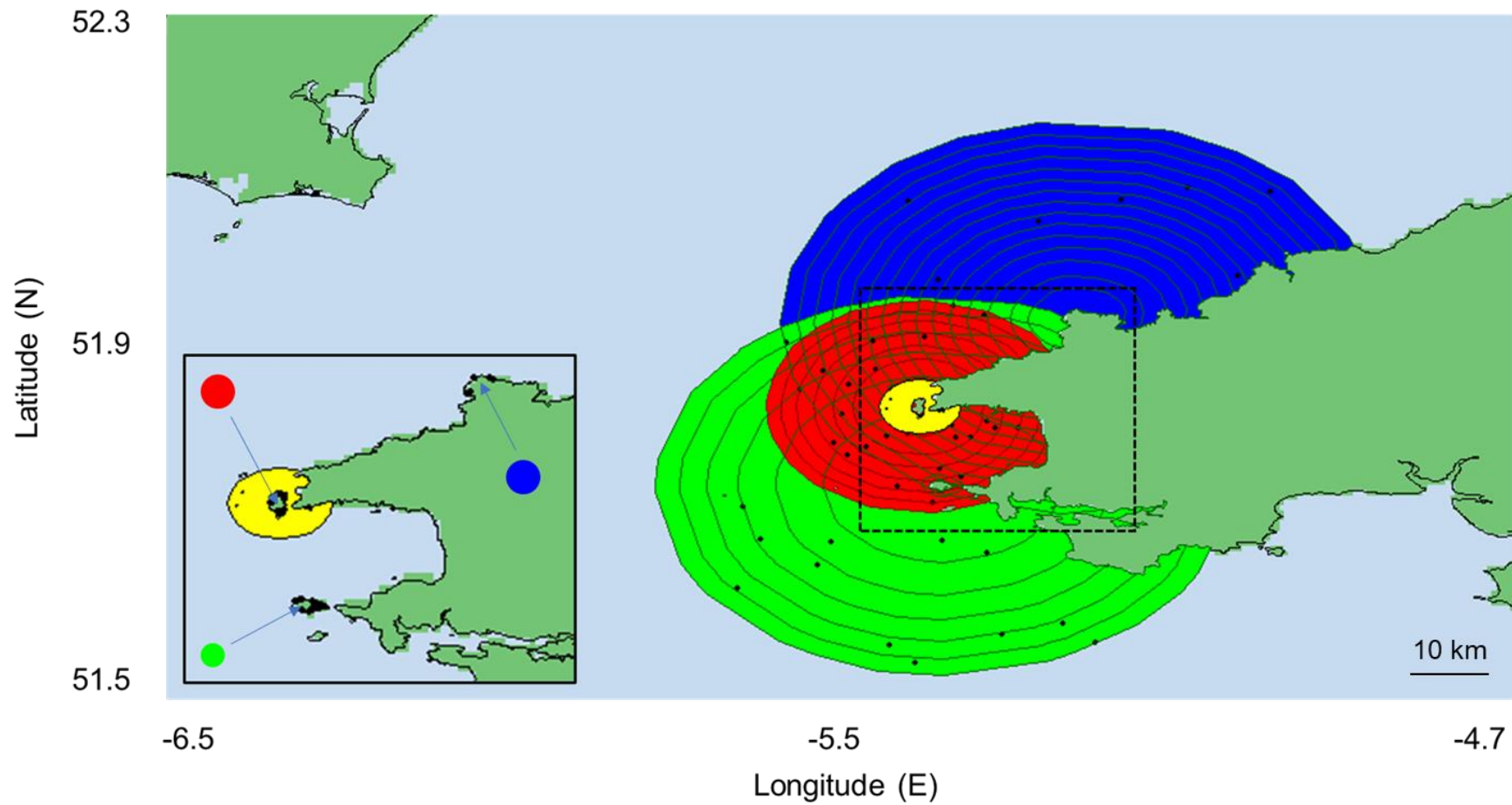


Fig. 2.3. Schematic diagram of the displacement kernels of grey seal pups dispersing from three sites in Pembrokeshire (Green = Skomer, Red = Ramsey, Blue = North Pembrokeshire; see text for details). The yellow area indicates a 500 m buffer zone around a planned TST site in the Ramsey Sound.

Table 2.1. Details of the non-linear models fitted to derive time-dependent displacement curves (i.e. 'dispersal kernels'). For full details of models and their parameters, refer to Börger & Fryxell, (2012).

Model	Name	Functional form	Model type	Biological interpretation
1	NullMod	$y = c$	Null (intercept only)	Stationary
2	SedMod	$y = \delta[1 - \exp(-\vartheta t)]$	Sedentary	Home-range movement
3	Linear	$y = 4Dt$	Linear	Diffusive movement
4	PowerC	$y = Dt^a$	Diffusive power	Diffusive movement
5	PowerCb	$y = t^a$	Power	Diffusive movement
6	ExponMod	$y = D * \exp(t)$	Exponential	Diffusive movement
7	DispMod	$y = \frac{\delta}{1 + \exp\left[\frac{(\theta - t)}{\varphi}\right]}$	Logistic	Dispersal movement
8	ReturnMod	$y = \frac{\delta}{1 + \exp\left[\frac{(\theta_1 - t)}{\varphi_1}\right]} + \frac{-\delta}{1 + \exp\left[\frac{(\theta_2 - t)}{\varphi_2}\right]}$	Double logistic	Dispersal and return
9	MixReturn	$y = \frac{\delta_1}{1 + \exp\left[\frac{(\theta_1 - t)}{\varphi_1}\right]} + \frac{-\delta_2}{1 + \exp\left[\frac{(\theta_2 - t)}{\varphi_2}\right]}$	Double logistic	Dispersal and return)

2.3.3 Drivers of displacement distance reached

To test hypotheses relating to the drivers of dispersal distance reached, I modelled log-transformed displacement distance against time (measured in days since birth to account for the differences in the timing of dispersal) using linear-mixed effects models, assuming gaussian errors. Given that some grey seal pups are known make initial exploratory movements before briefly returning to their natal site prior to dispersal (Thompson, 2012), displacement distance can often increase over short timescales, followed by a mixture of short and long distances being observed over intermediate timescales, and subsequently relatively long distances over extended timescales. I hence used a third-order polynomial function to account for this non-linear shape; this third-order polynomial also very closely reflected the shape of an equivalent generalized additive model (GAM) fit to the data.

As I was interested in sex-differences and differences between sites, I included sex and site as (factorial) fixed-effects. To test for the effect of differences in weather conditions (and hence, sea conditions), I included the North Atlantic Oscillation (NAO) as a (continuous) fixed effect; these data were sourced from the Climate Prediction Center, NOAA. I assumed a linear response to the NAO as this has been demonstrated in other fledgling marine megafauna taxa dispersing from their natal sites (Barros et al., 2013). The NAO represents the difference in atmospheric pressure at sea level between the Iceland Low and the Azores High. More positive values indicate a stronger difference in pressure resulting in more frequent storms across the Atlantic, with wind from the west dominating; negative values indicate a weaker difference in pressure, with fewer storms and wind from the east more prevalent (Hurrell, Kushnir, & Visbeck, 2001). The NAO accounts for variation in several relevant climate variables (including temperature, precipitation, and wind speed, amongst others) and has been shown to outperform local weather variables in explaining climate-driven variation in ecological processes including animal movement (Stenseth & Mysterud, 2005), thus representing an ecologically relevant measure for investigating seal pup dispersal across the Northeast Atlantic over several months. To ensure I used the most appropriate measure of the NAO, I compared 4 interpretations: 'astronomical' (monthly averages

from January through December); ‘biological’ (monthly averages of the 12 months following peak pupping season i.e. September to September); autumn (monthly averages from September through November) and autumn and winter (monthly averages from September through February). Model selection was undertaken by AIC to select the most appropriate NAO measure (Burnham & Anderson, 2004). Finally, to account for differences between years, I also included year as a random-effect. I used the ‘lmer’ function in the ‘lme4’ package in R to fit the linear-mixed effects models (Bates, Mächler, Bolker, & Walker, 2015). Finally, I obtained the most parsimonious model to explain the drivers of dispersal distance by stepwise simplification via backward selection of variables from the full model, undertaking model comparison using likelihood ratio tests (Crawley, 2007; Murtaugh, 2009).

As these data represent mark-resight records as opposed to detailed trajectories taken by individuals, I was not able to determine if the animals that were resighted at < 1 km from their mark location had not yet dispersed or had in fact dispersed and subsequently returned. Hence, the drivers of dispersal distance were examined for “dispersed” individuals only – defined as individuals found > 1 km from their mark location. Furthermore, one individual’s sex could not be determined and, as I was interested in testing sex differences, I discarded this datum, returning a final sub-sample of $n = 73$ individuals for this analysis (note that each individual contributed only one datum, the displacement distance).

2.4 Results

2.4.1 Quantification of natal dispersal in grey seal pups

184 seals were marked and resighted between 1956–1961 at between 3–317 days after birth, with a median (interquartile range) resighting age of 19.5 days (14–38 days). 74 individuals (40 %) were resighted at distances > 1 km at between 11–317 days after birth. Of these, 14 were resighted within 21 days after birth, having displaced between 1.4–41.8 km (mean = 9 km). The remaining 60 were resighted within 22–317 days after birth and were recorded

to have displaced between 1.5–964.3 km (mean = 130.1 km). 110 individuals (60 %) were resighted at ≤ 1 km from their original location at time periods ranging 3–160 days after birth. 94 of these had been resighted within 21 days, which is the typical maximum duration for post-natal weaning (Pomeroy, Fedak, Rothery, & Anderson, 1999). The other 16 individuals were resighted at between 22–160 days after birth (Table 2.2).

The distribution of displacement distances was heavy-tailed (Fig. 2.4c) and, for dispersed individuals only ($n = 76$), there was no directional preference for displacement (Rayleigh Test of Uniformity: $Z = 0.0187$, $p = 0.9745$) (Fig. 2.4b), with pups from all colonies dispersing widely across the UK (Fig. 2.4a). Most pups were resighted throughout Wales, the South West of England (Devon and Cornwall) and Southern Ireland (Wexford, Waterford, and Cork). Several pups from Ramsey and North Pembrokeshire displaced as far as France and Spain.

Table 2.2. Summary details of dispersed (> 1 km) and non-dispersed (≤ 1 km) individuals. Age represents the age at resighting. All percentages represent percentage of total.

Total ($n = 184$)			
Dispersed > 1 km $n = 74$ (40 %)		Non-dispersed ≤ 1 km $n = 110$ (60 %)	
Age ≤ 21 days $n = 14$ (8 %)	Age > 21 days $n = 60$ (33 %)	Age ≤ 21 days $n = 94$ (50 %)	Age > 21 days $n = 16$ (9 %)

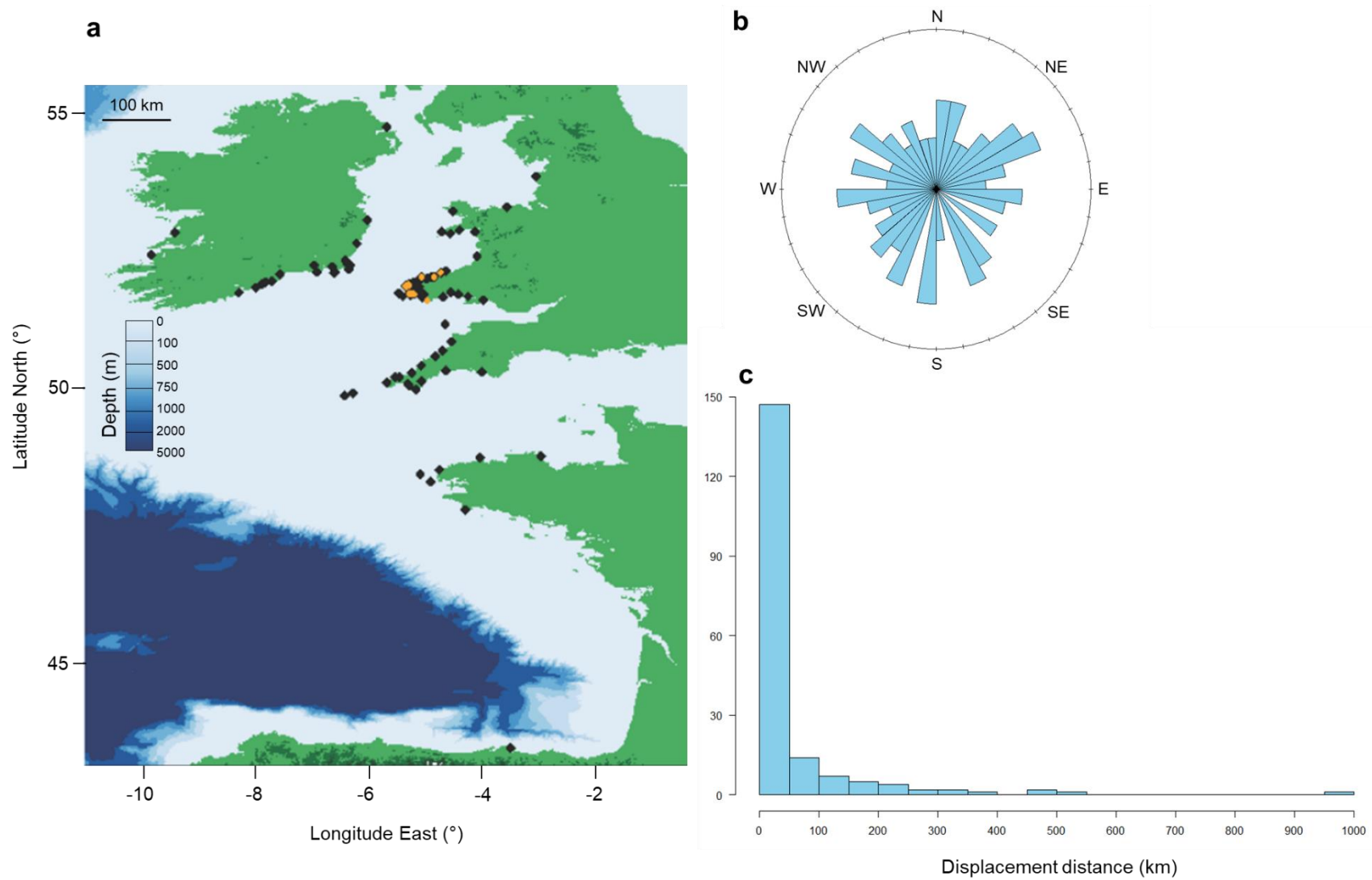


Fig. 2.4. (a) Map of grey seal pup mark locations (orange) and re-sighting locations (black) from ringing activities undertaken during 1956-1961 ($n = 184$). (b) Rose diagram of displacement headings ($^{\circ}$). (c) Frequency histogram of displacement distance (km).

2.4.2 Drivers of displacement distance reached

The best measure of the NAO was the biological annual average, outperforming competing models by 1.3–6.7 Δ AIC (Table 2.3). The most parsimonious linear model of displacement distance over time retained the full third-order polynomial function with year as a random-effect, plus the fixed-effects of sex, colony, NAO and an interaction between sex and NAO (Table 2.4). Inspection of model diagnostics indicated that all model assumptions were met for the distribution of residuals.

Displacement distance (log) increased as a function of days since birth (1.61 km d⁻¹, $t = 6.17$, $p < 0.001$) (Table 2.4; Fig. 2.5). The second- and third-order polynomial terms were highly significant ($p < 0.01$) in explaining the functional form of observed displacement distance over time. Displacement distance was not significantly different between sexes with females on average dispersing 1.47 km further than males ($t = - 1.213$, $p = 0.23$) (Table 2.4; Fig. 2.6). Pups dispersing from North Pembrokeshire covered the greatest distance followed by individuals from Ramsey, though this difference was not statistically significant (- 2.44 km, $t = - 1.899$, $p = 0.06$) (Table 2.4; Fig. 2.7). Individuals from Skomer displaced shorter distances, with a statistically significant reduction in distance compared to that of pups dispersing from North Pembrokeshire (- 2.89 km, $t = - 2.083$, $p < 0.05$) (Table 2.4; Fig. 2.7).

The effect of NAO was sex-dependent such that males increased the distance travelled in response to increases in the NAO index (1.57 km NAO⁻¹, $t = 2.62$, $p < 0.05$), whereas the distance travelled by females was reduced (- 1.51 km NAO⁻¹, $t = - 2.200$, $p < 0.05$) (Table 2.4; Fig. 2.8).

Table 2.3. Model comparisons of the most appropriate interpretation of North Atlantic Oscillation (NAO) values. See text for details.

NAO measure	df	AIC	ΔAIC	ω	k
Biological	13	267.7351	0	0.61825110	8
Autumn and Winter	13	269.0807	1.3456	0.31547847	8
Autumn	13	273.0067	5.2716	0.04430559	8
Astronomical	13	274.4100	6.6749	0.02196483	8

Table 2.4. Coefficients for the final model (reached by stepwise simplification) explaining the maximum displacement distance (log) in relation to the number of days elapsed (third-order polynomial), natal site (North Pembrokeshire, Ramsey, Skomer), sex, and the effect of the North Atlantic Oscillation (“Biological” NAO measure, see text). Models were fitted on $n = 73$ individuals that displaced > 1 km from their birth site. The estimates for each coefficient are relative to the baseline (Intercept) which represents the estimate for female pups from North Pembrokeshire.

Model:	logDist ~ Days + I(Days^2) + I(Days^3) + Colony + Sex + NAO + Sex:NAO + (1 Year)				
Parameter	Estimate	Std. Error	df	t	p
(Intercept)	5.82	0.51	38.84	11.45	<0.01
Days	1.61	0.26	63.73	6.17	<0.01
I((Days)^2)	-2.15	0.37	54.80	-5.90	<0.01
I((Days)^3)	0.46	0.10	59.91	4.50	<0.01
Ramsey	-0.89	0.47	63.00	-1.90	0.06
Skomer	-1.06	0.51	59.07	-2.08	0.04
Male	-0.39	0.32	63.83	-1.21	0.23
NAO	-0.42	0.19	11.10	-2.20	0.05
Male:NAO	0.87	0.33	62.62	2.62	0.01

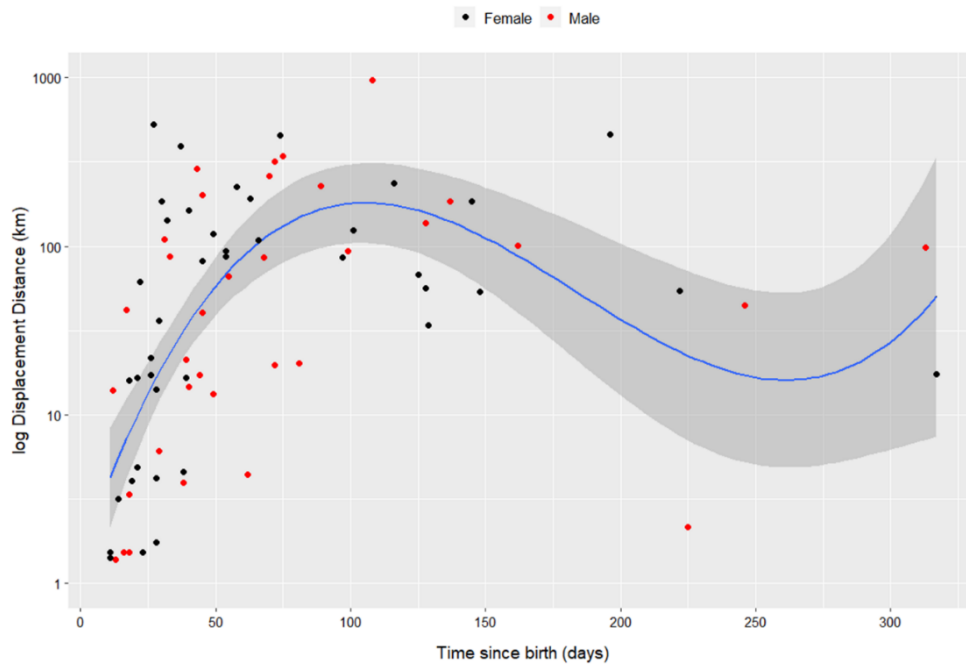


Fig. 2.5. Model predictions of log displacement distance (km) as a function of time since birth (days) for male (red) and female (black) grey seal pups displaced greater than 1 km from natal sites in Pembrokeshire (refer to 'Methods' for details) ($n = 73$).

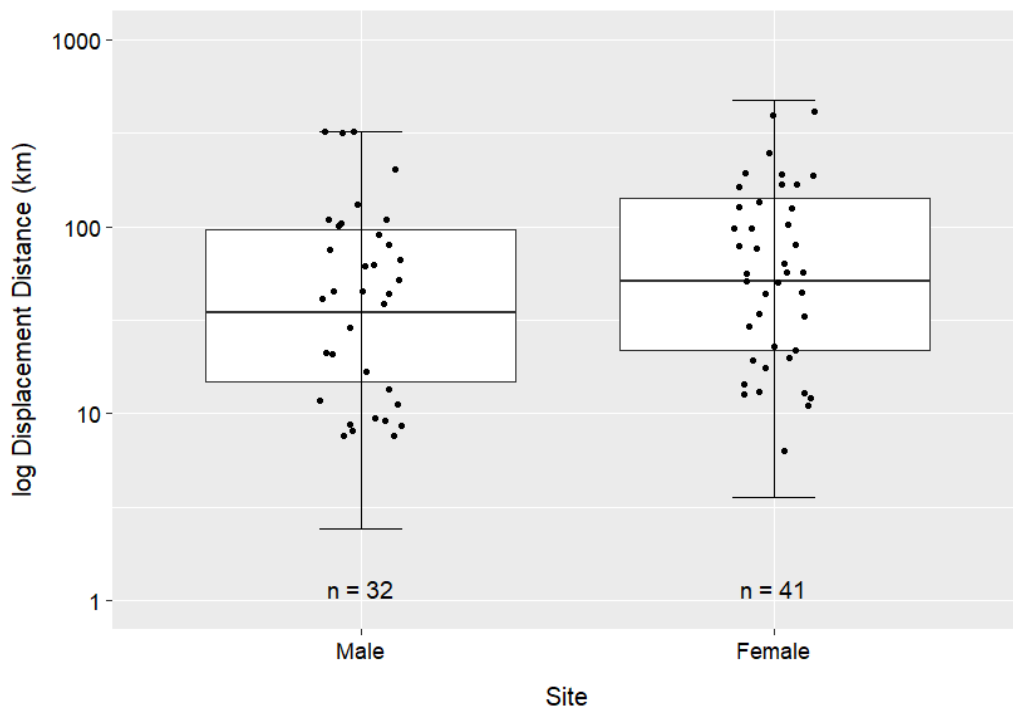


Fig. 2.6. Model predictions of log displacement distance (km) as a function of sex for grey seal pups displaced greater than 1 km from natal sites in Pembrokeshire (refer to text for details). There was no significant effect of sex (see Table 2.4).

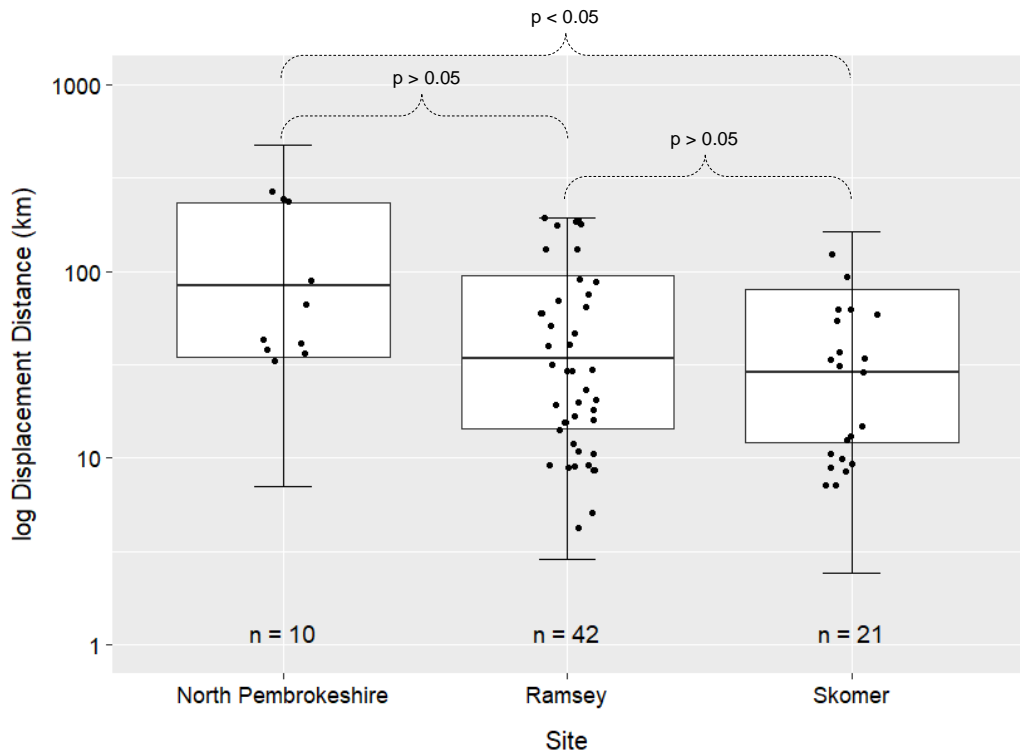


Fig. 2.7. Model predictions of log displacement distance (km) for grey seal pups displaced greater than 1 km from their respective natal sites in Pembrokeshire (refer to text for details).

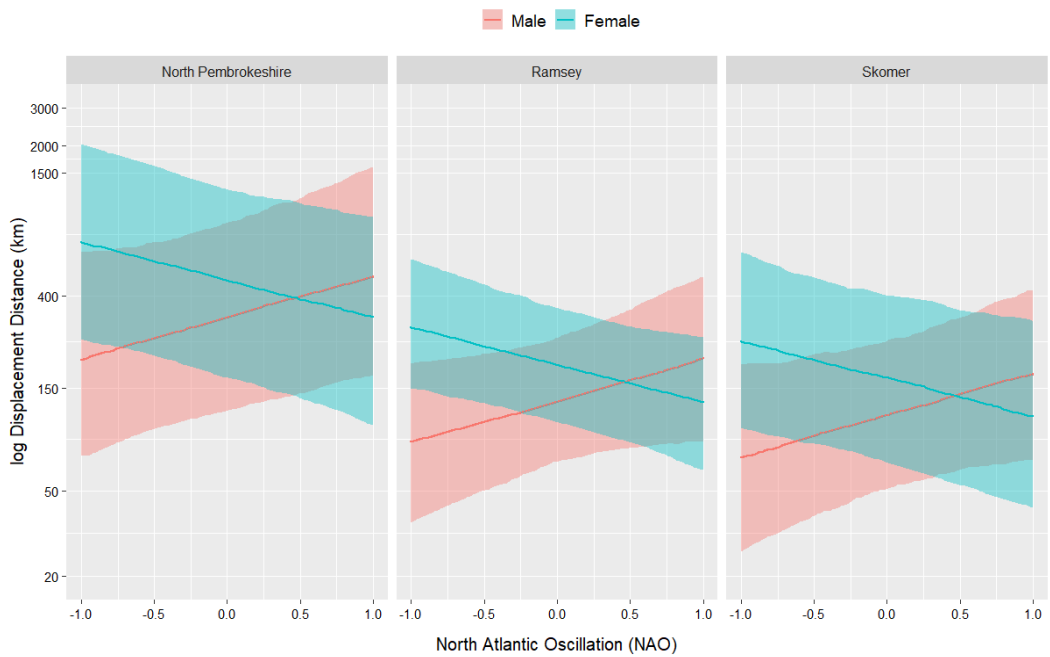


Fig. 2.8. The sex-dependent effect of North Atlantic Oscillation (NAO) values on displacement distance of grey seal pups (at 100 days after natal dispersal) from natal sites in Pembrokeshire (refer to text for details). Data shown are predictions from final model (Table 2.4) with 95 % confidence intervals (shaded regions) attained by bootstrapping ($n = 1000$ simulations).

2.4.3 Displacement over time and predicted overlap with a TST site

All displacement models fitted the data very well (range of CC statistic of 0.51–0.99 for the best fitting models; Table 2.5) and without model selection uncertainty (i.e. one single model achieved a clearly higher CC model fit statistic), except for Pembrokeshire females, where both the dispersal and diffusive models obtained near perfect fit (CC = 0.99). For the latter case, the diffusive model provided more biologically realistic parameter estimates and, importantly, for the timescale of the first 90 days the two curves were nearly identical (in accordance with both models obtaining a CC model fit value of 0.99). Consistent with the results of the dispersal distance analysis, the displacement curves differed between the sexes and colonies (Fig. 2.9), including diffusive, dispersal and return models (Table 2.2), with females generally dispersing sooner than males (except for the Pembrokeshire females).

Pups from North Pembrokeshire were predicted to have dispersed greater than 1 km from their natal site after an average of 18.5 days since birth (males = 21, females = 16) (Fig. 2.9). For pups from Skomer this was later (average of 32 days; males = 38, females = 26) and Ramsey was the latest (average of 43 days; males = 59, females = 27). The predictions of timing of overlap with the TST site for pups differed by sex: females from North Pembrokeshire were predicted to overlap between 59–61 days after birth whereas males sooner at 40–41 days; females from Ramsey were predicted to overlap between 26–27 days after birth, whereas males between 61–63 days. Females from Skomer were predicted to overlap at between 25–26 days whereas males slightly later at between 39–40 days.

The predictions from the displacement curves combined with daily pup counts (Fig. 2.10) demonstrated that a period of potentially highest risk – defined as a 30-day period when the greatest number of pups may overlap with the Ramsey Sound TST site – is between 88–117 days after 1st August; note that the first pups in Pembrokeshire are typically born from this date onwards, with peak pupping season occurring approximately 60–70 days after this; Bull et al., 2017).

Table 2.5. Concordance criterion (CC) values for each model used to derive time-dependent displacement curves.

site-sex Group	Model									Best Fit	Final Model*
	1	2	3	4	5	6	7	8	9		
	NullMod	SedMod	DispMod	ReturnMod	MixReturn	Linear	PowerC	PowerCb	ExponMod		
North Pembrokeshire Females	0.00	0.77	0.99	0.35	0.00	0.91	0.99*	0.93	0.89	DispMod	PowerC
North Pembrokeshire Males	0.00	0.50	0.66	0.83	0.71	0.19	0.36	0.20	0.01	ReturnMod	ReturnMod
Ramsey Females	0.00	0.45	0.64	0.72	0.26	0.25	0.36	0.26	0.00	ReturnMod	ReturnMod
Ramsey Males	0.00	0.32	0.52	0.40	0.41	0.24	0.27	0.23	0.01	DispMod	DispMod
Skomer Females	0.00	0.24	0.51	0.08	0.00	0.22	0.22	0.20	0.02	DispMod	DispMod
Skomer Males	0.00	0.53	0.68	0.60	0.00	0.52	0.52	0.51	0.06	DispMod	DispMod

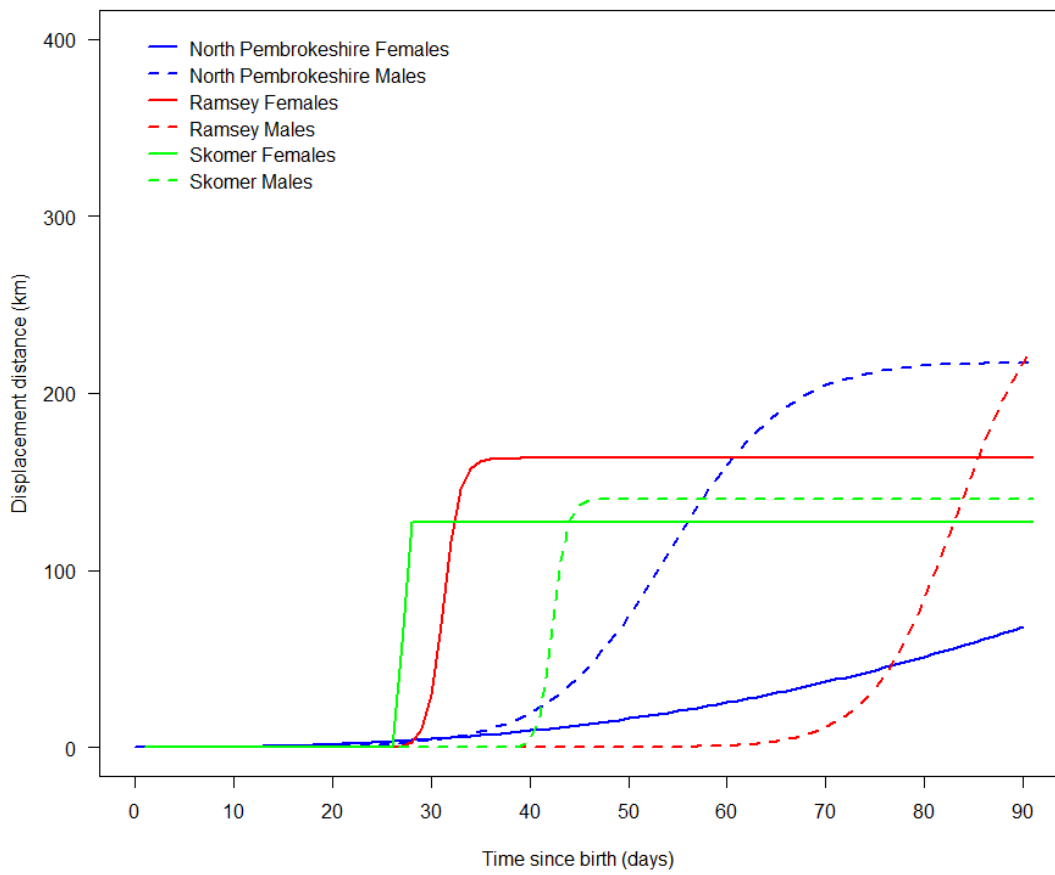


Fig. 2.9. Displacement predictions for the first 90 days since birth from the final models fitted for each site-sex group (see Table 2.1, 2.5–2.6).

Table 2.6. Predictions for the timing of overlap between seal pups and a nearby TST (see Fig. 2.9).

site-sex Group	Distance from TST (km)	Timing of overlap (days since birth)
North Pembrokeshire Females	25	59-61
North Pembrokeshire Males	25	40-41
Ramsey Females	2	26-27
Ramsey Males	2	61-63
Skomer Females	15	25-26
Skomer Males	15	39-40

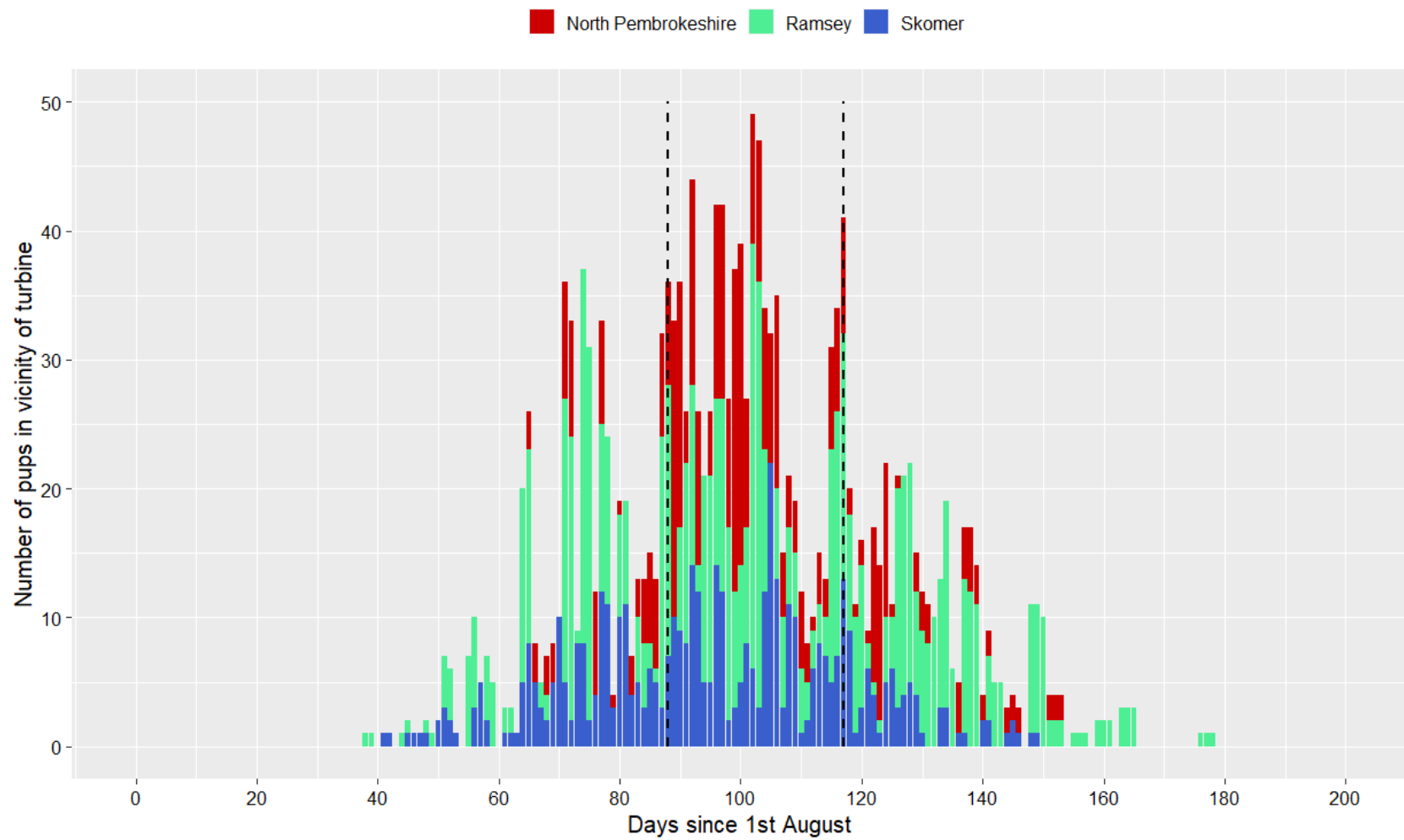


Fig. 2.10. The number of pups predicted to overlap with the vicinity of the Ramsey Sound TST site from the 1st August. The dotted lines indicate the 30-day period of greatest spatio-temporal overlap (see text for definition).

2.5 Discussion

This study demonstrates that newly weaned grey seal pups have the capacity to disperse large distances (> 950 km) within their first few months of life. There was no sex-difference in the distance dispersed by individuals, however there was an apparent sex-specific response to environmental conditions. Specifically, males displaced farther in response to more positive phases of the NAO, whereas females displaced shorter distances. There were also differences in the distance reached by animals dispersing from different natal sites, although effect sizes were small. I observed site- and sex-differences in the pattern of dispersal over time, including differences in the propensity to depart from the natal site. The model developed to predict the spatial overlap of grey seal pups over time with a nearby TST development site indicated that the greatest period of overlap occurred between approximately 3–4 months after the start of the pupping season. These findings have clear ramifications for our understanding of the dispersal of grey seal pups in their early life, and for developing appropriate conservation strategies to mitigate their risk of detrimental interaction with TSTs.

2.5.1 Quantification of displacement distance

The long-tail distribution of displacement distances by grey seals here mimics that seen in other dispersing marine organisms (Catalano et al., 2021; Martín-Vélez et al., 2021). The maximum displacement distance recorded (964 km) exceeds all other recorded displacement distances reached by grey seal pups undertaking natal dispersal from other regions; approximately 850 km by pups from Scotland (Carter et al., 2017); 739 km by pups from Norway (Bjørge et al., 2012); approximately 540 km by pups from North Wales (Carter et al., 2017); 444 km by pups from Germany (Peschko et al., 2019); and 300 km by pups from Iceland (Baylis et al., 2019). However, on average, the displacement distances reached by grey seal pups here are similar to those reported by pups dispersing from other areas. For example, Bjørge et al., (2002) reported a mean displacement distance of 120 km from pups dispersing from Norway while the individuals studied here dispersed 130 km on average. Greater

average displacement distances have however been seen in grey seal pups from other regions. Grey seals dispersing from Germany displaced an average of 173 km (Peschko et al., 2020). These results imply that differences in the displacement distance reached during natal dispersal by grey seal pups may be driven in part by regional differences. Indeed, other regional differences have been observed in the early life movements of grey seal pups, such as foraging trip distance which has been shown to be approximately 340 km (76 %) further in pups dispersing into the North Sea than those in the Celtic and Irish Seas (110 km; Carter et al., 2017). These results have important implications for the TST industry. Specifically, if the capacity of dispersal by grey seal pups from different regions varies, this means that grey seal pups from different regions will differ in their potential to reach sites of interest, such as TSEs (Thompson, 2012).

2.5.2 Drivers of dispersal distance, and displacement patterns over time

Day of departure from the natal site and dispersal propensity

Pups from all site-sex groups except North Pembrokeshire females were predicted to have a lag in their displacement prior to dispersing. Female pups from North Pembrokeshire dispersed in a more diffusive fashion, with their displacement distances best fitted by an exponential model. To date, only one other study (Baylis et al., 2019) has described the patterns of displacement over time in dispersing grey seal pups, albeit these were not quantified using the NSD approach. In Baylis et al., (2019), two distinct movement strategies were recorded. Pups either remained close to natal colonies (akin to a sedentary, home-range type movement) or dispersed. Of these movement types, only the latter was observed here. The fact that Baylis et al., (2019) examined only a study of $n = 5$ pups could have contributed to the observation of only two movement modes, suggesting sample size may be important for this.

Grey seal pups are expected to wean for 15–21 days (Pomeroy et al., 1999) followed by a post-weaning fast of 9–40 days on land prior to departure from the colony (Fedak & Anderson, 1982; Reilly, 1991; Speakman et al., 2007;

Noren et al., 2008; Bennett et al., 2010; 2013; Carter et al., 2017; 2019). While the day of departure for male pups from both Ramsey and Skomer was consistent with post-weaning fast durations recorded by Noren et al., (2008), all other pups were predicted to have displaced at least 1 km away from their natal site by 16–26 days after birth, thus allowing only ca. 0–11 days for a post-weaning fast. This suggests that pups in Pembrokeshire may not all necessarily behave in the same manner and in fact, some pups may have the capacity to become aquatic and even begin dispersing during their neonatal period.

Seminal works by Davies (1949) provide anecdotal accounts of pups entering the water from as early as a few hours after birth, and suggest that pups depart the beach immediately on completion of their moult, or at the end of lactation. This was later corroborated by Hewer (1974) who noted that some pups in Pembrokeshire left the beach and swam away immediately after moulting their lanugo. More recently, Jenssen et al., (2010) observed that pups in Norway often undertake neonatal aquatic dispersal, with several displacing of > 2 km at less than 10 days old and some reaching up to 12 km by less than 22 days old. The frequently cited 9–40 day post-weaning fast duration stems from research conducted only on pups from a total of three sites from two regions: Sable Island, Canada, and the Isle of May and North Rona, Scotland (Fedak & Anderson, 1982; Reilly, 1991; Bennett et al., 2007; Noren et al., 2008; Bennett et al., 2010). Importantly, these studies have not investigated pups from Pembrokeshire. Given that other regional differences exist in the post-weaning movements of grey seal pups (Carter et al., 2017), it is reasonable to deduce that regional differences could also be apparent in the duration of the post-weaning fast and thus the onset of natal dispersal.

The relatively high propensity to disperse by pups from North Pembrokeshire may be explained in part by the relatively high density of pups typically born here compared to the other sites studied (Saunders, 2008). However, if density-dependence was the driving factor for dispersal propensity, pups from Ramsey should exhibit a higher propensity to disperse than those from Skomer which was not the case. This suggests that broader factors not considered here, such as physical differences between sites (cf. Benjamins et al., 2015),

may drive variation in dispersal propensity. Differences in the day of departure and propensity to disperse have clear implications for the risks that pups may face in the context of interactions with TSTs, as these directly affect the age (and thus naivety and vulnerability; Thompson, 2012) at which pups may encounter devices.

Sex-differences in dispersal and the effect of the NAO

Despite grey seals not being sexually dimorphic at this life history stage, sex-specific ontogenetic differences in movement strategies are prevalent in the early life of grey seal pups (Carter et al., 2017) as well as in other juvenile pinnipeds (Lea et al., 2009; Jones et al., 2021). These are expected to provide a means of reducing competition between conspecifics. Indeed, Carter et al., (2017) demonstrated that foraging trip distance was sex-specific in the early life movements of pups from the Celtic and Irish Seas. These sex-differences were however modulated by environmental factors such as water depth, with males travelling to deeper waters further offshore compared to females who remained in more local, shallower waters (Carter et al., 2017). My results here however show that sex was not a significant driver of dispersal distance. Rather, sex-specific strategies were apparent in the response of grey seal pups to the NAO, which indicated that males displaced farther in conditions associated with stormier weather whereas female pups reduced their displacement distance.

Environmental conditions may modulate natal dispersal distance by affecting the motivation or capacity to disperse (Benard & McCauley, 2008). This has been seen in Northern fur seals where pups made use of favourable wind conditions for dispersal during extreme weather events (Lea et al., 2009), and in grey seals where the eastward flowing North Icelandic Irminger Current appeared to facilitate the eastward dispersal of pups from Iceland (Baylis et al., 2019). The NAO has been shown to have a substantial influence on the abundance of various benthic and pelagic prey species (Barros et al., 2012), including those such as sardine which can make up the diet of grey seal pups (Guisande et al., 2001; 2004). Importantly, sex-differences in habitat

preference (such as water depth) recorded for grey seal pups (Carter, 2018) are consistent with sex-differences in the choice of prey species (Carter, 2018). It may hence be possible that sex-specific targeting of different prey species whose abundance is affected by the NAO may drive variation in displacement differences between sexes. Indeed, such an effect was purported to drive the sex-specific response to the NAO in the displacement distance reached during dispersal by fledgling European Shags (Barros et al., 2012), where female displacement distance increased in NAO-positive years whilst male displacement distance reduced. Finally, stormy weather has also been shown to be responsible for the displacement of other juvenile marine megafauna to areas outside of their expected distribution (Monzon-Arguello et al., 2012), and stormy weather has also been shown to influence the sex-specific mortality of young seals (Ichihara, 1974).

Taken together, my results provide evidence that sex-specific responses to environmental conditions may exist in grey seal pups, complementing findings from existing studies (Carter et al., 2017). This suggests that understanding influential environmental conditions present at the time of weaning for grey seal pups may help to predict their displacement. In the context of the TST industry this is crucial, as this can help to determine the potential risk of grey seal pups reaching sites with TSTs, including whether there may be any sex-bias in this risk.

Site-specific differences in dispersal

Pinniped species are often observed to disperse greater distances from denser rookeries (Le Boeuf et al., 2011) in order to reduce the likelihood of competition with conspecifics. Indeed, Gaggiotti et al., (2012) has previously shown evidence of density-dependent dispersal in grey seals. Differences in seal density at the sites studied here may at least in part account for the differences in displacement distances observed; while it is important to note that density was not measured explicitly here, during an average pupping season sites in North Pembrokeshire support very high densities of individuals compared to Ramsey and Skomer (Saunders, 2008; Lock et al., 2016; Morgan, Morris, &

Stringell, 2018). For example, the “Red Wilderness” – a breeding beach in North Pembrokeshire – can support several hundred individuals (Saunders, 2008). Similarly, the fact that larger displacement distances (albeit only slightly larger) were observed by pups dispersing from Ramsey than Skomer is consistent with the typically greater number of pups born on the former compared to the latter (e.g. Lock et al., 2016; Morgan, Morris, & Stringell, 2018). Seals may have a preponderance to leave areas of higher density for risk of getting trampled by conspecifics; Le Boeuf & Briggs (1977) showed that there is higher mortality of seals at beaches with higher local seal density.

Site-specific variability in displacement patterns may also be driven by differences in environmental conditions (Singh et al., 2012) and resource heterogeneity (Couriot et al., 2018). All three sites studied here are either situated within or in close proximity to TSEs. Sites such as these display high topographic complexity and this complexity can vary over relatively fine-scales (Benjamins et al., 2015). Such variation has been shown to be key in influencing the movements of seals e.g. through variation in the distribution of resources (Benjamins et al., 2015; Lieber et al., 2018). Site-specific variation in the physical features of the marine environment has been previously shown to influence the movement strategies of grey seal pups; Carter (2018) showed that variation in the movement of weaned pups from West Wales was moderated by the percentage of mud and gravel in the seabed substrate. In line with these studies, my results suggest that, while effect sizes are relatively small, site-specific variation in dispersal may arise in response to site-specific differences in physical features of the marine environment, and possibly density. This provides support to the notion that site-specific analysis, including quantifying the densities of individuals at different sites and site-specific differences in physical features, is needed to predict dispersal and thus the potential overlap of animals with TSEs (Copping & Hemery, 2020). This is important for the TST industry, as establishing site-specific predictions of dispersal can help to estimate potential variation in risk between pups dispersing from different sites.

2.5.4 Predicted overlap with a nearby TST development site

The predicted spatio-temporal overlap of pups with the TST site was modulated by the timing of dispersal, the rate of displacement once pups had dispersed, and the distance of the colony from the TST site. Given their relatively large distance from the TST site, pups from North Pembrokeshire were predicted to overlap at a relatively older age compared to pups from other locations, even despite their relatively high dispersal propensity. Female pups from Skomer and Ramsey were predicted to overlap with the TST site at almost the same time (at between 25–27 days) and, owing to their relatively longer lag phase, males from Skomer and Ramsey were predicted to overlap with the TST site 4–24 days later.

I observed a clear time window of maximum overlap between pups and the TST site between 88–117 days after the start of the pupping season. This presents the 30-day period when the greatest number of pups may overlap with the TST site. TST developers planning to install devices in this area could consider this time as the highest risk period for grey seal pups and use this information to guide their mitigation strategies and monitoring procedures for device operations (Isaksson et al., 2021). One option to reduce potential detrimental impact (e.g. collision) with dispersing grey seal pups would be to limit the operation of TST devices during this period or employ more stringent monitoring strategies to detect potential pup and TST device interactions. Importantly, this “30-day risk period” is just one example of the ways that risk could be defined; legislators and the TST industry could work together to establish an agreed threshold to define operational protocols. For example, for the development of the first TST at the Ramsey Sound (the Deltastream™; Tidal Energy Limited, 2009), legislators permitted a set number of collisions to be detected with wild marine mammals before the turbine was shut down. Mitigation strategies should also consider the likelihood of seals reaching the depths required to come into contact with the TST and the subsequent likelihood of collision. While no depth usage data were available here, I note from other recent studies that grey seal pups are known to both frequently conduct diving behaviour (presumably for foraging) in TSEs (Thompson, 2012) and have the capacity reach depths of up to 40 m (Carter et al., 2017) within

the first few months of life; this depth is well within the range of most TSTs, including the site proposed for TST development in the Ramsey Sound (ca. 31.5 m; Tidal Energy Limited, 2009), suggesting that pups here could be at risk of collision.

Finally, the date of the start of the pupping season (i.e. phenology) can vary and certainly appears to have changed over time (Bull et al., 2017a). Specifically, the earliest pup born in the 1960s was on the 28th of August (Johnson, 1972); between 1992–2015 this date was between 1st–26th of August (Bull et al., 2017a); and in more recent years (2016–2020) the first pup has been born between July 30th –Aug 20th (Natural Resources Wales, *pers. comms.*). Hence, legislators and the TST industry must be aware that the period of maximum overlap needs to account for the start date of the pupping season. The date of the first pup born provides a relatively robust indication of when the peak pupping season will occur in any given year (between approx. 50–70 days later; Bull et al., 2017a).

2.5.5 Conclusions

In conclusion, my results provide greater understanding of grey seal pup dispersal including providing evidence of sex- and site-specific differences in dispersal distance, the pattern of displacement over time, and the propensity of dispersal. My results also suggest a sex-specific response to environmental conditions. The differences observed in grey seal pup dispersal may give rise to differences in the risk of overlap with nearby TST sites. Generally speaking, individuals that disperse the earliest and displace the most rapidly will be more likely to overlap with TST sites at a relatively young age and these may not necessarily be those individuals that are born closest to TST locations. Taken together, my results have two important implications for predicting the spatial overlap of dispersing grey seal pups with TSTs:

1. The risk of grey seal pup overlap with TSTs is likely to be sex-, region- and site-specific and so mitigation strategies must consider these sources of variation in their assessments.

2. The predictive modelling approach developed here can be used to model spatial overlap across sex- and site- groups and determine a time-period during which risks are elevated for grey seal pups at the population-level.

Lastly, the results presented here are the first quantitative predictions of grey seal pup spatial overlap with TSTs and are based on relatively old data. Providing new data are available – ideally large sample sizes of individual tracking data – future research will be able to refine these predictions. The modelling approach presented here can also be extended to grey seal pups dispersing from other regions where TST devices are common (e.g. Scotland), and indeed applied to other taxa. Future research may also consider how local-scale weather drives the movements of dispersing individuals (e.g. Mateos & Arroyo, 2011).

Chapter 3

Quantifying grey seal pup dispersal: Data and sample size requirements

“... seal calves are delightful animals, and marking them is a very pleasant occupation amid beautiful surroundings...
Catching adult seals is rather another matter...”
(Johnson 1955)



Fieldwork at Ramsey Island, Pembrokeshire. Accessing sites to capture seals requires the use of hard-bottomed zodiacs and heavy duty RHIBs (Photograph by William P. Kay).

3.1 Abstract

The emerging marine renewable energy industry presents new risks to marine megafauna, including potentially fatal collisions between animals and tidal stream turbines (TSTs). Understanding these risks requires an assessment of the broad-scale distribution of animals with areas targeted for development, including the spatial overlap between individuals and devices. Grey seal pups are an at risk group, especially during natal dispersal where they are naïve and vulnerable, and have been shown to make use of tidal stream environments (TSEs). Animal tracking methods are often used to quantify the movements of grey seal pups at sea but this method is limited in its ability to collect large sample sizes. This is problematic because grey seal pups display high inter-individual variation in their movements and so large sample sizes may be needed to make population-level inferences required for impact assessment. Here, using high-resolution tracking data from 12 individuals, I model the movements of grey seal pups during natal dispersal and compare displacement predictions to those generated from a large sample of ringing records in order to determine the data requirements for reliably estimating displacement. I demonstrate that individual variation in displacement over time can be explained by three movement modes (diffusion, dispersal, and return) with pups dispersing at three different scales (< 50 km; $> 50 \leq 150$ km; and > 150 km). Pups typically undertake exploratory behaviour relatively close to their natal site (within 50 km) for the first 30–70 days before moving offshore to sites as distant as 403.7 km. I show that individual-level model predictions from tracking data are consistent with predictions derived using population-level data. Using a resampling approach, I reveal that the mean and 25th percentile of displacement can be reliably estimated with a sample size of 5–14 pups, but that predicting upper limits of displacement requires data from more than 127 individuals. Finally, my findings suggest that a minimum recording duration of 200 days is required to reliably estimate displacement distance. My findings provide guidance for researchers attempting to investigate grey seal pup dispersal and their potential overlap with TSEs. This will aid researchers in providing robust predictions for environmental legislators to assess the risk of grey seal pups encountering TSTs.

3.2 Introduction

The emerging tidal stream energy industry presents an anthropogenic risk to marine megafauna (Copping & Hemery, 2020). Threats include, and are not limited to, fatal collision between animals and moving components of devices; disturbance from noise pollution or electromagnetic emissions; and changes to oceanography or habitat resulting in changes in the distribution of resources (Fox et al., 2018). Two important components in determining risk are estimating the broad-scale spatial overlap of animals with tidal stream environments (TSEs) (Waggitt & Scott, 2014), and understanding the fine-scale movements of animals within these locations (Copping et al., 2020). Novel animal tracking technologies (“tags”) have revolutionised the study of movements of marine megafauna in the wild (Hazen et al., 2012) and in recent years have been shown to be effective in studying the movements of animals in TSEs and avoidance responses to operational TSTs (e.g. Hastie et al., 2017; Joy et al., 2018; Onoufriou et al., 2021). In tandem, analytical frameworks have been developed to process the data that are obtained from tracking devices to generate spatial data that can be incorporated into environmental impact assessments (Isaksson et al., 2021).

Despite the potential of such research, the widespread use of tags is limited by the ethical, financial, and logistical constraints inherent to studying wild animals (Burger & Schaffer, 2008; Cagnacci, et al., 2010). Logistical challenges are particularly pertinent to studying marine megafauna as they are inherently difficult taxa to study; they spend much of their time at sea, often at long distances from the coast, and frequently below the surface where they are unable to be observed directly (Shillinger et al., 2012). To make matters worse, individual variation in the movements of marine megafauna is high (Hays et al., 2016) and so relatively large sample sizes ($30 < N < 100$) are needed in order to make population-level inferences (Hays et al., 2016; Sequeira et al., 2019). For studies examining the distribution of animals in specific environments such as TSEs this is made yet more difficult by the fact that not all animals studied will necessarily use the area of interest (Waggitt & Scott, 2014), thus requiring an even greater sample size of individuals.

Compared to tagging, visual survey methods, such as the use of theodolites, unmanned aerial vehicles, photographic approaches, and ID tags (e.g. bird rings) are commonly-used alternatives for collecting data on marine megafauna in coastal environments (Hoekendijk et al., 2015; Piwetz et al., 2018; Burke, Manley, & Bayley, 2020; Christiansen et al., 2020), and in recent years these methods have been augmented by more advanced technologies (Cole et al., 2019; Heal et al., 2021). These methods typically allow for the collection of greater sample sizes at relatively low logistical and financial cost, and with minimal to no ethical implications. However, they are only able to collect observations of animals whilst they are at the surface (Cole et al., 2019) and are limited in their ability to continuously track the movements that animals take when travelling between different, distant sites (Benjamins et al., 2015); for example, the movements of fledgling individuals dispersing from natal sites (Votier et al., 2011) or individuals travelling between breeding sites (Sayer et al., 2019). In the context of the TST industry, this information is crucial to understand how animals move between disparate tidal stream environments and for this, tag data are typically required. Moreover, while recent research has highlighted the potential for visual survey methods to examine the fine-scale movements of animals in TSEs (Cole et al., 2019), information is needed on how animals move whilst underwater, as this is key for determining collision risk (Hastie et al., 2019). While applications of active acoustic sonar (AAS) technology can provide useful insights, these methods provide data that are generally restricted to a range of tens of metres around a point of interest (such as a TST) and are limited in their ability to discriminate between species (Hastie, 2012).

An example of a marine megafauna species that is challenging to study, that covers long distances in the marine environment, and that is potentially at risk from detrimental interactions with TSTs, is the grey seal *Halichoerus grypus* (Carter et al., 2016). The life-history stage of most interest, especially in the context of TSTs, is the grey seal pup (Thompson, 2012). This is because as pups, grey seals can cover long distances during natal dispersal (Peschko et al., 2019) and have the capacity to reach distant TST sites (Chapter 2), as well as having been reported to make repeated use of TSEs (Thompson, 2012).

They are perceived to be at high risk from detrimental interaction with TSTs (Thompson, 2012) owing to the fact that they receive no parental guidance in their initial movements at sea and so are naïve to the threat of these devices (Wilson, et al., 2006). Moreover, grey seal pups suffer high mortality (up to 79 %) in their first year of life, with a large proportion (25 %) of this due to detrimental interaction with anthropogenic disturbance (Bjørge et al., 2002).

Recent studies of weaned grey seal pups have revealed important insights into the ontogeny of their behaviour and movement (Carter et al., 2017, 2019; Peschko et al., 2020), however no study to my knowledge is yet to quantify the “movement mode” (i.e. functional form of displacement; cf. Börger & Fryxell) of dispersing grey seal pups at the individual-level, in order to determine movement modes between individuals, analogous to work on juvenile seabirds (de Grissac et al., 2016). This is despite the fact that recent grey seal pup trajectories reveal distinct patterns of post-weaning movement, such as remaining close to their natal site, or dispersing to and settling in new areas (Peschko et al., 2020). These patterns, amongst others, are typically characterised by one of five different “movement modes”, namely dispersal, return, mixed-return, sedentary and diffusive (defined in Chapter 2 and see Börger and Fryxell, 2012). Classifying movement modes is a logical first step for understanding animal movement (Bastille-Rousseau et al., 2015) and is crucial for conservation management through being able to and reveal what an animal is doing (Morelle et a., 2017) and support predictions of space use over time (Killeen et al., 2014). In the context of TSTs, quantifying the movement modes of grey seal pups, and estimates of their displacement, is essential to predict the overlap of animals with devices (Chapter 2).

As pups, grey seals are large enough to bear tags and, while not having examined this directly, recent studies have tracked their movements in TSEs (e.g. Carter et al., 2017; 2019). However, the sample sizes of animals studied at different sites is typically low (~ 10 individuals; Carter et al., 2017). This is an issue because variation in animal behaviour in TSEs is typically high (Copping et al., 2020), driven in part by site-specific differences in physical features and variability in the distribution and abundance of resources (Benjamins et al., 2015; Levin, 1994). Moreover, variation in the movement of

pups during their early life is generally high, such as in their selection of foraging habitats (Carter, 2018), dive duration (Bennett et al., 2010), distance travelled (Peschko et al., 2020; Chapter 2), or movements through TSEs (Thompson, 2012). Sex-specific differences are also evident in some areas, such as in the environments targeted for foraging; female pups from West Wales demonstrated preference to shallow, sandy areas whilst males targeted deeper waters with more mud and gravel sediment (Carter et al., 2017; Carter, 2018). These differences have been suggested to be driven by a combination of inter-individual variation and strategies to provide sexual-segregation in the competition of resources, as seen in other juvenile seals (Jones et al., 2021).

High inter-individual variation and limited sample size creates problems with measuring and predicting population-level movements. An estimation of the sample size needed to robustly quantify variation in movement would thus be invaluable for those attempting to estimate overlap between vulnerable populations and potentially harmful developments, such as TSTs (Isaksson et al., 2021). In addition, tag deployments can last from a few days to many months (Carter et al., 2016), and grey seal pup behaviour develops gradually over time (Carter et al., 2019), and so it is crucial to understand what recording duration is required to make reliable inferences.

In Chapter 2, I demonstrated how quantifying the patterns of natal dispersal movements using a displacement modelling approach applied to population-level ringing data can help to inform strategies to mitigate collision risk of grey seal pups with TSTs. My aim here is to understand if smaller sample sizes of high-cost tracking data provide comparable estimates to those derived using relatively low-cost methods. To achieve this, I evaluate the natal dispersal of grey seal pups this time using high-resolution location data from 12 individuals tracked using Fastloc-GPS technology. My objectives were threefold:

1. Determine the “movement modes” (i.e. form of displacement) of individual grey seal pups dispersing from their natal sites and determine the recording duration required to reliably quantify this.
2. Evaluate the consistency of the estimates of displacement distance reached from the high-resolution sampling of the 12 individuals here, to

the estimates obtained from modelling population-level displacement using a large sample size ($n = 184$) from ringing records (Chapter 2).

3. Quantify the sample size required to robustly estimate grey seal pup displacement.

This information should aid researchers using tracking devices to design their studies appropriately to quantify the dispersal movements of grey seal pups in early life.

3.3 Methods

3.3.1 GPS telemetry data

12 grey seal pups were captured whilst hauled-out on beaches (Sharples, Moss, Patterson, & Hammond, 2012) at two pupping sites on the Welsh coast in 2009 and 2010 (Table 3.1; Fig. 3.1). Both sites, the Skerries in Anglesey (53.42 N, -4.61 E) and Ramsey in Pembrokeshire (51.86 N, - 5.34 E), are in very close proximity (< 1 km) to TSEs. Ramsey is a very important site for grey seal pups in Wales, with between 500–700 pups born annually (Strong et al., 2006); by comparison the Skerries boasts relatively few pups with around 15 pups born each year (Westcott & Stringell, 2003). The exact age (in days) of pups was not known, but all were observed to have been recently weaned and having not previously departed their natal colony. I hence assumed pup age to be 18 days old; the average age at weaning (range: 15–21; Noren et al., 2008).

Table 3.1. Deployment summary information. Sample sizes of pups tagged in site and year. Data for recording duration and number of fixes are given after data cleaning (see text).

Year	Deployment site	No. tagged seals			Recording duration (mean ± SD)	No. fixes (mean ± SD)
		f	m	Total		
2009	Skerries, Anglesey	1	2	3	208 ± 31	7536 ± 2221
	Ramsey, Pembrokeshire	0	0	0	NA	NA
2010	Skerries, Anglesey	4	1	5	199 ± 94	8785 ± 2410
	Ramsey, Pembrokeshire	2	2	4	185 ± 72	12683 ± 5234
Total		7	5	12		

Fastloc GPS-GSM tags (SMRU Instrumentation, University of St Andrews) were deployed on seals; a portion of fur behind the head on the back of the neck was cleaned with acetone and dried before the tag was glued in place (using RS Quick-Set Epoxy Adhesive (RS Components Ltd., UK) for 2009 deployments, and Loctite® 422™ Instant Adhesive super glue (Henkel, UK) for 2010 deployments). Capture, handling, and tag deployments were carried out by the Sea Mammal Research Unit in accordance with the Animals (Scientific Procedures) Act 1986 under UK Home Office project license #60/4009.

Tags were programmed to obtain a position fix every 20 min. I applied a speed filter to remove location estimates exceeding a speed threshold of 2 ms^{-1} (Carter et al., 2017) and removed further erroneous GPS location estimates by following the protocol outlined in Russell et al., (2015) (based on the number of satellites obtained for each position fix and residual error thresholds). Tags were expected to remain attached to the animals for up to 12 months before animals moulted and the tags detached (Carter et al., 2017).

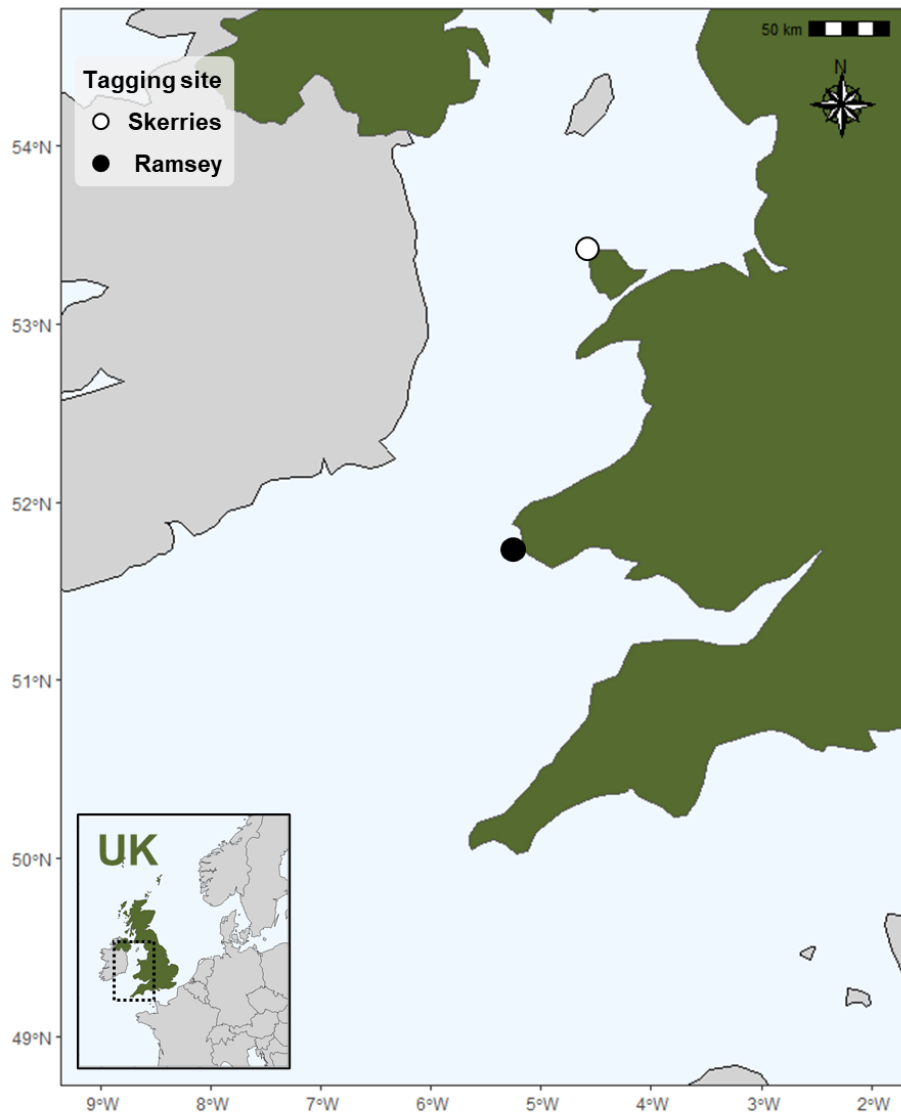


Fig. 3.1. Map showing the locations of pup tagging sites in Wales, UK.

3.3.2 Displacement modelling

As in Chapter 2, my aim was to model the displacement of individuals over time (this time using tracking data) and thus determine the patterns of movement of individuals. To achieve this, I once again implemented the displacement modelling approach outlined by Börger & Fryxell, (2012) to quantify the patterns of displacement of individuals over time. Specifically, I calculated the net-squared displacement (NSD) – the squared Euclidian distance, computed using the Haversine formula (i.e. great-circle distance) – from the start point for every position along each seal’s trajectory. The NSD is

a continuous-time-dependent movement statistic that provides fundamental insight into the distance moved by animals over time (Turchin, 1998; Nouvellet et al., 2009; Börger & Fryxell, 2012). In cases where straight-line distances from the start point were measured directly across land, I split tracks into segments and calculated the NSD from the respective start of each segment and summed these; this provides a more biologically appropriate assessment of the distance displaced from the natal colony through the water, as seals do not disperse across land (see Chapter 2). I obtained the average (i.e. expected) NSD value, termed the mean net-squared displacement (MSD), of each seal for each day (Börger and Fryxell, 2012).

As in Chapter 2, I classified seal movements into one of five movement modes: diffusive, sedentary (within home-range movements), dispersal, return, and mixed-return (Fig. 3.2). For ease of interpretation, I grouped return and mixed-return models under the general term 'returner' to represent individuals that moved back to, or close to, their respective start point. I fitted the models using a non-linear mixed-effects modelling approach implemented in the 'nlme' library in R, including all parameters (Table 3.2) as both fixed and random-effects (the latter to account for individual variability).

Table 3.2. Details of the non-linear models fitted to derive time-dependent displacement curves (i.e. 'dispersal kernels'). For full details of models and their parameters, refer to Börger & Fryxell, (2012). In all models, all parameters were included as both fixed and random effects. t represents the number of days since birth.

Model	Name	Functional form	Parameters	Biological interpretation
1	NullMod	$y = c$	c	Stationary
2	SedMod	$y = \delta[1 - \exp(-\vartheta t)]$	δ, ϑ	Home-range movement
3	Linear	$y = 4Dt$	D	Diffusive movement
4	PowerC	$y = Dt^a$	D, a	Diffusive movement
5	PowerCb	$y = t^a$	a	Diffusive movement
6	ExponMod	$y = D * \exp(t)$	D	Diffusive movement
7	DispMod	$y = \frac{\delta}{1 + \exp\left[\frac{(\theta - t)}{\varphi}\right]}$	δ, θ, φ	Dispersal movement
8	ReturnMod	$y = \frac{\delta}{1 + \exp\left[\frac{(\theta_1 - t)}{\varphi_1}\right]} + \frac{-\delta}{1 + \exp\left[\frac{(\theta_2 - t)}{\varphi_2}\right]}$	$\delta, \theta_1, \theta_2, \varphi_1, \varphi_2$	Dispersal and return
9	MixReturn	$y = \frac{\delta_1}{1 + \exp\left[\frac{(\theta_1 - t)}{\varphi_1}\right]} + \frac{-\delta_2}{1 + \exp\left[\frac{(\theta_2 - t)}{\varphi_2}\right]}$	$\delta, \theta_1, \theta_2, \varphi_1, \varphi_2$	Dispersal and return

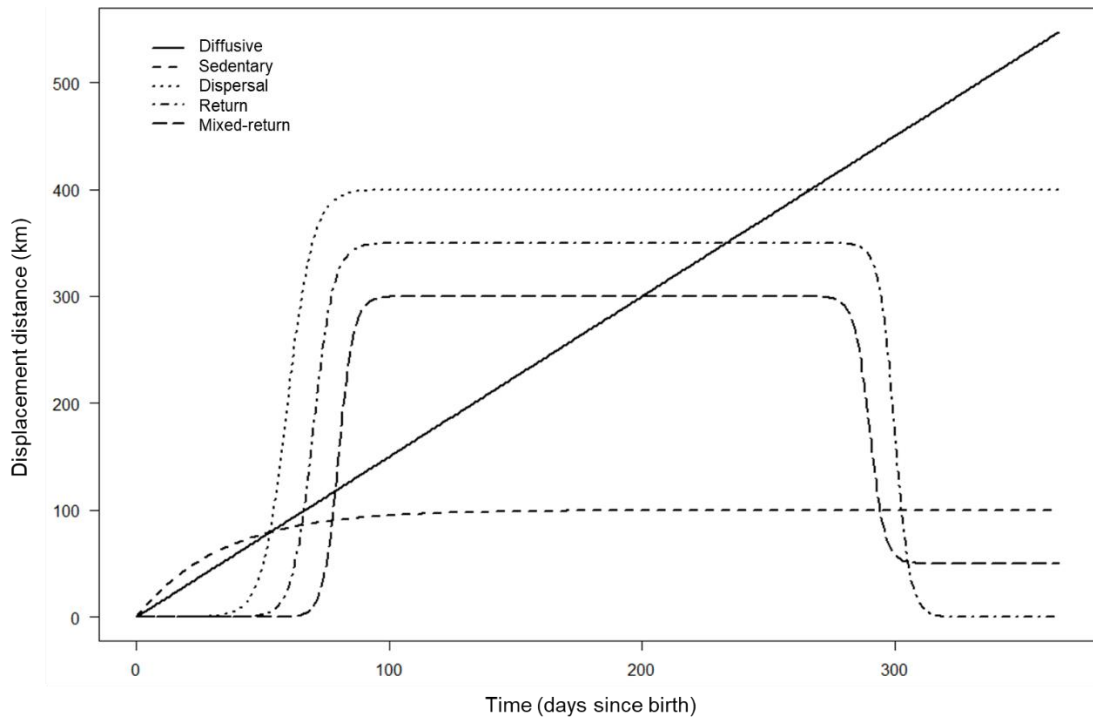


Fig. 3.2. Schematic diagram of displacement curves of the five movement modes considered (see Table 3.2 for equations).

Fitting models using non-linear mixed effects in this way can efficiently estimate the parameters of continuous, repeated measures of individuals (Pinheiro & Bates, 2000; Davidian & Giltinan, 2017) as it is robust to issues in sampling balance or missing data, and models are able to ‘borrow strength’ across individuals to derive appropriate parameter estimations (Pinheiro & Bates, 2000). Hence the use of this non-linear mixed-effects modelling approach is particularly appropriate here given the use of continuous tracking data with potentially high individual variation. However, in a few cases mixed model convergence can prove difficult; this is typical in fitting models where all parameters are included as mixed effects (Börger & Fryxell, 2012) or where the converged mixed model fits were inappropriate (see Appendix S2.1). To alleviate this, I also fitted the corresponding model at the individual-level; my goal was to ensure that the final model reached for each individual represented the most appropriate prediction given the data. In all cases, I assessed model fit for individual subjects using the concordance correlation (CC) coefficient (Huang et al., 2009), allowing therefore to select the best fitting model for each individual MSD curve whilst excluding models that were overfitted.

From the fitted NSD models I derived the following key displacement statistics for each individual (for full details see Appendix S2.2; Börger & Fryxell, 2012):

- Displacement distance at 30, 60, and 90 days .
- Maximum displacement (ϕ_1).
- The day individuals reached > 1 km displacement.
- The midpoint of dispersal (ϕ_2); i.e. the inflection point of dispersal.
- The dispersal scale parameter (ϕ_3); the time elapsed between reaching half and approximately $\frac{3}{4}$ of the maximum dispersal distance.
- The day that animals begin to disperse (ϕ_4); i.e. 'initiation'.
- The day at which individuals settle after dispersal (ϕ_5); i.e. 'settlement'.
- The distance travelled during 'transience' (ϕ_6); transience is the time period elapsed between initiation and settlement.
- The duration of transience (ϕ_7).
- The average rate of displacement during transience (ϕ_8).

These displacement statistics were also calculated from the model predictions derived in Chapter 2 for comparison. I also calculate the timing of any return journeys to determine the recording duration required to classify return movement modes (Appendix S3.2). To complement the displacement statistics above, I categorised each individual by their scale of displacement at 3 months old: (1) small scale movements – seals that displaced up to 50 km from their start point; (2) intermediate scale movements – seals that ranged between 50–150 km, typically displacing to different regions of Wales or to the closest shores of neighbouring countries of the UK and Ireland; and (3) large scale movements – seals which displaced > 150 km, moving to relatively distant areas of the UK such as the west of Ireland or the English south coast, and on towards the northern coast of France.

All analyses were undertaken using R (version 3.6.3 (2020-02-29); R Core Team, 2018).

3.3.3 Comparison of model predictions from individual- and population-level data

To understand the differences between the predictions made by models fitted to the high-resolution data from the 12 individuals here (hereon “GPS models”), to models fitted to the coarse data from the $n = 184$ individuals in Chapter 2 (hereon “ringing models”), I first visually assessed their similarities by plotting the predictions from each together across their full temporal range, and for the first 90 days. This qualitative assessment provided an initial indication of whether the shape and spatio-temporal extent covered by the models were agreeable or not. From this I also determined the proportion of GPS trajectories, and ringing data points, that fell outside of the extent covered by the ringing model predictions. To make quantitative comparisons, I inspected boxplots of the displacement statistics calculated in **3.3.2** to determine the extent of overlap between predictions.

3.3.4 Assessing sample size requirements

It was evident based on initial visual inspection of the model predictions that a small number of individuals from the ringing models displaced markedly further – within the same time period – than the 12 individuals studied here, presumably owing to a substantially larger sample size in the former which captured these particularly long-tailed displacements (e.g. Byrne et al., 2014). In order to determine how a reduced sample may have missed these “extreme” individuals, I used a bootstrapped simulation-based approach to evaluate how the distribution of displacement distances changed with sample size. Specifically, I took the empirical ringing data from the $n = 184$ grey seal pups presented in Chapter 2 and generated 1000 bootstrapped estimates (i.e. sampling with replacement) of displacement distance summary statistics – mean (μ), 25th and 75th percentile (p_{25} and p_{75} ; i.e. interquartile range (IQR)), 95th percentile (p_{95}), and max – from sample sizes ranging from 1–184 individuals.

To determine the recommended sample size to reliably estimate each summary statistic, I calculated at what sample size the mean (of 1000

bootstrapped estimates) stabilised to within $\pm 5\%$ of the estimate obtained from the maximum possible sample size of $n = 184$. To provide an indication of error, I also calculated at what sample size the range of the 95% confidence intervals (CIs) of each estimate stabilised to $\pm 10\%$.

3.4 Results

3.4.1 Summary of GPS telemetry data

I analysed GPS telemetry data from 12 individual seal pups from two sites on the Welsh coast with individual recording durations ranging from 98–335 days (Table 3.1; Fig. 3.3).

Pups dispersed from their natal colonies in Pembrokeshire and Anglesey to different sites across Wales, as well as to neighbouring regions in the UK and Ireland (Fig. 3.3; Appendix S3.3). Visual assessment of the trajectories showed that seals initially remained relatively close to their natal colony; following this, individuals either continued to remain at their original location, or moved away to new areas where they settled and from which they conducted central place foraging style movements (Fig. 3.3; Appendix S3.3). Pups tended to “hug” the coastline as they moved away from their natal site, with individuals rarely moving further than 30 km from nearest land. The cumulative distance swum by individuals ranged from 2502.6–14350.7 km over a period of between 98–336 days (Appendix S3.3).

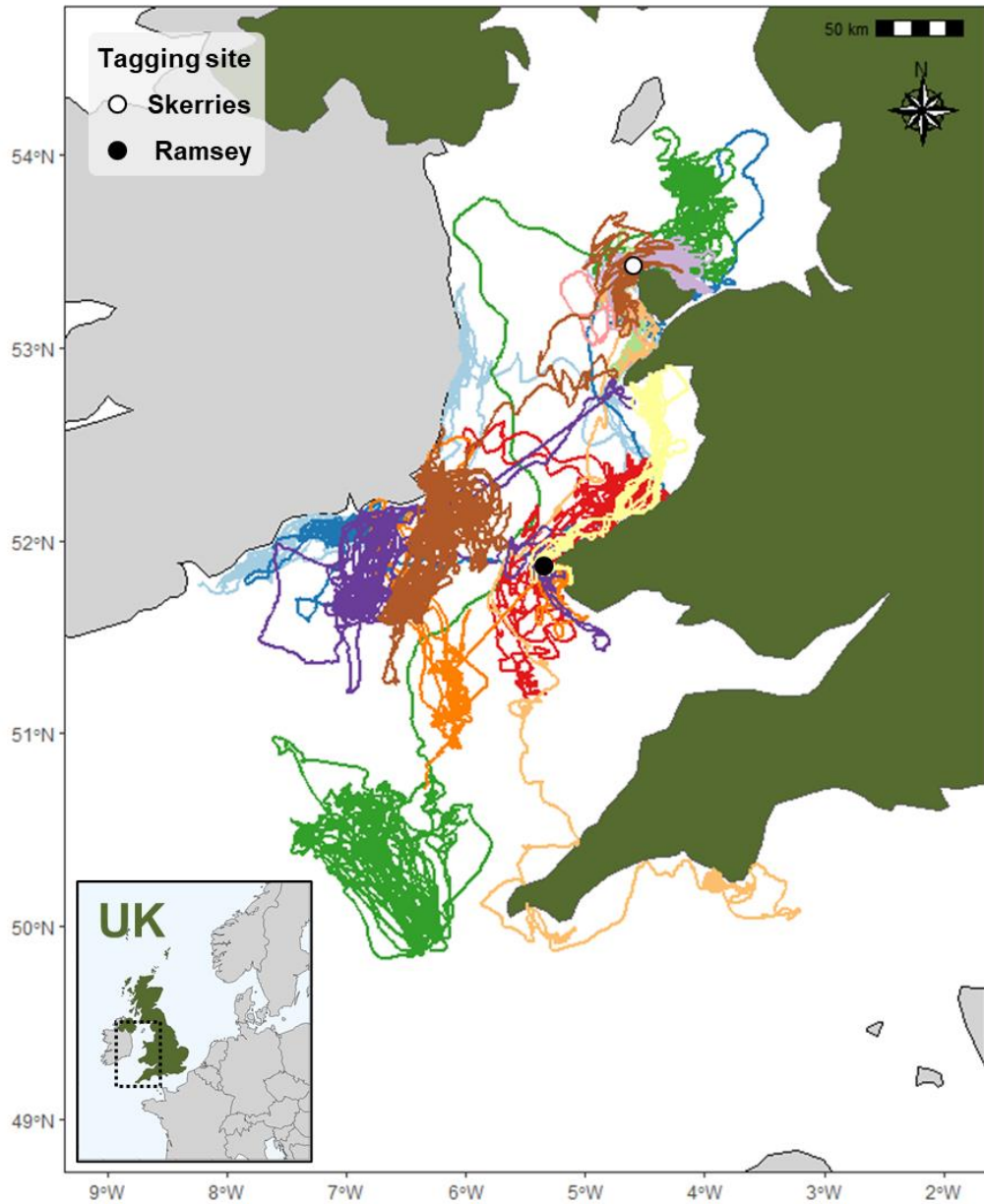


Fig. 3.3. Pup tagging sites (The Skerries, Isle of Anglesey; Ramsey Island, Pembrokeshire) and the pups' at-sea trajectories. Tracks show pup movements during their first year after weaning. Maps created using the 'ggmap' package in R (Kahle & Wickham, 2016). Pup trajectories are coloured individually.

3.4.2 Displacement models

CC values indicated that the displacement models were very well fitted for individuals classified as dispersers (mean \pm SD = 0.93 ± 0.07) and returners (0.86 ± 0.08), but less so for those classified as diffusive (0.49 ± 0.13) (Appendix S3.5). Individuals showed clear differences in their patterns of displacement away from their natal colonies (Table 3.3; Fig. 3.3; Appendix S3.3–S3.5). Movement modes included dispersal, return, mixed-return, and diffusive, and no individuals were classified as sedentary (Table 3.3). Of the 12 individuals, 4 (33 %) were classified as ‘dispersers’, 6 (50 %) as returners, and 2 (16.7 %) as ‘diffusive’. Individuals for which recording durations ranged from 98–212 days were classified as dispersers; 103–176 days as diffusive; and individuals with recording durations \geq 175 days were classified as returners or mixed-returners (Table 3.3; Appendix S3.4).

Displacement over time

Pups moved further than 1 km from their natal colony by 48.2 ± 37.5 (mean \pm SD) days since birth (Fig 4.4). At the extremes, 5 individuals had reached this distance by as early as 17–18 days old, and 1 individual not until 137 days since birth (Appendix S3.5).

10 individuals undertook an initial dispersal type displacement, initiated at 68.0 ± 42.0 days since birth. When these 10 individuals dispersed, they displaced to between 190.2 ± 126.7 km from their natal colony, increasing their displacement distance at a rate of 18.5 ± 12.5 km per day, and had settled at a new location by 80.8 ± 42.6 days since birth (Table 3.3; Appendix S3.5). 8 of these animals initiated their dispersal prior to 75 days old, and it was only beyond 175 days old after which some, but not all of these individuals, began to return (Fig. 3.4; Appendix S3.5). Specifically, only 6 of the 10 individuals that initially undertook dispersal subsequently made return movements to, or towards, home (Table 3.3; Fig. 3.4; Appendix S3.4). These individuals returned at 213.3 ± 53.2 days since birth following what was an extended period of settlement at their respective dispersal locations (lasting 135.2 ± 44.9 days (Table 3.3; Appendix S3.5). Of these 6 returners, the 5 classified as mixed-

returners showed greater variability in displacement distance during final settlement than the individual classified as a returner which, after having returned home to the Skerries, settled there with subsequently little movement away (Appendix S3.3–3.4).

Only 2 out of 10 individuals were classified as diffusive. These individuals increased their displacement distance from the natal site at a slower rate of 2.4 ± 0 km per day, reaching a maximum displacement distance of 35.8 ± 4.5 km (Table 3.3; Appendix S3.5).

Scale of displacement

By 3 months old, 4 individuals had undergone small scale displacements (< 50 km); 5 had made intermediate displacements ($> 50 \leq 150$ km); and 3 had made large scale displacements to > 150 km (Table 3.4).

Table 3.3. Estimates from fitted displacement over time models. Day 18, Day 30, Day 60, and Day 90 show the distance reached at 18, 30, 60, and 90 days since birth, respectively. “>1km” shows the day since birth by which individuals had displaced greater than 1 km from their natal site. For details of ϕ_1 - ϕ_8 refer to S4.2. “dsb” = days since birth.

ID	Movement mode	Sex	Site	CC	Day 18 (km)	Day 30 (km)	Day 60 (km)	Day 90 (km)	>1km (dsb)	ϕ_1 (km)	ϕ_2 (dsb)	ϕ_3 (days)	ϕ_4 (dsb)	ϕ_5 (dsb)	ϕ_6 (km)	ϕ_7 (days)	ϕ_8 (kmh)	Recording duration (days)
hg27-01-09	Mixed-return	M	SK	0.90	0.0	0.0	0.0	0.2	98	252	129.8	2.8	122	139	239.7	17	0.6	175
hg27-04-09	Dispersal	M	SK	0.96	0.0	0.0	99.8	219.1	52	219.1	61.1	0.8	59	64	208.5	5	1.7	212
hg27-07-09	Return	F	SK	0.85	0.0	0.0	27.0	51.5	56	49.1	60	0.4	59	62	46.8	3	0.6	237
hg29-11-10	Mixed-return	M	SK	0.98	0.0	0.0	0.0	0.0	137	380.6	163.4	2.2	157	171	362.1	14	1.1	336
hg29-13-10	Diffusive	F	SK	0.40	0.0	9.7	24.2	30.5	18	32.6	NA	NA	NA	NA	32.6	102	0.1	103
hg29-15-10	Mixed-return	F	R	0.72	1.4	31.5	63.8	63.8	17	63.8	32.1	1.9	27	38	60.7	11	0.2	262
hg29-16-10	Dispersal	F	SK	1.00	0.0	0.1	8.2	385.6	47	403.7	83.1	3	75	92	384	17	0.9	135
hg29-18-10	Dispersal	M	R	0.87	5.9	16.9	88.5	94.5	17	94.5	49.1	5.6	33	66	90	33	0.1	98
hg29-19-10	Diffusive	F	SK	0.58	0.0	10.3	22.9	28.1	18	39	NA	NA	NA	NA	39	175	0.1	176
hg29-21-10	Dispersal	M	R	0.87	0.0	0.0	105.9	105.9	38	105.9	46	0.8	44	49	100.7	5	0.8	157
hg29-22-10	Mixed-return	F	R	0.86	2.5	21.1	117.5	117.6	17	117.6	39.6	2.8	32	49	111.8	17	0.3	223
hg29-25-10	Mixed-return	F	SK	0.84	0.0	0.0	0.1	215.6	63	215.6	74.2	1	72	78	205.1	6	1.4	252
Average	NA	NA	NA	0.8	0.8	7.5	46.5	109.4	48.2	164.5	73.8	2.1	68.0	80.8	156.8	33.8	0.6	197.2
SD	NA	NA	NA	0.2	1.8	10.7	45.6	113.7	37.5	129.4	42.0	1.5	42.0	42.6	122.8	52.0	0.6	70.1

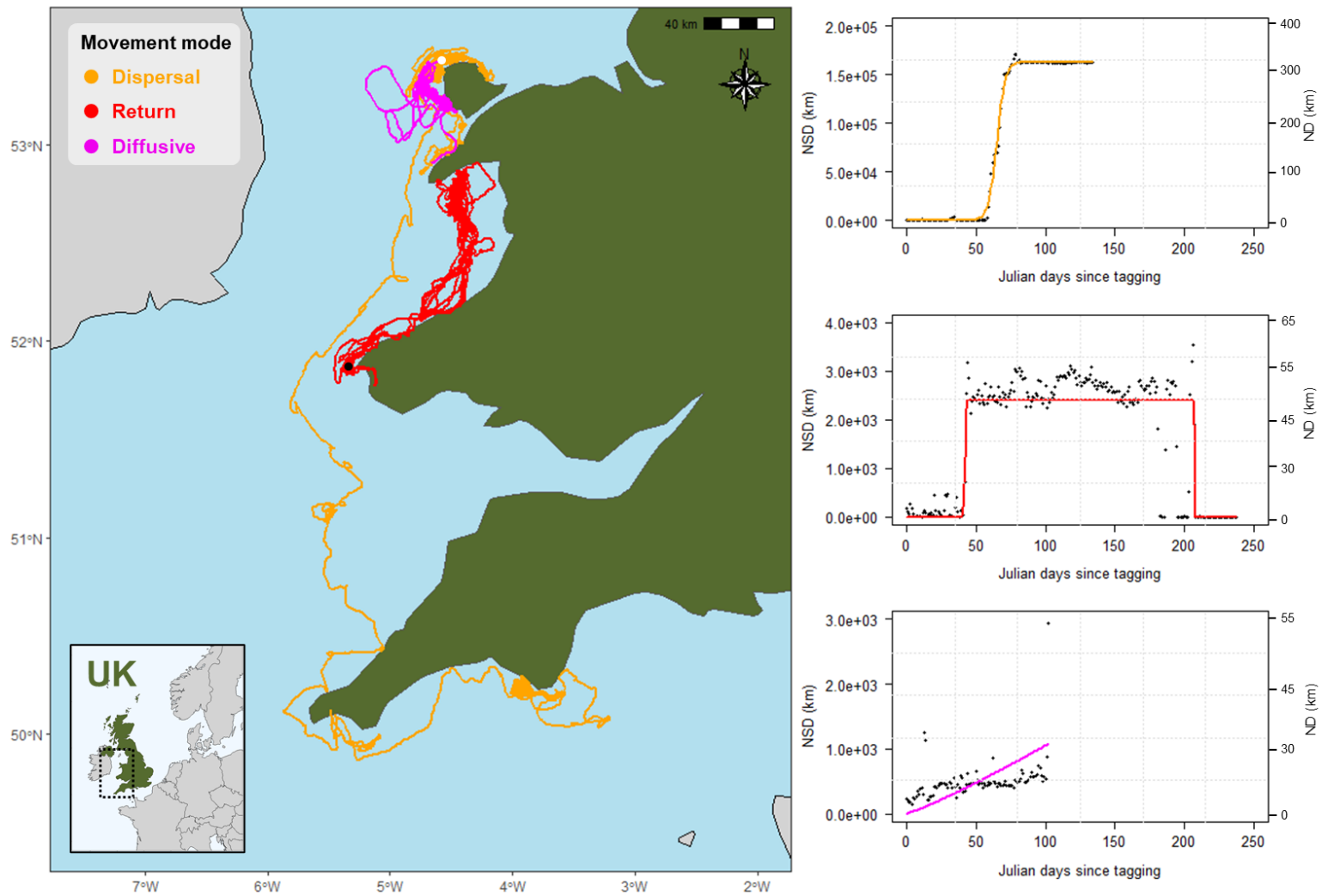


Fig. 3.4. Example individual pup trajectories (left) and typical NSD patterns (right). White dot = the Skerries tagging site; Black dot = Ramsey Island tagging site. See Appendix S3.3 and S3.4 for trajectories and NSD patterns respectively for all 12 individuals. Scale for net-displacement (ND) also shown.

Table 3.4. The scale of displacement at 3 months old for each individual grey seal pup.

Individual	Sex	Site	Movement mode	Displacement distance at 90 days (km)	Movement scale	Recording duration (days)
hg27-01-09	M	SK	Mixed-return	0.2	small	175
hg27-04-09	M	SK	Dispersal	219.1	large	212
hg27-07-09	F	SK	Return	51.5	intermediate	237
hg29-11-10	M	SK	Mixed-return	0	small	336
hg29-13-10	F	SK	Diffusive	30.5	small	103
hg29-15-10	F	R	Mixed-return	63.8	intermediate	262
hg29-16-10	F	SK	Dispersal	385.6	large	135
hg29-18-10	M	R	Dispersal	94.5	intermediate	98
hg29-19-10	F	SK	Diffusive	28.1	small	176
hg29-21-10	M	R	Dispersal	105.9	intermediate	157
hg29-22-10	F	R	Mixed-return	117.6	intermediate	223
hg29-25-10	F	SK	Mixed-return	215.6	large	252

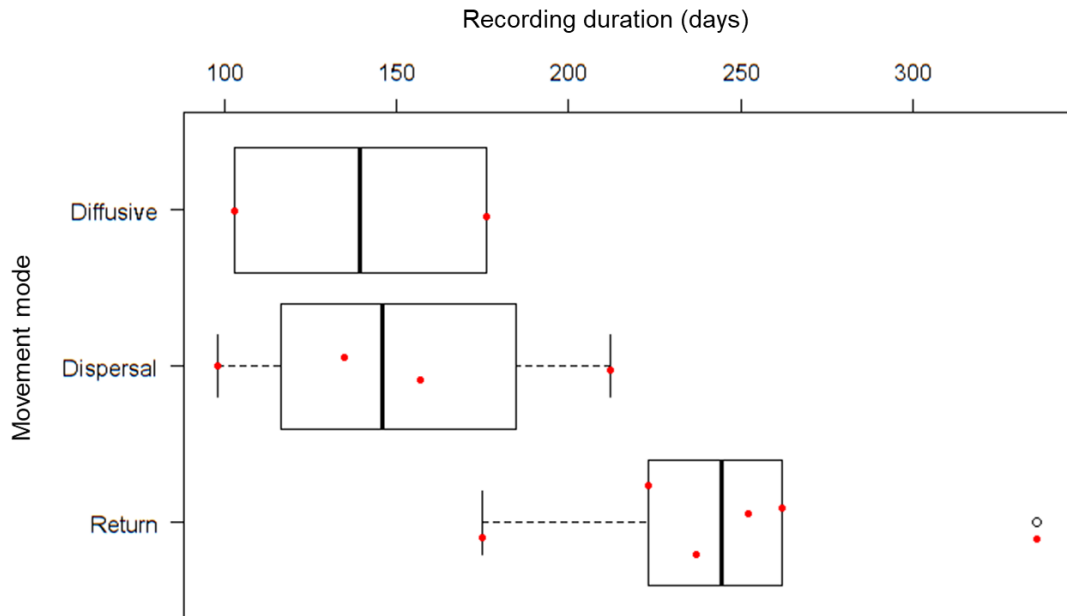


Fig. 3.5. The distribution of recording durations in days for movement mode classifications.

3.4.3 Displacement estimates from GPS- versus ringing-models

The predictions derived from models fit to the population-level data (“ringing models”) and the individual-level data (“GPS models”) returned broadly consistent predictions for the average displacement of seals over time (Fig. 3.6); assessed qualitatively, the functional forms of displacement fitted by both model types were markedly similar (Fig. 3.6–3.7), with early displacement predictions (≤ 70 days since birth) from all 12 GPS models falling within the 95 % confidence envelope derived from the ringing models (aside from a ca. 10 day period for 1 individual; Fig. 3.6). Fig 3.6–3.7 show that the 95% CIs of the population-level models derived from the ringing records (Chapter 2) capture most of the observed data points and model trajectories from the GPS data analysed here, except for those that dispersed particularly far in a short space of time. The GPS models predicted that, prior to 22 days old, pups would not move far from their place of birth; the earliest prediction for a pup to have displaced > 1 km was by 16 days old in the ringing models, and 17 days old in the GPS models (Appendix S3.5). Between 70–130 days since birth there was some divergence in predictions of small (< 50 km) displacement distances but broad agreement for medium ($> 50 \leq 150$ km) and large scale (> 150 km) displacements: The ringing model envelope indicated that animals had moved

away to between approximately 60–220 km from home whilst the GPS models predicted that most (10 out of 12) individuals had moved away, but to a wider range of displacement distances (between ca. 25–405 km), and 2 individuals were still yet to disperse. After 130 days since birth, predictions from both groups of models overlapped (but with a wider range of long distance dispersal for the ringing data), with only one individual prediction from the GPS models moving briefly beyond the upper 95 % CI limit of the ringing model confidence envelope (Fig. 3.6–3.7).

Boxplot comparisons indicated broad agreement in estimated displacement statistics between model types (Fig. 3.8–3.9; Appendix S3.5–3.6). For estimates of displacement distance, boxplots showed substantial overlap in all metrics except for distance at 90 days since birth (although whiskers overlapped) (Fig. 3.8). Displacement distance predictions from the ringing models were consistently higher and tended to have a longer-tailed distribution than those from GPS models (Fig. 3.8) but there was substantial overlap between predictions of the timing of displacement. The predictions from GPS models suggested longer time taken to reach > 1 km, with a longer-tailed distribution than the ringing models (Fig. 3.9), although predictions from the ringing models were well within the ranges predicted by the GPS models for all metrics estimated. There was also agreement between model types in the distributions of GOF values (i.e. CC scores), the rate of displacement during transience, and the scale parameter (Appendix S3.5–3.6).

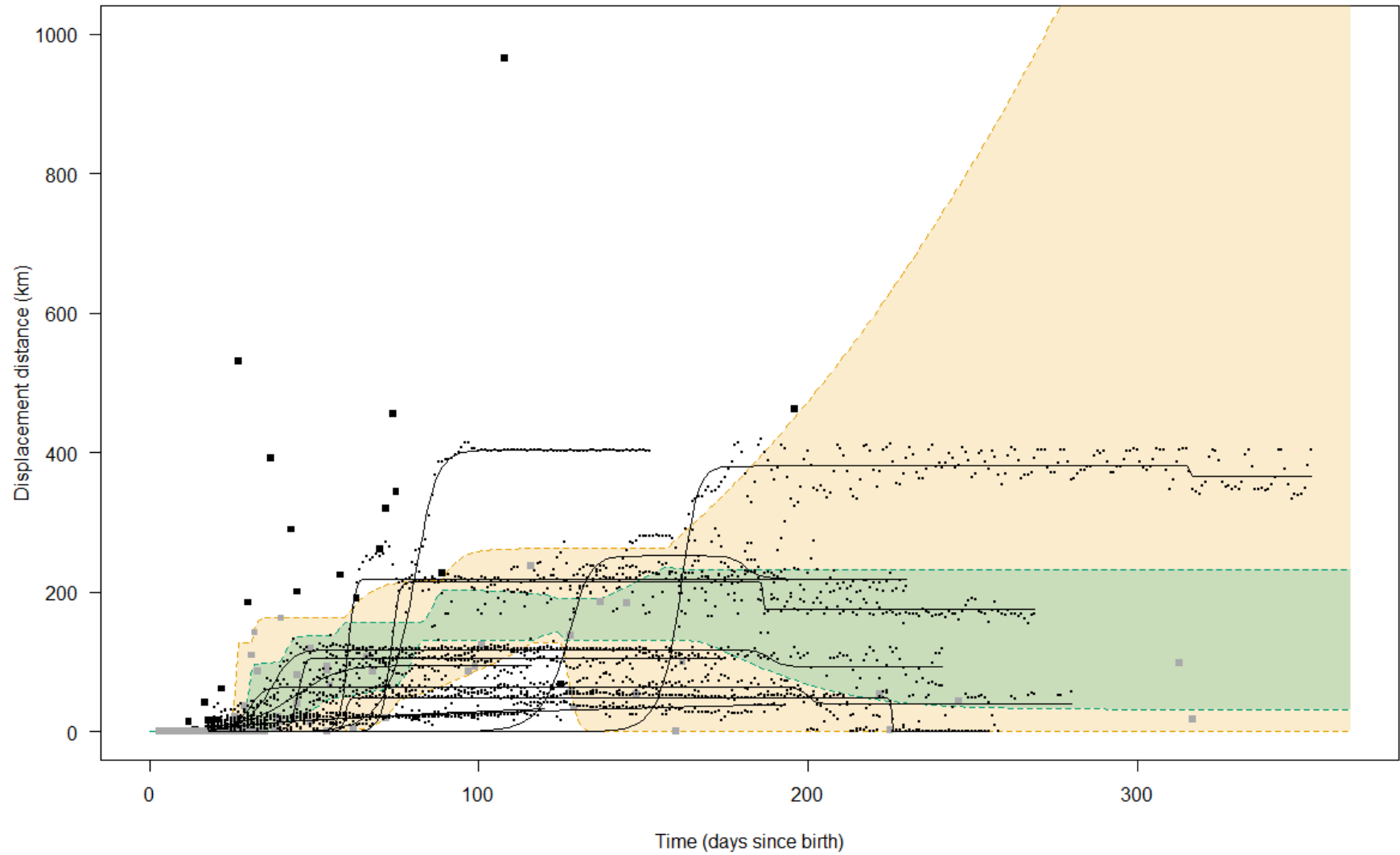


Fig. 3.6. Individual-level “GPS” models (black lines with small dots) overlaid with ringing record data from Chapter 2 (black and grey squares). The orange shaded region represents the 95 % CI of the population-level model predictions that were derived from the ringing records in Chapter 2 and the green shaded region shows the interquartile range of this. The ringing records that fell outside 95% CIs are shown as black squares and the ringing records that fell within are shown as grey squares. Also see Fig. 3.7.

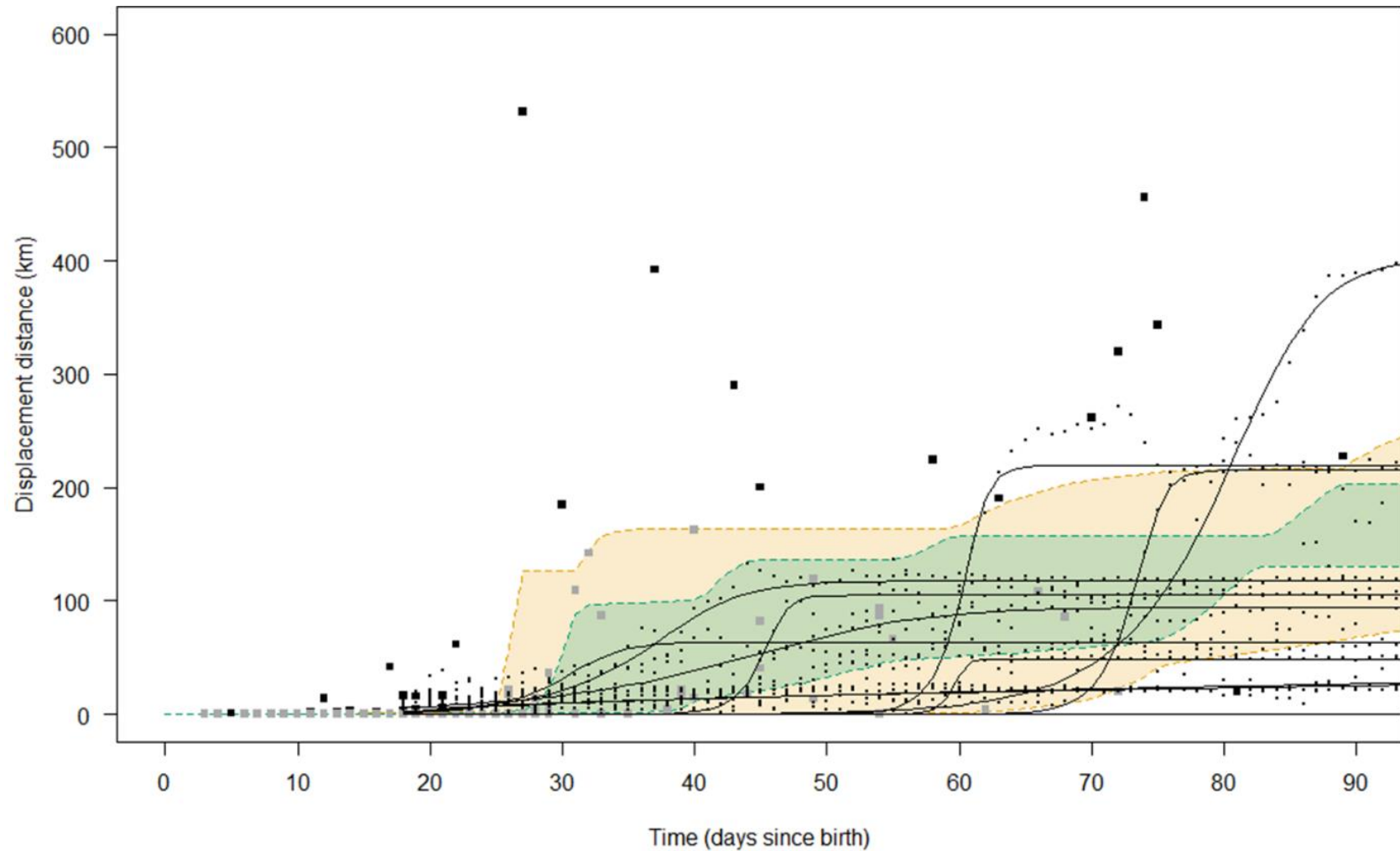


Fig. 3.7. Individual-level “GPS” models (black lines with small dots) overlaid with ringing record data from Chapter 2 (black and grey squares) for the first 90 days of displacement of grey seal pups after birth. The orange shaded region represents the 95 % CI of the population-level model predictions that were derived from the ringing records in Chapter 2 and the green shaded region shows the interquartile range of this. The ringing records that fell outside 95% CIs are shown as black squares and the ringing records that fell within are shown as grey squares. See Fig. 3.6 for full temporal range.

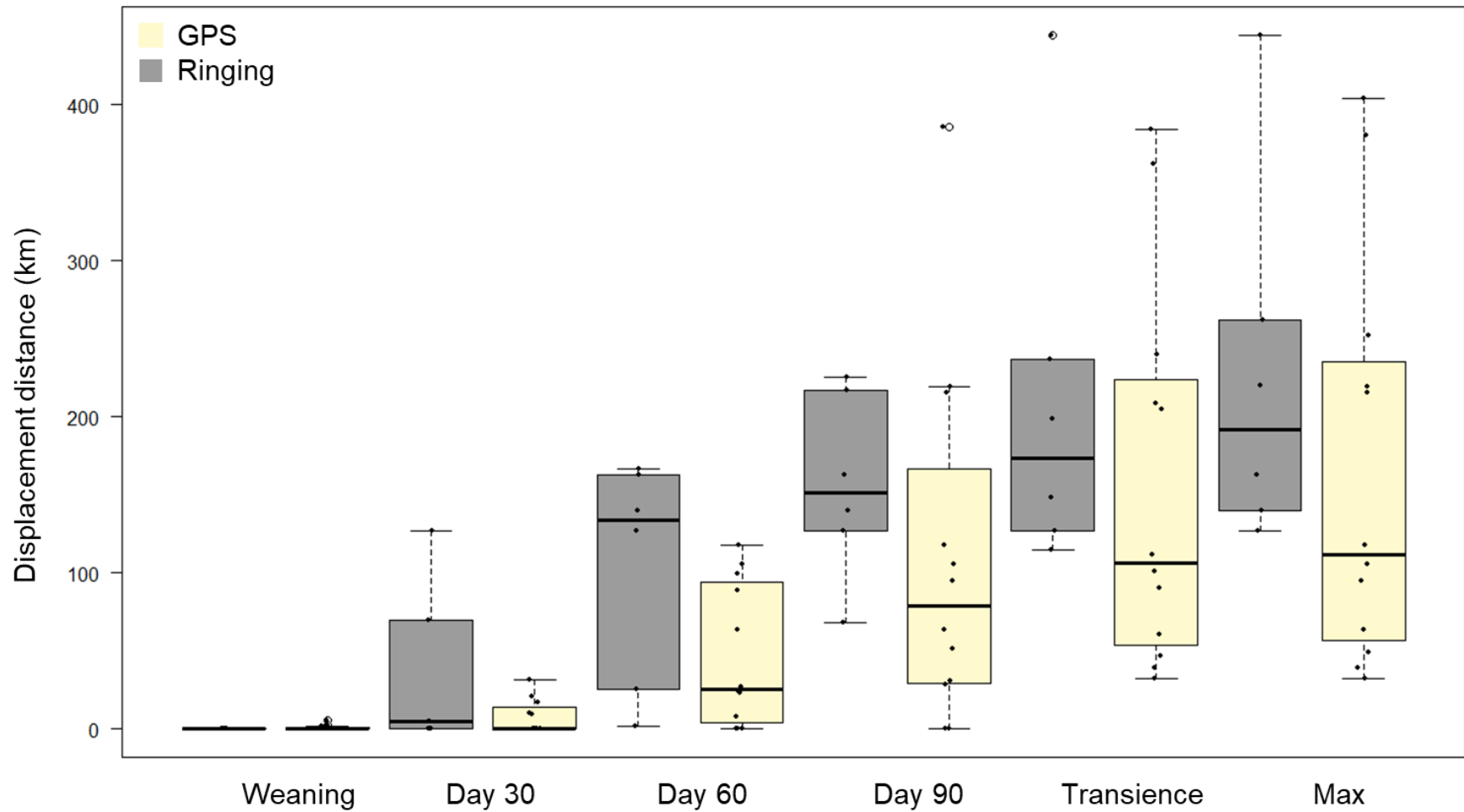


Fig. 3.8. The predicted displacement distances from models fitted to two data types (GPS data here; ringing data from Chapter 2) for different time periods since birth (from weaning to day 90), transience movements, and max displacement. Black dots show (jittered) data points. Comparisons of displacement distance at weaning was made for 18 days since birth (Noren et al., 2008).

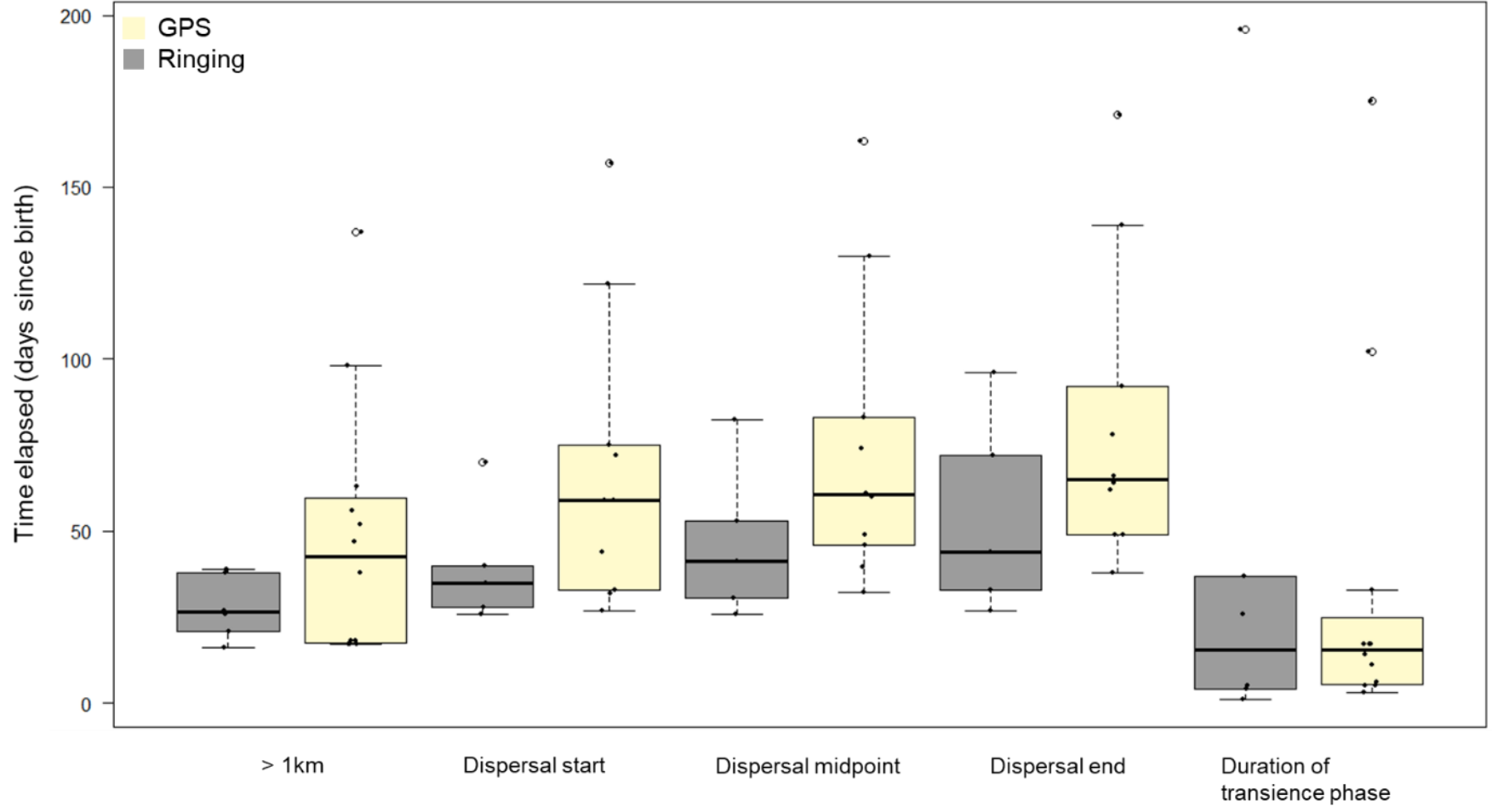


Fig. 3.9. The predicted time elapsed when key movement events were predicted to occur from the models fitted to two data types (GPS data here; ringing data from Chapter 2), and the duration of the transience and recording duration in days. Black dots show (jittered) data points.

3.4.4 Sample size analysis

32 (17.2 %) of the empirical displacement distances from the ringing data fell outside of the ringing model 95 % confidence envelope (Fig. 3.6) with 29 of these occurring within the first 90 days (Fig. 3.7). Of these 32 data points, 30 had reached a greater displacement distance than the empirical GPS data within the same timescale.

The bootstrapped power analyses showed a clear divide between how well summary statistics of displacement distances could be estimated with increasing sample size. Specifically, the mean of μ and p_{25} were well estimated (the mean stabilised to within ± 5 %) at low sample sizes ($n = 5$ and 14 , respectively; Fig. 3.10; Table 3.5). The mean of p_{75} , p_{95} , and max required a sample size an order of magnitude larger for reliable estimates ($n = 127$, 149 , and 170 , respectively; Fig. 3.10; Table 3.5). Obtaining reliable estimates (i.e. 95 % CIs stabilising to within ± 10 %) required greater sample sizes for μ , p_{75} , and p_{95} , (range: 164–184) except for p_{95} for which the required sample size did not change ($n = 14$; Fig. 3.10; Table 3.5). The 95 % CIs for bootstrapped estimates of the maximum displacement distance did not stabilise to within 10 % even with a maximum sample size of $n = 184$ (Fig. 3.10; Table 3.5).

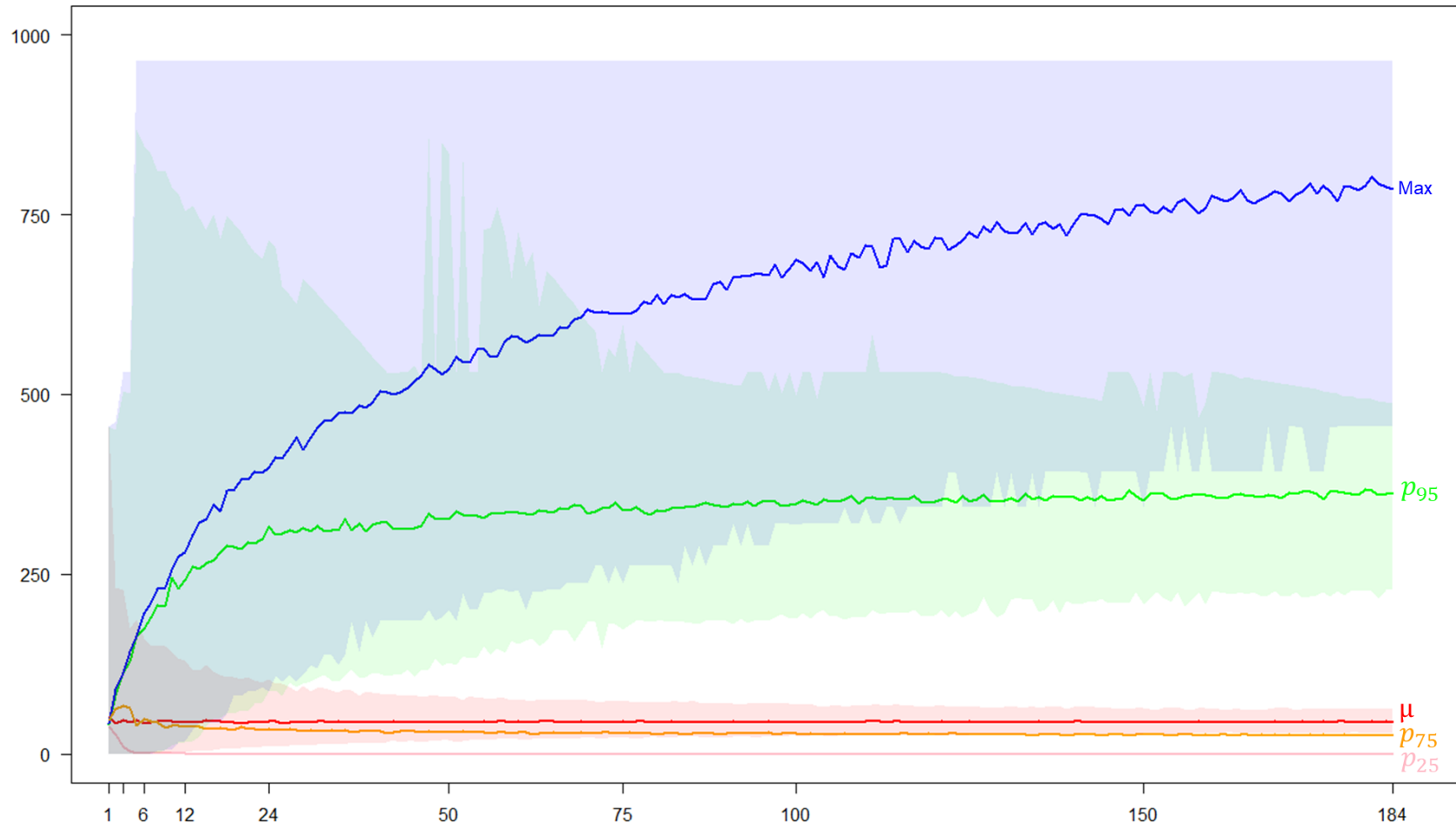


Fig. 3.10. Bootstrapped estimates of displacement distance summary statistics for varying sample sizes. For every sample size between 1–184, I subsampled that given number of displacement distances (1000 times with replacement) from the original $n = 184$ displacement distances in the ringing records (Chapter 2). With these I calculated for each summary statistic (Max, μ , p_{95} , p_{75} , p_{25}) the mean \pm 95 % CIs. The point at which the line stabilises for each metric indicates that no additional samples are needed to estimate that summary statistic of displacement distance. Lines tend to stabilise at relatively low sample sizes for all displacement metrics except the maximum displacement distance. Confidence intervals around the mean estimate of each metric become closer with increasing sample size.

Table 3.5. Results from bootstrapping analysis; sample sizes required to estimate varying summary statistics of displacement distance, and associated error (see Fig. 3.10).

Estimated summary statistic	Mean estimate at $n = 184$ (95 % CIs; km)	95 % CI range at $n = 184$ (km)	Sample size when mean estimate stabilises to within $\pm 5\%$	95 % CI range at stabilised mean (km)	Sample size when CI range stabilises at $\pm 10\%$
Max	786.3 (455.8–964.3)	508.5	149	572.2	-
μ	44.0 (29.1–60.9)	31.8	5	192.9	164
p_{95}	364.2 (227.6–487.9)	260.3	127	322.0	174
p_{75}	25.6 (11.5–56.2)	44.7	170	48.7	184
p_{25}	0 (0–0)	0	14	0	14

3.5 Discussion

My results highlight that whilst individual variation in grey seal pup movements is typically high in their first year, key differences between individuals can be well described by a set of fundamental movements modes (Morelle et al., 2017), providing timescales are taken into consideration. The predictions of displacement over time using a small sample size of GPS data were generally consistent with matching models fit to coarse, population-level ringing data (Chapter 2), providing validation that this analytical method is well suited for making predictions of displacement over time with both data types. Robust estimates of the mean displacement distance were obtainable with a sample as small as 5 individuals, however estimating the longer-tail of displacement required sample sizes two orders of magnitude larger. A recording duration of 200 days was required to reliably interpret the movement mode exhibited by individuals.

3.5.1 Quantifying patterns of displacement

Seals generally stayed close to the coastline (within 30 km) as they travelled away from their natal site, in line with behaviour seen by weaned individuals from other areas, such as those dispersing from Helgoland which stayed within a mean distance of 31.4 ± 10.9 km to shore ($n = 12$; Peschko et al., 2020). The differences in movement modes were characterised by three functional forms of displacement: dispersal, return, and diffusive. These findings concur with trends observed in grey seal pup natal dispersal from other breeding areas in the North East Atlantic, such as individuals born on the eastern coast of the UK which emigrate to the Wadden Sea and remain there (Brasseur et al., 2015; Carter et al., 2017), and those born in Helgoland which disperse to Britain, Denmark, and the Netherlands (Peschko et al., 2020). Baylis et al., (2019) documented two movement modes (dispersal and sedentary) for weaned grey seal pups from Iceland, however their sample of only $n = 5$ individuals may have led to the detection of only two movement modes. 2 pups (17%) here moved in a diffusive manner with trajectories consisting of meandering movements and a slow rate of increase in displacement distance

over time. Such movements are indicative of exploratory behaviour (Carter et al., 2017) which may provide an opportunity for individuals to learn how to navigate effectively (Breed et al., 2011), as seen in other juvenile marine megafauna; e.g. northern gannets (Votier et al., 2017). This is consistent with the observation that grey seal pups develop and refine their diving and foraging behaviour during their early life (Carter et al., 2017; 2019).

In their first few months of life (i.e. first 90 days) pups exhibited a range of movement scales. As with variation in movement modes, differences in movement scale may promote the reduction of foraging competition between conspecifics (Carter et al., 2017) as it enables individuals to distance themselves spatially from one another (de Grissac et al., 2016). Mechanisms such as targeting different substrate types have been suggested as potential drivers to reduce competition between grey seal pups (Carter, 2018). As for reducing competition between adult conspecifics, there is evidence to suggest that slightly older individuals (around 5 months old) are displaced from foraging grounds by adults (Breed et al., 2013). For pups however, resource competition with adults is expected to be relatively low. This is because dietary studies have shown that pups preferentially target lower trophic level species than adults (Carter, 2018). Movement away from the natal colony may also be linked to non-resource related aggressive interactions with adults, as grey seal bulls are well known to cannibalise pups (van Neer et al., 2019).

When individuals dispersed, they did so only for short durations and increased their displacement distance rapidly over time, using this movement to transit between their start point and a novel settlement location. Such direct travel to new locations could suggest that seals possess a degree of innate navigation (Åkesson & Weimerskirch, 2005; de Grissac et al., 2016); whilst further research is needed to fully evaluate this, strong navigational capabilities are well-recognised in adult grey seals (McClintock et al., 2012) and Carter et al., (2019) provided evidence that grey seal pups rapidly acquire adult-like behaviour. Once at the settlement location, the movements that seals undertook – repeated trips to and from land (Appendix S3.4) – resembles central place foraging behaviour typical of adults (McConnell et al., 1999). Presumably pups had dispersed to a suitable foraging ground (Carter et al.,

2016) and were returning to land in order to rest between foraging trips (McConnell et al., 1999).

Understanding the scales and movement modes of displacement of individuals is key for predicting the space-use of animals, including their potential overlap with TSEs. The results here reveal that a large proportion of animals undertake dispersal-like movement modes in their first few months, and that many return later, with clear implications with respect to the number of times that animals may encounter TSTs offshore. Moreover, the fact that animals appear to undertake central-place foraging like behaviour at settlement suggests that TSEs at these sites may be encountered often (Thompson, 2012).

3.5.2 Recording duration

Quantifying the movement modes of individuals is a key first step in understanding what proportion of individuals in a population behave in a certain way (Bastille-Rousseau et al., 2015), and clearly key to this is obtaining data for a long enough duration (Turchin, 1998). My results reinforce this, highlighting that (at least) the first 90 days represents a period of substantial variability in grey seal pup dispersal movements and is thus a critical period to study in order improve our understanding of the timings and movements of important biologically- and ecologically-relevant events for grey seal pups, such as the post-weaning fast, onset of dispersal, and transience behaviour amongst others. Other recent research supports this, with Carter et al., (2017) revealing that ontogeny of diving development continues to occur up to (and indeed beyond) this timeframe. This time period has also been shown to be key for other fledgling marine megafauna, with de Grissac et al., (2016) demonstrating that fundamental differences in movement modes can be observed within the first 3 months of life for juvenile petrels and albatross.

My results also demonstrate that recording duration needs to be sufficiently long to reliably quantify grey seal pup dispersal; specifically that the classification of movement mode reached may be susceptible to the duration over which an animal is recorded. The majority of individuals (10/12; 83 %) were observed to have initiated a dispersal by an average of 68 ± 42 days

since birth and reached their settlement location by around 80.8 ± 42.6 (range: 38–171) days. This would suggest a conservative limit of 175 days' recording duration is required to observe a dispersal event. Moreover, all individuals tracked for more than 175 days eventually returned to their natal site. This raises the critical question that if recording durations were at least this long for all individuals, would others have also been observed to return? Breeding site fidelity in adult grey seals is known to be high (Pomeroy et al., 1994; Twiss et al., 1994; Langley et al., 2020). Comparatively, the degree of philopatry that grey seal pups exhibit to their natal sites is inconsistent (Pomeroy et al., 2000); Allen et al., (1995) examined the genetic variability of grey seal colonies in Scotland and determined that philopatry to natal sites was likely to be common, however records have also shown that pups move permanently to sites up to 250 km away from the areas where they are born (Harwood, Anderson, & Curry, 1976). It is apparent from my results that grey seal pups dispersing from sites in Wales can and do return to their natal sites, but that detecting this is only possible with recording durations exceeding 175 days.

Crucially, the onset of each movement phase may occur at different times for different individuals, and for some individuals these phases may take a long time to occur. Taken together, my results indicate that grey seal pups typically spend the first ~ 30–70 days (from birth) within relatively close proximity (~ 50 km) to their natal site, undertaking exploratory behaviour (Carter et al., 2017). Following this, pups appear to undertake dispersal and settle at new locations for ~ 135 days after which many return to natal sites from 175 days since birth. In accordance with this, and in order to provide a degree of conservatism, I suggest that a minimum recording duration of 200 days is required to confidently determine movement modes and quantify displacement over time in dispersing grey seal pups. This output is crucial for researchers planning to study the displacement of grey seal pups over time and predict the spatial overlap of pups with anthropogenic impacts, such as TSTs (Copping et al., 2020). Indeed, without recording movements for a long enough duration, researchers may fail to acknowledge that there could be multiple periods in a grey seal pups' early life where they are at risk from interaction with TSTs; both on the outward and return leg of their dispersal. Unfortunately, typical tracking

devices deployed on grey seal pups far underachieve this, with fewer than 30 % of devices functioning successfully for this duration (Carter et al., 2017).

3.5.3 Comparing high-resolution data to low-resolution data

My comparison of displacement models fit to ringing records with those fit to GPS data highlights that overall there were a number of relatively extreme dispersers in the former than in the latter. This is expected, given the potential for increased variability with increasing sample size (Sequeira et al., 2019); specifically the increased probability of observing long-distance dispersal (Byrne et al., 2014). However, beyond 90 days, despite the small sample size, the displacement distance reached by some of the GPS-tracked individuals exceeded that of the predictions derived from the ringing models. This is because the latter are averaged across many more animals of which many are resighted at relatively short distances. In other words, the ringing model predictions are constrained by the large number of individuals that do not appear to move much (the real trajectories are of course not known). Conversely, as a proportion of the total number of individuals tracked, the GPS data contained a higher number of relatively long-distance dispersers. Hence, models fitted to larger sample sizes may converge on more conservative estimates of population-level displacement.

This result has clear implications for the management of grey seal pups and determining their risk of interaction with TSTs. For example, basing your predictions on a small number of extreme individuals may lead to adopting mitigation measures that are surplus to requirement, or that cannot be sufficiently resourced (Copping et al., 2020b). In contrast, it is also important to know if your predictions are conservative because it must also be a priority to protect any extreme individuals which disperse particularly far. Such individuals have high conservation value (Bartoń et al., 2019; Cozzi et al., 2020) as they likely represent the fittest individuals in the population and may be essential to maintaining genetic diversity or fuelling the recovery of dwindling populations through emigration (e.g. Brasseur et al., 2015).

Averaged over all individuals my results indicated that both sets of models return broadly similar estimates of displacement. Specifically, both sets of models shared consistent forms of displacement over time and remained appropriately conservative in their predictions of displacement for an average individual. Moreover, predictions from both sets of models predicted similar timings of displacement, transience rates and transience durations. This provides confidence that average predictions of displacement over time can be obtained from implementing the NSD modelling approach on both a large sample size of coarse data, as well as a smaller sample size of high-resolution tracking data, with important implications for designing tracking studies for grey seals (Sequeira et al., 2019).

This information is extremely useful for researchers intending to study the distribution grey seal pups, such as their overlap with TST sites, as it suggests that this modelling approach can be applied to both coarse data with high sample sizes and high-resolution data with low sample sizes in order to both to reliably predict displacement over time. This is something that has been successfully achieved for songbirds by combining geolocator tracking data with ringing archives (Heim et al., 2020). Importantly, when grey seals are tagged with tracking devices, they are almost always also marked using ID tags on their hind flippers (Carter, 2018; *pers. obs.*). These ID tags can provide resighting data for many years (Jeffries, Brown, & Harvey, 1993), even after tracking devices have fallen off (Sayer et al., 2019). Moreover, seals are often caught in large numbers (Mikkelsen et al., 2019) and while all can be marked with an ID tag, only a subset can be tagged with a tracking device. Flipper tags are also far lower cost and typically less invasive for the animal (van Neer et al., 2020; but see Saraux et al., 2011). The fact that this modelling approach could be applied to such data opens doors to a wealth of possibilities for studying grey seal pup displacement over time, including the opportunity to combine data from multiple tag types or indeed other marking efforts (e.g. dye marking; Westcott & Stringell, 2003). This complements recent other methodological developments to quantify the spatial overlap of wildlife with TSTs using tracking data (Isaksson et al., 2021).

3.5.4 Sample size requirements for predicting displacement distance

My sample size analysis revealed that recovering reliable estimates of summary statistics pertaining to the mean and lower bounds of displacement distance requires relatively small sample sizes (5–14 individuals), but that confidently predicting upper limits of displacement distance – maximum displacement distance, upper quartile and 95th percentile – requires data from many more individuals (127–170); plus many more for obtaining reliable estimates of associated error. This reinforces the notion that high sample sizes are needed to obtain a reasonable probability of detecting rare dispersal events (Hays et al., 2003; Byrne et al., 2014); for example, Sequeira et al., (2019) demonstrated that hundreds of tags were required to detect the colonization of a new site by green turtles.

The beauty of the approach presented here is that in future, recommended sample sizes can be reassessed in an adaptive way. Once tracking data are collected for greater numbers of individuals, especially over long timescales, these analyses can be repeated with further refinement, taking tag failure rates and varying timescales into account. Indeed, recording individuals for longer durations may well result in an even longer-tailed distribution of displacement distances (Appendix S3.8), requiring even greater sample sizes to fully understand variation over increasing timescales (Sequeira et al., 2019; Shimada et al., 2020). For now, the evidence points to the fact that more and longer data are required. This is in line with current recommendations for tagging marine megafauna (Sequeira et al., 2019; Shimada et al., 2020), and well within recommendations for terrestrial studies (Hebblewhite & Haydon, 2010).

The fact that estimating different summary statistics requires different sample sizes has important implications for practitioners making decisions regarding the conservation management of a population, in so far as selecting the appropriate metric of interest to base their assessments on, as well as for researchers wishing to collect more data using tracking devices to determine whether their sample size will be large enough to address their research question (Sequeira et al., 2019; Williams et al., 2020; Shimada et al., 2020).

Fortunately, progressively miniaturised tagging technologies are enabling researchers to tag ever increasing numbers of individuals (Williams et al., 2020) and the sample sizes suggested here are well within typical recommendations for telemetry studies on marine megafauna (Sequeira et al., 2019; Shimada et al., 2020). For grey seals specifically, numerous large historical records also exist which can supplement small sample sizes; for example, in addition to the ringing records studied in Chapter 2, a dedicated mark recapture programme was performed by Hall et al., (2001) to estimate postweaning survival of pups using 'hat tags' and mobile phone technology.

3.5.5 Conclusions

In conclusion, obtaining a better understanding of the movement patterns of grey seal pups is crucial for their conservation management both at the individual- and population-level, particularly in light of the growing number of potential anthropogenic impacts that might threaten young individuals, such as TST developments (Copping & Hemery, 2020). My findings demonstrate that variation in the dispersal movements of grey seal pups in their early life can be well explained by a set of fundamental movement modes, providing timescales are considered, and that the patterns of displacement over time can be consistently predicted using the NSD modelling approach using both large sample sizes of coarse data, and small sample sizes of high-resolution data. This provides new opportunities for researchers to investigate the distribution of grey seal pups over time and thus the spatial overlap of animals with TST devices. I also determine the sample size requirements for making predictions of key displacement statistics, and recommend a minimum tag recording duration of 200 days to reliably investigate grey seal movements during dispersal. These findings will support researchers to design experimental studies that appropriately quantify variation, and thus provide more robust predictions for legislators and the TST industry to support consenting processes. Finally, this work provides a baseline from which to conduct further hypothesis based research.

Chapter 4

Moving in a moving medium: Tidal drivers of harbour seal *Phoca vitulina* fine-scale movement and behaviour

“...all the animals belonging in the region of these currents are drawn in and fill it, often in such great quantities that one is tempted to believe it is not merely the mechanical influence of the narrow stream which has brought about such an accumulation...”
(Greeff, 1868)



Bobbing on the tide: A grey seal bull pauses to satisfy his curiosity with a stare, before disappearing into the tidal race at Ramsey Sound
(Photograph by William P. Kay).

4.1 Abstract

Quantifying the environmental drivers of variation in the movement and behaviour of wild animals is essential for informing their management. For marine megafauna, an understanding of how they use tidal currents is limited, yet this information is crucial for determining the potential impact of new anthropogenic threats associated with these hydrodynamic features, such as tidal stream turbines (TSTs). Here, I use a hidden Markov modelling framework to analyse the movement and behavioural responses of harbour seals (*Phoca vitulina*) to tidal currents using high-frequency GPS and dive data collected on 24 individuals from three sites in a tidal stream environment (TSE) in the North Sea. Results showed that rather than modulate their movements within behavioural states, seals instead switched behavioural strategies altogether in response to current conditions and the occurrence of tail-currents was key in modulating this. While behavioural state persistence was generally high (~ 80 %), tidal-currents increased the probability for seals to switch between behavioural states by approximately 30 %. Seals preferentially foraged in tail- as opposed to head-current conditions. No clear differences arose between sites and sexes, though juvenile responses were more acute than for adults, suggesting the former are more susceptible to currents, likely owing to their reduced movement capacity. The HMM framework indicated that 3 sets of discrete-valued random-effects (“behavioural contexts”) were required to account for individual-variation, or for variability driven by missing covariates. In the context of related research, my results suggest that depth-usage and diet are key factors that need to be further investigated to fully elucidate the use of tidal currents by harbour seals. The findings here have clear implications for the TST industry as they suggest that seals in these areas target tail-currents for foraging, putting them at risk from collision with operational devices.

4.2 Introduction

A growing body of evidence indicates that marine megafauna use tidal stream environments (TSEs) for important behaviours, including foraging and travelling (Benjamins et al., 2015, 2017; Hastie et al., 2016, 2017; Joy et al., 2018; Lieber et al., 2018; Lieber, Langrock, & Nimmo-Smith, 2021; Malinka et al., 2018; Onoufriou et al., 2021; Johnston et al., 2021; Gillespie et al., 2021). However, an understanding of how animals respond to physical features in TSEs (such as tidal currents) at fine spatio-temporal scales is relatively limited and remains a challenge (Hays et al., 2016; Hastie et al., 2019). Tidal stream environments are undergoing substantial change with the introduction of new marine renewable energy installations, especially tidal stream turbines (TSTs) (Copping et al., 2020). TSTs increase the risk of anthropogenic disturbance to marine megafauna (Copping et al., 2016; Joy et al., 2018; Walker, Morris, Stringell, & Taylor, 2019), with impacts that may include avoidance behaviour from key habitats, barrier effects, or direct collisions with devices (Hastie et al., 2017). To better understand the potential risks, an understanding of how animals behave in TSEs, and how they respond to fine-scale changes in tidal conditions, is key (Benjamins et al., 2015; Copping et al., 2016). Indeed, this information is required by TST developers as part of their Environmental Impact Assessments (Fox et al., 2018).

The movement of individuals is influenced by a range of biotic and abiotic external factors, including the evasion of predators (Breed et al., 2017) or anthropogenic threats (Nabe-Nielsen et al., 2018; van Beest et al., 2018), and responses to competitors (Waluda, Collins, Black, Staniland, & Trathan, 2010) or conspecifics (Wilson et al., 2015), however, it is purported that the distribution of resources (i.e. prey) is one of the strongest proximate drivers of movement (Zamon et al., 2001, 2003; Nathan et al., 2008; Stern & Friedlaender, 2017; Forcada, 2018). Optimal foraging theory (OFT) asserts that animals should modify their movement to minimise energetic expenditure whilst maximising energy gain (Pyke, 1984; Ydenberg et al., 1994). In the marine environment, prey are patchily distributed in time and space (Sims et al., 2008), and so too are the energetic costs of moving associated with obtaining them (Wilson, Quintana, & Hobson, 2012). Furthermore, the medium

that marine megafauna move through is itself moving, varying in its speed, direction, and turbulence, thus resulting in a dynamic energy landscape for animals to negotiate (Shepard et al., 2013).

This is particularly the case in TSEs, where flow regimes are heterogeneous and dynamic, changing spatio-temporally through the influence of localised tidal features and bathymetry-induced physical processes (Lieber et al., 2018). The energetic cost of moving against water currents is high, especially at fast velocities, because power costs are cubed as a function of speed (Wilson et al., 2002). However, tidal currents (and other regular hydrodynamic flow regimes) can generate predictable prey hotspots for predators (Lieber, Nimmo-Smith, Waggitt, & Kregting, 2019) and facilitate movements in the direction of tail-currents (Wilson et al., 2001). Hence, whilst the costs of operating in TSEs are high, so too can be the rewards, creating positive selection pressures for animals to adapt – or even specialise – their behaviours to exploit these resources.

An understanding of how marine megafauna behave in TSEs, and how they respond to fine-scale changes in tidal conditions, is essential for informing TST developers of the risks that devices pose (Benjamins et al., 2015; Copping et al., 2016). Greater understanding of, for example, how animals behave in head- or tail-currents, is useful in determining levels of risk (Copping et al., 2016) and can aid the TST industry to develop appropriate mitigation measures (e.g. operational strategies that coincide with -risk periods; Onoufriou et al., 2019; Chapter 2). An interesting study species for this general topic is the harbour seal (*Phoca vitulina*), a common apex marine predator species that inhabits coastal marine environments (Teilmann & Galatius, 2018). Harbour seals are central place foragers that are known to make use of TSEs (Hastie et al., 2016; Hastie et al., 2019). As such, harbour seals can often move in the near-vicinity of, and be capable of coming into direct contact with, local TST devices (Joy et al., 2018; Hastie et al., 2019). Harbour seals are perceived to be at risk of detrimental interaction with TSTs, such as through direct collision with moving parts of devices (Onoufriou et al., 2019).

Previous research on harbour seals has demonstrated that they, like many other marine megafauna, exhibit high between- and within-individual variability in their behaviour (Thompson et al., 1989; Cunningham et al., 2009; Sharples, et al., 2012; Hastie et al., 2016; Brandes et al., 2018; Heithaus et al., 2018; Sparling, Lonergan, & McConnell, 2018), as well as exhibiting differences in behaviour at different sites (Tollit et al., 1998; Wilson et al., 2014) or regions (Sharples et al., 2012); possibly in part due to local variations in environmental conditions, such as hydrodynamic features (Lieber, Nimmo-Smith, Waggitt, & Kregting, 2018). Hence, while there has been a recent increase in the number of publications investigating harbour seal movement and behaviour in TSEs (Hastie et al., 2016; Joy et al., 2018; Hastie et al., 2019; Onoufriou et al., 2021), further research is required both to obtain additional site-specific information and to fully quantify sources of variation, to develop a greater understanding of potential population-level responses (Copping et al., 2016; Copping & Hemery, 2020). Indeed, a common argument voiced by the MRE industry is that they require site-specific information to inform their consenting processes (Copping et al., 2016; ORJIP Ocean Energy, 2016; 2020; Copping & Hemery, 2020).

The Wadden Sea is a large tidal mudflat home to the largest population of harbour seals in Europe (SCOS, 2018). Seals here are frequently observed making use of tidal channels to travel between tidal inlets. The tidal current velocities are moderate to high (max: 1 ms^{-1} ; Luther, 1973; Anthony, 1995) with particularly strong currents in the tidal channels (max: 1.6 ms^{-1} ; Gräwe et al., 2016), and tidal ranges are large (~ 2.5 to 3.5 m; Stanev, Wölff, Burchard, Bolding, & Flöser, 2003). While the tidal current velocities here are typically insufficient for horizontal-axis TSTs, they can be exploited by other tidal stream energy devices, such as tidal kites. Indeed, numerous tidal energy prototypes have already been installed or trialled in the Wadden Sea, such as Torcado's tidal turbine (operational since 2015) and SeaCurrent's tidal kite (tested and operated in 2019) (Ocean Energy Systems, 2020), and there are plans to increase tidal stream energy development in all states surrounding the Wadden Sea coast in the coming years (Magagna & Uihlein, 2015).

Recently Clay et al., (2020) used hidden Markov models (HMMs) to demonstrate that wind speed and relative direction are important predictors of transitions between movement modes in albatrosses, providing evidence towards the general expectation that animals moving in highly dynamic mediums should flexibly adjust their movements to variable conditions in order to minimise movement costs. In this study, I applied this approach to harbour seal movements in TSEs in the Wadden Sea by combining high-resolution biologging data with modelled tidal data using a mixed, generalised HMM framework. This framework enabled me to quantify both within- and between-individual variation, as well as account for the effects of intrinsic (sex, age) and extrinsic (site) factors. I expected seals to respond dynamically to tidal currents (likely driven by predictable changes in prey distribution; Uda & Ishino, 1958; Riley, 1976; Wolanski & Hamner, 1988; Zamon, 2001, 2003; Genin, 2004). For example, the availability and predictability of prey should increase under head-currents, because increased water flow brings greater numbers of prey to the predator per unit of time (Zamon, 2001, 2003; Schwemmer et al., 2009; Williamson et al., 2019). Thus, I had three specific aims, which sought to quantify the effect of tidal currents on:

1. The probability of being in a given behavioural state (i.e. **stationary state probabilities; H_1**). Stationary state probabilities (SSPs) represent the probability of an animal being in a given state (at any time), under fixed covariate conditions (Leos-Barajas, Photopoulou, et al., 2017; Clay et al., 2020). Harbour seals have been observed to remain in narrow channels under high flow rates (Hastie et al., 2016), and swim both against (Joy et al., 2018) and with (Hastie et al., 2019) prevailing currents. Specific tactics in response to currents can serve to maximise foraging efficiency and minimise energy expenditure in accordance with an optimal foraging strategy (Krebs, 1978). Assuming seals followed an optimal foraging strategy, I would expect their behavioural states to match favourable tidal currents. Because the average current velocity of the study location examined here was similar to that seen during low current conditions in Joy et al., (2018), I hypothesized that seals would behave in the same manner. Specifically, Joy et al., (2018) observed

that seals swam into head-currents while foraging and utilised tail-currents for travelling. Thus I expected seals to forage in head-current conditions and travel using tail-currents, the latter in line with seals exploiting tail-currents to reduce their energy expenditure whilst travelling. As for resting states, I expected these to occur under slack conditions to prevent unwanted drift whilst seals were less active.

2. State-switching behaviour (i.e. **transition probabilities; H₂**). In line with the hypotheses derived for 1., I expected transitions to travelling states to be associated with tail-currents, transitions to foraging states to be associated with head-currents, and transitions to resting states to be associated with slack water. Moreover, I expected state-switching behaviour (i.e. the variability of switching to and from different states) to increase as the relative magnitude of head- or tail-currents increased, and conversely for behavioural state persistence to emerge under relatively slack conditions.
3. The movement characteristics within behavioural states (i.e. **state-dependent parameter distributions; H₃**). If seals utilised tidal currents as hypothesised in 1. and 2., I would expect them to adjust their movements (i.e. step lengths and turn angles) within behavioural states to accommodate these responses. Thus, I expected step lengths and directional persistence to increase under both head- and tail-currents (in the former so as to maintain their position against an oncoming flow; in the latter to maximise their distance travelled over time), and to be relatively unaffected in resting states (as seals should anyway utilise slack water periods for resting).

4.3 Methods

All data processing and analyses were performed in R version 3.6.3 (R Core Team, 2018).

4.3.1 Telemetry data

Dead-reckoning data loggers (DRs) were deployed on 30 harbour seals (6 females (4 pregnant), 24 males) at three haul-out sites in the German Bight (Helgoland (HE): 54.18°N, 7.86°E; Lorenzensplate (LP): 54.43°N, 8.60°E; and Rømø, Denmark (DK): 55.14°N, 8.44°E) between 2004–2006 as part of the MINOSplus project (Kellermann, Eskildsen, & Frank, 2006). The DRs (Driesen+Kern GmbH, Bad Bramstedt, Germany, 0.14 kg, 9 x 6.5 x 2.8 cm) recorded data at a 5 second sampling interval on multiple channels including dive depth, body posture and orientation, heading, temperature, and light, and stored these data on a 32 Mb flash drive at 16 bit resolution (Liebsch, 2006). ARGOS-linked satellite transmitters (SPOT3, Wildlife Computers, Washington, USA, 0.045 kg, 4.8 x 4.2 x 1.4 cm) were deployed in tandem to obtain location estimates, which were later used to correct for drift in the dead-reckoned trajectories (see Liebsch, 2006 and Wilson et al., 2007). The devices were secured within a custom-design flotation package made from epoxy glosscoat resin (Vosschemie, Uetersen, Germany) and hollow glass microspheres (Omega-Spheres ® Osthoff Omega Group, Norderstedt, Germany) mixed in a 70:30 ratio (Liebsch, 2006). This flotation package, hereon “tag”, was inserted into a neoprene sleeve which was glued using Devcon epoxy (Danvers, Massachusetts, USA) to the animal’s back (Liebsch, 2006). The tag was held in the sleeve by a nylon wire which would burn at a pre-determined time, acting as a mechanism to release the tag which would then float to the surface and wash up on shore; tags were recovered by beach-goers or by locating them using the ARGOS positions (Liebsch, 2006).

Seals were caught using seine nets deployed from boats, and restrained on land in hoop nets (Sharples et al., 2012). Prior to tagging, the tag attachment site was cleaned using seawater and acetone, before being dried with towels.

All capture, handling, and tagging procedures were performed under permit number V312-72241.121-19 (70-6/07) obtained from the Ministry of Energy, Agriculture, the Environment, Nature and Digitalization, Schleswig-Holstein, Germany.

4.3.2 Tidal data

I obtained tidal data for the German Bight from the Federal Maritime and Hydrographic Agency of Germany (Bundesamt für Seeschifffahrt und Hydrographie; BSH). These data were sourced from the BSH Operational Model v3, with a spatial resolution of 1 nautical mile and temporal resolution of 15 minutes. I utilised three dynamic tidal covariates from these data: sea surface elevation (SSE), zonal velocity (u), and meridional velocity (v). I extracted the values for each covariate, for each corresponding spatio-temporal coordinate in the seal trajectories, using the “*ncvar_get*” function in the R package “*ncdf4*”. I used the “*uv2ds*” function in the “*rWind*” package to convert the u and v to absolute tidal direction (d) and speed (s), and combined these to generate a tidal velocity vector (V_t). I determined the tidal state (a factorial covariate indicating the state of the tide experienced by each seal at each position) by calculating the difference in SSE for each location along a trip. Specifically, if the SSE at time t_n was greater than at t_{n+1} , then the tidal state was ebbing (“*ebb*”); if the opposite were true, the tide was flooding (“*flood*”). If there was no difference in SSE between t_n and t_{n+1} then the tide was “*slack*”. Using the absolute tidal velocity, I created a factorial covariate for tidal strength where velocity values $\leq 33^{\text{rd}}$ percentile were classed “*Low*”, values $\geq 66^{\text{th}}$ percentile were classed “*High*”, and values in between were classed “*Mid*”.

Due to data gaps in the model provided by the BSH, tidal data were not available for four dates: 21-04-2004, 15-10-2004, 14-11-2004, and 19-05-2004. I excluded these dates from analyses.

4.3.3 Data processing and calculating movement parameters

I downsampled the seal movement trajectories from 5 second to 15 minute resolution to match the resolution of my tidal data. Seals conducted varying numbers of foraging trips (see Table 4.1) and, to avoid analysing short excursions that may not be representative of typical foraging trips, I analysed only trips that were longer than 1 day. This reduced my sample size from 30 to 24 individuals, which conducted a total of 139 foraging trips. Of the 139 foraging trips, some trajectories extended further northwards than the spatial extent of my tidal data. I excluded any trajectories where $\geq 10\%$ of the seal locations were missing the respective tidal covariate data, which brought my final sample size down to 112 trips (Table 4.1).

I calculated the step lengths (S_t ; the Euclidian distance travelled between successively observed locations, $t_{n+1} - t_n$) and bearings (B_t ; the direction of travel recorded by the GPS between $t_{n+1} - t_n$) using the “*deg.dist*” and “*earth.bear*” functions respectively from the “*fossil*” package in R, based on the Haversine formula to account for the curvature of the earth. B_t was used to calculate turning angles (φ_t ; the change in direction between successive relocations). Movement velocity (V_g) was calculated by dividing S_t by the time interval $t_{n+1} - t_n$. I checked for erroneous records, defined as observations exceeding a speed threshold of 2 ms^{-1} (Carter et al., 2017), and found none.

4.3.4 Statistical analysis

To analyse the movement and behaviour of seals in response to tidal drivers I used hidden Markov models (HMMs) (Zucchini, MacDonald, & Langrock, 2017) implemented using the “*momentuHMM*” package in R (McClintock & Michelot, 2018).

I fitted a discrete-time, multivariate HMM to the location data by allocating one of three latent (i.e. “hidden”) states ($Z_t \in \{T, F, R\}$, where **T** denotes “travelling”, **F** denotes “foraging”, and **R** denotes “resting”), to each time interval along the trajectory ($t = 1, \dots, T$). Seals express a mixture of these three behavioural states as part of typical daily activity budgets (Mcclintock, Russell,

Matthiopoulos, & King, 2013; Russell et al., 2015; Leos-Barajas, Gangloff, et al., 2017; Carter et al., 2019). Following van Beest et al., (2019), my Markov chain was unobserved and first-order, meaning there were no *a priori* “known” states (cf. Carter et al., 2019), and the probability of being in any given state at time t was determined solely by the state at time t_{n-1} . Thus, the complete Markov chain for each trajectory was fully characterised by one-step state transition probabilities.

The three behavioural states were derived by their respective marginal component distributions of observed movement parameters (i.e. step lengths (S_t) and turn angles (φ_t): long step lengths with turn angles centred on zero (i.e. high directional persistence) nominally attributed to travelling (**T**), medium step lengths and an intermediate range in turn angles (moderate directional persistence) attributed to foraging (**F**), and short step lengths and a wide range in turn angles (low directional persistence) attributed to resting (**R**) (McClintock, et al., 2014; van Beest et al., 2019). Resting state movements may be conflated with similar movement patterns associated with periods of foraging if only S_t and φ_t are used to classify behavioural states (McClintock et al., 2013; Russell et al., 2015; Carter et al., 2019). Thus, I further characterised hidden states according to their component distributions of the proportion of time spent diving during each 15 min time interval ($\omega_{d,t}$). My multivariate HMM hence comprised three data streams: S_t , φ_t and $\omega_{d,t}$. For state-dependent component distributions of movement and dive parameters, I took: step length $S_t|Z_t = z \sim \text{Gamma}(\mu_z/\sigma_z, \sigma_z)$ where the (state-specific) mean step length parameter $\mu_z > 0$ and shape parameter $\sigma_z > 0$ for $Z_t \in \{\mathbf{T}, \mathbf{F}, \mathbf{R}\}$, turn angle $\varphi_t|Z_t = z \sim \text{wrapped Cauchy}(\mu_z, \gamma_z)$ with a mean of zero and a (state-specific) directional persistence parameter $0 < \gamma < 1$ for $Z_t \in \{\mathbf{T}, \mathbf{F}, \mathbf{R}\}$ (where 1 represents highly directional travel), and dive proportion $\omega_{d,t}|Z_t = z \sim \text{Beta}(\alpha_z, \beta_z)$ where both $\alpha > 0$ and $\beta > 0$ for $Z_t \in \{\mathbf{T}, \mathbf{F}, \mathbf{R}\}$ (McClintock, London, Cameron, & Boveng, 2017).

I considered the effect of up to four tidal covariates in my models: head-current component (V_c), tidal strength, tidal state, and tidal phase. V_c represents the head-current component vector of V_t (the magnitude of the tidal vector

experienced as either head- or tail-current; Appendix S4.2). Tidal phase was a continuous cyclical cosinor covariate which modelled the ebbing and flooding of the tide using two trigonometric functions, $\sin(\frac{2\pi t}{48})$ and $\cos(\frac{2\pi t}{48})$. I also included sex, site (Rømø, Lorenzensplate, or Helgoland), and age (adult or juvenile) as covariates. I modelled the effect of covariates on both the state-switching process and on the movement characteristics of behavioural states directly (Fig. 4.1; note I modelled covariate effects on S_t and φ_t only, and not on $\omega_{d,t}$; I included $\omega_{d,t}$ in my model only to improve behavioural state classification and my aims here were not to investigate covariate effects on dive proportion *per se*).

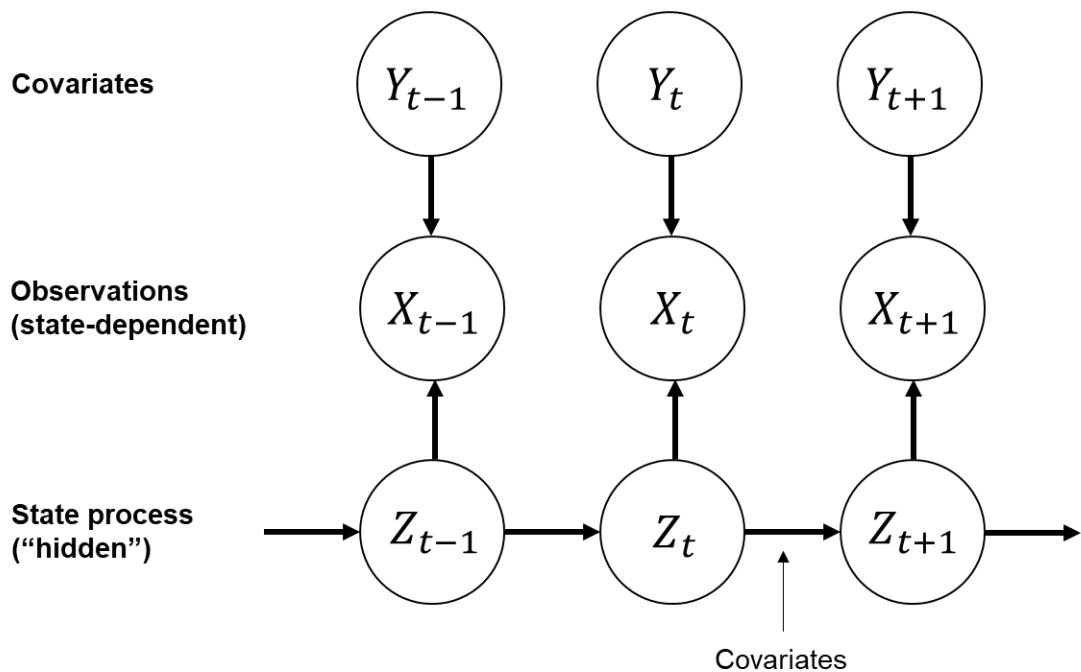


Fig. 4.1. Schematic of HMM dependence structure. X_t are the multivariate observed data (step lengths, turn angles, and dive proportion). Z_t is the behavioural state $Z_t \in \{T, F, R\}$ (travelling, foraging, resting) at time t . Y_t are the tidal and demographic covariates. Covariates also affected the state transition probabilities directly.

To account for both between- and within-individual variation in my models, I incorporated discrete-valued random-effects into the model structure by fitting them to the initial distribution and state transition probabilities (McClintock & Michelot, 2018). Thus, I included K "mixtures" in the model (up to a maximum of $K = 5$; DeRuiter et al., 2017). Given that their interpretation relates to

behaviour, I hereon refer to different mixtures as “behavioural contexts” (BCs; DeRuiter et al., 2017).

I fitted a total of 22 HMMs (Appendix S4.4) which included all covariate combinations as well as the two-way interactions between V_c and sex, V_c and site, and V_c and age. I also fitted models with two states (with one state resembling directional movement and a second state resembling area-restricted search; ARS) to check if the inclusion of a third state was justified. I used the forward algorithm (Zucchini et al., 2017) to conduct maximum likelihood estimation (MLE) utilising R’s built-in “nlm” optimisation routine (R Core Team, 2018). I checked for local maxima by refitting each HMM over a total of 10 iterations using a range of different, randomly selected starting parameter values $0 \leq \mu_z \leq 1.5$, $0 \leq \sigma_z \leq 1$, $0 \leq \gamma_z \leq 1$, $0 \leq \alpha_z \leq 100$, and $0 \leq \beta_z \leq 100$. To determine the best starting parameter values, I compared the maximum L values from all model iterations. Thus, I am confident that my final model represents the global maxima of L .

I selected the final model, including the number of behavioural contexts (BCs) and most appropriate tidal covariate, using the Akaike information criterion (AIC) (Appendix S4.4). To check for over-parameterisation, I compared AIC for models with reshuffled tidal covariate values. I checked that the assumptions of my final model were adequate through visual inspection of pseudo-residual plots (Appendix S4.5) and checked that state characteristics and sequences were biologically plausible, i.e. in line with reasonable expectations of harbour seal behaviour at sea (Mcclintock et al., 2013; Russell et al., 2015), and observations of the data (Carter et al., 2019). I used the Viterbi algorithm (Zucchini et al., 2017) to decode the most plausible sequence of states that gave rise to the observed data and assigned these to each respective time interval.

4.4 Results

I analysed seal movement data from a total of 112 foraging trips conducted by 24 individuals (8 from HE, 7 from LP, and 9 from DK) between April 2004 and September 2006 (Table 4.1). Individuals undertook between 1–16 trips each, providing a data duration of 57.4 ± 26.0 days, with trips lasting 4.67 ± 3.64 days (Table 4.1).

4.4.1 Summary of the HMM

The final model – which was very well supported ($-122.4 \Delta\text{AIC}$ versus the next best model; Appendix S4.4) – converged with three behavioural states consistent with biological expectations of typical harbour seal behaviour during foraging trips (Russell et al., 2015). Specifically, state 1 was classified by long step lengths ($\mu = 0.972$ km; 95 % CI: 0.966–0.979 km) and high directional persistence ($\gamma = 0.904$; 95 % CI: 0.900–0.909), indicative of travelling behaviour. State 2 featured intermediate step lengths ($\mu = 0.711$ km; 95 % CI: 0.705–0.717 km) and intermediate directional persistence ($\gamma = 0.740$; 95 % CI: 0.730–0.751), suggestive of foraging behaviour. State 3 showed the shortest step lengths ($\mu = 0.337$ km; 95 % CI: 0.330–0.343 km) and weakest directional persistence ($\gamma = 0.459$; 95 % CI: 0.442–0.476), consistent with resting behaviour (Fig. 4.2–4.3; Appendix S4.6–S4.7). Importantly, I note that differences in the means of these three states were negligible across all models considered, regardless of covariate combinations (or lack of covariate effects altogether), and across model fitting iterations (Appendix S4.4). This provides confidence that the final converged model is representative of the global optimum L .

The final model favoured the inclusion of head-current component (V_c) over the other tidal covariates considered and retained the full complexity of demographic covariate effects and their interactions with head-current component on both the state transition probabilities and movement parameters (Appendix S4.4). The final model had $K = 3$ BCs (BC1–3), i.e. three different patterns of state-switching behaviour (*sensu* DeRuiter et al., 2017). On

average (across all trips from all individuals), there was an almost equal probability of trips having been derived from each of BC1 (0.385) and BC2 (0.378), with a lower probability of trips derived from BC3 (0.237) (see later for details of each BC's characteristics). Whilst the model converged with $K = 3$ BCs, not all individuals undertook trips from each of these random-effect groups (see Appendix S4.11).

4.4.2 Summary of key responses to tidal currents

Harbour seals (*Phoca vitulina*) modulated their fine-scale movement and behaviour in response to tidal currents. Specifically, observed seal movement speeds increased in tail-currents and decreased in head-currents. Behavioural state persistence was generally high but decreased under tail-currents. Seals were more likely to switch to foraging under tail-currents and indeed were more likely to be foraging in tail-currents than head-currents. Variation between- and within-individuals was not well explained by the demographic covariates of site and sex, for which clear differences were not apparent. Juvenile responses were more acute than for adults. In the remainder of the results sections, I provide specific details of results as they relate to each of my aims (**H₁–H₃**) in turn.

Table 4.1. Details of the sub sample of 24 harbour seals (from 30 originally, see text and supporting information in Appendix S4.1 for details of the 6 individuals excluded) and the data collected from them used in this study. Note that female individuals at Helgoland were all pregnant.

Individual	Sex	Site	Age	Length (cm)	Mass (kg)	Tag date	Data duration (days)	Number of trips	Average trip duration (days; mean \pm SD)
DK03.05.-5	M	DK	Adult	178	91	Mar 2005	79	16	3.49 \pm 1.53
DK04.04.-2	M	DK	Adult	170	86	Apr 2004	94	2	3.68 \pm 0.56
DK05.06.-1	M	DK	Juvenile	NA	40	May 2006	55	1	10.09
DK05.06.-2	M	DK	Juvenile	130	35	May 2006	55	7	7.23 \pm 3.25
DK05.06.-4	M	DK	Juvenile	120	38	May 2006	81	4	11.35 \pm 5.78
DK09.04.-3	M	DK	Adult	148	NA	Sept 2004	28	4	4.91 \pm 1.06
DK09.04.-5	M	DK	Adult	155	66	Sept 2004	68	7	6.44 \pm 3.7
DK09.04.-6	M	DK	Adult	173	69	Sept 2004	63	10	3.19 \pm 1.75
DK11.05.-1	F	DK	Adult	156	82	Nov 2005	43	1	3.38
HE04.05.-1	F	HE	Adult	178	101	Apr 2005	18	1	1.66
HE04.05.-2	F	HE	Adult	155	98	Apr 2005	44	1	1.02
HE04.06.-4	F	HE	Adult	NA	NA	Apr 2006	57	5	1.57 \pm 0.23
HE04.06.-7	M	HE	Adult	160	95	Apr 2006	71	3	1.3 \pm 0.89
HE09.05.-2	M	HE	Adult	169	75	Sept 2005	21	2	2.67 \pm 2.16
HE09.06.-1	M	HE	Adult	160	73.5	Sept 2006	94	5	6.74 \pm 2.98
HE09.06.-2	M	HE	Adult	165	69	Sept 2006	94	4	1.62 \pm 0.52
HE09.06.-4	M	HE	Adult	160	73.5	Sept 2006	80	8	1.64 \pm 0.42
LP04.05.-2	F	LP	Adult	150	98	Apr 2005	74	10	4.35 \pm 2.49
LP04.05.-4	M	LP	Adult	150	42	Apr 2005	58	2	15.46 \pm 0.23
LP04.05.-5	M	LP	Adult	180	96	Apr 2005	20	2	2.88 \pm 0.6
LP04.05.-7	M	LP	Adult	174	93	Apr 2005	16	1	1.05
LP04.05.-8	M	LP	Adult	164	71	Apr 2005	18	1	3.02
LP04.06.-5	M	LP	Adult	170	80	Apr 2006	67	6	7.6 \pm 5.84
LP04.06.-8	M	LP	Adult	170	95	Apr 2006	79	9	5.72 \pm 3.29

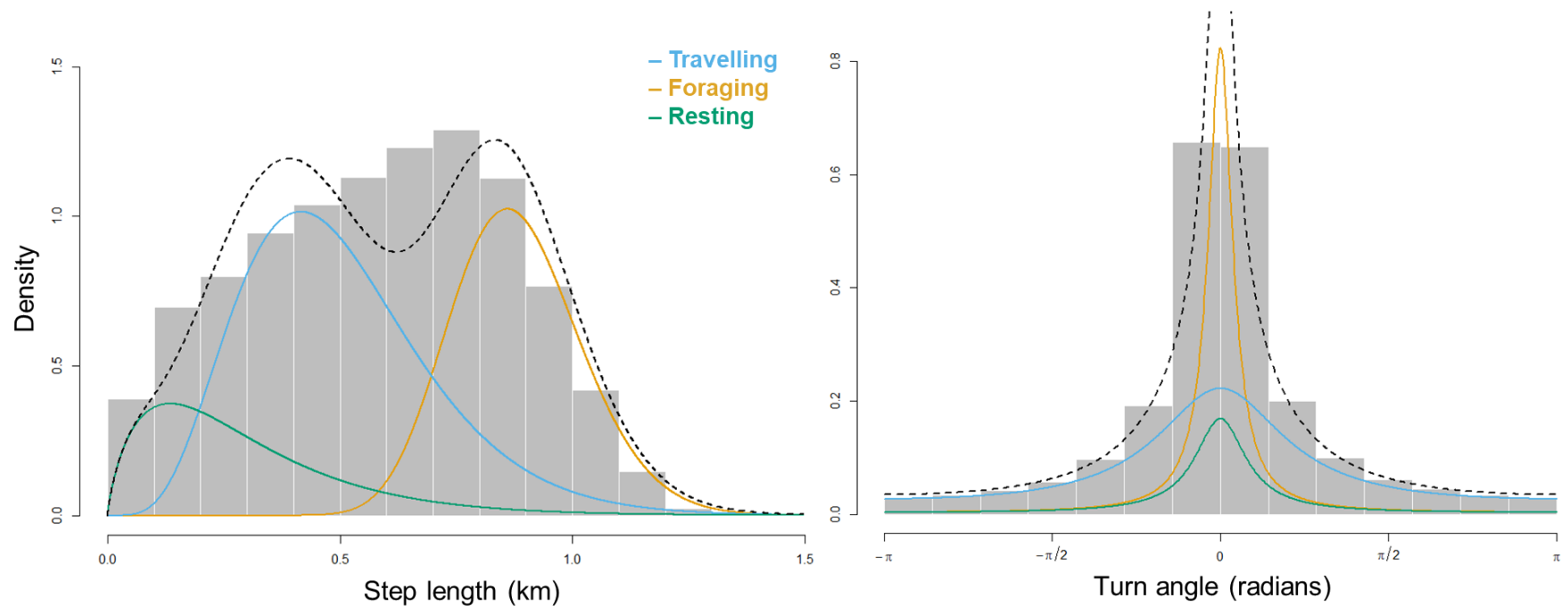


Fig. 4.2. State-dependent parameter distributions for the final HMM.

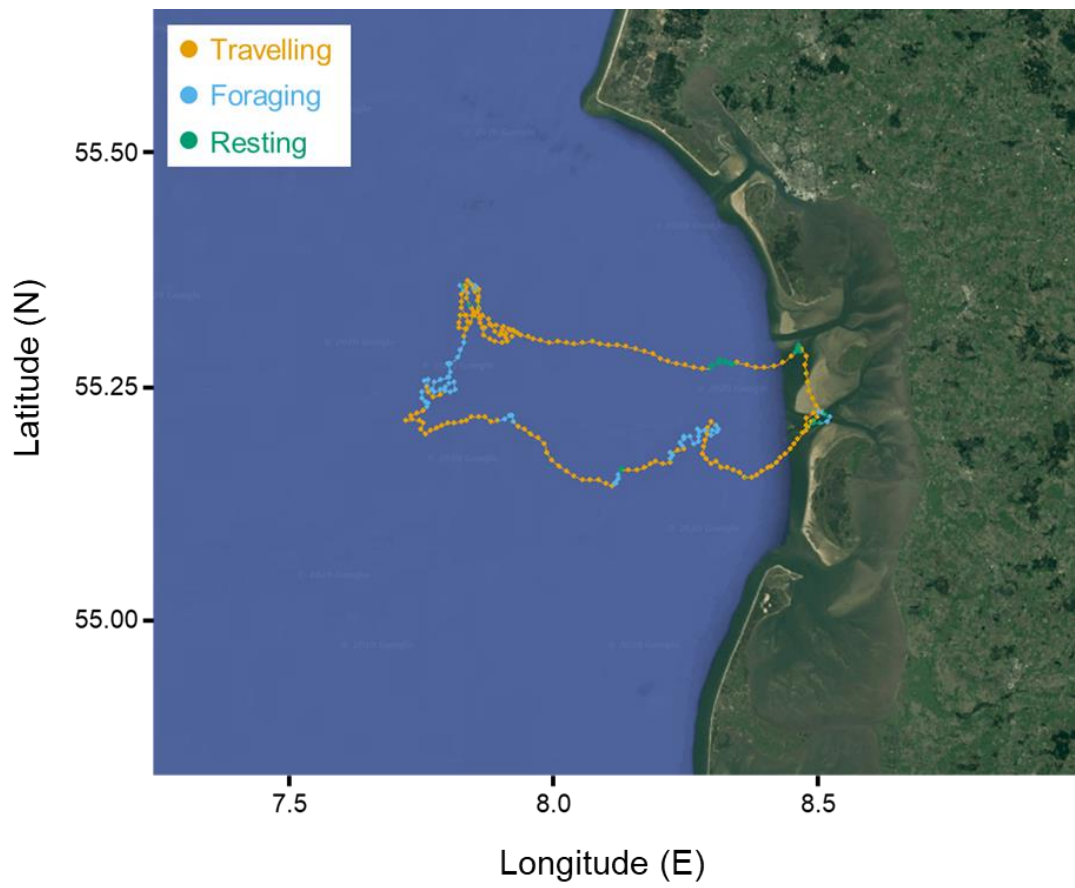


Fig. 4.3. Example trajectory with behavioural state assignments generated from generalised HMM (see Appendix S4.6 for all trajectories).

4.4.2 State-dependent distribution parameters (H₃)

Step length

Generally, seal movement speeds increased in tail-currents (i.e. step lengths became longer over the same duration) and decreased in head-currents. However, the effect sizes of these differences were small except for in resting states (Appendix S4.8). The standard deviation of step lengths (Appendix S4.7–4.8) increased in response to head-current component for travelling states (0.2 km) and decreased for resting states (-0.43 km); foraging states were unaffected (0.02 km; CI: -0.04–0.07 km).

Travelling state

The mean step length was 0.88 km (over a 15 min interval) for adults across all sites, 0.66 km for juveniles, and decreased with increasing head-current component (-0.089; CI: -0.132 – -0.046); and even more so for juveniles (-0.141; CI: -0.19 – -0.092; Fig. 4.4; Appendix S4.8).

Foraging state

The mean step length varied slightly for adults, across sites and sexes, as did the effect of head-current component (Fig. 4.4; Appendix S4.7–7.8). Specifically, females' mean step length was 0.06 km greater than males; HE individuals' mean step length was 0.13 km higher than for DK and LP, which were approximately equal (Fig. 4.4; Appendix S4.7–4.8); the mean was 0.22 km lower in juveniles as for the travelling state. Increasing head-current component gave rise to shorter mean step lengths for all except HE females, where the effect was opposite (Fig. 4.4; Appendix S4.7–4.8).

Resting state

In contrast to foraging, the resting state mean step length did not differ between sexes but differed between sites; 0.06 km greater for HE than DK individuals; 0.13 km shorter for LP individuals (Fig. 4.4; Appendix S4.7–4.8). Increasing head-current component gave rise to shorter step lengths (-0.5 km; CI: -0.7 – -0.3 km), especially for HE individuals (a further -0.3 km; CI: -0.4 – -0.1).

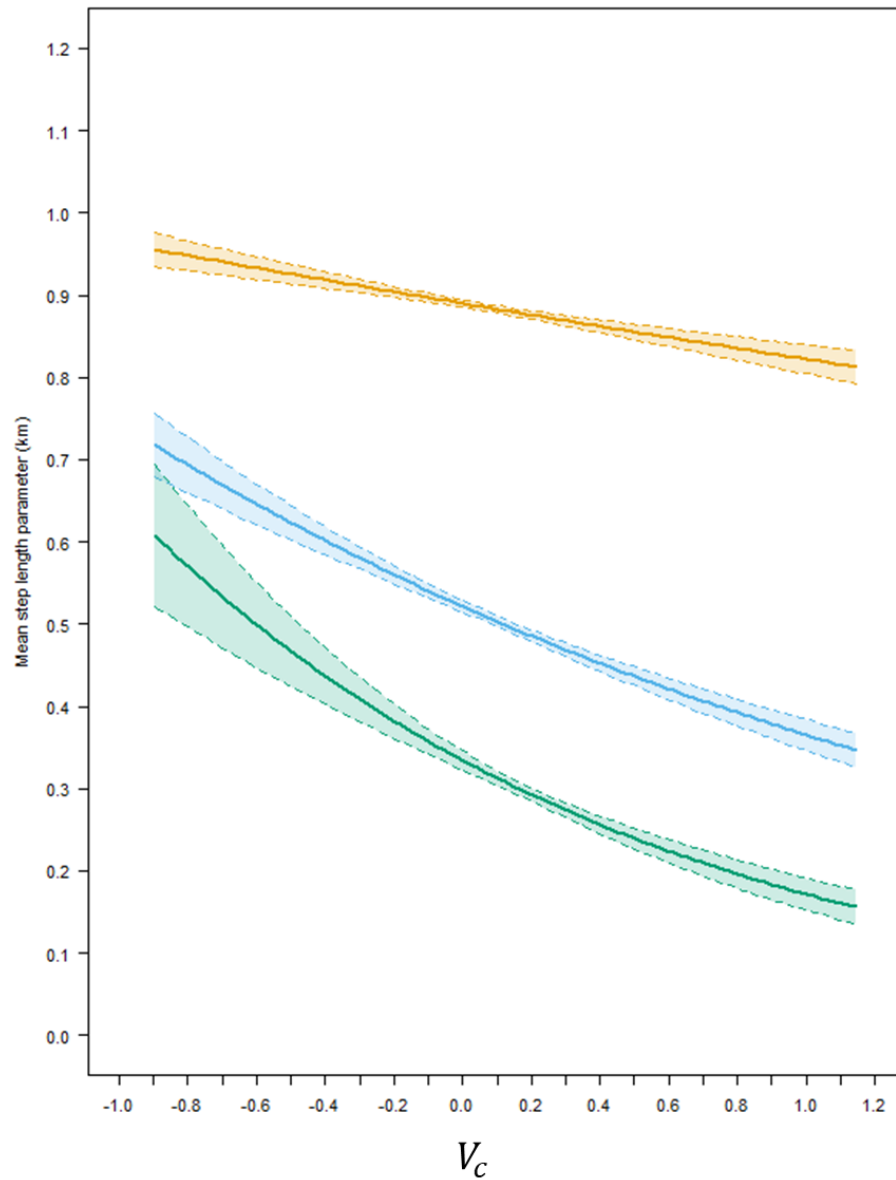


Fig. 4.4. Covariate effects on state dependent step length mean parameter as a function of head-current component (V_c). Coloured by decoded behavioural states (travelling, foraging, resting). Results shown highlight the typical response seen across all individuals studied (see text for comparisons). Solid lines show mean estimates with associated 95% CIs. More positive values of V_c indicate stronger head-currents, more negative values indicate stronger tail-currents. 0 indicates slack water.

Directional persistence

In contrast to step length, there were no general patterns in the response of directional persistence to tidal currents (Fig. 4.5). Directional persistence was markedly affected by head-current component (Fig. 4.5; Appendix S4.7–4.8) and varied between sexes, sites, and age classes.

Travelling state

Directional persistence decreased with V_c for both sexes in DK and LP and increased for HE (Fig. 4.5; Appendix S4.7–4.8); juveniles also saw a reduction, but overall had a higher mean than adults (0.1; CI: 0.02–0.2). DK adults had the highest mean, followed by HE (-0.27; CI: -0.37 – -0.16) and LP individuals (-0.5; CI: -0.58 – -0.46); Fig. 4.5; Appendix S4.7–4.8).

Foraging state

The mean for males was 0.2 higher than females; HE and LP had higher means than DK (by 1 and 0.27 respectively); juveniles had a higher mean (0.6; CI: 0.54–0.74) than adults (Fig. 4.5; Appendix S4.7–4.8). Greater head-current component decreased directional persistence for all groups except HE females (Fig. 4.5; Appendix S4.7–4.8).

Resting state

Directional persistence in the resting state was as variable across factorial groups as for foraging. Males had a greater mean than females (0.4; CI: 0.19–0.63); DK individuals were most persistent followed by HE (-0.2; CI: -0.37 – -0.06) and LP (-0.65; CI: -0.83 – -0.46); juveniles were lower than adults (-0.7; CI: -0.9 – -0.5). LP individuals increased their persistence in response to V_c ; females more so than males (Fig. 4.5; Appendix S4.7–4.8). DK females and juveniles also demonstrated a positive response to head-current component, although adult males were the opposite (Fig. 4.5; Appendix S4.7–4.8). HE individuals decreased their persistence in response to V_c , males more sharply than females (Fig. 4.5; Appendix S4.7–4.8).

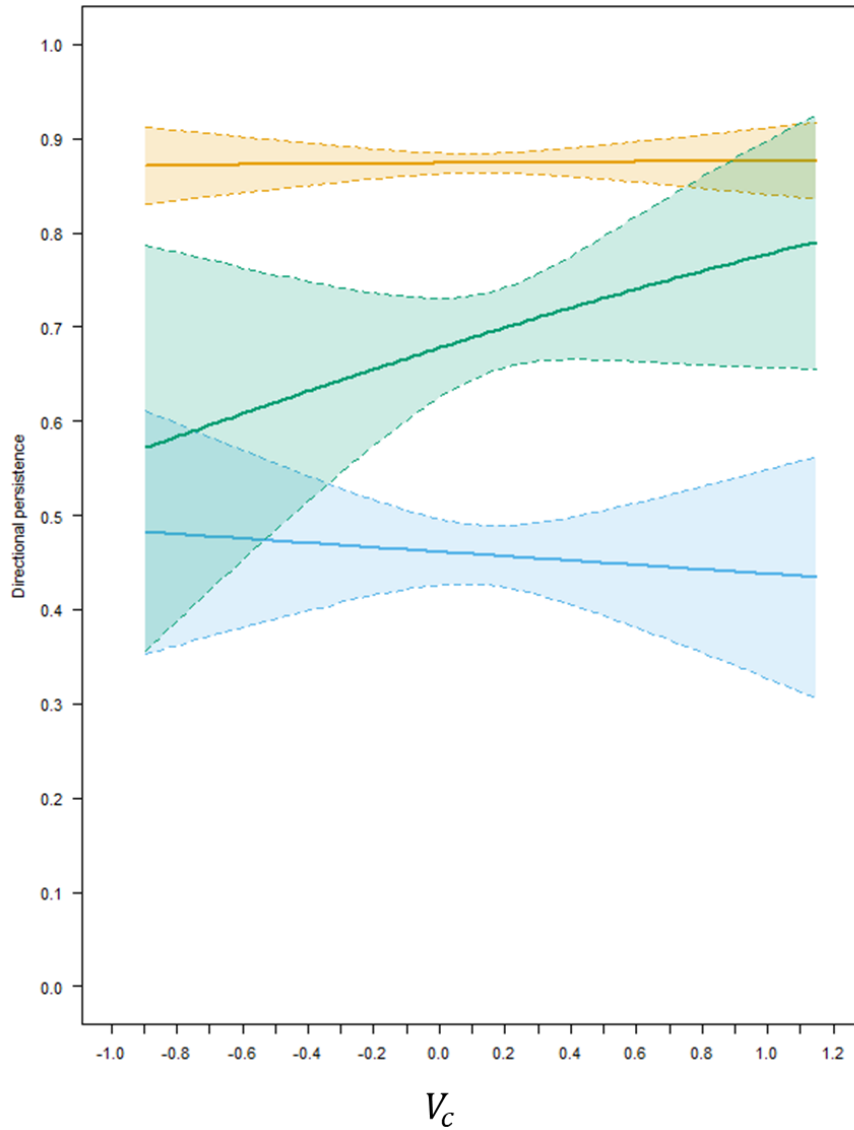


Fig. 4.5. Covariate effects on state dependent directional persistence parameter as a function of head-current component (V_c). Coloured by decoded behavioural state (travelling, foraging, resting). Results shown highlight the typical response seen across all individuals studied (see text for comparisons). Solid lines show mean estimates with associated 95% CIs. More positive values of V_c indicate stronger head-currents, more negative values indicate stronger tail-currents. 0 indicates slack water.

4.4.3 Stationary state probabilities (H_1)

Foraging state probability

The probability of being in a foraging state generally decreased under head-currents ($V_c > 0$) and increased in tail-currents ($V_c < 0$) and these trends were mostly consistent across BCs (Fig. 4.6; Appendix S4.9).

Exceptions to this rule were observed for LP males (in BC1 and BC3), LP females (BC3), DK males (both adults and juveniles) and females (BC2), and HE females (BC2); in these cases, the foraging SSP decreased both with increasing relative tail-currents and head-currents, with the highest probability under neutral tidal flow conditions, i.e. relatively weak or negligible head- or tail-currents (Fig. 4.6; Appendix S4.9).

Travelling state probability

Seals' travelling SSP varied widely in response to head-current component (Fig. 4.6; Appendix S4.9).

Specifically, in BC1, DK adult SSP peaked under mild head-currents (~ 0.3), decreasing further under increasing head-currents. For LP, males' travelling SSP was approximately equally likely under all current conditions (Fig. 4.6; Appendix S4.9), except at the extremes where the probability was highest and lowest for strong tail- and head-currents, respectively. In BC2, the SSP for DK individuals increased with tail-currents, with the lowest probability observed under neutral flow conditions; otherwise in BC2 only LP males varied from the norm with the SSP plateauing under moderate head-current conditions before decreasing. In BC3, DK adults' SSP showed no clear change in response to head-current component, with wide CIs (especially at the extremes), whilst for juveniles there was a clear, negative response, albeit with wide CIs under strong tail-currents (Appendix S4.9); for HE individuals the SSP decreased in response to head-currents; for LP individuals the travelling SSP peaked at the extremes for males, whilst females saw a steady increase in response to head-current component (Appendix S4.9).

Resting state probability

Resting SSPs demonstrated the greatest variability, with two patterns emerging across BCs (Fig. 4.6; Appendix S4.9):

First, the resting SSP was low to moderate ($0.05 < x < 0.6$) in tail-currents and increased under head-currents. Second, the resting SSP was highest under neutral flow or moderate head-currents, decreasing in both increased tail-currents and strong head-currents. Exceptions included LP females in BC1 and BC3; in both cases the SSP was highest in strong tail-currents, decreasing steadily to a minimum at neutral flow or weak head-currents before increasing slightly in greater head-currents (Fig. 4.6; Appendix S4.9). In LP males, SSP was equally low at the extremes of head-current component (between 0.05–0.1), with a plateau at mild tail-currents (Fig. 4.6; Appendix S4.9). Finally, the SSP for HE females plateaued in neutral flow and decreased with increasing tail- or head-currents, although CIs were very wide (Fig. 4.6; Appendix S4.9). For all states and across all BCs, CIs were consistently wider for females, likely due to relatively small sample size for this group; CIs for juveniles were relatively wide compared to adults for the travelling state only.

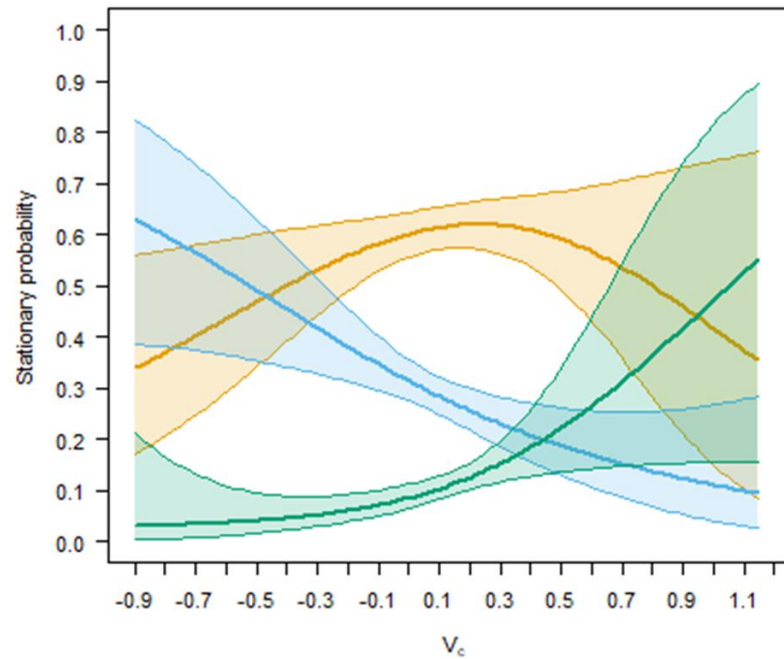


Fig. 4.6. Model-estimated stationary state probabilities for behavioural states (**travelling**, **foraging**, and **resting**) as a function of head-current component (V_c). Plots show 95 % CI. Results shown highlight the typical response seen across all individuals studied (see text for comparisons). More positive values of V_c indicate stronger head-currents, more negative values indicate stronger tail-currents. 0 indicates slack water.

4.4.4 Transition probabilities (H₂)

The initial distribution indicated that across BCs, it was 66–77 % likely that the first behavioural state for each individual was resting (Appendix S4.10). This was corroborated by visual observation of the trajectories (Fig. 4.3; Appendix S4.6).

Resting → Foraging

This probability of this transition was generally low and showed no consistent trend in response to head-current component (except decreasing in BC1), with wide CIs at the extremes (Fig. 4.4; Appendix S4.10).

Resting → Travelling

This transition probability was generally consistent across adults – decreasing with head-current component. For juveniles, the probability varied in response to V_c and according to BC; increasing in BC1, decreasing in BC3, and demonstrating no change in BC2 (Fig. 4.7; Appendix S4.10).

Travelling → Foraging

This probability decreased as a function of head-current component. Exceptions to this were juveniles in BC1 and LP females in BC1 and BC3, for which results were opposite (Fig. 4.7; Appendix S4.10).

Travelling → Resting

The probability of these transitions was generally very low and did not vary noticeably as a function of head-current component (Fig. 4.7; Appendix S4.10). The only exception to this was in BC1 where a small, linear increase in probability was observed under increasing head-currents for females and juveniles.

Foraging → Resting

Once in a foraging state, the probability of switching to resting was generally low under all current conditions. Exceptions were as follows: In BC1, the probability increased under tail-currents for HE and LP females; in BC2 decreasing head-current component increased the probability of switching for

adults, except HE females where the opposite occurred (Fig. 4.7; Appendix S4.10).

Foraging → Travelling

This transition probability was highly variable (Fig. 4.7; Appendix S4.10). Within BCs, males were more consistent than females. In BC1, the response to head-current component was negative for males and positive for females (except in HE where responses were both negative). In BC2, the probability increased in response to head-current component except for females in HE (no clear response) and LP (small decrease) (Appendix S4.10). Finally, in BC3, males showed the same trend as for BC1 whilst females showed a small increase in response to head-currents (Fig. 4.7; Appendix S4.10). Juveniles followed the adult pattern in BC1; in BC2 and BC3 the probability remained low under all current conditions (Fig. 4.7; Appendix S4.10).

Behavioural state persistence

The probability of remaining in a state (i.e. state “persistence”) was generally high but reduced in response to tail-currents. (Fig. 4.8; Appendix S4.10).

Exceptions to this were seen for juveniles and HE and LP females within BC3 for the travelling state; these showed a weak, linear decrease in response to head-current component (Appendix S4.10). In BC3, female foraging state persistence decreased in response to head-current component. For males in BC2, foraging state persistence plateaued around slack conditions and decreased under increasingly extreme head- and tail-currents; a trend also exhibited by LP females in BC1. Resting state persistence decreased for males in response to head-current component in BC2, and juveniles in BC1 (4.8–4.9; Appendix S4.10).

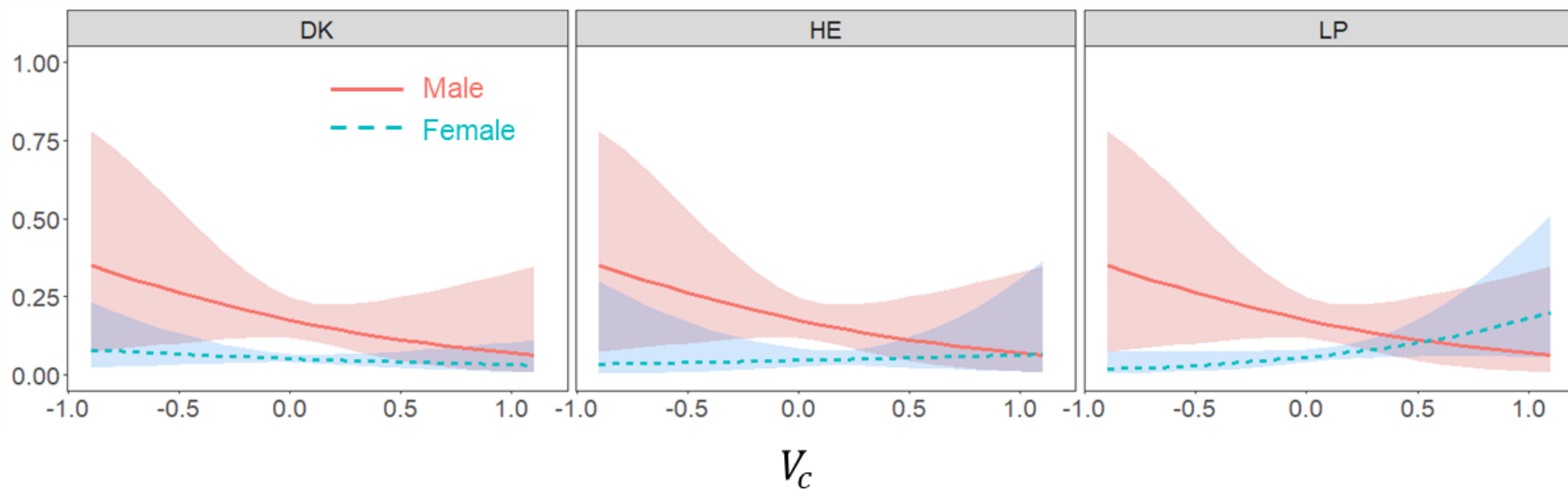


Fig. 4.7. Predicted transition probabilities as a function of head-current component (V_c) for the transition from travelling to foraging. Predictions made from the final hidden Markov model for seals of different sites and sexes (plot shows predictions for adults only). Plots show model-estimated coefficients plus 95% CI. See Appendix S4.10). Note that the two-way (sex:site) and three-way (V_c :sex:site) interactions are not included (Appendix S4.4). More positive values of V_c indicate stronger head-currents, more negative values indicate stronger tail-currents. 0 indicates slack water.

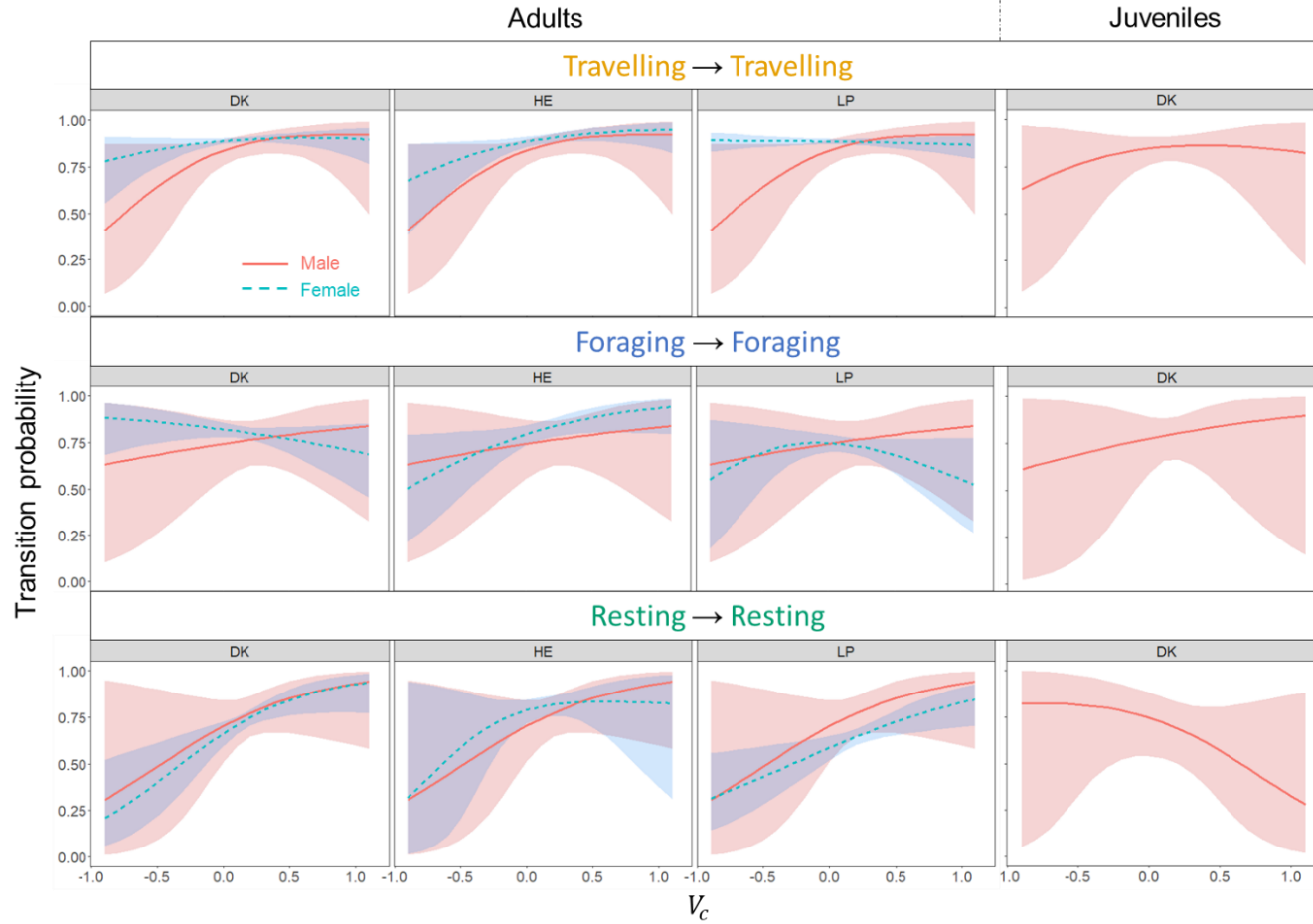


Fig. 4.8. Predicted behavioural state persistence probabilities as a function of head-current component (V_c) estimated from the final hidden Markov model, for seals of different sites, sexes, and age-class. Plots show model-estimated coefficients plus 95% CI. Results from BC1 shown (see text and Appendix S4.10). Note that the two-way (sex:site) and three-way (V_c :sex:site) interactions are not included (Appendix S4.4). More positive values of V_c indicate stronger head-currents, more negative values indicate stronger tail-currents. 0 indicates slack water.

4.4.5 Behavioural contexts and individual variation

Individuals generally exhibited a greater number of mixtures as the number of trips recorded increased (Fig. 4.9) but not for all: 6 individuals with ≥ 4 trips exhibited only one or two BCs, whereas others with < 4 trips exhibited all three. Individuals for which data were recorded from numerous trips generally showed a preference for a given BC; for example, individual “DK03.05.-5” (Table 4.1) conducted 16 trips, with 11 (69 %) of these being derived from BC1. At the other extreme, 7 individuals each with > 1 trip exhibited behaviours from only 1 BC, suggesting these individuals exhibited greater consistency in behaviour; the most consistent individual had all of its 8 trips from a single BC.

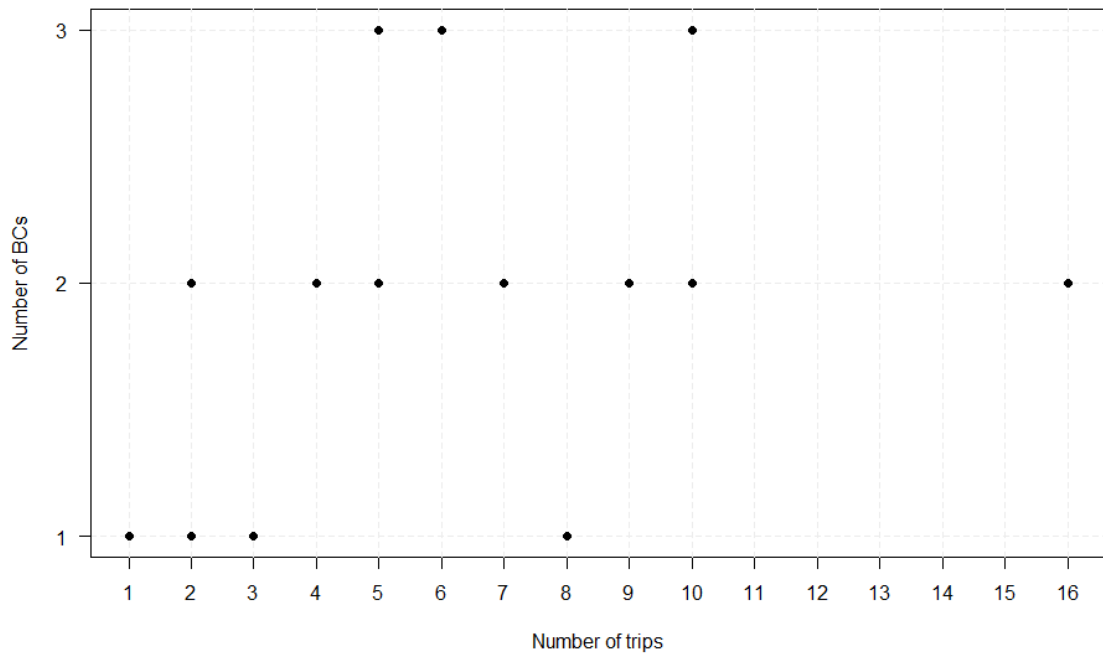


Fig. 4.9. Number of BCs utilised as a function of the number of trips recorded. Each data point represents a single individual (see Table 4.1)

4.5 Discussion

Results here demonstrated that tail-currents were key in modulating seal behaviour. While behavioural state persistence was high, the occurrence of tail-currents increased the probability of seals switching behavioural states. Contrary to my expectations, tail- as opposed to head-currents saw seals switch to foraging states and seals preferentially foraged in the former. Moreover, rather than adapt their movements within behavioural states, seals instead switched behavioural strategies altogether in response to current conditions. Individual variation was high, site- and sex-differences were small, and juveniles showed greater susceptibility to head-currents than adults.

Sex-differences have been documented in harbour seals' behaviour at sea, such that males typically conducted longer trips and dived to deeper depths than females (Thompson et al., 1998; Wilson et al., 2015). Differences are generally attributed to sexual dimorphism, as males are typically ca. 20 % (15 kg) heavier than females (Wilson et al., 2014). Here, however, females were ~ 17 % (16 kg) larger than males; this may have given rise to their slightly longer step lengths via an increased movement capacity (i.e. allometric scaling; Bonner & Peters, 1985). However, aside from this, differences between sexes were insignificant. It is, therefore, reasonable to deduce that any variation between individuals was most likely driven by individual variation rather than differences between demographic factors; this is supported by the fact that the best model had 3 'behavioural contexts', as these are responsible for "soaking up" variation that is not explained by modelled covariates. Individual variation in marine megafauna is typically high (Hays et al., 2016), and in the context of the TST industry, these results suggest that large sample sizes will be required to account for this (Chapter 3).

My results showed that seals do not appear to adjust their swim speed in response to currents, with small differences in observed movement speed likely only driven by variation in current speeds and not the actual swim speed of animals. This is highly plausible given that harbour seals are capable of sustaining swim speeds well above even the highest tidal current velocities experienced in the Wadden Sea (Davies et al., 1985). Such a finding has

important implications for understanding the movements of seals in TSEs, as it suggests – at least for the individuals studied here – that animals who operate in areas where the current velocities do not exceed their swimming capacity do not appear to actively vary their speed in response to currents.

Rather than modulate swim speed in response to currents, seals instead changed their behavioural state. Specifically, seals were more likely to switch behavioural state under tail-current conditions. In other words, the occurrence of tail-currents appeared to be the driving force for animals in deciding when to switch behaviour. In tail-current conditions seals predominantly switched to foraging behaviour. In contrast, state-probability and behavioural switching was not consistently associated with slack water or head-currents. This suggests that animals here appear to transit and rest under a range of current conditions but show a particular preference for foraging in tail-currents. Puffins have been observed to adopt a strategy such as this – exploiting tail-currents to aid drift through prey patches (Bennison et al., 2019). This finding has clear ramifications for the TST industry in this region, as it suggests that animals target tail-currents for foraging. Hence, animals will be carried towards operational devices when they are potentially distracted by foraging, putting them at increased risk of collision (Onoufriou et al., 2019). Compared to the switch from travelling to foraging, the transition from foraging to travelling was highly variable. This finding could be simply explained by seals switching back to travelling after becoming satiated, and thus deciding to travel to a nearby resting site for digestion (Russell et al., 2015).

Given that current velocities in my study area were similar to low current conditions in the Strangford Narrows, Northern Ireland (Joy et al., 2018), I expected seals to behave in the same manner; to move predominantly against currents (i.e. under head-current conditions) and certainly to use these for foraging. Instead, my results are in agreement with those presented by Hastie et al., (2019) who demonstrated that harbour seals' movements in Kyle Rhea, Scotland were generally in the same direction as the tide; this highlights a further example of regional differences in harbour seal behaviour. Likewise, the fact that seals here did not target periods of slack water for foraging contrasts the results found in Sparling et al., (2018), where seals presumably

targeted slack waters to forage on benthic prey when the energetic implications of movement through currents was minimal (see also Waggitt et al., 2016b). Regional differences in response to tidal currents have also been seen in harbour porpoise, which were more likely to perform foraging-like movements in areas of weak current velocities in the Wadden Sea (Stalder et al., 2020) and high current velocities in Wales (Pierpoint, 2008). Such findings suggest that researchers examining movements of animals in TSEs will almost certainly need to account for regional variation within species.

Depth usage appears to be a critically important and distinguishing factor in the response of harbour seals to tidal currents. Specifically, in Joy et al., (2018) harbour seals dived predominantly to the seafloor to forage on benthic prey, reaching depths of between 22.4–28.8 m, whereas in Hastie et al., (2019), seals dived notably shallower, most frequently to depths of 7–18 m to forage on pelagic prey. I did not model absolute dive depth here, but the same data (from the same individuals) were examined in Wilson et al., (2015), revealing that individuals dived to between 8.8–19 m i.e. to similar depths as in Hastie et al., (2019). Prey species composition and dietary studies from the Wadden sea have revealed that harbour seals predominantly forage on pelagic prey in both spring and autumn, shifting to benthic prey species in the summer (De La Vega et al., 2016); indeed, the majority of the data analysed here come from spring and autumn months (Table 4.1). This, combined with the fact that dives made by these individuals (see Wilson et al., 2015) were to relatively shallow depths for harbour seals (Gjertz, Lydersen, & Wiig, 2001; Eguchi & Harvey, 2005), suggests that individuals were foraging on pelagic prey, thus spending a relatively large proportion of time in mid-water or at the surface (Hastie et al., 2019). This is crucial because seals that spend more time in mid-water or at the surface are potentially more susceptible to drifting with currents (Hastie et al., 2019). In the context of these studies, my results point towards the notion that behavioural responses to tidal currents may be underpinned by the choice of prey species and the specialist (e.g. diving) strategies required to exploit them. Indeed, the harbour seals in Joy et al., (2018) – that predominantly dived to the seabed – were assumed to be exploiting a reduction in current velocity at the seafloor, enabling them to more easily maintain their position in head-

currents. This is a key point for researchers attempting to predict the risk of seals to TSTs, such that understanding the prey that animals eat at different sites may provide a good indication of how they will behave. This is particularly pertinent here because seals clearly utilised tail-currents for foraging which may put them at risk of collision with TSTs. It would hence be useful for future studies to prioritise the dietary analysis of animals that operate in TSEs.

Juveniles were more noticeably affected by head-currents than adults, especially whilst travelling; in particular, compared to adults, as relative head-current strength increased, juveniles' step lengths were shorter. Size-dimorphism is highly likely to have given rise to this. Indeed, juveniles in this study were around 60 % smaller than adults, which likely made them more susceptible to the effect of head-currents due to having a lower maximum swim speed threshold; adults generally moved at $\sim 0.94 \text{ ms}^{-1}$ (close to the minimum cost of transport estimates for adult harbour seals of $1\text{--}1.4 \text{ ms}^{-1}$; Davies, Williams & Kooyman, 1985), whereas juveniles generally moved at around $\sim 0.5 \text{ ms}^{-1}$. Thus, future studies examining the movement of seals in TSEs should control for the size of individuals.

Finally, the magnitude of individual variation in marine megafauna tracking datasets is often high (Carneiro et al., 2017) and the inclusion of additional BCs in this analysis served to improve model fit (Appendix S4.4; DeRuiter et al., 2017). My results indicated that individuals used markedly different numbers of BCs, with some displaying consistency across multiple trips, whilst others exhibited different BCs for each excursion. These findings have important methodological implications for researchers examining seal movements. In addition to collecting data from multiple individuals, collecting data from repeated trips within-individuals is essential to determine variability; even in very consistent individuals, a critical mass of data is required to appropriately quantify variation; likewise for individuals with high variability, numerous trips are required to determine the full extent of this.

Methodological limitations

In fitting two behavioural states that resemble ARS-like movements (foraging and resting) there is the possibility that some states will be conflated (Carter et al., 2019), even after accounting for time spent underwater (i.e. dive proportion; Russell et al., 2015). I observed that 15.8 % of time steps were assigned to resting which is well within the range of ~ 10–35 % reported by Russell et al., (2015).

Finally, the temporal resolution of my data and the resulting inferences are in line with other recent studies examining harbour seal responses to current conditions (Hastie et al., 2016; Joy et al., 2018). However, the spatial resolution is relatively coarse. Thus, while my results provide further novel ecological insight into how seals may respond to variations in tidal currents at relatively fine-scales, higher-resolution data would be beneficial to fully understand the very fine-scale responses of seals' to tidal currents, and the potential implications that this has for near-field interactions with TSTs (Copping & Hemery, 2020).

Chapter 5

Development and performance of a remote-release biologging tag for tracking the high-resolution movements of wild seals

“Not a year goes by without some public rumpus over seals”
(Hewer, 1974)



I restrain an adult harbour seal prior to release while photos are taken of the position of the attached animal tracking device (described in this Chapter). The seal is held in a hoop net with a damp cloth covering its head to keep it calm
(Photograph by William P. Kay).

5.1 Abstract

Tidal stream energy developments are increasing in the marine environment. Devices such as tidal stream turbines (TSTs) that are installed to generate energy pose threats to wild marine megafauna, such as seals, including collision risk. Studying the movements of seals at fine-scales in tidal stream environments (TSEs) and their near-field responses to TSTs is key to understanding the potential risk of detrimental interaction between animals and devices. The methods that are currently available to do this with sufficient resolution are however limited. The use of archival biologging devices offers a solution, however the cost of devices typically precludes their widespread application. Moreover, recovering archival tags deployed on seals is inherently difficult, and so far tags for many taxa have not demonstrated consistently reliable options for recovery. Here I present a new archival tag design for tracking the fine-scale, high-resolution 3D movements of wild seals. The tag incorporates multiple devices; a Fastloc-GPS, a triaxial inertial movement sensor, and a transmission unit for recovery (ARGOS SPOT or VHF tag). Tags were constructed using a combination of commercial devices and home-made units, including the innovative use of a Galvanic Timed Release (GTR) for a seal tag. At £3600 (~ \$4575), my tag offers superior functionality at a cost of approximately 3 times less than a commercial alternative. I deployed tags on free-ranging harbour and grey seals, collecting high-resolution movement data at 40 Hz for up to 14 days. Tags performed well, albeit with specific setbacks that are to be expected of novel deployments. These can be mitigated through further refinement. This novel tag design serves as a proof of concept, providing evidence that tagging seals in TSEs using a high-resolution archival tag recovered with a remote release mechanism is possible. The data obtained can be used to investigate seals in TSEs, including their near-field interactions with TSTs.

5.2 Introduction

The tidal stream energy sector is in its nascent stage compared to other sources of renewable energy (Chowdhury et al., 2020). However, tidal stream environments (TSEs) offer predictable and reliable sources of energy that can be exploited for electricity generation, and this has led to a large number of TSEs being proposed for tidal energy development worldwide, especially using tidal stream turbines. Tidal stream turbines (TSTs) operate in a fashion analogous to wind turbines, with rotating blades being driven by water currents (Copping et al., 2020). The deployment of such devices in the marine environment has led to concerns over the risks that they will pose to marine megafauna which may come into contact with them, with collision potentially resulting in severe or even fatal injury (Sparling et al., 2017; Fraser et al., 2018; Hastie et al., 2019; Onoufriou et al.; 2019; 2021).

Tidal stream environments are topographically complex, coastal habitats typically boasting fast tidal currents (Benjamins et al., 2015). The flow of water through these environments can be predictable (Cox et al., 2013), and as a result, marine megafauna are often attracted to these habitats for foraging opportunities (Uda & Ishino, 1958; Riley, 1976; Zamon 2001; 2003; Genin, 2004). Grey (*Halichoerus grypus*) and harbour (*Phoca vitulina*) seals, for example, have been shown to make use of TSEs as both foraging grounds (Thompson, 2012; Hastie et al., 2019; Onoufriou et al., 2021) and areas through which they travel (Thompson, 2012; Hastie et al., 2016; Carter et al., 2017). More generally, their residency patterns have typically been associated with tidally-mediated environments (Hastie et al., 2019; Leeney et al., 2010). Similar associations have also been observed in other species of marine megafauna (Wade et al., 2013; Benjamins et al., 2015; Waggitt et al., 2018; Cox et al., 2018; Gillespie et al., 2021). While the threat of TSTs pose risks to all taxa of marine megafauna (Copping et al., 2020), for grey and harbour seals this risk is expected to be particularly high. This is because the distribution and space-use of *H. grypus* and *P. vitulina* substantially overlaps with TSEs that have been proposed for TST developments (Carter et al., 2020). Interactions between seals and devices installed in these areas could cause displacement from these environments, create barriers to movement, or may result in

collisions (Hastie et al., 2016). The impact of which could potentially manifest in the exclusion of animals from important foraging habitat (Hastie et al., 2016), increased energetic costs associated with avoiding devices (Onoufriou, 2021), or mortality arising from collision (Onoufriou et al., 2019).

Determining the risks that TSTs pose to grey and harbour seals requires an understanding of seals' broad-scale spatial overlap with TSEs (e.g. Chapter 2; 3), fine-scale use of habitats when in these sites (Hastie et al., 2016; Chapter 4), and 'near field' interactions between animals and operational devices (Hastie et al., 2019). While our understanding of the broad- and fine-scale movements of seals in TSEs has increased over recent years (Hastie et al., 2016; 2019; Sparling et al., 2017; Lieber et al., 2018; Joy et al., 2018; Onoufriou et al., 2019; Chapter 2–4), information on the very fine-scale movements (< 100 m resolution; Waggitt & Scott, 2014) of individuals in TSEs and 'near-field responses' to TSTs is comparatively limited (Copping et al., 2020). This is in large part due to the inability to track seals underwater in high-resolution (Hastie et al., 2019; Copping et al., 2020; 2020b; Onoufriou, 2021). To date, only one study has examined the fine-scale underwater movements of (harbour) seals at 'near field' scales in TSEs, through the use of active acoustic sonar (AAS) (Hastie et al., 2019). This study revealed that harbour seals typically moved in the same direction as the current and that seals preferentially dived to within 14 m from the seabed, putting them at clear risk of collision with TSTs (Hastie et al., 2019). However, this study did not examine seal movements around operational TSTs and so was unable to detect near-field responses. This information is crucial for establishing estimates of risk (Copping & Hemery, 2020).

Various approaches have been used to track the movements of grey and harbour seals in TSEs, including visual survey methods (Lieber et al., 2018), active acoustic sonar (Hastie et al., 2019), and the use of GPS tracking devices (Hastie et al., 2016; 2019; Sparling et al., 2017; Joy et al., 2018; Onoufriou et al., 2021). While these methods can provide extremely useful insights into the movements of animals in TSEs, they are limited in their ability to study near-field responses to TSTs. Specifically, while visual surveys (e.g. Cole et al., 2019) and GPS tracking methods (e.g. Hastie et al., 2016) are able to infer the

movement paths taken by animals underwater they are unable to monitor these movements directly. GPS devices can be coupled with TDRs to concurrently record depth usage, but this still does not allow for 3D reconstruction of animal movement trajectories underwater (Planque et al., 2020). Moreover, while providing data of relatively high resolution (e.g. < 5 mins temporal resolution and between 18–70 m spatial resolution; Dujon et al., 2014), this resolution is insufficient to analyse interactions at close ranges to TSTs (Hastie et al., 2019) that may occur at second or even sub-second scales, hence precluding estimation of near-field evasion rates (Onoufriou, 2021). While AAS approaches have been shown to be effective in studying the near-field range movements of seals in TSEs (Hastie et al., 2019), they do not allow for estimation of fundamental movement metrics such as energetic expenditure (Wilson, Shepard & Liebsch, 2008) which are key to understand the implications of interactions with TSTs, such as the energetic costs of evasive manoeuvres (Onoufriou, 2021).

Currently, the only approach available to study seals in 3D underwater and at high-enough resolution to determine near-field responses to TSTs (and the full implications of this e.g. energetic costs) is to use multi-sensor biologging technologies such as tags containing triaxial accelerometers, magnetometers or gyrometers (Williams et al., 2020; Onoufriou, 2021). However, aside from their high cost being a restrictive factor (Kwok et al., 2017), a number of key drawbacks to the use of these technologies exist.

Multi-sensor loggers typically collect data at very high frequencies (> 40 Hz) resulting in a very large volume of data of which only summaries can be relayed via satellite (Cox et al., 2018). Such summary data unfortunately cannot be used to reconstruct animal trajectories at the resolutions required to elucidate near-field behaviour with TSTs (Onoufriou, 2021). Secondly, reconstructing trajectories from multi-sensor data is challenging when tracking animals moving through TSEs due to current-induced drift (Gaspar et al., 2006). This means that GPS devices must also be deployed in tandem to correct for positioning errors (Wilson et al., 2007). GPS devices are relatively large due to the power requirements associated with transmitting data, necessitating large batteries, and the constraints of appropriate tag size often

preclude the deployment of multiple devices (Wilson & McMahon, 2006). Alternatively, smaller Fastloc-GPS devices (e.g. Lotek's F5G 234A; 84 x 29 x 20 mm) can be deployed in tandem with other devices, whilst still minimising detrimental impact to the animal. However, these devices have reduced battery size which limits their ability to transmit their data, meaning that tags must be recovered, something that is notoriously difficult for wild seals (Wilson & Moss, *pers. comms.*). Nevertheless, tags can be built to 'pop-off' an animal for retrieval at sea, and there are several examples of successful tag recovery using such methods for other marine megafauna taxa (Gleiss et al., 2009; Block et al., 2011; Chapple et al., 2015; Lear & Whitney, 2016; Fossette et al., 2016; Whitmore et al., 2016; Whitney et al., 2016). However, consistently reliable applications of pop-off tags for seals have not yet been demonstrated.

In this Chapter I sought to tackle this multitude of challenges for tracking wild seals in TSEs. Specifically, my aim was to design a new tag that features a combination of multi-sensor and fastloc-GPS technology with an effective remote-release mechanism. In order to support investigations of the near-field responses to TSTs, this tag must be able to collect very high-resolution data on seals in 3D, including underwater, and be hydrodynamic in its design so as to minimize its impact on animals operating in TSEs (Kyte et al., 2019). The tag should be able to be built and assembled in-house using standard techniques, and be fully customisable to allow researchers to modify the design to meet their own requirements. Thus, I built and deployed 9 tags on wild harbour seals in the Wadden Sea and on grey seals in Wales. Here, I provide technological details of the tag that I developed, including a critical and transparent appraisal of its performance, and suggest areas for improvement. I also provide in the supplementary materials to this Chapter (Appendices S5.1–5.8), broader details of the factors to consider when building tags for tracking seals in TSEs. This information will facilitate researchers to track the very fine-scale movements of seals in TSEs in order to investigate near-field collision risk with operational TSTs.

5.3 Tag details

5.3.1 Tag requirements

My aim was to deploy high-resolution tracking tags for short durations (7–14 days) on seals in TSEs, to understand how they operation in fast flowing currents and provide evidence for the TST industry (Hastie et al., 2019). To achieve this, my tag required a tri-axial accelerometer to record movement, a pressure sensor to collect depth data, a fastloc-GPS device to correct for current-induced drift (Gaspar et al., 2006) and a transmitting unit to aid tag recovery (Table 5.1). The tag needed to remotely release from seals and transmit its location at the surface to aid recovery via VHF radio tracking or ARGOS transmissions (Carter et al., 2016), including with the use of a Goniometer for the latter (Barkley et al., 2020). Hence, the tags required a flotation package, an appropriate counter-balance, and a release mechanism. This meant that the tags could not be glued directly to the seal's pelage but rather a baseplate be used from which the tag could separate (e.g. Liebsch, 2004). The tag needed to be designed with hydrodynamics in mind to minimise drag (van der Hoop et al., 2014) but also robust and pressure-proof to protect it from physical damage.

5.3.2 Devices

I used a Daily Diary (DD; Wildbyte Technologies Ltd, Swansea, UK) multi-sensor logger to record triaxial acceleration powered by a 750mAh 3.6V Lithium Thionyl Chloride EVE cell (EVE Energy Co., Ltd, Guangdong, China) (Table 5.1). This device was selected because of its small size, low cost, and ability to sample at ultra-high frequencies (up to 800 Hz) and was programmed with a relatively high sampling frequency (40 Hz acceleration). The memory capacity of the DD (2 GB) and the battery life were spent in ~ 14 days. The DD was archival so needed to be recovered. The DD was connected to an ultra-small board-mounted pressure sensor (Mouser Electronics, High Wycombe, UK; Table 5.1). This pressure sensor is 2.75 times smaller than depth sensors

traditionally used in seal tags (e.g. Wilson et al., 2007), and recorded pressure at 4 Hz with 13 cm resolution.

To provide accurate positional information and correct for drift in dead-reckoning (Gaspar et al., 2006) I used the fastloc F3G 133A Marine GPS Datalogger (Sirtrack, Hastings, New Zealand; Table 5.1). This device was chosen based on its small size (Table 5.1) and was also archival. The fastloc-GPS provided a maximum temporal resolution of 2 minutes and was powered by an in-built, rechargeable battery, the duration of which was expected to last between 10–14 days. 2 of the 9 tags that I deployed did not contain a Sirtrack fastloc-GPS device (Table 5.2) as these were deployed in tandem with SMRU GPS-GSM tags (Sea Mammal Research Unit, University of St Andrews) which provided accurate GPS positional information.

To transmit tag position once the tag had detached (see later) I trialled two devices; a VHF transmitter (Sirtrack, Hastings, New Zealand) and an ARGOS Smart Position Only Tag (SPOT; Wildlife Computers, Redmond, USA) (Table 5.1). The former sent radio transmissions (1 second resolution) which are typically detectable at up to 20 km (Thompson & Miller, 1990), and the latter transmitted ARGOS locations (45 second resolution) detectable within 100 km. VHF and ARGOS transmitters had an expected battery life of 90 and 69 days, respectively.

All devices were superglued together inside a tag housing (see later) using Loctite® 422 Instant Adhesive (Bearing King Ltd, UK).

Table 5.1. Details of the components used in the tags. ⁱ Only one transmitter used per tag (ARGOS or VHF). ⁱⁱ GTRs can vary depending on duration of deployment; see [GT Products Marine](#). ⁱⁱⁱ Estimate. ^{iv} Price based on the setup incorporating the ARGOS transmitter. ^v Average.

Component	Details of specific model or material	Max dimensions (L x W x H; mm)	Mass (g)	Max Temporal Resolution	Battery duration (days)	Producer	Price per unit (exc. VAT) £	\$
Fastloc-GPS	F3G 133A	63 x 24 x 22	31	15 sec	14	Sirtrack, Hastings, New Zealand	1730	2198
SPOT ARGOS transmitter ⁱ	SPOT-363A	57 x 24 x 19	38	45 sec	60	Wildlife Computers, Redmond, USA	1340	1700
VHF transmitter ⁱ	V2G 152A (Core Marine Glue-On Transmitter)	40 x 20 x 10	16	1 sec	98	Sirtrack, Hastings, New Zealand	132	168
Daily Diary (IMU)	Slim Model	26 x 17 x 5	2	40 Hz	14	Wildbyte Technologies Ltd., Swansea, UK	490	623
IMU housing	30 mm Engineering Grade Translucent Polycarbonate Rod (Code: 4049500030)	76 x 30 x 20	30	NA	NA	Plasticstockist Bay Plastics Ltd, North Shields, UK	2 ⁱⁱⁱ	2.50 ⁱⁱⁱ
IMU housing screws (x2)	M2/A2/70 Stainless Steel Socket Cap Screw	2 x 2 x 10	<1	NA	NA	About Town Bolts, Brentwood, UK	0.05	0.06
IMU housing o-ring	Nitrile Bla 70 ShA	14 (internal diameter) 1.5 (cross section)	<1	NA	NA	Polymax, Bordon, UK	0.26	0.32
IMU battery	EF651625, LTC-7PN, 3.6 V, Lithium Thionyl Chloride, 750 mAh	26 x 17 x 7	8	NA	14	EVE Energy Co., Ltd, Guangdong, China	7 ⁱⁱⁱ	9 ⁱⁱⁱ
IMU Micro-SD Flash card	Example: Kingston MicroSDHC 8 GB	11 x 15 x 1	1.4	NA	NA	Kingston Technology, Middlesex, UK	2.99	3.73
Pressure sensor	MS5837-02BA01 Ultra-Small Pressure Sensor	3.3 x 3.3 x 2.75	<1	4 Hz	14	Mouser Electronics, High Wycombe, UK	16.50	21
Pressure sensor o-ring	No. 73515, High Quality O-ring Seal, Nitrile Rubber (NBR), 70 SHORES	1.8 (internal diameter) 0.8(cross section)	<1	NA	NA	Isoswiss Watchparts SA, Boécourt, Switzerland	0.41	0.51
Galvanic Timed Release (GTR)	G5 - 7 Day ⁱⁱ	46 x 11	6 ^v	NA	10-14	GT Products Marine, Ford, UK	1.40	1.80
Flotation	Microsphere-resin (cf. Whitmore et al., 2016; Appendix S5)	60 x 115 x 40	80 ^v	NA	NA	<i>Microspheres:</i> Omega-Spheres @ Osthoff Omega Group, Germany . <i>Resin:</i> Vosschemie, Uetersen, Germany	3.50 ⁱⁱⁱ	4.50 ⁱⁱⁱ
Tag	Floreon 3D PLA	130 x 50 x 30	45	NA	NA	Floreon, Sheffield, UK	3.50 ⁱⁱⁱ	4.50 ⁱⁱⁱ
Lead counterbalance	Code 3	1.32 (thickness) Diameter cut to measure	50 ^v	NA	NA	Roofing Superstore, Plymouth, UK	1 ⁱⁱⁱ	1.25 ⁱⁱⁱ
Baseplate	Floreon 3D PLA	115 x 75 x 3	18	NA	NA	Floreon, Sheffield, UK	0.80 ⁱⁱⁱ	1.00 ⁱⁱⁱ
Bungee cord	Venture Zone Premium Shock Cord	3 (diameter); length cut to measure	<1	NA	NA	Lightstock, Cranbrook, TN17 9EH (purchase via Amazon)	0.28 ⁱⁱⁱ	0.35 ⁱⁱⁱ
Total ^{iv}	NA	210 x 115 x 40	322.4 ^{iv, v}	NA	NA	NA	3599.74 ^{iv}	4571.58 ^{iv}

5.3.3 Tag design and flotation

The tag shape was designed using computer-aided design (CAD) with guidance from aerospace engineers (Evans and Naumann, *pers. comms.*). The final tag had maximum dimensions of 210 x 115 x 40 mm with a tapered design (Fig. 5.1) to mitigate drag impact. A small, raised section at the nose of the tag locked it into a baseplate. Tag housings were 3D-printed using a MakerBot Replicator+ from biodegradable 'Floreon' filament (Floreon, Hesse, UK). The tag design included an extension of the lower section at the rear (Fig. 5.2), creating a tray on which a float could be attached. The float was made following Liebsch (2006), with a 70:30 mixture of epoxy glosscoat resin (Vosschemie, Uetersen, Germany) and hollow glass microspheres (Omega-Spheres® Osthoff Omega Group, Germany). The float was wedge-shaped to aid stability at the surface and was painted orange for greater visibility when floating at sea (Fig. 5.1). I provide a step-by-step protocol for float preparation in Appendix S5.5.

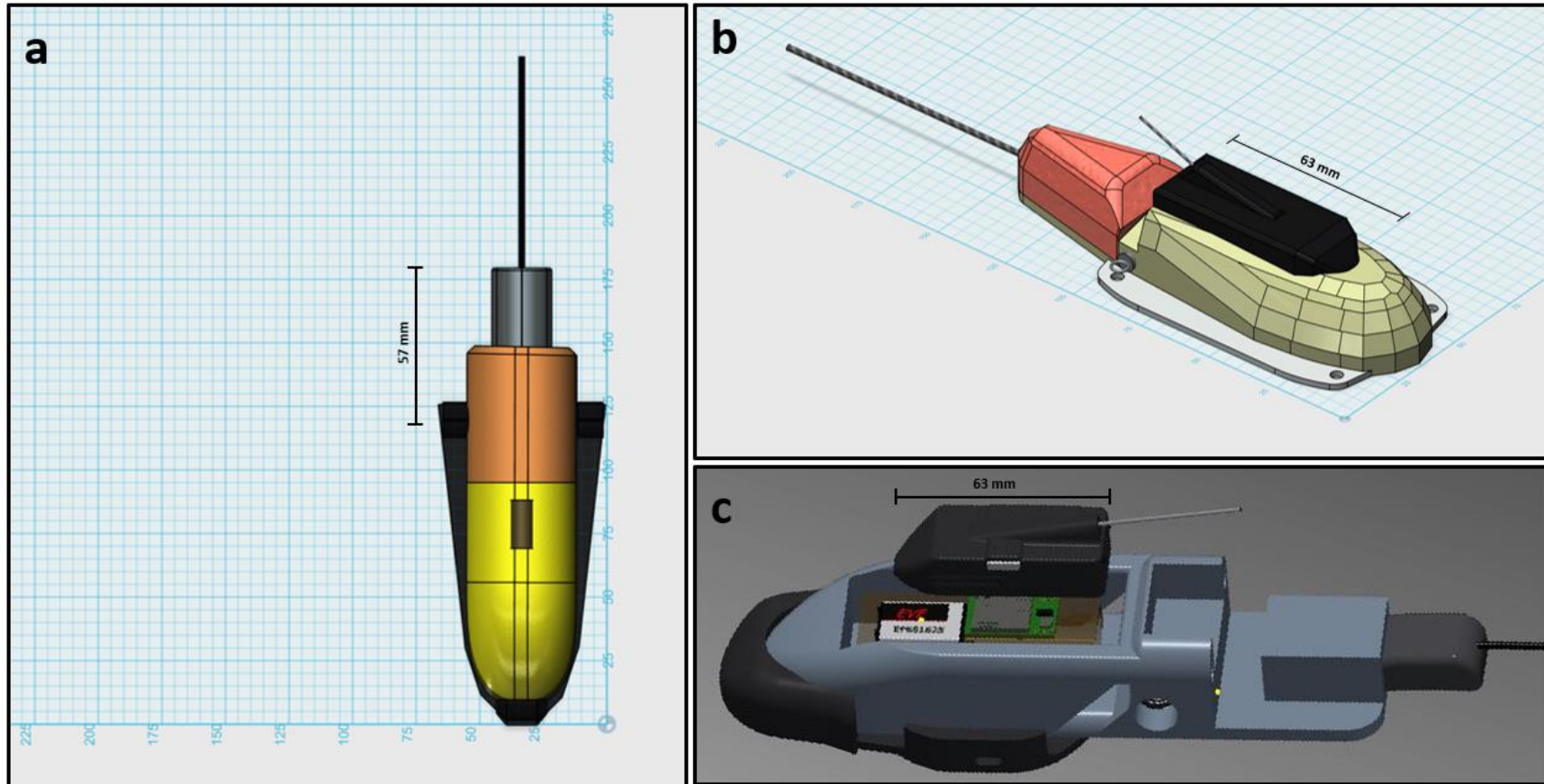


Fig. 5.1. Iterative tag designs were drawn using CAD software. (a) An early design for a tag comprising of only a SPOT (grey with antenna) and DD (DD not shown; positioned underneath). Orange section is the flotation device. Yellow is the 3D printed portion of the tag. Brown is the position of GTR. Black is baseplate. (b) A later design featuring a VHF transmitter set into an orange float at the rear (antenna visible only; extruding backwards). Yellow is 3D printed portion. DD not shown (positioned underneath the Fastloc-GPS; black). Baseplate in light grey at bottom with galvanic release positioned at tag midsection (grey). (c) Final design (shown with VHF device as transmitting unit; grey, rear). Turquoise is 3D printed portion. Fastloc-GPS (dark grey) shown raised above DD (for aid of visualisation, later sunk down into DD housing groove). Float not shown here but this was added on to the rear portion of the tag, engulfing the VHF device. Baseplate with raised sides and contoured edges shown in black at bottom. GTR positioned at bottom, midpoint in circular cavity.

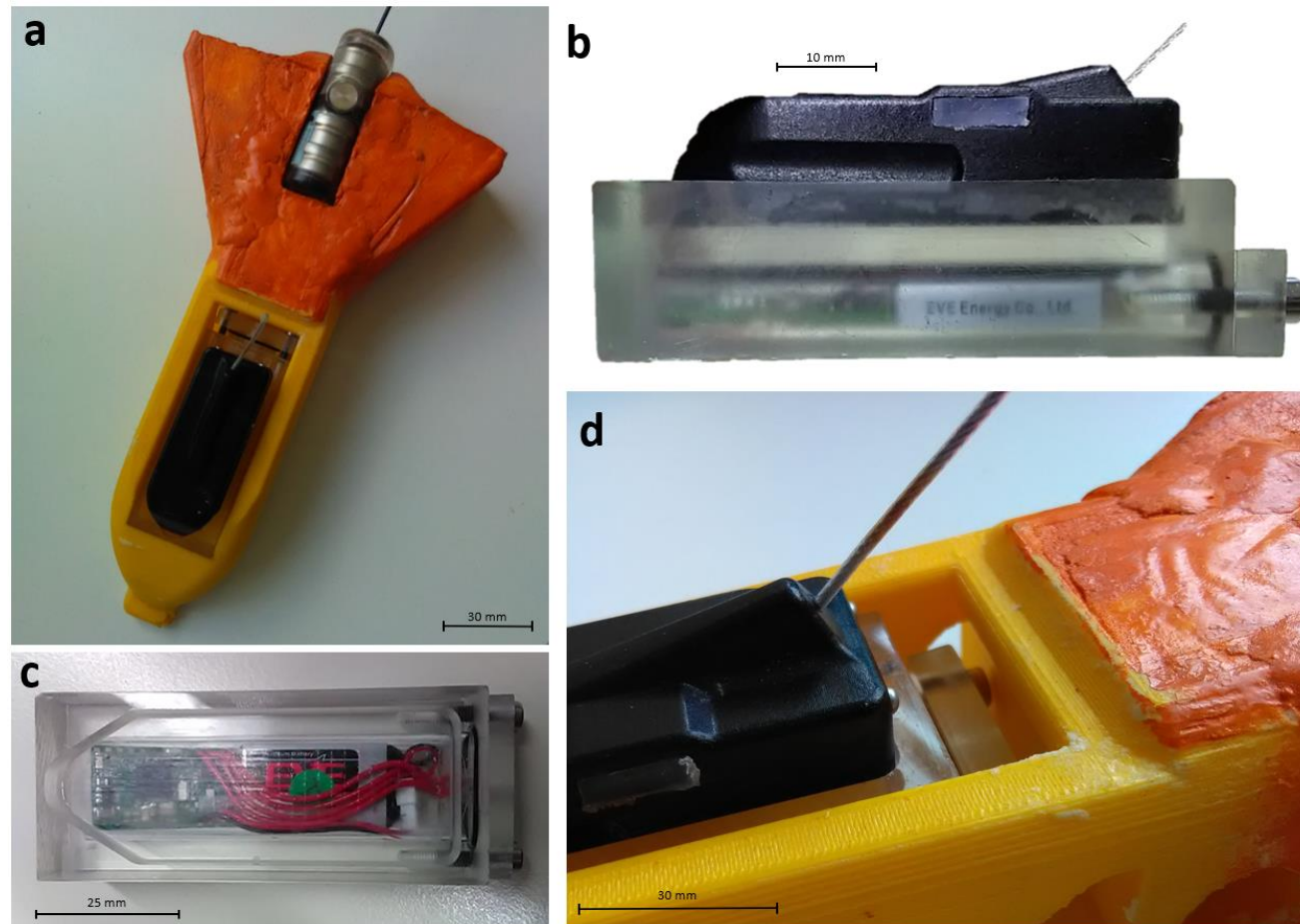


Fig. 5.2. The final tag design featuring the SPOT device as the transmitting unit (instead of the VHF transmitter). (a) Complete tag featuring SPOT at rear and DD forward underneath Fastloc-GPS device. (b) Arrangement of DD (below) and Fastloc-GPS (black) devices in DD housing. The DD was accessed via the rear screw, and the Fastloc-GPS device could be programmed via a USB connection hidden by a silicone bung (light grey, top). (c) DD only shown in transparent polycarbonate housing highlighting wiring; 4 wires at top (all red) run over the battery to the rear pressure sensor, 2 wires at bottom (1 black, 1 red) run to the white battery connector. (d) Close-up of DD housing and Fastloc-GPS device positioned in central cavity of the tag. A groove was cut in the side of the tag to let water drain to enable correct functioning of the SWS and pressure sensor onboard the Fastloc-GPS and DD respectively.

5.3.4 Baseplate and release mechanism

The baseplate consisted of a small plate with a raised frontal section housing a groove for the nose of the tag to fit into (Fig. 5.3). Two raised side sections with slots were incorporated into the design to hold the release mechanism (Fig. 5.4). Both the raised front and side sections were contoured to encourage the smooth reattachment of water flow over the top and along the sides of the completed tag.

The release mechanism consisted of a GTR (GT Marine Products, UK) placed within a small cavity towards the rear of the tag (Fig. 5.4). This connected the tag to the baseplate via elastic bungee (3 mm) cord (VentureZone, UK). The bungee cord was secured at the raised side sections using cable ties (Fig. 5.4). The cords were tightly tensioned, forcing the nose of the tag into the raised groove at the front of the baseplate; holding it in place even when considerable force was applied in the aft direction. This secure attachment was essential to prevent the tag from moving independently of the animal when moving through water as this would generate unwanted noise in the data, or worse, risk early detachment of the tag. The slight downward angling of the bungee cord served to hold the tag downwards on to the baseplate, preventing it from lifting.

The diameter of the GTR shrinks over time due to corrosion (Whitmore et al., 2016) and the tightly tensioned bungee cord compensated for this. Ample free space was provided around the GTR to allow debris to wash out of the cavity following corrosion. The mechanism worked such that once the GTR had corroded completely, the two bungee cords retracted, drawing the eyelets of the GTR out from the cavity and allowing the tag to free itself from the baseplate.

The GTRs used were variable in their expected corrosion rates and were selected based on the ambient water temperature and salinity expected during deployment (Appendix S5.8), as well as accounting for anticipated haul-out behaviour of seals (20–30% of their time; see Leeney et al., 2010 and references therein). This is because the GTR only corrodes whilst submerged in seawater.

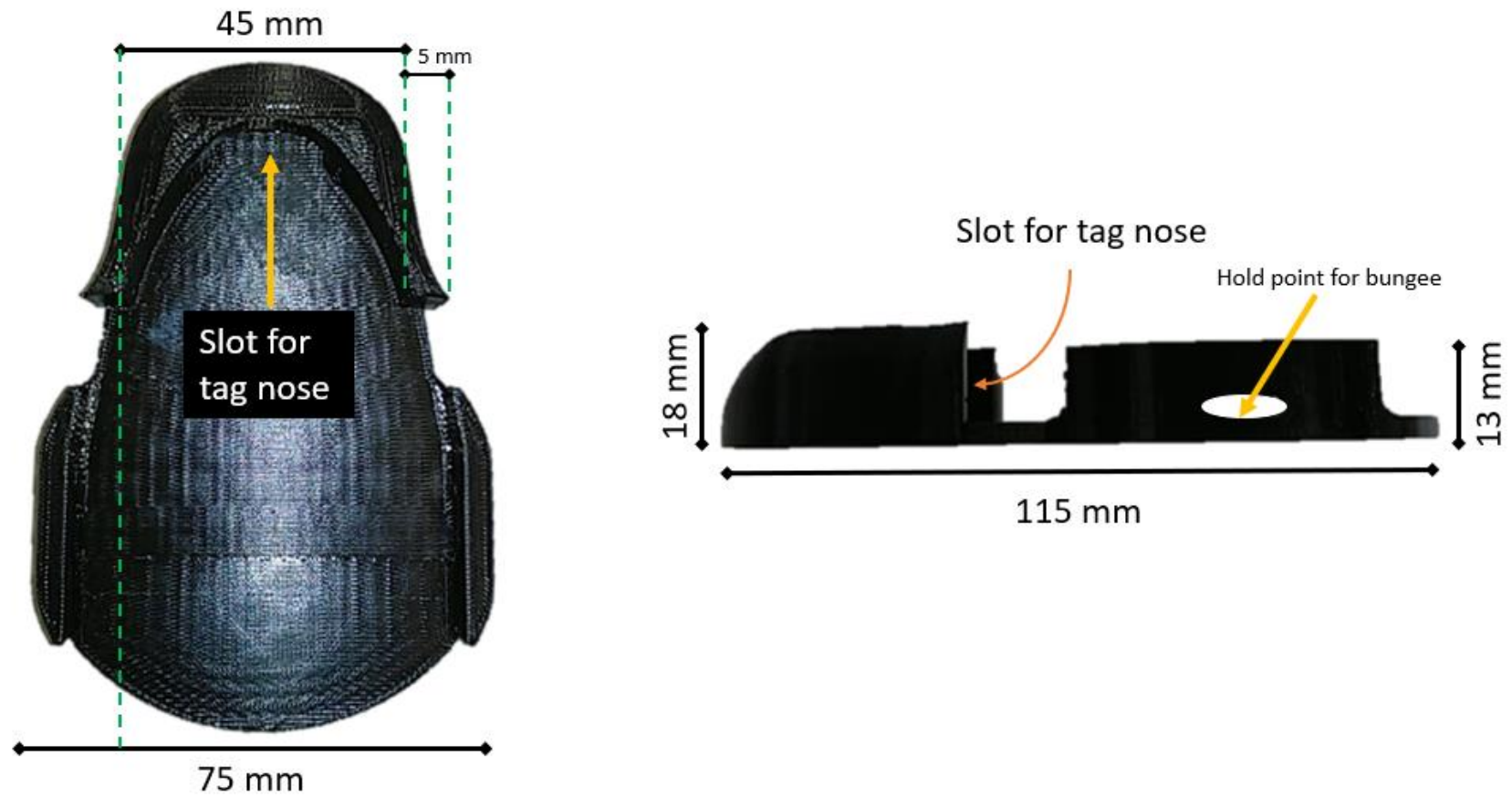


Fig. 5.3. Final baseplate design as 3D printed in Floreon 3D. Note the smoothing contours of the raised sections designed to increase reattachment of water flow.



Fig. 5.4. Attachment of the tag housing to the baseplate using release mechanism. (1) GTR positioned in cavity and secured to raised side sections via bungee threaded through the GTR eyelet (2) The bungee was cut to measure here and secured in position using a cable tie. (3) Open side section to allow water to drain. (4) The nose of the tag slots into a groove in the baseplate. Insets (a), (b), and (c) show side, front, and top profiles, respectively.

5.3.5 Tag deployments¹

Harbour seals were caught on land using seine nets (Jeffries et al., 1993) at Lorenzensplate (54.43 N, 8.62 E; Fig. 5.5) under the licensing and permits of ITAW, Büsum (Permit No. Az V312-72241.121-19 (70-6/07) and V244-3986/2017 (17-3/14) of the Ministry of Energy, Agriculture, Environment and Rural Areas of Schleswig–Holstein, Germany). Grey seals were caught at Ramsey (51.86 N, - 5.34 E; Fig. 5.5) in hoop nets using rush and grab techniques (Sharples et al., 2012) under the licensing and permits of the Sea Mammal Research Unit (SMRU), St Andrews (UK Home Office license #60/4009 in accordance with the Animals Scientific Procedures Act 1986). The tag, via the baseplate, was glued directly to seal's pelage between the shoulder blades (Fig. 5.6) using superglue (Loctite® 422 Instant Adhesive). When attaching the tag to the seal's pelage, downward pressure was applied on the tag for 7–10 minutes (whilst the animal was restrained) to ensure the glue was well set (Nachtsheim, *pers. comms.*).

I deployed 9 tags in total: 7 on harbour seals in Lorenzensplate, Germany, and 2 on grey seals in Ramsey, Wales (Table 5.2). In addition to the GTR release mechanism, the baseplate of tags 8 and 9 were glued to a piece of hardboard which was itself glued directly to the seal's pelage. This was an experimental setup, suggested by SMRU, to test if the hardboard would slowly disintegrate over time allowing the baseplate to detach prior to the seal's annual moult.

In an attempt to recover the tags, 15 extensive search efforts were undertaken via foot (12) or on boat (3) with active VHF, UHF or ARGOS tracking (Table 5.3). The search efforts for tags deployed in Germany covered from Büsum to Vejers, whilst for tags deployed in Wales this covered between Skomer and Ramsey Island. Unlike for the tags deployed with SPOT transmitters (tags 5–9), tags deployed with VHF transmitters (tags 1–4) did not provide any remote indication of their whereabouts prior to undertaking search efforts, as these tags did not transmit their location to satellites (this was also the case in tags deployed with SPOTs if these devices failed). Recovery efforts for these were

¹ Note that in addition to the 9 tags described in the main text, I deployed three additional tags of an earlier design in October 2017; all details of these are outlined in Appendix S5.4.

hence based on *a priori* understanding of seal movement patterns from previous tagging projects conducted in these regions. Specifically, adult harbour seals tend to remain within the Wadden sea area for 5–7 days before heading northwards to undertake foraging trips, returning to their start point after 16–19 days (Liebsch, 2006; Chapter 4). Adult grey seals tagged in Ramsey were expected to stay relatively close to their point of origin, conducting central place foraging trips to no more than 50 km offshore for around 7–10 days at a time (Carter & Moss, *pers. comms.*). Tags deployed with SPOT transmitters could provide real-time position information to guide search efforts. If SPOT tags failed, searches were conducted in line with the strategy for VHF tags. In addition to these 15 active search efforts, I also relied on opportunistic tag recovery by members of the public. Accordingly, I labelled the underside of each tag with details of a return address and telephone number to contact to claim a reward should a member of the public have found a tag (Fig. 5.7; Appendix S5.4).

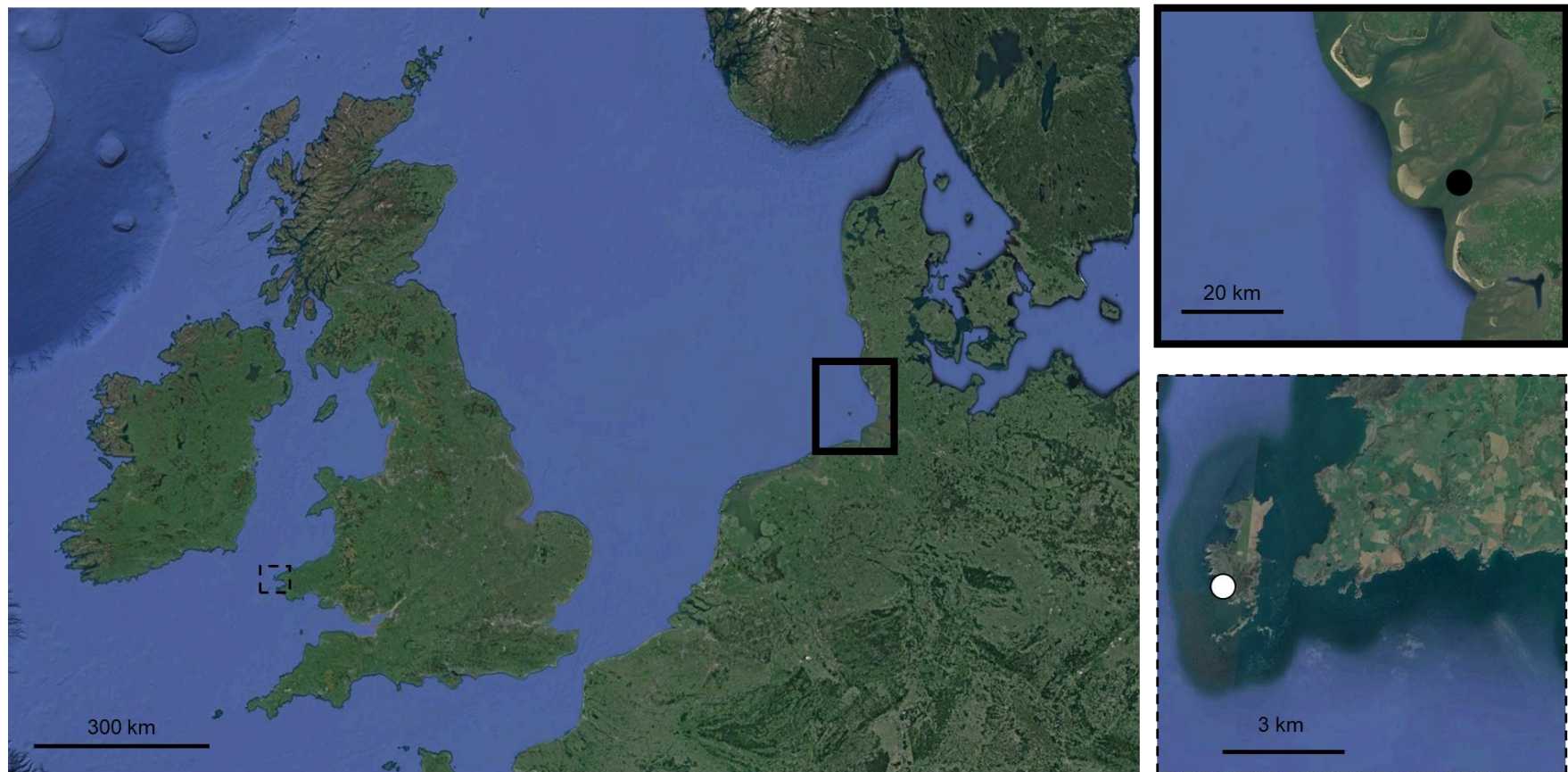


Fig. 5.5. Tagging sites of seals. Top right: Lorenzensplate (54.43 N, 8.62 E; black dot). Bottom right: Ramsey (51.86 N, - 5.34 E; white dot).



Fig. 5.6. Deployment of tag on harbour seal. Tag with SPOT transmitter shown in (a), tag with VHF transmitter shown in (b)-(e). (a) Gluing tag to pelage. (b) Tag glued to restrained seal. (c) Seal with tag moving across land. (d) Seal with tag entering water. (e) Seal with tag swimming at surface. All work undertaken in line with Permit No. Az V312- 72241.121-19 (70-6/07) and V244-3986/2017 (17-3/14) of the Ministry of Energy, Agriculture, Environment and Rural Areas of Schleswig-Holstein, Germany.

5.4 Evaluation

5.4.1 General tag characteristics

The combined mass (in air) of the tag, complete with all electronic devices, baseplate, and release mechanism, was 322.4 g; lighter than or similar to biologging tags typically deployed on grey and harbour seals that range between 305–680 g (median = 370 g) (Carter et al., 2016; SMRU Instrumentation). The tag weight was equivalent to 0.1 % of an average adult grey seal (325 kg; Hall & Russell, 2018) and 0.2 % of an average adult harbour seal (165 kg; Teilmann & Galatius, 2018); considerably below the 5 % recommended tag mass limit (Casper, 2009). The tag displaced 280 ml of water and required a lead counterbalance weighing 50 g (included in the 322.4 g total) to make it sink. The tag had a buoyant force of 0.34 N, equating to 0.1 % of the buoyancy of an average adult grey seal (-34.2 N; Beck, Bowen, & Iverson, 2000); well within the 5 % change in buoyancy that could be considered to have significant impact (Grusha & Patterson, 2005; Gleiss et al., 2009)². The total cost of the device (Table 5.1) was 64 % less than a commercially purchased equivalent (Mikkelsen, *pers. comms.*; cf. Mikkelsen et al., 2019). The custom-built float was approximately 0.5 % the cost of a commercial equivalent (Wildlife Computers, *pers. comms.*).

The tags were robust and durable. All pressure tests conducted prior to deployment were successful, with no water ingress. The tags that were recovered were found to be in good condition with only minimal abrasions or cosmetic damage (Fig. 5.7). The floats of these tags were in good condition suggesting that the flotation and buoyancy of tags were not at risk during deployment. That said, I cannot determine the potential failure of tags that were not recovered, and it is notable that only the tags deployed on harbour seals, in a TSE environment with soft-sediment, were later recovered (see 5.4.2). It is possible that tags deployed on the rocky shores inhabited by (the

² To my knowledge there are no quantitative values in existing literature for average harbour seal buoyancy. However, like grey seals, they are (qualitatively) noted as being slightly negatively buoyant (Ramasco et al., 2014). As the buoyant force of my tag was similar in magnitude to comparable tags deployed on *P. vitulina* (Mikkelsen et al., 2019), I anticipated that the tag would not notably affect the buoyancy of harbour seals.

considerably larger) grey seals suffered some damage. The reward labels were in good condition on the tags recovered except for one tag (tag 7) which showed a relatively greater sign of wear (Fig. 5.7), though the essential details remained clearly visible for the tag to be returned by the member of the public who discovered it. All of the tags that were recovered showed no signs of water ingress (but see Appendix S5.4 for issues with other tags trialled), and all electronic devices were fully functional in post-recovery testing.



Fig. 5.7. Recovery condition of tags. (a) Tag 2 recovered near Westerheversand Lighthouse. (b) top and (c) bottom of tag 4 showing minimal abrasions after recovery at Nordstrand. (d) Tag 7 recovered at Westerhever. Inset: Close up shows the abrasions to the tag reward label. (e) Tag 7 close up of Fastloc-GPS showing minor cosmetic damage.

5.4.2 Release mechanism

Of the 4 tags recovered, 2 detached after their expected duration of 6.5–9 days, 1 tag after 7 hours and the other sometime within the 48 hours (Table 5.2). I observed a small deposition of salt crystals inside the cavity two tag housings owing to the GTR drying out. This may have contributed to a slightly extended attachment duration. Tag detachment after 7 hours is disappointing given the successful retention of other tags. However, the premature release of 1 tag was likely influenced by the fact that constraints during fieldwork meant that insufficient time was available to allow the glue to set when attaching the device to the animal.

One tag deployed on a grey seal in Ramsey Island suffered a premature release. *H. grypus* are approximately 110 kg heavier than *P. vitulina* on average, and on Ramsey Island they haul-out on rocky beaches or in caves, whereas the harbour seals in Lorenzensplate haul-out on sandy shores. Thus the risk of tag damage is greater in the former than the latter. The tag deployed using only the hardboard release mechanism remained attached to the animal for several weeks. This tag was never recovered so I am unable to evaluate if the hardboard served as a viable attachment and release mechanism.

Table 5.2. Tag deployment and summary information. Further details provided in text. All tags listed here were of the final design type including either a VHF or SPOT transmitter. Note that three additional tags of an earlier design were deployed prior to these (in October 2017); these are detailed in Appendix S5.4.

Tag	Transmitter	Baseplate ³	GTR	Species	Region	Age	Sex	Deployed	Recovered	Data	Issues	Positives
1	VHF	Large	D4	<i>P. vitulina</i>	Lorenzensplate	Adult	M	18/04/2018	NA	NA	NA	NA
2	VHF	Large	D4	<i>P. vitulina</i>	Lorenzensplate	Adult	M	18/04/2018	09/05/2018	Fastloc-GPS (7 days) DD (8 days)	DD malfunction after 20 hours	GTR released as expected. Good condition.
3	VHF	Large	D4	<i>P. vitulina</i>	Lorenzensplate	Adult	F	18/04/2018	NA	NA	NA	NA
4	VHF	Large	D4	<i>P. vitulina</i>	Lorenzensplate	Adult	M	18/04/2018	25/05/2018	Fastloc-GPS (7 hours) DD (13 days)	Premature release hence Fastloc-GPS and DD only 7 hours	Tag in good condition.
5	SPOT	Small	D6	<i>P. vitulina</i>	Lorenzensplate	Adult	F	13/09/2018	NA	ARGOS (7 days)	SPOT failed after 7 days	NA
6	SPOT	Small	D6	<i>P. vitulina</i>	Lorenzensplate	Adult	F	13/09/2018	NA	ARGOS (13 days)	SPOT failed after 13 days	NA
7	SPOT	Small	D6	<i>P. vitulina</i>	Lorenzensplate	Adult	F	13/09/2018	25/09/2018	ARGOS (19 days) Fastloc-GPS (9 days) DD (6 days)	Logging hours set to 144.	GTR released as expected. Good condition.
8	SPOT	Small + Hardboard	D4	<i>H. grypus</i>	Ramsey	Adult	M	18/04/2019	19/04/2019	ARGOS (20.5 days)	Premature release.	NA
9	SPOT	Small + Hardboard	D4	<i>H. grypus</i>	Ramsey	Adult	F	18/04/2019	NA	NA	SPOT failed	NA

³ For further details about each baseplate, see Appendix S5.6.

Table 5.3. Details of search efforts and tag recoveries. Land searches (L) and boat searches (B). Details of the search efforts for the three tags deployed in October 2017, including a search by plane, are provided in Appendix S5.4.

Date	Search	Tracking	Details
26/04/18	L1	VHF	Searched various places along the dike between Büsum and Lorenzensplate. Strong but intermittent VHF signal picked up from tag 3 and weak signals from tags 1 and 2 at Husum Bay. Nothing heard from tag 4.
02/05/18	L2	VHF	Searched between Sankt Peter-Ording and Westerhever. Tag 2 heard again but no others.
03/05/18	B1	VHF	Searched between Sankt Peter-Ording and Westerhever. Tag 2 heard again and a few signals from tags 1, 3 and 4 though these were coming from different directions. The signal from tag 2 was clear but locating the signal proved difficult.
04/05/18	L3	VHF	Searched between Westerhever and Lorenzensplate. Clear signal again from tag 2 by Westerheversand Lighthouse, with a possible faint signal from tag 1 between Westerhever and Lorenzensplate.
09/05/18	L4	VHF	Searched Westerhever, specifically towards the lighthouse to try to find tag 2. Clear signal from tag 2 which was recovered near Westerheversand Lighthouse.
17/05/18	L5	VHF	Searched the dike around Nordstrand. No signals detected from any of tags 1, 3 or 4.
25/05/18	NA	NA	Tag 4 recovered by beachgoers at Nordstrand.
09/06/18	L6	VHF	Searched along the dike as far north as Sylt but nothing heard from tags 1 or 3.
25/09/18	L7	UHF	Searched Westerhever and found tag 7 but did not hear either of tags 5 or 6.
07/10/18	L8	UHF Goniometer	Search the dike as far north as Sylt. Heard a signal from tag 6 from Sylt when stood on the mainland. Specifically, pings every 90s (haul-out mode) were heard which suggested the tag was dry.
10/10/18	L9	UHF Goniometer	Searched between Hörnum and Westerland. Heard the signal again from tag 6 but this time every 45s which suggested the tag was in the water again.
18/10/18	L10	UHF Goniometer	Searched as far north as Sylt but could not detect a signal from any of the tags.
24/10/18	L11	UHF Goniometer	Searched Sankt Peter-Ording, Osterhever and Nordstrand. No signals detected.
06/11/18	B2	UHF Goniometer	Searched by boat along the coastline from Sylt to Røm but did not detect signals from any tag.
05/12/18	L12	UHF Goniometer	Search from Vejers to Rømmø but no signals detected.
19/04/19	NA	NA	Tag 9 recovered in Porth Lleuog by Ramsey warden during walk around the island.
12/05/19	B3	UHF Goniometer	Searched St Bride's Bay between Skomer and Ramsey islands. Tag 9 was heard numerous times but it was difficult to localise the signal and get an accurate direction. Entered several caves including both capture site and another dense haul-out but nothing to be found.

5.4.3 Tag recovery

Of the 4 tags that were recovered, 2 of these were found via active recovery efforts and 2 were found by members of the public. Of these, 2 out of 5 tags with SPOT transmitters were recovered whereas 2 out of 4 tags with VHF tags were retrieved. A further 4 tags were detected on one occasion or more but were not found. 1 tag was never detected and was not found. Tags were detectable during 8 (53 %) of the recovery efforts undertaken (Table 5.3). When detected, VHF transmissions were received at a range of up to 25 km. However, analysis of the trajectories of tags that were not detected but were later recovered demonstrated that several were within 10 km offshore yet went undetected. One tag that was later recovered had no fastloc-GPS data after it had washed up on the beach, suggesting that it had remained wet; this would have prevented it from collection position estimates as these are only attempted when the device is dry (i.e. when animals are at the surface). SPOT tag performance was relatively poor with tags frequently ceasing to uplink positions to satellites after 6–32 days.

5.4.4 Data collected and seal movements

Data obtained

Most of the tags (6 of 9; 66%) collected usable high-resolution data for between 7 hours to 20.5 days although 3 tags collected no data or partly malfunctioned (Table 5.2). All tags that were physically recovered (4 of 9) had collected data on all devices, although some errors in data acquisition occurred (Table 5.2).

Tags recorded DD data ranging from 20–334 hours (Table 5.4; Fig. 5.9). DDs enabled the collection of high-resolution 3D movement data from individuals in TSEs (Fig. 5.9), and provided insights into the post-release behaviour of grey and harbour seals. Tag 7 collected 144 hours of data (Table 5.3) but should have collected more – this was a result of human error in programming the maximum recording duration, not an error with the device *per se*. 2 of the DDs recovered had suffered from device error (Table 5.2); one minor and one severe. In the minor case, small episodes of “flatlining” were observed in one

channel of the data record suggesting that the DD was experiencing issues in functionality (Fig. 5.9). In the severe case, after 16.5 hours of tracking time the DD ceased to function with complete flatlining of data across all channels (Table 5.2), albeit the recording duration of this DD totalled 334 hours (Table 5.4).

Fastloc-GPS data were collected over 156–216 hours (Table 5.2, 5.4) and showed no errors in the data acquired (Fig. 5.8). Likewise ARGOS data acquired were without fault, with recording durations lasting 168–492 hours (Table 5.2, 5.4; Fig. 5.10).

Table 5.4. Recording durations of tag deployments. For details, see text and Tables 5.2, 5.4.

Tag	Recording duration (days)		
	Daily Diary	Fastloc-GPS	ARGOS SPOT Tag
2	0.83	7	NA
4	13.9	6.5	NA
5	NA	NA	7
6	NA	NA	13
7	0.25	216	19
8	NA	NA	20.5

Seal movements

Seals tracked from Lorenzensplate moved a total distance of between 3–86.9 km from the tagging site (Fig. 5.8) and conducted trips out to sea reaching 9–75 km offshore as well as conducting periods of rest on land. Individuals were seen to make extensive use of the tidal channel at the edge of the Lorenzensplate sandbank, moving back and forth through this area (Fig. 5.8) and diving to depths of between 0.5–28.8 m (Fig. 5.9). Seals spent a maximum of 26.9 % of their time hauled-out. Data obtained from the seal tagged in Ramsey demonstrated that it travelled as far as 18 km offshore into the St George’s channel.

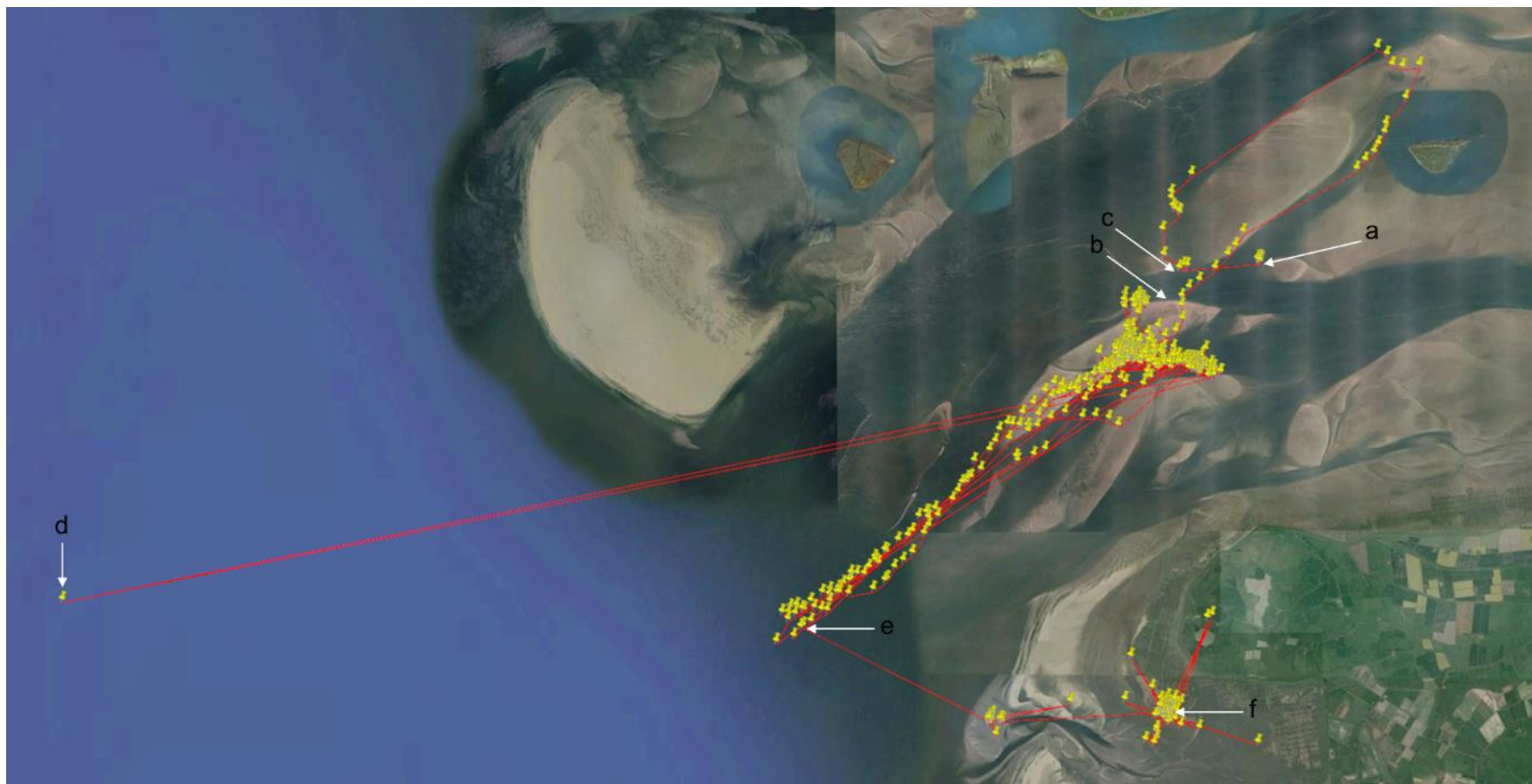


Fig. 5.8. Example of a fastloc-GPS trajectory (collected by tag 2). (a) Locations collected whilst on board the tagging vessel 2 hours prior to tagging. (b) The location of the tagging site (54.439167 N, 8.643889 E). (c) The location of the first GPS position collected by the tag whilst attached to the animal indicating that the animal swam immediately north from the tagging site after release. This position was collected 19 mins after the animal first entered the water. (d) Erroneous record. (e) The final GPS location collected before the tag detached from the animal. (f) The location where the tag was eventually recovered at Westerhever.

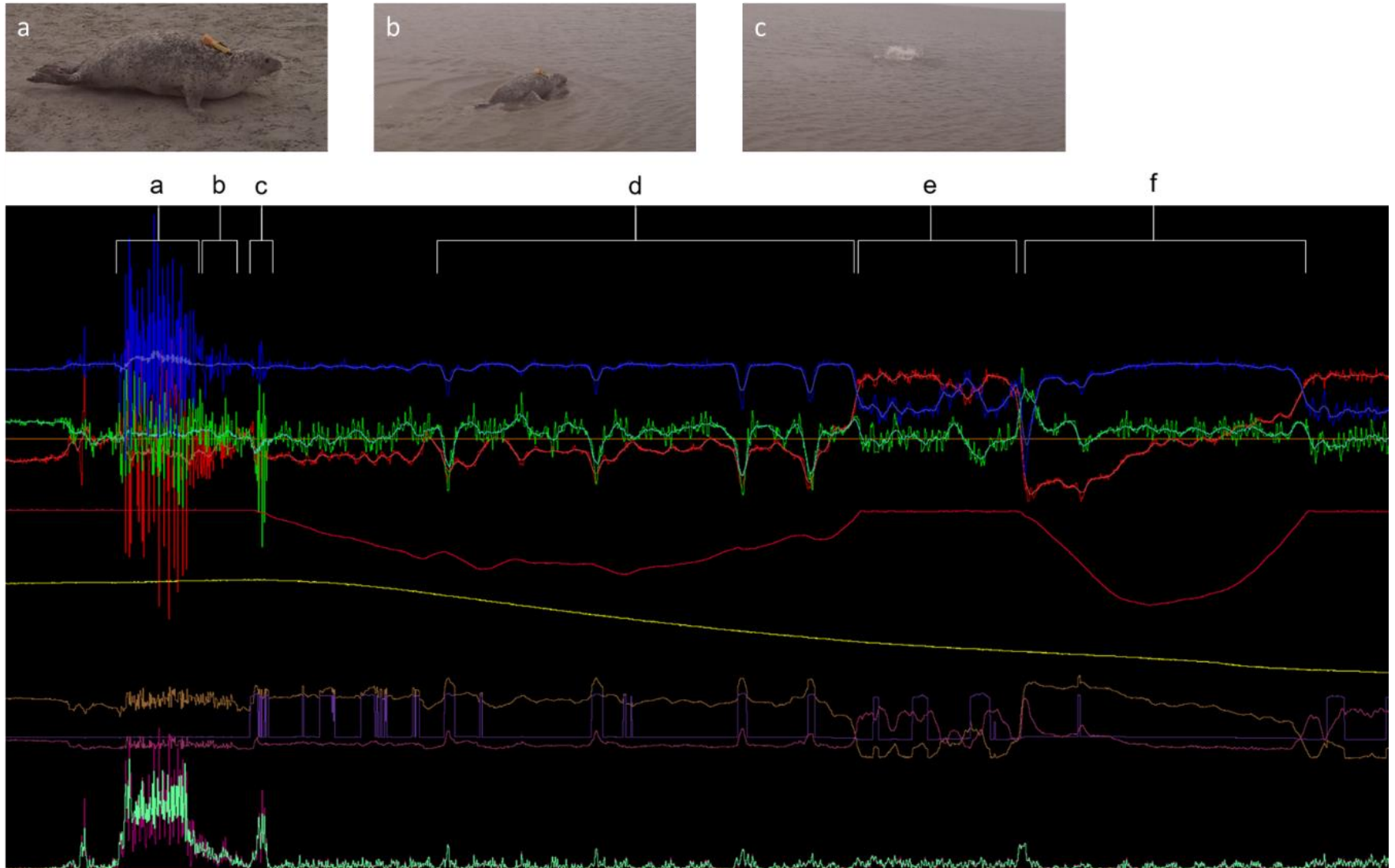


Fig. 5.9. Figure legend overleaf.

Fig. 5.9. Example of high-resolution 3D data obtained from Daily Diary (DD). These data show the moments of a seal immediately after it was released. Full trace is 5 minutes long. Data channels from top to bottom: Blue, acceleration Z (heave); green, acceleration Y (sway); red, acceleration X (surge); red, pressure; yellow, temperature; brown, magnetometry X; purple, magnetometry Y; magenta, magnetometry Z; dark magenta, raw VeDBA; light green, VeDBA smoothed. (a) Seal moving across land immediately after release with relatively high surge, heave, and VeDBA. (b) Seal entering water at shallow depths (tag not yet submerged). Surge and heave decrease as the seal utilises sway motion for forward propulsion. (c) Seal reaches depth at which it can swim normally and bursts forward with high sway from side-to-side tail flipper beats. Note the beginning of occasional flatlining of the magnetometry Y channel (see text). (d) On its first dive after release the seal's sway is relatively high compared to its subsequent dive indicative of rapid movement away from the capture site. The magnetometry is also relatively stable which would suggest the animal was heading in a straight line away from the tagging site. (e) The seal surfaces after its first dive. Note the change in posture from horizontal to vertical, indicated by the swap in position between blue and red channels; the seal surfaced head up. Simultaneously the magnetometry X and Z channels flip indicating the seal had turned 180° to look back at the tagging site. (f) Second dive following release with relatively lower activity and sway, suggesting less urgent swimming. The interpretations made at sections (a), (b) and (c) are validated by a video recording collected simultaneously (stills shown above).

5.5 Discussion

Innovations in practical tools are at the forefront of gaining knowledge for furthering ecology and conservation science (Börger, 2016). In recent years, advancements in, and the miniaturization of, biologging technologies have revolutionised the ability of researchers to study animal movement and behaviour in the wild (Wilmers et al., 2015). Studying the movements of wild marine megafauna in TSEs has become of key interest in recent years because of the growing number of tidal stream energy generating devices such as TSTs being installed in coastal waters (Hastie et al., 2019). These present new anthropogenic threats to wild animals, such as in the form of collision risk (Copping et al., 2020). Understanding the movements of wild animals in TSEs and their potential interactions with TSTs is therefore crucial for assessing the levels of risk (Copping et al., 2016).

A relatively large body of information already exists on the broad- and fine-scale movements of marine megafauna in TSEs (Benjamins et al., 2015; Waggitt et al., 2016; 2017; Lieber et al., 2018; Joy et al., 2018; Hastie et al., 2019; Copping et al., 2020; Isaksson et al., 2020; Onoufriou et al., 2017). However, a paucity of information is available on the very fine-scale movements of individuals in these environments and their near-field behaviour in response to TSTs (Waggitt & Scott, 2014; Hastie et al., 2019; Onoufriou, 2021). With the exception of the use of AAS (Malinka et al., 2018; Hastie et al., 2019), this lack of information stems largely from the inability of methods to study animals with the resolution needed to observe and quantify these behaviours (Hastie et al., 2019; Copping & Hemery, 2020). Here I have attempted to bridge this gap by designing and building a new tag for tracking the very fine-scale 3D movements of wild seals. In particular, the tag that I have developed makes inroads towards three key issues associated with studying the movements of seals in TSEs.

Collection of (vast quantities of) high-resolution data

This tag offers the potential to collect and retrieve vast quantities of high-resolution data, including data on the 3D movements of seals. Such data are urgently required by researchers studying animals in TSEs in order to understand the very-fine scale movements of animals and their near-field responses to operational TSTs (Hastie et al., 2019). Traditional GPS tags are not able to do this, as the need to transmit data to satellites means that only relatively small volumes of data can be obtained (Williams et al., 2020). Tag technology has advanced dramatically in recent years (Holton et al., 2021), and while there are now numerous biologging tags that are able to collect comparably large data volumes, none have yet been demonstrated to be remotely recoverable from wild seals. Hence, although the recovery rate of tags here was poorer than hoped, this tag presents a crucial proof of concept and provides a starting point for future studies (Sequeira et al., 2019).

Combining advanced, multi-sensor loggers with fastloc-GPS

The tag designed here provides the opportunity to combine multiple, independent tracking devices in a single housing. This facilitates the use of multi-sensor loggers (i.e. accelerometers, magnetometers, etc.; Williams et al., 2020) to quantify high-resolution trajectories, together with fastloc-GPS devices that provide accurate positional information. This is key to studying animals in TSEs, as the dynamic nature of these environments means that tags will be susceptible to large drift error (Gaspar et al., 2006; Onoufriou, 2021). Deploying multiple concurrent devices on animals in tandem is not new (Wilmers et al., 2015). Indeed, multiple separate devices have previously been deployed together on individual animals (e.g. Mosser et al., 2014). However, this has predominantly been undertaken in studies examining large, terrestrial taxa (Mosser et al., 2014; Wilson et al., 2014; Williams et al., 2014). Moreover, combining both high-resolution accelerometry sensors and fastloc-GPS devices on marine megafauna has only been achieved by attaching these devices separately rather than combining them in a single package (Wilson, et al., 2015). This has clear implications for animal welfare, as the attachment of

multiple devices results in increased detriment to the individual through increased tagging effort, additional attachment points, and increased drag (Andrews et al., 2019). Recent years have seen “combined accelerometer-GPS” tags, such as Axy-trek dataloggers (Technosmart Europe S.R.L) deployed on marine megafauna (e.g. Scopoli’s shearwaters *Calonectris diomedea*; Cianchetti-Benedetti et al., 2018). However the fundamental distinction between these tags and the one presented here is that the former includes standard GPS whereas the latter includes fastloc-GPS technology. This is crucial, because fastloc-GPS technology is essential for tracking animals that are only observed fleetingly at the surface, such as seals (Carter et al., 2016).

The cost of tags and recovery

The high cost of commercial tags used to research seals (~ £10,000 per unit; Mikkelsen, *pers. comms.*) can preclude their widespread use. Keeping tag cost down is key to obtaining sufficient sample sizes (Rafiq et al., 2019; Sequeira et al., 2019) and this is essential for studying animals in TSEs where variation between environments and between individuals is high (Benjamins et al., 2015; Chapter 2–3). Whilst the cost of the tag presented here is not inexpensive, its cost is approximately one-third of commercial alternatives.

However, it is not just the cost of a unit that is important, recovery rates must also be considered. I suffered a tag loss of 56 %. This suggests that the cost of my tag must at least be doubled if it is to be compared to other available alternatives. Further, the recovery efforts required to retrieve the devices here are non-trivial, often involving high cost for the charter of vessels and associated personnel (Whitmore et al., 2016). Previous studies utilising remote release tags have demonstrated substantially greater recovery rates. For example, Lear & Whitney, (2016) were able to recover 97.4 % of their tags at distances of up to 231 km. These exceptional recovery rates reduced the total effective cost to \$535 per animal studied, 87 % less expensive than the cost for the same work to be undertaken using irretrievable satellite tags (\$4200 per individual; Lear & Whitney, 2016). The tag that I have developed here is the

first of its kind, and with proof of concepts such as these it is typical to obtain low recovery rates (Sequeira et al., 2019). Thus, with future refinements to this tag design – in particular ensuring that the performance of transmitters used for recovery is improved – it may well be possible to achieve much higher recovery rates. This would create a wealth of new opportunities for studying seals in TSEs.

5.6 Perspectives

In lieu of setbacks, my successes provide tentative evidence that tagging seals in TSEs using a remote-release tag is possible, exemplifying the trend of deploying a small number of novel devices in an effort to guide future research (Sequeira et al., 2019). Indeed, the multi-sensor data that I was able to collect are amongst the highest resolution data that exist for wild seals in the areas studied, and indeed for seals in TSEs generally (Onoufriou, 2021). With further refinement, the tag presented here has the potential to be used with even greater success. Moreover, the utility of the data collected can be enhanced by pooling them with data from tags deployed on other animals in the same areas (e.g. Ferreira et al., 2020).

The variation of seal movements in TSEs is high (Benjamins et al., 2015; Sparling et al., 2017; Joy et al., 2018; Lieber et al., 2018; Hastie et al., 2019; Onoufriou et al., 2021). In light of this, *a priori* information on the behaviour of animals in these environments may be initially required to determine whether tracking seals with the tags presented here will be worthwhile. This is because there is no guarantee that animals will enter a study site of interest (Waggitt & Scott, 2014) and being able to anticipate where animals will go is crucial to supporting tag recovery efforts. Moreover, the dynamic nature of TSEs may make recovering tags even more challenging as strong tidal currents could cause tags to drift over long distances, and turbulent conditions make the operation of research vessels difficult (Benjamins et al., 2015).

Future research efforts utilising this tag would benefit from undertaking further study to determine the factors that drive the performance transmitting units.

This was a key limiting factor in the tag presented here, with at least 60 % of SPOT transmitters malfunctioning early. In particular, a combination of both a VHF and SPOT transmitters could improve the ability to recover tags even if one of the transmitters fails.

Chapter 6

Minimising the impact of biologging devices: Using Computational Fluid Dynamics for optimising tag design and positioning

“If this trend continues unabated for the next 15 years... it will be possible to carry out sophisticated aerodynamic design with very small teams, and with the members not necessarily at the same location. Designers in such an era will have the opportunity to fully explore their creative ideas.”
(Jameson & Vassberg, 2001)



A harbour seal departs from the beach after being tagged with a biologging device
(Photograph by Dominik A. Nachtsheim).

6.1 Abstract

Studying the impacts of new anthropogenic threats to marine megafauna (such as tidal stream turbines; TSTs) requires the use of externally attached biologging devices to track individuals in the wild. However, attaching tags to such streamlined taxa can substantially increase the drag experienced by animals, with potentially severe implications for the individuals being studied, as well as introducing bias to the data that are collected. Despite dramatic increases in the sophistication of biologging technology, progress in reducing the impact of tags on animals is less obvious, notwithstanding the implications for animal welfare. Existing guidelines focus on tag weight (e.g. the '5 % rule') but ignore the hydrodynamic drag experienced by aquatic organisms. This can be considerable, especially for animals moving in fast flowing tidal stream environments (TSEs). Designing tags to minimise impact for animals moving in TSEs is not trivial, as the drag impact depends on the position of the tag on the animal, as well as its shape and dimensions. Here, I demonstrate the capabilities of computational fluid dynamics (CFD) modelling to optimise the design and positioning of biologgers on marine megafauna, using the grey seal (*Halichoerus grypus*) as a model species. Specifically, I investigate the effects of (i) tag form, (ii) tag size and (iii) tag position and quantify drag impact under frontal hydrodynamic forces, as encountered by seals swimming at sea. By comparing a conventional vs. a streamlined tag, I show that the former can induce up to 22 % larger drag for a swimming seal; to match the drag of the streamlined tag, the conventional tag would have to be reduced in size by 50 %. For the conventional tag, the drag induced can differ by up to 11 % depending on the position along the seal's body, whereas for the streamlined tag this difference amounts to only 5 %. Given these substantial effects, I conclude that the drag impact of tags must be used as an additional metric for determining if tags are ethical. To facilitate this, I provide a step-by-step guide to assist researchers in quantifying the drag impact of their own devices. This work can directly support researchers studying marine megafauna in TSEs by minimizing the impact of tags on animals.

6.2 Introduction

The growth of the tidal energy industry in response to the need to reduce fossil fuel emissions has created new anthropogenic threats for marine megafauna (Copping et al., 2020). For example, animals may come into contact with novel devices such as tidal stream turbines (TSTs), potentially resulting in displacement behaviour from key habitats (Hastie et al., 2019) or fatal collision (Onoufriou et al., 2019). Establishing the likelihood of risks to marine megafauna is critical to support the tidal energy industry to develop responsibly by informing environmental impact assessments (Copping et al., 2020b).

In recent decades, the use of biologging devices to gather information on the behaviour, movement and physiology of animals has increased substantially (Hussey et al., 2015). In addition to collecting vast amounts of movement and behavioural data (Heylen & Nachtsheim 2018), biologging devices can collect oceanographic data (Roquet et al., 2017; Treasure et al., 2017), and other environmental measures, such as ambient noise levels (Mikkelsen et al., 2019). Studies using biologging devices have revealed some of the most extreme feats of animal biology, such as the deepest dive (2992 m by the Cuvier's Beaked Whale *Ziphius cavirostris*; Schorr et al., 2014) and the longest migration (80,000 km by the Arctic tern *Sterna paradisaea*; Egevang et al., 2010). Biologging studies have also proven to be essential in improving species conservation (Fraser et al., 2018). Crucially for the TST industry, biologging data can be used to track the movements of animals in tidal stream environments (TSEs) where devices are planning to be installed. Indeed, data collected from tags attached to animals can be used to quantify the overlap of animals with TSTs (Isaksson et al., 2021).

However, the attachment of devices to animals is not without consequence for the animals carrying them (Thorstad et al., 2001; Vandenabeele et al., 2014; Bodey et al., 2017; Wilson et al., 2018). Tag-induced detriment has often been attributed to tag weight (Kenward 2001) which has driven researchers to work within weight-defined bounds (Casper 2009). Indeed, researchers often select their study animals based on the size or weight requirements for the tags, rather than trying to optimise tags for a given species or size class; though

there are examples of specific developments made for very small animals (Stidsholt et al., 2018). Despite this, most studies using tags have so far largely failed to take advantage of technological advancements to reduce the impact of tags on animals (Portugal & White 2018). Crucially, for projects involving tags on aquatic animals, the focus on weight by most existing tag guidelines – e.g. the 3 % or 5 % rule (Casper 2009) – ignores hydrodynamic impacts (most notably drag) which are key in modulating energy expenditure and behaviour during swimming (Culik & Wilson 1991; Cornick et al., 2006; Rosen et al., 2017; van der Hoop et al., 2018). For example, the relative drag of tags with poorly designed hydrodynamics can be up to 60 % greater (Shorter et al., 2014). In addition, increasing the drag of animals being studied may lead to biased data which is not representative of wild individuals (Ropert-Coudert et al., 2000; Barron et al., 2010; Lear et al., 2018). For example, captive dolphins tagged with biologging devices were shown to reduce their speed by 11 % whilst wearing a tag (van der Hoop et al., 2014). Increases in drag thus also raises important ethical concerns for the animal being tagged (Wilson & McMahon 2006). Issues associated with increases in drag are particularly pertinent when studying animals that move in fast-flowing conditions such as those encountered in TSEs because drag is cubed as a function of speed (Wilson, Ropert-Coudert, & Kato, 2002). Thus, examining the impact of drag for animals that move in TSEs is key (Kyte et al., 2019).

Designing minimal-impact tags and testing drag in real systems is however not trivial, as the impact of drag is a complex function of both the position of the tag on the animal as well as its shape and dimensions (Bannasch et al., 1994; Vandenabeele et al., 2015). One approach to assess the effects of tag-induced drag is by *in-situ* modification of the shape and positioning of tags deployed on a subject animal whilst in wind or flume tunnels, or in captivity (Culik et al., 1994; van der Hoop et al., 2014; Shorter et al., 2017). Assessing tags in isolation in wind tunnels is also a viable approach (Vandenabeele et al., 2015). These approaches are beneficial insofar as during live experiments it is possible to observe how animals react to tags under real operational conditions (cf. Pavlov & Rashad 2012; van der Hoop et al., 2018), as well as assessing animal energetics, kinetics and biomechanics, and changes in these

over time (Geertsen et al., 2004; Ropert-Coudert et al., 2007; Rosen et al., 2017; van der Hoop et al., 2018). However, experimental approaches are limited in that they are very time consuming and labour intensive, wind or flume tunnels are not always accessible, and the use of live animals raises ethical concerns and requires appropriate licensing (Kyte et al., 2018). Furthermore, the logistical constraints of working with very large taxa (e.g. cetaceans) often make *in-situ* experiments impractical.

An alternative to experimental approaches uses computational fluid dynamics (CFD) to assess tag-induced drag (Kyte et al., 2018). CFD is the primary tool for virtual design and drag modelling within the aerospace industry (Jameson & Vassberg, 2001) and is notable in being able to model drag with the accuracy of results comparable to physical experiments (Tyagi & Sen, 2006; Jagadeesh et al., 2009; Vassberg et al., 2014); for example Shorter et al., (2014) demonstrated that CFD simulation predictions of tag-induced drag agreed with experimental assessments. Of particular value is that CFD analysis can be implemented quickly and efficiently and can gather repeated, comprehensive measures on hydrodynamic aspects of tag design. As such, CFD analysis can aid the prototyping of biologging tags prior to manufacture by estimating their effects in a virtual environment without the need for experiments (Pavlov et al., 2007; Kyte et al., 2018). Indeed, CFD has the potential to revolutionise biologging tag design (Heylen & Nachtsheim, 2018).

The use of CFD to examine tag design and impact has grown within the biologging community since the mid-2000s (Pavlov et al., 2007) (see Appendix S6.1 for a brief review). Some commercial tag manufacturers utilise CFD to assess tags during product development, though results from these studies are often not published. Indeed, the use of CFD to examine tag-induced drag remains relatively limited in peer-reviewed literature, and its full potential may not yet have been realised. Specifically, while there have been several advances in the use of CFD to design tags and quantify their impact (Appendix S6.1), no publication has yet examined an approach which simultaneously considers device size (Vandenabeele et al., 2015), shape (Shorter et al., 2014) and positioning along the animal's body (Bannasch et al., 1994; Vandenabeele et al., 2014).

Here I address this gap and support ecologists to realise the full potential of CFD for improving tag design and assessing tag-induced drag. Specifically, I (i) evaluate how tag-induced drag varies with device shape, size, and positioning on the animal, (ii) exemplify the efficacy of CFD for tag design, and (iii) provide step-by-step instructions for ecologists to use CFD to efficiently assess the drag impact of biologging tags (Appendix S6.3); facilitating effective, future interdisciplinary collaborations with engineers. This should lead to refined methods for studying animals in TSEs using biologging devices.

6.3 Methods

In addition to this section, I provide a step-by-step guide to modelling the drag impact of tags with CFD simulations using ANSYS FLUENT™, version R15.0 (ANSYS, Inc., Pennsylvania, USA) (Appendix S6.3).

6.3.1 Construction of geometries

I used computer aided design (CAD) software (Autodesk® Inventor LT™, Autodesk Inc., California, USA) to construct and manipulate seal and tag geometries. Note that any modern 3D CAD software package will allow the geometric manipulations necessary to reproduce this work. For the purpose of this study, two tag geometries were considered. The first represented a traditional GPS tag for seals (tag A), as used in Hazekamp et al., (2010), measuring 10 x 7 x 4 cm (length x width x height). The second geometry represented a streamlined tag designed by me (tag B), measuring 11 x 10 x 4 cm. Both tags were designed to contain multiple biologging sensors capable of recording high-resolution data on seal movements and behaviour in TSEs.

The seal geometry was obtained from Hazekamp et al., (2010) in IGES (.igs) format and converted into a solid body for integration with the tag geometries. I chose to use the seal and tag A geometries from Hazekamp et al., (2010) in order to facilitate direct comparison of results. Importantly, the results from CFD simulations (see later) will depend on (and be specific to) the chosen size

of the animal geometry, hence the geometry should be an appropriate reflection of the real animal being studied. My seal geometry was 1734 mm long – within the range of a typical adult female grey seal (McLaren 1993). My main aim was to exemplify the CFD method by assessing effects of size, shape, and position of the main body design of two tags on induced drag. Hence, to maintain simplicity in the CFD modelling (Kyte et al., 2018), external features such as the antennae were removed from both tag geometries (see appendices S6.2 and S6.4 for details).

To prepare the geometries ahead of export to the CFD mesh generation process, I used CAD ‘cleaning’ software (CADfix, International TechneGroup, Inc., Ohio, USA) to ensure that the combined seal-tag solid body was ‘watertight’. This is necessary to allow the subsequent modelling of drag effects of the tag at different positions along the animal’s body.

6.3.2 CFD simulations

I undertook mesh generation, pre-processing and CFD simulations also within ANSYS Fluent™. I first undertook a mesh convergence study to determine the appropriate mesh resolutions required for the simulations. I generated a surface mesh (Fig. 6.1), encompassing the seal body and tag, composed of a finely resolved mesh for the fluid boundary layer around the seal (Fig. 6.1 (a)), and a further (coarser) volume mesh for the remainder of the volume around the seal body (Fig. 6.1(b)) (see Appendix S6.4 for further details). The surface mesh provided the input to ANSYS Fluent’s numerical solver to simulate the flow and determine flowfield properties, such as turbulence, around the animal body under different freestream conditions, and to compute force coefficient outputs. Importantly, the assumption was made that a steady-state solution existed for each (non-dynamic) case, which allows for local time integration within the CFD solver, as a precise time history of the solution was not necessary.

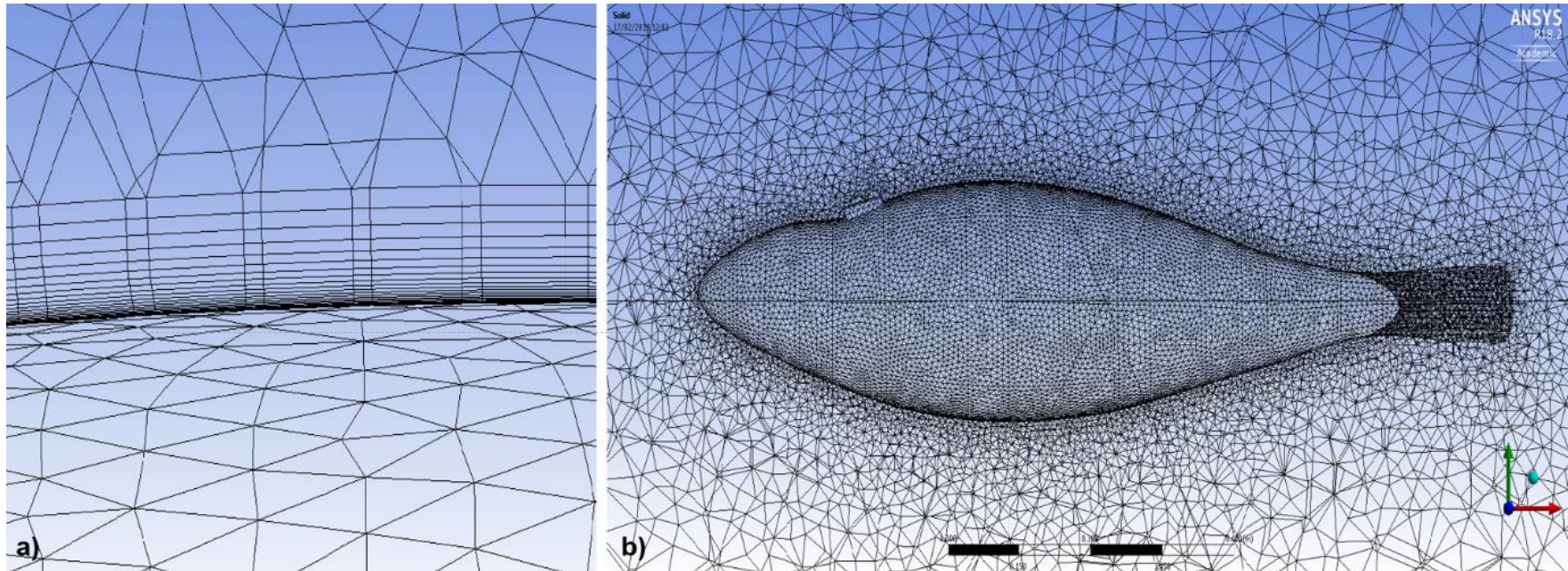


Fig. 6.1. Example of a computational fluid dynamics (CFD) mesh used in this study showing (a) the surface triangulation and 'inflation layers' used to capture the thin boundary layer flow close to the seal surface and (b) the surface grid over the seal and tag, along with a centreline 'slice' through the volume mesh.

Flow visualisations were obtained using the software package EnSight and ANSYS PostProcessing (ANSYS, Inc., Pennsylvania, USA), to provide a qualitative description of the underlying fluid dynamics causing the force coefficient responses observed. A summary of the CFD process is provided in Fig. 6.2 (and refer to Appendix S6.4 for specific details; see also Appendix S6.3).

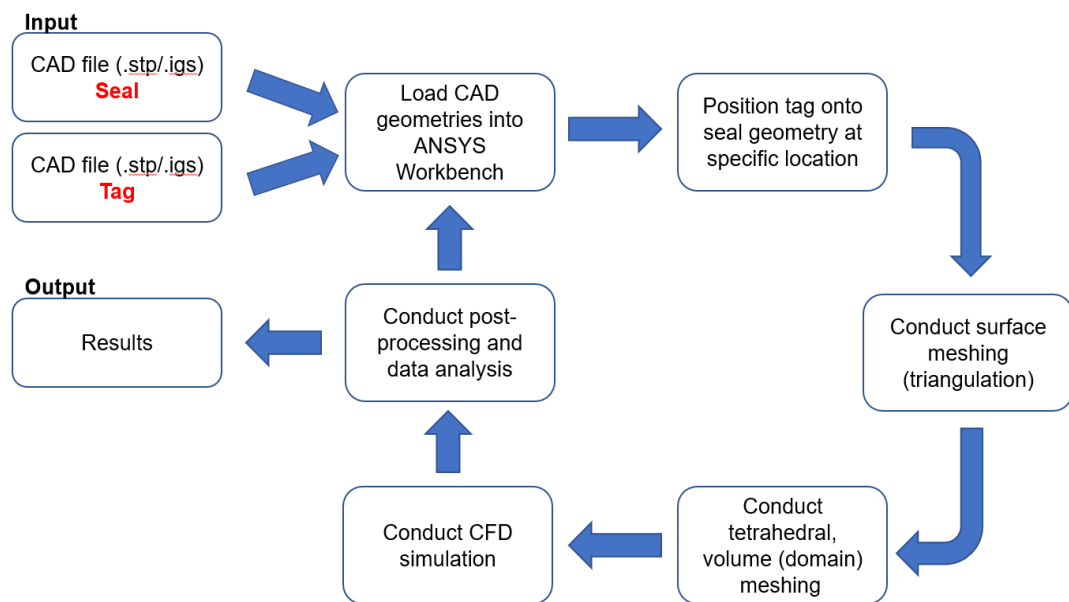


Fig. 6.2. Summary of the computational fluid dynamics (CFD) methodology used for running flow simulations within Ansys Workbench. A detailed step-by-step guide of this process is provided in Appendix S6.3.

Simulations were undertaken using a range of flow speeds (1, 3, 5, 7 and 9 ms^{-1}). These were selected because they are within the typical speeds that seals will encounter when swimming at sea, including resultant speeds – i.e. the resultant combination of seal velocity and current velocity – when seals swim into an oncoming flow (Hazekamp et al., 2010; Kyte et al., 2018; Hastie et al., 2019). This can frequently occur when seals move through TSEs (Hastie et al., 2019). I computed non-dimensional force coefficients in order to verify that non-dimensionalised outputs were insensitive to the absolute input freestream velocity across this range; indeed, all force coefficients collapsed onto a single curve across this speed range, indicating that the force coefficient

response was independent of freestream speed, and that my results remained consistent across the range of velocities modelled. In other words, I verified that the optimum position for each tag was consistent across the full range of velocities investigated i.e. the velocity used to subsequently test for the effects of tag shape, size, and positioning, did not bias these investigations. Thus, a velocity of 5 ms⁻¹ was selected for further investigation because I was particularly interested in the drag effects and performance of tags when flow speed was relatively high; such speeds may be encountered by seals swimming in TSEs (Hastie et al., 2019). For example, seals moving in the Ramsey Sound may experience currents of up to 3 ms⁻¹ (Malinka et al., 2018). Grey seals can swim at up to 2 ms⁻¹ (Gallon et al., 2007) meaning that seals travelling directly into currents could encounter resultant speeds of 5 ms⁻¹.

In line with Pavlov & Rashad (2012) my model was assumed to represent an animal swimming at a constant speed in a rectilinear fashion. While at sea, seals undertake a range of complex 3D motions (Mitani et al., 2003) and move at varying speeds (Williams 2018). Hence, my results cannot account for the full range of movement that a seal exhibits, but instead focus on the predominant forward motion of straight line swimming that seals undertake during transit (Davis et al., 2001). These simplifications are necessary due to the added complexity of modelling the highly unsteady and interacting effects of fluid flow around a non-rigid, moving body (Adkins & Yan 2006); while these analyses are possible and certainly interesting for future studies, they require the use of unsteady, fluid-structure interaction CFD modelling techniques (Adkins & Yan 2006) and were unnecessary for my aims (see also Kyte et al., 2018).

The output from the CFD simulations was the non-dimensional drag coefficient (C_d) for each seal and tag combination. The Reynolds number, Re , of the flow simulations, defined as

$$Re = \frac{\rho VL}{\mu} \quad (1)$$

where ρ is the fluid density (1028 kg m⁻³), V is the freestream flow velocity (5 m s⁻¹), L is the seal length (1734 mm) and μ is the dynamic viscosity of salt water (1.09 x 10⁻³ Pa·s), was 8.2 x 10⁶.

All non-dimensional drag coefficients, C_d , defined as

$$C_d = \frac{D}{\frac{1}{2}\rho V^2 A} \quad (2)$$

where D is the absolute drag value (in Newtons) of each seal and tag combination, were determined for each tag type, at nine discrete positions along the seal's dorsal surface, under frontal flow (zero angle of attack) using the seal frontal area, A (0.134 m^2), as the reference. The nine positions studied ranged from the seal's neck (position 1; 216 mm from the nose) to 1080 mm from the nose (position 9) (Fig. 6.3). These positions were selected as they provide relevant comparisons in the context of tagging grey seals in the wild. Specifically positions 1, 2, and 3 are the most commonly used positions to attach devices to seals (Sharples et al., 2012); positions 4, 5 and 6 are rarely used (Fedak et al., 1983); and positions 7, 8, and 9 were anticipated to be the most hydrodynamic (Bannasch et al., 1994). The comparisons of C_d values are for the combined seal-tag body.

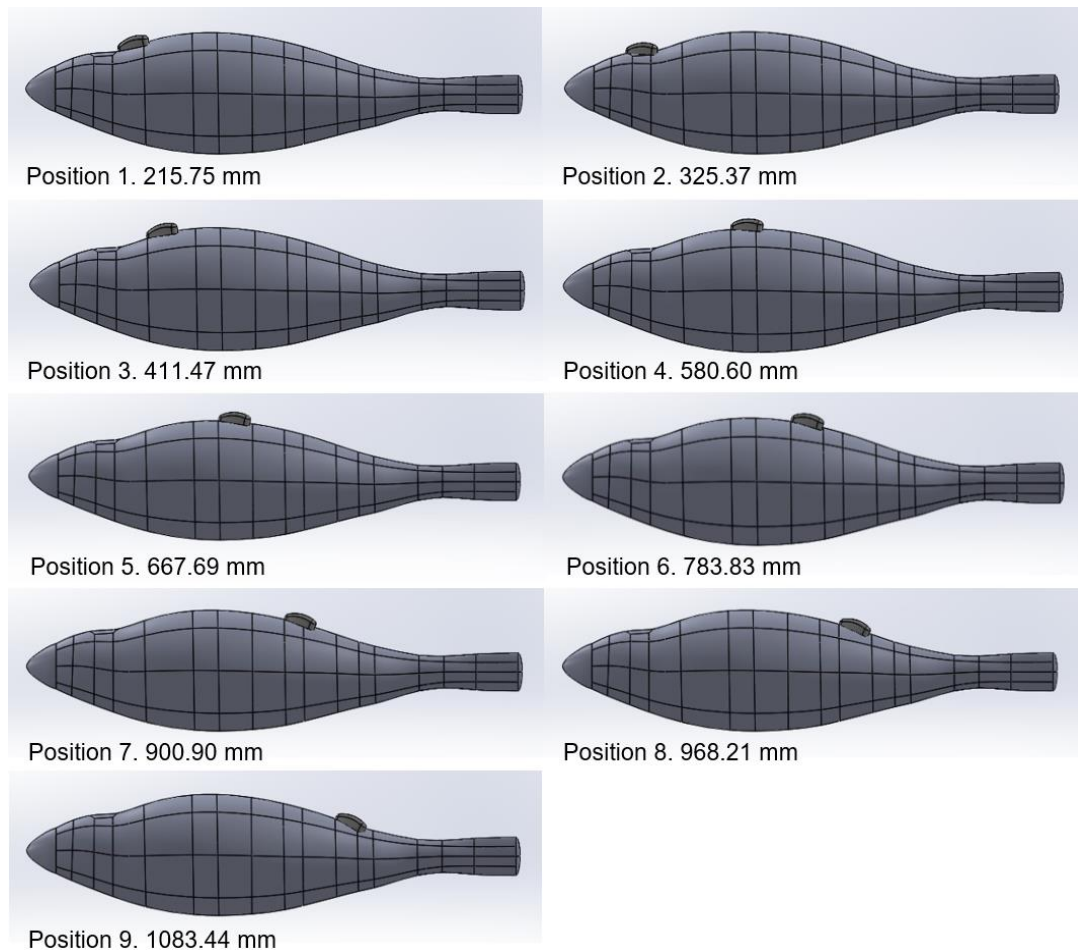


Fig. 6.3. Nine discrete tag positions (distance in mm from nose) along the model seal dorsal surface considered in the computational fluid dynamics (CFD) modelling.

6.3.3 The effect of tag size, shape, and position on tag-induced drag

To examine the effect of tag size, I used the non-dimensional drag coefficient (C_d), hereon “drag”, obtained from the CFD solver, to predict by how much the standard tag (A) would need to be decreased in size in order to reduce its absolute drag penalty to the same value of the more hydrodynamic tag B (under the same flow conditions). Thus, via a process of linear re-scaling, I iteratively reduced the size of tag A to reach the equivalent drag penalty to that of tag B.

I used a paired t-test to examine the effect of tag shape on tag-induced drag (i.e. mean drag over the full range of nine positions modelled). To test the effect of tag positioning *per se* I modelled drag as a function of position using a linear fixed-effects model (testing both linear and polynomial (quadratic and cubic)

relationships to account for potential non-linear effects of position), including tag type (A or B) as a fixed-effect (to account for shape effects), interacting with position. I used step-wise model selection to compare the full model (with an interaction between tag shape and position) versus the intercept only model, as well as comparing cubic versus quadratic polynomial functions for the position covariate, retaining the former in both cases. All analyses were performed using R version 3.5.1 (R Core Team 2018).

6.4 Results

6.4.1 Turbulence and pressures generated by tags with contrasting shape

Tag A, a standard tag, commonly used for seals and other marine mammals, with a non-streamlined shape, induced considerably more turbulent distortions, particularly in the wake of the device, than the streamlined tag B, with the reattachment point of the lowest, smooth streamline passing over tag A 20 % further downstream from the base of the tag than in the case of tag B (Fig. 6.4). This delayed reattachment of streamlined flow resulted in a turbulent wake region that was approximately 30 % larger (when viewed transversely). This type of drag is often referred to as 'base drag' (Suliman et al., 2009) and was one of the major contributors to the increased drag of tag A. Specifically, turbulent flow creates mixing between different layers of otherwise smooth, laminar flow, resulting in irregular fluctuations in pressure (Pope, 2000). There were also stagnant flow regions on the upper side of tag A which were not evident on tag B (Fig. 6.4). These stagnant regions (due to the less streamlined upper surface of tag A) contributed to increased drag by reducing the flow to zero (Pope, 2000). The peak pressure on the front of tag A was 15 % higher than that on tag B and the high pressure region on tag A (see red area in Fig. 6.4) was 65 % larger than that on tag B. There was also evidence of a considerable, low pressure (blue) region, generating suction, on the upper surface of tag A which was not present on tag B. The general form of the regions of high and low pressure across the tags was consistent across all positions for both tag shapes (Fig. 6.4).

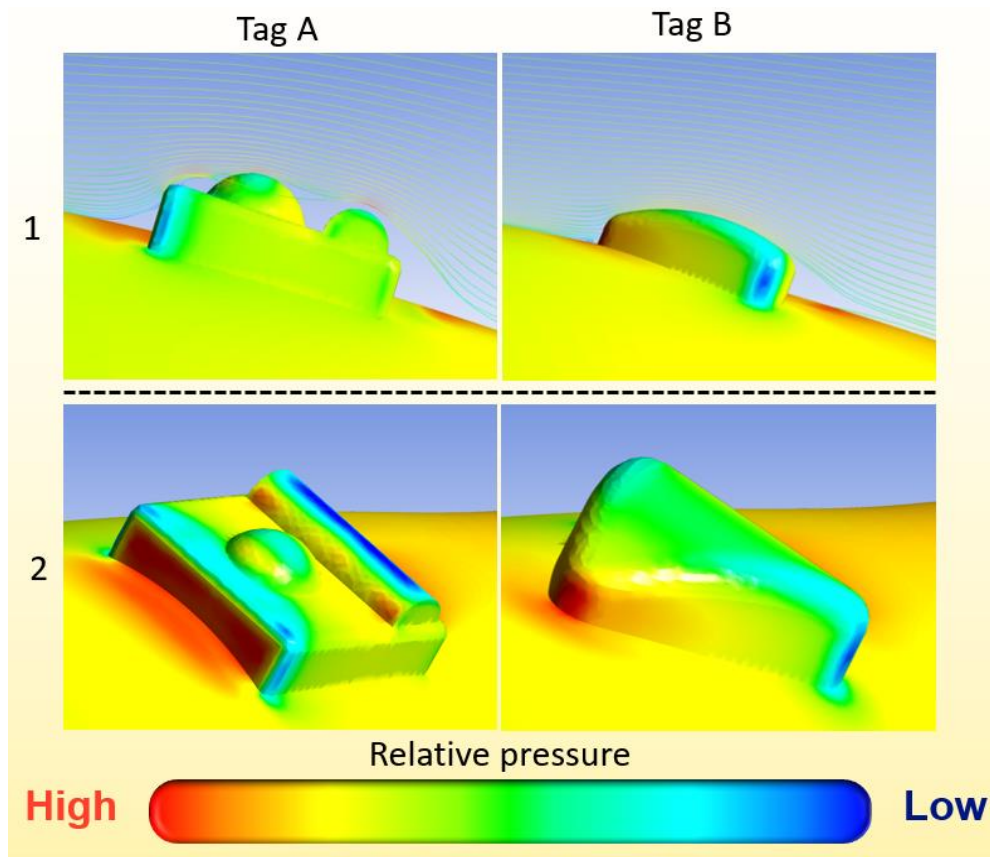


Fig. 6.4. Turbulence (visualized via velocity coloured streamlines) and pressure differentials (rows 1 and 2, respectively) for tag A (first column) and tag B (second column) modelled at 5 m/s flow speed. Rows 1 and 2 present the tag viewed in transverse profile and frontal profile, respectively.

6.4.2 Shape and size effects on drag experienced by tagged animals

Tag A produced an 18.5 % greater mean percentage drag increase than tag B across the full range of positions studied ($t = 16.012$, $df = 8$, $p < 0.001$) (Table 6.1), with a maximum percentage increase of 22.3 % greater than tag B (at position 6) (Table 6.2). These results mean that tag A would require a ca. 50 % linear scaling reduction in size to reduce its drag penalty to that of tag B; i.e. from 10 x 7 x 4 cm to 5 x 3.5 x 2 cm. It is also worth noting that tag B is the preferred option for lower absolute drag despite it being markedly larger than tag A.

Table 6.1. The dimensions, volume, drag coefficient (C_d) (mean \pm standard deviation) and percentage increase in C_d over the baseline case (seal with no tag) (mean \pm standard deviation) of tag designs A and B. Means and percentage increase of drag are calculated over the range of positions tested (1-9).

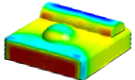
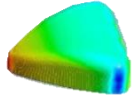
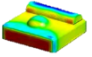
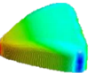
Tag	Form	Dimensions (L x W x H; cm)	Volume (cm ³)	Drag coefficient (C_d) (mean \pm SD)	Drag coefficient % increase over the baseline (no tag) case (mean \pm SD)
A		10 x 7 x 4	280	0.075 \pm 0.002	27.4 \pm 4.2
B		11 x 10 x 4	440	0.064 \pm 0.001	8.9 \pm 1.8

Table 6.2. The drag force (N), power requirement (W), drag coefficient (C_d), and percentage increase of C_d and C_i (lift coefficient) over the baseline case (seal with no tag), across all positions. Note that negative C_i values equates to downforce (see Appendix S6.5 for details). Results shown are for the simulations at 5 ms^{-1} but apply equally across all swim speeds tested (see Methods for details).

	Tag	Position	Position (mm)	Drag (N)	Power (W)	Drag coefficient (C_d)	C_d increase over baseline case (seal with no tag) (%)	Lift coefficient (C_i)	C_i increase over baseline case (seal with no tag) (%)
	None	NA	NA	101.3	506.6	0.0588	NA	0.00259	NA
	A	1	215.75	125.1	625.5	0.0726	23.5	0.00614	137.2
	A	2	325.37	122.5	612.3	0.0711	20.9	0.00430	66.1
	A	3	411.47	127.0	635.0	0.0737	25.3	0.00492	90.0
	A	4	580.60	132.5	662.6	0.0769	30.8	0.00366	41.3
	A	5	667.69	133.8	669.1	0.0777	32.1	0.00078	-69.7
	A	6	783.83	133.9	669.5	0.0777	32.1	0.00157	-39.4
	A	7	900.90	131.7	658.3	0.0764	29.9	0.00005	-98.1
	A	8	968.21	130.6	653.1	0.0758	28.9	-0.00257	-199.2
	A	9	1083.44	125.1	625.5	0.0726	23.5	-0.00004	-101.7
	B	1	215.75	108.4	542.1	0.0629	7.0	-0.00039	-115.2
	B	2	325.37	109.8	548.8	0.0637	8.3	0.00194	-25.1
	B	3	411.47	112.0	560.0	0.0650	10.5	0.00113	-56.4
	B	4	580.60	113.4	566.9	0.0658	11.9	0.00075	-71.1
	B	5	667.69	112.0	560.0	0.0650	10.5	-0.00057	-121.8
	B	6	783.83	111.3	556.6	0.0646	9.9	-0.00067	-125.8
	B	7	900.90	109.8	548.8	0.0637	8.3	0.00062	-76.3
	B	8	968.21	108.9	544.5	0.0632	7.5	0.00025	-90.3
	B	9	1083.44	107.9	539.4	0.0626	6.5	0.00188	-27.4

6.4.3 Position effects on drag experienced by tagged animals

The positioning of tags had a marked impact on their drag (Fig. 6.5) (Tag A: $F_3 = 25.253$, $p < 0.001$; Tag B: $F_3 = 10.362$, $p < 0.001$). Positions 2 and 9 (on the dorsal surface at the neck, and between the shoulder blades respectively; corresponding to 215.75 mm and 1083.44 mm from the tip (nose) of the model), were optimum for tag A and tag B, respectively (Fig. 6.5). The drag varied as a cubic function of position, and this effect differed by tag type ($p = 0.002$). Drag was greatest around the mid-point of the dorsal surface on the model seal (specifically, positions 5 and 6 for tag A, and positions 3 and 4 for tag B) (Fig. 6.5; Table 6.2). Importantly, the variability in tag-induced drag between attachment positions was markedly greater in tag A, with drag values ranging from 0.071 to 0.078; equating to an increase in drag penalty, compared to a seal with no tag, of + 20.8 % to + 32.1 %, with a maximum drag penalty difference of 11.3 % between positions 2 and 6. For tag B these values ranged from 0.063 to 0.066, equating to an increase in drag of + 6.5 % to + 11.9 %, with a maximum difference of 5.4 % between positions 4 and 9 (Table 6.2). Accordingly, the coefficient of variation in drag for tag A (3.31 %) was almost double that of tag B (1.71 %).

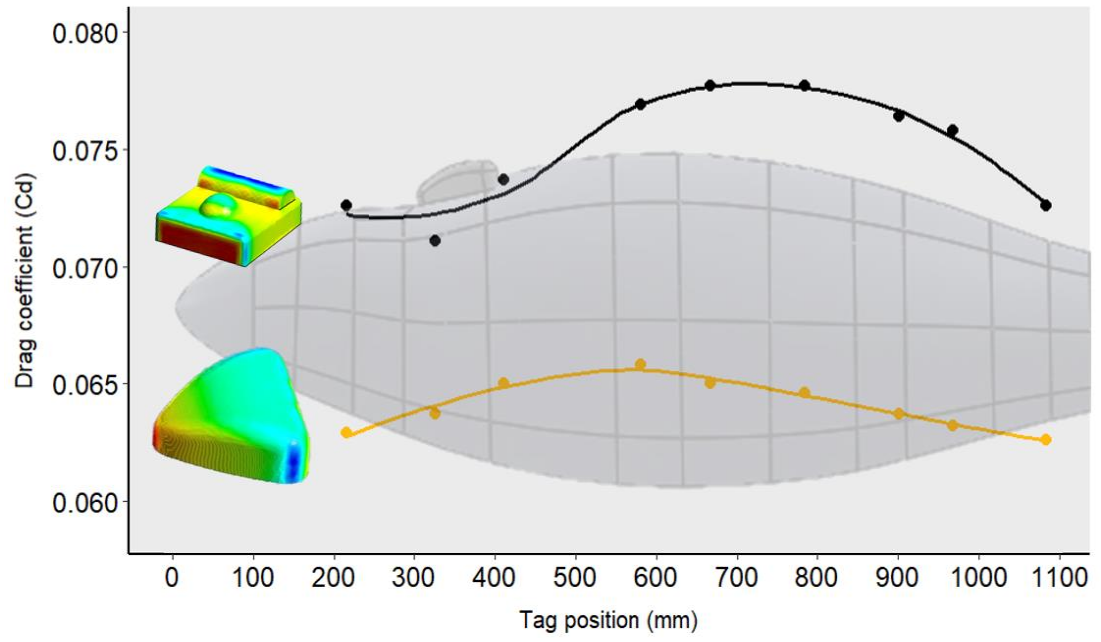


Fig. 6.5. The drag coefficient (C_d) of tag designs A and B and changes in C_d along the length of the model seal.

6.5 Discussion

6.5.1 Effect of tag shape and size

My results have exemplified that tag shape may be more influential than size *per se* in generating increased drag for tagged animals, with the considerably larger but more hydrodynamically designed tag (B) giving rise to a lower drag penalty than the smaller tag A. This result is in agreement with Balmer et al., (2014) who demonstrated that the size of tags was an insignificant driver of overall drag, with only a 1.2 % increase in drag between the smallest (25 mm) and largest (38.6 mm) tags studied. Thus, I propose that shape should be considered more systematically in tag design. Moreover, achieving the reduction in size that would be necessary to reduce drag without instead designing a more streamlined form (here a reduction in size of tag A by ca. 50 %) is often not possible due to limitations in the size of electronic components and batteries. On the contrary, my results suggest there may be scope to increase the size of tags, within reason (Fig. 5.6), providing that their form ultimately leads to a reduction in drag (cf. Shorter et al., 2014; Fiore et al., 2017). It is however important to note that the effect of tag-induced drag is likely to be greater as the ratio of tag to animal volume increases (Kyte et al., 2018), and minimising tag frontal cross-sectional area should also be undertaken where possible (Rosen et al., 2017). Ultimately, to reduce drag, tags should be designed to be more streamlined in line with the contours of the animal being tagged, to achieve smooth flow reattachment downstream of the tag. For this, an increase in size (and thus volume and/or cross-sectional area) could be justified. Certainly, seen in this light, the persistent stated aim to simply "miniaturise" biologging devices may be too simplistic (Portugal & White 2018).

The fact that tag A exhibited greater drag than tag B is in accordance with other CFD and wind tunnel research examining tags on seals (Kyte et al., 2019), cetaceans (Fiore et al., 2017) and birds (Vandenabeele et al., 2014), such that greater turbulent flow distortions and larger pressure differentials caused by poor hydrodynamics contributed to increased drag. I note that the absolute drag values observed in my study are larger than those obtained in Kyte et al.,

(2018), who modelled tag-induced drag on a similarly sized harp seal. This can be attributed to the large difference in flow velocities used in the simulations; Kyte et al., (2018) used a maximum flow velocity of 1.7 ms^{-1} whereas my simulations used 5 ms^{-1} . The differences in speeds examined reflect the fact that here I consider resultant speeds as experienced by a seal moving at maximum speed (2 ms^{-1} ; Gallon et al., 2007) into a 3 ms^{-1} tidal current (Malinka et al., 2018). Importantly, when scaled to non-dimensional drag, my values are in line with that work. Similarly, when comparing my work to Hazekamp et al., (2010) I found similar yet quantitatively different results. Specifically, Hazekamp et al., (2010) observed a 13.8 % increase in drag, whereas I saw an increase of 23.5 %. This difference is expected because Hazekamp et al., (2010) ran their simulations using the $k-\epsilon$ turbulence model, which tends to underpredict the drag impact of a tag (see Kyte et al., 2018 and Appendix S6.2 for further details).

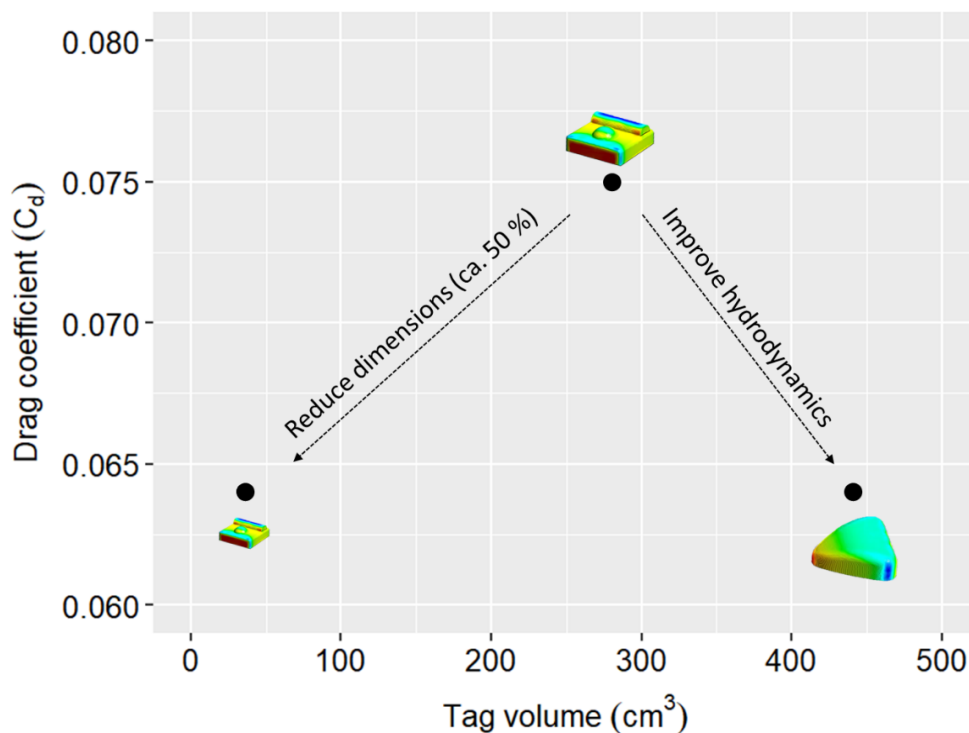


Fig. 6.6. Tag drag coefficient (C_d) as a function of tag volume (cm^3) (see Table 6.1 for dimensions). Data points are shown as black dots alongside schematic representations of tags. The two options for drag reduction are to reduce the tag dimensions or improve the hydrodynamic design.

6.5.2 Effect of tag positioning

Device positioning is crucial in determining tag-induced drag, as evidenced by the non-linear relationship between drag and tag position. This concurs with the results of Vandenabeele et al., (2014) who observed strong and non-linear effects of tag position on induced drag on a model cormorant in a wind tunnel. Similarly, Tudorache et al., (2014) documented that for swimming eels tagged with biologging devices, placement of a tag in a non-optimum position could result in a 15 % reduction in critical swimming speed and a significant increase in oxygen consumption rate while swimming. My results further showed that the effect of tag positioning on drag is significantly dependent upon the shape of the tag, and that the variability in the effect of tag positioning for tag B is almost half that for tag A. This demonstrates that improving hydrodynamic design can reduce the impact of positioning *per se* on device-induced drag. Moreover, even though tag B was larger than tag A, its drag impact was less; this suggests that tag size becomes less important providing that you design a tag with a hydrodynamic shape.

In practice, the choice of tag positioning will depend on the form of the animal and is compounded by the fact that the positioning of a tag can affect both the quality and quantity of data collected (Watson & Granger 1998; Jones et al., 2011). For example, GPS data from marine megafauna can only be obtained when individuals surface for a long enough duration to receive a satellite fix (Carter et al., 2016), and for this reason tags are routinely placed on areas of the animal that are exposed most frequently and for the longest periods, for example on the head of pinnipeds (Lake et al., 2006). In such cases, researchers must consider the trade-offs of successful data acquisition with device effects, or consider how they might modify their tags to achieve a more balanced outcome (Jones et al., 2011); for example, researchers could consider using alternative technologies, such as fastloc-GPS devices, that require only very short durations at the surface (< 1 s) to acquire satellite fixes (Dujon et al., 2014), so that tags can be placed at optimum (i.e. drag-minimising) positions on the animal that are exposed for shorter durations.

6.5.3 Drag impact: A revised metric for tracking wild animals

Most existing guidelines for tag impact do not advise on appropriate tag size, placement positions, or configurations (Rosen et al., 2017), and many are relatively naïve to the impacts of drag that are most relevant to marine applications. For example, the European Parliament and Council Directive 2010/63/EU on the protection of animals used for scientific purposes (2010) OJ L276/34 (EU, 2010) simply lists the application of external telemetry devices as a “mild severity procedure”, and makes no explicit reference to any quantifiable impact, such as the relative weight of the device or tag-induced drag. Similarly, the guidelines for the care and use of wildlife set out by the Canadian Council on Animal Care (CCAC, 2003) refer only to minimizing telemetry device weight (guideline 28) and the Animal Welfare Act of the United States Department of Agriculture includes no information on the use of telemetry devices on animals for scientific research (USDA, 2017). The National Marine Fisheries Service (NOAA Fisheries) provides permits to tag marine megafauna, and evaluates tag impact using extensive criteria, including the location of the tag, maximum tag footprint, tag mass, and tag size, amongst others (NOAA Fisheries, 2019). However, there is no mention of tag-induced drag, nor any advice for how to assess this. Only two exceptions can be found: the UK Joint Working Group on Refinement’s (JWGR) report on refinements in telemetry procedures (Morton et al., 2003) notes that minimizing drag is essential, suggesting that tags should be streamlined. Similarly, the US Fisheries and Wildlife Service insists that researchers must minimize tag-induced drag (USFWS, 2017). This includes, amongst other criteria, that the tag must have a low profile and be streamlined, and must be placed in appropriate positions.

The USFWS is the only body to propose a quantitative metric for drag, such that it is unlikely to approve studies using tags where devices increase drag by more than 10 %. However, given that recent research has demonstrated that a tag which induces an average of only 7 % additional drag can result in up to an 11 % difference in swim speed (van der Hoop et al., 2014), I propose here that approving tags which introduce up to 10 % drag is not sufficiently conservative. Rather, I suggest that a 5 % total increase in drag should be the

maximum supported by future studies. Meeting this standard would bring the maximum accepted percentage impact of tag drag in line with that of the benchmark '5 %' rule for tag mass (Casper, 2009).

6.5.4 Future work and the usefulness of CFD

This work has demonstrated the value of an interdisciplinary approach, harnessing engineering techniques to design minimal impact tags and efficiently assess their relative drag loading. While CFD has previously been utilised to measure the impact of tags (Appendix S6.1), its use has largely been limited to researchers with substantial prior CFD modelling expertise (Kyte et al., 2018). Indeed, there is currently limited advice for researchers who are developing their own tags on how to quantify the drag of their tags and hence how to minimise impact. Hence, in addition to demonstrating the importance of tag design, I fill this gap by providing a step-by-step guide that ecologists can follow to assess tag-induced drag in a quick and efficient manner using CFD techniques (Appendix S6.3). This will support more researchers to measure and report on the drag-impact of their tags and ultimately contribute to developing best practice. The methods in this guide are standard for aeronautical design (Jameson & Vassberg 2001) and should facilitate new opportunities for collaboration between engineers and ecologists – particularly for novice users of CFD techniques.

Researchers planning on using CFD techniques must however be aware of its limitations. CFD relies on approximate, numerical solutions to the governing fluid dynamic equations, and so there will always be some discrepancies in absolute force predictions between independent studies; for example, I have highlighted some key comparisons between my results and those of similar works (Hazekamp et al., 2010; Kyte et al., 2018). I provide necessary further detail on the limitations of CFD in Appendix S6.2, which I encourage the reader to consult for guidance.

Chapter 7

Conclusions

“Slowly and painfully we are gathering the facts that will one day enable us to arrange the details of the life of the seals into a connected story.”
(Matthews 1979)



Harbour seals are caught as part of annual tagging and monitoring fieldwork in Lorenzensplate, Germany (Photograph by Stephanie Groß)

7.1 Context and rationale

In my review of the literature in Chapter 1, I identified that the movements of marine megafauna in tidal stream environments (TSEs) are relatively poorly understood, and that the development of tidal stream turbine (TST) devices to combat climate change presents new anthropogenic threats (Copping et al., 2020), creating an urgent need for research to inform Environmental Impact Assessments and aid the TST industry to meet its consenting requirements (ORJIP Ocean Energy, 2020). I learnt that the risk that TSTs pose are particularly acute for seals, as their distribution typically overlaps with TSEs targeted for the installation of these devices (Carter et al., 2020) and because seals are known to frequent TSEs, including at a young age (Thompson, 2012; Lieber et al., 2018). Research is required at three spatial scales (broad, fine, and near-field; cf. Waggitt & Scott, 2014) and studies to date have been limited in their locations, spatio-temporal extent, species, age-class, or sample size (Benjamins et al., 2015). In particular, studies that have recorded the very fine-scale, 3D movements of marine megafauna in TSEs are almost entirely lacking. This is fundamentally linked to the fact that there are a paucity of methods and instruments available to track animals in sufficient resolution (Copping & Hemery, 2020). This is an issue because this research is crucial in determining the movement of animals in TSEs and their responses to TST devices, including near-field evasive behaviours. Existing knowledge gaps and limitations have raised a number of key priorities for research:

- (i) Improve understanding of the spatio-temporal use of TSEs by marine megafauna and their potential overlap with TSTs.
- (ii) Determine the frequency and consequences of far-field responses to, and near-field interactions with, TSTs (including collision) at both the individual- and population-level.
- (iii) Improve the methods and instruments used to measure (i) and (ii).
- (iv) Refine the techniques used to assess and manage the risks of any detrimental interaction(s) between animals and devices, and
- (v) Obtain baseline data for sites and species where data are lacking (including tidal energy lease sites where devices have not yet been installed).

The general aim of my thesis was hence to quantify how marine megafauna move in TSEs. As well as provide new ecological insights that are useful to the TST industry, I sought to contribute novel research methods to support what remains a frontier subject in movement ecology. In doing so, I sought to use the understanding and methods developed to improve the management of TST devices in order to mitigate potential impacts on these taxa. For my study system I focused on two species of seal, living in coastal regions of the Irish, Celtic and North Sea, where several previous or ongoing research projects enabled me to utilise previously accumulated data as well as capture and tag wild animals for further data collection. These regions exhibit relatively moderate ($\sim 1 \text{ ms}^{-1}$) to fast flowing (3 ms^{-1}) tidal currents and are areas where TST devices have already been installed or are planned for future development.

In order to understand the broad-scale (1 – 10 km) spatial overlap of seals with TSEs, I first had to quantify the contribution of intrinsic and extrinsic factors on the movement of individuals, as these animals move over large scales across coastal and oceanic environments (Russell et al., 2015; Jones et al., 2015; Vincent et al., 2017). Given the general lack of information on early-life movements of seals (Carter et al., 2016), coupled with the notion that young individuals are the most naïve and vulnerable to anthropogenic stressors (Thompson, 2012; Luck et al., 2020), I first applied novel methods to a large, existing record of the early life movements of pups. I (a) digitised a large dataset of historic ringing records on grey seal pup movements from colonies on the Welsh coast (Kay et al., 2020); then (b) developed a new approach to obtain predictive displacement kernels of seal pup movements over their first year of independence at sea, quantified the relative contribution of environmental drivers, individual-variation and demographic covariates on displacement, and combined the movement predictions with count data, to predict the spatio-temporal overlap risk of pups with an existing TST site. I then (c) utilised fine-scale GPS movement data (also from grey seal pups on the Welsh coast) to validate my analysis of the ringing records, as well as address fundamental trade-offs in sampling design and intensity for quantifying dispersal.

These first works enabled me to examine the potential for broad-scale overlap of seal pups with TSEs and predict when individuals could overlap with TST sites. I was also able to generate clear recommendations to estimate displacement. Importantly, in their early life, grey seal pups behave very differently to adults, although quickly develop the movement capacities to match their older conspecifics (Carter et al., 2019). Hence, it was crucial in these first chapters to develop methods that could be broadly applied to different aged individuals, as well as animals from other taxa. I achieved this by developing new analytical methods to utilise existing data such as those obtained from marking studies. Importantly, this can include photo-ID and visual survey data that are routine for monitoring seals and other marine megafauna (Sayer et al., 2019; Heal et al., 2021).

Following this, I (d) sought to investigate seals' use of TSEs at relatively fine-scales. I therefore applied a state-of-the-art hidden Markov model (HMM) to dead-reckoned ARGOS trajectories and dive data of adult harbour seals to identify how they change their movements and behaviour in response to tidal currents, and the degree of individual behavioural variability in this. For this I used an existing dataset of seals tracked in the mid-2000s, further exemplifying the benefits of applying new statistical tools to older data.

Finally, as the tools to study wild seals in very-fine scales underwater and their responses to TSTs are extremely limited (Hastie et al., 2019; Onoufriou, 2021), I sought to develop methods to track seal movements in high-resolution underwater and better understand how seals operate in TSEs. To do this I (e) designed a new tag to sample high-frequency multivariate biologging data from seals in TSEs, and (f) developed a new approach to quantify and minimise the tag-induced drag impact of these devices, something which is crucial for animals that move in fast-flowing environments.

In the remainder of this chapter I provide a summary of the key contributions made in addressing these objectives, their wider implications with respect to understanding seal ecology in TSEs and their interactions with TST devices, and their potential applications for the TST industry. I also suggest directions for future research.

7.2 Broad-scale overlap with TSEs

A key research objective established from **Chapter 1** was to provide further information on the broad-scale overlap of marine megafauna with tidal stream environments (TSEs). Thus, in **Chapter 2** I examined the drivers of variation in the scales and patterns of grey seal pup displacement during natal dispersal, using a dataset of $n = 246$ individuals. I implemented a least-cost path function in a novel context to calculate the distance travelled by seals at sea, revealing a large degree of individual variation in dispersal distance (by nearly three orders of magnitude; 3–964.3 km), and used linear mixed effects models to investigate the factors that generated variation in this. I showed that natal dispersal is far-ranging and that the displacement distance reached by pups is driven by time, differences between sites, and sex-dependent responses to weather conditions, however no fixed-effect was observed for sex *per se*. Most interestingly of all, the displacement distance reached by grey seal pups during natal dispersal was well predicted by a climatic variable, the North Atlantic Oscillation (NAO).

Following this, I employed a second, novel analytical method to predict the patterns of grey seal pup displacement over time, by taking displacement models originally designed to model individual-level displacement (Börger & Fryxell, 2012) and applying these to population-level data. I demonstrated that, at the population-level, seal pup dispersal is exhibited by at least three movement strategies (diffusive, dispersal, and return). Importantly, I learnt that seal pups from some sites begin to disperse earlier than previous estimates had suggested (as young as 16 days old), and that once they disperse, seal pups increase their displacement distance rapidly from their natal colony. This has clear implications for the age at which pups may encounter TST devices, as pups are known to use TSEs during early life (Thompson, 2012). My results further indicated that some individuals begin to return towards their natal colony after around 115 days after birth. These findings have clear implications for the management of seal populations, suggesting that differences in the strategies of sub-populations need to be accounted for (Gaggiotti et al., 2002),

along with the impacts of weather (Lea et al., 2009). Crucially for the TST industry, the displacement patterns of pups can inform nearby developments of the potential encounter rates of pups over time. To exemplify this, I applied a final new method by combining my predictions of displacement over time with recent pup count data to predict the potential number of individuals in the vicinity of a TST site, and for what period. I revealed site-specific differences but demonstrated a clear window of maximum overlap occurring between 88–117 days after the onset of the pupping season. These results can provide clear mitigation strategies for the TST industry, such as in recommending time periods where the operation of devices can be reduced to minimise risk of collision. This mitigation strategy could be easily incorporated into an Adaptive Management framework (Copping & Hemery, 2020). As well as providing new ecological insights and methodological tools that support the TST industry, these two chapters showcased how valuable an old dataset can be. In fact, prior to undertaking these analyses I had manually digitised the historical ringing data from its original, hand-written record.

In **Chapter 3**, I aimed to quantify individual-variability in grey seal pup dispersal using high-resolution Fastloc-GPS data. In doing so, I sought to validate the population-level predictions of displacement over time made in Chapter 2 with individual-level predictions of dispersal. I followed the same displacement modelling and evaluation approach as in Chapter 2 and my results suggested broad agreement in displacement distance and time parameters, suggesting that, as well as their intended use for individual-level data, there is promise in applying the displacement approach of Börger and Fryxell (2012) to population-level data. Seal pups tended to “hug” the coastline as they displaced from their natal site, serendipitously providing support for the use of the least-cost path function in Chapter 2 to derive seal trajectories, and revealing further insights into the potential use of TSEs by grey seal pups (Thompson, 2012). Results also alluded to density-dependent or tidal drivers of dispersal propensity, with pups from the dense Ramsey colony displacing sooner than those at the Skerries. However, empirical counts of grey seal pups born at beaches during the years studied were not explicitly factored into the modelling approach, and this is a refinement that would be useful for future

research. As in Chapter 2, individual-level movement patterns also returned three movement modes (a mixture of diffusive, dispersal, and return strategies), and predictions of displacement over time also indicated that some pups dispersed from their natal sites very soon after weaning. Importantly, except for a few extreme individuals, the 95 % model confidence envelope predicted by the population-level ringing models was well-matched to the individual-level GPS model predictions. I concluded with the recommendation that a minimum recording duration of 200 days is needed to obtain credible data on the movement strategies of pups in early life and help to determine the proportion of movement modes within a population (Fryxell et al., 2008). Importantly, return movements to natal colonies could expose grey seal pups to a second episode of overlap risk with TST devices within their first year of life, suggesting that management strategies of pups need to account for both an initial dispersal and a return phase. Finally, I conducted a bootstrapping analysis to determine the sample size required to reliably estimate displacement distance, concluding this to be over 150 individuals for metrics that are typically useful for practitioners to designate areas of conservation. Moreover, I highlighted how large sample sizes are key to detecting very large-scale dispersal, which is typically undertaken by the fittest individuals within a population that have high conservation value (Cozzi et al., 2020).

Results from this Chapter have best practice implications for future research on seal pups as they suggest that large sample sizes may be required (as suggested also for other marine megafauna, see Sequeira et al., 2019). This is a non-trivial issue, as tagging such large sample sizes requires huge effort. Fortunately, as evidence from Chapter 2, the method of Börger & Fryxell, (2012) can be applied to even very coarse data such as those obtained from routine marking efforts, and even very old data can provide good predictions of grey seal pup space use today. Thus, there is great promise in analysing datasets collected over recent years, for which also local-scale weather covariates are available, to investigate displacement; indeed, another new opportunity for future research. Finally, this chapter also suggested that data over substantial periods are required for each individual, especially for determining risk of overlap with TSTs. Notably, the long recording period

required will mean that tags will need to be designed to minimise their impact (an issue on which I also contributed new work, as detailed later).

7.3 Fine-scale movements in TSEs

In having made novel ecological and methodological contributions to the study of broad-scale overlap of seals with TSTs, I sought to analyse relatively fine-scale data typically obtained from tagging studies to determine the influence of tides on seal movement and behaviour. Therefore, in **Chapter 4** I analysed the movements of harbour seals in the Wadden Sea, a TSE proposed for TST developments. Chapter 1 had highlighted the lack of understanding relating to site-specific differences and individual-variation in seals' responses to head- and tail-currents; Chapters 2 and 3 had also highlighted a large degree of individual variation in the movements of seals (albeit for grey seal pups). Thus, I focused my research on addressing these issues. Chapter 1 had further emphasised that refinements to the methods of studying such responses and accounting for such variation were necessary, and so in Chapter 4 I made use of a cutting-edge, mixed, generalised hidden Markov modelling framework (cf. DeRuiter et al., 2017; Carter et al., 2019) to exemplify how these could be used to answer this research question using high-resolution tracking data.

To do so, I used for this Chapter a large and existing high-resolution dataset of seal movements and diving behaviour from the North Sea collected between 2004–2006. I used vector component calculations to calculate the relative strength of tidal currents for each step along each seals' trajectories, using data from a relatively coarse hydrodynamic model from the German Hydrographic Institute. I considered several tidal metrics that could affect seal movements and concluded that the head-current component (a vector providing an indication of both the strength and direction of tidal current relative to seal movements) best explained the underlying variation in the data (see also Onoufriou et al., 2021). I classified movements along seal trajectories into one of three behavioural states (resting, foraging, or travelling), based the underlying distribution of their step lengths, turn angles, and proportion of time spent diving, and modelled these in response to tidal currents, accounting also

for the fixed-effects of sex, site, and age-class. Specifically, I modelled covariate effects on the probability of states occurring, the probability of transitioning between states, and the distribution of movement parameters within behavioural states. Furthermore, I used discrete-valued random-effects (DeRuiter et al., 2017) to provide a quantitative indication of the amount of unexplained within- and between-individual variation.

Results demonstrated that harbour seals adjusted their behaviour in response to tidal currents and that the occurrence of tail-currents specifically was key in modulating this. Seals preferentially exploited tail-currents for foraging and this was consistent across site- and sex-groups, with individual variation likely responsible for explaining unaccounted for variability in the data. My results demonstrated that harbour seals in my study behaved in a manner analogous to individuals in a fast-flowing (4 ms^{-1}) TSE in Kyle Rhea, Scotland (Hastie et al., 2019) despite the tidal velocities in the Wadden Sea being much closer to the $\leq 1 \text{ ms}^{-1}$ low current velocities (amongst others) experienced by seals in the Strangford Narrows, Northern Ireland. This led me to believe that observed movement differences in response to tidal-currents may be modulated by depth usage and the associated availability of prey, which is likely to vary across regions and between sites (Benjamins et al., 2015).

Understanding how seals move in TSEs is key for the management of TSTs, and this Chapter provides novel information on how seals may move and modify their behaviour in response to tidal currents in areas not previously studied. This Chapter provides the first example of tidal drivers of harbour seal movements and behaviour in the Wadden Sea, as well as providing quantification of the degree of individual variability in responses to tidal currents, crucial for predicting population-level responses. More generally, the results in this Chapter can offer new insights into optimal foraging strategies, thus potentially providing a much broader contribution to our understanding of the ecology of seals in TSEs. Finally, in applying today's methods to data from the mid-2000s, I yet again highlight how new cutting-edge analytical techniques applied to old data can maximise the value of the latter. My results also provide an historical baseline for seal movements and behaviour in

response to tidal currents in the Wadden Sea, which can be compared to future research following TST installation.

The results presented here manifest in a number of valuable applied implications for the TST industry intending to operate devices in TSEs and for researchers intending to study this. Specifically, (i) likely due to the homogenous topography of the Wadden Sea, site-differences in behavioural responses to tidal currents in this region are negligible, however, (ii) individual variation is high, allometric effects are clear, and regional differences with other areas are apparent, the latter potentially being modified by the prey species targeted and depth-usage required to exploit them. This means that (iii) large sample sizes will need to be studied, ideally from all life history stages, and this should include dietary analysis. Finally, and most tangibly for TST developments here and elsewhere, (iv) seals preferentially targeted tail-currents for foraging. This information is critical to predict where an animal will be, which direction it is likely to be heading in, and what it may be doing if it encounters a TST, with major implications for modelling collision risk (Onoufriou et al., 2019; Horne et al., 2021).

Finally, despite having learnt much about the responses of seals to tidal currents, my understanding was still restricted by the spatial (1 nmi) and temporal (15 min) resolution of my data. This reiterates the need to collect very high-resolution data, for which I hope the tag I subsequently developed in Chapter 5 and the data obtained from these will contribute to in future. In future work, I plan to extend the analysis here to incorporate absolute dive depth and jaw-sensor data as additional data streams in HMMs to model attempted prey capture events and further refine estimates of foraging activity (Liebsch et al., 2007).

7.4 Tag developments for tracking animals in TSEs

Having established some of the key drivers of broad-scale overlap of animals with TSEs, and investigated a key example of relatively fine-scale drivers in these environments, I now sought to address the technological development

needs identified in Chapter 1, by designing and building a new tag to track the very fine-scale 3D movements of seals underwater, which I present in **Chapter 5**. This tag presents a new approach to seal tag design by incorporating multiple sensors in a modular and flexible design, with a galvanic remote-release attachment mechanism. In this Chapter I present an evaluation of my tag, including full justification of the sensors chosen and techniques used to build the device, and the design workflow to reach my final tag design. While the final tag is approximately a third of the price of off-the-shelf commercial devices, and boasts superior functionality to many available alternatives, it remains archival in its method of data acquisition, and thus relies on relatively arduous and expensive fieldwork efforts for recovery. Nevertheless, providing tags can be retrieved, the device provides the ability to record very fine-scale movements of animals in TSEs, including correcting for drift-error in dead-reckoning, and can remotely release from wild subjects before floating to the surface to transmit its location.

While I was successful in recovering only a limited number of tags from field deployments, these have critical value as a proof of concept (Sequeira et al., 2019) and the data collected can be used to begin reconstructing the 3D fine-scale movements of seals in TSEs, providing a baseline for future research. Indeed, these data have already been shared with other members of the International Bio-Logging Society. Moreover, my efforts suggest that further refinement of the tag, especially of key aspects like improving the performance of transmitters, supported by a more systematic recovery effort (e.g. Lear & Whitney, 2016), would offer real potential for this deployment approach.

In order to support other researchers in developing tags, in additional supplementary materials I provide an exhaustive table of factors and a comprehensive flowchart of factors to consider when building tags for marine megafauna, as well as a step-by-step guide to building floatations from standard materials. This Chapter is an exemplar of the notion that the greater involvement that researchers and practitioners have in designing tags, the greater awareness they will have of the engineering issues and correct functioning procedures associated with devices; this is crucial to achieving successful deployments and appropriate interpretation of the data (Holton et

al., 2021). More broadly, this Chapter makes important contributions to the reporting of the challenges in tag design; a key issue raised at a recent best practice workshop in tagging cetaceans and pinnipeds (Kay et al., *In Prep*).

Another important aspect related to designing tags for marine megafauna concerns their drag impact on the tagged animals. It has long been known that tags deployed on marine animals can have adverse effects on their energetics (Bannasch et al., 1994), and ultimately on populations (Saraux et al., 2011). Drag impact increases with speed (Vandenabeele et al., 2015), and hence fast-moving animals, or animals moving in fast-moving mediums such as TSEs, will suffer particular detriment. It was for this reason, amongst several others, that I originally aimed to collect high-resolution data over only short-term deployments in Chapter 5. However, my results from Chapter 3 indicated that to reliably assess other behaviours in these environments, tags would need to be attached for longer durations. If the tags designed in Chapter 5 were to be refined for longer deployments then I would need some way to assess their impact and improve their design. Hence, in **Chapter 6** I sought to develop methods to optimise the design of tags and minimise their hydrodynamic impact. Alongside this project, the Integrated Bio-logging Framework (IBF) that I had contributed to (Williams et al., 2020) had strongly recommended that researchers employ interdisciplinary approaches, and I thus identified this as an excellent opportunity to do just that. In Chapter 6 I present an example of an interdisciplinary collaboration between ecologists and aerospace engineers to improve the hydrodynamic performance of tags on seals to minimize their drag impact using computational fluid dynamics (CFD). I published this chapter in *Methods in Ecology and Evolution* and showed that tag-induced drag is a complex factor of the size, shape, and positioning of the device. This work contributes directly to best practice in the deployment of tags on marine megafauna, especially for animals in TSEs which operate in high drag environments; I concluded with the suggestion that the reporting of drag values in future studies is needed to improve guidelines for monitoring tag impact, and that tags should ideally inflict no more than an additional 5 % drag. To facilitate this, I created a step-by-step guide for

ecologists to employ CFD modelling techniques to design and measure the impact of their tags.

7.5 Final conclusions

Global increases in the development and installation of TST devices are expected to affect marine megafauna in numerous, detrimental ways. Impacts need to be identified and mitigated if we are to achieve sustainable management of natural marine resources. For this, an understanding of how marine megafauna make use of the TSEs targeted by the TST industry is crucially needed. This thesis suggests that the movements and behaviour of seals in TSEs are driven by a combination of measurable (and in some cases predictable), demographic and environmental factors, and that the conservation strategies developed to manage the interaction between individuals and populations with TSTs must consider site- and region-specific differences, and account for wide inter-individual variation. My results also highlight the importance of considering age-classes separately in management strategies. To address these challenges, my thesis contributes novel tools for studying marine megafauna in TSEs, new baseline data of their movements in these habitats, and new methodological applications for analysing the data obtained. Further work is required to elucidate the full extent of variability of marine megafauna movements, and threats of TST developments, in these numerous but unique environments, and such future work will benefit from developing new tools, sharing data, and embracing research frameworks to ensure that their efforts fit the needs of practitioners.

References

- Abrahms, B., Aikens, E. O., Armstrong, J. B., Deacy, W. W., Kauffman, M. J., & Merkle, J. A. (2020). Emerging Perspectives on Resource Tracking and Animal Movement Ecology. *Trends in Ecology & Evolution*, 2777, 1–13. doi:10.1016/j.tree.2020.10.018
- Abrahms, B., Welch, H., Brodie, S., Jacox, M. G., Becker, E. A., Bograd, S. J., ... Hazen, E. L. (2019). Dynamic ensemble models to predict distributions and anthropogenic risk exposure for highly mobile species. *Diversity and Distributions*, ddi.12940. doi:10.1111/ddi.12940
- Adachi, T., Costa, D. P., Robinson, P. W., Peterson, S. H., Yamamichi, M., Naito, Y., & Takahashi, A. (2017). Searching for prey in a three-dimensional environment: hierarchical movements enhance foraging success in northern elephant seals. *Functional Ecology*, 31(2), 361–369. doi:10.1111/1365-2435.12686
- Adcock, T. A. A., Draper, S., Houlsby, G. T., Borthwick, A. G. L., & Serhadlioglu, S. (2013). The available power from tidal stream turbines in the Pentland Firth. *Proceedings of the Royal Society A: Mathematical, Physical and Engineering Sciences*, 469(2157), 20130072. doi:10.1098/rspa.2013.0072
- Adkins, D., & Yan, Y. Y. (2006). CFD simulation of fish-like body moving in viscous liquid. *Journal of Bionic Engineering*, 3(3), 147–153. doi:10.1016/S1672-6529(06)60018-8
- Afán, I., Navarro, J., Grémillet, D., Coll, M., & Forero, M. G. (2019). Maiden voyage into death: are fisheries affecting seabird juvenile survival during the first days at sea? *Royal Society Open Science*, 6(1), 181151. doi:10.1098/rsos.181151
- Åkesson, S., & Weimerskirch, H. (2005). Albatross long-distance navigation: Comparing adults and juveniles. *Journal of Navigation*, 58(3), 365–373. doi:10.1017/S0373463305003401
- Allen, A. M., Månsson, J., Sand, H., Malmsten, J., Ericsson, G., & Singh, N. J. (2016). Scaling up movements: from individual space use to population patterns. *Ecosphere*, 7(10), e01524. doi:10.1002/ecs2.1524
- Allen, A. M., & Singh, N. J. (2016). Linking Movement Ecology with Wildlife Management and Conservation. *Frontiers in Ecology and Evolution*, 3, 155. doi:10.3389/fevo.2015.00155
- Allen, P. J., Amos, W., Pomeroy, P. P., & Twiss, S. D. (1995). Microsatellite variation in grey seals (*Halichoerus grypus*) shows evidence of genetic differentiation between two British breeding colonies. *Molecular Ecology*, 4(6), 653–662. doi:10.1111/J.1365-294X.1995.TB00266.X
- Allen, R. M., Metaxas, A., & Snelgrove, P. V. R. (2018). Applying Movement Ecology to Marine Animals with Complex Life Cycles. *Annual Review of Marine Science*, 10(1), 19–42. doi:10.1146/annurev-marine-121916-063134
- Andersen, S. M., Teilmann, J., Dietz, R., Schmidt, N. M., & Miller, L. A. (2014). Disturbance-induced responses of VHF and satellite tagged harbour seals. *Aquatic Conservation: Marine and Freshwater Ecosystems*, 24(5), 712–723.
- Anderwald, P., Evans, P., Dyer, R., Dale, A., Wright, P., & Hoelzel, A. (2012). Spatial scale and environmental determinants in minke whale habitat use

- and foraging. *Marine Ecology Progress Series*, 450, 259–274. doi:10.3354/meps09573
- Andrews, R., Baird, R., Calambokidis, J., Goertz, C. E., Gulland, F. M., Heide-Jorgensen, M.-P., ... Zerbini, A. (2019). Best practice guidelines for cetacean tagging, *Journal of Cetacean Rescue and Management*, 20(1), 27–66.
- Anthony, D. (1995). A Simple Model for Current Speed in Tidal Channels. *Geografisk Tidsskrift-Danish Journal of Geography*, 95(1), 12–18. doi:10.1080/00167223.1995.10649359
- Arranz, P., Benoit-Bird, K. J., Friedlaender, A. S., Hazen, E. L., Goldbogen, J. A., Stimpert, A. K., ... Tyack, P. L. (2019). Diving Behavior and Fine-Scale Kinematics of Free-Ranging Risso's Dolphins Foraging in Shallow and Deep-Water Habitats. *Frontiers in Ecology and Evolution*, 7(March), 1–15. doi:10.3389/fevo.2019.00053
- Avila, I. C., Kaschner, K., & Dormann, C. F. (2018). Current global risks to marine mammals: Taking stock of the threats. *Biological Conservation*, 221, 44–58. doi:10.1016/j.biocon.2018.02.021
- Bagchi, S., Singh, N. J., Briske, D. D., Bestelmeyer, B. T., McClaran, M. P., & Murthy, K. (2017). Quantifying long-term plant community dynamics with movement models: implications for ecological resilience. *Ecological Applications*, 27(5), 1514–1528. doi:10.1002/eap.1544
- Balmer, B. C., Wells, R. S., Howle, L. E., Barleycorn, A. A., McLellan, W. A., Ann Pabst, D., ... Zolman, E. S. (2014). Advances in cetacean telemetry: A review of single-pin transmitter attachment techniques on small cetaceans and development of a new satellite-linked transmitter design. *Marine Mammal Science*, 30(2), 656–673. doi:10.1111/mms.12072
- Band, B., Sparling, C., Thompson, D., Onoufriou, J., Martin, E. S., & West, N. (2016). Refining estimates of collision risk for harbour seals and tidal turbines. *Scottish Marine and Freshwater Science*, 7(17), 133. doi:10.7489/1786-1
- Bannasch, R., Wilson, R. P., & Culik, B. (1994). Hydrodynamic aspects of design and attachment of a back-mounted device in penguins. *The Journal of Experimental Biology*, 194(1), 83–96.
- Barkley, A. N., Broell, F., Pettitt-Wade, H., Watanabe, Y. Y., Marcoux, M., & Hussey, N. E. (2020). A framework to estimate the likelihood of species interactions and behavioural responses using animal-borne acoustic telemetry transceivers and accelerometers. *Journal of Animal Ecology*, 89(1), 146–160. doi:10.1111/1365-2656.13156
- Barrett-Lennard, L., Matkin, C., Durban, J., Saulitis, E., & Ellifrit, D. (2011). Predation on gray whales and prolonged feeding on submerged carcasses by transient killer whales at Unimak Island, Alaska. *Marine Ecology Progress Series*, 421, 229–241. doi:10.3354/meps08906
- Barron, D. G., Brawn, J. D., & Weatherhead, P. (2010). Meta-analysis of transmitter effects on avian behaviour and ecology. *Methods in Ecology and Evolution*, 1(2), 180–187. doi:10.1111/j.2041-210X.2010.00013.x
- Barros, Á., Álvarez, D., & Velando, A. (2013). Climate Influences Fledgling Sex Ratio and Sex-Specific Dispersal in a Seabird. *PLoS ONE*, 8(8), e71358. doi:10.1371/journal.pone.0071358
- Bartoń, K. A., Zwijacz-Kozica, T., Zięba, F., Sergiel, A., & Selva, N. (2019). Bears without borders: Long-distance movement in human-dominated

- landscapes. *Global Ecology and Conservation*, 17, e00541. doi:10.1016/j.gecco.2019.e00541
- Bastille-Rousseau, G., Potts, J. R., Yackulic, C. B., Frair, J. L., Hance Ellington, E., Blake, S., ... Blake, S. (2015). Flexible characterization of animal movement pattern using net squared displacement and a latent state model. *Movement Ecology*, 4(1), 15. doi:10.1186/s40462-016-0080-y
- Bates, D., Mächler, M., Bolker, B., & Walker, S. (2015). Fitting Linear Mixed-Effects Models Using lme4. *Journal of Statistical Software*, 67(1). doi:10.18637/jss.v067.i01
- Baylis, A. M. M., Þorbjörnsson, J. G., dos Santos, E., & Granquist, S. M. (2019). At-sea spatial usage of recently weaned grey seal pups in Iceland. *Polar Biology*, 42(11), 2165–2170. doi:10.1007/s00300-019-02574-5
- Beck, C. A., Bowen, W. D., & Iverson, S. J. (2000). Seasonal changes in buoyancy and diving behaviour of adult grey seals. *The Journal of Experimental Biology*, 203(15), 2323–30.
- Benard, M. F., & McCauley, S. J. (2008). Integrating across life-history stages: Consequences of natal habitat effects on dispersal. *American Naturalist*, 171(5), 553–567. doi:10.1086/587072
- Benjamins, S., Dale, A., Hastie, G., Waggitt, J., Lea, M.-A., Scott, B., & Wilson, B. (2015). Confusion Reigns? A Review of Marine Megafauna Interactions with Tidal-Stream Environments. In *Oceanography and Marine Biology: An Annual Review*, 53, 1–54. doi:10.1201/b18733-2
- Benjamins, S., Dale, A., Van Geel, N., & Wilson, B. (2016). Riding the tide: Use of a moving tidal-stream habitat by harbour porpoises. *Marine Ecology Progress Series*, 549, 275–288. doi:10.3354/meps11677
- Benjamins, S., van Geel, N., Hastie, G., Elliott, J., & Wilson, B. (2017). Harbour porpoise distribution can vary at small spatiotemporal scales in energetic habitats. *Deep Sea Research Part II: Topical Studies in Oceanography*, 141, 191–202. doi:10.1016/j.dsr2.2016.07.002
- Bennett, K. A., Hammill, M., & Currie, S. (2013). Liver glucose-6-phosphatase proteins in suckling and weaned grey seal pups: structural similarities to other mammals and relationship to nutrition, insulin signalling and metabolite levels. *Journal of Comparative Physiology B*, 183(8), 1075–1088.
- Bennett, K. A., McConnell, B. J., Moss, S. E. W., Speakman, J. R., Pomeroy, P. P., & Fedak, M. A. (2010). Effects of Age and Body Mass on Development of Diving Capabilities of Gray Seal Pups: Costs and Benefits of the Postweaning Fast. *Physiological and Biochemical Zoology*, 83(6), 911–923. doi:10.1086/656925
- Bennett, K. A., Speakman, J. R., Moss, S. E. W. W., Pomeroy, P., Fedak, M. A., Moss, S. E. W. W., ... Fedak, M. A. (2007). Effects of mass and body composition on fasting fuel utilisation in grey seal pups (*Halichoerus grypus Fabricius*): An experimental study using supplementary feeding. *Journal of Experimental Biology*, 210(17), 3043–3053.
- Bennison, A., Quinn, J. L., Debney, A., & Jessopp, M. (2019). Tidal drift removes the need for area-restricted search in foraging Atlantic puffins. *Biology Letters*, 15(7), 20190208.
- Bidder, O. R., Walker, J. S., Jones, M. W., Holton, M. D., Urge, P., Scantlebury, D. M., ... Wilson, R. P. (2015). Step by step: reconstruction of terrestrial animal movement paths by dead-reckoning. *Movement Ecology*, 3(1), 23.

- doi:10.1186/s40462-015-0055-4
- Bir, G. S., Lawson, M. J., & Li, Y. (2011). Structural Design of a Horizontal-Axis Tidal Current Turbine Composite Blade. In *ASME 30th International Conference on Ocean, Offshore, and Arctic Engineering*.
- Bjørge, A., Oien, N., Hartvedt, S., Bothun, G., & Bekkby, T. (2002). Dispersal and bycatch mortality in Gray *Halichoerus grypus*, and harbor *Phoca vitulina*, seals tagged at the Norwegian coast. *Marine Mammal Science*, 18(4), 963–976.
- Block, B. A., Jonsen, I. D., Jorgensen, S. J., Winship, A. J., Shaffer, S. A., Bograd, S. J., ... Costa, D. P. (2011). Tracking apex marine predator movements in a dynamic ocean. *Nature*, 475(7354), 86–90. doi:10.1038/nature10082
- Bodey, T. W., Cleasby, I. R., Bell, F., Parr, N., Schultz, A., Votier, S. C., & Bearhop, S. (2017). A phylogenetically controlled meta-analysis of biologging device effects on birds: Deleterious effects and a call for more standardized reporting of study data. *Methods in Ecology and Evolution*, 12(10), 3218–3221. doi:10.1111/2041-210X.12934
- Bonner, N., & Peters, R. H. (1985). *The Ecological Implications of Body Size*. Cambridge University Press. doi:10.2307/2403351
- Bordino, P. (2002). Movement patterns of franciscana dolphins (*Pontoporia blainvillei*) in Bahia Anegada, Buenos Aires, Argentina. *Latin American Journal of Aquatic Mammals*, 1(1), 71–76. doi:10.5597/LAJAM00011
- Börger, L. (2016). Editorial: Stuck in motion? Reconnecting questions and tools in movement ecology. *Journal of Animal Ecology*, 85(1), 5–10. doi:10.1111/1365-2656.12464
- Börger, L., Bijleveld, A. I., Fayet, A. L., Machovsky-Capuska, G. E., Patrick, S. C., Street, G. M., ... Vander Wal, E. (2020). Biologging Special Feature. *Journal of Animal Ecology*, 89(1), 6–15. doi:10.1111/1365-2656.13163
- Börger, L., & Fryxell, J. (2012). Quantifying individual differences in dispersal using net squared displacement. In J. Clobert (Ed.), *Dispersal Ecology and Evolution* (First Edit, pp. 222–230). Oxford University Press.
- Bowen, D. (2016). *Halichoerus grypus*. *The IUCN Red List of Threatened Species 2016: E.T9660A45226042*.
- Bowen, W. D., den Heyer, C. E., McMillan, J. I., & Iverson, S. J. (2015). Offspring size at weaning affects survival to recruitment and reproductive performance of primiparous gray seals. *Ecology and Evolution*, 5(7), 1412–1424.
- Bowler, D. E., & Benton, T. G. (2005). Causes and consequences of animal dispersal strategies: relating individual behaviour to spatial dynamics. *Biological Reviews*, 80(2), 205–225. doi:10.1017/S1464793104006645
- Boyd, J. M., Lockie, J. D., & Hewer, H. R. (1962). The breeding colony of grey seals on North Rona, 1959. *Proceedings of the Zoological Society of London*, 138(2), 257–278.
- Brandes, L. C. R., Graham, I., Hastie, G., & Thompson, P. (2018). Repeatability & foraging consistency of harbour seals in the Moray Firth, NE Scotland [Conference Abstract #BE07]. *32nd Conference of the European Cetacean Society, La Spezia, Italy, 6-10 April*.
- Brandon, J. R., Punt, A. E., Moreno, P., & Reeves, R. R. (2017). Toward a tier system approach for calculating limits on human-caused mortality of marine mammals. *ICES Journal of Marine Science*, 74(3), 877–887.

- doi:10.1093/icesjms/fsw202
- Bras, Y. Le, Jouma'a, J., & Guinet, C. (2017). Three-dimensional space use during the bottom phase of southern elephant seal dives. *Movement Ecology*, 5(1), 18. doi:10.1186/s40462-017-0108-y
- Brasseur, S. M. J. M., van Polanen Petel, T. D., Gerrodette, T., Meesters, E. H. W. G., Reijnders, P. J. H., & Aarts, G. (2015). Rapid recovery of Dutch gray seal colonies fueled by immigration. *Marine Mammal Science*, 31(2), 405–426. doi:10.1111/mms.12160
- Braune, B. M., & Gaskin, D. E. (1982). Feeding ecology of nonbreeding populations of larids off Deer Island, New Brunswick. *The Auk*, 99(1), 67–76.
- Breed, G. A., Matthews, C. J. D., Marcoux, M., Higdon, J. W., Le Blanc, B., Petersen, S. D., ... Ferguson, S. H. (2017). Sustained disruption of narwhal habitat use and behavior in the presence of Arctic killer whales. *Proceedings of the National Academy of Sciences of the United States of America*, 114(10), 2628–2633. doi:10.1073/pnas.1611707114
- Breed, G., Bowen, W., & Leonard, M. (2011). Development of foraging strategies with age in a long-lived marine predator. *Marine Ecology Progress Series*, 431, 267–279. doi:10.3354/meps09134
- Brown, D. D., Kays, R., Wikelski, M., Wilson, R., & Klimley, A. (2013). Observing the unwatchable through acceleration logging of animal behavior. *Animal Biotelemetry*, 1(1), 20. doi:10.1186/2050-3385-1-20
- Brown, R. F., & Mate, B. R. (1983). Abundance, movements, and feeding habits of harbor seals, *Phoca vitulina*, at Netarts and Tillamook Bays, Oregon. *Fishery Bulletin*, 81(2), 291–301.
- Bull, J. C., Börger, L., Franconi, N., Banga, R., Lock, K., Newman, P., ... Stringell, T. (2017). Temporal trends and phenology in grey seal (*Halichoerus grypus*) pup counts at Skomer, Wales. *Natural Resources Wales Evidence Report No. 217*.
- Burger, A. E., & Schaffer, A. S. (2008). Application of tracking and data-logging technology in research and conservation of seabirds. *The Auk*, 125(2), 253–264.
- Burke, B., Manley, P., & Bayley, S. (2020). Migration and wintering of first-year Llesse Black-backed Gulls *Larus fuscus graellsii* from two Irish colour-ringing projects. *Irish Birds*, 42, 112–116.
- Burnham, K. P., & Anderson, D. R. (2004). Multimodel Inference: Understanding AIC and BIC in Model Selection. *Sociological Methods & Research*, 33(2), 261–304.
- Byrne, A. W., Quinn, J. L., O'Keeffe, J. J., Green, S., Paddy Sleeman, D., Wayne Martin, S., & Davenport, J. (2014). Large-scale movements in European badgers: has the tail of the movement kernel been underestimated? *Journal of Animal Ecology*, 83(4), 991–1001. doi:10.1111/1365-2656.12197
- Byrne, M. E., Holland, A. E., Bryan, A. L., & Beasley, J. C. (2017). Environmental conditions and animal behavior influence performance of solar-powered GPS-GSM transmitters. *The Condor*, 119(3), 389–404. doi:10.1650/condor-16-76.1
- Cade, D. E., Barr, K. R., Calambokidis, J., Friedlaender, A. S., & Goldbogen, J. A. (2017). Determining forward speed from accelerometer jiggle in aquatic environments. *The Journal of Experimental Biology*, 221(2).

- doi:10.1242/jeb.170449
- Cagnacci, F., Boitani, L., Powell, R. A., & Boyce, M. S. (2010). Animal ecology meets GPS-based radiotelemetry: a perfect storm of opportunities and challenges. *Philosophical Transactions of the Royal Society B: Biological Sciences*, 365(1550), 2157–2162. doi:10.1098/rstb.2010.0107
- Cairns, D. K., & Schneider, D. C. (1990). Hot spots in cold water: feeding habitat selection by thick-billed murre. *Studies in Avian Biology*, 14, 52–60.
- Camphuysen, C. J., Fox, A. D., Leopold, M. F., & Petersen, I. K. (2004). Towards standardised seabirds at sea census techniques in connection with environmental impact assessments for offshore wind farms in the UK. *Report by Royal Netherlands Institute for Sea Research and the Danish National Environmental Research Institute Commissioned by Cowrie Ltd.*
- Canadian Council on Animal Care. (2003). CCAC Guidelines on: The Care and Use of Wildlife. *Canadian Council on Animal Care, Ottawa, Ontario, Canada.*
- Carneiro, A. P. B., Bonnet-Lebrun, A. S., Manica, A., Staniland, I. J., & Phillips, R. A. (2017). Methods for detecting and quantifying individual specialisation in movement and foraging strategies of marine predators. *Marine Ecology Progress Series*, 578, 151–166. doi:10.3354/meps12215
- Carter, M. I. D. (2018). From pup to predator: ontogeny of foraging behaviour in grey seal (*Halichoerus grypus*) pups. *PhD Thesis*. doi:10.1016/j.electstud.2004.07.005
- Carter, M. I. D., McClintock, B. T., Embling, C. B., Bennett, K. A., Thompson, D., & Russell, D. J. F. (2019). From pup to predator; generalized hidden Markov models reveal rapid development of movement strategies in a naïve long-lived vertebrate. *Oikos*, 129(5), 630–642. doi:10.1111/oik.06853
- Carter, M.I.D., Bennett, K. A., Embling, C. B., Hosegood, P. J., & Russell, D. J. F. (2016). Navigating uncertain waters: a critical review of inferring foraging behaviour from location and dive data in pinnipeds. *Movement Ecology*, 4(1), 1–20. doi:10.1186/s40462-016-0090-9
- Carter, M. I. D., Boehme, L., Duck, C. D., Grecian, W. J., Hastie, G. D., Mcconnell, B. J., ... Russell, D. J. F. (2020). Habitat-based predictions of at-sea distribution for grey and harbour seals in the British Isles Report to BEIS. *OESEA-16-76/OESEA-17-78.*
- Carter, M. I. D., Russell, D. J. F., Embling, C. B., Blight, C. J., Thompson, D., Hosegood, P. J., & Bennett, K. A. (2017). Intrinsic and extrinsic factors drive ontogeny of early-life at-sea behaviour in a marine top predator. *Scientific Reports*, 7(1), 1–14. doi:10.1038/s41598-017-15859-8
- Casper, R. M. (2009). Guidelines for the instrumentation of wild birds and mammals. *Animal Behaviour*, 78(6), 1477–1483. doi:10.1016/j.anbehav.2009.09.023
- Catalano, K. A., Dedrick, A. G., Stuart, M. R., Puritz, J. B., Montes, H. R., & Pinsky, M. L. (2021). Quantifying dispersal variability among nearshore marine populations. *Molecular Ecology*, 30(10), 2366–2377. doi:10.1111/mec.15732
- Chapman, C. A., & Reyna-hurtado, R. (2019). Why Movement Ecology Matters. In C. A. Chapman & R. Reyna-hurtado (Eds.), *Movement Ecology of Neotropical Forest Mammals* (pp. 1–3). Springer, Cham.

- Chapple, T. K., Gleiss, A. C., Jewell, O. J. D., Wikelski, M., & Block, B. A. (2015). Tracking sharks without teeth: a non-invasive rigid tag attachment for large predatory sharks. *Animal Biotelemetry*, 3(1), 14. doi:10.1186/s40317-015-0044-9
- Chenoweth, E., Gabriele, C., & Hill, D. (2011). Tidal influences on humpback whale habitat selection near headlands. *Marine Ecology Progress Series*, 423, 279–289.
- Chilvers, B. L., Corkeron, P. J., Blanshard, W. H., Long, T. R., & Martin, A. R. (2001). A new VHF tag and attachment technique for small cetaceans. *Aquatic Mammals*, 27(1), 11–15.
- Chowdhury, M. S., Rahman, K. S., Selvanathan, V., Nuthammachot, N., Suklueng, M., Mostafaeipour, A., ... Techato, K. (2020). Current trends and prospects of tidal energy technology. *Environment, Development and Sustainability*, 23(6), 8179–8194. doi:10.1007/s10668-020-01013-4
- Christiansen, F., Nielsen, M. L. K., Charlton, C., Bejder, L., & Madsen, P. T. (2020). Southern right whales show no behavioral response to low noise levels from a nearby unmanned aerial vehicle. *Marine Mammal Science*, 36(3), 953–963. doi:10.1111/mms.12699
- Cianchetti-Benedetti, M., Dell’Omo, G., Russo, T., Catoni, C., & Quillfeldt, P. (2018). Interactions between commercial fishing vessels and a pelagic seabird in the southern Mediterranean Sea. *BMC Ecology*, 18(1), 54. doi:10.1186/s12898-018-0212-x
- Clark, P. E., Johnson, D. E., Kniep, M. A., Jermann, P., Huttash, B., Wood, A., ... Titus, K. (2006). An advanced, low-cost, GPS-based animal tracking system. *Rangeland Ecology and Management*, 59(3), 334–340. doi:10.2111/05-162R.1
- Claudet, J., Osenberg, C. W., Domenici, P., Badalamenti, F., Milazzo, M., Falcón, J. M., ... Planes, S. (2010). Marine reserves: Fish life history and ecological traits matter. *Ecological Applications*, 20(3), 830–839. doi:10.1890/08-2131.1
- Clay, T. A., Joo, R., Weimerskirch, H., Phillips, R. A., Ouden, O. Den, Clusellatruillas, M. B. S., ... Patrick, S. C. (2020). Sex-specific effects of wind on the flight decisions of a sexually dimorphic soaring bird. *Journal of Animal Ecology*, 89(8), 1811–1823. doi:10.1111/1365-2656.13267
- Clobert, J., Le Galliard, J. F., Cote, J., Meylan, S., & Massot, M. (2009). Informed dispersal, heterogeneity in animal dispersal syndromes and the dynamics of spatially structured populations. *Ecology Letters*, 12(3), 197–209.
- Cole, E.-L., Waggitt, J. J., Hedenstrom, A., Piano, M., Holton, M. D., Börger, L., & Shepard, E. L. C. (2018). The Ornithodolite as a tool to quantify animal space use and habitat selection; a case study with birds diving in tidal waters. *Integrative Zoology*, 10, 267–281. doi:10.1111/1749-4877.12327
- Computers Inc, W. (2017). SPOT Tag User Guide. Redmond, WA, USA.
- Copeland, H. E., Sawyer, H., Monteith, K. L., Naugle, D. E., Pocewicz, A., Graf, N., & Kauffman, M. J. (2014). Conserving migratory mule deer through the umbrella of sage-grouse. *Ecosphere*, 5(9), 1–16. doi:10.1890/ES14-00186.1
- Copping, A. E., Freeman, M. C., Gorton, A. M., & Hemery, L. G. (2020). Risk Retirement—Decreasing Uncertainty and Informing Consenting

- Processes for Marine Renewable Energy Development. *Journal of Marine Science and Engineering* 2020, 8(3), 172. doi:10.3390/JMSE8030172
- Copping, A. E., Hemery, L. G., Overhus, D. M., Garavelli, L., Freeman, M. C., Whiting, J. M., ... Tugade, L. G. (2020). Potential environmental effects of marine renewable energy development—the state of the science. *Journal of Marine Science and Engineering*, 8(11), 1–18.
- Copping, A., & Hemery, L. (2020). *OES-Environmental 2020 State of the Science Report: Environmental Effects of Marine Renewable Energy Development Around the World. Report for Ocean Energy Systems (OES)*.
- Copping, A., Sather, N., Hannah, L., Whiting, J., Zydlewski, G., Staines, G., ... Masden, E. (2016). Annex IV 2016 State of the Science Report: Environmental Effects of Marine Renewable Energy Development Around the World.
- Copping, A., Gear, M., Jepsen, R., Chartrand, C., & Gorton, A. (2017). Understanding the potential risk to marine mammals from collision with tidal turbines. *International Journal of Marine Energy*, 19, 110–123. doi:10.1016/j.ijome.2017.07.004
- Cornick, L. A., Inglis, S. D., Willis, K., & Horning, M. (2006). Effects of increased swimming costs on foraging behavior and efficiency of captive Steller sea lions: Evidence for behavioral plasticity in the recovery phase of dives. *Journal of Experimental Marine Biology and Ecology*, 333(2), 306–314. doi:10.1016/j.jembe.2006.01.010
- Council, Marine Energy (2019). *UK Marine Energy 2019. A New Industry. Scottish Renewables* (Vol. 1).
- Couriot, O., Hewison, A. J. M., Saïd, S., Cagnacci, F., Chamailié-Jammes, S., Linnell, J. D. C., ... Morellet, N. (2018). Truly sedentary? The multi-range tactic as a response to resource heterogeneity and unpredictability in a large herbivore. *Oecologia*, 187(1), 47–60. doi:10.1007/s00442-018-4131-5
- Cox, S. L., Orgeret, F., Gesta, M., Rodde, C., Heizer, I., Weimerskirch, H., & Guinet, C. (2018). Processing of acceleration and dive data on-board satellite relay tags to investigate diving and foraging behaviour in free-ranging marine predators. *Methods in Ecology and Evolution*, 9(1), 64–77. doi:10.1111/2041-210X.12845
- Cox, S., Scott, B., & Camphuysen, C. (2013). Combined spatial and tidal processes identify links between pelagic prey species and seabirds. *Marine Ecology Progress Series*, 479, 203–221. doi:10.3354/meps10176
- Cozzi, G., Behr, D. M., Webster, H. S., Claase, M., Bryce, C. M., Modise, B., ... Ozgul, A. (2020). African Wild Dog Dispersal and Implications for Management. *The Journal of Wildlife Management*, 84(4), 614–621. doi:10.1002/jwmg.21841
- Crawley, M. J. (2007). *The R Book. The R Book*. doi:10.1002/9780470515075
- Croxall, J. P., & Prince, P. A. (1996). Potential interactions between wandering albatrosses and longline fisheries for patagonian toothfish at South Georgia. *CCAMLR Science*, 3, 101–110.
- Culik, B. M., Bannasch, R., & Wilson, R. P. (1994). External devices on penguins: How important is shape? *Marine Biology*, 118, 353–357.
- Culik, B., & Wilson, R. P. (1991). Swimming energetics and performance of instrumented adelic penguins (*Pygoscelis adeliae*). *Journal of*

- Experimental Biology*, 158, 355–368.
- Cunningham, L., Baxter, J. M., & Boyd, I. L. (2010). Variation in harbour seal counts obtained using aerial surveys. *Journal of the Marine Biological Association of the United Kingdom*, 90(8), 1659–1666. doi:10.1017/S002531540999155X
- Cunningham, L., Baxter, J. M., Boyd, I. L., Duck, C. D., Lonergan, M., Moss, S. E., & McConnell, B. (2009). Harbour seal movements and haul-out patterns: implications for monitoring and management. *Aquatic Conservation: Marine and Freshwater Ecosystems*, 19(4), 398–407. doi:10.1002/aqc.983
- Daunt, F., Afanasyev, V., Adam, A., Croxall, J. P., & Wanless, S. (2007). From cradle to early grave: juvenile mortality in European shags *Phalacrocorax aristotelis*; results from inadequate development of foraging proficiency. *Biology Letters*, 3(4), 371–374. doi:10.1098/rsbl.2007.0157
- Davidian, M., & Giltinan, D. M. (2017). *Nonlinear Models for Repeated Measurement Data*. Routledge. doi:10.1201/9780203745502
- Davies, R. W., Williams, T. M., & Kooyman, G. L. (1985). Swimming metabolism of yearling and adult harbor seals *Phoca vitulina*. *Physiological Zoology*, 58(5), 590–596.
- Davies, J. L. (1949). Observations on the Grey Seal (*Halichoerus grypus*) at Ramsey Island, Pembrokeshire. *Proceedings of the Zoological Society of London*, 119(3), 673–692. doi:10.1111/j.1096-3642.1949.tb00896.x
- Davis, R. W., Fuiman, L. A., Williams, T. M., & Le Boeuf, B. J. (2001). Three-dimensional movements and swimming activity of a northern elephant seal. *Comparative Biochemistry and Physiology - A Molecular and Integrative Physiology*, 129(4), 759–770. doi:10.1016/S1095-6433(01)00345-2
- Dawson, T. M., Formia, A., Agamboué, P. D., Asseko, G. M., Boussamba, F., Cardiec, F., ... Maxwell, S. M. (2017). Informing Marine Protected Area Designation and Management for Nesting Olive Ridley Sea Turtles Using Satellite Tracking. *Frontiers in Marine Science*, 4, 312. doi:10.3389/fmars.2017.00312
- de Boer, M. N., Simmonds, M. P., Reijnders, P. J. H., & Aarts, G. (2014). The Influence of Topographic and Dynamic Cyclic Variables on the Distribution of Small Cetaceans in a Shallow Coastal System. *PLoS ONE*, 9(1), e86331. doi:10.1371/journal.pone.0086331
- de Grissac, S., Börger, L., Guitteaud, A., & Weimerskirch, H. (2016). Contrasting movement strategies among juvenile albatrosses and petrels. *Scientific Reports*, 6(1), 26103. doi:10.1038/srep26103
- De La Vega, C., Lebreton, B., Siebert, U., Guillou, G., Das, K., Asmus, R., & Asmus, H. (2016). Seasonal variation of harbor Seal's diet from the wadden sea in relation to prey availability. *PLoS ONE*, 11(5), 1–21. doi:10.1371/journal.pone.0155727
- Del Caño, M., Quintana, F., Yoda, K., Dell'Omo, G., Blanco, G. S., & Gómez-Laich, A. (2021). Fine-scale body and head movements allow to determine prey capture events in the Magellanic Penguin (*Spheniscus magellanicus*). *Marine Biology*, 168(6), 84. doi:10.1007/s00227-021-03892-1
- DeMaster, D. P., Fowler, C. W., Perry, S. L., & Richlen, M. F. (2001). Predation and competition: The impact of fisheries on marine-mammal populations

- over the next one hundred years. *Journal of Mammalogy*, 82(3), 641-651.
- DeRuiter, S. L., Langrock, R., Skirbutas, T., Goldbogen, J. A., Calambokidis, J., Friedlaender, A. S., & Southall, B. L. (2017). A multivariate mixed hidden Markov model for blue whale behaviour and responses to sound exposure. *The Annals of Applied Statistics*, 11(1), 362–392. doi:10.1214/16-AOAS1008
- Dickinson, E. R., Stephens, P. A., Marks, N. J., Wilson, R. P., & Scantlebury, D. M. (2020). Best practice for collar deployment of tri-axial accelerometers on a terrestrial quadruped to provide accurate measurement of body acceleration. *Animal Biotelemetry*, 8(1), 1-8. doi:10.1186/s40317-020-00198-9
- Dujon, A. M., Lindstrom, R. T., & Hays, G. C. (2014). The accuracy of Fastloc-GPS locations and implications for animal tracking. *Methods in Ecology and Evolution*, 5(11), 1162–1169. doi:10.1111/2041-210X.12286
- Dunn, D. C., Harrison, A.-L., Curtice, C., DeLand, S., Donnelly, B., Fujioka, E., ... Halpin, P. N. (2019). The importance of migratory connectivity for global ocean policy. *Proceedings of the Royal Society B: Biological Sciences*, 286(1911), 20191472. doi:10.1098/rspb.2019.1472
- Egevang, C., Stenhouse, I. J., Phillips, R. A., Petersen, A., Fox, J. W., & Silk, J. R. D. (2010). Tracking of Arctic terns *Sterna paradisaea* reveals longest animal migration. *Proceedings of the National Academy of Sciences*, 107(5), 2078–2081. doi:10.1073/pnas.0909493107
- Eguchi, T., & Harvey, J. T. (2005). Diving behavior of the pacific harbour seal (*Phoca vitulina Ricardii*) in Monterey Bay, California. *Marine Mammal Science*, 21(2), 283–295. doi:10.1111/j.1748-7692.2005.tb01228.x
- Elliott, J. T. (2004). *Seabird and cetacean distribution in relation to tidal activity within the Gulf of Corryvreckan, Scotland*. MSc Thesis, University of Aberdeen, Scotland, UK.
- Embling, C. B., Gillibrand, P. A., Gordon, J., Shrimpton, J., Stevick, P. T., & Hammond, P. S. (2010). Using habitat models to identify suitable sites for marine protected areas for harbour porpoises (*Phocoena phocoena*). *Biological Conservation*, 143(2), 267–279. doi:10.1016/j.biocon.2009.09.005
- Embling, C. B., Illian, J., Armstrong, E., van der Kooij, J., Sharples, J., Camphuysen, K. C. J., & Scott, B. E. (2012). Investigating fine-scale spatio-temporal predator-prey patterns in dynamic marine ecosystems: A functional data analysis approach. *Journal of Applied Ecology*, 49(2), 481–492.
- Estes, J. A., Heithaus, M., McCauley, D. J., Rasher, D. B., & Worm, B. (2016). Megafaunal Impacts on Structure and Function of Ocean Ecosystems. *Annual Review of Environment and Resources*, 41, 83-116. doi:10.1146/annurev-environ-110615-085622
- Estes, J. A., Terborgh, J., Brashares, J. S., Power, M. E., Berger, J., Bond, W. J., ... Wardle, D. A. (2011). Trophic downgrading of planet earth. *Science*, 333(6040).
- EU. (2010). Directive 2010/63/EU Of The European Parliament and of the Council of 22 September 2010 On the Protection of Animals used for Scientific Purposes. *Official Journal of the European Union*, L276, 33–79.
- Evans, B. J., Hassan, O., Jones, J. W., Morgan, K., & Remaki, L. (2009). Simulating Steady State and Transient Aerodynamic Flows Using

- Unstructured Meshes and Parallel Computers. In M. M. Hafez, K. Oshima, & D. Kwak (Eds.), *Computational Fluid Dynamics Review 2010* (pp. 1–28). World Scientific, New Jersey.
- Evans, B. J., Hassan, O., Jones, J. W., Morgan, K., & Remaki, L. (2011). Computational fluid dynamics applied to the aerodynamic design of a land-based supersonic vehicle. *Numerical Methods for Partial Differential Equations*, 27(1), 141–159. doi:10.1002/num.20644
- Fancy, S. G., Pank, L. F., Douglas, D. C., Curby, C. H., Garner, G. W., Amstrup, S. C., & Regelin, W. L. (1988). Satellite telemetry: a new tool for wildlife research and management. *United States Fisheries Wildlife Resources Publication, No. FWS-PU(1–54)*.
- Fedak, M. A., & Anderson, S. S. (1982). The energetics of lactation: accurate measurements from a large wild animal, the grey seal (*Halichoerus grypus*). *Journal of Zoology, London*, 198, 473–479. doi:10.1111/jzo.1982.198.4.473
- Fedak, M. a, Anderson, S. S., & Curry, M. G. (1983). Attachment of a radio tag to the fur of seals. *Journal of Zoology*, 200(2), 298–300. doi:10.1111/j.1469-7998.1983.tb05794.x
- Ferreira, L. C., Thums, M., Fossette, S., Wilson, P., Shimada, T., Tucker, A. D., ... Whiting, S. D. (2020). Multiple satellite tracking datasets inform green turtle conservation at a regional scale. *Diversity and Distributions*, 27(2), 249-266. doi:10.1111/ddi.13197
- Field, I. C., Bradshaw, C. J. A., Burton, H. R., Sumner, M. D., & Hindell, M. A. (2005). Resource partitioning through oceanic segregation of foraging juvenile southern elephant seals (*Mirounga leonina*). *Oecologia*, 142(1), 127–135. doi:10.1007/s00442-004-1704-2
- Field, I. C., Harcourt, R. G., Boehme, L., De Bruyn, P. J. N., Charrassin, J. B., McMahon, C. R., ... Hindell, M. A. (2012). Refining instrument attachment on phocid seals. *Marine Mammal Science*, 28(3), 325–332.
- Fiore, G., Anderson, E., Garborg, C. S., Murray, M., Johnson, M., Moore, M. J., ... Shorter, K. A. (2017). From the track to the ocean: Using flow control to improve marine bio-logging tags for cetaceans. *PLoS ONE*, 12(2), 1–19.
- Foley, C. J., & Sillero-Zubiri, C. (2020). Open-source, low-cost modular GPS collars for monitoring and tracking wildlife. *Methods in Ecology and Evolution*, 11(4), 553–558. doi:10.1111/2041-210X.13369
- Forcada, J. (2018). Distribution. *Encyclopedia of Marine Mammals*, 259–262. doi:10.1016/B978-0-12-804327-1.00106-0
- Fossette, S., Witt, M. J., Miller, P., Nalovic, M. A., Albareda, D., Almeida, A. P., ... Godley, B. J. (2014). Pan-Atlantic analysis of the overlap of a highly migratory species, the leatherback turtle, with pelagic longline fisheries. *Proceedings of the Royal Society B: Biological Sciences*, 281(1780), 20133065. doi:10.1098/rspb.2013.3065
- Fossette, S., Katija, K., Goldbogen, J. A., Bograd, S., Patry, W., Howard, M. J., ... Gleiss, A. C. (2016). How to tag a jellyfish? A methodological review and guidelines to successful jellyfish tagging. *Journal of Plankton Research*, 38, 1347–1363. doi:10.1093/plankt/fbw073
- Fox, C. J., Benjamins, S., Masden, E. A., & Miller, R. (2018). Challenges and opportunities in monitoring the impacts of tidal-stream energy devices on marine vertebrates. *Renewable and Sustainable Energy Reviews*, 81,

- 1926–1938.
- Fraenkel, P. L. (2006). Tidal Current Energy Technologies. *Ibis*, *148*, 145–151. doi:10.1111/j.1474-919X.2006.00518.x
- Fraser, K. C., Davies, K. T. A., Davy, C. M., Ford, A. T., Flockhart, D. T. T., & Martins, E. G. (2018). Tracking the conservation promise of movement ecology. *Frontiers in Ecology and Evolution*, *6*, 150. doi:10.3389/fevo.2018.00150
- Gaggiotti, O. E., Jones, F., Lee, W. M., Amos, W., Harwood, J., & Nichols, R. A. (2002). Patterns of colonization in a metapopulation of grey seals. *Nature*, *416*(6879), 424–427. doi:10.1038/416424a
- Gallon, S. L., Sparling, C. E., Georges, J.-Y., Fedak, M. A., Biuw, M., & Thompson, D. (2007). How fast does a seal swim? Variations in swimming behaviour under differing foraging conditions. *Journal of Experimental Biology*, *210*(18), 3285–3294. doi:10.1242/jeb.007542
- Gaspar, P., Georges, J.-Y. J., Fossette, S., Lenoble, A., Ferraroli, S., Le Maho, Y., & Maho, Y. Le. (2006). Marine animal behaviour: neglecting ocean currents can lead us up the wrong track. *Proceedings of the Royal Society B: Biological Sciences*, *273*(1602), 2697–2702. doi:10.1098/rspb.2006.3623
- Geertsen, B. M., Teilmann, J., Kastelein, R. a, Vlemmix, H. N. J., & Miller, L. A. (2004). Behaviour and physiological effects of transmitter attachments on a captive harbour porpoise (*Phocoena phocoena*). *Journal of Cetacean Research and Management*, *6*(2), 139–146.
- Genin, A. (2004). Bio-physical coupling in the formation of zooplankton and fish aggregations over abrupt topographies. *Journal of Marine Systems*, *50*, 3–20.
- Gill, Jr., R. E., & Hall, J. D. (1983). Use of Nearshore and Estuarine Areas of the Southeastern Bering Sea by Gray Whales (*Eschrichtius robustus*). *Arctic*, *36*(3). doi:10.14430/arctic2276
- Gillespie, D., Palmer, L., Macaulay, J., Sparling, C., & Hastie, G. (2021). Harbour porpoises exhibit localized evasion of a tidal turbine. *Aquatic Conservation: Marine and Freshwater Ecosystems*. doi:10.1002/AQC.3660
- Gills, B., & Morgan, J. (2020). Global Climate Emergency: after COP24, climate science, urgency, and the threat to humanity. *Globalizations*, *17*(6), 885–902.
- Gjertz, I., Lydersen, C., & Wiig, Ø. (2001). Distribution and diving of harbour seals (*Phoca vitulina*) in Svalbard. *Polar Biology*, *24*(3), 209-214. doi:10.1007/s0030000000197
- Gleiss, A. C., Norman, B., Liebsch, N., Francis, C., & Wilson, R. P. (2009). A new prospect for tagging large free-swimming sharks with motion-sensitive data-loggers. *Fisheries Research*, *97*(1–2), 11–16. doi:10.1016/j.fishres.2008.12.012
- Goetz, F. W., Jasonowicz, A. J., & Roberts, S. B. (2018). What goes up must come down: Diel vertical migration in the deep-water sablefish (*Anoplopoma fimbria*) revealed by pop-up satellite archival tags. *Fisheries Oceanography*, *27*(2), 127–142. doi:10.1111/fog.12239
- Goldbogen, J. A., Hazen, E. L., Friedlaender, A. S., Calambokidis, J., DeRuiter, S. L., Stimpert, A. K., & Southall, B. L. (2015). Prey density and distribution drive the three-dimensional foraging strategies of the largest

- filter feeder. *Functional Ecology*, 29(7), 951–961. doi:10.1111/1365-2435.12395
- Gottwald, J., Zeidler, R., Friess, N., Ludwig, M., Reudenbach, C., & Nauss, T. (2019). Introduction of an automatic and open-source radio-tracking system for small animals. *Methods in Ecology and Evolution*, 10(12), 2163–2172. doi:10.1111/2041-210X.13294
- Gräwe, U., Flöser, G., Gerkema, T., Duran-Matute, M., Badewien, T. H., Schulz, E., & Burchard, H. (2016). A numerical model for the entire Wadden Sea: Skill assessment and analysis of hydrodynamics. *Journal of Geophysical Research: Oceans*, 121(7), 5231–5251. doi:10.1002/2016JC011655
- Grecian, W. J., Masden, E. A., Hammond, P. S., Owen, E., Daunt, F., Wanless, S., & Russell, D. J. F. (2018). Man-made structures and Apex Predators: Spatial interactions and overlap (MAPS). Final report to INSITE.
- Greig, D. J., Gulland, F. M. D., Harvey, J. T., Lonergan, M., & Hall, A. J. (2018). Harbor seal pup dispersal and individual morphology, hematology, and contaminant factors affecting survival. *Marine Mammal Science*, 35(1), 187–209. doi:10.1111/mms.12541
- Grusha, D. S., & Patterson, M. R. (2005). Quantification of drag and lift imposed by pop-up satellite archival tags and estimation of the metabolic cost to cownose rays (*Rhinoptera bonasus*). *Fishery Bulletin*, 103(1), 63–70.
- Guisande, C., Vergara, A. R., Riveiro, I., & Cabanas, J. M. (2004). Climate change and abundance of the Atlantic-Iberian sardine (*Sardina pilchardus*). *Fisheries Oceanography*, 13(2), 91–101. doi:10.1046/j.1365-2419.2003.00276.x
- Guisande, C., Cabanas, J. M., Vergara, A. R., & Riveiro, I. (2001). Effect of climate on recruitment success of Atlantic Iberian sardine *Sardina pilchardus*. *Marine Ecology Progress Series*, 223, 243–250.
- Hall, A. J., & Russell, D. J. F. (2018). Gray Seal. In *Encyclopedia of Marine Mammals*, 52, 420–422. Elsevier. doi:10.1016/b978-0-12-804327-1.00139-4
- Halpern, B. S., Frazier, M., Potapenko, J., Casey, K. S., Koenig, K., Longo, C., ... Walbridge, S. (2015). Spatial and temporal changes in cumulative human impacts on the world's ocean. *Nature Communications*, 6, 1–7. doi:10.1038/ncomms8615
- Halpern, B. S., Walbridge, S., Selkoe, K. A., Kappel, C. V., Micheli, F., D'Agrosa, C., ... Watson, R. (2008). A Global Map of Human Impact on Marine Ecosystems. *Science*, 319(5865), 948–952. doi:10.1126/science.1149345
- Harnos, A., Fehérvári, P., & Csörgő, T. (2015). Hitchhikers' guide to analysing bird ringing data. *Ornis Hungarica*, 23(2), 163–188. doi:10.1515/orhu-2015-0018
- Harris, M. P., Bogdanova, M. I., Daunt, F., & Wanless, S. (2012). Using GPS technology to assess feeding areas of Atlantic Puffins *Fratercula arctica*. *Ringling & Migration*, 27(1), 43–49. doi:10.1080/03078698.2012.691247
- Harrison, A. L., Costa, D. P., Winship, A. J., Benson, S. R., Bograd, S. J., Antolos, M., ... Block, B. A. (2018). The political biogeography of migratory marine predators. *Nature Ecology and Evolution*, 2(10), 1571–1578. doi:10.1038/s41559-018-0646-8

- Harwood, J., Anderson, S. S., & Curry, M. G. (1976). Branded Grey seals (*Halichoerus grypus*) at the Monach Isles, Outer Hebrides. *Journal of Zoology*, 180(4), 506–508. doi:10.1111/j.1469-7998.1976.tb04698.x
- Harwood, J., & Prime, J. H. (1978). Some Factors Affecting the Size of British Grey Seal Populations. *The Journal of Applied Ecology*, 15(2), 401. doi:10.2307/2402600
- Hastie, G. D. (2012). *Tracking marine mammals around marine renewable energy devices using active sonar. SMRU Ltd report URN:12D/328 to the Department of Energy and Climate Change, SMRU, St. Andrews.*
- Hastie, G. D., Bivins, M., Coram, A., Gordon, J., Jepp, P., MacAulay, J., ... Gillespie, D. (2019). Three-dimensional movements of harbour seals in a tidally energetic channel: Application of a novel sonar tracking system. *Aquatic Conservation: Marine and Freshwater Ecosystems*, 29(4), 564–575. doi:10.1002/aqc.3017
- Hastie, G. D., Russell, D. J. F., Benjamins, S., Moss, S., Wilson, B., & Thompson, D. (2016). Dynamic habitat corridors for marine predators; intensive use of a coastal channel by harbour seals is modulated by tidal currents. *Behavioral Ecology and Sociobiology*, 70(12), 2161–2174. doi:10.1007/s00265-016-2219-7
- Hastie, G. D., Russell, D. J. F., Lepper, P., Elliott, J., Wilson, B., Benjamins, S., & Thompson, D. (2017). Harbour seals avoid tidal turbine noise: Implications for collision risk. *Journal of Applied Ecology*, 55(2), 684–693. doi:10.1111/1365-2664.12981
- Hastie, G. D., Wu, G.-M., Moss, S., Jepp, P., J., M., Lee, A., & Gillespie, D. (2019). Automated detection and tracking of marine mammals: a novel sonar tool for monitoring effects of marine industry. *Aquatic Conservation: Marine and Freshwater Ecosystems*, 29, 119–130. doi:10.1002/aqc.3103
- Hawkes, C. (2009). Linking movement behaviour, dispersal and population processes: Is individual variation a key? *Journal of Animal Ecology*, 78(5), 894–906. doi:10.1111/j.1365-2656.2009.01534.x
- Hays, G. C., Bradshaw, C. J. A., James, M. C., Lovell, P., & Sims, D. W. (2007). Why do Argos satellite tags deployed on marine animals stop transmitting? *Journal of Experimental Marine Biology and Ecology*, 349(1), 52–60. doi:10.1016/j.jembe.2007.04.016
- Hays, G. C., Bastian, T., Doyle, T. K., Fossette, S., Gleiss, A. C., Gravenor, M. B., ... Sims, D. W. (2012). High activity and Lévy searches: jellyfish can search the water column like fish. *Proceedings of the Royal Society B: Biological Sciences*, 279(1728), 465–473. doi:10.1098/rspb.2011.0978
- Hays, G. C., Bailey, H., Bograd, S. J., Bowen, W. D., Campagna, C., Carmichael, R. H., ... Sequeira, A. M. M. (2019). Translating Marine Animal Tracking Data into Conservation Policy and Management. *Trends in Ecology and Evolution*, 34(5), 459–473. doi:10.1016/j.tree.2019.01.009
- Hays, G. C., Broderick, A. C., Godley, B. J., Luschi, P., & Nichols, W. J. (2003). Satellite telemetry suggests high levels of fishing-induced mortality in marine turtles. *Marine Ecology Progress Series*, 262, 305–309. doi:10.3354/meps262305
- Hays, G. C., Ferreira, L. C., Sequeira, A. M. M., Meekan, M. G., Duarte, C. M., Bailey, H., ... Thums, M. (2016). Key Questions in Marine Megafauna Movement Ecology. *Trends in Ecology and Evolution*, 31(6), 463–475. doi:10.1016/j.tree.2016.02.015

- Hays, G. C., & Hawkes, L. A. (2018). Satellite Tracking Sea Turtles: Opportunities and Challenges to Address Key Questions. *Frontiers in Marine Science*, 5. doi:10.3389/fmars.2018.00432
- Hays, G. C., Mortimer, J. A., Rattray, A., Shimada, T., & Esteban, N. (2021). High accuracy tracking reveals how small conservation areas can protect marine megafauna. *Ecological Applications*. doi:10.1002/eap.2418
- Hazekamp, A. A. H., Mayer, R., & Osinga, N. (2010). Flow simulation along a seal: The impact of an external device. *European Journal of Wildlife Research*, 56(2), 131–140. doi:10.1007/s10344-009-0293-0
- Hazen, E. L., Abrahms, B., Brodie, S., Carroll, G., Jacox, M. G., Savoca, M. S., ... Bograd, S. J. (2019). Marine top predators as climate and ecosystem sentinels. *Frontiers in Ecology and the Environment*, 17(10), 565–574. doi:10.1002/fee.2125
- Hazen, E. L., Maxwell, S. M., Bailey, H., Bograd, S. J., Hamann, M., Gaspar, P., ... Shillinger, G. L. (2012). Ontogeny in marine tagging and tracking science: Technologies and data gaps. *Marine Ecology Progress Series*, 457, 221–240. doi:10.3354/meps09857
- Heal, M., Hoover, B. A., & Waggitt, J. J. (2021). Using rangefinder binoculars to measure the behaviour and movement of European Shags *Phalacrocorax aristotelis* in coastal environments. *Bird Study*, 1–6.
- Hebblewhite, M., & Haydon, D. T. (2010). Distinguishing technology from biology: a critical review of the use of GPS telemetry data in ecology. *Philosophical Transactions of the Royal Society B: Biological Sciences*, 365(1550), 2303–2312. doi:10.1098/rstb.2010.0087
- Heerah, K., Cox, S. L., Blevin, P., Guinet, C., & Charrassin, J.-B. (2019). Validation of dive foraging indices using archived and transmitted acceleration data: the case of the Weddell seal. *Front Ecol Environ*, 7(30), 1–15. doi:10.3389/fevo.2019.00030
- Heim, W., Heim, R. J., Beermann, I., Burkovskiy, O. A., Gerasimov, Y., Ktitorov, P., ... Kamp, J. (2020). Using geolocator tracking data and ringing archives to validate citizen-science based seasonal predictions of bird distribution in a data-poor region. *Global Ecology and Conservation*, 24, e01215. doi:10.1016/j.gecco.2020.e01215
- Heithaus, M. R., Dill, L. M., & Kiszka, J. J. (2018). Feeding Strategies and Tactics. In *Encyclopedia of Marine Mammals* (Vol. 70, pp. 354–363). Elsevier. doi:10.1016/b978-0-12-804327-1.00126-6
- Heithaus, M. R., Frid, A., Wirsing, A. J., & Worm, B. (2008). Predicting ecological consequences of marine top predator declines. *Trends in Ecology and Evolution*, 23(4), 202–210. doi:10.1016/j.tree.2008.01.003
- Hewer, H. R. (1974). *British Seals*. (M. Davies, J. Huxley, J. Gilmour, & K. Mellanby, Eds.). Collins, St. James Place, London.
- Hewer, H. R. H. (1955). Notes on the marking of Atlantic seals in Pembrokeshire. *Proceedings of the Zoological Society of London*, 13(1), 66–80.
- Heylen, B. C., & Nachtsheim, D. A. (2018). Bio-telemetry as an Essential Tool in Movement Ecology and Marine Conservation. In S. Jungblut, V. Liebich, & M. Bode (Eds.), *YOUMARES 8 – Oceans Across Boundaries: Learning from each other* (pp. 83–107). Cham: Springer International Publishing. doi:10.1007/978-3-319-93284-2_7
- Hicks, J. L., O'Hara Hines, R. J., Schreer, J. F., & Hammill, M. O. (2004).

- Correlation of depth and heart rate in harbour seal pups. *Canadian Journal of Zoology*. doi:10.1139/Z04-087
- Hill, R. (2011). A Remote Release Device for Marine Mammal Electronic Tags. *Wildlife Computers, Inc.*, 1–18.
- Hobbs, R. C., Laidre, K. L., Vos, D. J., Mahoney, B. A., & Eagleton, M. (2005). Movements and Area Use of Belugas, *Delphinapterus leucas*, in a Subarctic Alaskan Estuary. *Arctic*, 58(4), 331–340.
- Hobday, A. J., Arrizabalaga, H., Evans, K., Nicol, S., Young, J. W., & Weng, K. C. (2015). Impacts of climate change on marine top predators: Advances and future challenges. *Deep-Sea Research Part II: Topical Studies in Oceanography*, 113, 1–8. doi:10.1016/j.dsr2.2015.01.013
- Hoekendijk, J. P. A., de Vries, J., van der Bolt, K., Greinert, J., Brasseur, S., Camphuysen, K. C. J., & Aarts, G. (2015). Estimating the spatial position of marine mammals based on digital camera recordings. *Ecology and Evolution*, 5(3), 578–589. doi:10.1002/ece3.1353
- Holm, K. J., & Burger, A. E. (2002). Foraging Behavior and Resource Partitioning by Diving Birds during Winter in Areas of Strong Tidal Currents. *Waterbirds: The International Journal of Waterbird Biology*, 25(3), 312–325.
- Holton, M. D., Wilson, R. P., Teilmann, J., & Siebert, U. (2021). Animal tag technology keeps coming of age: an engineering perspective. *Philosophical Transactions of the Royal Society B: Biological Sciences*, 376(1831). doi:10.1098/rstb.2020.0229
- Holyoak, M., Casagrandi, R., Nathan, R., Revilla, E., & Spiegel, O. (2008). Trends and missing parts in the study of movement ecology. *Proceedings of the National Academy of Sciences*, 105(49), 19060–19065. doi:10.1073/pnas.0800483105
- Hooten, M. B., Johnson, D. S., McClintock, B. T., & Morales, J. M. (2017). *Animal Movement*. Boca Raton: CRC Press, doi:10.1201/9781315117744
- Horne, J. K. (2000). Acoustic approaches to remote species identification: a review. *Fisheries Oceanography*, 9(4), 356–371. doi:10.1046/j.1365-2419.2000.00143.x
- Horne, N., Culloch, R. M., Schmitt, P., Lieber, L., Wilson, B., Dale, A. C., ... Kregting, L. T. (2021). Collision risk modelling for tidal energy devices: A flexible simulation-based approach. *Journal of Environmental Management*, 278(July 2020). doi:10.1016/j.jenvman.2020.111484
- Horning, M., Andrews, R. D., Bishop, A. M., Boveng, P. L., Costa, D. P., Crocker, D. E., ... Womble, J. N. (2019). Best practice recommendations for the use of external telemetry devices on pinnipeds. *Animal Biotelemetry*, 7, 1–17. doi:10.1186/s40317-019-0182-6
- Horning, M., Haulena, M., Rosenberg, J. F., & Nordstrom, C. (2017). Intraperitoneal implantation of life-long telemetry transmitters in three rehabilitated harbor seal pups. *BMC Veterinary Research*, 13(1), 139. doi:10.1186/s12917-017-1060-1
- Horning, M., Haulena, M., Tuomi, P. A., Mellish, J.-A. E. A. E., Goertz, C. E., Woodie, K., ... Boveng, P. L. (2017). Best practice recommendations for the use of fully implanted telemetry devices in pinnipeds. *Animal Biotelemetry*, 5(1), 13. doi:10.1186/s40317-017-0128-9
- Huang, S., Meng, S. X., & Yang, Y. (2009). Assessing the goodness of fit of forest models estimated by nonlinear mixed-model methods. *Canadian*

- Journal of Forest Research*, 39(12), 2418–2436. doi:10.1139/x09-140
- Hückstädt, L. A., Schwarz, L. K., Friedlaender, A. S., Mate, B. R., Zerbini, A. N., Kennedy, A., ... Costa, D. P. (2020). A dynamic approach to estimate the probability of exposure of marine predators to oil exploration seismic surveys over continental shelf waters. *Endangered Species Research*, 42, 185–199. doi:10.3354/ESR01048
- Hunt, G. L., Mehlum, F., Russel, R. W., Irons, D., Decker, B., & Becker, P. H. (1999). Physical processes, prey abundance, and the foraging ecology of seabirds. In *22nd International Ornithological Congress. Durban*.
- Hunt Jr, G. L., Russell, R. W., Coyle, K. O., & Weingartner, T. (1998). Comparative foraging ecology of planktivorous auklets in relation to ocean physics and prey availability. *Marine Ecology Progress Series*, 167, 241–259.
- Hurrell, J. W., Kushnir, Y., & Visbeck, M. (2001). The North Atlantic Oscillation. *Science*, 291(5504), 603–605. doi:10.1126/science.1058761
- Hussey, N. E., Kessel, S. T., Aarestrup, K., Cooke, S. J., Cowley, P. D., Fisk, A. T., ... Whoriskey, F. G. (2015). Aquatic animal telemetry: A panoramic window into the underwater world. *Science*, 348(6240). doi:10.1126/science.1255642
- Ichihara, T. (1974). Possible effect of surface wind force on the sex-specific mortality of young fur seal in the eastern Pacific. *Bull. Far Seas. Fish. Res. Lab.*, 11, 1–8.
- Ingram, S. N., Walshe, L., Johnston, D., & Rogan, E. (2007). Habitat partitioning and the influence of benthic topography and oceanography on the distribution of fin and minke whales in the Bay of Fundy, Canada. *Journal of the Marine Biological Association of the United Kingdom*, 87(1), 149–156.
- Intergovernmental Panel on Climate Change. (2014). *Climate Change 2014: Mitigation of Climate Change*, (Cambridge University Press: Cambridge, UK).
- Isaksson, N., Cleasby, I. R., Owen, E., Williamson, B. J., Houghton, J. D. R., Wilson, J., & Masden, E. A. (2021). The use of animal-borne biologging and telemetry data to quantify spatial overlap of wildlife with marine renewables. *Journal of Marine Science and Engineering*, 9(3), 1–32. doi:10.3390/jmse9030263
- Isaksson, N., Masden, E. A., Williamson, B. J., Costagliola-Ray, M. M., Slingsby, J., Houghton, J. D. R., & Wilson, J. (2020). Assessing the effects of tidal stream marine renewable energy on seabirds: A conceptual framework. *Marine Pollution Bulletin*, 157, 111314. doi:10.1016/j.marpolbul.2020.111314
- Isojunno, S., Matthiopoulos, J., & Evans, P. (2012). Harbour porpoise habitat preferences: robust spatio-temporal inferences from opportunistic data. *Marine Ecology Progress Series*, 448, 155–170. doi:10.3354/meps09415
- Jagadeesh, P., Murali, K., & Idichandy, V. G. (2009). Experimental investigation of hydrodynamic force coefficients over AUV hull form. *Ocean Engineering*, 36, 113–118.
- Jahncke, J., Coyle, K. O., Zeeman, S. I., Kachel, N. B., & Hunt Jr., G. L. (2005). Distribution of foraging shearwaters relative to inner front of SE Bering Sea. *Marine Ecology Progress Series*, 305, 219–233. doi:10.3354/MEPS305219

- Jameson, A., & Vassberg, J. (2001). Computational fluid dynamics for aerodynamic design: Its current and future impact. In *39th Aerospace Sciences Meeting and Exhibit*. Reston, Virginia: American Institute of Aeronautics and Astronautics. doi:10.2514/6.2001-538
- Jeffries, S. J., Brown, R. F., & Harvey, J. T. (1993). Techniques for capturing, handling and marking harbour seals. *Aquatic Mammals*, *19*, 21-21.
- Johnson, A. L. (1955). Seal catching. *Nature in Wales: The Quarterly Journal of the West Wales Field Society*, *1*(2), 54–56.
- Johnson, A. L. (1972). Seal Markings. *Nature in Wales: The Quarterly Journal of the West Wales Field Society*, *13*(2), 66–80.
- Johnston, D. T. (2019). Investigating the foraging ecology of black guillemots *Cepphus grylle* in relation to tidal stream turbines and marine protected areas. *Doctoral Thesis*.
- Johnston, D. T., Furness, R. W., Robbins, A. M. C. C., Tyler, G., Taggart, M. A., & Masden, E. A. (2018). Black guillemot ecology in relation to tidal stream energy generation: An evaluation of current knowledge and information gaps. *Marine Environmental Research*, *134*, 121-129. doi:10.1016/j.marenvres.2018.01.007
- Johnston, D. T., Furness, R., Robbins, A., Tyler, G., McIlvenny, J., & Masden, E. (2021). Tidal stream use by black guillemots *Cepphus grylle* in relation to a marine renewable energy development. *Marine Ecology Progress Series*, *669*, 201–212. doi:10.3354/meps13724
- Johnston, D. W., Thorne, L., & Read, A. (2005). Fin whales *Balaenoptera physalus* and minke whales *Balaenoptera acutorostrata* exploit a tidally driven island wake ecosystem in the Bay of Fundy. *Marine Ecology Progress Series*, *305*, 287–295. doi:10.3354/meps305287
- Jones, E. L., McConnell, B. J., Smout, S., Hammond, P. S., Duck, C. D., Morris, C. D., ... Matthiopoulos, J. (2015). Patterns of space use in sympatric marine colonial predators reveal scales of spatial partitioning. *Marine Ecology Progress Series*, *534*, 235–249. doi:10.3354/meps11370
- Jones, K. A., Ratcliffe, N., Votier, S. C., Lisovski, S., Bonnet-Lebrun, A.-S., & Staniland, I. J. (2021). Sexual segregation in juvenile Antarctic fur seals. *Oecologia*. doi:10.1007/s00442-021-04983-y
- Jones, T., Bostrom, B., Carey, M., Imlach, B., Mikkelsen, J., Ostafichuk, P., ... Jones, D. (2011). Determining Transmitter Drag and Best-Practice Attachment Procedures for Sea Turtle Biotelemetry. *NOAA Technical Memorandum, NMFS-SWFSC*.
- Joo, R., Picardi, S., Boone, M. E., Clay, T. A., Patrick, S. C., Romero-Romero, V. S., & Basille, M. (2020). A decade of movement ecology. *arXiv preprint arXiv:2006.00110*.
- Joslin, J., Polagye, B., & Parker-Stetter, S. (2014). Development of a stereo-optical camera system for monitoring tidal turbines. *Journal of Applied Remote Sensing*, *8*(1), 083633. doi:10.1117/1.JRS.8.083633
- Jouma'a, J., Le Bras, Y., Picard, B., & Guinet, C. (2017). Three-dimensional assessment of hunting strategies in a deep diving predator, southern elephant seal *Mirounga leonina*. *Marine Ecology Progress Series*, *573*, 255–268.
- Joy, R., Wood, J. D., Sparling, C. E., Tollit, D. J., Copping, A. E., & McConnell, B. J. (2018). Empirical measures of harbor seal behavior and avoidance of an operational tidal turbine. *Marine Pollution Bulletin*, *136*, 92–106.

- Kahle, D., & Wickham, H. (2016). ggmap: Spatial Visualization with ggplot2. *The R Journal*, 5(1), 144–161.
- Katzner, T. E., & Arlettaz, R. (2020). Evaluating Contributions of Recent Tracking-Based Animal Movement Ecology to Conservation Management. *Frontiers in Ecology and Evolution*, 7, 519. doi:10.3389/fevo.2019.00519
- Kauhala, K., Korpinen, S., Lehtiniemi, M., & Raitaniemi, J. (2019). Reproductive rate of a top predator, the grey seal, as an indicator of the changes in the Baltic food web. *Ecological Indicators*, 102, 693–703. doi:10.1016/j.ecolind.2019.03.022
- Kavelaars, M. M., Baert, J. M., Stienen, E. W. M., Shamoun-Baranes, J., Lens, L., & Müller, W. (2020). Breeding habitat loss reveals limited foraging flexibility and increases foraging effort in a colonial breeding seabird. *Movement Ecology*, 8(1), 45. doi:10.1186/s40462-020-00231-9
- Kay, W. P., Bull, J. C., Mortlock, E., Stringell, T. B., Lock, K. M., & Borger, L. (2020). Eighteen years of capture-mark-recapture (CMR) data of grey seal pups, *Halichoerus grypus*, from Pembrokeshire, Wales. Retrieved from <https://libcat.naturalresources.wales/folio/?oid=124164>
- Kay, W. P., Naumann, D. S., Bowen, H. J., Withers, S. J., Evans, B. J., Wilson, R. P., ... Börger, L. (2019). Minimizing the impact of biologging devices: Using computational fluid dynamics for optimizing tag design and positioning. *Methods in Ecology and Evolution*, 2019, 1–12. doi:10.1111/2041-210X.13216
- Kays, R., Crofoot, M. C., Jetz, W., & Wikelski, M. (2015). Terrestrial animal tracking as an eye on life and planet. *Science*, 348(6240). doi:10.1126/science.aaa2478
- Keen, K. A., Beltran, R. S., Pirotta, E., & Costa, D. P. (2021). Emerging themes in Population Consequences of Disturbance models. *Proceedings of the Royal Society B: Biological Sciences*, 288(1957), 20210325. doi:10.1098/rspb.2021.0325
- Kellermann, A., Eskildsen, K., & Frank, B. (2006). The MINOS project: Ecological assessments of possible impacts of offshore wind energy projects. In *Progress in Marine Conservation in Europe: NATURA 2000 Sites in German Offshore Waters*. doi:10.1007/3-540-33291-X_15
- Kenward, R. (2001). *A manual for wildlife radio tagging*. Academic Press.
- King, S. L., Schick, R. S., Donovan, C., Booth, C. G., Burgman, M., Thomas, L., & Harwood, J. (2015). An interim framework for assessing the population consequences of disturbance. *Methods in Ecology and Evolution*, 6(10), 1150–1158. doi:10.1111/2041-210X.12411
- Kirschvink, J. L. (1997). Homing in on vertebrates. *Nature*, 390(6658), 339–340. doi:10.1038/36986
- Krebs, J. R. (1978). Optimal foraging: decision rules for predators. *Behavioural Ecology: An Evolutionary Approach*, 23–63.
- Kreeger, T. J., & Arnemo, J. M. (2012). *Handbook of Wildlife Chemical Immobilization* (4th ed.). Wyoming: Wildlife Pharmaceuticals.
- Kwok, R. (2017). Field Instruments: Build it yourself. *Nature*, 545(7653), 253–255. doi:10.1038/nj7653-253a
- Kyte, A., Pass, C., Pemberton, R., Sharman, M., & McKnight, J. C. (2019). A computational fluid dynamics (CFD) based method for assessing the hydrodynamic impact of animal borne data loggers on host marine

- mammals. *Marine Mammal Science*, 35(2), 364–394. doi:10.1111/mms.12540
- Ladd, C., Jahncke, J., Hunt Jr., G. L., Coyle, K. O., & Stabeno, P. J. (2005). Hydrographic features and seabird foraging in Aleutian Passes. *Fisheries Oceanography*, 14(178–195).
- Lake, S., Burton, H., & Wotherspoon, S. (2006). Movements of adult female Weddell seals during the winter months. *Polar Biology*, 29(4), 270–279. doi:10.1007/s00300-005-0050-0
- Langley, I., Rosas da Costa Oliver, T., Hiby, L., Stringell, T. B., Morris, C. W., O’Cadhla, O., ... Pomeroy, P. P. (2020). Site use and connectivity of female grey seals (*Halichoerus grypus*) around Wales. *Marine Biology*, 167(6), 86. doi:10.1007/s00227-020-03697-8
- Langton, R., Davies, I. M., & Scott, B. E. (2011). Seabird conservation and tidal stream and wave power generation: Information needs for predicting and managing potential impacts. *Marine Policy*, 35(5), 623–630. doi:10.1016/j.marpol.2011.02.002
- Largey, N., Cook, A. S., Thaxter, C. B., McCluskie, A., Stokke, A. G., Wilson, B., & Masden, E. A. (2021). Methods to quantify avian airspace use in relation to wind energy development. *Ibis*, 163(3), 747–764. doi:10.1111/ibi.12913
- Le Boeuf, B. J., & Briggs, K. T. (1977). The cost of living in a seal harem. *Mammalia*, 41(2). doi:10.1515/mamm.1977.41.2.167
- Le Boeuf, B. J., Condit, R., Morris, P. A., & Reiter, J. (2011). The northern elephant seal (*Mirounga angustirostris*) rookery at año nuevo: A case study in colonization. *Aquatic Mammals*, 37(4), 486–501. doi:10.1578/AM.37.4.2011.486
- Lea, M.-A., Johnson, D., Ream, R., Sterling, J., Melin, S., & Gelatt, T. (2009). Extreme weather events influence dispersal of naive northern fur seals. *Biology Letters*, 5(2), 252–257. doi:10.1098/rsbl.2008.0643
- Lear, K. O., Gleiss, A. C., & Whitney, N. M. (2018). Metabolic rates and the energetic cost of external tag attachment in juvenile blacktip sharks *Carcharhinus limbatus*. *Journal of Fish Biology*, 93(2), 391–395. doi:10.1111/jfb.13663
- Lear, K. O., & Whitney, N. M. (2016). Bringing data to the surface: recovering data loggers for large sample sizes from marine vertebrates. *Animal Biotelemetry*, 4(1), 12. doi:10.1186/s40317-016-0105-8
- Leeney, R. H., Broderick, A. C., Mills, C., Sayer, S., Witt, M. J., & Godley, B. J. (2010). Abundance, distribution and haul-out behaviour of grey seals (*Halichoerus grypus*) in Cornwall and the Isles of Scilly, UK. *Journal of the Marine Biological Association of the United Kingdom*, 90(5), 1033–1040. doi:10.1017/S0025315409991512
- Leos-Barajas, V., Gangloff, E. J., Adam, T., Langrock, R., van Beest, F. M., Nabe-Nielsen, J., & Morales, J. M. (2017). Multi-scale Modeling of Animal Movement and General Behavior Data Using Hidden Markov Models with Hierarchical Structures. *Journal of Agricultural, Biological and Environmental Statistics*, 22(3), 232–248. doi:10.1007/s13253-017-0282-9
- Leos-Barajas, V., Photopoulou, T., Langrock, R., Patterson, T. A., Watanabe, Y. Y., Murgatroyd, M., & Papastamatiou, Y. P. (2017). Analysis of animal accelerometer data using hidden Markov models. *Methods in Ecology and*

- Evolution*, 8(2), 161–173. doi:10.1111/2041-210X.12657
- Levin, S. A. (1994). Patchiness in marine and terrestrial systems: from individuals to populations. *Philosophical Transactions - Royal Society of London, B*, 343(1303). doi:10.1098/rstb.1994.0013
- Lewis, M., Neill, S. P., Robins, P. E., & Hashemi, M. R. (2015). Resource assessment for future generations of tidal-stream energy arrays. *Energy*, 83, 403–415. doi:10.1016/j.energy.2015.02.038
- Li, S., Akamatsu, T., Dong, L., Wang, K., Wang, D., & Kimura, S. (2010). Widespread passive acoustic detection of Yangtze finless porpoise using miniature stereo acoustic data-loggers: A review. *The Journal of the Acoustical Society of America*, 128(3), 1476. doi:10.1121/1.3455829
- Lieber, L., Langrock, R., & Nimmo-Smith, W. A. M. (2021). A bird's-eye view on turbulence: seabird foraging associations with evolving surface flow features. *Proceedings of the Royal Society B: Biological Sciences*, 288(1949), rspb.2021.0592. doi:10.1098/rspb.2021.0592
- Lieber, L., Nimmo-Smith, W. A. M., Waggitt, J. J., & Kregting, L. (2018). Fine-scale hydrodynamic metrics underlying predator occupancy patterns in tidal stream environments. *Ecological Indicators*, 94, 397–408. doi:10.1016/j.ecolind.2018.06.071
- Lieber, L., Nimmo-Smith, W. A. M., Waggitt, J. J., & Kregting, L. (2019). Localised anthropogenic wake generates a predictable foraging hotspot for top predators. *Communications Biology*, 2(1), 123. doi:10.1038/s42003-019-0364-z
- Liebsch, N. S. (2006). Hankering back to ancestral pasts: constraints on two pinnipeds, *Phoca vitulina* & *Leptonychotes weddellii* foraging from a central place. *PhD Dissertation*, 161.
- Liebsch, N., Wilson, R. P., Bornemann, H., Adelung, D., & Plötz, J. (2007). Mouthing off about fish capture: Jaw movement in pinnipeds reveals the real secrets of ingestion. *Deep-Sea Research Part II: Topical Studies in Oceanography*, 54(3–4), 256–269. doi:10.1016/j.dsr2.2006.11.014
- Lindström, J. (1999). Early development and fitness in birds and mammals. *Trends in Ecology and Evolution*, 14(9), 343–348. doi:10.1016/S0169-5347(99)01639-0
- Lock, K., Burton, M., Newman, P., & Jones, J. (2016). Skomer Marine Conservation Zone Project Status Report 2016. *NRW Evidence Report No. 197*, 117.
- Lockley, R. M. (1958). Seal Marking, 1957. *Nature in Wales: The Quarterly Journal of the West Wales Field Society*, 4(1), 537–543.
- Löhner, R., & Oñate, E. (2004). A general advancing front technique for filling space with arbitrary objects. *International Journal for Numerical Methods in Engineering*, 61(12), 1977–1991. doi:10.1002/nme.1068
- Lossent, J., Lejart, M., Folegot, T., Clorennec, D., Di Iorio, L., & Gervaise, C. (2018). Underwater operational noise level emitted by a tidal current turbine and its potential impact on marine fauna. *Marine Pollution Bulletin*, 131, 323–334. doi:10.1016/j.marpolbul.2018.03.024
- Lotze, H. K., Tittensor, D. P., Bryndum-Buchholz, A., Eddy, T. D., Cheung, W. W. L., Galbraith, E. D., ... Worm, B. (2019). Global ensemble projections reveal trophic amplification of ocean biomass declines with climate change. *Proceedings of the National Academy of Sciences*, 116(26), 12907–12912. doi:10.1073/pnas.1900194116

- Lowry, L. (2016). *Phoca vitulina*. *The IUCN Red List of Threatened Species*.
- Lowther, A. D., Ahonen, H., Hofmeyr, G., Oosthuizen, W. C., Nico De Bruyn, P. J., Lydersen, C., & Kovacs, K. M. (2015). Reliability of VHF telemetry data for measuring attendance patterns of marine predators: A comparison with time depth recorder data. *Marine Ecology Progress Series*, 538, 249–256. doi:10.3354/meps11504
- Luck, C., Cronin, M., Gosch, M., Healy, K., Cosgrove, R., Tully, O., ... Jessopp, M. (2020). Drivers of spatiotemporal variability in bycatch of a top marine predator: First evidence for the role of water turbidity in protected species bycatch. *Journal of Applied Ecology*, 57(2), 219–228. doi:10.1111/1365-2664.13544
- Luther, G. (1973). UWL 'Helgoland' - an underwater laboratory for rough sea conditions. *Helgoländer Wiss. Meeresunters*, 24, 45–53.
- Lydersen, C., Martin, A., Kovacs, K., & Gjertz, I. (2001). Summer and autumn movements of white whales *Delphinapterus leucas* in Svalbard, Norway. *Marine Ecology Progress Series*, 219, 265–274. doi:10.3354/meps219265
- Machovsky-Capuska, G. E., & Raubenheimer, D. (2020). The Nutritional Ecology of Marine Apex Predators. *Annual Review of Marine Science*, 12(1), 361–387. doi:10.1146/annurev-marine-010318-095411
- Madin, E. M. P., Dill, L. M., Ridlon, A. D., Heithaus, M. R., & Warner, R. R. (2016). Human activities change marine ecosystems by altering predation risk. *Global Change Biology*, 22(1), 44–60. doi:10.1111/gcb.13083
- Magagna, D., & Uihlein, A. (2015). Ocean energy development in Europe: Current status and future perspectives. *International Journal of Marine Energy*, 11, 84–104. doi:10.1016/j.ijome.2015.05.001
- Malinka, C., Gillespie, D., Macaulay, J., Joy, R., & Sparling, C. (2018). First in situ passive acoustic monitoring for marine mammals during operation of a tidal turbine in Ramsey Sound, Wales. *Marine Ecology Progress Series*, 590, 247–266. doi:10.3354/meps12467
- Mansfield, A. W. (1967). Distribution of the Harbor Seal, *Phoca vitulina* Linnaeus, in Canadian Arctic Waters. *Journal of Mammalogy*, 48(2), 249. doi:10.2307/1378028
- Marine Energy Wales. (2020). *State of the Sector 2020: Economic Benefits for Wales*.
- Martin-Short, R., Hill, J., Kramer, S. C., Avdis, A., Allison, P. A., & Piggott, M. D. (2015). Tidal resource extraction in the Pentland Firth, UK: Potential impacts on flow regime and sediment transport in the Inner Sound of Stroma. *Renewable Energy*, 76, 596–607. doi:10.1016/j.renene.2014.11.079
- Martín-Vélez, V., van Leeuwen, C. H. A., Sánchez, M. I., Hortas, F., Shamoun-Baranes, J., Thaxter, C. B., ... Green, A. J. (2021). Spatial patterns of weed dispersal by wintering gulls within and beyond an agricultural landscape. *Journal of Ecology*, 109(4), 1947–1958. doi:10.1111/1365-2745.13619
- Mateos, M., & Arroyo, G. M. (2011). Ocean surface winds drive local-scale movements within long-distance migrations of seabirds. *Marine Biology*, 158(2), 329–339. doi:10.1007/s00227-010-1561-y
- Maxwell, S. M., Hazen, E. L., Bograd, S. J., Halpern, B. S., Breed, G. A., Nickel, B., ... Costa, D. P. (2013). Cumulative human impacts on marine

- predators. *Nature Communications*, 4(1), 2688. doi:10.1038/ncomms3688
- Mazzaro, L., & Dunn, J. (2009). Descriptive account of long-term health and behavior of two satellite-tagged captive harbor seals *Phoca vitulina*. *Endangered Species Research*, 10(1), 159–163. doi:10.3354/esr00190
- McClintock, B. T., Johnson, D. S., Hooten, M. B., Ver Hoef, J. M., & Morales, J. M. (2014). When to be discrete: The importance of time formulation in understanding animal movement. *Movement Ecology*, 2(1), 1–14. doi:10.1186/s40462-014-0021-6
- McClintock, B. T., King, R., Thomas, L., Matthiopoulos, J., McConnell, B. J., & Morales, J. M. (2012). A general discrete-time modeling framework for animal movement using multistate random walks. *Ecological Monographs*, 82(3), 335–349. doi:10.1890/11-0326.1
- McClintock, B. T., London, J. M., Cameron, M. F., & Boveng, P. L. (2017). Bridging the gaps in animal movement: Hidden behaviors and ecological relationships revealed by integrated data streams. *Ecosphere*, 8(3). doi:10.1002/ecs2.1751
- McClintock, B. T., & Michelot, T. T. T. T. (2018). momentuHMM: R package for generalized hidden Markov models of animal movement. *Methods in Ecology and Evolution*, 9(6), 1518–1530. doi:10.1111/2041-210X.12995
- McClintock, B. T., Russell, D. J. F., Matthiopoulos, J., & King, R. (2013). Combining individual animal movement and ancillary biotelemetry data to investigate population-level activity budgets. *Ecology*, 94(4), 838–849. doi:10.1890/12-0954.1
- McConnell, B. J., Fedak, M. a., Lovell, P., & Hammond, P. S. (1999). Movements and foraging of grey seals in the North sea. *The Journal of Applied Ecology*, 36, 573–590. doi:10.1046/j.1365-2664.1999.00429.x
- McGowan, J., Beger, M., Lewison, R. L., Harcourt, R., Campbell, H., Priest, M., ... Possingham, H. P. (2017). Integrating research using animal-borne telemetry with the needs of conservation management. *Journal of Applied Ecology*, 54(2), 423–429. doi:10.1111/1365-2664.12755
- McIntyre, T. (2014). Trends in tagging of marine mammals: a review of marine mammal biologging studies. *African Journal of Marine Science*, 36(4), 409–422.
- McLaren, I. A. (1993). Growth in pinnipeds. *Biological Reviews*, 68(1), 1–79.
- Mendes, S., Turrell, W., Lütkebohle, T., & Thompson, P. (2002). Influence of the tidal cycle and a tidal intrusion front on the spatio-temporal distribution of coastal bottlenose dolphins. *Marine Ecology Progress Series*, 239, 221–229. doi:10.3354/meps239221
- Mikkelsen, L., Johnson, M., Wisniewska, D. M., van Neer, A., Siebert, U., Madsen, P. T., & Teilmann, J. (2019). Long-term sound and movement recording tags to study natural behavior and reaction to ship noise of seals. *Ecology and Evolution*, 9(5), 2588-2601. doi:10.1002/ece3.4923
- Mitani, Y., Sato, K., Ito, S., Cameron, M. F., Siniff, D. B., & Naito, Y. (2003). A method for reconstructing three-dimensional dive profiles of marine mammals using geomagnetic intensity data: results from two lactating Weddell seals. *Polar Biology*, 26(5), 311–317. doi:10.1007/s00300-003-0487-y
- Møller, A. P., Flensted-Jensen, E., & Mardal, W. (2006). Dispersal and climate change: A case study of the Arctic tern *Sterna paradisaea*. *Global Change*

- Biology*, 12(10), 2005–2013. doi:10.1111/j.1365-2486.2006.01216.x
- Monzon-Arguello, C., Dell'Amico, F., Moriniere, P., Marco, A., Lopez-Jurado, L. F., Hays, G. C., ... Lee, P. L. M. (2012). Lost at sea: genetic, oceanographic and meteorological evidence for storm-forced dispersal. *Journal of The Royal Society Interface*, 9(73), 1725–1732. doi:10.1098/rsif.2011.0788
- Morelle, K., Bunnefeld, N., Lejeune, P., & Oswald, S. A. (2017). From animal tracks to fine-scale movement modes: a straightforward approach for identifying multiple spatial movement patterns. *Methods in Ecology and Evolution*, 8(11), 1488–1498. doi:10.1111/2041-210X.12787
- Morgan, L. H., Morris, C. W., & Stringell, T. B. (2018). Grey Seal Pupping Phenology on Ynys Dewi/Ramsey Island, Pembrokeshire. *NRW Evidence Report No. 156*, 23.
- Morton, D. B., Editor, P. H., Bevan, R., Heath, K., Kirkwood, J., Pearce, P., ... Webb, A. (2003). Refinements in telemetry procedures. 7th report of the BVAAWF/FRAME/RSPCA/UFWA Joint Working Group on Refinement, Part A. *Laboratory Animals*, 37, 261–299.
- Mosser, A. A., Avgar, T., Brown, G. S., Walker, C. S., & Fryxell, J. M. (2014). Towards an energetic landscape: broad-scale accelerometry in woodland caribou. *Journal of Animal Ecology*, 83(4), 916–922. doi:10.1111/1365-2656.12187
- Mozo, R., Alabart, J. L., Rivas, E., & Folch, J. (2019). New method to automatically evaluate the sexual activity of the ram based on accelerometer records. *Small Ruminant Research*, 172, 16–22. doi:10.1016/j.smallrumres.2019.01.009
- Murtaugh, P. A. (2009). Performance of several variable-selection methods applied to real ecological data. *Ecology Letters*, 12(10), 1061–1068. doi:10.1111/j.1461-0248.2009.01361.x
- Myers, R. A., Baum, J. K., Shepherd, T. D., Powers, S. P., & Peterson, C. H. (2007). Cascading effects of the loss of apex predatory sharks from a coastal ocean. *Science*, 315(5820), 1846–1850. doi:10.1126/science.1138657
- Nabe-Nielsen, J., van Beest, F. M., Grimm, V., Sibly, R., Teilmann, J., & Thompson, P. M. (2018). Predicting the impacts of anthropogenic disturbances on marine populations. *Conservation Letters*, 11(5), 1–8. doi:10.1111/conl.12563
- Nathan, R., Getz, W. M., Revilla, E., Holyoak, M., Kadmon, R., Saltz, D., & Smouse, P. E. (2008). A movement ecology paradigm for unifying organismal movement research. *Proceedings of the National Academy of Sciences*, 105(49), 19052–19059. doi:10.1073/pnas.0800375105
- Nathan, R., & Giuggioli, L. (2013). A milestone for movement ecology research. *Movement Ecology*, 1(1), 1. doi:10.1186/2051-3933-1-1
- Nichols, B. S., Leubner-Metzger, G., & Jansen, V. A. A. (2020). Between a rock and a hard place: adaptive sensing and site-specific dispersal. *Ecology Letters*, 23(9), 1370–1379. doi:10.1111/ele.13564
- NOAA Fisheries. (2019). *Marine Mammal Scientific Research and Enhancement Permit Application OMB No. 0648-0084*.
- Noren, S. R., Boness, D. J., Iverson, S. J., McMillan, J., & Bowen, W. D. (2008). Body Condition at Weaning Affects the Duration of the Postweaning Fast in Gray Seal Pups (*Halichoerus grypus*). *Physiological and Biochemical*

- Zoology*, 81(3), 269–277. doi:10.1086/528777
- Nouvellet, P., Bacon, J. P. P., & Waxman, D. (2009). Fundamental Insights into the Random Movement of Animals from a Single Distance-Related Statistic. *The American Naturalist*, 174(4), 506–514. doi:10.1086/605404
- Nuijten, R. J. M., Gerrits, T., Shamoun-Baranes, J., & Nolet, B. A. (2020). Less is more: On-board lossy compression of accelerometer data increases biologging capacity. *Journal of Animal Ecology*, 89(1), 237–247.
- Nuuttila, H. K., Thomas, L., Hiddink, J. G., Meier, R., Turner, J. R., Bennell, J. D., ... Evans, P. G. H. (2013). Acoustic detection probability of bottlenose dolphins, *Tursiops truncatus*, with static acoustic dataloggers in Cardigan Bay, Wales. *The Journal of the Acoustical Society of America*, 134(3), 2596–2609. doi:10.1121/1.4816586
- Ocean Energy Systems. (2017). OES Annual Report 2016. *The Executive Committee of Ocean Energy Systems*, 1–188.
- Ocean Energy Systems. (2018). OES Annual Report 2017. *The Executive Committee of Ocean Energy Systems*, 1–154.
- Ocean Energy Systems. (2019). OES Annual Report 2018. *Annual Report*, 1–146.
- Ocean Energy Systems. (2020). *OES Annual Report 2019*.
- Onoufriou, J., Brownlow, A., Moss, S., Hastie, G., & Thompson, D. (2019). Empirical determination of severe trauma in seals from collisions with tidal turbine blades. *Journal of Applied Ecology*, 56(7), 1712–1724.
- Onoufriou, J., Russell, D. J. F., Thompson, D., Moss, S. E., & Hastie, G. D. (2021). Quantifying the effects of tidal turbine array operations on the distribution of marine mammals: Implications for collision risk. *Renewable Energy*, 180, 157–165.
- ORJIP Ocean Energy. (2016). *The Forward Look; an Ocean Energy Environmental Research Strategy for the UK*.
- ORJIP Ocean Energy. (2020). Wave and Tidal Stream Critical Evidence Needs. *Report to: The Crown Estate, Crown Estate Scotland, Marine Scotland, Welsh Government, Scottish Natural Heritage and Natural Resources Wales*, (November), Issued by Aquatera Ltd, MarineSpace Ltd and EMEC.
- Osinga, N., Nussbaum, S. B., Brakefield, P. M., & Udo de Haes, H. A. (2012). Response of common seals (*Phoca vitulina*) to human disturbances in the Dollard estuary of the Wadden Sea. *Mammalian Biology*, 77(4), 281–287.
- Pavlov, V. V., Wilson, R. P., & Lucke, K. (2007). A new approach to tag design in dolphin telemetry: Computer simulations to minimise deleterious effects. *Deep-Sea Research Part II: Topical Studies in Oceanography*, 54(3–4), 404–414. doi:10.1016/j.dsr2.2006.11.010
- Pavlov, V. V., & Rashad, A. M. (2012). A non-invasive dolphin telemetry tag: Computer design and numerical flow simulation. *Marine Mammal Science*, 28(1), 16–27. doi:10.1111/j.1748-7692.2011.00476.x
- Peck-Richardson, A., Lyons, D., Roby, D., Cushing, D., & Lerczak, J. (2018). Three-dimensional foraging habitat use and niche partitioning in two sympatric seabird species, *Phalacrocorax auritus* and *P. penicillatus*. *Marine Ecology Progress Series*, 586, 251–264. doi:10.3354/meps12407
- Pelc, R., & Fujita, R. M. (2002). Renewable energy from the ocean. *Marine Policy*, 26(6), 471–479.
- Peschko, V., Müller, S., Schwemmer, P., Mercker, M., Lienau, P.,

- Rosenberger, T., ... Garthe, S. (2020). Wide dispersal of recently weaned grey seal pups in the Southern North Sea. *ICES Journal of Marine Science*, 2019. doi:10.1093/icesjms/fsaa045
- Phillips, R. A., Xavier, J. C., & Croxall, J. P. (2003). Effects of satellite transmitters on albatrosses and petrels. *The Auk*, 120(4), 1082–1090.
- Photopoulou, T., Lovell, P., Fedak, M. A., Thomas, L., & Matthiopoulos, J. (2015). Efficient abstracting of dive profiles using a broken-stick model. *Methods in Ecology and Evolution*. doi:10.1111/2041-210X.12328
- Pierpoint, C. (2008). Harbour porpoise (*Phocoena phocoena*) foraging strategy at a high energy, near-shore site in south-west Wales, UK. *Journal of the Marine Biological Association of the United Kingdom*, 88(6), 1167–1173. doi:10.1017/S0025315408000507
- Pinheiro, J. C., & Bates, D. M. (2000). *Mixed-effects models in S and S-Plus: Statistics and Computing*. Springer-Verlag, New York.
- Pirotta, E., Mangel, M., Costa, D. P., Goldbogen, J., Harwood, J., Hin, V., ... New, L. (2019). Anthropogenic disturbance in a changing environment: modelling lifetime reproductive success to predict the consequences of multiple stressors on a migratory population. *Oikos*, 128(9), 1340–1357. doi:10.1111/oik.06146
- Piwetz, S., Gailey, G., Munger, L., Lammers, M. O., Jefferson, T. A., & Würsig, B. (2018). Theodolite tracking in marine mammal research: From Roger Payne to the present. *Aquatic Mammals*, 44(6), 683–693. doi:10.1578/AM.44.6.2018.683
- Planque, Y., Huon, M., Caurant, F., Pinaud, D., & Vincent, C. (2020). Comparing the horizontal and vertical approaches used to identify foraging areas of two diving marine predators. *Marine Biology*, 167(2), 25. doi:10.1007/s00227-019-3636-8
- Pomeroy, P. P., Anderson, S. S., Twiss, S. D., & McConnell, B. J. (1994). Dispersion and site fidelity of breeding female grey seals (*Halichoerus grypus*) on North Rona, Scotland. *Journal of Zoology*. doi:10.1111/j.1469-7998.1994.tb05275.x
- Pomeroy, P. P., Fedak, M. A., Rothery, P., & Anderson, S. (1999). Consequences of maternal size for reproductive expenditure and pupping success of grey seals at North Rona, Scotland. *Journal of Animal Ecology*, 68(2), 235–253. doi:10.1046/j.1365-2656.1999.00281.x
- Pomeroy, P. P., Green, N., Hall, A. J., Walton, M., Jones, K., & Harwood, J. (1996). Congener-specific exposure of grey seal (*Halichoerus grypus*) pups to chlorinated biphenyls during lactation. *Canadian Journal of Fisheries and Aquatic Sciences*, 53(7), 1526–1534. doi:10.1139/f96-087
- Ponganis, P. J. (2015). Diving Physiology of Marine Mammals and Seabirds. *Diving Physiology of Marine Mammals and Seabirds*. doi:10.1017/CBO9781139045490
- Pope, S. B. (2000). *Turbulent Flows*. Cambridge University Press. doi:10.1017/CBO9780511840531
- Portugal, S. J., & White, C. R. (2018). Miniaturisation of biologgers is not alleviating the 5% rule. *Methods in Ecology and Evolution*, 1(1), 1–2. doi:10.1111/2041-210X.13013
- Pyke, G. H. (1984). Optimal Foraging Theory: A Critical Review. *Annual Review of Ecology and Systematics*. doi:10.1146/annurev.es.15.110184.002515

- R Core Team. (2018). R: A Language and Environment for Statistical Computing. Vienna, Austria. Retrieved from <https://www.r-project.org/>
- Rafiq, K., Appleby, R. G., Edgar, J. P., Jordan, N. R., Dexter, C. E., Jones, D. N., ... Cochrane, M. (2019). OpenDropOff: An open-source, low-cost drop-off unit for animal-borne devices. *Methods in Ecology and Evolution*, 10(9), 1517–1522. doi:10.1111/2041-210X.13231
- Ragen, T. J., Antonelis, G. A., & Kiyota, M. (1995). Early Migration of Northern Fur Seal Pups from St. Paul Island, Alaska. *Journal of Mammalogy*, 76(4), 1137–1148. doi:10.2307/1382605
- Raya Rey, A., Bost, C. A., Schiavini, A., & Pütz, K. (2010). Foraging movements of Magellanic penguins *Spheniscus magellanicus* in the Beagle Channel, Argentina, related to tide and tidal currents. *Journal of Ornithology*, 151(4), 933–943. doi:10.1007/s10336-010-0531-y
- Rayment, W., Clement, D., Dawson, S., Slooten, E., & Secchi, E. (2011). Distribution of Hector's dolphin (*Cephalorhynchus hectori*) off the west coast, South Island, New Zealand, with implications for the management of bycatch. *Marine Mammal Science*, 27(2), 398–420. doi:10.1111/j.1748-7692.2010.00407.x
- Ream, R. R., Sterling, J. T., & Loughlin, T. R. (2005). Oceanographic features related to northern fur seal migratory movements. *Deep Sea Research Part II: Topical Studies in Oceanography*, 52(5–6), 823–843. doi:10.1016/j.dsr2.2004.12.021
- Reilly, J. J. (1991). Adaptations to prolonged fasting in free-living weaned gray seal pups. *The American Journal of Physiology*, 260(2 Pt 2), R267-72. doi:10.1152/ajpregu.1991.260.2.R267
- Riley, G. A. (1976). A model of plankton patchiness. *Limnology and Oceanography*, 21, 873–880.
- Riotte-Lambert, L., & Matthiopoulos, J. (2020). Environmental Predictability as a Cause and Consequence of Animal Movement. *Trends in Ecology & Evolution*, 35(2), 163–174. doi:10.1016/j.tree.2019.09.009
- Rivalan, P., Barbraud, C., Inchausti, P., & Weimerskirch, H. (2010). Combined impacts of longline fisheries and climate on the persistence of the Amsterdam Albatross *Diomedea amsterdamensis*. *Ibis*, 152(1), 6–18. doi:10.1111/j.1474-919X.2009.00977.x
- Roche, R. C., Walker-springett, K., Robins, P. E., Jones, J., Veneruso, G., Whitton, T. A., Piano, M., Ward, S. L., ... King, J. W. (2016). Research priorities for assessing potential impacts of emerging marine renewable energy technologies: Insights from developments in Wales (UK). *Renewable Energy*. doi:10.1016/j.renene.2016.08.035
- Ropert-Coudert, Y., Knott, N., Chiaradia, A., & Kato, A. (2007). How do different data logger sizes and attachment positions affect the diving behaviour of little penguins? *Deep-Sea Research Part II: Topical Studies in Oceanography*, 54(3–4), 415–423. doi:10.1016/j.dsr2.2006.11.018
- Ropert-Coudert, Y., Bost, C., Handrich, Y., Bevan, R. M., Butler, P. J., Woakes, A. J., & Le Maho, Y. (2000). Impact of Externally Attached Loggers on the Diving Behaviour of the King Penguin. *Physiological and Biochemical Zoology*, 73(4), 438–444. doi:10.1086/317743
- Roquet, F., Boehme, L., Block, B., Charrassin, J.-B., Costa, D., Guinet, C., ... Fedak, M. A. (2017). Ocean Observations Using Tagged Animals.

- Oceanography*, 30(2), 139–139. doi:10.5670/oceanog.2017.235
- Rosen, D. A. S., Gerlinsky, C. G., & Trites, A. W. (2017). Telemetry tags increase the costs of swimming in northern fur seals, *Callorhinus ursinus*. *Marine Mammal Science*, 1–18. doi:10.1111/mms.12460
- Runge, C. A., Martin, T. G., Possingham, H. P., Willis, S. G., & Fuller, R. A. (2014). Conserving mobile species. *Frontiers in Ecology and the Environment*, 12(7), 395–402. doi:10.1890/130237
- Russell, D. J. F., Brasseur, S. M. J. M., Thompson, D., Hastie, G. D., Janik, V. M., Aarts, G., ... McConnell, B. (2014). Marine mammals trace anthropogenic structures at sea. *Current Biology*, 24(14), R638–R639. doi:10.1016/j.cub.2014.06.033
- Russell, D. J. F., McClintock, B. T., Matthiopoulos, J., Thompson, P. M., Thompson, D., Hammond, P. S., ... McConnell, B. J. (2015). Intrinsic and extrinsic drivers of activity budgets in sympatric grey and harbour seals. *Oikos*, 124(11), 1462–1472. doi:10.1111/oik.01810
- Sæther, B.-E. E., Coulson, T., Grøtan, V., Engen, S., Altwegg, R., Armitage, K. B., ... Weimerskirch, H. (2013). How Life History Influences Population Dynamics in Fluctuating Environments. *The American Naturalist*, 182(6), 743–759. doi:10.1086/673497
- Sala, J. E., Wilson, R. P., & Quintana, F. (2014). Foraging effort in Magellanic penguins: balancing the energy books for survival? *Marine Biology*, 162(3), 501–514. doi:10.1007/s00227-014-2581-9
- Sampaio, E., & Rosa, R. (2020). Climate Change, Multiple Stressors, and Responses of Marine Biota, 264–275. doi:10.1007/978-3-319-95885-9_90
- Saroux, C., Le Bohec, C., Durant, J. M., Viblanc, V. A., Gauthier-Clerc, M., Beaune, D., ... Le Maho, Y. (2011). Reliability of flipper-banded penguins as indicators of climate change. *Nature*, 469(7329), 203–208. doi:10.1038/nature09630
- Saunders, D. (2008). Ronald Mathias Lockley (1903-2000). *Ibis*, 143(1), 167–168. doi:10.1111/j.1474-919X.2001.tb04183.x
- Sayer, S., Allen, R., Hawkes, L. A., Hockley, K., Jarvis, D., & Witt, M. J. (2019). Pinnipeds, people and photo identification: the implications of grey seal movements for effective management of the species. *Journal of the Marine Biological Association of the United Kingdom*, 99(5), 1221–1230. doi:10.1017/S0025315418001170
- Schofield, G., Dimadi, A., Fossette, S., Katselidis, K. A., Koutsoubas, D., Lilley, M. K. S., ... Hays, G. C. (2013). Satellite tracking large numbers of individuals to infer population level dispersal and core areas for the protection of an endangered species. *Diversity and Distributions*, 19(7), 834–844. doi:10.1111/ddi.12077
- Schorr, G. S., Falcone, E. A., Moretti, D. J., & Andrews, R. D. (2014). First Long-Term Behavioral Records from Cuvier's Beaked Whales (*Ziphius cavirostris*) Reveal Record-Breaking Dives. *PLoS ONE*, 9(3), e92633. doi:10.1371/journal.pone.0092633
- Schwemmer, P., Adler, S., Guse, N., Markones, N., & Garthe, S. (2009). Influence of water flow velocity, water depth and colony distance on distribution and foraging patterns of terns in the Wadden Sea. *Fisheries Oceanography*, 18(3), 161–172. doi:10.1111/j.1365-2419.2009.00504.x
- SCOS. (2018). Scientific Advice on Matters Related to the Management of

- Seal Populations: 2018. *Special Committee on Seals (SCOS) Main Advice Report*.
- SCOS. (2020). Scientific Advice on Matters Related to the Management of Seal Populations: 2020. *Special Committee on Seals (SCOS) Main Advice Report*, 1–223.
- Scott, B. E., Webb, A., Palmer, M. R., Embling, C. B., & Sharples, J. (2013). Fine scale bio-physical oceanographic characteristics predict the foraging occurrence of contrasting seabird species; Gannet (*Morus bassanus*) and storm petrel (*Hydrobates pelagicus*). *Progress in Oceanography*, 117, 118–129. doi:10.1016/j.pocean.2013.06.011
- Seals and fish stocks in the North-East Atlantic. (2010). *European Parliament*.
- Senko, J., Nelms, S., Reavis, J., Witherington, B., Godley, B., & Wallace, B. (2020). Understanding individual and population-level effects of plastic pollution on marine megafauna. *Endangered Species Research*, 43, 234–252. doi:10.3354/esr01064
- Sequeira, A. M. M., Heupel, M. R., Lea, M. A., Eguíluz, V. M., Duarte, C. M., Meekan, M. G., ... Hays, G. C. (2019). The importance of sample size in marine megafauna tagging studies. *Ecological Applications*, 29(6), e01947. doi:10.1002/eap.1947
- Sergio, F., Caro, T., Brown, D., Clucas, B., Hunter, J., Ketchum, J., ... Hiraldo, F. (2008). Top Predators as Conservation Tools: Ecological Rationale, Assumptions, and Efficacy. *Annual Review of Ecology, Evolution, and Systematics*, 39(1), 1–19. doi:10.1146/annurev.ecolsys.39.110707.173545
- Sharples, R. J., Moss, S. E., Patterson, T. A., & Hammond, P. S. (2012). Spatial variation in foraging behaviour of a marine top predator (*Phoca vitulina*) determined by a large-scale satellite tagging program. *PLoS ONE*, 7(5). doi:10.1371/journal.pone.0037216
- Shepard, E. L. C., Wilson, R. P., Rees, W. G., Grundy, E., Lambertucci, S. A., & Vosper, S. B. (2013). Energy landscapes shape animal movement ecology. *American Naturalist*. doi:10.1086/671257
- Shepard, E., Wilson, R., Quintana, F., Gómez Laich, A., Liebsch, N., Albareda, D., ... McDonald, D. (2008). Identification of animal movement patterns using tri-axial accelerometry. *Endangered Species Research*, 10, 47–60. doi:10.3354/esr00084
- Shillinger, G. L., Bailey, H., Bograd, S. J., Hazen, E. L., Hamann, M., Gaspar, P., ... Spotila, J. R. (2012). Tagging through the stages: Technical and ecological challenges in observing life histories through biologging. *Marine Ecology Progress Series*, 457, 165–170. doi:10.3354/meps09816
- Shimada, T., Thums, M., Hamann, M., Limpus, C. J., Hays, G. C., FitzSimmons, N. N., ... Meekan, M. G. (2020). Optimising sample sizes for animal distribution analysis using tracking data. *Methods in Ecology and Evolution*, 2020(September), 1–10. doi:10.1111/2041-210X.13506
- Shorter, A., Murray, M., Johnson, M., Moore, M., & Howle, L. (2014). Drag of suction cup tags on swimming animals: Modeling and measurement. *Marine Mammal Science*, 30(2), 726–746. doi:10.1111/mms.12083
- Shorter, A., Shao, Y., Ojeda, L., Barton, K., Rocho-Levine, J., van der Hoop, J., & Moore, M. (2017). A day in the life of a dolphin: Using bio-logging tags for improved animal health and well-being. *Marine Mammal Science*, 33(3), 785–802. doi:10.1111/mms.12408

- Sikes, R. S. (2016). 2016 Guidelines of the American Society of Mammalogists for the use of wild mammals in research and education: *Journal of Mammalogy*, 97(3), 663–688. doi:10.1093/jmammal/gyw078
- Sims, D. W., Southall, E. J., Humphries, N. E., Hays, G. C., Bradshaw, C. J. A., Pitchford, J. W., ... Metcalfe, J. D. (2008). Scaling laws of marine predator search behaviour. *Nature*. doi:10.1038/nature06518
- Skubel, R. A., Wilson, K., Papastamatiou, Y. P., Verkamp, H. J., Sulikowski, J. A., Benetti, D., & Hammerschlag, N. (2020). A scalable, satellite-transmitted data product for monitoring high-activity events in mobile aquatic animals. *Animal Biotelemetry*, 8(1), 1–14. doi:10.1186/s40317-020-00220-0
- Slater, P. J. B. (1976). Tidal rhythm in a seabird. *Nature*, 264.5587, 636–638.
- Solsona Berga, A., Wright, A. J., Galatius, A., Sveegaard, S., & Teilmann, J. (2015). Do larger tag packages alter diving behavior in harbor porpoises? *Marine Mammal Science*, 31(2), 756–763. doi:10.1111/mms.12179
- Spalart, P., & Allmaras, S. (1994). A one-equation turbulence model for aerodynamic flows. *La Recherche Aeronautique*, 1, 5. doi:10.2514/6.1992-439
- Sparling, C., Lonergan, M., & Mcconnell, B. (2018). Harbour seals (*Phoca vitulina*) around an operational tidal turbine in Strangford Narrows: No barrier effect but small changes in transit behaviour. *Aquatic Conservation: Marine and Freshwater Ecosystems*, 28(1), 194–204. doi:10.1002/aqc.2790
- Stabeno, P. J., Kachel, D. G., Kachel, N. B., & Sullivan, M. E. (2005). Observations from moorings in the Aleutian Passes: temperature, salinity and transport. *Fisheries Oceanography*, 14(s1), 39–54. doi:10.1111/j.1365-2419.2005.00362.x
- Stafford, K. M., Okkonen, S. R., & Clarke, J. T. (2013). Correlation of a strong Alaska Coastal Current with the presence of beluga whales *Delphinapterus leucas* near Barrow, Alaska. *Marine Ecology Progress Series*, 474, 287–297. doi:10.3354/meps10076
- Stalder, D., Van Beest, F. M., Sveegaard, S., Dietz, R., Teilmann, J., & Nabe-Nielsen, J. (2020). Influence of environmental variability on harbour porpoise movement. *Marine Ecology Progress Series*, 648, 207–219. doi:10.3354/meps13412
- Stanev, E. V., Wölff, J. O., Burchard, H., Bolding, K., & Flöser, G. (2003). On the circulation in the East Frisian Wadden Sea: Numerical modeling and data analysis. *Ocean Dynamics*, 53(1), 27–51. doi:10.1007/s10236-002-0022-7
- Stenseth, N. C., & Mysterud, A. (2005). Weather packages: Finding the right scale and composition of climate in ecology. *Journal of Animal Ecology*, 74(6), 1195–1198. doi:10.1111/j.1365-2656.2005.01005.x
- Stern, S. J., & Friedlaender, A. S. (2017). Migration and Movement. *Encyclopedia of Marine Mammals*, (2003), 602–606. doi:10.1016/b978-0-12-804327-1.00173-4
- Stidsholt, L., Johnson, M., Beedholm, K., Jakobsen, L., Kugler, K., Brinkløv, S., ... Madsen, P. T. (2018). A 2.6-g sound and movement tag for studying the acoustic scene and kinematics of echolocating bats. *Methods in Ecology and Evolution*, 0–2. doi:10.1111/2041-210X.13108
- Stirling, I. (1980). The Biological Importance of Polynyas in the Canadian

- Arctic. *Arctic*, 33(2). doi:10.14430/arctic2563
- Strong, P. G., Lerwill, J., Morris, S. R., & Stringell, T. B. (2006). *Pembrokeshire marine SAC grey seal monitoring 2005*. CCW Marine Monitoring Report (Vol. 26).
- Suliman, M. A., Mahmoud, O. K., Al-Sanabawy, M. A., & Abdel-Hamid, O. E. (2009). Computational investigation of base drag reduction for a projectile at different flight regimes. *Paper: ASAT-13-FM-05, 13th International Conference on Aerospace Science and Aviation Technology, Military Technical College, Kobry Elkobbah, Cairo, Egypt*.
- Suryan, R. M., & Harvey, J. T. (1998). Tracking harbour seals (*Phoca vitulina richardsi*) to determine dive behavior, foraging activity, and haul-out site use. *Marine Mammal Science*, 14(2), 361–372. doi:10.1111/j.1748-7692.1998.tb00728.x
- Sveegaard, S., Andreassen, H., Mouritsen, K. N., Jeppesen, J. P., Teilmann, J., & Kinze, C. C. (2012). Correlation between the seasonal distribution of harbour porpoises and their prey in the Sound, Baltic Sea. *Marine Biology*, 159(5), 1029–1037. doi:10.1007/s00227-012-1883-z
- Sydeman, W. J., Poloczanska, E., Reed, T. E., & Thompson, S. A. (2015). Climate change and marine vertebrates. *Science*. doi:10.1126/science.aac9874
- Takei, Y., Suzuki, I., Wong, M. K. S., Milne, R., Moss, S., Sato, K., & Hall, A. (2016). Development of an animal-borne blood sample collection device and its deployment for the determination of cardiovascular and stress hormones in phocid seals. *American Journal of Physiology - Regulatory Integrative and Comparative Physiology*, 311(4), R788–R796. doi:10.1152/ajpregu.00211.2016
- Taormina, B., Bald, J., Want, A., Thouzeau, G., Lejart, M., Desroy, N., & Carlier, A. (2018). A review of potential impacts of submarine power cables on the marine environment: Knowledge gaps, recommendations and future directions. *Renewable and Sustainable Energy Reviews*, 96, 380–391. doi:10.1016/J.RSER.2018.07.026
- Taormina, B., Laurans, M., Marzloff, M. P., Dufournaud, N., Lejart, M., Desroy, N., ... Carlier, A. (2020). Renewable energy homes for marine life: Habitat potential of a tidal energy project for benthic megafauna. *Marine Environmental Research*, 161, 105131. doi:10.1016/j.marenvres.2020.105131
- Teilmann, J., & Galatius, A. (2018). Harbor Seal. In *Encyclopedia of Marine Mammals* (pp. 451–455). Elsevier. doi:10.1016/B978-0-12-804327-1.00145-X
- Thompson, D. (2012). *Assessment of Risk to Marine Mammals from Underwater Marine Renewable Devices in Welsh waters (on behalf of the Welsh Government), Phase 2: Studies of Marine Mammals in Welsh High Tidal Waters, Annex 1 Movements and Diving Behaviour of Juvenile Grey Seals*.
- Thompson, D., Hammond, P. S., Nicholas, K. S., & Fepak, M. A. (1991). Movements, diving and foraging behaviour of grey seals (*Halichoerus grypus*). *Journal of Zoology*, 224(2), 223–232. doi:10.1111/j.1469-7998.1991.tb04801.x
- Thompson, D., Onoufriou, J., Brownlow, A., & Morris, C. (2016). Data based estimates of collision risk: an example based on harbour seal tracking

- data around a proposed tidal turbine array in the Pentland Firth. *Scottish Natural Heritage Comissioned Report No. 900*, (9), 41.
- Thompson, D., Duck, C. D., Morris, C. D., & Russell, D. J. F. (2019). The status of harbour seals (*Phoca vitulina*) in the UK. *Aquatic Conservation: Marine and Freshwater Ecosystems*, 29(S1), 40–60. doi:10.1002/AQC.3110
- Thompson, P. M., Fedak, M. A., McConnell, B. J., & Nicholas, K. S. (1989). Seasonal and Sex-Related Variation in the Activity Patterns of Common Seals (*Phoca vitulina*). *The Journal of Applied Ecology*, 26(2), 521. doi:10.2307/2404078
- Thompson, P. M., Kovacs, K. M., & McConnell, B. J. (1994). Natal dispersal of harbour seals (*Phoca vitulina*) from breeding sites in Orkney, Scotland. *Journal of Zoology*, 234(4), 668–673. doi:10.1111/j.1469-7998.1994.tb04873.x
- Thompson, P. M., Mackay, A., Tollit, D. J., Enderby, S., & Hammond, P. S. (1998). The influence of body size and sex on the characteristics of harbour seal foraging trips. *Canadian Journal of Zoology*, 76(6), 1044–1053. doi:10.1139/z98-035
- Thompson, P. M., McConnell, B. J., Tollit, D. J., Mackay, A., Hunter, C., & Racey, P. A. (1996). Comparative Distribution, Movements and Diet of Harbour and Grey Seals from Moray Firth, N. E. Scotland. *The Journal of Applied Ecology*, 33(6), 1572. doi:10.2307/2404795
- Thompson, P. M., & Miller, D. (1990). Summer Foraging Activity and Movements of Radio-Tagged Common Seals (*Phoca vitulina*. L.) in the Moray Firth, Scotland. *The Journal of Applied Ecology*, 27(2), 492–501. doi:10.2307/2404296
- Tidal Energy Limited. (2009). *DeltaStream Demonstrator Project Ramsey Sound, Pembrokeshire*.
- Tinker, M. T., Bodkin, J. L., Ben-David, M., & Estes, J. A. (2018). Otters: *Enhydra lutris* and *Lontra felina*. *Encyclopedia of Marine Mammals*, (1972), 664–671. doi:10.1016/B978-0-12-804327-1.00188-6
- Tollit, D. J., Black, A. D., Thompson, P. M., Mackay, A., Corpe, H. M., Wilson, B., ... Parlane, S. (1998). Variations in harbour seal *Phoca vitulina* diet and dive-depths in relation to foraging habitat. *Journal of Zoology*, 244(2), 209–222. doi:10.1111/j.1469-7998.1998.tb00026.x
- Treasure, A., Roquet, F., Ansoorge, I. J., Bester, M., Boehme, L., Bornemann, H., ... de Bruyn, P. J. N. (2017). Marine mammals exploring the oceans pole to pole: A review of the MEOP Consortium. *Oceanography*, 30(2), 132–138. doi:10.5670/oceanog.2017.234
- Tudorache, C., Burgerhout, E., Brittiijn, S., & Van Den Thillart, G. (2014). The effect of drag and attachment site of external tags on swimming eels: Experimental quantification and evaluation tool. *PLoS ONE*, 9(11), 1–10. doi:10.1371/journal.pone.0112280
- Turchin, P. (1998). Quantitative Analysis of Movement. *Measuring and Modeling Population Redistribution in Animals and Plants*. Sinauer Associates.
- Twiss, S. D., Pomeroy, P. P., & Anderson, S. S. (1994). Dispersion and site fidelity of breeding male grey seals (*Halichoerus grypus*) on North Rona, Scotland. *Journal of Zoology*, 233(4), 683–693. doi:10.1111/j.1469-7998.1994.tb05374.x
- Tyagi, A., & Sen, D. (2006). Calculation of transverse hydrodynamic

- coefficients using computational fluid dynamic approach. *Ocean Engineering*, 33, 798–809.
- Uda, M., & Ishino, M. (1958). Enrichment patterns resulting from eddy systems in relation to fishing grounds. *J Tokyo Univ Fish*, 44, 105–129.
- United States Department of Agriculture (USDA). (2017). Animal Welfare Act and Animal Welfare Regulations Blue Book. *Animal and Plant Health Inspection Service (APHIS)*, (January).
- USFWS. (2017). *Federal Fish and Wildlife Permit Application OMB No. 1018-0093*.
- van Beest, F. M., Mews, S., Elkenkamp, S., Schuhmann, P., Tsolak, D., Wobbe, T., ... Langrock, R. (2019). Classifying grey seal behaviour in relation to environmental variability and commercial fishing activity - a multivariate hidden Markov model. *Scientific Reports*, 9(1), 5642. doi:10.1038/s41598-019-42109-w
- van Beest, F. M., Teilmann, J., Hermanssen, L., Galatius, A., Mikkelsen, L., Sveegaard, S., ... Nabe-Nielsen, J. (2018). Fine-scale movement responses of free-ranging harbour porpoises to capture, tagging and short-term noise pulses from a single airgun. *Royal Society Open Science*, 5(1), 170110. doi:10.1098/rsos.170110
- van der Hoop, J. M., Fahlman, A., Hurst, T., Rocho-Levine, J., Shorter, K. A., Petrov, V., & Moore, M. J. (2014). Bottlenose dolphins modify behavior to reduce metabolic effect of tag attachment. *Journal of Experimental Biology*, 217(23), 4229–4236. doi:10.1242/jeb.108225
- van der Hoop, J. M., Fahlman, A., Shorter, K. A., Gabaldon, J., Rocho-Levine, J., Petrov, V., & Moore, M. J. (2018). Swimming Energy Economy in Bottlenose Dolphins Under Variable Drag Loading. *Frontiers in Marine Science*, 5, 465. doi:10.3389/fmars.2018.00465
- van Der Hoop, Julie M., Moore, M. J., Barco, S. G., Cole, T. V. N., Daoust, P. Y., Henry, A. G., ... Solow, A. R. (2013). Assessment of Management to Mitigate Anthropogenic Effects on Large Whales. *Conservation Biology*, 27(1), 121–133. doi:10.1111/j.1523-1739.2012.01934.x
- van Etten, J. (2017). R Package gdistance: Distances and Routes on Geographical Grids. *Journal of Statistical Software*, 76(13). doi:10.18637/jss.v076.i13
- van Neer, A., Gross, S., Kesselring, T., Wohlsein, P., Leitzen, E., & Siebert, U. (2019). Behavioural and pathological insights into a case of active cannibalism by a grey seal (*Halichoerus grypus*) on Helgoland, Germany. *Journal of Sea Research*, 148–149, 12–16. doi:10.1016/j.seares.2019.03.004
- van Neer, A., Rubio-Garcia, A., Gross, S., Salazar-Casals, A., Arriba-Garcia, A., Wohlsein, P., & Siebert, U. (2020). An innovative approach for combining marking of phocid seals with biopsy sampling using a new type of livestock ear tags. *Journal of Marine Animals and Their Ecology*, 12(1).
- van Parijs, S. M., Hastie, G. D., & Thompson, P. M. (1999). Geographical variation in temporal and spatial vocalization patterns of male harbour seals in the mating season. *Animal Behaviour*, 58(6), 1231–1239. doi:10.1006/anbe.1999.1258
- van Parijs, S. M., Thompson, P. M., & Tollit, D. J. (1997). Distribution and activity of male harbour seals during the mating season, *Animal Behaviour*, 54(1): 35-43.

- Vandenabeele, S., Grundy, E., Friswell, M., Grogan, A., Votier, S., & Wilson, R. (2014). Excess baggage for birds: Inappropriate placement of tags on gannets changes flight patterns. *PLoS ONE*, 9(3). doi:10.1371/journal.pone.0092657
- Vandenabeele, S. P., Shepard, E. L. C., Grémillet, D., Butler, P. J., Martin, G. R., & Wilson, R. P. (2015). Are bio-telemetric devices a drag? Effects of external tags on the diving behaviour of great cormorants. *Marine Ecology Progress Series*, 519, 239–249. doi:10.3354/meps11058
- Vanderlaan, A. S. M., & Taggart, C. T. (2007). Vessel collisions with whales: The probability of lethal injury based on vessel speed. *Marine Mammal Science*, 23(1), 144–156. doi:10.1111/J.1748-7692.2006.00098.X
- Vassberg, J. C., Tinoco, E. N., Mani, M., Rider, B., Zickuhr, T., Levy, D. W., ... Murayama, M. (2014). Summary of the Fourth AIAA Computational Fluid Dynamics Drag Prediction Workshop. *Journal of Aircraft*, 51(4), 1070–1089. doi:10.2514/1.C032418
- Vermeer, K., Szabo, I., & Greisman, P. (1987). The relationship between plankton-feeding Bonaparte's and Mew Gulls and tidal upwelling at Active Pass, British Columbia. *Journal of Plankton Research*, 9(3), 483–501. doi:10.1093/plankt/9.3.483
- Vincent, C., Huon, M., Caurant, F., Dabin, W., Deniau, A., Dixneuf, S., ... Ridoux, V. (2017). Grey and harbour seals in France: Distribution at sea, connectivity and trends in abundance at haulout sites. *Deep-Sea Research Part II: Topical Studies in Oceanography*, 141(April), 294–305. doi:10.1016/j.dsr2.2017.04.004
- Votier, S. C., Fayet, A. L., Bearhop, S., Bodey, T. W., Clark, B. L., Grecian, J., ... Patrick, S. C. (2017). Effects of age and reproductive status on individual foraging site fidelity in a long-lived marine predator. *Proceedings of the Royal Society B: Biological Sciences*, 284(1859), 20171068. doi:10.1098/rspb.2017.1068
- Votier, S. C., Grecian, W. J., Patrick, S., & Newton, J. (2011). Inter-colony movements, at-sea behaviour and foraging in an immature seabird: results from GPS-PPT tracking, radio-tracking and stable isotope analysis. *Marine Biology*, 158(2), 355–362. doi:10.1007/s00227-010-1563-9
- Wade, H. M., Masden, E. A., Jackson, A. C., & Furness, R. W. (2012). Which seabird species use high-velocity current flow environments? Investigating the potential effects of tidal-stream renewable energy developments. *BOU Mar. Renewables Birds*. doi:10.13140/2.1.2530.6885
- Wade, H. M. (2015). Investigating the potential effects of marine renewable energy developments on seabirds. *PhD Dissertation*, September 2015, 1-417.
- Waggitt, J. J., & Scott, B. E. (2014). Using a spatial overlap approach to estimate the risk of collisions between deep diving seabirds and tidal stream turbines: A review of potential methods and approaches. *Marine Policy*, 44, 90–97. doi:10.1016/J.MARPOL.2013.07.007
- Waggitt, J. J., Cazenave, P. W., Torres, R., Williamson, B. J., & Scott, B. E. (2016). Quantifying pursuit-diving seabirds' associations with fine-scale physical features in tidal stream environments. *Journal of Applied Ecology*, 53(6), 1653–1666. doi:10.1111/1365-2664.12646
- Waggitt, J. J., Cazenave, P. W., Torres, R., Williamson, B. J., & Scott, B. E.

- (2016b). Predictable hydrodynamic conditions explain temporal variations in the density of benthic foraging seabirds in a tidal stream environment. *ICES Journal of Marine Science*, 73(10), 2677-2686.
- Waggitt, J. J., Evans, P. G. H., Andrade, J., Banks, A. N., Boisseau, O., Bolton, M., ... Hiddink, J. G. (2020). Distribution maps of cetacean and seabird populations in the North-East Atlantic. *Journal of Applied Ecology*, 57(2), 253–269. doi:10.1111/1365-2664.13525
- Waggitt, J. J., Robbins, A. M. C., Wade, H. M., Masden, E. A., Furness, R. W., Jackson, A. C., & Scott, B. E. (2017). Comparative studies reveal variability in the use of tidal stream environments by seabirds. *Marine Policy*, 81(March), 143–152. doi:10.1016/j.marpol.2017.03.023
- Walker, K. A., Trites, A. W., Haulena, M., & Weary, D. M. (2012). A review of the effects of different marking and tagging techniques on marine mammals. *Wildlife Research*, 39(1), 15. doi:10.1071/WR10177
- Walker, R. J., Morris, C., Stringell, T. B., & Taylor, N. (2019). Marine Renewable Energy: Current Research and Evidence Gaps on Impacts on Marine Mammals. Proceedings from the European Cetacean Society Conference 2018 Workshop, La Spezia, Italy. (pp. 1–27).
- Walton, R., Baxter, R., Bunbury, N., Hansen, D., Fleischer-Dogley, F., Greenwood, S., & Schaepman-Strub, G. (2019). In the land of giants: habitat use and selection of the Aldabra giant tortoise on Aldabra Atoll. *Biodiversity and Conservation*, 28(12), 3183–3198. doi:10.1007/s10531-019-01813-9
- Waluda, C. M., Collins, M. A., Black, A. D., Staniland, I. J., & Trathan, P. N. (2010). Linking predator and prey behaviour: contrasts between Antarctic fur seals and macaroni penguins at South Georgia. *Marine Biology*, 157(1), 99–112. doi:10.1007/s00227-009-1299-6
- Wang, Z., Quintanal, J., & Corral, R. (2017). Accelerating advancing layer viscous mesh generation for 3D complex configurations. *Procedia Engineering*, 203, 128–140. doi:10.1016/j.proeng.2017.09.797
- Wanless, S., Gremillet, D., & Harris, M. P. (1998). Foraging Activity and Performance of Shags *Phalacrocorax aristotelis* in Relation to Environmental Characteristics. *Journal of Avian Biology*, 29(1), 49. doi:10.2307/3677340
- Watanuki, Y., Daunt, F., Takahashi, A., Newell, M., Wanless, S., Sato, K., & Miyazaki, N. (2008). Microhabitat use and prey capture of a bottom-feeding top predator, the European shag, shown by camera loggers. *Marine Ecology Progress Series*, 356, 283–293. doi:10.3354/meps07266
- Watson, K. P., & Granger, R. A. (1998). Hydrodynamic effect of a satellite transmitter on a juvenile green turtle (*Chelonia mydas*). *Journal of Experimental Biology*, 201(17), 2497–2505.
- Weimerskirch, H. (2009). *30 years of wildlife tracking with ARGOS – Editorial.* (ed. H. Ferro), p. 3. CLS, Cape Town, South Africa.
- Westcott, S. M., & Stringell, T. B. (2003). Grey seal pup production for North Wales, 2002. *Bangor, CCW Marine Monitoring Report No. 5*, 1–55.
- Whitmore, B. M., White, C. F., Gleiss, A. C., & Whitney, N. M. (2016). A float-release package for recovering data-loggers from wild sharks. *Journal of Experimental Marine Biology and Ecology*, 475(February), 49–53. doi:10.1016/j.jembe.2015.11.002
- Whitney, N. M., White, C. F., Gleiss, A. C., Schwieterman, G. D., Anderson,

- P., Hueter, R. E., & Skomal, G. B. (2016). A novel method for determining post-release mortality, behavior, and recovery period using acceleration data loggers. *Fisheries Research*, 183(November), 210–221. doi:10.1016/j.fishres.2016.06.003
- Wikelski, M., & Kays, R. (2019). Movebank: archive, analysis and sharing of animal movement data. Retrieved 26 February 2019, from www.movebank.org
- Wildermann, N., Sasso, C., Gredzens, C., & Fuentes, M. M. P. B. (2020). Assessing the effect of recreational scallop harvest on the distribution and behaviour of foraging marine turtles. *Oryx*, 54(3), 307–314. doi:10.1017/S0030605318000182
- Williams, H. J., Holton, M. D., Shepard, E. L. C. C., Largey, N., Norman, B., Ryan, P. G., ... Wilson, R. P. (2017). Identification of animal movement patterns using tri-axial magnetometry. *Movement Ecology*, 5(1), 1–14. doi:10.1186/s40462-017-0097-x
- Williams, H. J., Taylor, L. A., Benhamou, S., Bijleveld, A. I., Clay, T. A., Grissac, S., ... Börger, L. (2020). Optimizing the use of biologgers for movement ecology research. *Journal of Animal Ecology*, 89(1), 186–206. doi:10.1111/1365-2656.13094
- Williams, T. M. (2018). Swimming. In *Encyclopedia of Marine Mammals* (pp. 970–979). Elsevier. doi:10.1016/B978-0-12-804327-1.00256-9
- Williams, T. M., Wolfe, L., Davis, T., Kendall, T., Richter, B., Wang, Y., ... Wilmers, C. C. (2014). Instantaneous energetics of puma kills reveal advantage of felid sneak attacks. *Science*, 346(6205), 81–85. doi:10.1126/science.1254885
- Williamson, B., Fraser, S., Williamson, L., Nikora, V., & Scott, B. (2019). Predictable changes in fish school characteristics due to a tidal turbine support structure. *Renewable Energy*, 141, 1092–1102. doi:10.1016/j.renene.2019.04.065
- Wilmers, C. C., Estes, J. A., Edwards, M., Laidre, K. L., & Konar, B. (2012). Do trophic cascades affect the storage and flux of atmospheric carbon? An analysis of sea otters and kelp forests. *Frontiers in Ecology and the Environment*, 10(8), 409–415. doi:10.1890/110176
- Wilmers, C. C., Nickel, B., Bryce, C. M., Smith, J. A., Wheat, R. E., & Yovovich, V. (2015). The golden age of bio-logging : how animal- borne sensors are advancing the frontiers of ecology. *Ecology*, 96(7), 1741–1753. doi:10.1890/14-1401.1
- Wilson, B., Batty, R. S., Daunt, F., & Carter, C. (2006). *Collision risks between marine renewable energy devices and mammals, fish and diving birds. Report to the Scottish Executive. Scottish Association for Marine Science, Oban, Scotland, PA37 1QA.*
- Wilson, B., Benjamins, S., & Elliott, J. (2013). Using drifting passive echolocation loggers to study harbour porpoises in tidal-stream habitats. *Endangered Species Research*, 22(2), 125–143. doi:10.3354/esr00538
- Wilson, K., Lance, M., Jeffries, S., & Acevedo-Gutiérrez, A. (2014). Fine-Scale Variability in Harbor Seal Foraging Behavior. *PLoS ONE*, 9(4), e92838. doi:10.1371/journal.pone.0092838
- Wilson, K., Littnan, C., Halpin, P., & Read, A. (2017). Integrating multiple technologies to understand the foraging behaviour of Hawaiian monk seals. *Royal Society Open Science*, 4(3), 160703.

- doi:10.1098/rsos.160703
- Wilson, R. P. (2004). Antennae on transmitters on penguins: balancing energy budgets on the high wire. *Journal of Experimental Biology*, 207(15), 2649–2662. doi:10.1242/jeb.01067
- Wilson, R. P., Sala, J. E., Gómez-Laich, A., Ciancio, J., & Quintana, F. (2015). Pushed to the limit: Food abundance determines tag-induced harm in penguins. *Animal Welfare*, 24(1), 37–44. doi:10.7120/09627286.24.1.037
- Wilson, R. P. (1992). Can we determine when marine endotherms Feed? A Case Study With Seabirds. *Journal of Experimental Biology*, 167, 267–275.
- Wilson, R. P., Grundy, E., Massy, R., Soltis, J., Tysse, B., Holton, M., ... Butt, T. (2014). Wild state secrets: Ultra-sensitive measurement of micro-movement can reveal internal processes in animals. *Frontiers in Ecology and the Environment*, 12(10), 582–587. doi:10.1890/140068
- Wilson, R. P., Holton, M. D., Walker, J. S., Shepard, E. L. C., Scantlebury, D. M., Wilson, V. L., ... Jones, M. W. (2016). A spherical-plot solution to linking acceleration metrics with animal performance, state, behaviour and lifestyle. *Movement Ecology*, 4(1), 22. doi:10.1186/s40462-016-0088-3
- Wilson, R. P., Holton, M., Wilson, V. L., Gunner, R., Tysse, B., Wilson, G. I., ... Scantlebury, D. M. (2018). Towards informed metrics for examining the role of human-induced animal responses in tag studies on wild animals. *Integrative Zoology*. doi:10.1111/1749-4877.12328
- Wilson, R. P., Liebsch, N., Gómez-Laich, A., Kay, W. P., Bone, A., Hobson, V. J., & Siebert, U. (2015). Options for modulating intra-specific competition in colonial pinnipeds: the case of harbour seals (*Phoca vitulina*) in the Wadden Sea. *PeerJ*, 3, e957. doi:10.7717/peerj.957
- Wilson, R. P., & McMahon, C. R. (2006). Measuring devices on wild animals: What constitutes acceptable practice? *Frontiers in Ecology and the Environment*, 4(3), 147–154. doi:10.1890/1540-9295(2006)004
- Wilson, R. P., Quintana, F., & Hobson, V. J. (2012). Construction of energy landscapes can clarify the movement and distribution of foraging animals. *Proceedings of the Royal Society B: Biological Sciences*. doi:10.1098/rspb.2011.1544
- Wilson, R. P., Ropert-Coudert, Y., & Kato, A. (2002). Rush and grab strategies in foraging marine endotherms: The case for haste in penguins. *Animal Behaviour*. doi:10.1006/anbe.2001.1883
- Wilson, R. P., Shepard, E. L. C., & Liebsch, N. (2008). Prying into the intimate details of animal lives: Use of a daily diary on animals. *Endangered Species Research*, 4(1–2), 123–137. doi:10.3354/esr00064
- Wilson, R. P., Spairani, H. J., Coria, N. R., Culik, B. M., & Adelung, D. (1990). Packages for Attachment to Seabirds: What Color Do Adelie Penguins Dislike Least? *Journal of Wildlife Management*, 54(3), 447–451. doi:10.2307/3809657
- Wilson, R. P., Williams, H. J., Holton, M. D., di Virgilio, A., Börger, L., Potts, J. R., ... Scantlebury, D. M. (2020). An “orientation sphere” visualization for examining animal head movements. *Ecology and Evolution*, (February), 1–12. doi:10.1002/ece3.6197
- Wilson, R. P., Liebsch, N., Davies, I. M., Quintana, F., Weimerskirch, H., Storch, S., ... McMahon, C. R. (2007). All at sea with animal tracks; methodological and analytical solutions for the resolution of movement.

- Deep Sea Research Part II: Topical Studies in Oceanography*, 54(3–4), 193–210. doi:10.1016/j.dsr2.2006.11.017
- Wisniewska, D. M., Johnson, M., Teilmann, J., Siebert, U., Galatius, A., Dietz, R., & Madsen, P. T. (2018). High rates of vessel noise disrupt foraging in wild harbour porpoises (*Phocoena phocoena*). *Proceedings of the Royal Society B: Biological Sciences*, 285(1872), 20172314. doi:10.1098/rspb.2017.2314
- Witte, M., Hanke, W., Wieskotten, S., Miersch, L., Brede, M., Dehnhardt, G. and Leder, A. (2012). On the wake flow dynamics behind harbor seal vibrissae—a fluid mechanical explanation for an extraordinary capability. *Nature-inspired fluid mechanics*, 271-289. Springer, Berlin, Heidelberg.
- Wolanski, E., & Hamner, W. M. (1988). Topographically controlled fronts in the ocean and their biological influence. *Science*, 241.4862, 177–181.
- Ydenberg, R. C., Welham, C. V. J., Schmid-Hempel, R., Schmid-Hempel, P., & Beauchamp, G. (1994). Time and energy constraints and the relationships between currencies in foraging theory. *Behavioral Ecology*, 5(1), 28–34.
- Young, J. W., Hunt, B. P. V., Cook, T. R., Llopiz, J. K., Hazen, E. L., Pethybridge, H. R., ... Anela Choy, C. (2015). The trophodynamics of marine top predators: Current knowledge, recent advances and challenges. *Deep Sea Research Part II: Topical Studies in Oceanography*, 113, 170–187. doi:10.1016/j.dsr2.2014.05.015
- Zacharias, M. A., & Roff, J. C. (2001). Use of focal species in marine conservation and management: A review and critique. *Aquatic Conservation: Marine and Freshwater Ecosystems*. doi:10.1002/aqc.429
- Zamon, J. E. (2001). Seal predation on salmon and forage fish schools as a function of tidal currents in the San Juan Islands, Washington, USA. *Fisheries Oceanography*, 10(4), 353–366. doi:10.1046/j.1365-2419.2001.00180.x
- Zamon, J. E. (2003). Mixed species aggregations feeding upon herring and sandlance schools in a nearshore archipelago depend on flooding tidal currents. *Marine Ecology Progress Series*, 261(1), 243–255. doi:10.3354/meps261243
- Zeppelin, T., Pelland, N., Sterling, J., Brost, B., Melin, S., Johnson, D., ... Ream, R. (2019). Migratory strategies of juvenile northern fur seals (*Callorhinus ursinus*): bridging the gap between pups and adults. *Scientific Reports*, 9(1). doi:10.1038/s41598-019-50230-z
- Zucchini, W., MacDonald, I. L., & Langrock, R. (2017). *Hidden Markov Models for Time Series: an introduction using R*. Chapman and Hall/CRC.

Appendix I: Supplementary material for Chapter 1

Contents

Appendix S1: Global distribution of grey and harbour seals

Appendix S1: Global distribution of grey and harbour seals

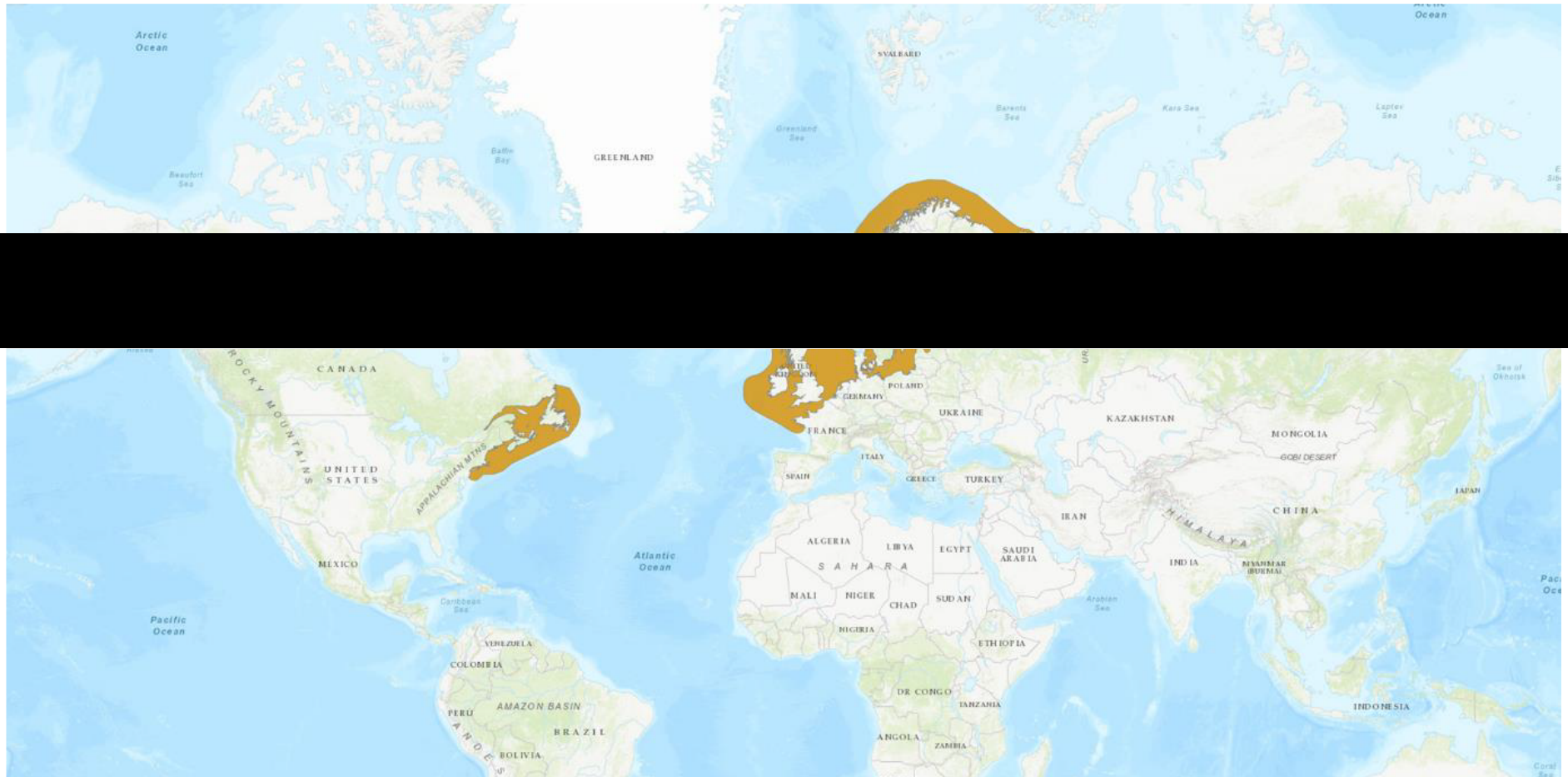


Fig. S1.1. Global distribution of the grey seal *Halichoerus grypus* (Bowen, 2016).



Fig. S1.2. Global distribution of the harbour seal *Phoca vitulina* (Lowry, 2016).

Appendix II: Supplementary material for Chapter 2

Contents

Appendix S2: Supplementary results for Chapter 2

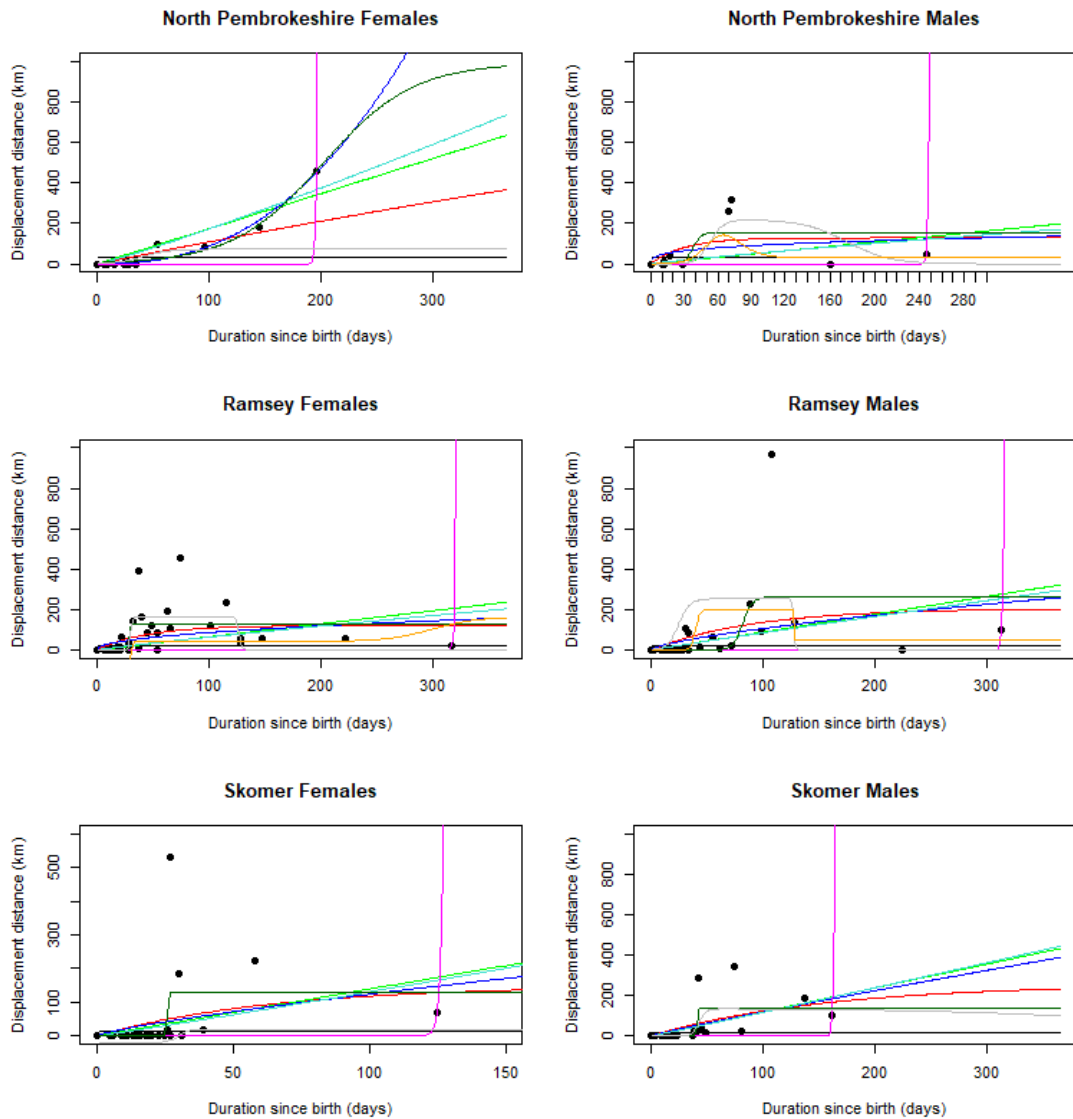


Fig. S2.1. All fitted displacement models. Note the almost identical displacement pattern between the dispersal model versus the diffusive model for North Pembrokeshire Females. Black line: null model (intercept only); red: sedentary model; light green: linear model; blue: diffusive (PowerC) model; turquoise: diffusive (PowerC2) model; magenta: diffusive (exponential) model; dark green: dispersal model; grey: return model; orange: mixed-return model.

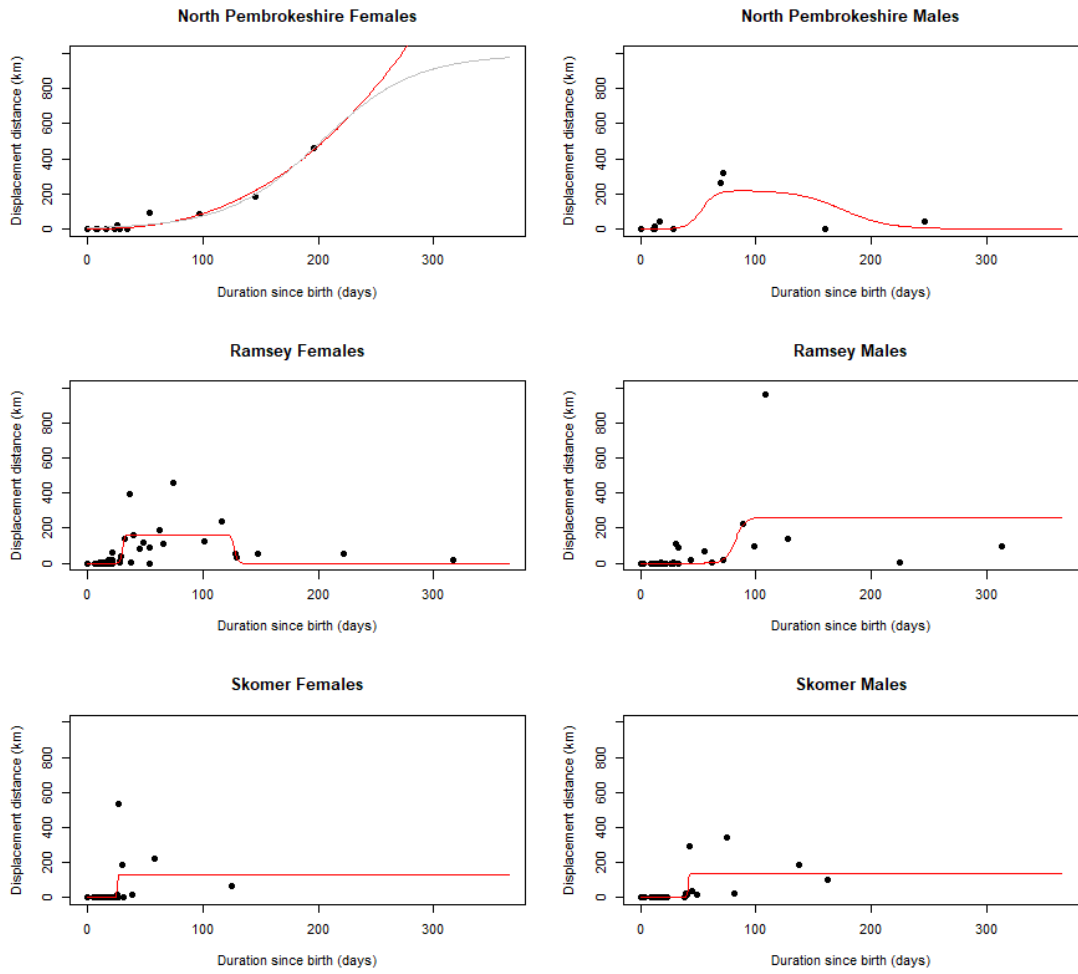


Fig. S2.2. Fitted displacement models. Red line shows the final model in each case and in the case of North Pembrokeshire Females (top-left panel) the best fitting (but excluded) model is shown in grey.

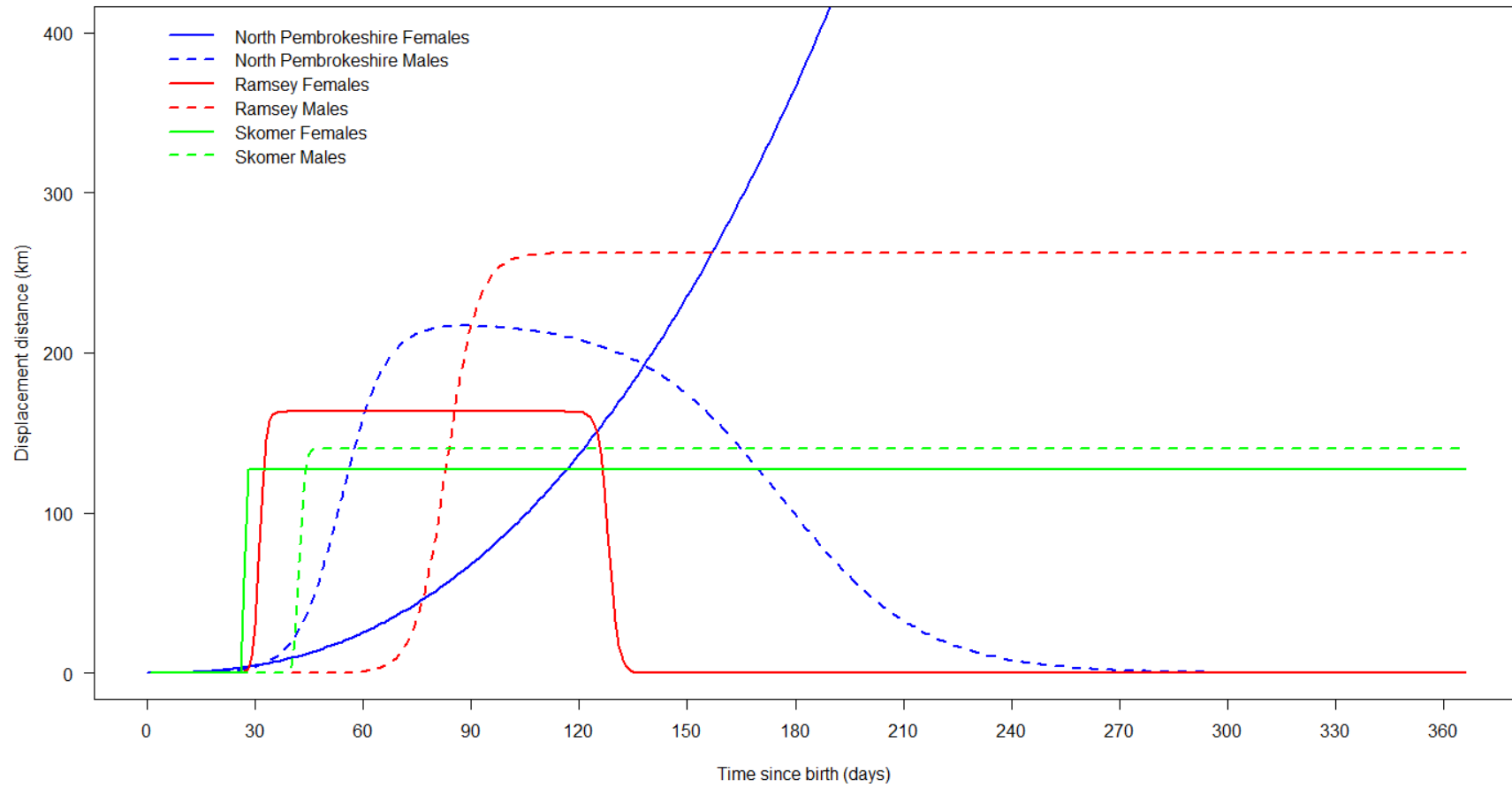


Fig. S2.3. All final displacement models plotted over a period of 1 year.

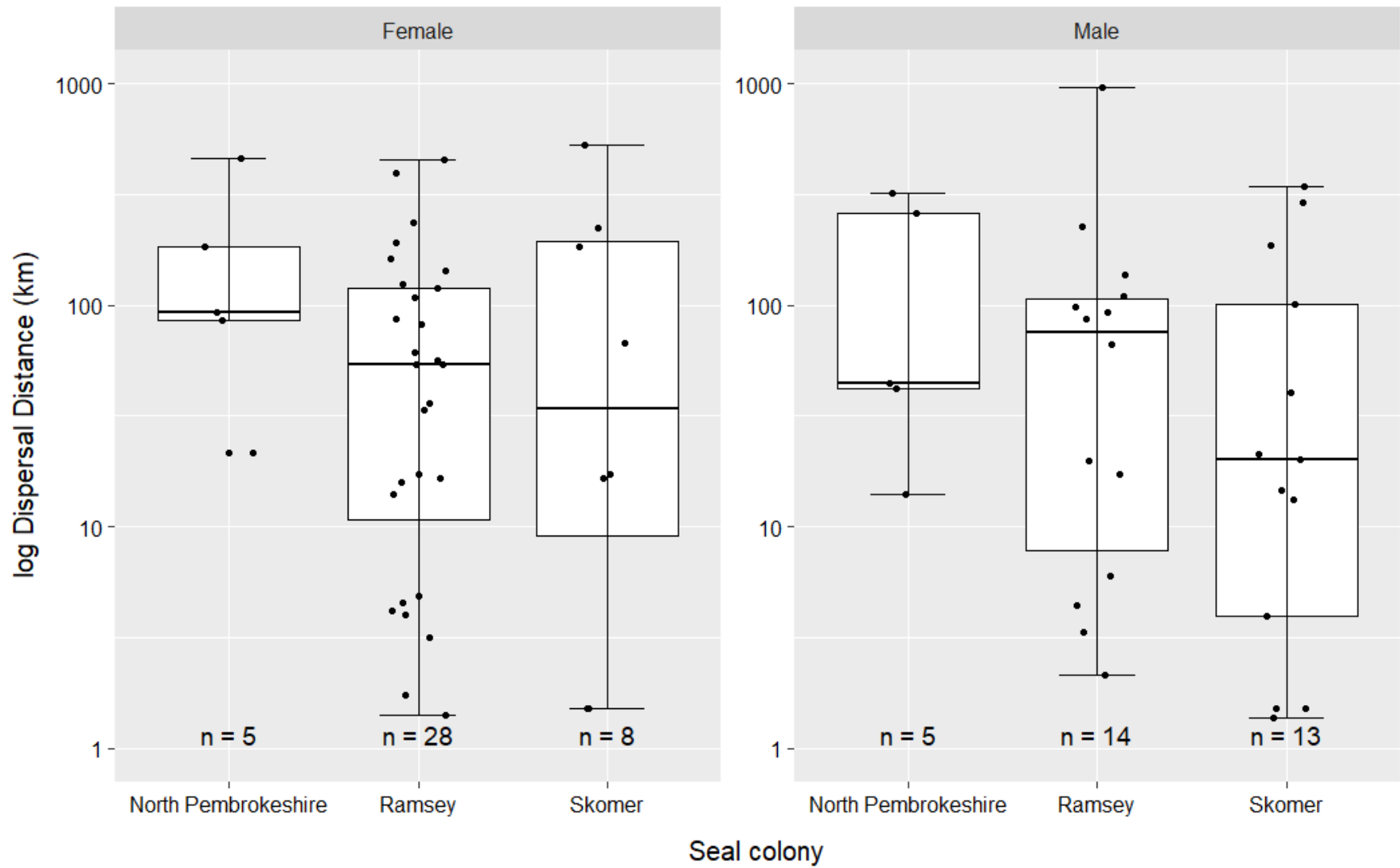


Fig. S2.4. log Displacement distance by [colony, sex] group.

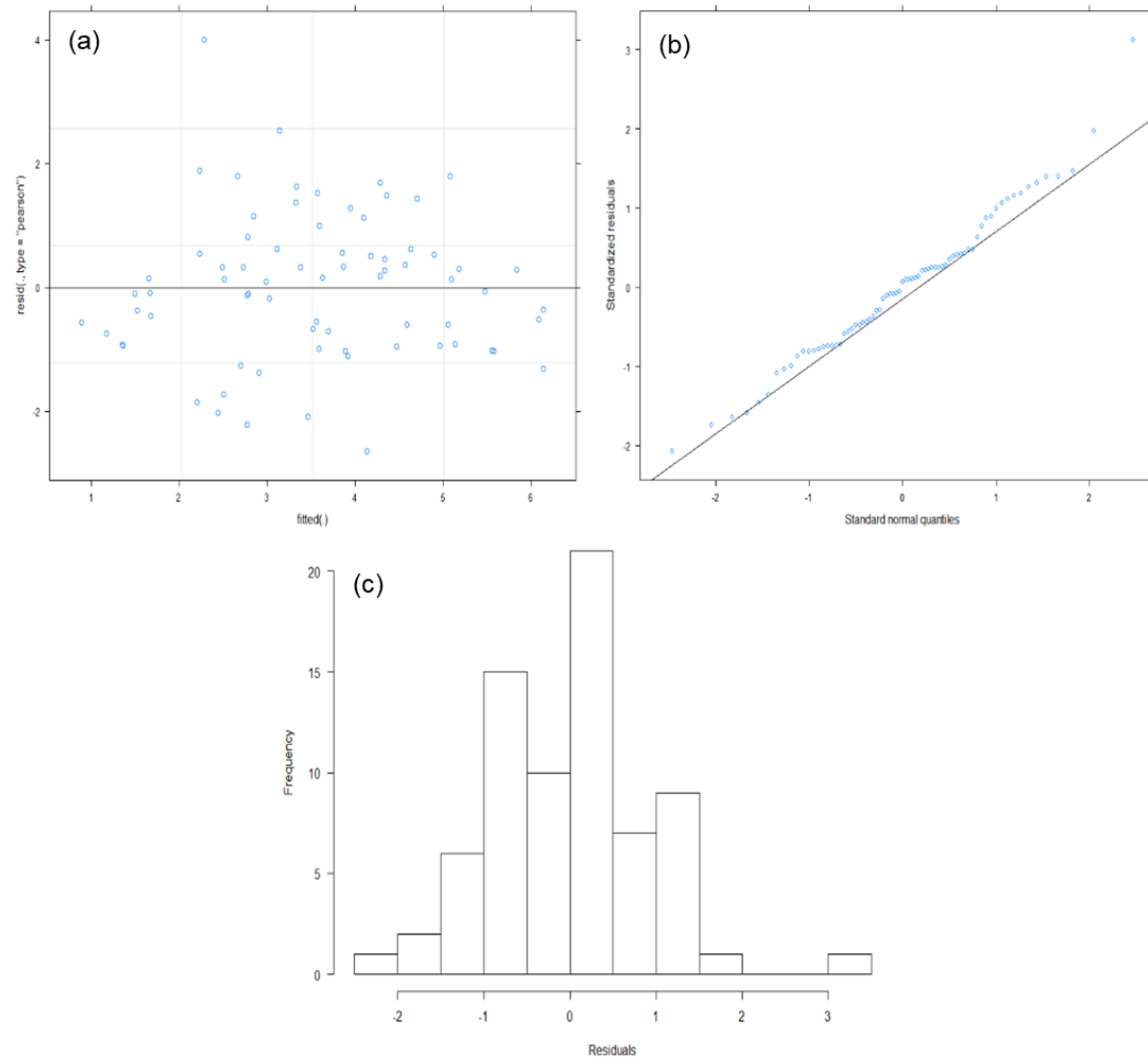


Fig. S2.5. Model diagnostics of the final displacement distance model reached by stepwise simplification (Table 2.4). (a) Residuals vs. fitted values. (b) Normal Q-Q plot. (c) Histogram of residuals.

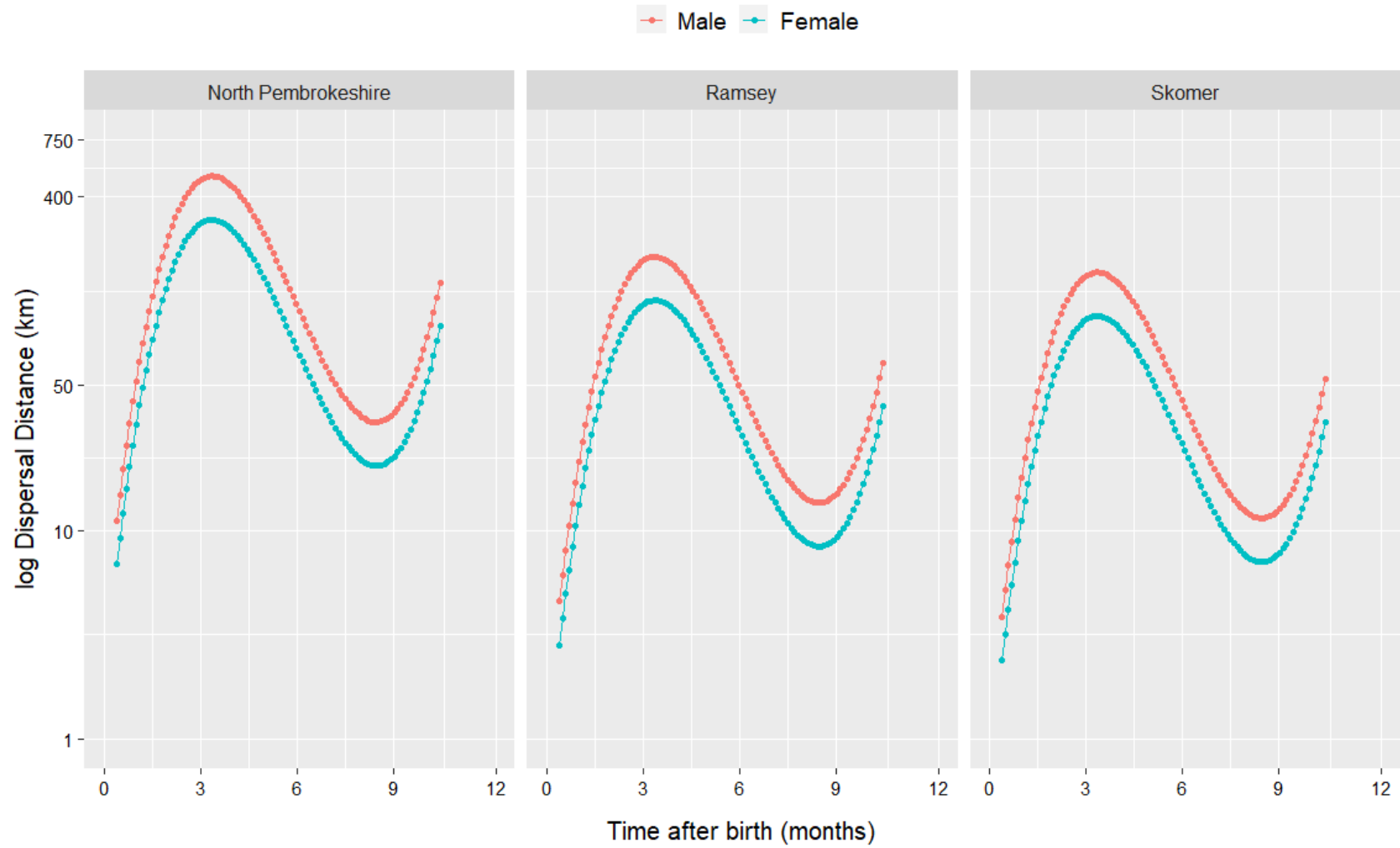


Fig. S2.6. Predicted displacement distance reached at different time periods for pups from each [colony, sex] group when NAO = 1.

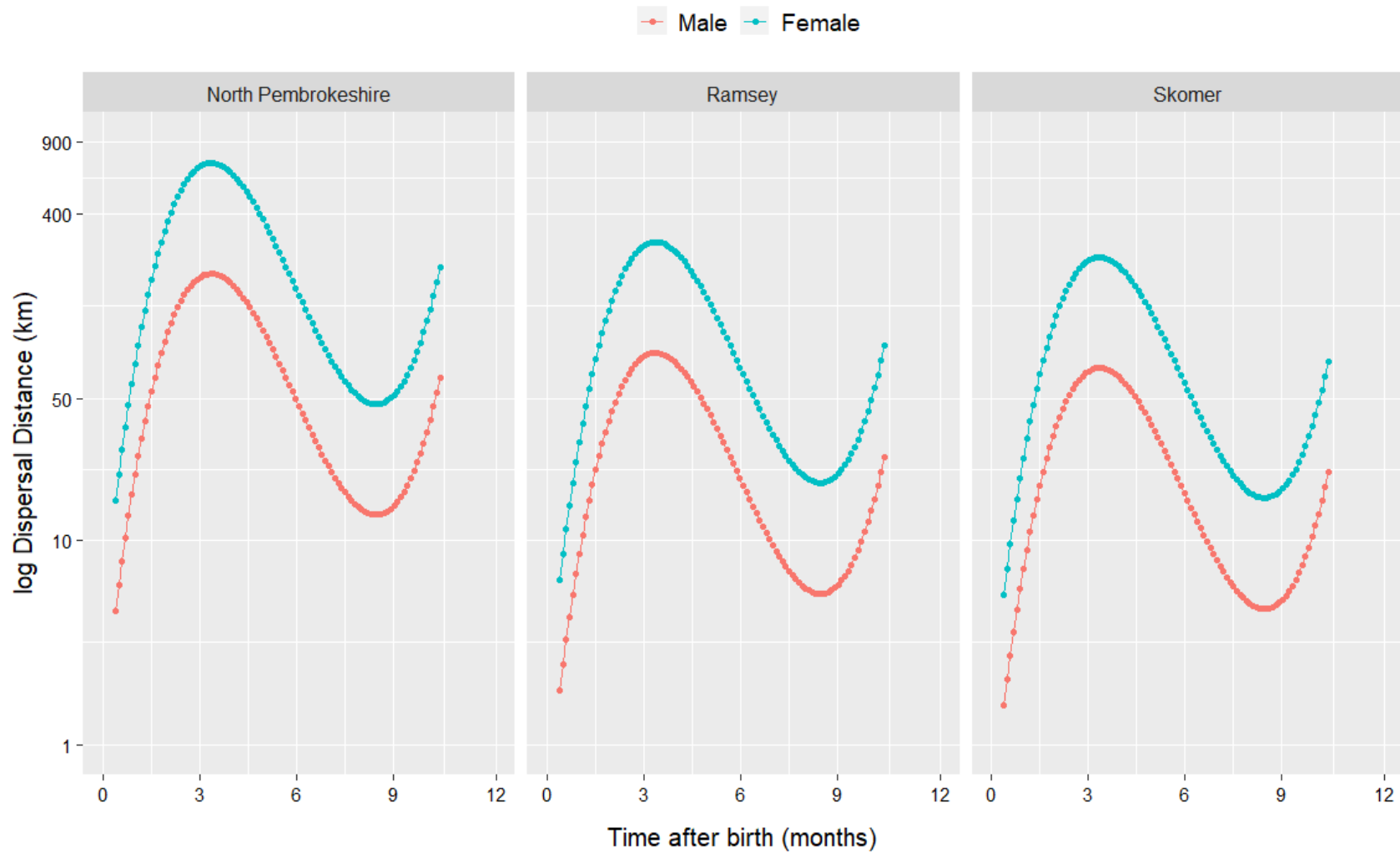


Fig. S2.7. Predicted displacement distance reached at different time periods for pups from each [site, sex] group when NAO = -1.

Table S2.8. Sample size distribution of pups from each sex-site group.

Sex	North Pembrokeshire	Ramsey	Skomer
Male	10	46	27
Female	13	53	33
Unknown	0	2	0

Appendix III: Supplementary material for Chapter 3

Contents

Appendix S3.1: Model fitting rules and considerations

Appendix S3.2: Displacement statistics

Appendix S3.3: Grey seal pup movement trajectories and distance travelled

Appendix S3.4: Individual-level model fits

Appendix S3.5: Parameter estimates from fitted displacement models

Appendix S3.6: Additional comparisons between models of different data types

Appendix S3.7: CC values of displacement models and model rule violations

Appendix S3.8: Maximum displacement versus recording duration

Appendix S3.1: Model fitting rules and considerations

I evaluated the support from the data for each of the displacement models using the concordance correlation (CC) coefficient. In addition to this, when fitting the models, I followed a number of rules to determine that the final model chosen for each individual was appropriate, as follows:

- (i) All estimated model parameters must be estimated within the limits of the temporal range of the empirical data (i.e., no extrapolation).
- (ii) Predicted maximum daily displacement rates must not exceed the empirical rate of displacement for any given individual, nor exceed the maximum expected velocity threshold for weaned grey seal pups (2 ms^{-1} ; Carter et al., 2017). Predicted maximum daily displacement rates were calculated directly from fitted model values post-hoc and were checked manually to ensure they were not too fast (Appendix S3.2).
- (iii) The model fit must correctly resemble its expected functional form (for example, occasionally the mixed-return model would converge on a 'return' asymptote that was greater than the estimate for the initial dispersal asymptote, resulting in an incorrect functional form).
- (iv) Fitted values must not be negative, as it is not possible to reach a negative distance away from the start point.
- (v) The model fit must clearly resemble the displacement pattern of the empirical data.

Appendix S3.2: Displacement statistics

Table S3.2. Displacement statistics derived from the fitted NSD models (see Fig. S3.2, Appendix S3.5, and Börger & Fryxell (2012) for further details).

Parameter	Name	Description and derivation
ϕ_1	Maximum displacement	The maximum displacement distance reached. For dispersal, sedentary, return, and mixed-return models this is equal to the asymptote.
ϕ_2	Midpoint of dispersal	The inflection point of the dispersal sigmoid curve. Present only in dispersal, return and mixed-return models.
ϕ_3	Dispersal scale parameter	This parameter controls the rate of increase of the linear distance in the dispersal curve; it determines the time elapsed between reaching half and approximately 3/4 of the asymptote (Börger & Fryxell, 2012). By rearranging the dispersal equation, it can be shown that $\phi_2 \pm 3\phi_3$ defines the start and end points of the dispersal transience phase, respectively. Present only in dispersal, return and mixed-return models. Not the same as predicted maximum daily displacement rate (see Appendix S3.1).
ϕ_4	Dispersal initiation	Start of the dispersal transience phase ($\phi_4 = \phi_2 - 3\phi_3$). Present only in dispersal, return and mixed-return models. ϕ_4 is within 5 % of the start distance.
ϕ_5	Dispersal settlement	End of the dispersal transience phase ($\phi_5 = \phi_2 + 3\phi_3$). Present only in dispersal, return and mixed-return models. ϕ_5 is within 5 % of the asymptotic distance.
ϕ_6	Dispersal transience distance	The displacement distance moved between the start and end of the dispersal transience phase. For nomadic and sedentary models this is equal to the maximum displacement.
ϕ_7	Dispersal transience duration	The duration of the dispersal transience phase ($\phi_7 = \phi_5 - \phi_4$). For nomadic models this is the total duration of movement; for sedentary models this is the duration before reaching asymptote.
ϕ_8	Dispersal transience displacement rate	Average displacement rate during dispersal transience ($\phi_8 = \phi_6 / \phi_7$). Not that this is different to the predicted maximum daily displacement rate (see Appendix S3.1).
ϕ_9	Return displacement	The return displacement distance moved. In return models this is equal to the asymptote; in mixed-return models this value is different to the asymptote. Not present in dispersal, nomadic, or sedentary models.
ϕ_{10}	Midpoint of return	The inflection point of the return sigmoid curve. Not present in dispersal, nomadic, or sedentary models.
ϕ_{11}	Return scale parameter	This parameter controls the rate of decrease of the linear distance in the return curve. By rearranging the return equation, it can be shown that $\phi_{10} \pm 3\phi_{11}$ defines the start and end points of the return transience, respectively. Present only in return and mixed-return models.

Parameter	Name	Description and derivation
ϕ_{12}	Return initiation	Start of the return transience phase ($\phi_{12} = \phi_{10} - 3\phi_{11}$). Present only in return and mixed-return models. ϕ_{12} is within 5 % of the start of the dispersal settlement distance.
ϕ_{13}	Return settlement	End of the return transience phase ($\phi_{13} = \phi_{10} + 3\phi_{11}$). Present only in return and mixed-return models. ϕ_{13} is within 5 % of the return settlement distance.
ϕ_{14}	Return transience distance	The displacement distance moved between the start and end of the return transience phase. Present only in return and mixed-return models.
ϕ_{15}	Return transience duration	The duration of the return transience phase ($\phi_{15} = \phi_{13} - \phi_{12}$). Present only in return and mixed-return models.
ϕ_{16}	Return transience displacement rate	Average displacement rate during return transience ($\phi_{16} = \phi_{14}/\phi_{15}$).
ϕ_{17}	Return settlement distance	The displacement distance from the colony that the animal returns to. Present only in return and mixed-return models.
ϕ_{18}	Settlement duration	The time elapsed between reaching and subsequently departing the dispersal settlement distance ($\phi_{18} = \phi_{12} - \phi_5$).

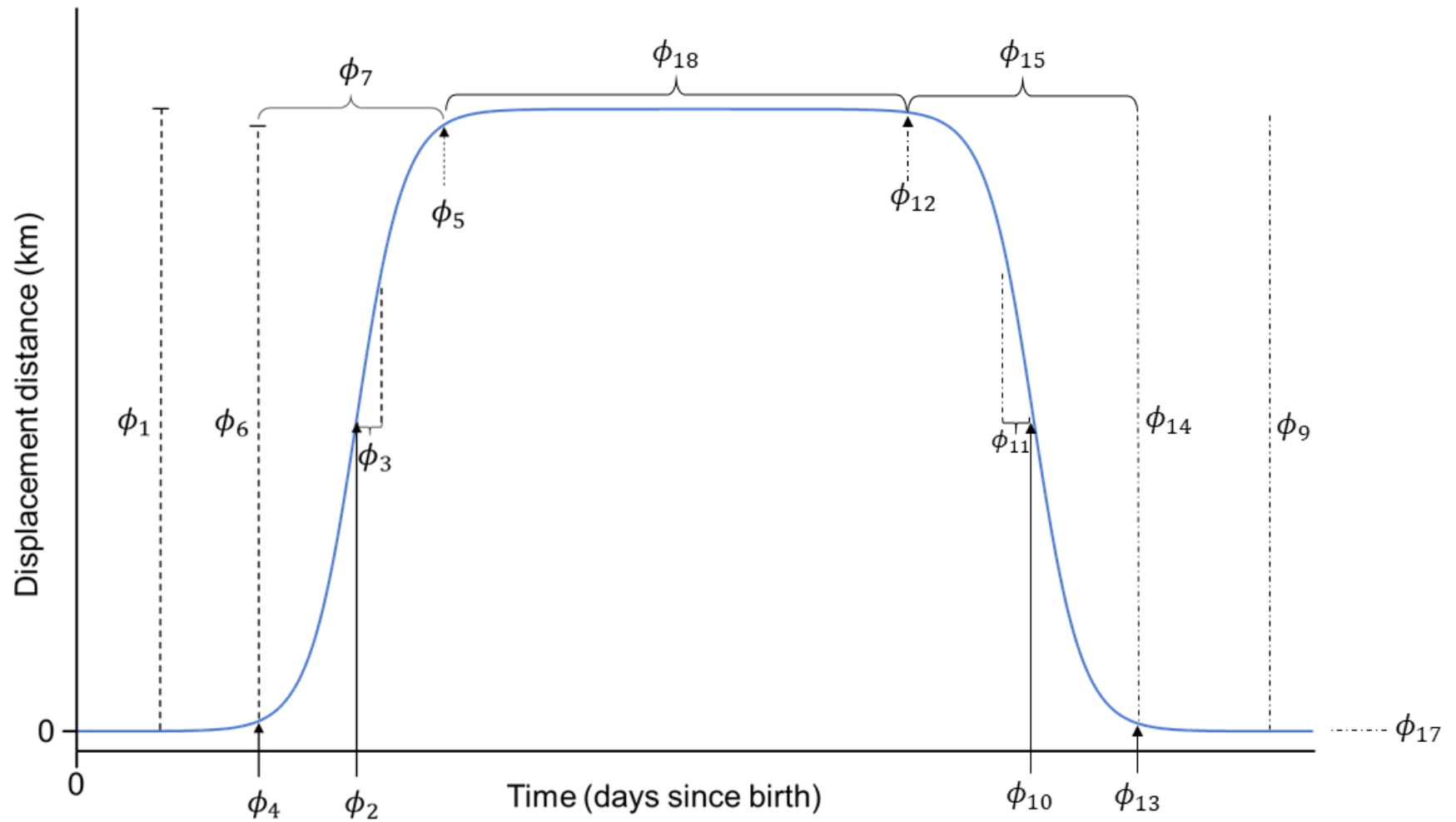


Fig. S3.2. Schematic diagram of return movement model showing two sigmoidal displacements between a distant location (settlement distance; asymptote) and the start point (0 km). The first sigmoidal displacement to the asymptote is considered the dispersal movement, with the second considered the return movement; note for dispersal models only the first displacement occurs, and for mixed-return models the return movement reaches a different (smaller) asymptote. See Table S3.3 for details of parameters $\phi_1 - \phi_{18}$. Parameters ϕ_8 and ϕ_{16} not shown in the figure; these are the rate of displacement of the first and second sigmoid, respectively.

Appendix S3.3: Grey seal pup movement trajectories and distance travelled

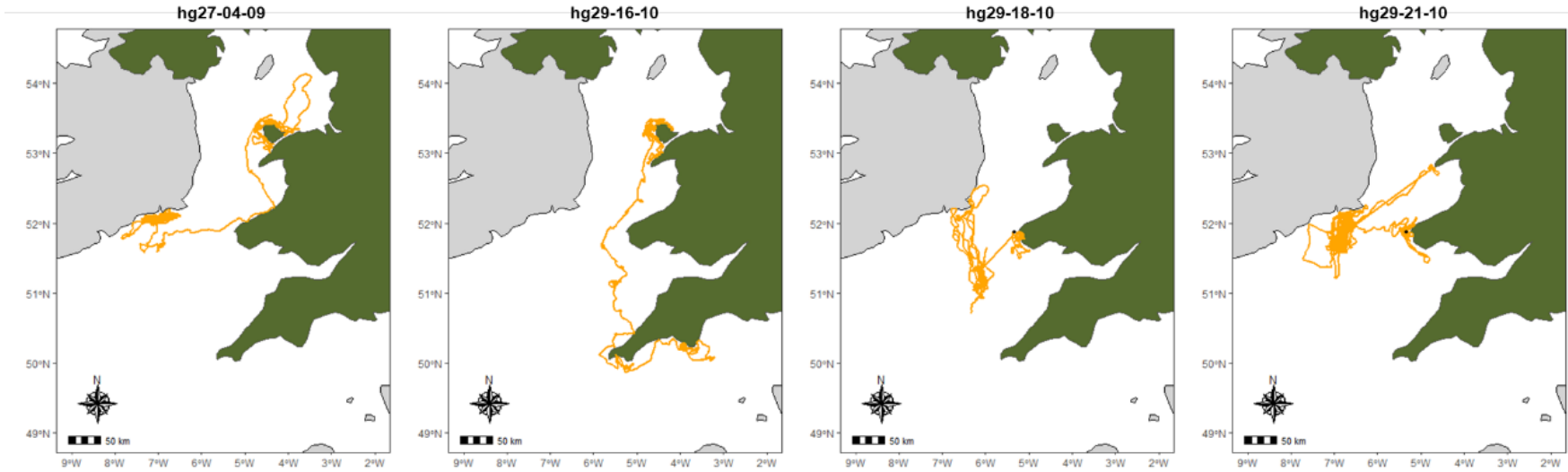


Fig. S3.3.1. Movement trajectories of pups classified as dispersers. White dot = Skerries tagging site; black dot = Ramsey.

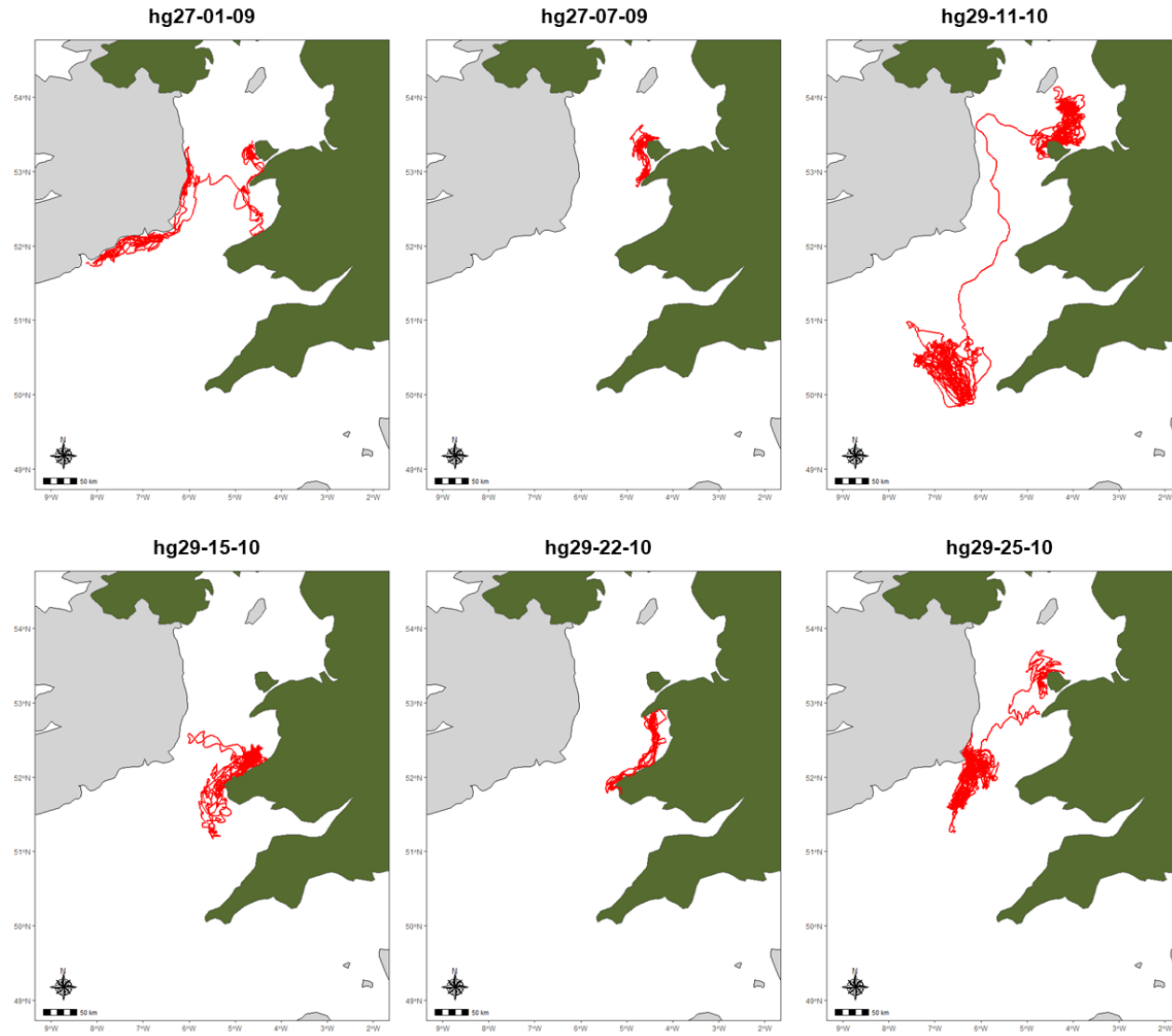


Fig. S3.3.2. Movement trajectories of pups classified as returners. White dot = Skerries tagging site; black dot = Ramsey.

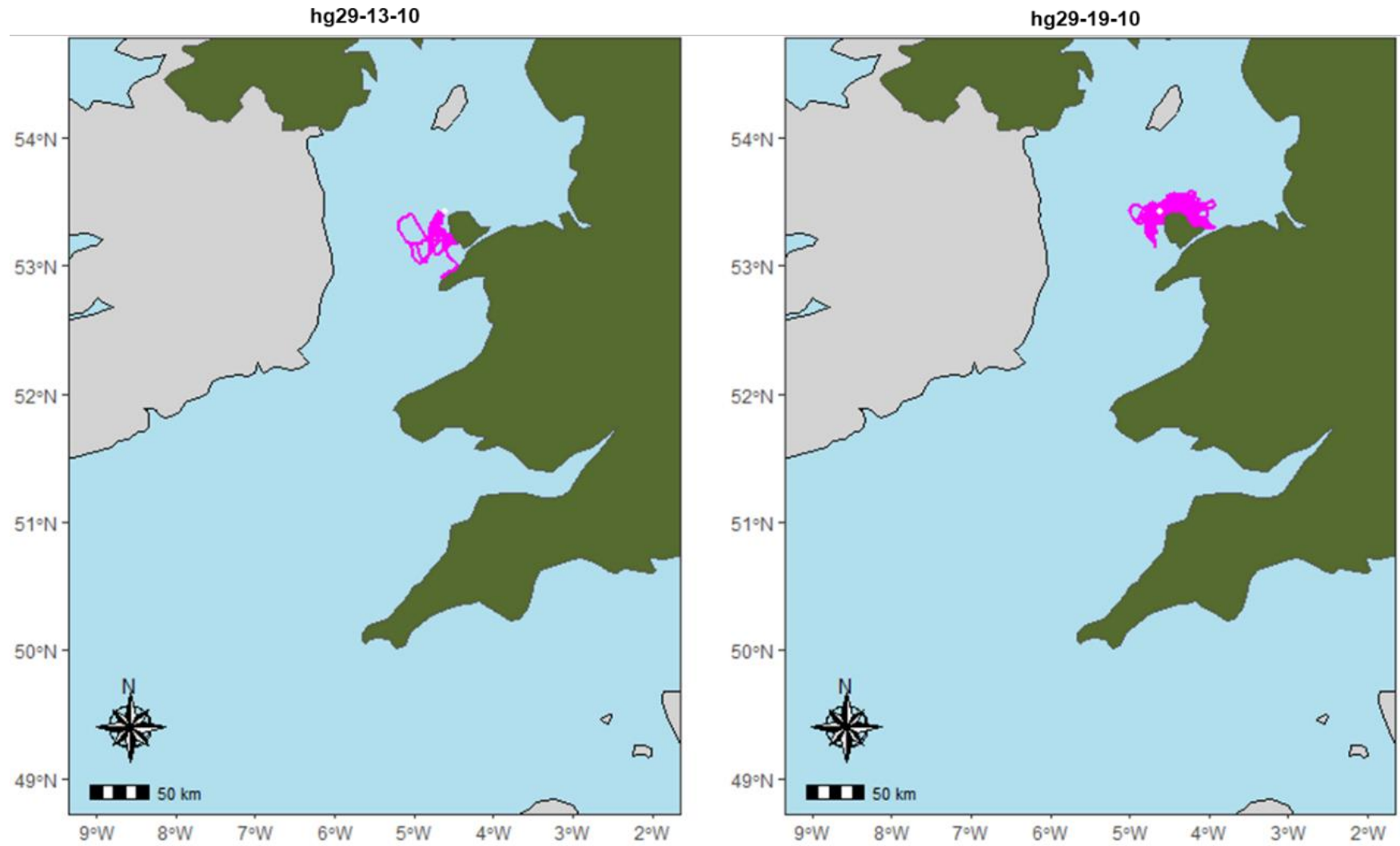


Fig. S3.3.3. Movement trajectories of pups classified as diffusive. White dot = Skerries tagging site.

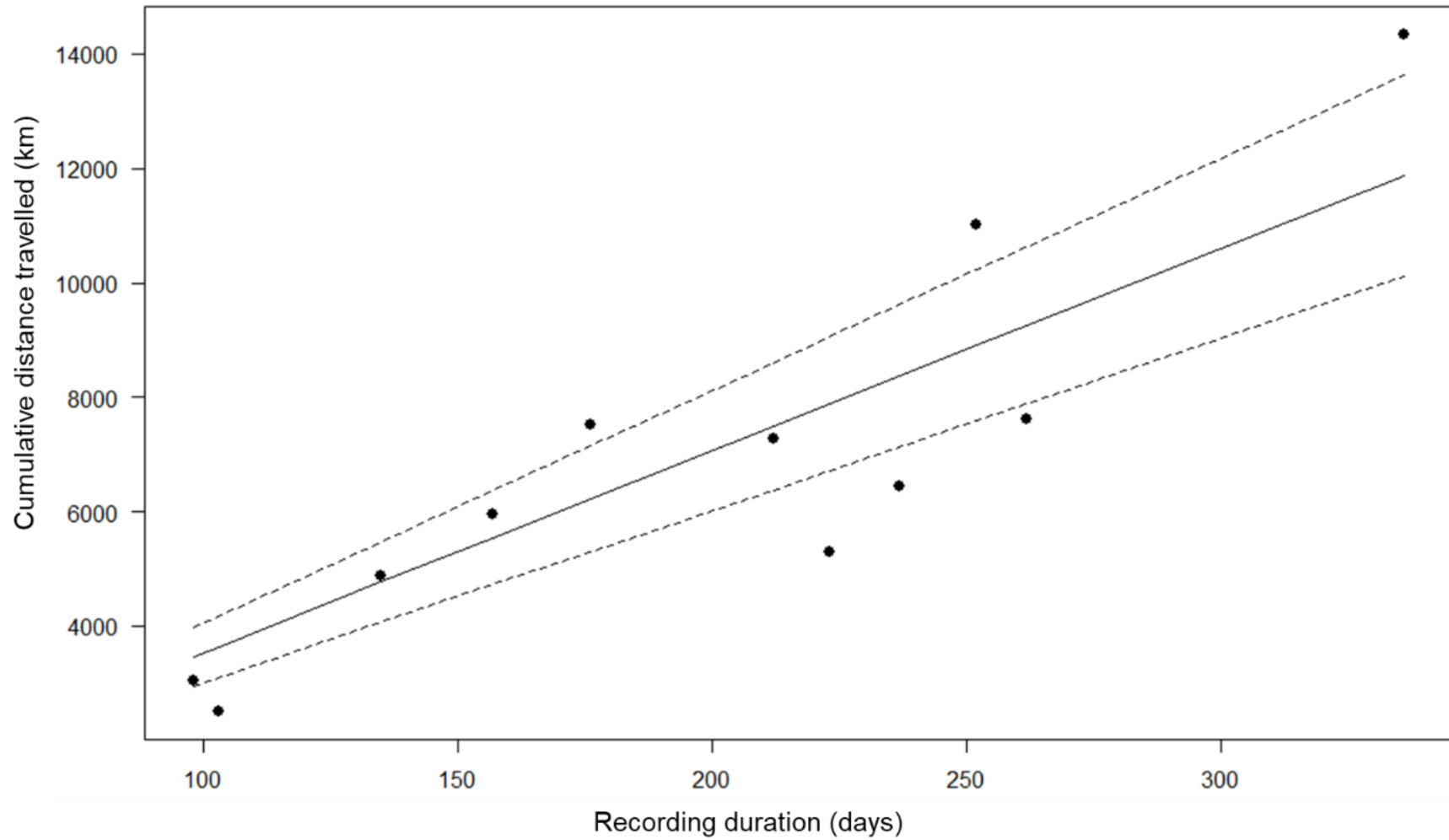


Fig. S3.3.4. Cumulative distance travelled by each individual as a function of their recording duration. Note that cumulative distance does not equal displacement distance but rather the total distance swum through the water during the full trajectory. Model fit from linear model shown (\pm 95 % CI); intercept constrained to zero. Cumulative distance increased by 35.4 km per day (95 % CI: 30.1 – 40.6 km; $t_{(10)} = 15.03$, $p < 0.01$; $R^2 = 0.96$).

Appendix S3.4: Individual-level model fits

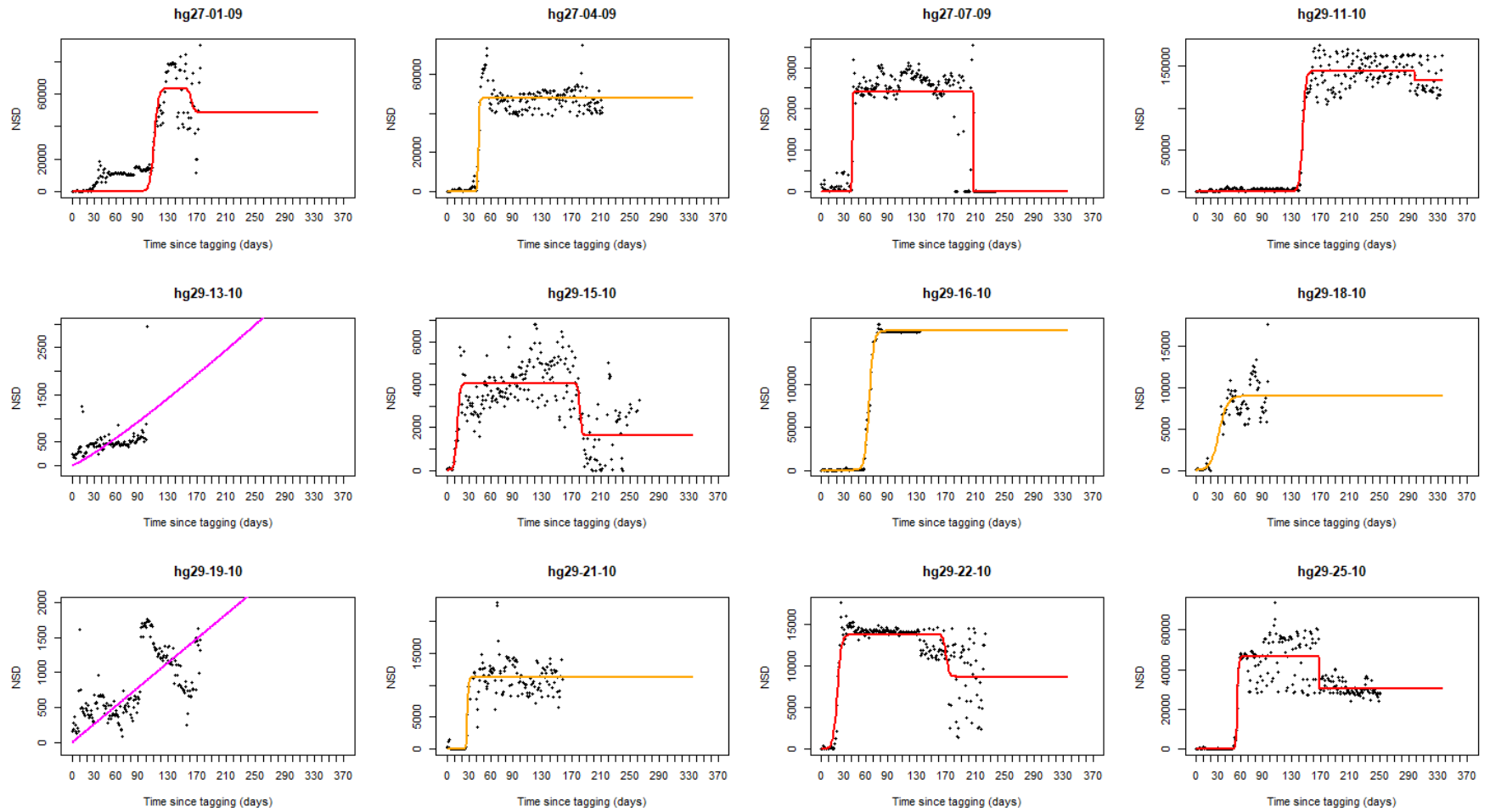


Fig. S3.4.1. Empirical data and model fits for best fitting movement models for each individual (orange = dispersal, red = return, magenta = diffusive).

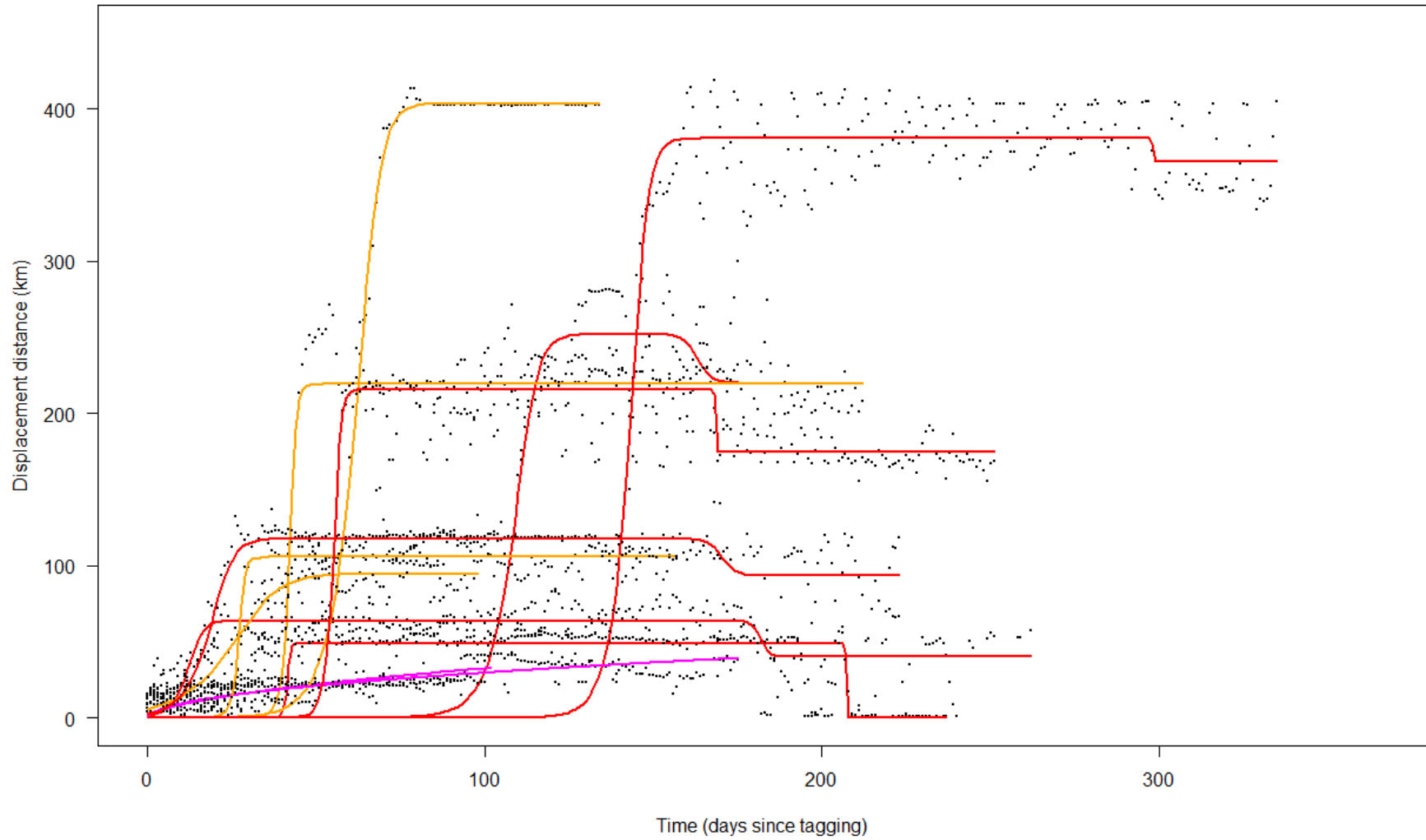


Fig. S3.4.2. Empirical data and model fits for best fitting movement models for each individual (orange = dispersal, red = return, magenta = diffusive). All models shown together on same plot for comparison of scales and recording duration.

Appendix S3.5: Parameter estimates from fitted displacement models

Table S3.5.1 Estimates from fitted displacement models. Both the individual-level models studied here, and the population-level models (Chapter 2) are shown (separated by $\phi_1 - \phi_8$). For details of $\phi_1 - \phi_8$ refer to S3.2. “dsb” = days since birth, NPF = North Pembrokeshire Females, NPM = North Pembrokeshire Males, RF = Ramsey Females, RM = Ramsey Males, SF = Skomer Females, SM = Skomer Males.

ID	Movement mode	Sex	Site	CC	Day 18 (km)	Day 30 (km)	Day 60 (km)	Day 90 (km)	>1km (dsb)	ϕ_1 (km)	ϕ_2 (dsb)	ϕ_3 (days)	ϕ_4 (dsb)	ϕ_5 (dsb)	ϕ_6 (km)	ϕ_7 (days)	ϕ_8 (kmh)	Recording duration (days)
hg27-01-09	Mixed-return	M	SK	0.90	0.0	0.0	0.0	0.2	98	252	129.8	2.8	122	139	239.7	17	0.6	175
hg27-04-09	Dispersal	M	SK	0.96	0.0	0.0	99.8	219.1	52	219.1	61.1	0.8	59	64	208.5	5	1.7	212
hg27-07-09	Return	F	SK	0.85	0.0	0.0	27.0	51.5	56	49.1	60	0.4	59	62	46.8	3	0.6	237
hg29-11-10	Mixed-return	M	SK	0.98	0.0	0.0	0.0	0.0	137	380.6	163.4	2.2	157	171	362.1	14	1.1	336
hg29-13-10	Diffusive	F	SK	0.40	0.0	9.7	24.2	30.5	18	32.6	NA	NA	NA	NA	32.6	102	0.1	103
hg29-15-10	Mixed-return	F	R	0.72	1.4	31.5	63.8	63.8	17	63.8	32.1	1.9	27	38	60.7	11	0.2	262
hg29-16-10	Dispersal	F	SK	1.00	0.0	0.1	8.2	385.6	47	403.7	83.1	3	75	92	384	17	0.9	135
hg29-18-10	Dispersal	M	R	0.87	5.9	16.9	88.5	94.5	17	94.5	49.1	5.6	33	66	90	33	0.1	98
hg29-19-10	Diffusive	F	SK	0.58	0.0	10.3	22.9	28.1	18	39	NA	NA	NA	NA	39	175	0.1	176
hg29-21-10	Dispersal	M	R	0.87	0.0	0.0	105.9	105.9	38	105.9	46	0.8	44	49	100.7	5	0.8	157
hg29-22-10	Mixed-return	F	R	0.86	2.5	21.1	117.5	117.6	17	117.6	39.6	2.8	32	49	111.8	17	0.3	223
hg29-25-10	Mixed-return	F	SK	0.84	0.0	0.0	0.1	215.6	63	215.6	74.2	1	72	78	205.1	6	1.4	252
Average	NA	NA	NA	0.8	0.8	7.5	46.5	109.4	48.2	164.5	73.8	2.1	68.0	80.8	156.8	33.8	0.6	197.2
SD	NA	NA	NA	0.2	1.8	10.7	45.6	113.7	37.5	129.4	42.0	1.5	42.0	42.6	122.8	52.0	0.6	70.1
NPF	Diffusive	F	N	0.99	0.0	4.7	25.5	68.1	16.0	444.9	NA	NA	NA	NA	444.9	196.0	0.09	196
NPM	Return	M	N	0.83	0.0	4.6	166.5	216.8	21.0	220.1	53.1	6.1	35.0	72.0	199.0	37.0	0.22	246
RF	Return	F	R	0.72	0.0	69.7	163.2	163.2	26.0	163.2	30.4	0.8	28.0	33.0	148.0	5.0	1.23	317
RM	Dispersal	M	R	0.52	0.0	0.0	1.5	225.1	38.0	262.4	82.3	4.3	70.0	96.0	237.0	26.0	0.38	313
SF	Dispersal	F	S	0.51	0.0	127.1	127.1	127.1	27.0	127.1	26.0	0.0	26.0	27.0	115.0	1.0	4.79	125
SM	Dispersal	M	S	0.68	0.0	0.0	140.2	140.2	39.0	140.2	41.4	0.7	40.0	44.0	127.0	4.0	1.32	162
Average	NA	NA	NA	0.71	0.0	34.4	104.0	156.8	27.8	226.3	46.6	2.4	39.8	54.4	211.8	44.8	1.34	226.5
SD	NA	NA	NA	0.18	0.0	48.2	65.7	58.9	9.2	118.6	22.5	2.7	17.8	29.0	123.1	75.4	1.77	79.3

Table S3.5.2 Estimates of “downward” sigmoid from fitted displacement models (for return and mixed-return models only). Both the individual-level models studied here, and the population-level models (Chapter 3), are shown (separated by ~~rows~~). For details of $\phi_9 - \phi_{17}$ refer to Appendix S3.2. NPM = North Pembrokeshire Males, RF = Ramsey Females.

ID	Movement mode	Sex	Site	CC	ϕ_9 (km)	ϕ_{10} (dsb)	ϕ_{11} (days)	ϕ_{12} (dsb)	ϕ_{13} (dsb)	ϕ_{14} (dsb)	ϕ_{15} (dsb)	ϕ_{16} (dsb)	ϕ_{17} (dsb)	ϕ_{18} (days)	Recording duration (days)
hg27-01-09	Mixed-return	M	SK	0.90	252	180.9	2.1	175	188	239.7	13	0.8	220.2	53	175
hg27-07-09	Return	F	SK	0.85	49.1	225.1	0.1	225	226	46.8	1	1.9	0	166	237
hg29-11-10	Mixed-return	M	SK	0.98	380.6	316.1	0.1	316	317	362.1	1	15.1	365.6	159	336
hg29-15-10	Mixed-return	F	R	0.72	49.5	199.6	1.3	196	204	47.1	8	0.2	40.2	169	262
hg29-22-10	Mixed-return	F	R	0.86	71.5	188.2	2.1	182	195	68	13	0.2	93.3	150	223
hg29-25-10	Mixed-return	F	SK	0.84	126.1	186.1	0.1	186	187	120	1	5	174.9	114	252
Average	NA	NA	NA	0.86	154.8	216	0.9	213.3	219.5	147.3	6.2	3.9	149	135.2	274.5
SD	NA	NA	NA	0.09	134.5	51.5	1	53.2	49.9	128	5.9	5.8	134	44.9	53.0
NPM	Return	M	N	0.83	220.1	175.0	19.5	117	234	199.0	117	0.07	0.0	82	246
RF	Return	F	R	0.72	163.2	127.2	1.3	124	132	148.0	8	0.77	0.0	96	317
Average	NA	NA	NA	0.78	191.7	151.1	10.4	120.5	183.0	173.5	62.5	0.42	0.0	89	281.5
SD	NA	NA	NA	0.08	28.4	23.9	9.1	3.5	51.0	25.5	54.5	0.35	0.0	9.9	50.2

Appendix S3.6: Additional comparisons between models of different data types

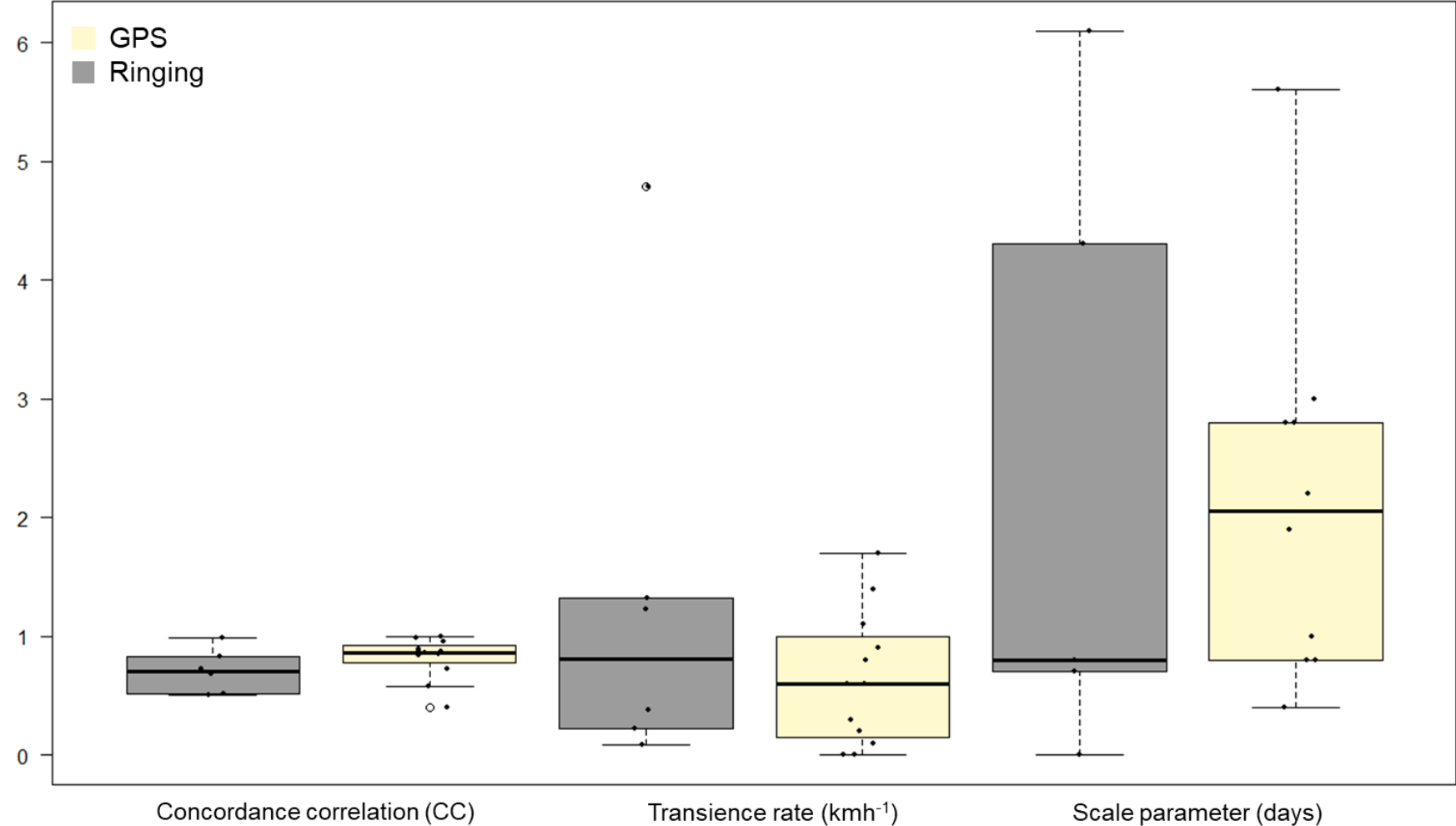


Fig. S3.6. Distribution of model statistics and parameter estimates derived from models fitted to population-level (“Ringing”; $n = 6$) and individual-level (“GPS”; $n = 12$) data. Black dots show (jittered) data points.

Appendix S3.7: CC values of displacement models and model rule violations

Table S3.7.1. Concordance Correlation (CC) coefficient values (3 sig. fig.) for each of the displacement models fitted to the 12 individuals (mixed models). The number after each model specifies the number of parameters included as random-effects. The model with the highest CC value is in **bold**. The final model chosen for each individual is in **red**. Models with greater CC than the respective final chosen model for each individual but which violated model fitting rules (see Appendix S3.1) are indicated with an asterisk. Refer to Table S3.7.2 for models fit at the individual level.

Model	hg27-01-09	hg27-04-09	hg27-07-09	hg29-11-10	hg29-13-10	hg29-15-10	hg29-16-10	hg29-18-10	hg29-19-10	hg29-21-10	hg29-22-10	hg29-25-10
NullMod	0.000	0.000	0.000	0.000	0.000	0.000	0.000	0.000	0.000	0.000	0.000	0.000
Linear	0.734	0.625	-0.036	0.803	0.392	-0.088	0.831	0.803	0.581	0.560	0.013	0.391
PowerC	0.762	0.591	-0.065	0.816	0.396	-0.108	0.853	0.791	0.571	0.526	-0.016	0.358
PowerC2	0.807	0.390	-0.172	0.760	0.128	-0.178	0.807	0.640	0.263	0.356	-0.084	0.185
DispMod1	0.814	0.499	-0.080	0.877	0.423*	-0.124	0.832	0.701	0.513	0.380	-0.070	0.331
DispMod2	0.888	0.946	0.477	0.982	0.240	0.321	0.998	0.872	0.373	0.861	0.702	0.830
DispMod3	0.892	0.956	0.488	0.982	0.232	0.343	0.999	0.869	0.374	0.868	0.724	0.839
SedMod1	0.472	0.362	-0.002	0.285	0.011	-0.007	0.097	0.581	0.015	0.340	0.009	0.377
SedMod2	0.140	0.114	0.030	0.087	0.007	0.048	0.043	0.644	0.012	0.652	0.493	0.124
ReturnMod1	0.811	0.485	-0.098	0.886	0.424*	-0.136	0.828	0.702	0.504	0.377	-0.079	0.308
ReturnMod2	0.888	0.945	0.486	0.982	0.247	0.316	0.999	0.873*	0.692*	0.860	0.699	0.836
ReturnMod3	0.435	0.698	0.174	0.528	-0.116	0.135	0.914	0.597	0.091	0.471	0.087	0.739
ReturnMod4	0.893	0.957*	0.798	0.983	0.216	0.576	0.999*	0.867	0.276	0.870*	0.873*	0.905
MixReturn1	0.778	0.597	0.288	0.874	-0.007	0.320	0.845	0.665	0.003	0.706	0.417	0.494
MixReturn2	0.665	0.698	0.597	0.982	0.250	0.396	0.993	0.541	0.600*	0.543	0.324	0.856
MixReturn3	0.897	0.944	0.791	0.982	0.242	0.668	0.999	0.873*	0.424	0.860	0.859	0.913
MixReturn4	0.682	0.740	0.509	0.982	0.207	0.479	-0.039	0.731	0.559*	0.580	0.499	0.851
MixReturn5	0.910*	0.956	0.337	0.982	0.197	0.253	0.999	0.805	0.345	0.862	0.725	0.904
HighestCC	MixReturn5	ReturnMod4	ReturnMod4	ReturnMod4	ReturnMod1	MixReturn3	ReturnMod4	ReturnMod2	ReturnMod2	ReturnMod4	ReturnMod4	MixReturn3
ChosenMod	MixReturn3	NA	NA	NA	PowerC	NA	NA	NA	Linear	NA	MixReturn3	NA

Table S3.7.2. Concordance Correlation (CC) coefficient values (3 sig. fig.) for each of the displacement models fitted to the 12 individuals (individual models). The model with the highest CC value is in **bold**. The final model chosen for each individual is in **red**; this is the model with the highest CC value and one that did not violate the rules for model fits (see Appendix S3.1). DNC = Did Not Converge. Refer to Table S3.7.1 for mixed model equivalents.

Model	hg27-01-09	hg27-04-09	hg27-07-09	hg29-11-10	hg29-13-10	hg29-15-10	hg29-16-10	hg29-18-10	hg29-19-10	hg29-21-10	hg29-22-10	hg29-25-10
NullMod	0.000	0.000	0.000	0.000	0.000	0.000	0.000	0.000	0.000	0.000	0.000	0.000
Linear	0.734	0.625	-0.035	0.803	0.373	-0.088	0.831	0.802	0.572	0.559	0.013	0.391
PowerC	0.808	0.674	0.081	0.816	0.258	0.065	0.870	0.800	0.527	0.602	0.184	0.425
PowerCb	0.807	0.391	-0.101	0.760	0.369	-0.133	0.807	0.656	0.527	0.356	-0.082	0.185
DispMod	0.891	0.956	0.510	0.982	0.194	0.327	0.999	0.873	0.579	0.868	0.724	0.839
SedMod	0.273	0.756	0.269	0.767	0.189	0.247	0.602	0.817	0.559	0.703	0.496	0.565
ReturnMod	0.904*	0.958*	0.854	0.983	0.229	0.597	DNC	DNC	0.353	0.871*	0.877*	0.907
MixReturn	0.872	0.956	0.904*	0.984	0.184	0.723	0.999*	0.870	0.152	0.858	0.881*	0.921
HighestCC	ReturnMod	ReturnMod	MixReturn	MixReturn	Linear	MixReturn	MixReturn	DispMod	DispMod	ReturnMod	MixReturn	MixReturn
ChosenMod	NA	DispMod	ReturnMod	MixReturn	NA	MixReturn	DispMod	DispMod	NA	DispMod	NA	MixReturn

Table S3.7.3. Record of model fitting rule violations (see Appendix S3.1) for candidate models with greater CC values than the respective chosen model (see Tables S3.7.1 and S3.7.2).

Individual	Model	Description of model fitting rules violations
hg27-01-09	MixReturn5	Violated rule (iii); did not resemble the correct functional form of a mixed-return model (consisted of two positive sigmoid curves).
	ReturnMod	Violated rules (iii) and (i); did not resemble the correction functional form of a return model (did not include an extended period of settlement); model not complete within the temporal range of the empirical data.
hg27-04-09	ReturnMod4	Violated rules (i) and (iv); model not complete within the temporal range of the empirical data; minimum value negative.
	ReturnMod	Violated rules (i) and (iv); model not complete within the temporal range of the empirical data; minimum value negative.
hg27-07-09	MixReturn	Violated rule (iv); minimum value negative.
hg29-11-10	NA	NA
hg29-13-10	ReturnMod1	Violated rule (i); model not complete within the temporal range of the empirical data.
	DispMod1	Violated rule (i); model not complete within the temporal range of the empirical data.
hg29-15-10	NA	NA
hg29-16-10	ReturnMod4	Violated rule (i); model not complete within the temporal range of the empirical data.
	MixReturn	Violated rule (i); model not complete within the temporal range of the empirical data.
hg29-18-10	ReturnMod2	Violated rule (i); model not complete within the temporal range of the empirical data.
	MixReturn3	Violated rule (i); model not complete within the temporal range of the empirical data.
hg29-19-10	ReturnMod2	Violated rule (i); model not complete within the temporal range of the empirical data.
	MixReturn2	Violated rule (v); model is does not clearly represent the pattern of the empirical data - the animal is moving around a lot without a consistent pattern (i.e., transience).
	MixReturn4	Violated rule (v); model is does not clearly represent the pattern of the empirical data - the animal is moving around a lot without a consistent pattern (i.e., transience).
hg29-21-10	ReturnMod4	Violated rule (i); model not complete within the temporal range of the empirical data.
	ReturnMod	Violated rule (i); model not complete within the temporal range of the empirical data.
hg29-22-10	ReturnMod4	Violated rule (i); model not complete within the temporal range of the empirical data.
	ReturnMod	Violated rule (iv); minimum value negative.
	MixReturn	Violated rule (iv); minimum value negative.
hg29-25-10	NA	NA

Appendix S3.8: Maximum displacement versus recording duration

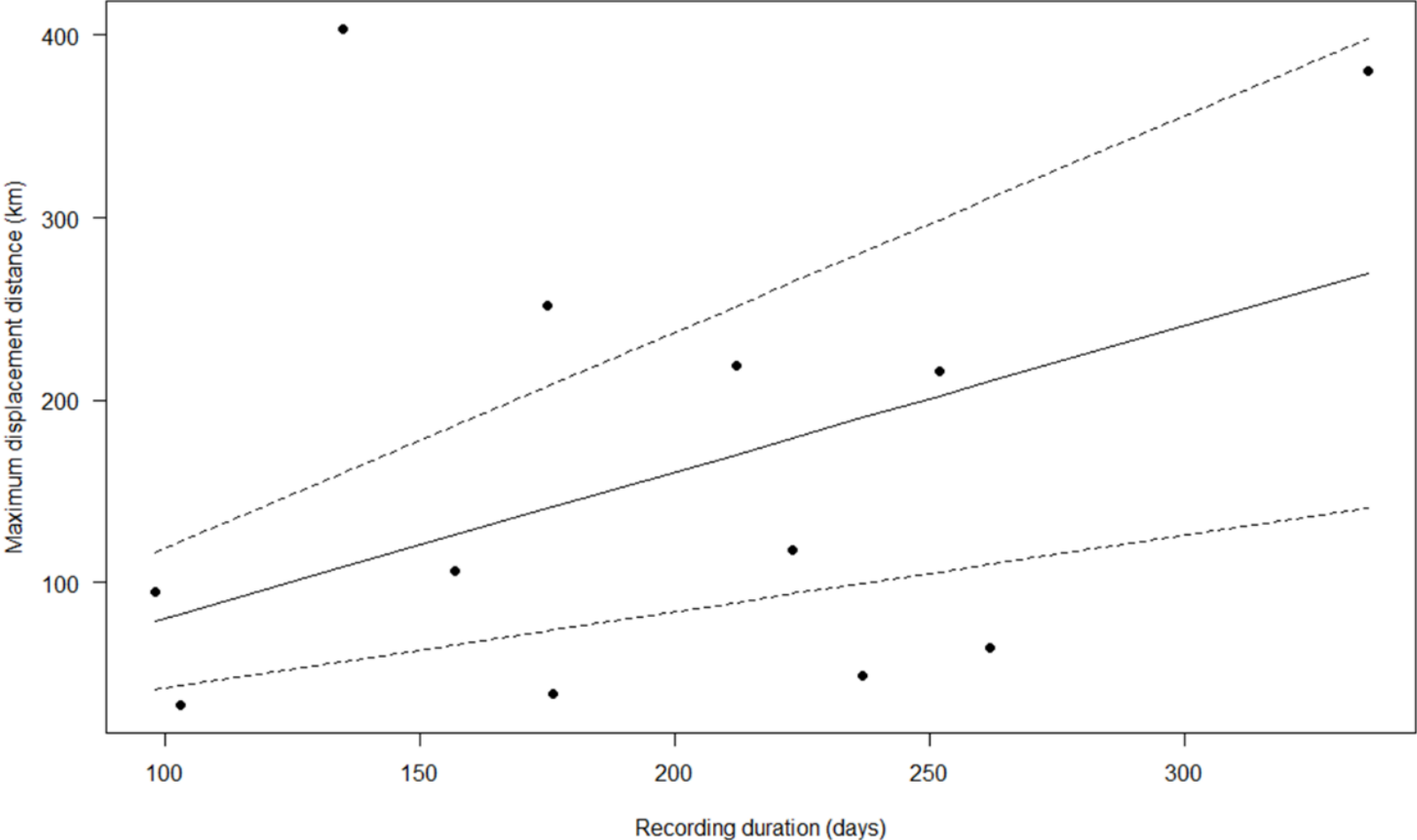


Fig. S3.8. Maximum displacement distance reached by each individual as a function of their recording duration. Model fit from linear model shown (\pm 95 % CI); intercept constrained to zero. Maximum displacement distance increased by 0.8 km per day (95 % CI: 0.42 - 1.19 km; $t_{(11)} = 4.62$, $p < 0.01$; $R^2 = 0.66$).

Appendix IV: Supplementary material for Chapter 4

Contents

Appendix S4.1: Details of 6 individuals excluded from analysis

Appendix S4.2: Vector component calculations

Appendix S4.3: Individual differences in observed movement variables

Appendix S4.4: Details of HMMs considered

Appendix S4.5: Pseudo-residual plots of final HMM

Appendix S4.6: Seal area usage trajectories

Appendix S4.7: State-dependent distribution parameter estimates

Appendix S4.8: Regression coefficients for state-dependent parameter estimates

Appendix S4.9: Regression coefficients for stationary state probabilities

Appendix S4.10: Regression coefficients for transition probabilities

Appendix S4.11: Examples of foraging trips with apparent drift whilst resting

Appendix S4.1: Details of 6 individuals excluded from analysis

Table S4.1. Tagging details of the 6 individuals excluded from the analyses (cf. Table 7.1; main text).

Individual	Sex	Site	Age	Tag date	Number of trips	Average trip duration (days; mean \pm SD)
HE04.06.-1	M	Helgoland, Germany (HE)	Adult	10/04/2006	15	0.60 \pm 0.20
HE04.06.-8	M	Helgoland, Germany (HE)	Adult	10/04/2006	3	0.66 \pm 0.35
HE09.05.-3	M	Helgoland, Germany (HE)	Adult	27/09/2005	1	0.24 \pm 0
LP04.06.-3	F	Lorenzensplate, Germany (LP)	Adult	19/04/2006	1	0.82 \pm 0
LP10.05.-1	M	Lorenzensplate, Germany (LP)	Adult	12/10/2005	1	0.51 \pm 0
LP10.05.-5	M	Lorenzensplate, Germany (LP)	Adult	12/10/2005	1	0.32 \pm 0

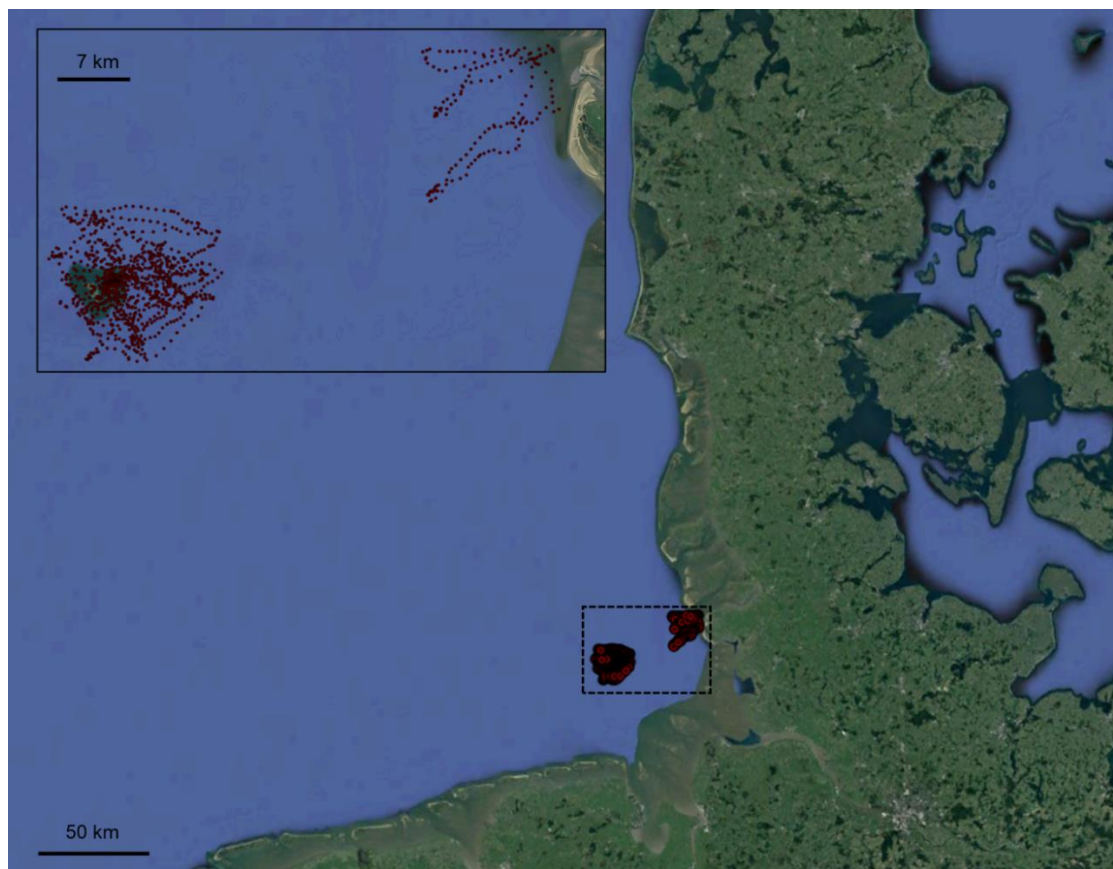


Fig S4.1. Trajectories of the 6 individuals excluded from the analyses showing area usage.

Appendix S4.2: Vector component calculations

When tracking marine animals swimming through the water the trajectories observed are manifestations of the combination of the animal's swimming motion and the effect of ocean currents (Gaspar et al., 2006). To understand how seals responded to currents, I was interested in modelling the seals' voluntary swim vectors – rather than their resultant movement vectors – against tide vectors. Hence, using the observed ground speed vector (V_g) and known tide speed vector (V_t), I calculated each animal's voluntary swim speed vector (V_s) for each step along their trajectories, as follows:

$$V_s = \sqrt{V_g^2 + V_t^2 + 2V_gV_t \cos \theta_1} \quad \text{Eqn. 7.1}$$

where θ_1 is the relative angle between V_g and V_t (Fig. S4.2). I calculated the relative angle between V_t and V_s as follows:

$$\theta_2 = \frac{\arccos(V_s^2 + V_t^2 - V_g^2)}{\pi/180} \quad \text{Eqn. 7.2}$$

Finally, I calculated the head-current component (V_c) of the tidal vector using:

$$V_c = V_t \cos \theta_3 \quad \text{Eqn. 7.3}$$

Where positive values of V_c represented head-current and negative values represented tail-currents.

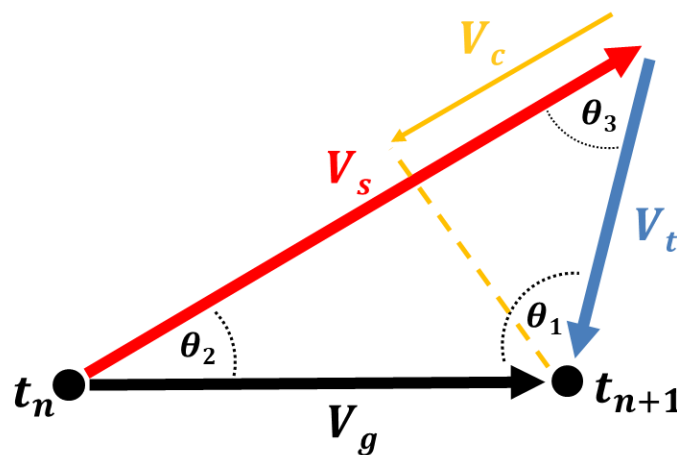


Fig. S4.2. Schematic of vector calculations between two consecutive positions on a trajectory, where V_g is the ground track speed vector, V_t is the tide speed vector, V_s is the seal swim speed vector, and V_c is the head-current component.

Appendix S4.3: Individual differences in observed movement variables

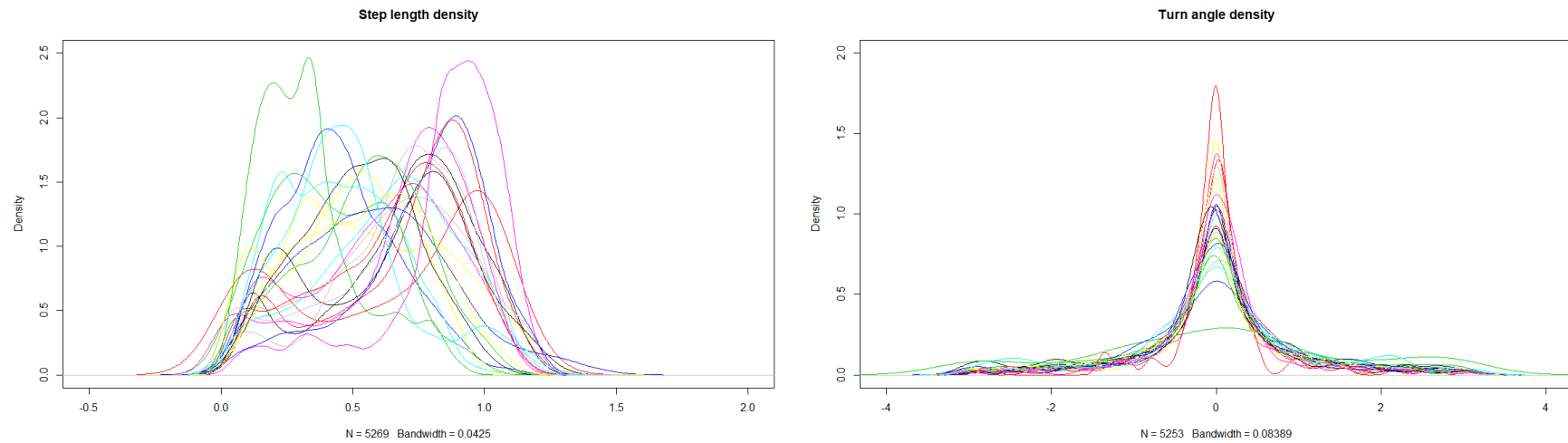


Fig. S4.3. Individual differences in step length and turn angle density. Each individual is individually coloured.

Appendix S4.4: Details of HMMs considered

Table S4.4. AIC scores and log-likelihood for the models considered examining covariate effects on transition probabilities and movement parameters with varying numbers of mixtures. The Δ AIC is the difference in AIC score for each model compared to the model represented in row 1. The model in row 1 has only two states (an ARS state and a directional state). ^(S)i indicates covariate values randomly shuffled. HC = head-current component (V_c)

Covariate effects on transition probabilities	Covariate effects on movement parameters	log L	K	AIC	Δ AIC
~1	~1	9115.5	1	-18205.0	0
~1	~1	23653.5	1	-47261.0	-29056
~HC	~1	23684.7	1	-47311.4	-29106.4
~sex	~1	23719.8	1	-47381.5	-29176.5
~site	~1	23831.1	1	-47592.3	-29387.3
~tState	~1	23669	1	-47268.0	-29063
~HC*sex	~1	23767.1	1	-47452.2	-29247.2
~HC*site	~1	23900.3	1	-47694.6	-29489.6
~tState*sex	~1	23740.3	1	-47374.7	-29169.7
~tState*site	~1	23861.4	1	-47580.8	-29375.8
~HC:sex:site	SL μ = ~HC:sex:site SL σ = ~1 TA μ = ~1 TA γ = ~HC:sex:site	25415.6	3	-50461.3	-32256.3
~HC+sex+site+age	SL μ = ~HC+sex+site+age SL σ = ~HC TA μ = ~1 TA γ = ~HC+sex+site+age	26832.1	1	-53492.3	-35287.3
~HC+sex+site+age+HC:sex	SL μ = ~HC+sex+site+age+HC:sex SL σ = ~HC	26872.6	1	-53549.2	-35344.2

Covariate effects on transition probabilities	Covariate effects on movement parameters	log L	K	AIC	Δ AIC
	TA $\mu = \sim 1$ TA $\gamma = \sim \text{HC} + \text{sex} + \text{site} + \text{age} + \text{HC} : \text{sex}$				
$\sim \text{HC} + \text{sex} + \text{site} + \text{age} + \text{HC} : \text{site}$	SL $\mu = \sim \text{HC} + \text{sex} + \text{site} + \text{age} + \text{HC} : \text{site}$ SL $\sigma = \sim \text{HC}$ TA $\mu = \sim 1$ TA $\gamma = \sim \text{HC} + \text{sex} + \text{site} + \text{age} + \text{HC} : \text{site}$	26901.7	1	-53583.4	-35378.4
$\sim \text{HC} + \text{sex} + \text{site} + \text{age} + \text{HC} : \text{age}$	SL $\mu = \sim \text{HC} + \text{sex} + \text{site} + \text{age} + \text{HC} : \text{age}$ SL $\sigma = \sim \text{HC}$ TA $\mu = \sim 1$ TA $\gamma = \sim \text{HC} + \text{sex} + \text{site} + \text{age} + \text{HC} : \text{age}$	26869.9	1	-53543.8	-35338.8
$\sim \text{HC} + \text{sex} + \text{site} + \text{age} + \text{HC} : \text{sex} + \text{HC} : \text{site}$	SL $\mu = \sim \text{HC} + \text{sex} + \text{site} + \text{age} + \text{HC} : \text{sex} + \text{HC} : \text{site}$ SL $\sigma = \sim \text{HC}$ TA $\mu = \sim 1$ TA $\gamma = \sim \text{HC} + \text{sex} + \text{site} + \text{age} + \text{HC} : \text{sex} + \text{HC} : \text{site}$	26934.2	1	-53624.5	-35419.5
$\sim \text{HC} + \text{sex} + \text{site} + \text{age} + \text{HC} : \text{sex} + \text{HC} : \text{age}$	SL $\mu = \sim \text{HC} + \text{sex} + \text{site} + \text{age} + \text{HC} : \text{sex} + \text{HC} : \text{age}$ SL $\sigma = \sim \text{HC}$ TA $\mu = \sim 1$ TA $\gamma = \sim \text{HC} + \text{sex} + \text{site} + \text{age} + \text{HC} : \text{sex} + \text{HC} : \text{age}$	26909.7	1	-53599.4	-35394.4
$\sim \text{HC} + \text{sex} + \text{site} + \text{age} + \text{HC} : \text{site} + \text{HC} : \text{age}$	SL $\mu = \sim \text{HC} + \text{sex} + \text{site} + \text{age} + \text{HC} : \text{site} + \text{HC} : \text{age}$ SL $\sigma = \sim \text{HC}$ TA $\mu = \sim 1$ TA $\gamma = \sim \text{HC} + \text{sex} + \text{site} + \text{age} + \text{HC} : \text{site} + \text{HC} : \text{age}$	26927.3	1	-53610.5	-35405.5
$\sim \text{HC} + \text{sex} + \text{site} + \text{age} + \text{HC} : \text{sex} + \text{HC} : \text{site} + \text{HC} : \text{age}$	SL $\mu = \sim \text{HC} + \text{sex} + \text{site} + \text{age} + \text{HC} : \text{sex} + \text{HC} : \text{site} + \text{HC} : \text{age}$ SL $\sigma = \sim \text{HC}$ TA $\mu = \sim 1$ TA $\gamma = \sim \text{HC} + \text{sex} + \text{site} + \text{age} + \text{HC} : \text{sex} + \text{HC} : \text{site} + \text{HC} : \text{age}$	26960.2	1	-53652.3	-35447.3
$\sim \text{HC} + \text{sex} + \text{site} + \text{age} + \text{HC} : \text{sex} + \text{HC} : \text{site} + \text{HC} : \text{age}$	SL $\mu = \sim \text{HC} + \text{sex} + \text{site} + \text{age} + \text{HC} : \text{sex} + \text{HC} : \text{site} + \text{HC} : \text{age}$ SL $\sigma = \sim \text{HC}$ TA $\mu = \sim 1$ TA $\gamma = \sim \text{HC} + \text{sex} + \text{site} + \text{age} + \text{HC} : \text{sex} + \text{HC} : \text{site} + \text{HC} : \text{age}$	27328.1	2	-54262.1	-36057.1
$\sim \text{HC} + \text{sex} + \text{site} + \text{age} + \text{HC} : \text{sex} + \text{HC} : \text{site} + \text{HC} : \text{age}$	SL $\mu = \sim \text{HC} + \text{sex} + \text{site} + \text{age} + \text{HC} : \text{sex} + \text{HC} : \text{site} + \text{HC} : \text{age}$ SL $\sigma = \sim \text{HC}$ TA $\mu = \sim 1$ TA $\gamma = \sim \text{HC} + \text{sex} + \text{site} + \text{age} + \text{HC} : \text{sex} + \text{HC} : \text{site} + \text{HC} : \text{age}$	27452.3	3	-54384.5	-36179.5

Covariate effects on transition probabilities	Covariate effects on movement parameters	log L	K	AIC	ΔAIC
	TA $\mu = \sim 1$ TA $\gamma = \sim \text{HC} + \text{sex} + \text{site} + \text{age} + \text{HC}:\text{sex} + \text{HC}:\text{site} + \text{HC}:\text{age}$				
$\sim \text{HC}^{(s)} + \text{sex} + \text{site} + \text{age} + \text{HC}^{(s)}:\text{sex} + \text{HC}^{(s)}:\text{site} + \text{HC}^{(s)}:\text{age}$	SL $\mu = \sim \text{HC}^{(s)} + \text{sex} + \text{site} + \text{age} + \text{HC}^{(s)}:\text{sex} + \text{HC}^{(s)}:\text{site} + \text{HC}^{(s)}:\text{age}$ SL $\sigma = \sim \text{HC}^{(s)}$ TA $\mu = \sim 1$ TA $\gamma = \sim \text{HC}^{(s)} + \text{sex} + \text{site} + \text{age} + \text{HC}^{(s)}:\text{sex} + \text{HC}^{(s)}:\text{site} + \text{HC}^{(s)}:\text{age}$	26847.6	3	-53175.3	-34970.3

Appendix S4.5: Pseudo-residual plots of final HMM

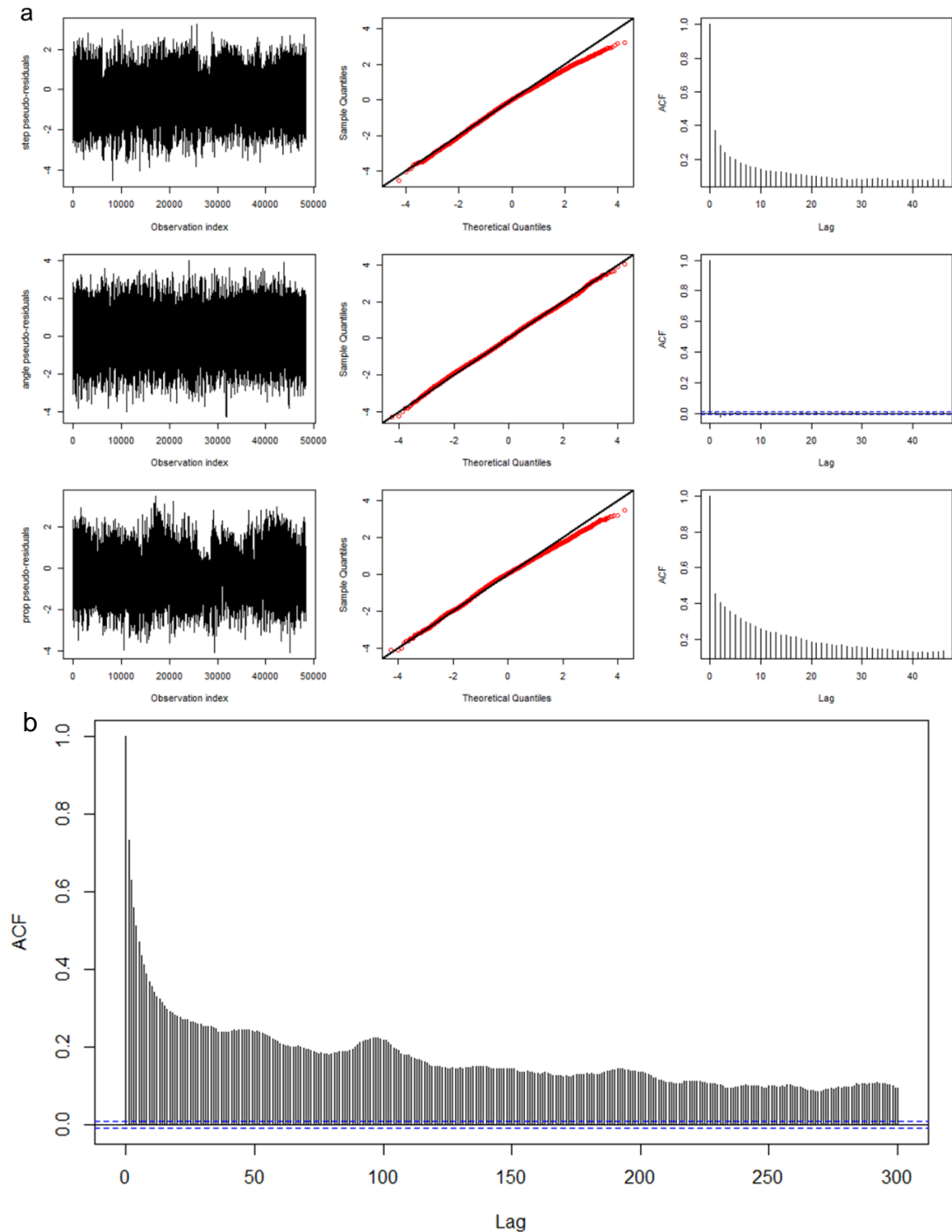


Fig S4.5. a) Pseudo-residual, quartile-quartile and autocorrelation function plots for step length (top row), turn angle (middle row), and dive proportion (bottom row) from the final model. b) ACF plot shown for step length with lag of 300, demonstrating autocorrelation pattern every c. 96 steps corresponding to 24 hours (15 min sampling frequency).

Appendix S4.6: Seal area usage trajectories

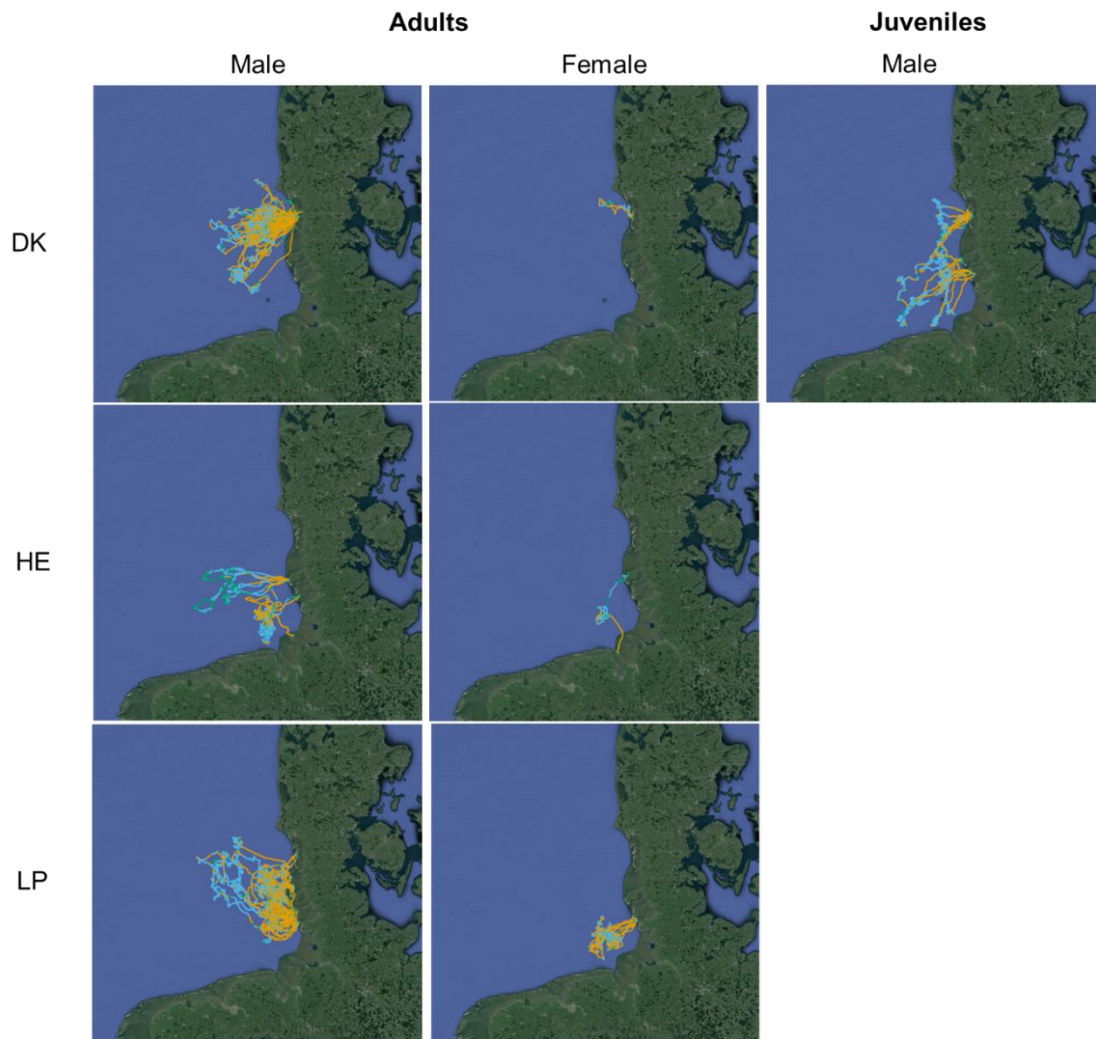


Fig. S4.6. Trajectories of all trips from all seals split by factorial groupings. Coloured by decoded behavioural state (travelling, foraging, and resting) from fitted HMM.

Appendix S4.7: State-dependent distribution parameter estimates

Table S4.7 State-dependent distribution parameter estimates (and 95 % confidence intervals) for final 3-state HMM. The mean turn angle parameter (μ) was constrained to zero (hence == 0) whereas all other parameters were estimated. Values are based on mean covariate values.

Variable	State 1 (<i>T</i>)	State 2 (<i>F</i>)	State 3 (<i>R</i>)
Step length	$\mu = 0.88$ (0.876, 0.885)	$\mu = 0.497$ (0.491, 0.504)	$\mu = 0.306$ (0.298, 0.314)
	$\sigma = 0.14$ (0.139, 0.142)	$\sigma = 0.206$ (0.203, 0.209)	$\sigma = 0.222$ (0.217, 0.228)
Directional persistence	$\mu == 0$	$\mu == 0$	$\mu == 0$
	$\gamma = 0.872$ (0.867, 0.876)	$\gamma = 0.474$ (0.458, 0.49)	$\gamma = 0.753$ (0.736, 0.77)
Dive prop.	$\alpha = 97.537$ (93.838, 101.235)	$\alpha = 66.081$ (64.266, 67.895)	$\alpha = 2.345$ (2.257, 2.432)
	$\beta = 15.716$ (15.187, 16.245)	$\beta = 14.654$ (14.275, 15.033)	$\beta = 1.942$ (1.865, 2.019)

Appendix S4.8: Regression coefficients for state-dependent parameter estimates

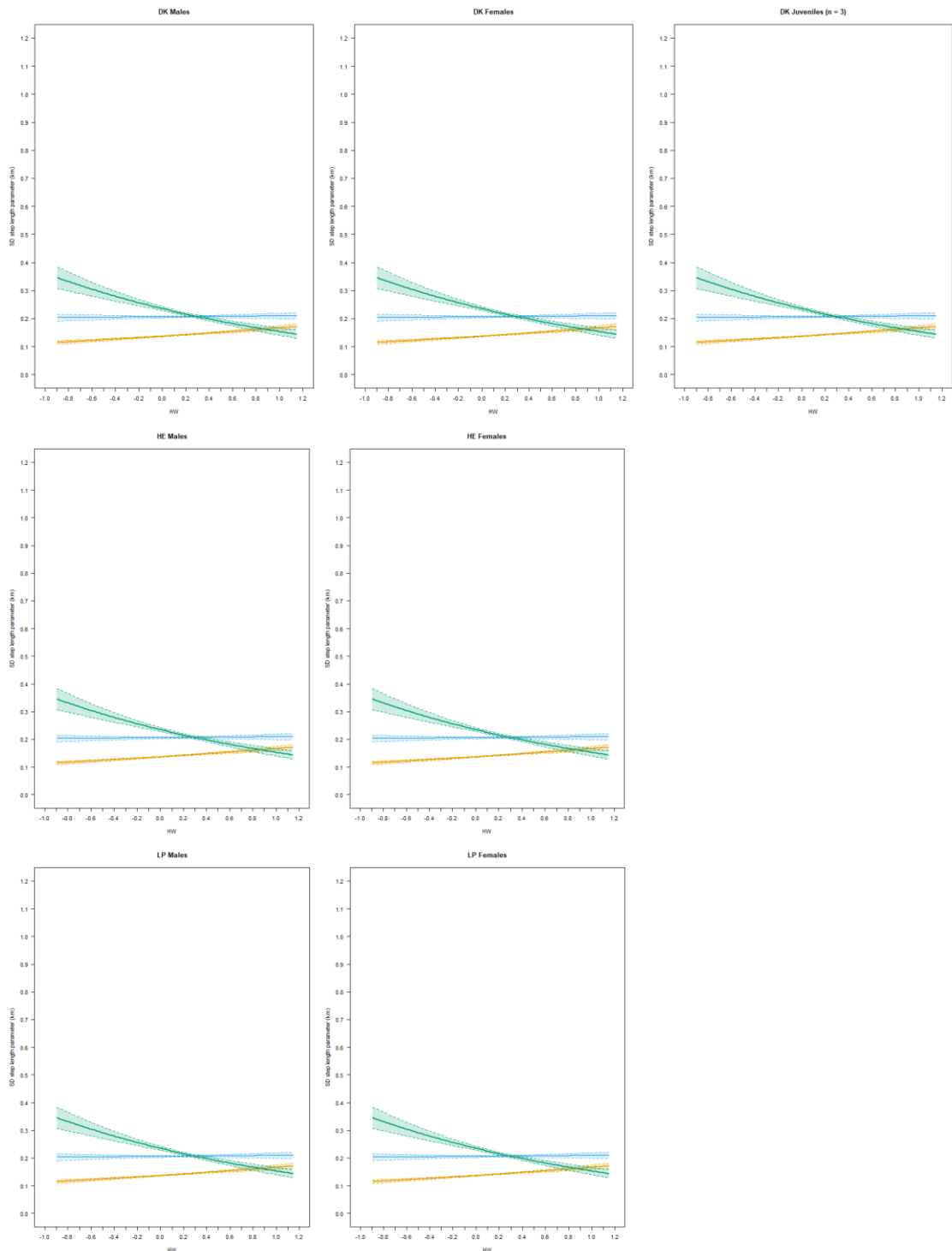


Fig. S4.8. Covariate effects on state dependent step length SD parameter. Coloured by decoded behavioural state (travelling, foraging, and resting). Solid lines show mean estimates with associated 95% CIs

Table S4.8.1. Regression coefficients for state-dependent step length distribution parameter estimates (and 95 % confidence intervals) for final 3-state HMM. Intercept refers to when HC = 0.13, sex = F, site = DK (Rømø, Denmark). *Confidence intervals encompassing zero; considered a relatively unimportant effect. HC = head-current component (V_c).

Variable	State 1 (<i>T</i>)	State 2 (<i>F</i>)	State 3 (<i>R</i>)
Step Length (μ):Intercept	-0.097 (-0.109, -0.085)	-0.589 (-0.62, -0.558)	-1.09 (-1.147, -1.033)
Step Length (μ):HC	-0.089 (-0.132, -0.046)	-0.118 (-0.215, -0.021)	-0.504 (-0.715, -0.293)
Step Length (μ):sexM	-0.02 (-0.031, -0.009)	-0.061 (-0.089, -0.033)	-0.005 (-0.053, 0.044)*
Step Length (μ):siteHE	-0.072 (-0.085, -0.059)	0.127 (0.105, 0.149)	0.069 (0.029, 0.109)
Step Length (μ):siteLP	-0.048 (-0.055, -0.041)	-0.013 (-0.03, 0.005)*	-0.132 (-0.174, -0.09)
Step Length (μ):agejuvenile	-0.221 (-0.233, -0.209)	-0.23 (-0.251, -0.209)	0.003 (-0.05, 0.056)*
Step Length (μ):HC:sexM	0.01 (-0.028, 0.048)*	-0.238 (-0.319, -0.158)	-0.162 (-0.334, 0.009)*
Step Length (μ):HC:siteHE	0.025 (-0.021, 0.071)*	0.152 (0.074, 0.231)	-0.284 (-0.44, -0.128)
Step Length (μ):HC:siteLP	0.008 (-0.021, 0.037)*	0.019 (-0.052, 0.091)*	0.028 (-0.132, 0.188)*
Step Length (μ):HC:agejuvenile	-0.141 (-0.19, -0.092)	0.028 (-0.05, 0.106)*	0.3 (0.129, 0.472)
Step Length (σ) Intercept	-1.989 (-2.004, -1.975)	-1.581 (-1.597, -1.566)	-1.447 (-1.477, -1.416)
Step Length (σ):HC	0.196 (0.143, 0.25)	0.016 (-0.04, 0.071)*	-0.429 (-0.53, -0.328)

Table S4.8.2. Regression coefficients for state-dependent turn angle distribution parameter estimates (and 95 % confidence intervals) for final 3-state HMM. Intercept refers to when HC = 0, sex = F, site = DK (Rømø, Denmark). * Confidence intervals encompassing zero. HC = head-current component (V_c).

Variable	State 1 (T)	State 2 (F)	State 3 (R)
TA Concentration (γ):Intercept	1.936 (1.836, 2.037)	-0.155 (-0.296, -0.014)	0.744 (0.502, 0.986)
TA Concentration (γ):HC	0.023 (-0.33, 0.377)*	-0.094 (-0.587, 0.399)*	0.508 (-0.297, 1.314)*
TA Concentration (γ):sexM	-0.004 (-0.097, 0.089)*	0.183 (0.057, 0.31)	0.409 (0.19, 0.628)
TA Concentration (γ):siteHE	-0.266 (-0.372, -0.159)	1.004 (0.893, 1.114)	-0.214 (-0.365, -0.062)
TA Concentration (γ):siteLP	-0.524 (-0.584, -0.463)	0.266 (0.18, 0.353)	-0.645 (-0.826, -0.464)
TA Concentration (γ):agejuvenile	0.108 (0.024, 0.192)	0.641 (0.546, 0.736)	-0.707 (-0.934, -0.48)
TA Concentration (γ):HC:sexM	-0.143 (-0.451, 0.165)*	-0.898 (-1.3, -0.496)	-0.802 (-1.484, -0.12)
TA Concentration (γ):HC:siteHE	0.446 (0.082, 0.81)	0.707 (0.291, 1.123)	-0.935 (-1.511, -0.36)
TA Concentration (γ):HC:siteLP	-0.028 (-0.27, 0.213)*	-0.235 (-0.616, 0.146)*	0.787 (0.151, 1.423)
TA Concentration (γ):HC:agejuvenile	-0.173 (-0.513, 0.168)*	-0.206 (-0.591, 0.179)*	0.751 (0.006, 1.496)

Appendix S4.9: Regression coefficients for stationary state probabilities

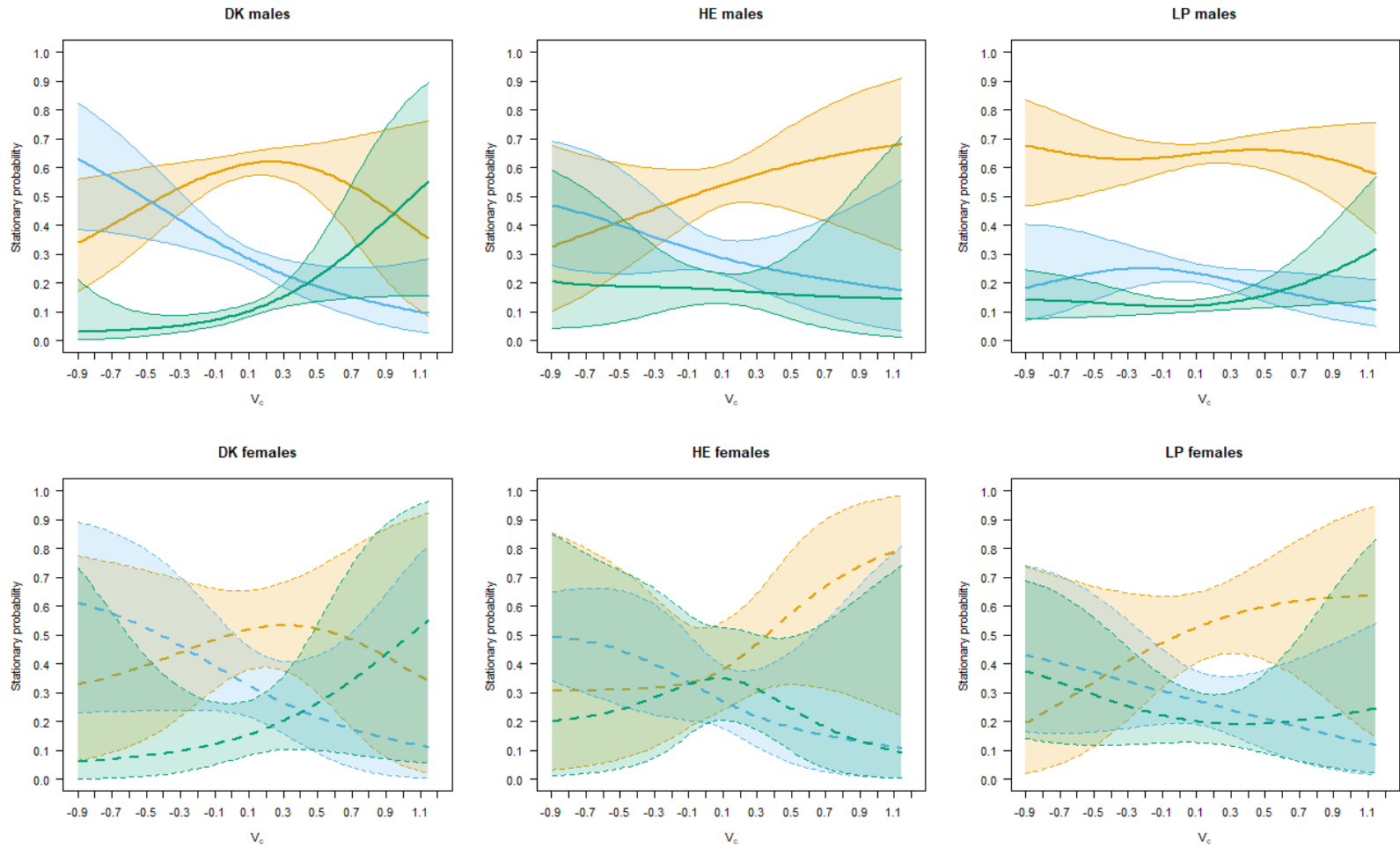


Fig. S4.9.1. Model-estimated stationary state probabilities for behavioural states (travelling, foraging, and resting) as a function of V_c for each state-sex group (adults only) for BC1. Plots show 95% CI. Note that the two-way (sex:site) and three-way (V_c :sex:site) interactions are not included (Appendix S4.4).

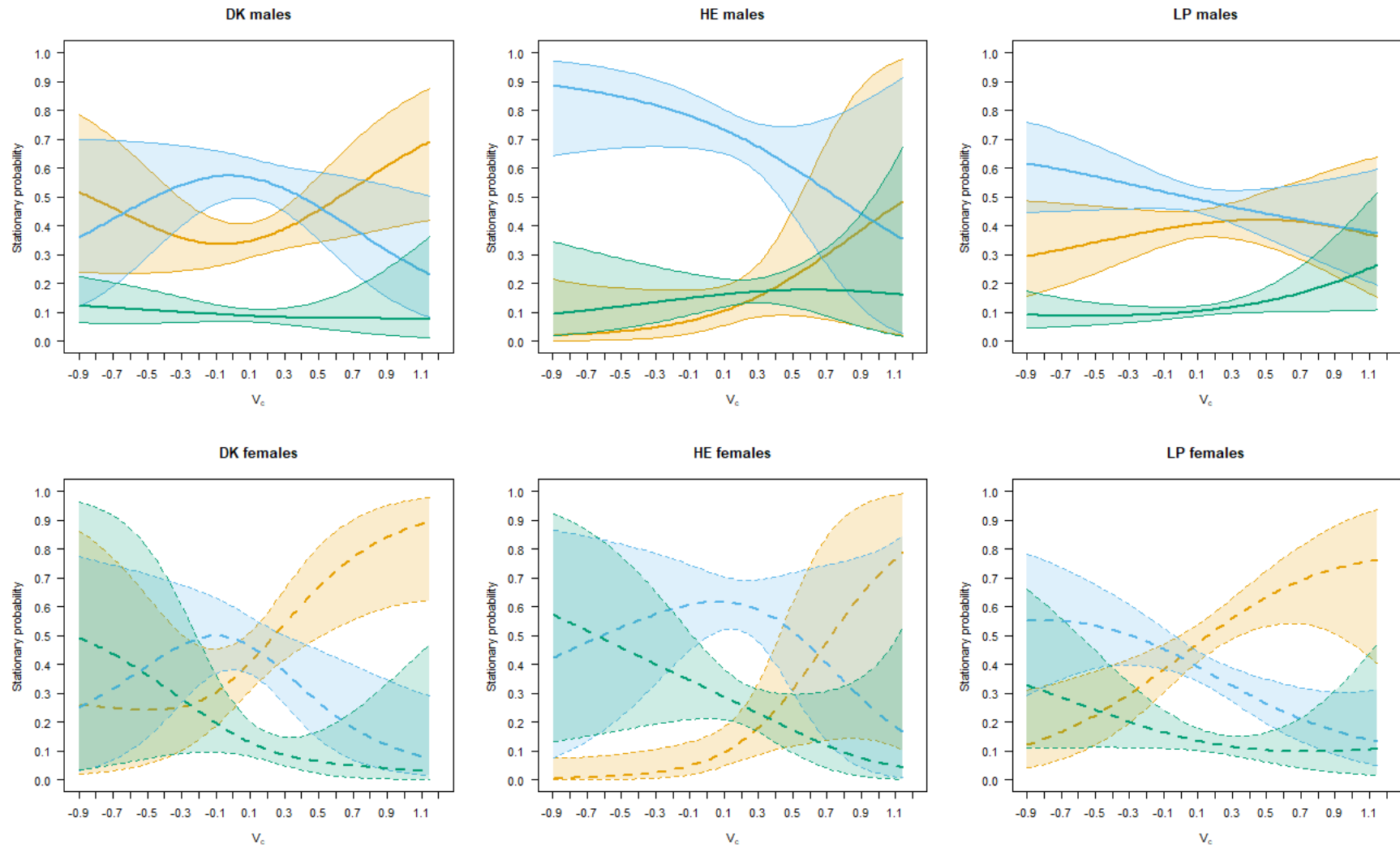


Fig. S4.9.2. Model-estimated stationary state probabilities for behavioural states (travelling, foraging, and resting) as a function of V_c for each state-sex group (adults only) for BC2. Plots show 95% CI. Note that the two-way (sex:site) and three-way (V_c :sex:site) interactions are not included (Appendix S4.4).

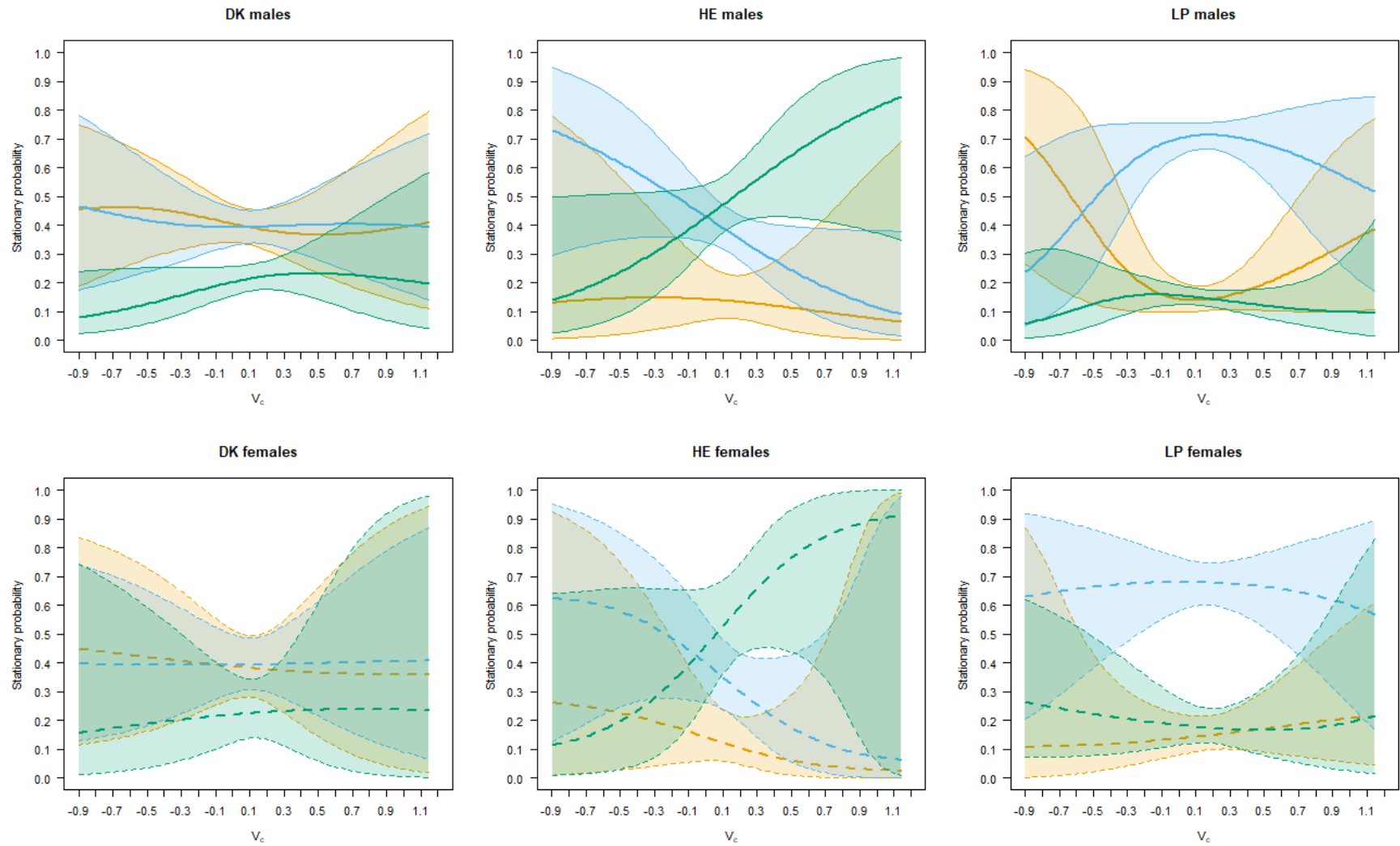


Fig. S4.9.3. Model-estimated stationary state probabilities for behavioural states (travelling, foraging, and resting) as a function of V_c for each state-sex group (adults only) for BC3. Plots show 95% CI. Note that the two-way (sex:site) and three-way (V_c :sex:site) interactions are not included (Appendix S4.4).

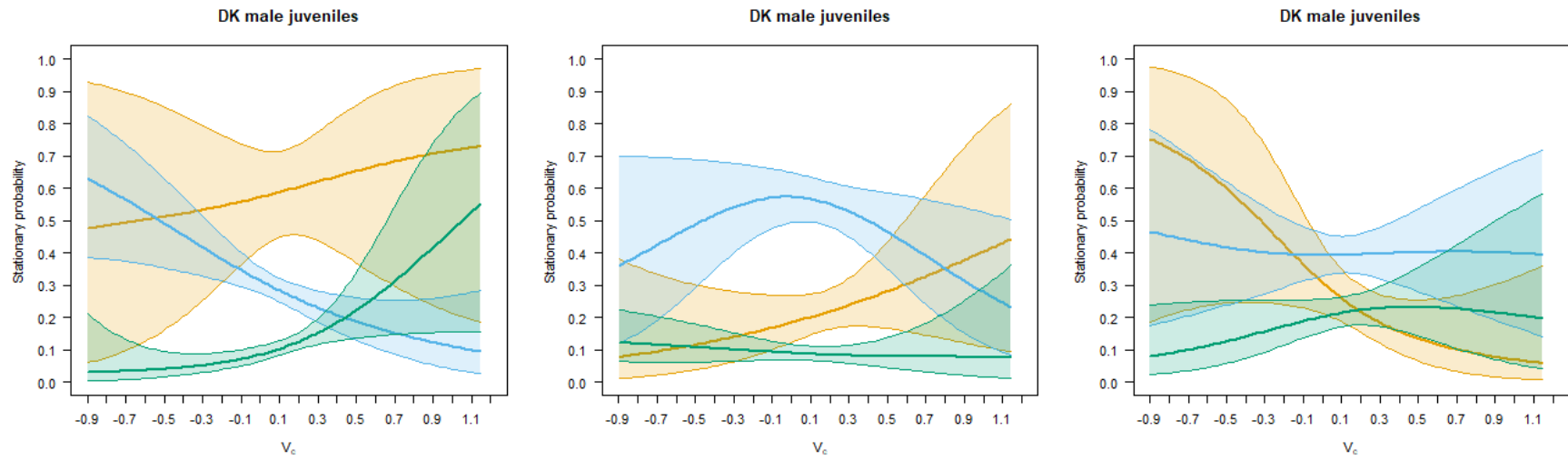


Fig. S4.9.3. Model-estimated stationary state probabilities for behavioural states (travelling, foraging, and resting) as a function of V_c for DK male juveniles (each column represents a different behavioural context; BC1-BC3). Plots show 95% CI. Note that the two-way (sex:site) and three-way (V_c :sex:site) interactions are not included (Appendix S4.4).

Appendix S4.10: Regression coefficients for transition probabilities

Table S4.10.1. Model-estimated regression coefficients for transition probabilities for each mix (and 95 % confidence intervals) for final 3-state HMM. Intercept refers to when HC = 0.13 (mean), sex = F, site = DK, age = adult. Where confidence intervals did not encompass zero, the covariate was considered to have a notable effect on the transition between respective states; ↑ = positive, ↓ = negative, and × = no effect. Covariate effects that were consistent in the direction of their effect (or lack of) across mixtures are indicated ✓; those that were not were indicated ✗. HC = head-current component (V_c).

Covariate	State transition	Mixture			Effect			Consistent across mixtures
		1	2	3	1	2	3	
(Intercept)	1 → 2	-1.89 (-2.579, -1.201)	-2.445 (-2.856, -2.034)	-1.508 (-1.954, -1.062)	↓	↓	↓	✓
	1 → 3	-3.185 (-4.444, -1.926)	-4.119 (-4.993, -3.245)	-3.185 (-4.308, -2.062)	↓	↓	↓	✓
	2 → 1	-1.351 (-2.327, -0.374)	-2.959 (-3.488, -2.43)	-1.527 (-2.157, -0.898)	↓	↓	↓	✓
	2 → 3	-2.433 (-3.47, -1.396)	-3.418 (-3.903, -2.933)	-2.638 (-3.177, -2.099)	↓	↓	↓	✓
	3 → 1	-2.071 (-3.595, -0.547)	-2.728 (-3.879, -1.577)	-2.552 (-3.915, -1.189)	↓	↓	↓	✓
	3 → 2	-1.211 (-2.267, -0.155)	-2.569 (-3.281, -1.858)	-2.227 (-2.926, -1.529)	↓	↓	↓	✓
HC	1 → 2	-2.488 (-4.925, -0.052)	-0.84 (-2.678, 0.997)	-1.052 (-2.967, 0.864)	↓	×	×	✗
	1 → 3	0.524 (-2.664, 3.712)	-0.47 (-3.495, 2.554)	-0.384 (-4.42, 3.651)	×	×	×	✓
	2 → 1	-0.702 (-3.156, 1.752)	2.512 (0.554, 4.469)	-1.442 (-4.065, 1.181)	×	↑	×	✗
	2 → 3	-0.151 (-4.619, 4.316)	-2.222 (-4.317, -0.127)	-0.697 (-2.91, 1.515)	×	↓	×	✗
	3 → 1	-1.256 (-5.475, 2.962)	-0.47 (-3.867, 2.927)	-0.102 (-7.177, 6.973)	×	×	×	✓
	3 → 2	-2.044 (-6.275, 2.188)	1.326 (-0.984, 3.636)	-1.144 (-4.095, 1.807)	×	×	×	✓
sexM	1 → 2	-0.562 (-1.216, 0.092)	-0.212 (-0.518, 0.094)	-1.35 (-1.804, -0.896)	×	×	↓	✗
	1 → 3	-0.049 (-1.273, 1.176)	0.974 (0.154, 1.794)	-0.088 (-1.238, 1.063)	×	↑	×	✗
	2 → 1	-0.311 (-1.244, 0.623)	-0.437 (-0.849, -0.025)	-1.396 (-2.036, -0.757)	×	↓	↓	✗
	2 → 3	-1.085 (-1.933, -0.237)	-0.036 (-0.421, 0.349)	-0.353 (-0.826, 0.121)	↓	×	×	✗
	3 → 1	0.927 (-0.557, 2.412)	1.424 (0.334, 2.515)	0.192 (-1.227, 1.611)	×	↑	×	✗
	3 → 2	-0.469 (-1.404, 0.467)	1.094 (0.549, 1.64)	-0.153 (-0.811, 0.505)	×	↑	×	✗
siteHE	1 → 2	0.146 (-0.249, 0.542)	0.765 (0.128, 1.402)	-0.159 (-0.831, 0.513)	×	↑	×	✗
	1 → 3	-0.299 (-0.974, 0.376)	-0.87 (-2.797, 1.057)	-3.525 (-9.735, 2.685)	×	×	×	✓
	2 → 1	-0.171 (-0.683, 0.342)	-1.469 (-2.732, -0.205)	-1.229 (-1.926, -0.532)	×	↓	↓	✗
	2 → 3	1.232 (0.488, 1.975)	0.709 (0.226, 1.193)	0.007 (-0.491, 0.505)	↑	↑	×	✗

Covariate	State transition	Mixture			Effect			Consistent across mixtures
		1	2	3	1	2	3	
siteLP	3 → 1	-0.754 (-1.436, -0.073)	-1.439 (-2.71, -0.168)	-4.466 (-7.174, -1.757)	↓	↓	↓	✓
	3 → 2	-0.444 (-1.222, 0.335)	0.47 (-0.243, 1.184)	-0.624 (-1.183, -0.065)	x	x	↓	✗
	1 → 2	-0.134 (-0.434, 0.165)	0.423 (0.074, 0.771)	0.073 (-0.354, 0.501)	x	↑	x	✗
	1 → 3	0.295 (-0.076, 0.667)	-0.071 (-0.534, 0.391)	-0.666 (-1.476, 0.143)	x	x	x	✓
	2 → 1	0.205 (-0.208, 0.619)	0.989 (0.582, 1.395)	-1.703 (-2.322, -1.085)	x	↑	↓	✗
	2 → 3	1.261 (0.554, 1.968)	0.953 (0.581, 1.326)	0.045 (-0.337, 0.427)	↑	↑	x	✗
	3 → 1	0.328 (-0.129, 0.785)	-0.089 (-0.729, 0.551)	-0.952 (-1.704, -0.2)	x	x	↓	✗
agejuvenile	3 → 2	0.351 (-0.296, 0.998)	1.177 (0.597, 1.757)	1.105 (0.583, 1.627)	x	↑	↑	✗
	1 → 2	0.209 (-0.548, 0.965)	-0.302 (-0.775, 0.171)	-0.294 (-1.019, 0.431)	x	x	x	✓
	1 → 3	0.634 (-0.239, 1.508)	-0.45 (-1.05, 0.15)	-0.605 (-1.444, 0.234)	x	x	x	✓
	2 → 1	0.408 (-0.507, 1.323)	-1.159 (-1.937, -0.381)	-0.991 (-1.827, -0.154)	x	↓	↓	✗
	2 → 3	-1.741 (-8.361, 4.88)	0.108 (-0.342, 0.558)	-0.066 (-0.555, 0.423)	x	x	x	✓
	3 → 1	-0.319 (-1.553, 0.916)	-0.951 (-1.66, -0.242)	-0.336 (-1.118, 0.446)	x	↓	x	✗
	3 → 2	-0.552 (-2.116, 1.012)	0.515 (-0.077, 1.106)	0.627 (-0.043, 1.297)	x	x	x	✓
HC:sexM	1 → 2	1.236 (-0.915, 3.386)	0.257 (-0.987, 1.502)	0.533 (-1.215, 2.281)	x	x	x	✓
	1 → 3	0.256 (-2.654, 3.167)	-0.299 (-2.974, 2.376)	-0.064 (-4.01, 3.881)	x	x	x	✓
	2 → 1	1.44 (-0.786, 3.666)	-1.066 (-2.458, 0.325)	1.508 (-0.828, 3.843)	x	x	x	✓
	2 → 3	-0.023 (-3.251, 3.205)	0.239 (-1.198, 1.676)	0.985 (-0.741, 2.712)	x	x	x	✓
	3 → 1	-1.318 (-5.267, 2.631)	-2.141 (-5.07, 0.788)	-2.41 (-9.491, 4.672)	x	x	x	✓
	3 → 2	0.8 (-2.937, 4.537)	-1.544 (-3.095, 0.007)	1.805 (-0.901, 4.511)	x	x	x	✓
HC:siteHE	1 → 2	-0.453 (-2.217, 1.312)	-2.164 (-4.987, 0.659)	0.839 (-1.716, 3.394)	x	x	x	✓
	1 → 3	-0.565 (-2.898, 1.768)	0.066 (-6.276, 6.408)	-1.125 (-3.517, 1.267)	x	x	x	✓
	2 → 1	-1.812 (-3.754, 0.129)	-1.537 (-5.152, 2.079)	0.971 (-2.052, 3.995)	x	x	x	✓
	2 → 3	-1.74 (-5.332, 1.851)	2.813 (0.903, 4.723)	0.075 (-2.122, 2.271)	x	↑	x	✗
	3 → 1	2.894 (-0.042, 5.829)	2.31 (-1.294, 5.914)	0.358 (-8.101, 8.817)	x	x	x	✓
	3 → 2	-1.908 (-6.416, 2.6)	0.421 (-1.87, 2.712)	-2.338 (-4.563, -0.113)	x	x	↓	✗
HC:siteLP	1 → 2	1.089 (-0.251, 2.429)	-0.803 (-2.399, 0.794)	1.827 (0.076, 3.578)	x	x	↑	✗
	1 → 3	-0.299 (-1.812, 1.213)	1.06 (-0.882, 3.003)	1.348 (-1.857, 4.552)	x	x	x	✓
	2 → 1	0.49 (-1.082, 2.063)	-1.877 (-3.546, -0.208)	2.709 (0.123, 5.296)	x	↓	↑	✗
	2 → 3	-2.015 (-5.721, 1.691)	1.38 (-0.389, 3.15)	-0.919 (-2.735, 0.898)	x	x	x	✓

Covariate	State transition	Mixture			Effect			Consistent across mixtures
		1	2	3	1	2	3	
HC:agejuvenile	3 → 1	1.219 (-0.627, 3.066)	0.818 (-1.723, 3.358)	-0.581 (-4.095, 2.932)	x	x	x	✓
	3 → 2	0.178 (-2.275, 2.632)	-1.452 (-3.531, 0.626)	-0.405 (-2.348, 1.537)	x	x	x	✓
	1 → 2	-0.577 (-3.958, 2.804)	0.426 (-1.586, 2.439)	1.672 (-1.565, 4.908)	x	x	x	✓
	1 → 3	0.109 (-3.218, 3.436)	-1.128 (-3.565, 1.308)	1.903 (-1.498, 5.303)	x	x	x	✓
	2 → 1	-1.603 (-5.772, 2.567)	-0.372 (-3.062, 2.319)	0.002 (-3.053, 3.057)	x	x	x	✓
	2 → 3	-0.383 (-1.119, 0.353)	2.045 (0.132, 3.959)	-0.1 (-2.069, 1.869)	x	↑	x	✗
	3 → 1	4.727 (1.067, 8.386)	2.503 (-0.033, 5.038)	-1.113 (-4.54, 2.314)	↑	x	x	✗
	3 → 2	0.649 (-5.191, 6.49)	0.579 (-1.463, 2.622)	-0.931 (-3.119, 1.257)	x	x	x	✓

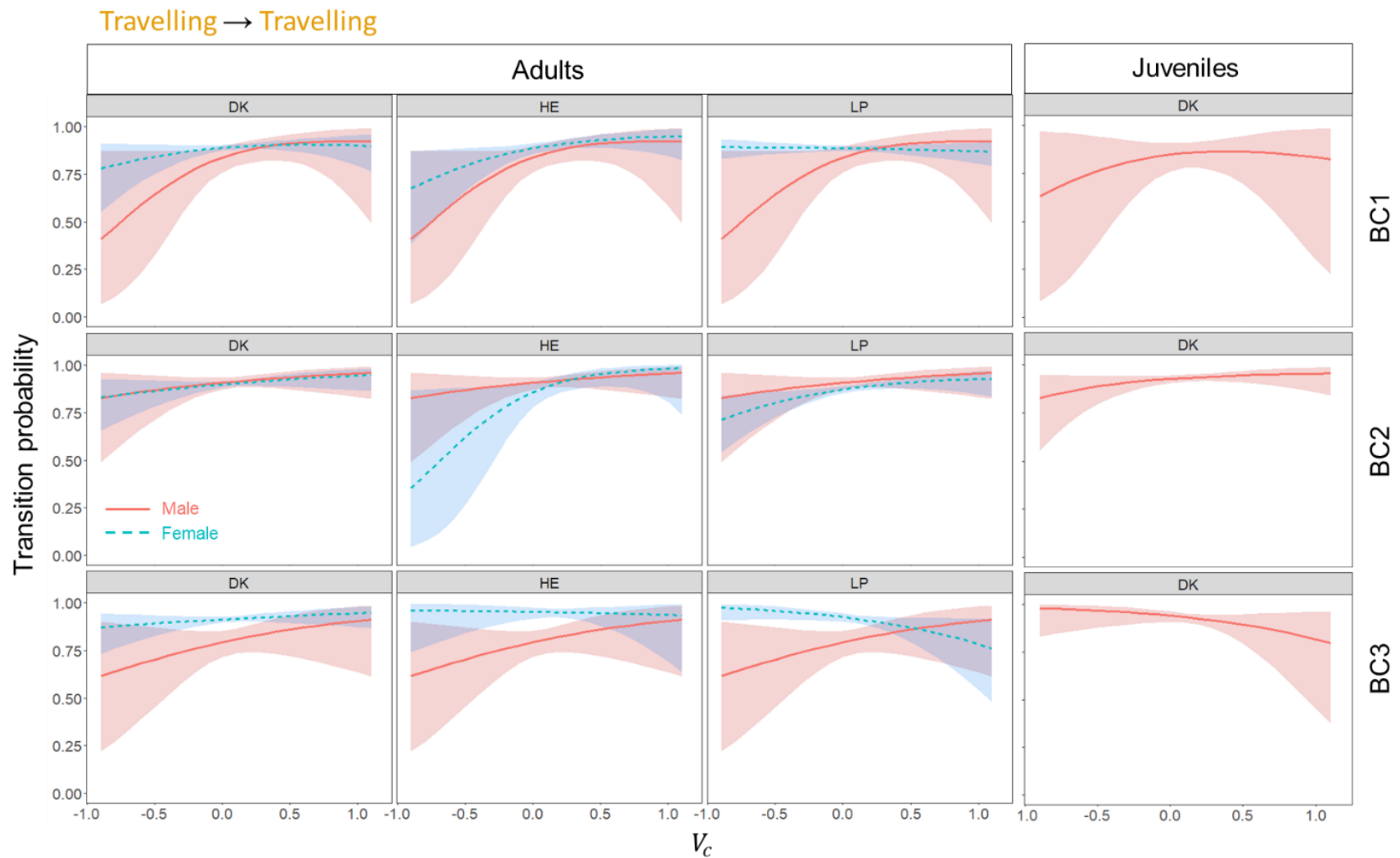


Fig. S4.10.1. Transition probabilities as a function of V_c estimated from the final hidden Markov model, for seals of different sites, sexes, and age-class. Specific state transition indicated top-left. Plots show model-estimated coefficients plus 95% CI. Note that the two-way (sex:site) and three-way (V_c :sex:site) interactions are not included (Appendix S4.4).

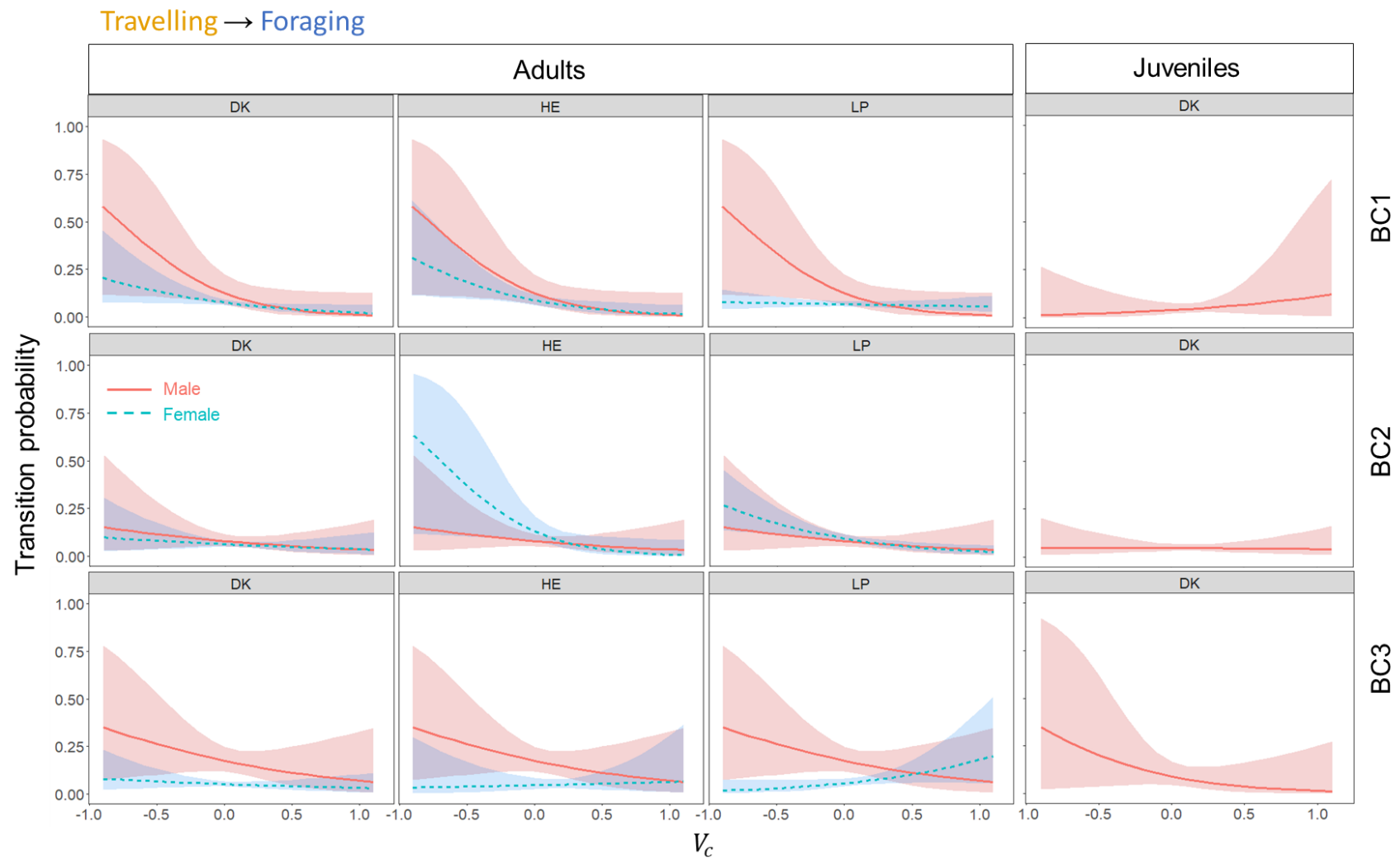


Fig. S4.10.2. Transition probabilities as a function of V_c estimated from the final hidden Markov model, for seals of different sites, sexes, and age-class. Specific state transition indicated top-left. Plots show model-estimated coefficients plus 95% CI. Note that the two-way (sex:site) and three-way (V_c :sex:site) interactions are not included (Appendix S4.4).

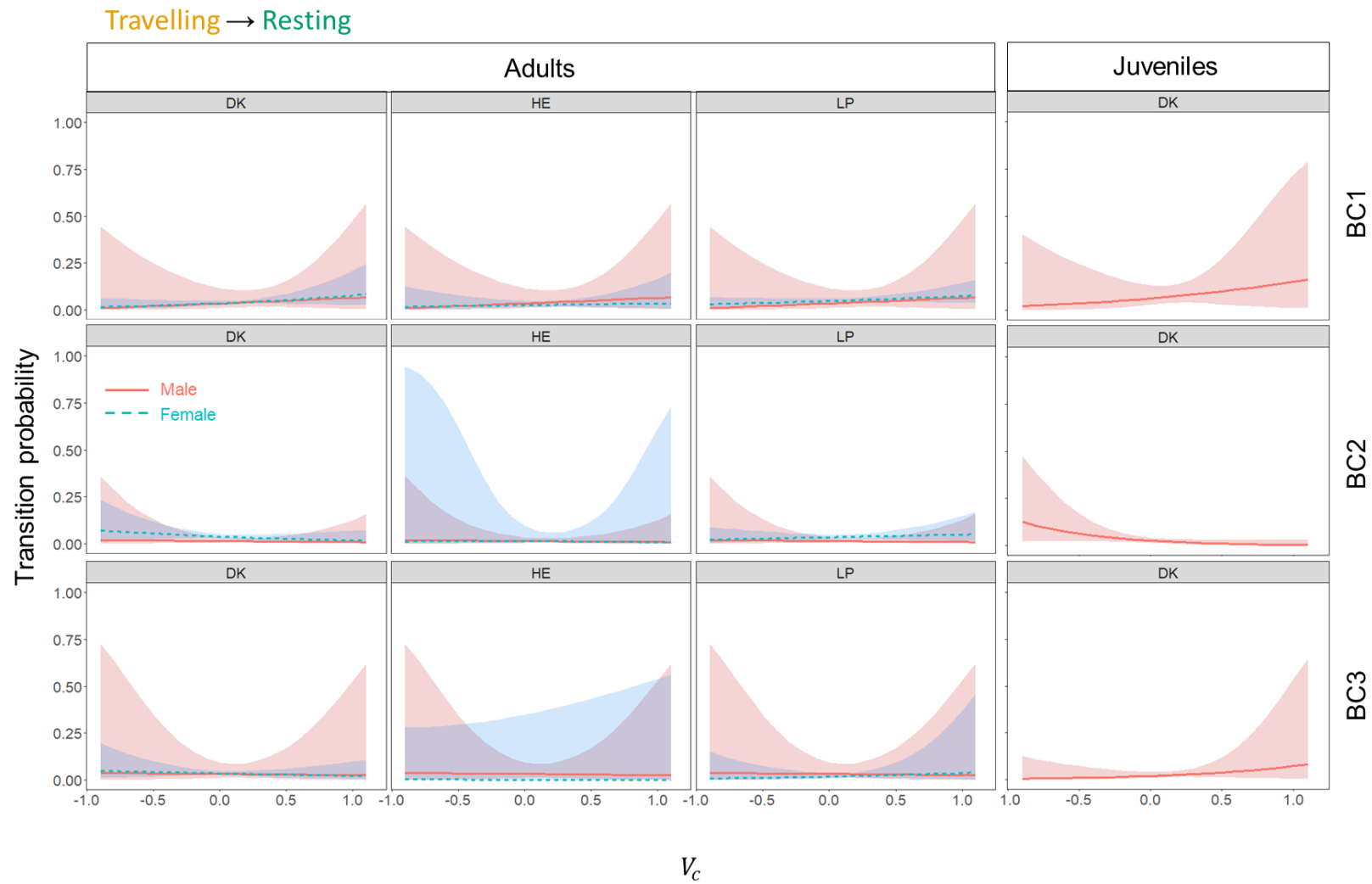


Fig. S4.10.3. Transition probabilities as a function of V_c estimated from the final hidden Markov model, for seals of different sites, sexes, and age-class. Specific state transition indicated top-left. Plots show model-estimated coefficients plus 95% CI. Note that the two-way (sex:site) and three-way (V_c :sex:site) interactions are not included (Appendix S4.4).

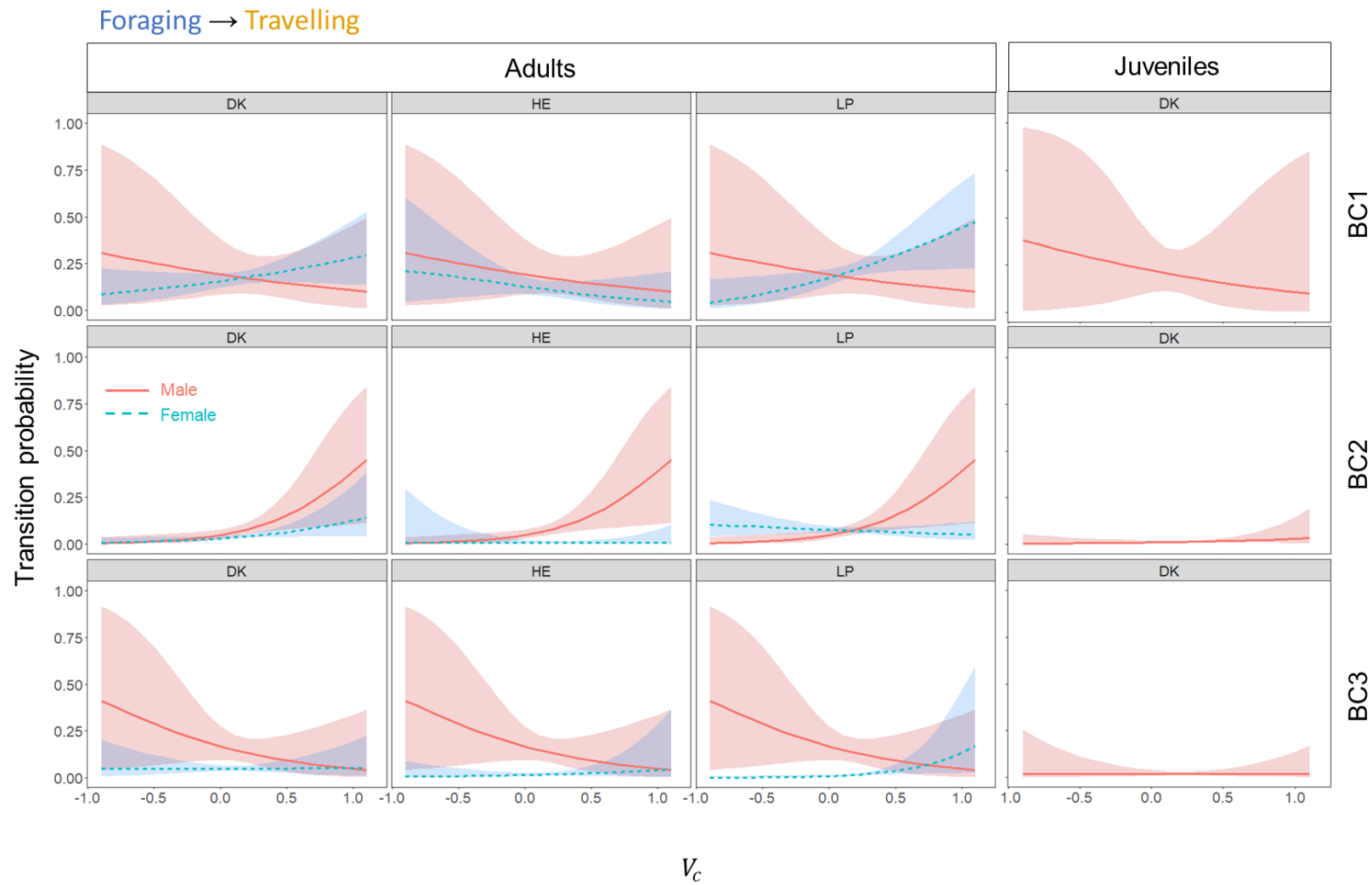


Fig. S4.10.4. Transition probabilities as a function of V_c estimated from the final hidden Markov model, for seals of different sites, sexes, and age-class. Specific state transition indicated top-left. Plots show model-estimated coefficients plus 95% CI. Note that the two-way (sex:site) and three-way (V_c :sex:site) interactions are not included (Appendix S4.4).

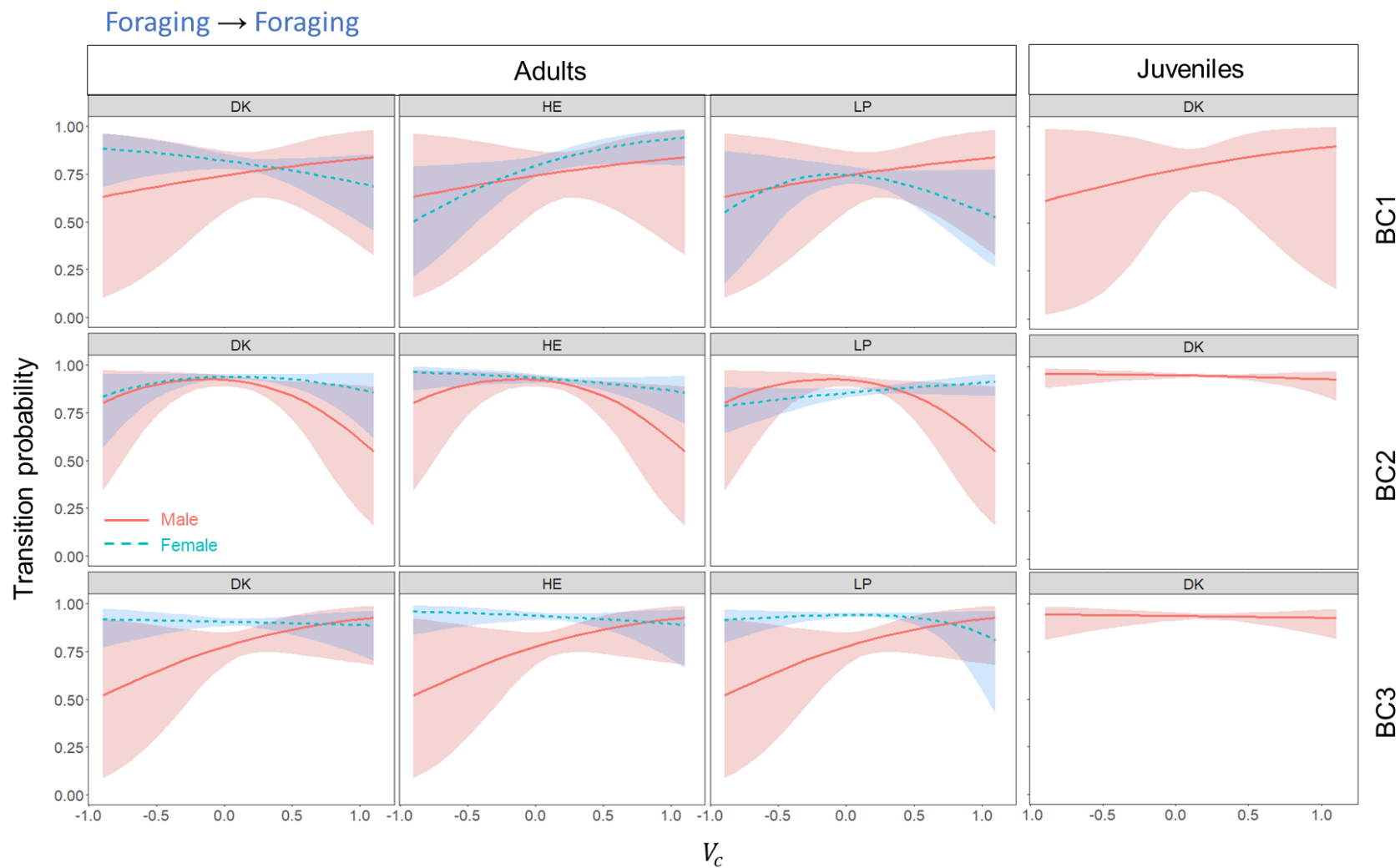


Fig. S4.10.5. Transition probabilities as a function of V_c estimated from the final hidden Markov model, for seals of different sites, sexes, and age-class. Specific state transition indicated top-left. Plots show model-estimated coefficients plus 95% CI. Note that the two-way (sex:site) and three-way (V_c :sex:site) interactions are not included (Appendix S4.4).

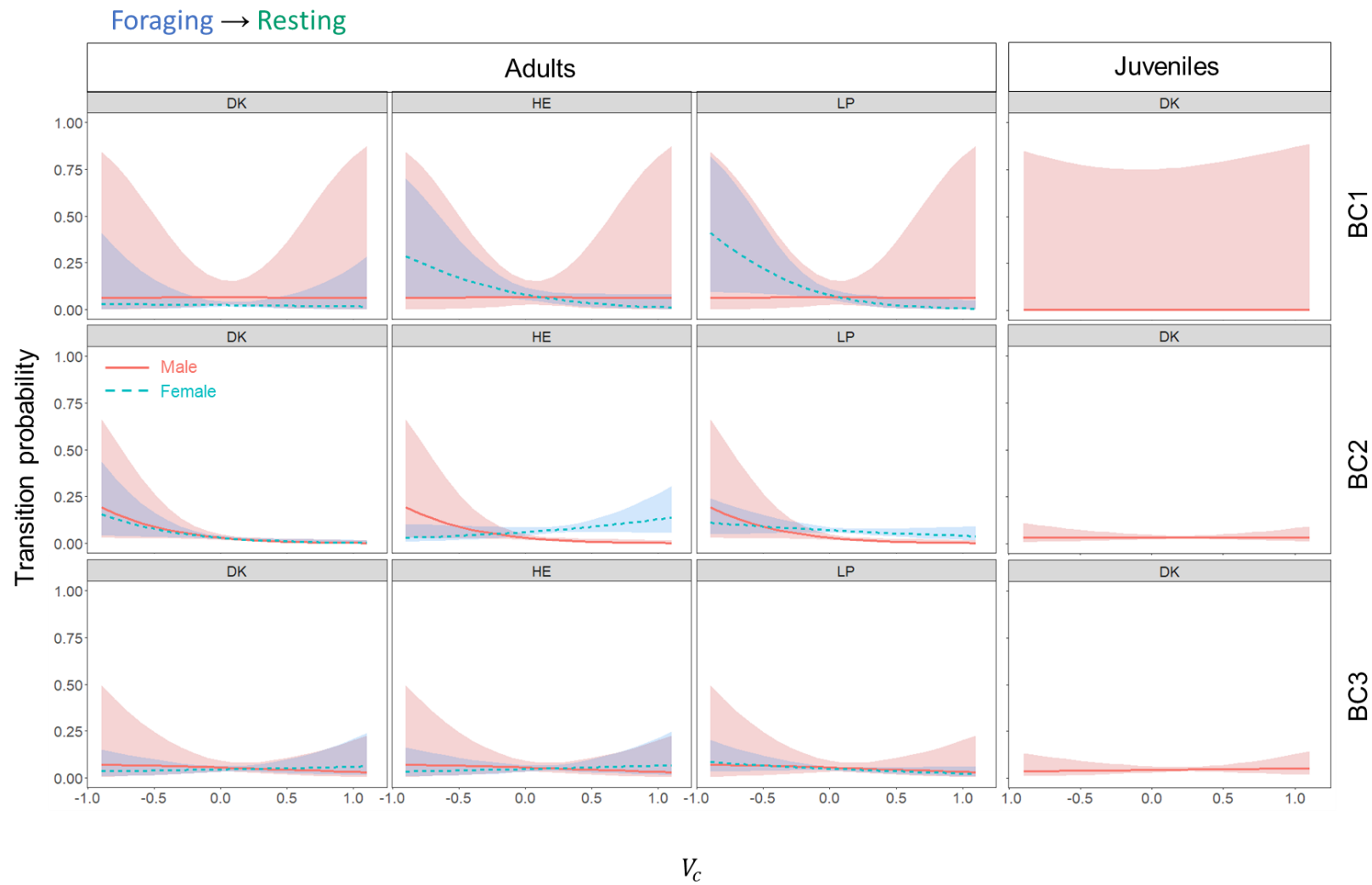


Fig. S4.10.6. Transition probabilities as a function of V_c estimated from the final hidden Markov model, for seals of different sites, sexes, and age-class. Specific state transition indicated top-left. Plots show model-estimated coefficients plus 95% CI. Note that the two-way (sex:site) and three-way (V_c :sex:site) interactions are not included (Appendix S4.4).

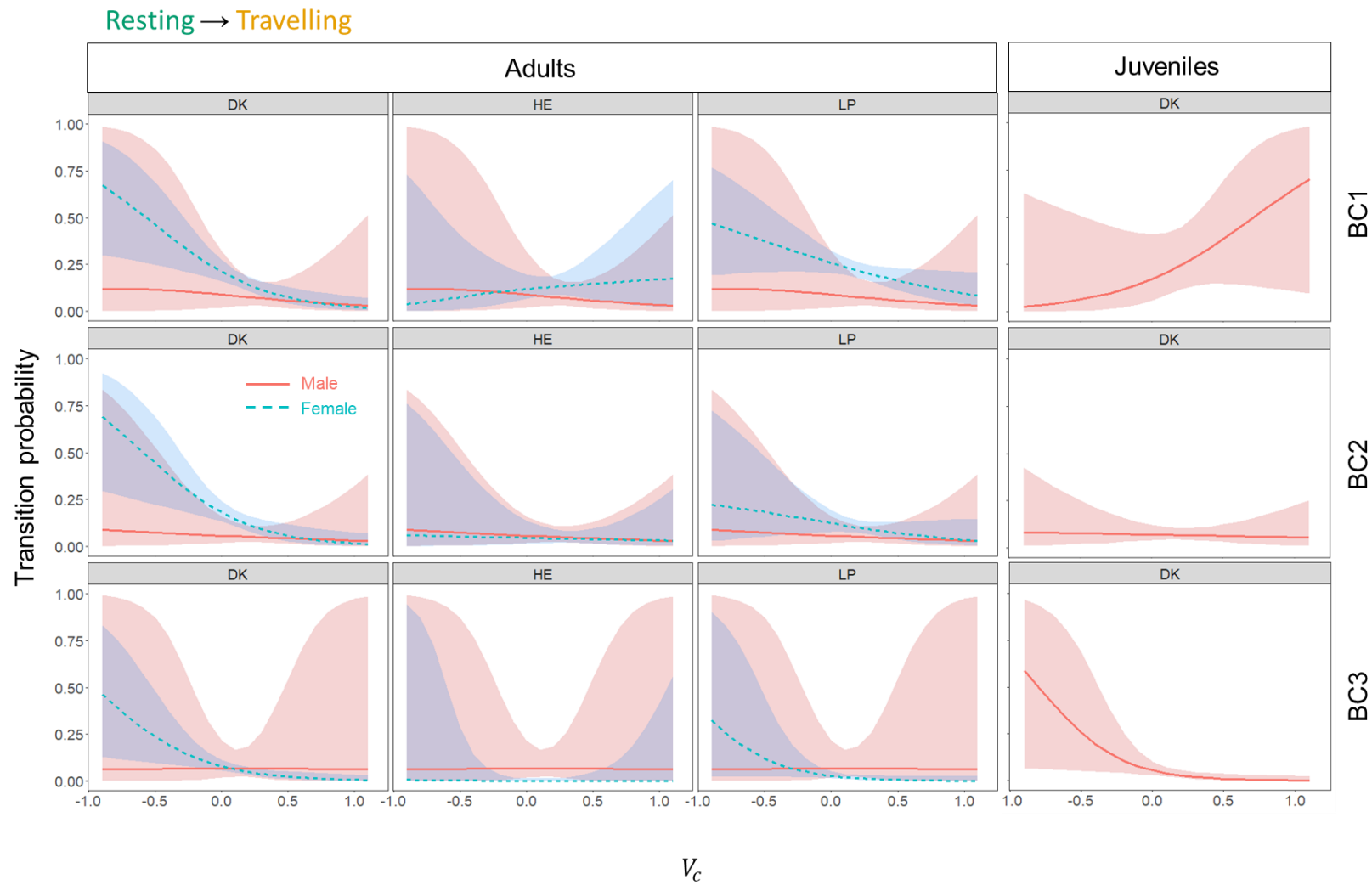


Fig. S4.10.7. Transition probabilities as a function of V_c estimated from the final hidden Markov model, for seals of different sites, sexes, and age-class. Specific state transition indicated top-left. Plots show model-estimated coefficients plus 95% CI. Note that the two-way (sex:site) and three-way (V_c :sex:site) interactions are not included (Appendix S4.4).

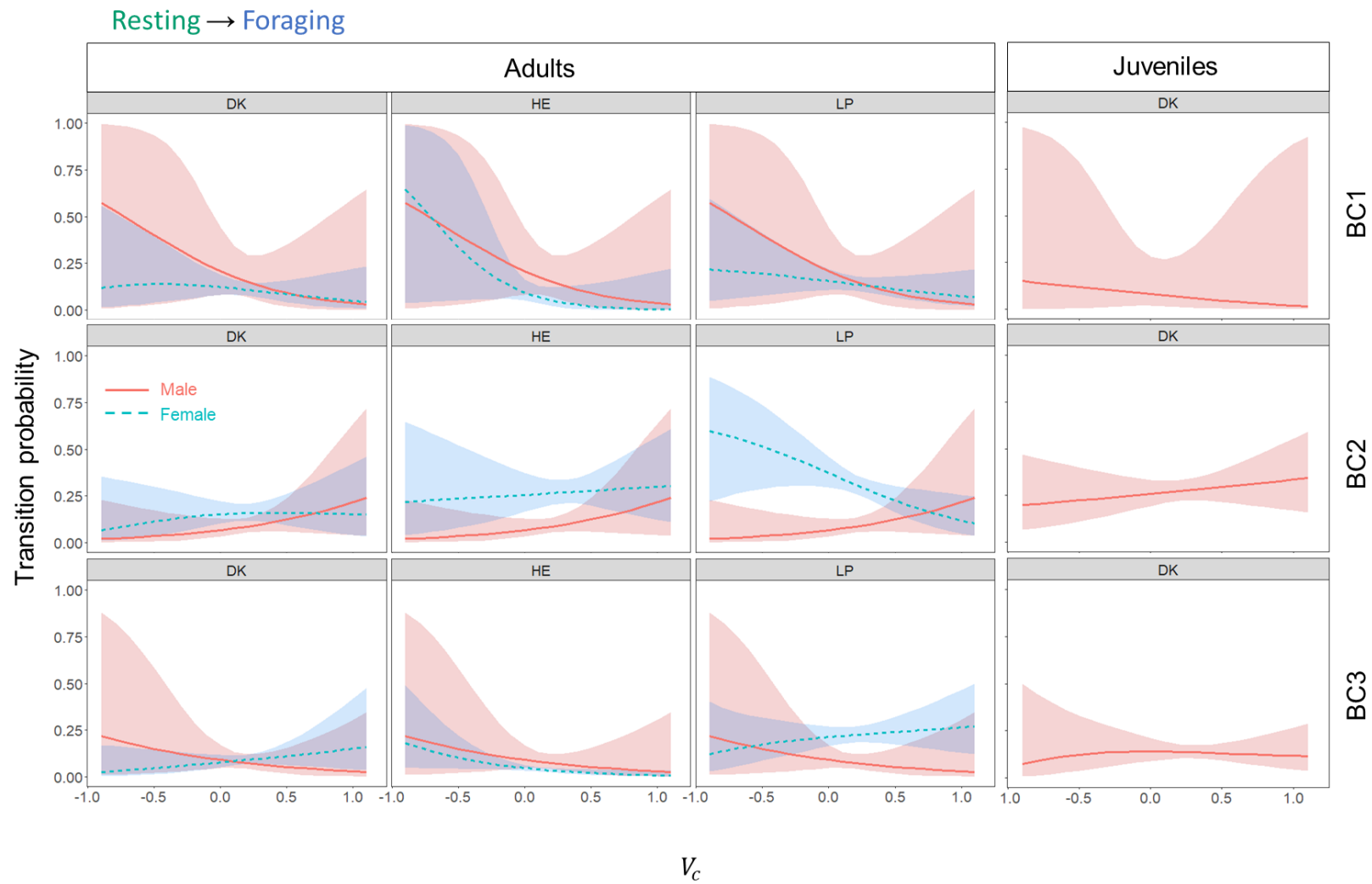


Fig. S4.10.8. Transition probabilities as a function of V_c estimated from the final hidden Markov model, for seals of different sites, sexes, and age-class. Specific state transition indicated top-left. Plots show model-estimated coefficients plus 95% CI. Note that the two-way (sex:site) and three-way (V_c :sex:site) interactions are not included (Appendix S4.4).

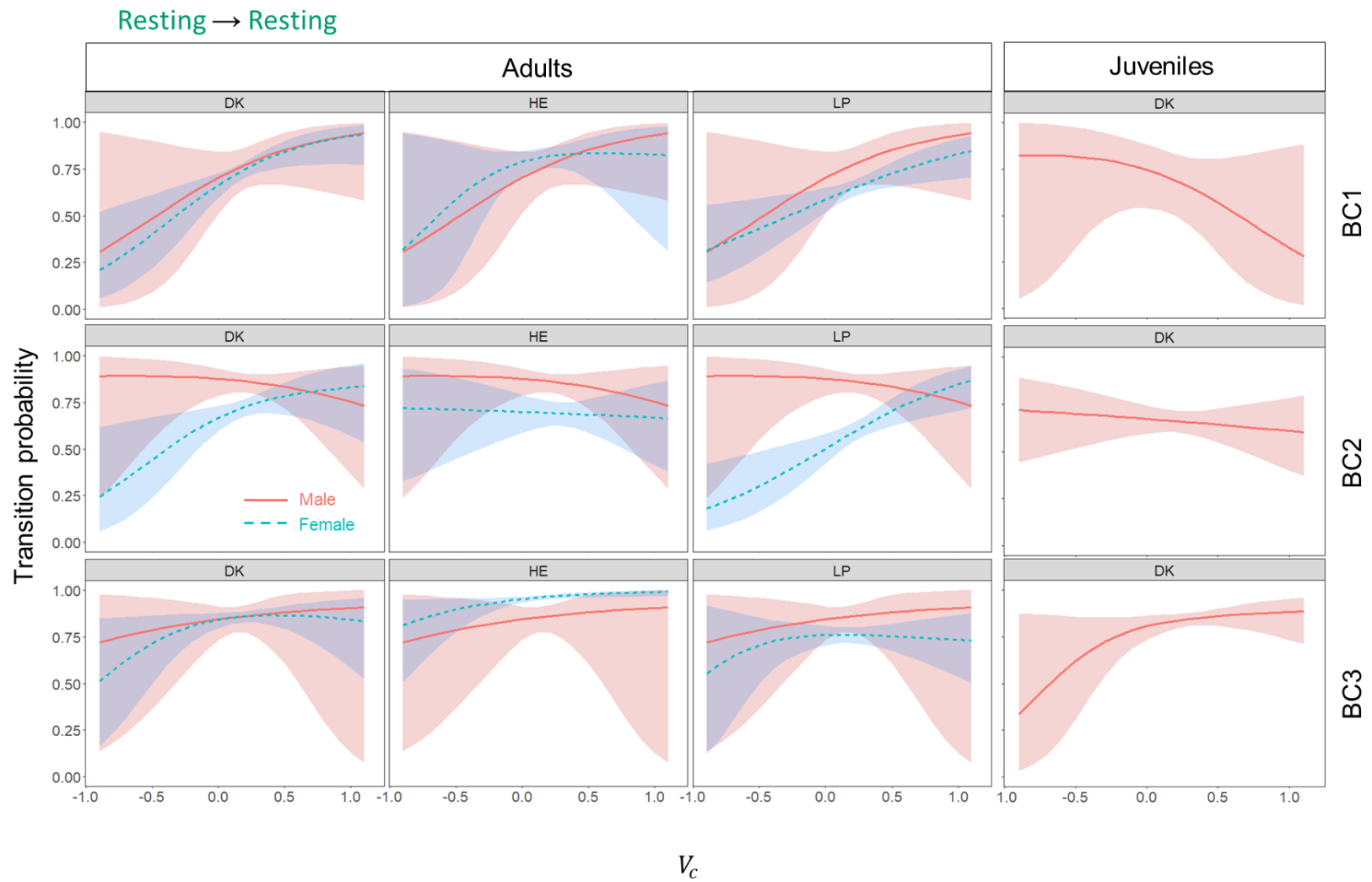


Fig. S4.10.9. Transition probabilities as a function of V_c estimated from the final hidden Markov model, for seals of different sites, sexes, and age-class. Specific state transition indicated top-left. Plots show model-estimated coefficients plus 95% CI. Note that the two-way (sex:site) and three-way (V_c :sex:site) interactions are not included (Appendix S4.4).

Table S4.10.2. Estimated initial state distributions from the final HMM ($N = 3, K = 3$).

Behavioural context	State 1 (<i>T</i>)	State 2 (<i>F</i>)	State 3 (<i>R</i>)
1	0.09	0.14	0.77
2	0.34	0.00	0.66
3	0.20	0.10	0.70

Appendix S4.11: Examples of foraging trips with apparent drift whilst resting.

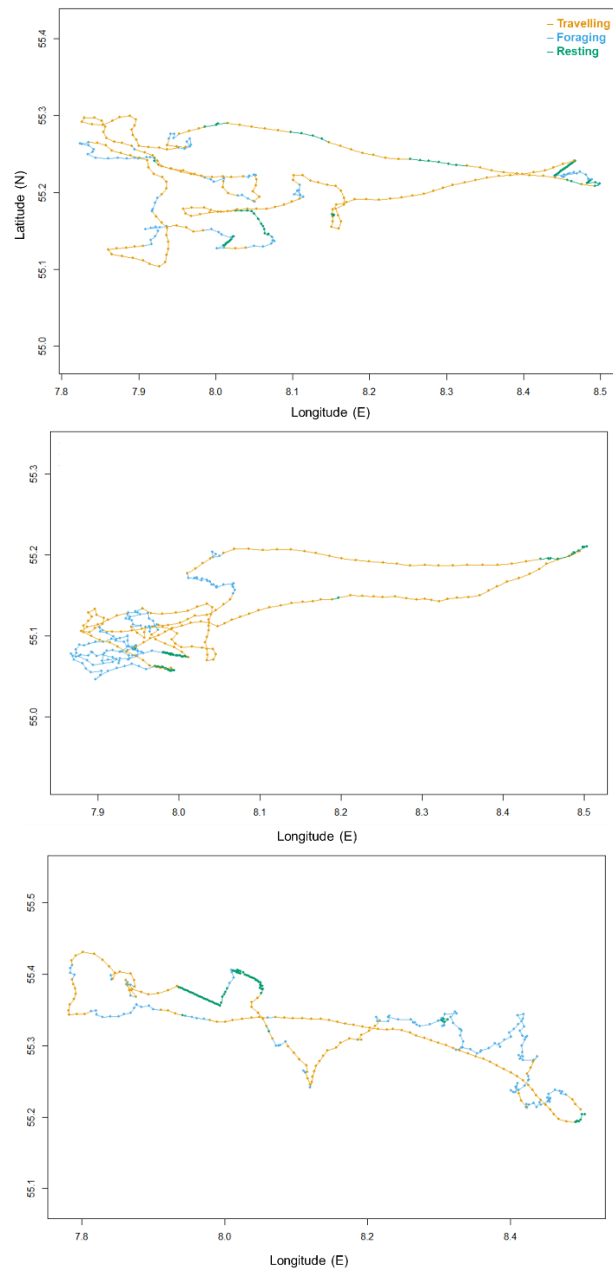


Fig. S4.11. Three foraging trips coloured by behavioural state, highlighting clear examples of highly directional drift whilst resting (green steps).

Appendix V: Supplementary material for Chapter 5

Contents

Appendix S5.1: Factors to consider when developing and constructing a biologging device

Appendix S5.2: Lessons learnt through building tags

Appendix S5.3: Fastloc-GPS performance

Appendix S5.4: Previous tag design and appraisal

Appendix S5.5: Float preparation protocol

Appendix S5.6: Baseplate designs and appraisals

Appendix S5.7: Example data recording sheet for logging tag design and deployment details

Appendix S5.8: Additional tag details

Appendix S5.1: Factors to consider when developing and constructing a biologging device

For many researchers studying animal movement and behaviour using biologging devices, purchasing “off-the-shelf” tags is not feasible, be it due to financial constraints or the fact that the devices that are on offer may not come with all of the functionalities that are required to address a specific research question. As a result, researchers often turn to the strategy of building their own devices. This can bring a number of benefits, including that tags can be designed to be bespoke to the research project, can incorporate custom-functionality, and costs are generally reduced. This is important because tag design is intrinsically linked to study design (Williams et al., 2020). Researchers also become more familiar with their devices, which aids them in better understanding the deployment of their devices and the data that are subsequently collected (Holton et al., 2021). It is also an excellent learning opportunity which develops key skills in problem solving and can reportedly make the researcher more versatile (Kwok, 2017). However, building biologging devices is challenging, and ecologists and biologists may lack the necessary engineering experience and expertise to do so. This means that researchers must work together with technicians and engineers to support them in their tag development and construction. Despite this support, researchers typically come across numerous hurdles during the process of their tag development, and more often than not these hurdles are common across individuals.

While many reviews exist to highlight the versatility in tag design and device type (Williams et al., 2020 and references therein), until recently only a paucity of studies offered guidance on how to design and construct tags, or indeed a list of necessary considerations when doing so. The *Method in Ecology and Evolution* journal's newly established “Practical Tools” publication type provides an online space for articles that offer this type of guidance (e.g. Gottwald et al., 2019; Rafiq et al., 2019; Foley & Sillero-Zubiri, 2020), though

greater numbers of these publications are required to cover the breadth of devices available and challenges therein.

One of the key challenges in tag building and design is in identifying all of the potential factors that need to be considered at the outset, and how they may interplay with one another. Gaining an holistic understanding of all of the complex issues that need to be addressed, prior to the start of device design and production, can be helpful; it will mitigate problems arising later in the design process, and in turn can reduce the number of iterative tag designs that are required. With hindsight, this can certainly be said for the tag described in this Chapter. Indeed, the process of developing this tag has brought about many learning opportunities with which I have created a comprehensive list of the considerations that need to be made. Table S5.1 below outlines these considerations with relevant examples from the literature, highlighting the trials and tribulations and lessons learnt from my own tag development process. I hope that this resource will serve as a useful and exhaustive guide for researchers who are commencing new research projects and may be starting the process of developing new tags from a position of limited understanding. Table S5.1 is presented as a comprehensive flowchart: Fig. S5.1.

This resource directly addresses a view expressed at a recent tagging workshop convened at the World Marine Mammal Conference (WMMC) in December 2019 (Kay, Zerbini & Andrews, *In Prep*). Specifically, several attendees noted their reason(s) for attendance as to: “learn the basics in tagging, including the methods”, “learn about the current state of tag attachment and if there was a place online to find such information”, “[have] a discussion about tag design”, “become more familiar with, and improve basic knowledge of, the pros and cons of different tagging methods”, “hear what considerations are being made by other researchers and manufacturers to minimise the impact of their designs”. Hence, I anticipate that, in particular, early career stage researchers will find this guide useful, and that also for more

experienced researchers this could serve as a valuable inventory for revision and reflection purposes.

Table S5.1. (overleaf) Factors to consider when developing and building a biologging device

Factor	Details, considerations, and examples
Class I. Study animal	Example: Grey seal (<i>Halichoerus grypus</i>).
A. Type	The specific requirements for tag design may change depending on if your study animal is domesticated or in captivity or is in the wild. Note that the behaviours that animals exhibit, as well as the performance of tagging systems, may vary substantially between captive/domestic and wild animals (Brown, Kays, Wikelski, Wilson, & Klimley, 2013).
1. Captive/domesticated	When working with captive animals the researcher is often more able to remove or change the tag at a later date. Hence, temporary attachment methods may be preferred. Example: Takei et al., (2016) attached a blood sampler to a captive seal via a temporary Velcro patch glued to the animal's back. Animals in captivity can be regularly monitored and deleterious tag effects can be resolved in-situ.
2. Wild	Example: Wild animals often cannot be recaptured hence tags will require a transmitting component in order to later establish their whereabouts so that the tag can be retrieved.
B. Location	The primary location or environment that your study animal inhabits will determine many factors of your final tag design. For example, when tagging animals that inhabit deep oceans tags must be waterproof and able to withstand pressure. The environment may also determine specific sensors that are advantageous to incorporate into your final tag design.
1. Terrestrial	Example: If your study species inhabits a woodland, it is useful to consider how canopy cover may affect the performance of tag components, such as GPS, light sensors, or solar panels (e.g. Byrne, Holland, Bryan, & Beasley, 2017).
2. Avian	Example: When tagging flying animals, it is often useful to include an altimeter in the final tag design.
3. Aquatic	Example: When tagging aquatic animals, it is often useful to include a barometric pressure sensor to record depth.
4. Other	Animals that are generally not restricted to one single terrain type or mode of transport e.g. seabirds that make use of land, water, and air. Many complicating factors must be considered in the tag design for these animals including drag, buoyancy, waterproofing, robustness, weight, colour, etc.

Factor	Details, considerations, and examples
C. Specifics	Specifics of the animal(s) you intend to tag. For example: size, mass, age, condition, sex. Are any animals to be excluded from tagging (e.g. juveniles, pregnant individuals, individuals in poor condition). Also consider the size or mass of the animal relative to the tag that it will bear. Example: Tags developed for grey seals may have substantially different impacts depending on whether tags are deployed on adults (weighing ~ 200 kg) to weaned pups (~ 50 kg).
D. Other	Are there any other special considerations for your study animal pertaining to its biology or ecology? Example: Sea otters are exceptional in that they are the only marine mammal without a layer of insulating blubber (Tinker, Bodkin, Ben-David, & Estes, 2018). This makes attaching external telemetry devices to the fur difficult, because doing so may severely compromise an individual's ability to thermoregulate; sea otters are generally equipped with implantable devices, or with flipper tags (Walker et al., 2012). Example: The animal spends a lot of time in shaded environments; a solar recharging panel would not be effective (e.g. Walton et al., 2019). Example: Animals that fight conspecifics (e.g. Mozo, Alabart, Rivas, & Folch, 2019). If so, is there a risk that the tag could come prematurely detached or damaged - do you need to consider making the tag more robust?
Class II. Animal welfare	In all cases the welfare of the animal must be considered. Also consider the potential disturbance to conspecifics in the form of i) general disturbance (e.g. disturbance to other adults in a colony), and ii) specific disturbance (e.g. if the research requires the tagging of adults nursing young, will the young animals be affected? Example: Seal pups can be separated from their mothers if disturbed (Osinga, Nussbaum, Brakefield, & Udo de Haes, 2012). Consider the cumulative effects of other samples (e.g. biological) being taken during the tagging process; blood, faeces, urine, semen, hair, skin, blubber etc.

Factor	Details, considerations, and examples
A. Capture and handling	<p>What are the stresses and risks associated with the capture and handling of animals necessary for the deployment of tags? Must the animal be captured and restrained at all? If so, by what means and for what duration? Is it necessary to subdue the animal e.g. using sedatives, during the tag deployment? Will tag deployment differ for a sedated versus a non-sedated animal? Can the tag be deployed without the need for the capture and direct handling of the animal at all? For example, can tags be deployed remotely e.g. using darting techniques (Horning et al., 2019). Remotely attaching tags often means the final tag positioning is more subject to chance. Will the final tag design require a second recapture of the animal to retrieve the device? If so, what are the cumulative stresses and risks associated with this?</p>
B. Tag impacts	<p>The impact of tags includes both the potential harms associated with the deployment and attachment of tags <i>per se</i>, as well as the impacts post-attachment.</p>
1. Drugs	<p>Consider whether the deployment of tags require anaesthesia or sedation (cf. Kreeger & Arnemo, 2012).</p>
2. Surgical	<p>Consider whether the deployment of tags requires surgical procedures, leading to surgical stress (both during and post-operative).</p>
3. Direct damage	<p>Consider the potential for direct damage caused by the tag being attached to the animal. For example: wound breakdown, chronic adhesions, lesions, seroma, skin damage, lacerations, burns, hair loss, or abrasions to skin, fur, or feathers (Field et al., 2012).</p>
4. Physiological	<p>Consider the wider physiological effects of attaching a tag to an animal. For example, extra load incurred by bearing the tag could affect the animal's energetic balance because of the extra power requirements to carry that burden. Similarly, disturbance to heat transfer (e.g. in sea otters) may give rise to changes in metabolic requirements for homeothermy.</p>

Factor	Details, considerations, and examples
5. Weight	Consider the overall weight of the device for the animal to bear both for the resulting energetic implications as well as the weight of the device creating pressure in a specific area leading to direct damage (see II.B.3 in this table). Increased weight caused by the tag may preclude an animal from performing normal behaviours, or from performing the same behaviours for the same length of time as an untagged animal. Tags should not exceed 3 % of the mass of the tagged animal (Casper, 2009).
6. Drag	Increased hydro- or aerodynamic drag induced by wearing the tag may give rise to greater energetic costs of swimming or flying for aquatic and avian animals respectively (Kay et al., 2019; Chapter 6). Increases in shear loading forces associated with increased drag may also lead to potential direct damage at the site of tag attachment (Fiore et al., 2017). Increased drag may preclude the ability for the tagged animal to reach its maximum movement speed or prevent that animal performing normal behaviours.
7. Buoyancy	Energetic implications of increased or decreased buoyancy as well as shear loading forces leading to potential damage at the site of attachment.
8. Lift/downthrust	Energetic implications of generating increased lift or downthrust.
9. Biofouling	Devices may be prone to biofouling over time, especially in long deployments (Hays, Bradshaw, James, Lovell, & Sims, 2007). Biofouling could lead to greater tag weight, or changes to tag buoyancy, lift or drag over time. For example, audio interference from acoustic pingers (the noise generated from acoustic pingers may cause detriment to the tagged animal directly as well as alter prey/predators to the animal's presence). Brightly coloured tags have been shown to draw attention from conspecifics (e.g. Wilson, Spairani, Coria, Culik, & Adelung, 1990). Is a biofouling agent required - is this non-toxic?

Factor	Details, considerations, and examples
10. Size	Tags must not be made so large that they might preclude normal behaviours. For example, Aldabra giant tortoise (<i>Aldabrachelys gigantea</i>) often enter caves to avoid direct sunlight (Walton et al., 2019). Attaching a very large tag to the carapace of an individual may prevent it from entering caves, or risk damage to the tag. Tags may affect the mobility of specific body parts. For example, animals tagged with large collars may find the movement of their neck to be restricted.
11. Noise/emissions	If your tag produces sound, consider the effect that this may have on the study animal, or its prey, predators, or conspecifics. Example: acoustic pingers; consider the sound source, signal duration, frequency (bandwidth), duration of exposure, etc.
12. Other individuals	Consider that attachment of tags to animals may draw unwanted attention to them from conspecifics or their prey or predators.
C. Deployment duration	Deployment duration is a key factor in determining tag impact and animal welfare. In many cases, impacts that would be benign or perhaps not even occur over short deployments may be more severe if the tag is attached for a longer duration. For example, long duration tags are more likely to suffer from biofouling (Hays et al., 2007).
1. Short	Example: up to 24-hour deployments of accelerometers on wild dogs in captivity.
2. Medium	Example: up to 3 week-long deployments of pop-off satellite tags on harbour seals.
3. Long	Example: 6-month deployment of satellite data relay loggers (SDRLs) on grey seals.
Class III. Research objectives	The final tag design will ultimately need to be developed to meet the specific objectives of the research.
A. Data required	What types of data are required? Hence what different sensor components must the tag contain? How much data are required and hence what sampling frequency, duty cycling, and battery duration are necessary? For a review, see Williams et al., (2020).

Factor	Details, considerations, and examples
1. Sampling frequency	Increased sampling frequency generates greater volumes of data. However important consideration must be made with respect to the trade-off between device memory capacity and battery life. Additionally, whilst many tags can store large volumes of data, those same volumes of data cannot necessarily be transmitted via satellite (Cox et al., 2018). Hence, if large volumes of data are to be collected, tags must often be made to be recoverable to download the data directly. Is the sampling frequency high enough to detect the behaviours of interest in your study?
2. Number of individuals	Is it possible to address the research question appropriately using the data from tags that collect large volumes of data but only from a small number of individuals? The answer to this question will determine, for example, whether it is more appropriate to tag a handful of individuals with tags that collect large and comprehensive data, or if it is better to use a cruder tag which can be deployed on a greater number of individuals. For example: when developing tags for use on marine predators, consider referring to Sequeira et al., (2019) for information regarding sample size.
3. Data types	Capture-mark-recapture (CMR), magnetometry, accelerometry, audio, visual, environmental (pressure, temperature, humidity, light), speed, position, internal conditions (e.g. stomach temperature or heart rate), defecation rates. See Williams et al., (2020) for a comprehensive list.
4. Data abstraction	Will the data collected by the tag be abstracted in any way whilst the tag is still on the animal (e.g. Photopoulou, Lovell, Fedak, Thomas, & Matthiopoulos, 2015), or will all data be recorded raw and processed at a later date? If so, what data do you wish to retain?

Factor	Details, considerations, and examples
5. Duty cycling	How can you program the tag to ensure that the duty cycling allows the data that is useful to you to be recorded? There are numerous trade-offs to consider with respect to device memory capacity and battery life (Holton et al., <i>In Press</i>). Video cameras draw substantial power and the footage captured requires a large memory capacity, hence duty cycling a camera to capture only useful data is a strategy to mitigate these; for example, turning on a video camera when acceleration goes above a certain threshold to attempt to capture footage to specific activities such as prey capture attempts. Duty cycling may also affect successful component functioning. For example, when recording aquatic animals that surface only briefly to breathe using GPS devices, care must be taken to ensure that duty cycling does not prevent successful position fixes being obtained. Duty cycling can also be used for data abstraction, data download, and device recovery purposes through setting patterns on the transmission rate of tags. Generally, changes in duty cycling will affect the duration the tag can be deployed and/or the size of the tag, through having to accommodate appropriate memory and battery capacities.
Class IV. Device requirements	In addressing class I-III the final tag design will accrue a number of specific requirements that it must meet. Further to those already listed, there are many other factors that should be considered in the preparation of the final device.
A. Device category (a)	Device category (a) refers to whether the tag will be an internal or external device. For the former, will the tag be implanted internally or ingested by the animal?
1. Internal	Device can be surgically implanted e.g. beneath the skin (subcutaneous) or deeper (such as directly in the heart in the case of heart rate loggers) (Horning et al., 2017). Other internal sensors are ingested, such as stomach temperature sensors (Wilson, 1992). A common example of implantable sensors is subcutaneous coded acoustic pingers for fish (Horne, 2000).
2. External	Many devices such as those which transmit to or receive data from satellites must be externally attached, such as VHF or GPS tags. Further considerations of this are provided in IV.F .

Factor	Details, considerations, and examples
3. Mixture or both	In few cases, elements of the device will be implanted and other parts exposed (e.g. Takei et al., 2016). It may be the case that two or more separate devices are attached to the animal with these being a combination of standalone internal and external devices (e.g. Liebsch, Wilson, Bornemann, Adelung, & Plötz, 2007). If using multiple devices, consider the cumulative impacts of tags and consider how multiple tags can be positioned most appropriately to minimise these impacts (Jones et al., 2011).
B. Device category (b)	Device category (b) refers to whether the tag will be an archival unit, a transmitting unit, or a combination of both. The decision here is linked closely to III.A.
1. Archival	Consideration must be made as to whether or not any data recorded should be collected and only stored on board the device (e.g. written to a flash memory card). If this is the case, the device must later be recovered to download the data.
2. Transmitting	Data can be transmitted from devices to local base stations (e.g. via the mobile phone GSM network) or to orbiting satellites (e.g. ARGOS). Transmitting devices, particularly those that transmit to distant satellites, often require far greater battery capacity in order to do so, and especially if the data packets are large.
2. Mixture	It may be that both archival and transmitting units are used on the animal either separately or together as part of the complete device, as demonstrated herein.
B. Physical properties	Ensuring that the physical properties of your tag meet the requirements of the environment that it will be subjected to is crucial.
1. Buoyancy	If the tag is likely to enter the water at some point during the deployment, what is the inherent buoyancy of the device? What is the buoyancy of the device relative to the animal? If the tag is a pop-off device, will it be buoyant enough when it has detached from the animal to be able to float to the surface and be recovered? Example: This Chapter, or pop-off tags for elasmobranchs (Whitmore et al., 2016).

Factor	Details, considerations, and examples
2. Durability	Is the tag durable and robust enough to protect it from direct impact damage? e.g. biting from predators or conspecifics, or the tag being knocked against rocks etc. If not, how much damage can the device sustain before functioning failure. In the case of a pop-off device, if the tag is damaged, will it still be able to be recovered?
3. Proofing	The device must be proofed against the environmental conditions: water ingress, pressure, humidity, temperature, UV, dust, salt residue, biofouling, snow cover. Is the device sufficiently proofed for short and long duration deployments? Example: proofing with epoxy glosscoat resin (Vosschemie, Uetersen, Germany).
4. Opacity	Does the housing need to be transparent and exposed to light in order for certain functionalities or sensors to work e.g. light sensor, solar panel.
5. Shape	The overall device shape or form will affect aero- or hydrodynamics. Hence, once a final tag design is agreed in terms of its components and characteristics, can its shape be further improved? Consider if the improvements to tag shape require an increase in size and weight (cf. Kay et al., 2019; Chapter 6).
6. Size	Size must be sufficient to accommodate all required electronic components and another features (e.g. base plate and release mechanism). Consider if the final dimensions and frontal surface area are appropriate for the animal (Solsona Berga, Wright, Galatius, Sveegaard, & Teilmann, 2015). Consider the footprint of the tag on the animal.
7. Ferrous contents	Check if ferrous materials interfere with magnetic sensors (magnetometers) or on-board compass (Bidder et al., 2015). Is there a risk that ferrous material could affect magnetoreception in animals?
8. Smoothing	Is the surface of the tag smooth or rough? i.e., is it likely to cause abrasions? Are all sharp edges rounded off to mitigate lacerations?
9. Materials	Are materials non-toxic and hypoallergenic? Are all materials inert to the environment that they will be exposed to? Will the tag be coated in a biofouling agent?

Factor	Details, considerations, and examples
10. Colour	Consider how the colour of the device may affect the behaviour of the tagged animal or its predators, prey, or conspecifics. Example: Wilson et al., (1990) observed that black tags were preferable for penguins. Alternatively, more vibrant colours may assist recovery of the device. For marine deployments, consider how the colour may change with varying light attenuation at depth.
11. Weight	Mass in air or in water. Mass of tag relative to animal. Adherence to the 3 or 5 % rule (Casper, 2009).
C. Components	Tags are comprised of multiple electronic components which each require consideration.
1. Interference	Will multiple components interfere with one-another? For example, a magnetic mandibular sensor could interfere with a magnetometer, or transmitting components may interfere with one another.
2. Battery	Will the battery be rechargeable or replaceable? What is the battery capacity? Consider the trade-offs between battery size and device memory capacity. This requires careful consideration together with the device's sampling frequency and current draw.
3. Release mechanism	If the tag is a pop-off device, what release mechanism will be used? Examples include galvanic-timed releases (GTRs) or burn wires (Whitmore et al., 2016; Mikkelsen et al., 2019; main text). Will the release mechanism work passively (e.g. GTRs) or will it be pre-determined (e.g. electronic burn wire circuit)? Will the release mechanism be manual (e.g. triggered by remote VHF) or automatic (e.g. GTR)? Define the duration after which the release mechanism should trigger and consider how this duration complements your research objectives and battery requirements, memory capacity etc.
4. Sensors	These will depend on the research objectives. For example: magnetometry, accelerometry, speed, environmental, intra-mandibular angle sensor (IMASEN), stomach temperature logger, defecation logger, position sensors (GPS, Fastloc-GPS, radio, dead-reckoning). For a guide, see Williams et al., (2020).
5. Sensor protection	Protection from short-circuiting using guronic casting resin or similar.
6. Sensor orientation	In which orientation do sensors need to be mounted. This is particularly important for triaxial sensors, gyrometers, and transmitting units.

Factor	Details, considerations, and examples
7. Sensor functioning	Careful and extensive consideration needs to be made for sensor functioning. For example, in marine deployments, the surfacing time of animals will affect the viability of satellite transmissions and GPS location estimates. Similarly, dead-reckoning sensors will accrue error over time, and water currents will affect dead-reckoned trajectories. Magnetism will affect magnetometry. Appropriate testing is required. Do some sensors need to be specially adapted for use? Example: In this Chapter I adapt an on-board pressure sensor for use as an external sensor.
8. Base plate	If the tag is a pop-off device, it will presumably release itself from a baseplate. In this case, how will the tag be affixed to the base plate? How large is the base plate? What material is the base plate made from, and what is its durability? Are the materials biodegradable? How long will the base plate remain on the animal for?
9. Labelling	If possible, allow room somewhere on the tag to include a label providing information of that tag (e.g. project ID, return address, reward label etc.).
D. Orientation of device	Knowing how you intend to orientate the device on the animal is important, particularly for the functioning of sensors such as compasses, accelerometers, magnetometers, and gyrometers.
1. On the animal	What is the optimum orientation of the device on the animal? Minimum considerations should include hydrodynamics and sensor functioning.
2. Off the animal	Is a specific orientation required for the device when it is not on the animal? Consider for example pop-off devices that must transmit from the ground or afloat once they have detached from the animal. Example: Pop-off tags for elasmobranchs (Whitmore et al., 2016). Is a counter-balance required? Ensure if using magnetoreceptors that any counterbalance is not ferrous. Is the device self-righting?
E. Positioning of device	Positioning of the device on the animal is important for device functioning, impact on the animal, and feasibility for tag deployment. The positioning of the device is often a trade-off between the optimum position for the animal and the optimum position for device functioning (Kay et al., 2019; Chapter 6).

Factor	Details, considerations, and examples
1. Optimum for animal	e.g. aerodynamic or hydrodynamic positioning. Example: tags on penguins are commonly placed towards the tail on the dorsal surface to minimise drag (Bannasch et al., 1994). Tag positioning should not impede movement (e.g. tags should not restrict head or neck movement).
2. Optimum for device	Appropriate positioning for optimum device function e.g. do any antennae need to be exposed and facing an appropriate direction whilst on the animal or following detachment?
F. Attachment	Will the tag be attached directly to the animal or will it be attached e.g. via a tether or baseplate?
1. Ring	Example: Cattle ear tags, flipper tags, bird rings. Can the tag serve a purpose further than just identification, e.g. biopsy sampling (van Neer et al., 2020). Is the ring metal or plastic?
2. Collar	Researchers must consider the potential for independent movement of the collar relative to the movement of the animal. Consider potential for the collar to restrict movement or pose a snag hazard. Collars may create abrasions, hence careful consideration of appropriate materials (e.g. silastic) and smoothing is necessary. Appropriate elasticity required for potential changes in animal morphology. Example: Collar deployments on quadrupedal mammals (Dickinson, Stephens, Marks, Wilson, & Scantlebury, 2020).
3. Harness	Considerations are similar to those for collar attachments (IV.F.2).
4. Glue	The tag could be glued directly to the animal or via other means e.g. mesh (Mazzaro & Dunn, 2009), baseplate (Peck-Richardson, Lyons, Roby, Cushing, & Lerczak, 2018), or neoprene webbing (Liebsch, 2006), amongst others. Various glue types are available e.g. epoxies or superglue. Consider glue properties: Exothermic, quick setting etc. Consider the duration required for glue to set and therefore animal handling durations. Methods for gluing e.g. dabbing on to fur and massaging in. Removal of glue at a later date e.g. captive animals. Long-lasting effects of glue e.g. hardening leading to hard edges which can become sharp and lacerate skin. Does glue penetrate beneath the fur and stick to the skin? Can glue restrict how free movement of skin?

Factor	Details, considerations, and examples
5. Suction-cup	Generally used for cetacean applications only. Often only viable for short- to medium-term attachment durations. Potential for tags to move during deployment. The force of suction-cups must be enough to overcome drag and lift forces. It is necessary to consider the potential lift forces generated by the tag and the effects this may have on pressure loading on the skin (potentially resulting in bruising or blistering at the attachment site). Example: (Shorter et al., 2014)
6. Baseplate or mesh	Attaching tags to meshes has been commonplace for deployments on seals, however meshes have been demonstrated to increase abrasions compared to alternative attachment methods (Field et al., 2012). If using a baseplate, consider the added weight of this.
7. Bolts	Example: Tags bolted to the dorsal fin in deployments on cetaceans (Andrews et al., 2019). Consider the obvious implications of the invasiveness of this attachment method, and the resulting potential for infection at the attachment site.
8. Clamp	This type of attachment method typically involves a spring-loaded clamp with friction pads or spikes to hold a tag in place. Example: Tags clamped to the dorsal fin of elasmobranchs (Gleiss et al., 2009).
9. Downforce	Specific to deployments of tags on free-swimming, continuously moving organisms such as elasmobranchs whereby the tag is held on to the animal via resultant hydrodynamic downforce while the animal swims (e.g. Pavlov & Rashad, 2012)
G. Data recovery	Data from devices can be recovered either remotely via transmission telemetry or recovered manually from archival devices.
1. Remote download	Data transmission via local base station (e.g. Clark et al., 2006) or satellite (Fancy et al., 1988).
2. Animal recapture	Difficulty and stress involved in animal recapture. Easier with certain species e.g. nesting birds, pinnipeds returning to ice holes. Example: Penguins returning to their nest (Sala, Wilson, & Quintana, 2014).
3. Pop-off	Data may be stored in an archival tag which remotely releases from the animal. Data are recovered by recovery of the device and subsequent data download.

Factor	Details, considerations, and examples
4. Recovery effort	The recovery effort associated with different data recovery methods is highly variable. Data that are downloaded via remote download can be active or passive. For example, you may need to login to satellite portals to retrieve data (active) or data may be sent automatically to the recipient via email (passive). Animal recapture involves large amounts of effort which may include tracking animals using recent satellite locations and/or radio telemetry. Recovery effort for data from pop-off devices can vary from active searching for tags on foot, via plane, or via boat. All recovery efforts involve a degree of monitoring post-deployment.
H. Preparation and functioning	There will be a range of requirements in terms of device preparation and functioning depending on the complexity of the tag and its sensors. For example, some “off-the-shelf” tags cannot be modified, whereas homemade or bespoke tags may have complex programming features such as duty cycling.
1. Calibration	In the field or in the lab. Consider the varying magnetism at calibration sites compared to deployment sites and the potential effects on magnetoreceptors. Consider clock off-sets. Difficulty of calibration in the field – preparation of tag in the field may mean an animal has to be restrained for longer while the device is set up.
2. Programming	Check that the device has been programmed correctly.
3. Testing	Check that all components of the devices been tested. This includes both electronic components and auxiliary components such as release mechanisms or attachment methods. Ensure that tags are tested in conditions that will be similar to expected deployment conditions – e.g. in marine applications, expected salinity, temperature, pressure. If the tag is required to float at the surface with positive buoyancy for an extended period, make sure to conduct this test over appropriate time periods.. It may be the case that water ingress over time compromises the buoyancy and/or float orientation of the device (see Appendix S5.2). Consider replicating animal behaviour in testing, for example accounting for seal haul-out cycles when testing saltwater corrosive release mechanisms.

Factor	Details, considerations, and examples
4. Device activation	How will the device be activated? If devices are being activated by a manual switch e.g. a physical or magnetic switch, is the switch accessible once the device is fully constructed and all components have been assembled? Alternatively, the device could be activated automatically by a saltwater switch (SWS) – note that the tag design needs to be built appropriately so that a SWS functions correctly; see the design of the tag presented herein – or by a pre-determined duty cycling procedure (e.g. a timestamp). Finally, devices could be activated remotely via a transmitted signal (e.g. radio frequency) – ensure that no other transmitting units interfere with one another.
5. Priming	Numerous satellite transmitting devices need to be, and benefit from being, primed before deployment. This means that tags are switched on in the near vicinity of the animal capture location to collect some initial location estimates which aids the tag's location filtering algorithms. Always read instruction manuals for your device components and conduct trial missions before deployment in the field.
6. On-board processing	Consider on-board processing of data (Cox et al., 2018)
7. User friendly	Can the device be programmed and set up ready to deploy with minimal expertise or using simple instructions? Does the user require advanced prior knowledge? Is there bespoke software associated with setting up the device? What technical support is available to the user in the event of malfunction? Can devices be reset in the field? Does a reset require a laptop or internet connection?
8 Updates	Software or firmware updates. Are all device components fully up to date?
9. Retrieval	What is required to retrieve the data from the device once the device has been recovered? Consider any additional equipment required (e.g. tracking equipment).
10. Reusability	Is the device reusable in its entirety or can only certain components be recycled? For example, can disposable batteries be replaced, or rechargeable batteries recharged.
11. Data and memory	Ensure that the device will not overwrite previously stored data. Ensure that there is enough memory capacity in the device to collect all of the data required.
12. Sterilisation	How will the tag (and associated equipment) be sterilised prior to deployment on animals?

Factor	Details, considerations, and examples
13. Documentation	Adequate documentation is required to ensure all tag details are recorded. Example: Appendix S5.7. Good time keeping is paramount. Photographic or video evidence of tag deployments is strongly recommended.
Class V. Device cost	The cost of devices is often one of the key considerations for many researchers. Keeping costs to a minimum is important, especially if the research requires a large sample size.
A. General	These are the general costs that a researcher is likely to incur that are directly associated with the tag unit(s). These include components and parts, updates, malfunctions, and other miscellaneous costs.
1. Components	Cost of individual components. Replaceable components e.g. batteries. Number of uses. Likelihood of device recovery.
2. Updates	Cost for software or firmware updates (including licensing costs).
3. Malfunctions	Costs associated with fixing malfunctions.
4. Miscellaneous	Delivery fees, import tax, insurance, bulk order discounts.
B. Services subscriptions	For some services, a subscription fee is required (e.g. ARGOS satellite network).
1. Satellite fees	Example: The ARGOS satellite network charges a €15 monthly fee per active platform (tag), plus €4 per day for any transmitting platform.
2. Software fees	Fees to purchase and update licenses for use of service subscriptions.
C. Additional equipment	Additional equipment may be required for the correct functioning or testing of your device.
1. Recovery tools	Example: ARGOS transmitting tags can be recovered locally but may require specialised satellite tracking equipment – a Goniometer.
2. Building materials	Depending on how your device is constructed, there may be costs associated with consumables (see Table 5.1). Example: Guronic casting resin may be used to seal electronics from water ingress.
D. Deployment costs	There are substantial costs associated with field deployment efforts which need to be considered in the costing of a tag.

Factor	Details, considerations, and examples
E. Recovery costs	Same as V.D. Additionally, consider costs involved in offering a reward for device retrieval by a member of the public e.g. Hays et al., (2012) offered members of the public a £25 reward for finding their tags.
Class VI. Deployment	
A. Conditions	Can the device be deployed in all conditions? e.g. wind, rain. Consider how many tags can be deployed in the same deployment and thus the number of animals that need to be captured at a time versus the number of required capture attempts.
B. Equipment	What other equipment is required to deploy the device? e.g. laptop for programming, boat for reaching animal capture site.
C. Personnel	Are any other personnel required for the deployment of the device, or can it be done singlehandedly? Vets, animal capturers, licensee holders, coxswains, towers. Ensure that the team will have the skills and experience necessary to deploy the device(s) or if so ensure that training is undertaken prior to deployment.
D. Magnetic field	The earth's magnetic field changes continuously. If you are using magnetometers in your tag it will be important to consider the earth's magnetic field in the deployment locale during the deployment period.
E. Practice	If possible, conduct full trial runs with the devices to ensure you are well versed in how they will be deployed. Note this builds on the tag-specific preparations listed in IV.H.
Class V. Miscellaneous	
A. Unit delivery	Consider the lead times on items when purchasing. Do not leave purchasing your tag equipment until the last minute as some manufacturers may take several weeks to deliver. Consider the varying stock of tags that manufacturers may have; this may vary seasonally (e.g. typically high demand leading up to and during Summer fieldwork seasons).

Factor	Details, considerations, and examples
B. Permitting and licensing	Ensure that your tag meets any specific requirements outlined by relevant permits or licensing restrictions for your research. For example, it may be that permits preclude you from deploying tags with explosive release mechanisms.
C. Futureproofing/patenting	Consider how you might design your tag in such a way that it can be used again, or easily adapted, in future by you and other researchers. Once your device is well tested and has been proven to be successful, consider patenting your device.

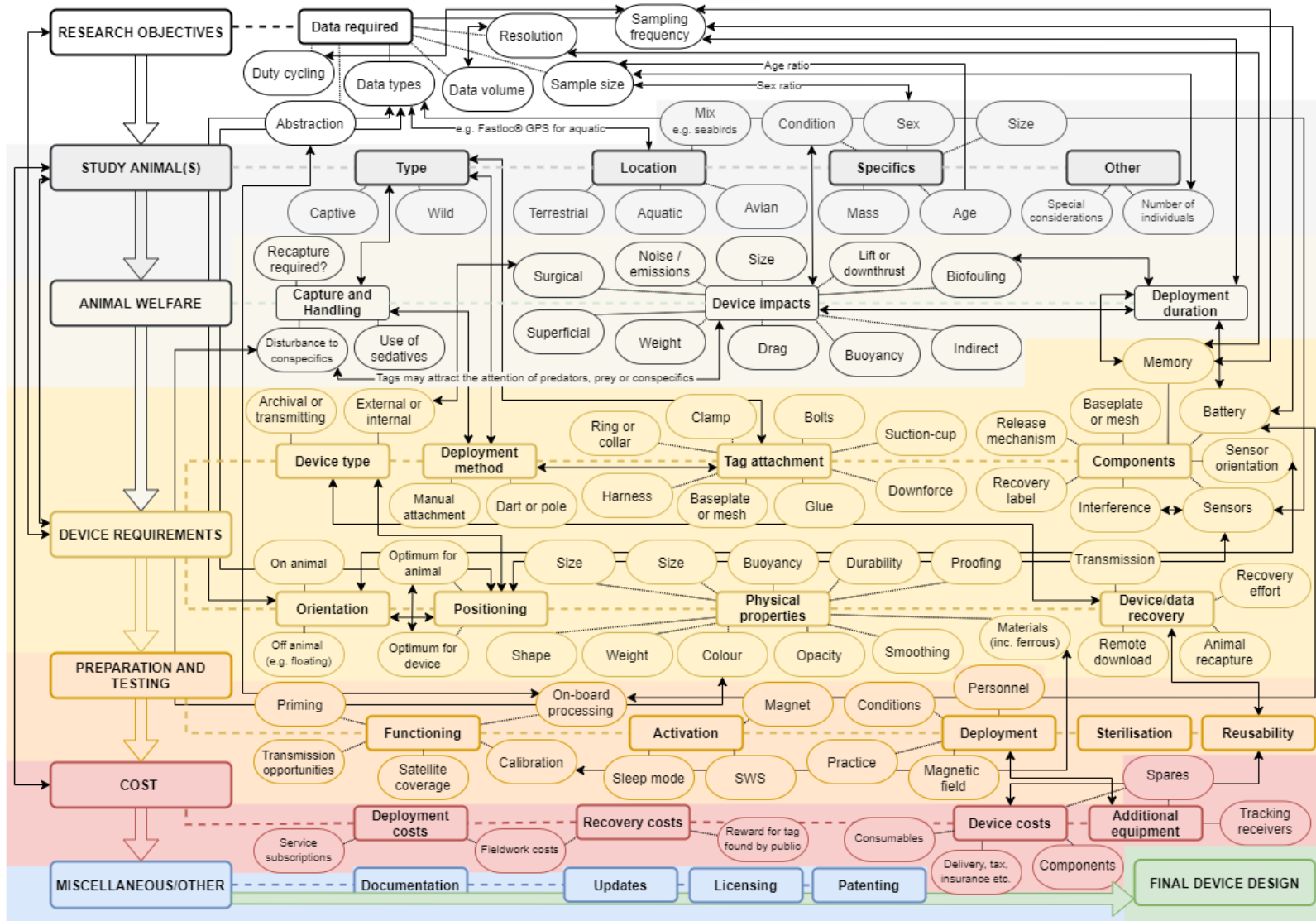


Fig. S5.1. Flowchart highlighting all of the considerations required when developing tags and the links between them (see Table S5.1).

Appendix S5.2: Lessons learnt through constructing tags

In addition to the list of considerations outlined in Table S5.1, the process of development and construction of the tag presented herein expectedly gave rise to a number of teething issues which are not easily described in the form of an inventory. The challenges of these lessons learnt, if not readily described, are likely to stall progress again in future for other researchers who may be naïve to them. Indeed, a recent best practices in tagging workshop highlighted the need to report more frequently on things that “went wrong”. While some – but not all – of the lessons learnt are notably minor and hence may be considered trivial, they nevertheless limit progress. There is always the risk that others in future might repeat these mistakes, and hence it is therefore preferable to anticipate them from the outset. The following short list highlights both a number of lessons learnt that others could avoid in future, as well as a few useful tips and tools:

- **Electronics wiring:** It is sensible and hence inevitable to size up a tag housing to accommodate the constraints that the main electronic components require and design it so that it is “made to measure”. For example, for my tag I developed a housing to accommodate the Daily Diary IMU (26 x 17 x 5 mm) and a battery (26 x 17 x 7 mm). The researcher must however make sure to provide some additional room to allow for the wiring!
- **Component insulation:** Guronic can be used to insulate electronic components. This will prevent them from water ingress as well as providing some additional protection from direct physical damage.
- **Component movement:** I found that in some cases electronic components were moving inside their housings independently of the movement of the animal. This movement, commonly referred to as “jiggle” (cf. Cade, Barr, Calambokidis, Friedlaender, & Goldbogen, 2017), is particularly consequential in tags that measure fine-scale movement at high sampling frequencies, such as accelerometers or magnetometers (Williams et al., 2020). This movement is generally not wanted and one of the most efficient ways I was able to deal with it was to surround the electronic components within the housing with semi-

rigid packaging foam (STPE200 Ethafoam, eFoam, UK). This has the potential to reduce the noise in the data produced by stochastic motion of tag components.

- **SD card teething issues:** When programming SD cards, always be aware of potential “lock” switches. These are manual switches which prevent formatting or overwriting.
- **GTR corrosion:** If GTRs are positioned inside a cavity, ensure there is ample clearance around the GTR to allow sufficient water flow equally across it. This will ensure that corrosion rates are accurate and prevent the build-up of corroding material residue (Fig. S5.2). The tag shown in Fig. S5.2 had been submerged in a saltwater tank for 24 hours. However, note that the water here was stationary, and the residue was easily flushed out when water flow was initiated; only very little build-up of corroding material residue was observed under test conditions with water flow; this highlights the importance of testing under expected field conditions (Appendix S5.1: **IV.H.3**).
- **GTR disconnection:** When the GTR corrodes and the link breaks, the eyelets should retract from the housing allowing the tag to separate from the baseplate. In one test however I observed that the eyelets became stuck inside the GTR cavity. To overcome this, ensure that there is ample room for the eyelets to retract. I achieved this by filing down the entrance to the cavity at both sides to allow greater room for the eyelets to exit and make it so that the route the bungee cord pulled the eyelet out of the cavity was along a rounded corner.
- **Tag flotation:** The overall housing of the tag presented herein was porous to water however water ingress was slow. This was not an issue as far as the electronic components were concerned as each of these were contained within their own separate housings which were integrated into the overall tag housing. One issue which did arise however was that, in testing the flotation of the tag, I found that tags were initially presenting as being buoyant but over an extended time period - as water made its way into the tag housing - they began to sink below the surface. I hence further encourage researchers to conduct

tests of their tags that are comparable to real field deployments; if the tag is required to float at the surface with positive buoyancy for an extended period, make sure to conduct this test over appropriate time periods.



Fig. S5.2. An example of GTR corrosion build up.

Appendix S5.3: Fastloc-GPS performance

Test deployments

Note that all Fastloc-GPS devices were tested in the following tests. These include the Fastloc-GPS devices deployed in both my final tag design (presented in the main text) and my first tag design (Appendix S5.4).

- Test 1; 163 m; Cefn Bryn trig point; 51.587579 N, -4.175104 E:

General

Time device due to start	09:00:00
Time first fix attempted	09:00:15
Expected number of fix attempts	144
Number of fixes attempted	144
Proportion of fixes attempted	100 %
Number of fixes obtained	111
Proportion of fixes obtained versus fixes attempted	77 %

Spatial error

	(m)
Minimum	1.4
Lower quartile	16.5
Median	30.3
Upper quartile	45.1
Maximum	987
Mean	76.5
Variance	24.7
Standard Deviation	157.2

- Test 2; 0 m; Swansea Bay 1; 51.606931 N, -3.978508 E:

General

Time device due to start	09:01:00
Time first fix attempted	09:01:09
Expected number of fix attempts	110
Number of fixes attempted	110
Proportion of fixes attempted	100 %
Number of fixes obtained	90
Proportion of fixes obtained versus fixes attempted	81.8 %

Spatial error

(m)

Minimum	2.1
Lower quartile	17.9
Median	28.8
Upper quartile	42.3
Maximum	434.9
Mean	44
Variance	3.74
Standard Deviation	61.2

- Test 3; 0 m; Swansea Bay 1; 51.6067 N, -3.978283 E:

General

Time device due to start	14:30:00
Time first fix attempted	14:30:08
Expected number of fix attempts	200
Number of fixes attempted	200
Proportion of fixes attempted	100 %
Number of fixes obtained	144
Proportion of fixes obtained versus fixes attempted	72 %

Spatial error

(m)

Minimum	1.7
Lower quartile	13.3
Median	21.7
Upper quartile	39.6
Maximum	861.4
Mean	42.6
Variance	7.2
Standard Deviation	84.8

- Test 4; 5 - 75 m; Coastal route; Start: 51.571605 N, -3.986582 E:

General

Time device due to start	13:30:00
Time first fix attempted	13:30:18
Expected number of fix attempts	120
Number of fixes attempted	120
Proportion of fixes attempted	100 %
Number of fixes obtained	94
Proportion of fixes obtained versus fixes attempted	78.3 %

Spatial error

(m)

Minimum	0.81
Lower quartile	4.68
Median	15.1
Upper quartile	53.3
Maximum	229
Mean	33.93
Variance	2043.2
Standard Deviation	45.2

Wild deployments

- Tag 2

Time device first entered water	10:32:24
Time first fix attempted	10:51:00
Maximum potential number of fix attempts ⁴	4754
Number of fixes attempted	1099
Proportion of fixes attempted	23.1 %
Number of fixes obtained	693
Proportion of fixes obtained versus fixes attempted	63 %

- Tag 4

Time device first entered water	11:33:00
Time first fix attempted	11:36:29
Maximum potential number of fix attempts ⁶	208
Number of fixes attempted	128
Proportion of fixes attempted	61.5 %
Number of fixes obtained	59
Proportion of fixes obtained versus fixes attempted	46.1 %

- Tag 7

Time device first entered water	10:31:56
Time first fix attempted	10:32:33
Maximum potential number of fix attempts ⁶	6625
Number of fixes attempted	2374
Proportion of fixes attempted	35.8 %
Number of fixes obtained	1268
Proportion of fixes obtained versus fixes attempted	53.4 %

- Tag A

Time device first entered water	10:49:20
Time first fix attempted	11:08:52
Maximum potential number of fix attempts ⁶	1370
Number of fixes attempted	790
Proportion of fixes attempted	57.7 %
Number of fixes obtained	616
Proportion of fixes obtained versus fixes attempted	78 %

- Tag C

Time device first entered water	11:34:51
Time first fix attempted	11:45:47
Maximum potential number of fix attempts ⁶	4706
Number of fixes attempted	2464
Proportion of fixes attempted	52.4 %
Number of fixes obtained	1715
Proportion of fixes obtained versus fixes attempted	69.6 %

Appendix S5.4: Previous tag design and appraisal

The tag design presented herein is the final product following iterative design iterations over the course of two years. With each modification to the design lessons were learnt and built upon. In this supplementary note I present details of an earlier tag design and the lessons learnt which led to the development of the final tag design presented in the main text, appraising the limitations and my justification for adapting the design.

My first tag design incorporated the same animal tracking devices as the final tag design presented in the main text – a daily diary (DD), Fastloc-GPS, and VHF transmitter – with the exception of the pressure sensor which was a PA-4LD 30 bar pressure sensor (Keller Ltd., Dorchester, UK) measuring 4 x 11 (diameter) mm. The structure and shape of the tag, arrangement of the devices, and the release mechanism were different to the final tag design (Fig. S5.4.1). Specifically, the tag was made entirely from flotation mixture with no 3D printed sections (see main text and Table 6.1), and was near-triangular in shape with tapering from the nose; this shape was drawn up using CAD software as for the tags described in the main text and measured 11 × 10 × 4 cm. All three animal tracking devices were positioned side by side and were set into the flotation mixture, being glued in place with super glue. The DD housing measured 55 x 35 x 30 mm (including the rear plug and screws) and in this case the DD was positioned above the battery inside the housing. The GTR was positioned at the nose of the tag in a small cavity and was fixed to a thin (1 mm), polycarbonate baseplate using two cable ties which ran from the nose to the rear of the tag. When the GTR corroded, the tag would become completely free to detach from the animal and float to the surface, though the cable ties and baseplate would remain. The underside of the tag included a 25.3 g lead counterbalance just off centre which allowed the tag to float at the surface with the VHF transmitter exposed (Fig. S5.4.1). The tag weighed 290 g in air (including the lead counterbalance) and had a buoyant force of 0.36 N.

I deployed 3 tags (A, B, and C) of this design on harbour seals in Lorenzensplate on the 10th October 2017 (Table S5.4.1) using the same methods as described in the main text. All tags were deployed with D4 model

GTRs in 13 °C waters (see main text) and were expected to remain attached to the animals for 5.5–6.5 days. Devices were programmed with the same programming schedule as for tags deployed in April 2018 (see main text). To aid recovery of the devices, a public message was posted to a local online nature conservation group to ask for volunteers to look out for my tags washing up on the Wadden Sea coastline. 4 search efforts were conducted including by land, sea, and air (Table S5.4.2; Fig. S5.4.2) but no transmissions were detected on any search effort. Two tags were eventually recovered – one on the 27th October in Houvig Strand, Denmark (tag B) and another on the 14th November (tag A) in St. Peter Ording. Both tags were recovered by beachgoers. Interestingly, from the Fastloc-GPS data collected, I predict that tag A would have been drifting near Süderoogsand on the 17th October when a search was being conducted by land, and had washed up on Süderoogsand by the 19th October colleagues were searching by boat – passing the location within a distance of 3–4 km. However, the tag was not detected on either occasion. This performance of the VHF transmitter was disappointing but I cannot rule out the potential for signal attenuation if the VHF antenna was wet or buried (see main text). Based on the Fastloc-GPS data I anticipate that no tags were in the vicinity of the search on the 27th October. On the 7th November a search was conducted by plane from Büsum, Germany to Limfjord, Denmark at up to 20 km offshore (Fig. S5.2). Based on the location and date of its discovery, I speculate that it is highly likely for this search effort to have passed tag C, but the tag was not detected.

Both tags A and C were in good condition on recovery except for the DD in tag C which had suffered from water intrusion and was corroded. I suspect that this was due to the o-ring not having sealed sufficiently (either because the o-ring was too thin, or because not enough silicone grease had been applied). All other devices were in good condition and functioned normally in post-recovery testing. Unfortunately, the DDs in both tags had malfunctioned during deployment and I was unable to obtain any data that were usable. Specifically, the data resembled flatlines on all recording channels (Fig. S5.4.3; main text). The Fastloc-GPS data from tag A lasted 1 day and 19 hours, suggesting the tag had released prematurely at this time. The data showed that the seal

remained in the vicinity of the tagging site for 1 day before heading 46 km south west to, presumably, conduct a foraging trip. There is a break in the GPS data here for 7 days before a cluster of positions were collected at the sandbank just north of Süderoogsand for the following three days. Interestingly, this tag was eventually found at St. Peter Ording some 25 km south of this position. I suspect the tag had been washed up on the beach and was eventually re-floated on the tide and drifted southwards (Fig. S5.4.4). The Fastloc-GPS data from tag C lasted 6 days and 10 hours, indicating that the tag remained attached for the correct duration. The data show that the seal remained in Lorenzensplate for two days before conducting a foraging trip to 20 km offshore. The seal returned to Lorenzensplate for two more days before rapidly travelling northwards 75 km towards Sylt. The tag appears to have detached halfway along this route. The tag was eventually found a further 115 km north (Fig. S5.4.5).

From developing, building, and deploying these tags I learnt a number of lessons that aided me in my development of the final tag design presented in the main text. In particular, this first tag design had a number of distinct pros and cons in contrast to my final design, as follows:

Pros

- In being made entirely out of flotation mixture, this tag design was more robust to damage than my final design.
 - It was relatively easy to accommodate GTRs of larger sizes without requiring an increase in tag size – to do this you would simply need to mill out a larger cavity at the nose of the tag.

Cons

- Not enough room to include a SPOT transmitter
- Correct floating orientation (for when the tag had detached from the animal) was relatively difficult to achieve well and likely would be even more difficult to achieve if attempting to include a SPOT transmitter due to the counterbalance required.
- The tag being made entirely out of flotation mixture meant that a greater amount of work was required to prepare the tags both in terms of

constructing the tag out of resin and microspheres, and in milling the cavities to set the electronic devices.

- The tags required a larger amount of unrecyclable resources (particularly resin and microspheres) which also created greater wastage from the construction process.
- I was not happy with how secure the tag was using the GTR and cable tie attachment method. In particular, there was quite a lot of lateral movement in the tag which would have created noise in the IMU data as well as potentially risk early detachment.
- When the tag had detached, the cable ties remained on the baseplate until the baseplate fell off during the annual moult. This risked entanglement issues to the animal. Compared to my final tag design, the cable ties would not have slipped freely as easily had the animal become entrapped.
- In attaching the release mechanism, I noted that the nose and rear of the baseplate lifted up slightly if the cable ties were too tightly tensioned. This jeopardised the ability for the glue to set the baseplate to the seal's pelage. Moreover, a small lip at the front of the baseplate would likely increase drag and hence affect hydrodynamic performance of the tag as well as risk early detachment.
- The routing of the cable ties through the baseplate and back to the GTR (see Fig. S5.4.1 c–d) meant that cable ties were pressing directly on to the pelage of the seal.
- The surface area of the baseplate was substantially larger meaning that a greater amount of glue needed to be applied.
- The flexibility of the baseplate meant that it bowed slightly around the curvature of the seal's pelage which meant that the tag did not sit level on the baseplate.

In addition to the list of pros and cons above, the key reason for choosing to design a more elongated tag was based on the malfunctioning of both DD devices in tags A and C. Specifically, it was possible that the very close proximity of the VHF transmitter to the DD device may have caused the

malfunction (Wilson, *pers. comms.*). Interestingly, in all of the tests that I conducted, this was not the case. Nevertheless, this type of transmitter interference has been documented previously (Wilson, *pers. comms.*). Hence, to rule out any potential interference, I specifically designed my next tag (presented in the main text) such that the VHF (or SPOT) transmitter were positioned further away from DD device.

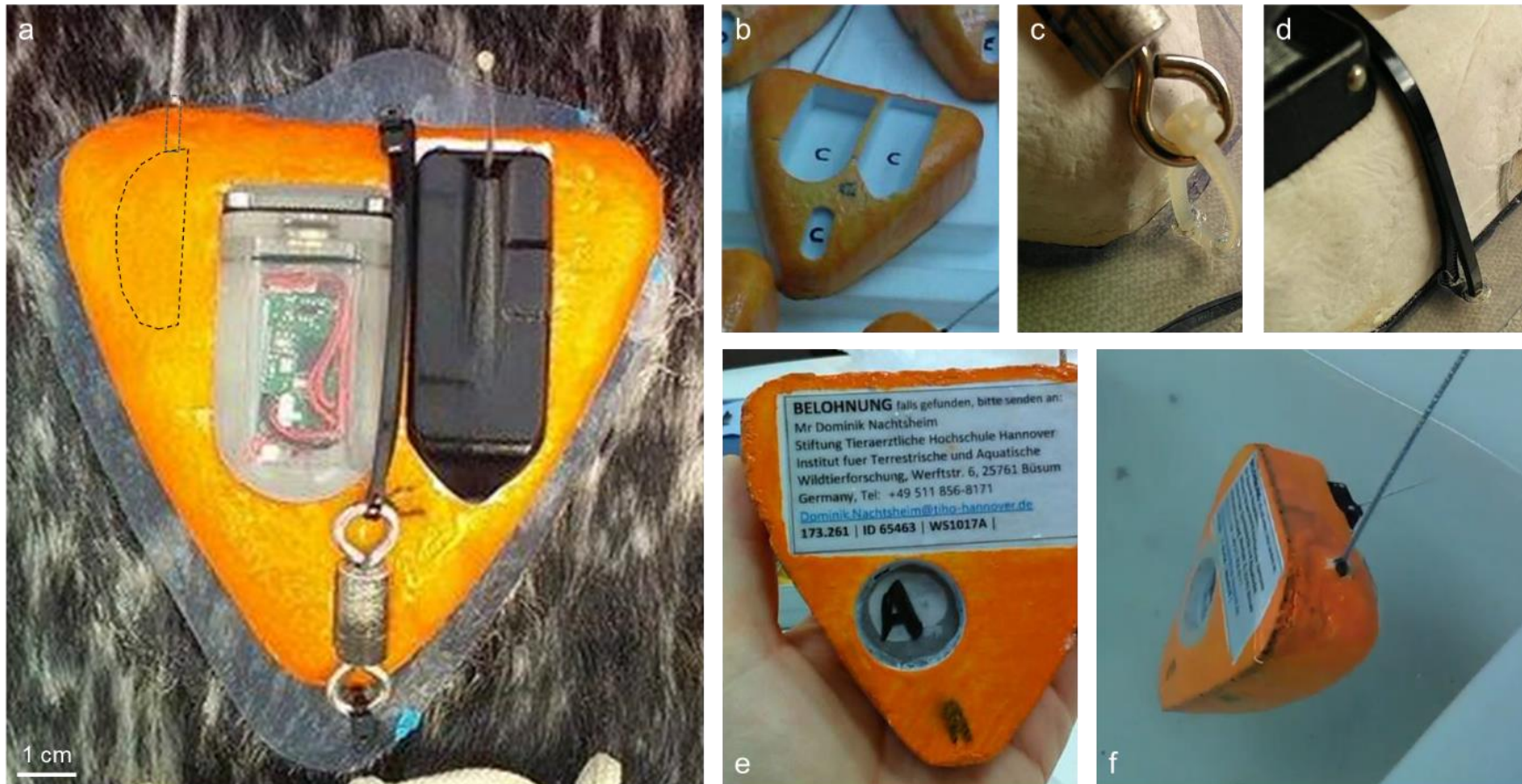


Fig. S5.4.1. The first seal tag design. (a) Tag attached to a harbour seal. The GTR (grey) is positioned at the nose, Fastloc-GPS (black) positioned on the right, DD (green in transparent housing) positioned just off centre and VHF positioned on left inside flotation mixture (dotted outline indicates position). (b) Tag shown prior to devices being glued into place. (c) View of the cable tie attaching the front of the baseplate to the GTR. (d) View of the cable tie attaching the rear of the baseplate to the GTR. One of the Fastloc-GPS' saltwater switch sensors are also visible. (e) underside of the tag showing the reward label and the lead counterbalance. (f) The floating orientation of the tag exposing the VHF transmitter.

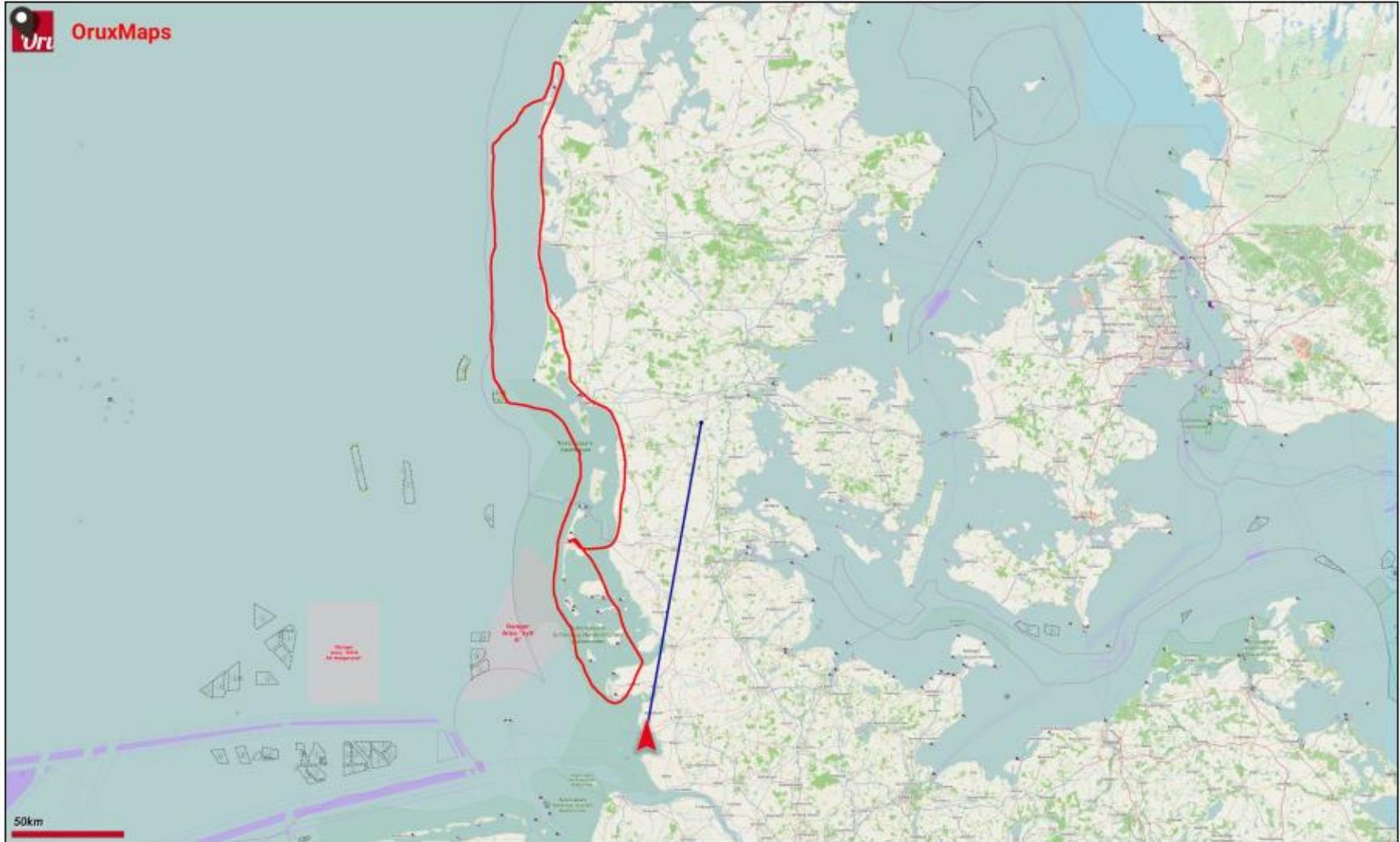


Fig. S5.4.2. The search route taken by plane from Büsum to Limfjord on the 7th November to attempt to detect the tags via VHF.

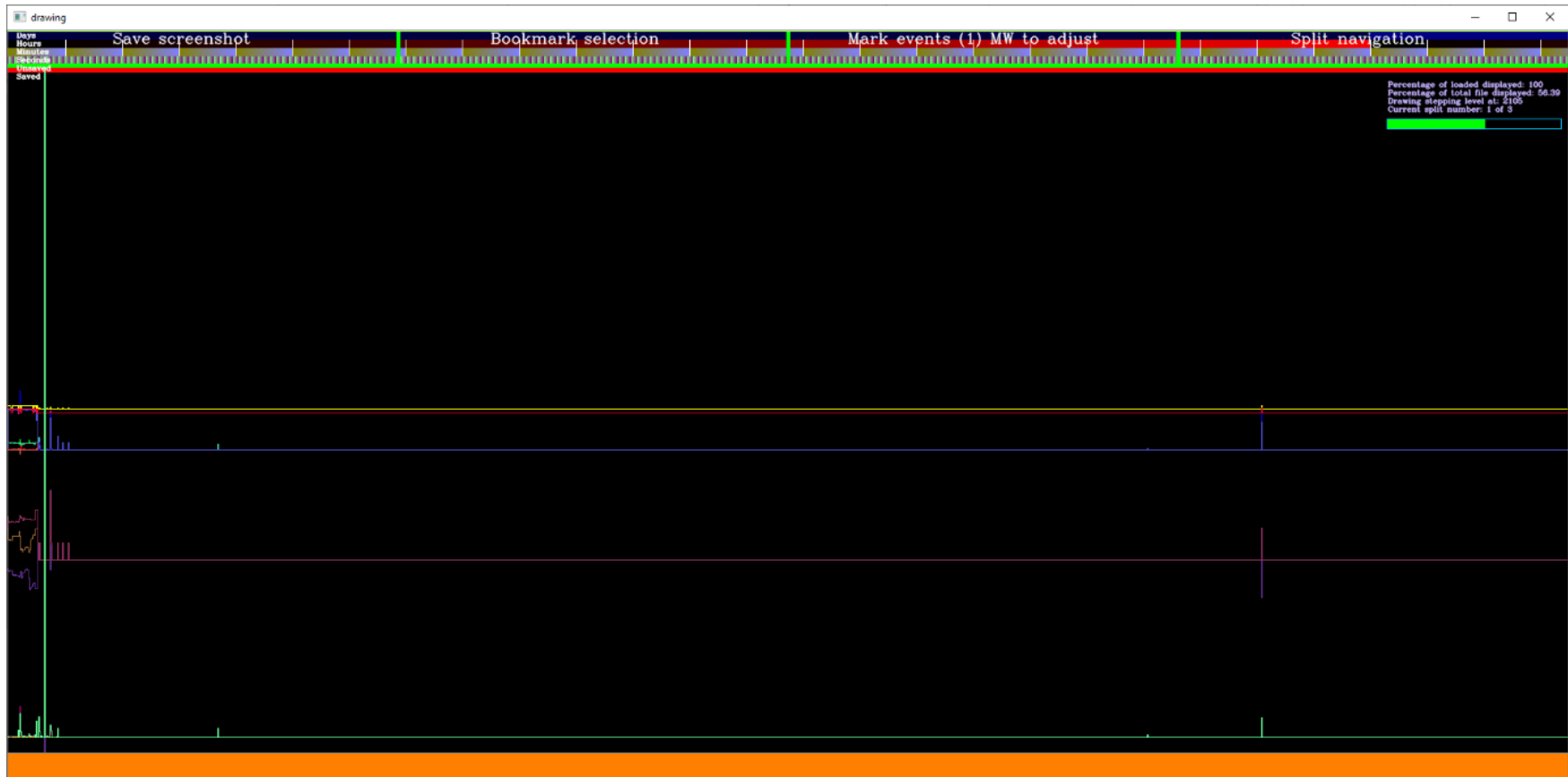


Fig. S5.4.3. An example of the data collected by the DDs which malfunctioned in both tags A and C.



Fig. S5.4.4. Fastloc-GPS trajectory collected by tag A. (a) The location of the tagging site (54.439167 N, 8.643889 E). (b) The suspected location of tag detachment. (c) GPS locations detected from when the tag is presumed to have washed up at the beach north of Suderoogsand. (d) The approximate location of tag recovery.

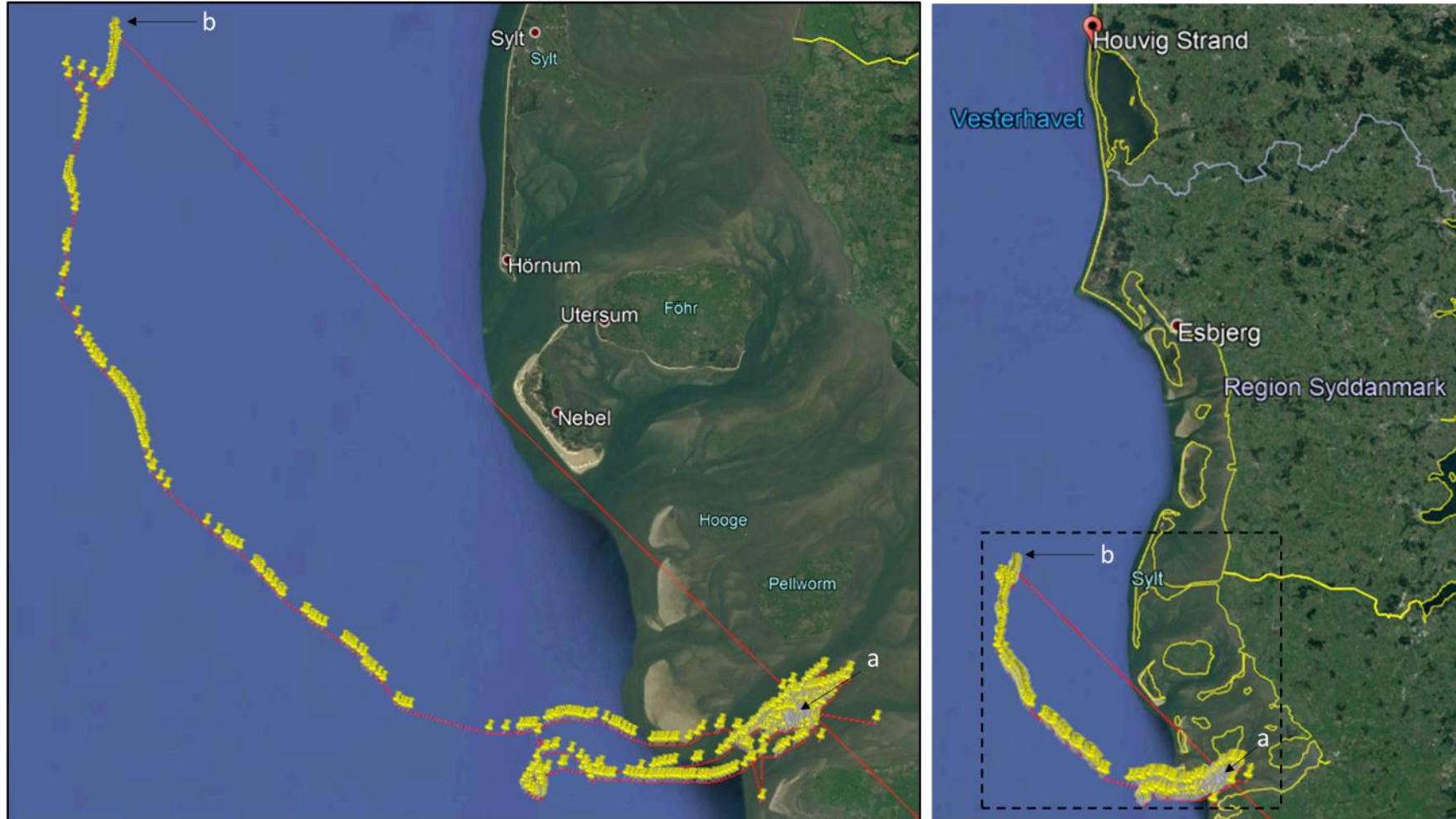


Fig. S5.4.5. Fastloc-GPS trajectory collected by tag C. Left panel shows zoomed section for ease of viewing the recorded trajectory. Right panel shows location of final tag recovery at Houvig Strand, Denmark (a) The location of the tagging site (54.439167 N, 8.643889 E). (b) The suspected location of tag detachment. The red line extended south west after the end of the trajectory results from an erroneous record.

Table S5.4.1. Tag deployment and summary details of the three first design tags deployed in October 2017.

ID	Transmitter	Baseplate	GTR	Species	Region	Age	Sex	Deployed	Recovered	Data	Issues	Positives
A	VHF	Polycarbonate	D4	<i>P. vitulina</i>	Lorenzensplate	Adult	M	10/10/2017	14/11/2017	Fastloc-GPS (2 days) DD (2 days)	DD malfunction Premature release	Tag in good condition.
C	VHF	Polycarbonate	D4	<i>P. vitulina</i>	Lorenzensplate	Adult	F	10/10/2017	27/10/2017	Fastloc-GPS (6.5 days) DD (11 hours)	Saltwater intrusion DD malfunction	GTR released as expected
D	VHF	Polycarbonate	D4	<i>P. vitulina</i>	Lorenzensplate	Adult	F	10/10/2017	NA	NA	NA	NA

Table S5.4.2. Search and recovery efforts for the three tags deployed in October 2017.

Date	Search	Tracking	Details
17/10/17	L1	VHF	Searched various places along the Lorenzensplate coastline. Nothing heard from tags A, B, or C.
19/10/17	B1	VHF	Searched various places along the Lorenzensplate coastline. Nothing heard from tags A, B, or C.
27/10/17	L2	VHF	Searched the coastline from Lorenzensplate to Rømø. Nothing heard from tags A, B, or C.
07/11/17	P1	VHF	Covered the entire coastline from Büsum, Germany to Limfjord, Denmark, including 20 km offshore (Fig. S3.2). Nothing heard from tags A, B, or C.

Appendix S5.5: Float preparation protocol

The following protocol outlines step-by-step instructions for the construction of a custom flotation package for biologging devices used in marine deployments. The two main components required for the float are epoxy glosscoat resin and Omega-Spheres ®; these are combined in a 7:3 mix ratio (Liebsch, 2006) producing a mixture with an approximate density of 0.33 (g/ml). Note that the epoxy glosscoat resin itself consists of two components: Parts A and B which need to be mixed in a 10:4 ratio. In summary, the method involves combining these two components before packing the resultant mixture into a float mould (Fig. S5.5a). Dummy casts or blocks are fitted to leave room for tag components to sit after the flotation mixture has set (Fig. S5.5b).

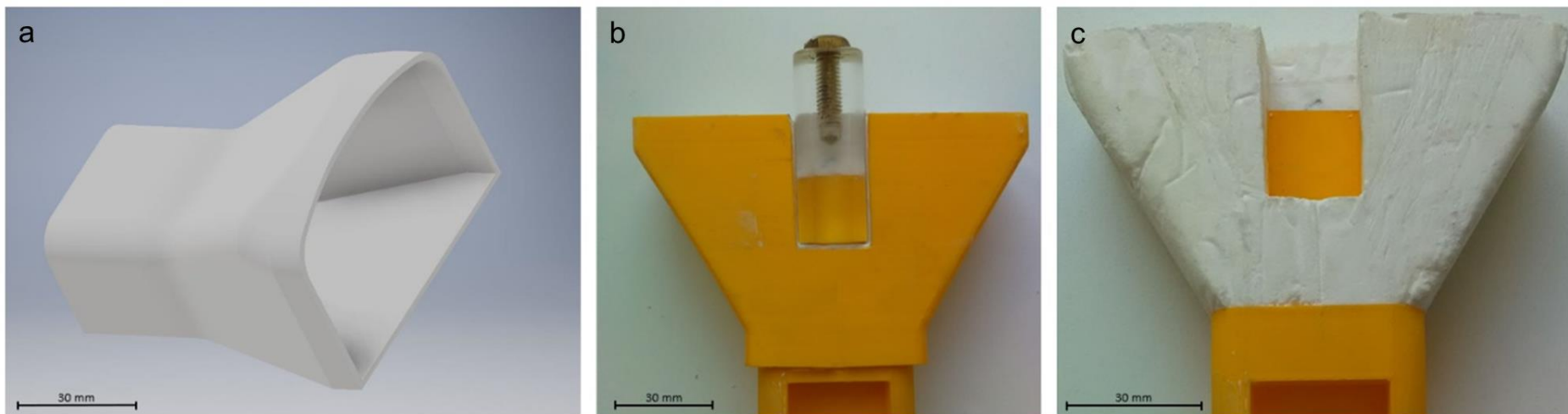


Fig. S5.5. (a) An example of a 3D printed mould in which the flotation mixture was packed. CAD software (Autodesk® Inventor LT™, Autodesk Inc., California, USA) was used to design the mould. This software can also tell you the internal volume of the mould. (b) A tag with a mould encasing the rear of the tag. A polycarbonate dummy block is fitted in place of where the SPOT tag will later sit. Both the mould and the dummy block are wrapped in taugt clingfilm and sprayed with Ease Release 200™ prior to the mixture being packed into the mould. (c) A finished flotation. Note the creases that are left from the clingfilm. There is an obvious cavity leftover from where the dummy block was fitted.

Equipment:

Materials/tools	Supplier
Epoxy glosscoat (fibreglass resin)	http://www.vosschemie.eu/
Omega-Spheres® (hollow glass microspheres)	http://www.elminas.com/osthoff-omega-group/?lang=en .
Ease Release™ 200 (release agent)	http://www.benam.co.uk
Float mould (e.g. made from Floreon 3D PLA)	http://floreon.com
Dummy casts or blocks (e.g. made from Engineering Grade Translucent Polycarbonate Rod)	http://www.plasticstockist.com/
Weighing scale (precision: 0.1 g)	Various
PVC Clingfilm (Caterwrap) and Sellotape	Various
Pouring container (x 2)	Various
Large container or mixing bowl	Various
Wooden mixing sticks	Various
Personal Protective Equipment e.g. disposable gloves, mask, lab coat	Various

Instructions:

Work to be conducted in a fume cupboard. Full PPE to be worn; disposable gloves, mask, and lab coat. Note it is recommended to wear two pairs of disposable gloves as it is convenient to remove one pair halfway through the protocol (see below)

Step 1: Calculate the mass (m) of the resin and microspheres required for the mould (Fig. S3.1) using $m = V * \rho$; where V is the mould volume and ρ is the mixture density.

- e.g. for a 300 ml mould, $m = 300 * 0.33$, therefore a total of ~100 g mix is required.

Step 2: Calculate the mass of constituent parts (resin and microspheres) in 7:3 ratio.

- Resin: $(100 \text{ g} \div 10) * 7 = 70 \text{ g}$
- Microspheres: $(100 \text{ g} \div 10) * 3 = 30 \text{ g}$

Step 3: Due to its high viscosity, when mixing the epoxy glosscoat resin in a later step (Step X), some of the mixture is likely to stick to its pouring container. Hence, it is advisable to use some extra resin which is in addition to the amount

that has been calculated in Step 2. From experience, an additional 5 g is ample. Thus,

- Resin: $70 \text{ g} + 5 \text{ g} = 75 \text{ g}$

Step 4: Calculate the mass of constituent parts of resin required to make up 75 g total:

- Part A: $(75 \text{ g} \div 14) * 10 = 53.6 \text{ g}$
- Part B: $(75 \text{ g} \div 14) * 4 = 21.4 \text{ g}$

Step 5: Weigh out parts A and B each into separate, pourable containers. Do not mix yet.

Step 6: In a large mixing bowl or container, weigh out the required microspheres and spread them evenly. Do not add the resin yet.

Step 7: Prepare your mould and dummy block(s). Specifically, wrap clingfilm tightly around the mould and dummy block(s); make sure to cover all edges. Ensure as best as you can that the clingfilm is laid taught so that air pockets and creases do not form; Sellotape can be helpful for this.

Step 8: Once wrapped in clingfilm, generously spray both the mould and dummy block(s) with the release agent (Ease Release 200™). This will prevent the flotation mixture from sticking directly to the mould or dummy block(s) and hence assist later with their removal. Then, position the dummy block(s) correctly in the mould ready to be filled with flotation (Fig. S5.5b).

Step 7: Mix resin parts A and B together using a wooden mixing stick. Make sure that the components are very well mixed - consider mixing continuously for at least 1 minute. Note that the pot time (i.e. duration in which it can be used) after the two parts have been combined is between 30 - 40 minutes at 20 °C. Hence, once mixed, immediately pour the resin evenly over the microspheres. Take care to ensure you pour only the required amount of total resin (e.g. in this example 70 g).

Step 8: Carefully mix the resin and microspheres. Be careful not to mix too vigorously otherwise you may cause the powdered microspheres to puff out of the container. Mix the components using your hands, making sure to bind it all together. Once mixed, providing you donned two pairs of gloves from the outset it is convenient at this point to remove your top layer of gloves.

Step 9: With your clean pair of gloves, pick up the mould (with dummy block(s) in place) in one hand, and use the other hand to pack the mixture into the mould (Fig. S5.5b). You want to make sure that the mixture is well compacted into the mould.

Step 10: Leave to set at 20 °C for a minimum of 8 hours setting time by which point the mould should be dry and well set. At this point, wearing appropriate PPE, it is safe to remove the flotation mixture from the mould, and remove the dummy block(s) (Fig. S5.5c). Do not touch the mixture prior this (i.e. while it is still setting) as you will likely leave surface irregularities.

Step 11: Inspect the flotation to see that there are no obvious faults; often if the clingfilm is not pulled tightly enough creases and bubbles can form which will cause the mould to present with surface irregularities (small grooves etc.). To rectify any irregularities, repeat steps 1-10 using only a small amount of mixture, and use this to fill any holes and tidy up the flotation. Again, leave this to set for a minimum of 8 hours at 20 °C.

Step 12: Note that the total curing time required for epoxy glosscoat resin at 20 °C is 8 days, or 6 hours at 50 °C (e.g. in a laboratory oven). It is hence strongly advised to prepare your flotations well in advance of your fieldwork deployment date, e.g. 10 days prior. For further details on setting and curing times, consult the epoxy glosscoat resin technical data sheet and safety data sheets, as well as any instructions provided by the supplier.

Step 13: Once you are happy that your flotation is fully cured, you can now spray it with a chosen colour paint.

Appendix S5.6: Baseplate design and appraisals

Similar to the process of design iteration that I undertook in developing my final tag design, the baseplate that I used underwent a series of design iterations. Here I present and appraise each baseplate design in turn.

Baseplate 1

The first baseplate was designed to be used together with my first tag design (Appendix S5.4). This baseplate was made from 1 mm polycarbonate sheet and cut to measure to match the footprint of the tag. The baseplate extended approximately 5 mm further around the footprint of the tag to ensure that the super glue used to attach the baseplate to the seal's pelage did not accidentally glue the tag directly to the baseplate (Fig. S5.6.1). The baseplate's slightly larger footprint was also required to provide room for the cable ties used to hold the GTR in place (Fig. S5.4.1). This baseplate was used in the deployment of tags A, B, and C in October 2017. The appraisal of this baseplate is presented in Appendix S5.4.

Baseplate 2

The second baseplate I designed (Fig. S5.6.2) was to be used with the final tag design (see main text). This baseplate was printed using a 3D printer from Floreon 3D and measured 170 x 75 x 18 mm. The baseplate had a tapered nose which was contoured appropriately to complement the shape of the tag and had a slot in the nose for the tag to fit into. The baseplate featured two small, raised sections at the rear to prevent the tag from moving laterally as well as two raised sections at the side with holes to hold the bungee cord in place for the release mechanism. This baseplate was used in the deployment of tags 1–4 in April 2018.

From deploying this baseplate, I learnt that the raised sections at the rear of the tag were not required, as the bungee cord if tensioned tightly enough mitigated lateral movement of the tag. The overall size of the baseplate was also more than necessary and I hence determined that this could be substantially reduced in size, which would reduce the surface area for gluing. I was also concerned that the two raised sections at the front of the baseplate

were not strong enough to hold the release mechanism, as when preparing the tags for deployment I observed one of these to break.

Baseplate 3 (final)

My final baseplate design is described in the main text. This baseplate was used together with my final tag design (see main text). Compared to my second baseplate design, I substantially reduced the length of this design to minimise the surface area required for gluing and contoured the rear edge of the baseplate to remove any sharp corners that could have caused lacerations. I also modified the raised sections at the side to make these thicker for extra strength and more appropriately contoured to encourage smooth reattachment of water flow to minimise hydrodynamic drag (Kay et al., 2019). This baseplate was used in the deployment of tags 5–7 in September 2018 and tags 8 and 9 in April 2019.

Experimental baseplate

In the April 2019 deployments I deployed tags 8 and 9 with an experimental hardboard baseplate recommended by SMRU. The reason for this was that I hoped that as well as the tag itself becoming detached, the baseplate would also detach prior to the annual moult as the hardboard took on water and deteriorated. I used 1 mm hardboard and cut this to measure the same shape as my baseplate. I cut shallow grooves into the hardboard to encourage the absorption of water. my baseplate was glued directly to this hardboard before the whole unit was glued to the seal's pelage. I discuss the performance of this baseplate in the main text.

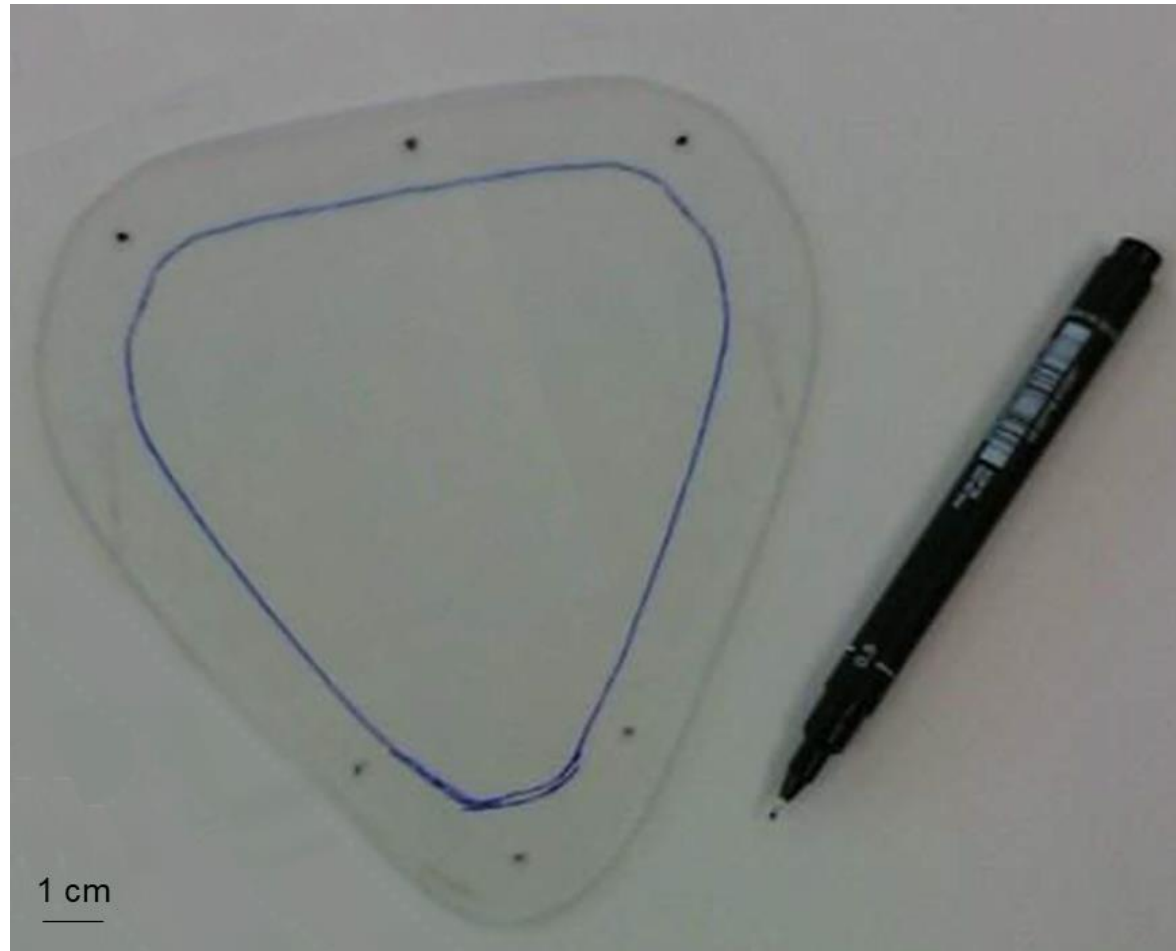


Fig. S5.6.1. My first baseplate design (baseplate 1) made out of thin (1 mm) polycarbonate sheet.



Fig. S5.6.2. (a) My second baseplate design. (b) A tag deployed in the April 2018 deployments with a VHF transmitter using baseplate 2.

Appendix S5.7: Example data recording sheet for logging tag design and deployment details

SLAM Seal Capture Sheet Project ID: _____		Date: _____	Location: _____	Data custodian: _____
resin_float ID: _____ float_photo: Yes/No weight: _____ length: _____ width: _____ thickness: _____ buoyancy: _____ resin:beads_ratio: _____ coat: _____ DD_housing_orientation_in_float: _____ GPS_housing_orientation_in_float: _____ VHF_housing_orientation_in_float: _____	Daily_Diary DD_ID: _____ DD_photo: Yes/No weight: _____ length: _____ width: _____ wall_thickness: _____ DD_housing_type: _____ attachment_to_float/animal: _____ DD_longitudinal_rotation_in_housing: _____ DD_lateral_rotation_in_housing: _____ DD_vertical_rotation_in_housing: _____ battery_size: _____ start_voltage: _____ pressure_sensor: _____ vosschemie: Yes/No			
baseplate_ID: _____ baseplate_type: _____ attachment_to_float: _____ weight: _____ length: _____ width: _____ thickness: _____	Animal ID: _____ alternative_ID: _____ Sex: _____ Age_class: _____ age_estimate: _____ birth_year: _____ pit_tag_ID: _____ mortality: Yes/No species: _____			
Capture_info location: _____ date: _____ capture_start_time: _____ latitude: _____ longitude: _____ capture_method: _____	DD_calibration operator: _____ calibration_location: _____ Time_DD_turned_on: _____ acc_calibration_start_time: _____ calibration_outdoor: Yes/No mag_calibration_start_time: _____ far_from_metal: Yes/No compass_calibration_start: _____ DD_north_orientated: Yes/No DD_lay_down_time: _____ utc_time_sync: Yes/No Timezone: _____ Notes			
Animal handling and deployment operator(s): _____ process_start_time: _____ sedation: Yes*/No DD_on_animal_time: _____ eye_drops: Yes/No eye_drug: _____ animal_release_time: _____ eye_cover: Yes/No start_monitoring_time: _____ total_weight: _____ net_weight: _____ seal_weight: _____ time_tag_wet: _____ seal_length: _____ length_type: _____ balance_type: _____ circumference: _____ tag_attachment_type: _____ glue_used: _____ glue_setting_duration: _____ attachment_position: _____ photo: Yes/No tag_longitudinal_rotation_on_animal: _____ video: Yes/No tag_lateral_rotation_on_animal: _____ tag_vertical_rotation_on_animal: _____ release_latitude: _____ release_longitude: _____ behaviour_during_capture: _____ release_behaviour: _____ seal_condition: _____ natural_marks: _____				

Page _____ of _____

Sheet ID: _____

*Sedatives and anaesthesia					
drug	dose	route	time	Immob. degree	response

<p>GPS_configuration ID: midpoint_latitude: midpoint_longitude: midpoint_height: computer_timezone: computer_time_accurate: Yes/No configured_in_country: Yes/No date_configured: time_configured: Position_update_rate: Maximum_dive_duration: SWS_num: Haulout_duration: start_date: start_time: UHF_beacon_channel: UHF_download_rate: battery_size: solar_recharging: Yes/No expected_lifetime: battery_%: SWS_free_in_float: Yes/No GPS_antenna_free: Yes/No GPS_active_10_red_light_display: Yes/No bung_silicone_grease: Yes/No offline_configuration: Yes/No vendor:</p>	<p>DD_configuration ID: configuration_date: board_software: Code_line: acc_data: Yes/No acc_freq: mag_data: Yes/No mag_freq: temp_data: Yes/No temp_freq: pressure_data: Yes/No pressure_freq:</p>
<p>Injectables oxytocin: antibiotic: isotope_num: isotope_0hr: isotope_3hr:</p>	<p>VHF_configuration ID: frequency: vendor: model: battery_life: ping_rate: time_on: tested_on: Yes/No</p>
	<p>Samples and veterinary procedures plasma: serum: blood: milk: faecal_lavage: stomach_lavage: rectal: vaginal: nasal: oral: eye: saliva: hair: skin: tooth: whisker: blubber: urine: photo(s): Yes/No video(s): Yes/No veterinary_procedures:</p>

Notes

Appendix S5.8: Additional tag details

Devices, programming, and priming

Inertial movement unit

I used a Daily Diary (DD; Wildbyte Technologies Ltd, Swansea, UK; Table 5.1) as the IMU device which recorded triaxial acceleration, triaxial magnetometry, temperature and pressure (Wilson et al., 2008), albeit the latter was superseded by the TDR. This IMU was selected because of its small size, relatively low cost, and high functionality and customizability including being able to sample at high frequencies (up to 800 Hz). Given my aim of collecting short term, high-resolution data, the DD was programmed with a relatively high sampling frequency (40 Hz acceleration, 13 Hz magnetometry, and 4 Hz temperature) and was programmed to start collecting data via activation with a magnet. This meant the DDs could be switched on in “sleep mode” and glued in place within the tag housing prior to animal capture; a magnet could then activate the DD immediately prior to tag deployment. Once activated, DDs recorded data continuously with no duty cycling. To power the device, I used a 750mAh 3.6V Lithium Thionyl Chloride EVE cell (EVE Energy Co., Ltd, Guangdong, China; Table 5.1). Both the memory capacity of the DD (2 GB) and the battery life were spent in approximately 14 days. Data were stored on a 2 GB micro SD card (Table 5.1) and, as the DD was not capable of transmitting its data to satellites, this device needed to be recovered. The DD was connected to an ultra-small board-mounted pressure sensor (Mouser Electronics, High Wycombe, UK; Table 5.1) to obtain pressure data. This sensor was mounted externally (see later). This pressure sensor is 2.75 times smaller than Keller depth sensors traditionally used on seal tags of this kind (e.g. Wilson et al., 2007), and recorded pressure at 4 Hz at 13 cm resolution, with the data fed into the DD and stored on the SD card.

GPS for accurate positional information

To provide accurate positional information and correct for drift in dead-reckoning (Wilson et al., 2007) I included a Fastloc-GPS device. I chose the

F3G 133A Marine GPS Datalogger (Sirtrack, Hastings, New Zealand; Table 5.1). This small device is archival in the sense that it is not able to transmit to orbiting satellites, meaning it too needed to be recovered to download the data (however it is possible to program this device to transmit via UHF to a local base station; F3B 139A UHF Base Station, Sirtrack). It was necessary to choose this model of Fastloc-GPS as any satellite transmitting equivalent was too large to deploy in tandem with other devices. In any case, I was already required to recover the tag in order to retrieve the DD. I programmed the Fastloc-GPS to have a maximum temporal resolution of 2 minutes, reduced to 2 hours when animals were hauled-out; assessed by a saltwater switch (SWS) detecting that the device had been dry for more than 30 minutes. The Fastloc-GPS devices were powered by an in-built, rechargeable battery. With these programming settings, the most conservative estimate for battery duration was 7.1 days however this prediction assumed fixes were obtained every 2 mins and did not account for haul-out mode savings; I expected the Fastloc-GPS to last between 10-14 days. Tags 8 and 9 did not contain a Sirtrack Fastloc-GPS device (Table 5.3) as these tags were deployed in tandem with SMRU GPS-GSM tags (Sea Mammal Research Unit, University of St Andrews) which provided accurate GPS positional information.

Transmitting units

I considered two options for transmitting devices to aid tag recovery (Table 5.1); a VHF transmitter (Sirtrack, Hastings, New Zealand) or an ARGOS Smart Position Only Tag (SPOT; Wildlife Computers, Redmond, USA). The former sent continuous radio transmissions (1 second resolution)⁵ which could be triangulated by a handheld receiver, and the latter provided satellite locations (up to 45 second resolution when wet, or 90 second when hauled-out; defined by 50 % dry for over 5 minutes) that could be viewed online via the ARGOS tracking web portal or the Wildlife Computers tag portal, and on mobile via the

⁵ Note that tag 1 was fitted with a VHF transmitter with a unique duty cycling for experimental purposes. This VHF transmitter was programmed to send continuous 1 second transmissions for the first two hours after activation, followed by a 7-day period of silence. After this period, the tag would send 1 second transmissions continuously and indefinitely until the battery depleted.

ARGOS Collecte Localisation Satellites (CLS) app “CLS View”. The ARGOS transmissions were expected to be detectable to within a few miles using a Goniometer (Goetz, Jasonowicz, & Roberts, 2018). Additionally, the SPOT transmitted an Ultra-High Frequency (UHF) radio transmission which could be detected within a more local range (of several kilometres).

The VHF transmitters had an expected battery life of 90 days and required no pre-deployment programming or preparation, only to be switched on via activation with a magnet. The SPOTs were deployed in self-start mode and activated automatically when saltwater was detected. In tags 1-7 (Table 5.3) the SPOTs began attempting transmissions immediately on activation, however the SPOTs in tags 8-9 had a 14-day delayed start to prevent possible interference with SMRU’s GPS-GSM tags (Appendix S5.1: **IV.C.1**) which they were deployed together in tandem with; I expected the tags to have released by no later than 14 days hence deemed it safe for the SPOTs to begin transmitting uplinks after this time. The SPOTs only attempted uplinks when tags were at the surface (either when the animal surfaced to breathe or when the tag had released from the baseplate and was floating). While on the animal (in “at-sea” mode), the SPOTs were programmed to send a maximum of 40 uplinks per hour with a minimum uplink interval of 45 seconds. If the SWS detected that the device was dry 50 % of the time during a 5 minute window then it would enter “haul-out” mode and send a maximum of 40 uplinks per hour with a 90 second minimum uplink interval; haul-out settings also applied when the tag had released from the animal and was floating at the surface, because the SWS remained dry. The SPOT device would return to at-sea mode if the SWS detected that the device had been wet 85 % of the time in any 5 minute window. Uplinks were only attempted during the 12 hours of the day during when orbiting satellites were passing over the study site as predicted by CLS ARGOS Pass Prediction Software (<http://www.argos-system.org/>); between 06:00–12:00 and 15:00–19:00 for deployments in Germany, and between 07:00–12:00 and 17:00–22:00 for deployments in Wales (Table 5.3). To conserve battery power the SPOTs only uplinked positional data to satellites and did not send any summary data of percentage dry timelines or time at temperature, as these summary statistics were

expected to be obtained by the DD. The SPOTs' UHF pinger sent transmissions every 2 seconds (only whilst the tag was dry). The SPOT battery capacity provided 33,000 uplinks which at the maximum possible transmission frequency gave a minimum expected battery duration of 68.75 days (as for the Fastloc-GPS devices, this is also a conservative estimate as it excludes haul-out mode savings and assumes the device operates continuously at its maximum temporal resolution, which is unlikely).

Device priming

Prior to deployment, SPOT devices were primed in a location near to their eventual deployment location; priming improves positional estimates because the Kalman filtering algorithm uses measurements from both current and previous satellite passes to calculate position estimates (Wildlife Computers Inc, 2017). SPOTs deployed in Lorenzensplate (Table 5.3) were primed in Büsum (54.128159 N, 8.867239 E). SPOTs deployed in Wales were not primed so as to prevent possible interference with SMRU GPS-GSM tags (Appendix S5.1).

Once all devices had been programmed, tested, and primed, they were superglued permanently inside the tag housing using Loctite® 422 Instant Adhesive (Bearing King Ltd, UK).

Device tests

Daily Diaries

I tested DDs in circumstances similar to those expected during deployment. Specifically, I logged data continuously for up to 14 days including in a saltwater pressure chamber (see below), and moving outdoors along a 7 km coastal route (Fig. S5.1).

Pressure sensors

Pressure sensors were tested to a maximum pressure of 7 bar in a pressure test chamber. I checked that sensors were detecting small changes in pressure by forcing air into the small cavity where the pressure sensor was held in the back of the DD housing.

Fastloc-GPS devices

I tested the accuracy of Fastloc-GPS position fixes using three different methods. First, I allowed the devices to collect data while stationary in a dry, open environment clear of any obstructions, at relatively high altitude (163 m; Cefn Bryn trig point; 51.587579 N, -4.175104 E; Fig S5.2); I expected that these would be optimum conditions for position acquisition. Second, I tested device performance at sea level in a saltwater bath. Specifically, I submerged the device in saltwater before raising it approximately 5–10 cm out of the water momentarily (no more than 1 second) according to a regular schedule in line with its sampling frequency (e.g. every 2 minutes). This was to simulate the surfacing behaviour of the device while attached to seals – at worst the device should breach the surface very briefly (for 1 second or less) as seals pitch forward to dive underwater (van Neer, *pers. comms.*). Two tests of this kind were conducted on the beach at Swansea Bay (51.606931 N, -3.978508 E and 51.6067 N, -3.978283 E; Fig. S5.3-5.4). Finally, I tested the device along a 7 km coastal route (Fig. S5.1) by walking with the device affixed to the top of a

cap. For further details of these tests (including specific programming schedules), see Appendix S5.2.

Transmitter tests

I tested both the SPOT and VHF transmitters to determine their detection range and, for the SPOT tags only, their transmission location accuracy. For the VHF, I tested the range at sea level from 2.5–22.4 km in Swansea and Camarthen Bay, UK (Fig. S5.5). Specifically, to ensure the tags were not lost during testing, I monitored the tag while it floated freely in shallow water at the beach, whilst L. Börger travelled to distant sites with a VHF receiver to track the device. I also tested the ability to detect the tag from on board a boat from up to 3 km south of Büsum harbour, Germany (Fig. S5.6). For this test I secured the tag on a short tether (2 m) from a fixed buoy so that it could float freely at sea while the boat travelled away.

For the SPOT tags, I tested the detection range of both the ARGOS uplink signal and the UHF transmission using a Goniometer (Collecte Localisation Satellites SA - CLS, Ramonville-Saint-Agne, France) and wideband handheld scanning UHF receiver (model: AOR AR-8200 MK3), respectively. Specifically, I placed a transmitting SPOT tag on the dike at Büsum (54.133675 N, 8.921741 E) and tested its detection from a range of 1 m–11.5 km (Fig. S5.6). I also placed a transmitting SPOT tag at the Institute for Terrestrial and Aquatic Wildlife (ITAW), Büsum (54.128160 N, 8.867253 E) and stopped several times en route to Sylt to search for the transmissions, up to a maximum distance of 90 km (Fig. S5.6). I tested the SPOT tags both whilst they were dry on land (prone orientation), and whilst they were floating in a saltwater bath (vertical orientation).



Fig. S5.1. 7 km coastal-urban route (yellow line) used for testing Fastloc-GPS devices and DDs. Yellow markers show the position fixes obtained by the Fastloc-GPS device (data from one example test shown). Blue marker shows start location of GPS device (51.571605 N, -3.986582 E). Black rings shown for scale (5-50 m radius). Inset: Zoomed in section of data collected by the tag whilst it was positioned stationary on the harbour wall.

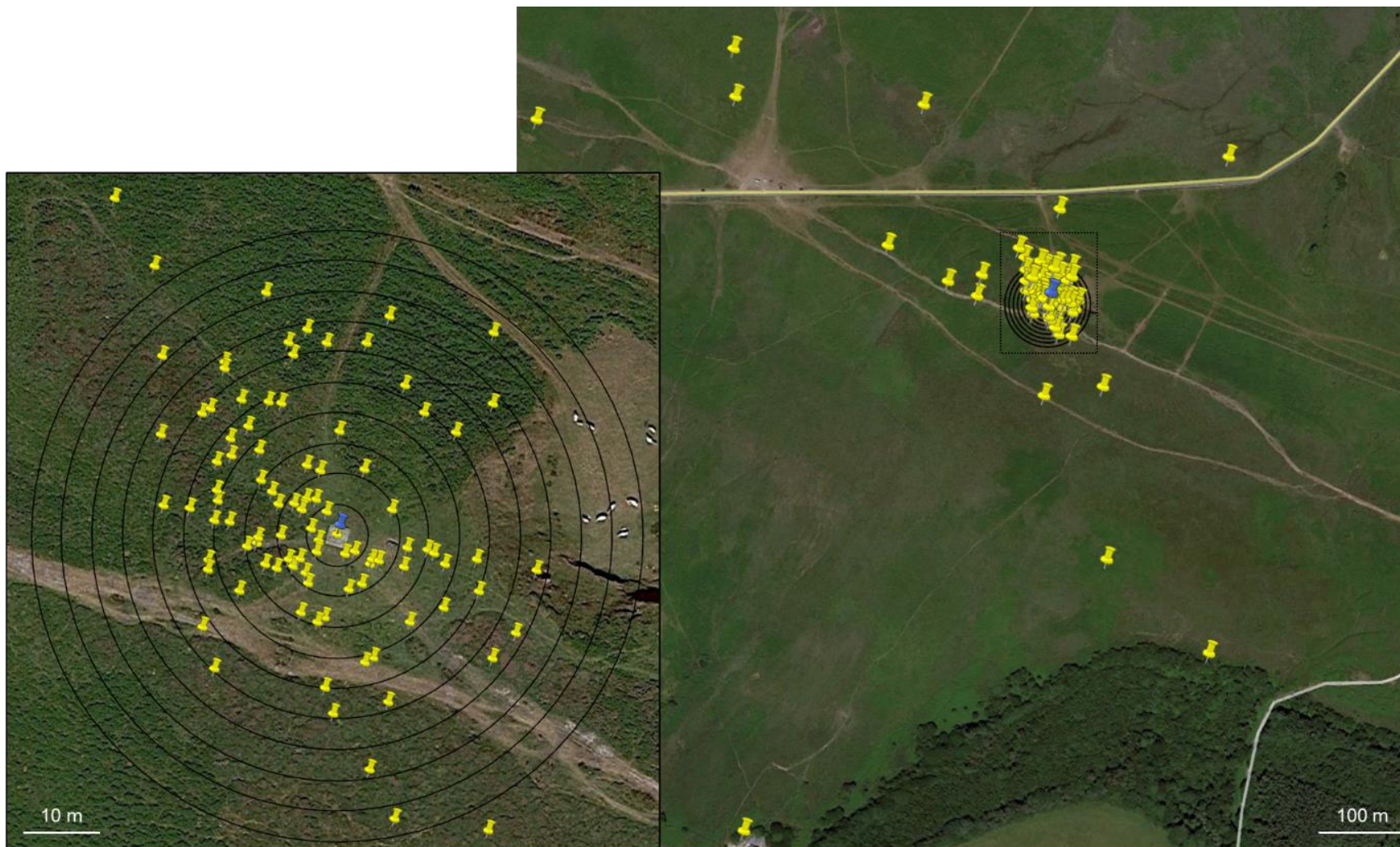


Fig. S5.2. Fastloc-GPS position acquisition accuracy test at Cefn Bryn trig point (see text). Blue marker shows the location of the GPS device (51.587579 N, -4.175104 E). Yellow markers show position fixes obtained. Black rings radiating from the GPS position are shown for scale (5-50 m radius). Inset left: Zoomed in section to highlight close cluster of position fixes.

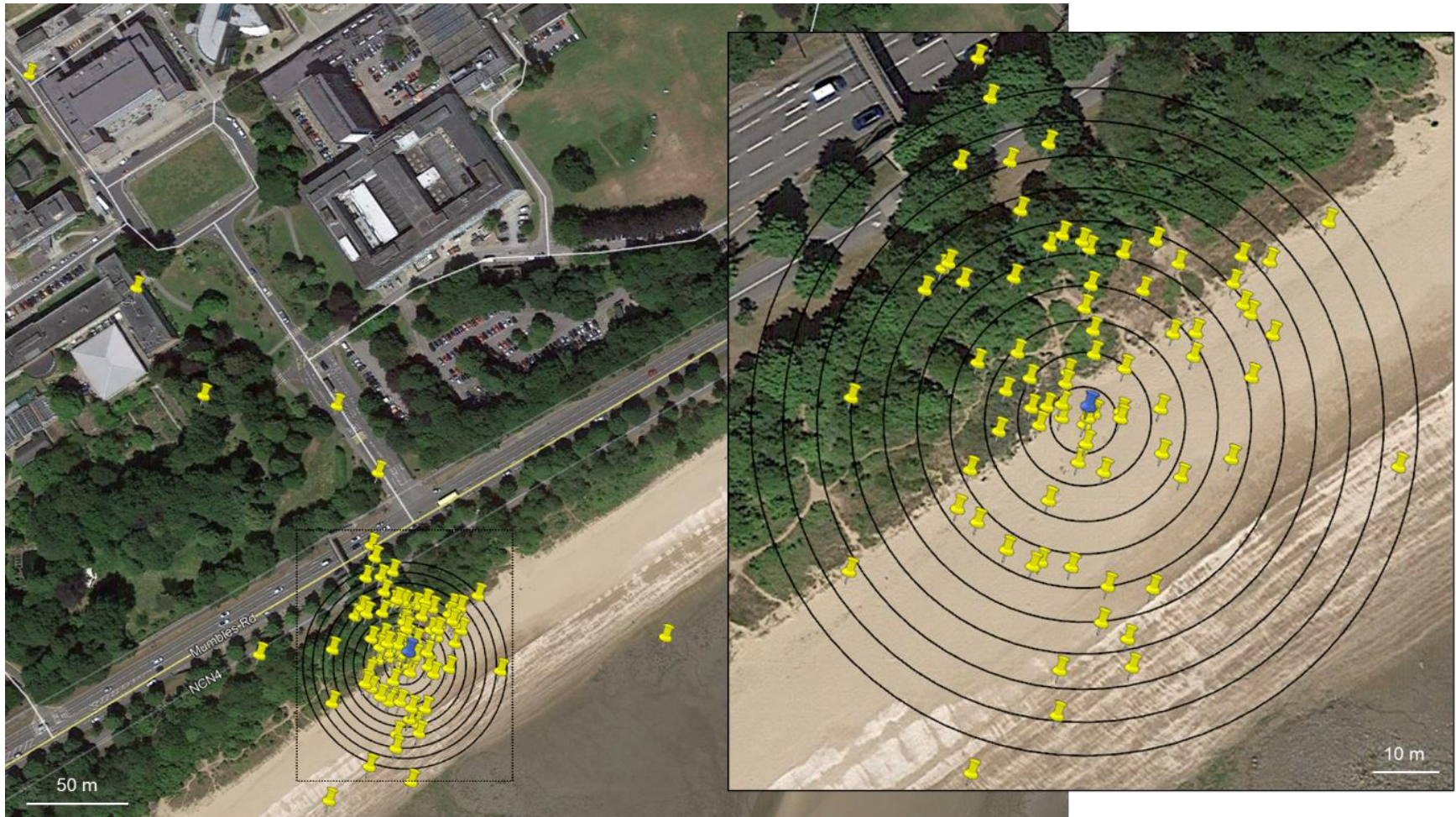


Fig. S5.3. Fastloc-GPS position acquisition accuracy test (1 of 2) at Swansea Bay (see text). Blue marker shows true location of GPS device (51.606931 N, -3.978508 E). Yellow markers show position fixes obtained. Black rings radiating from the GPS position shown for scale (5-50 m radius). Inset right: Shows cluster of position fixes around the location of the GPS device.

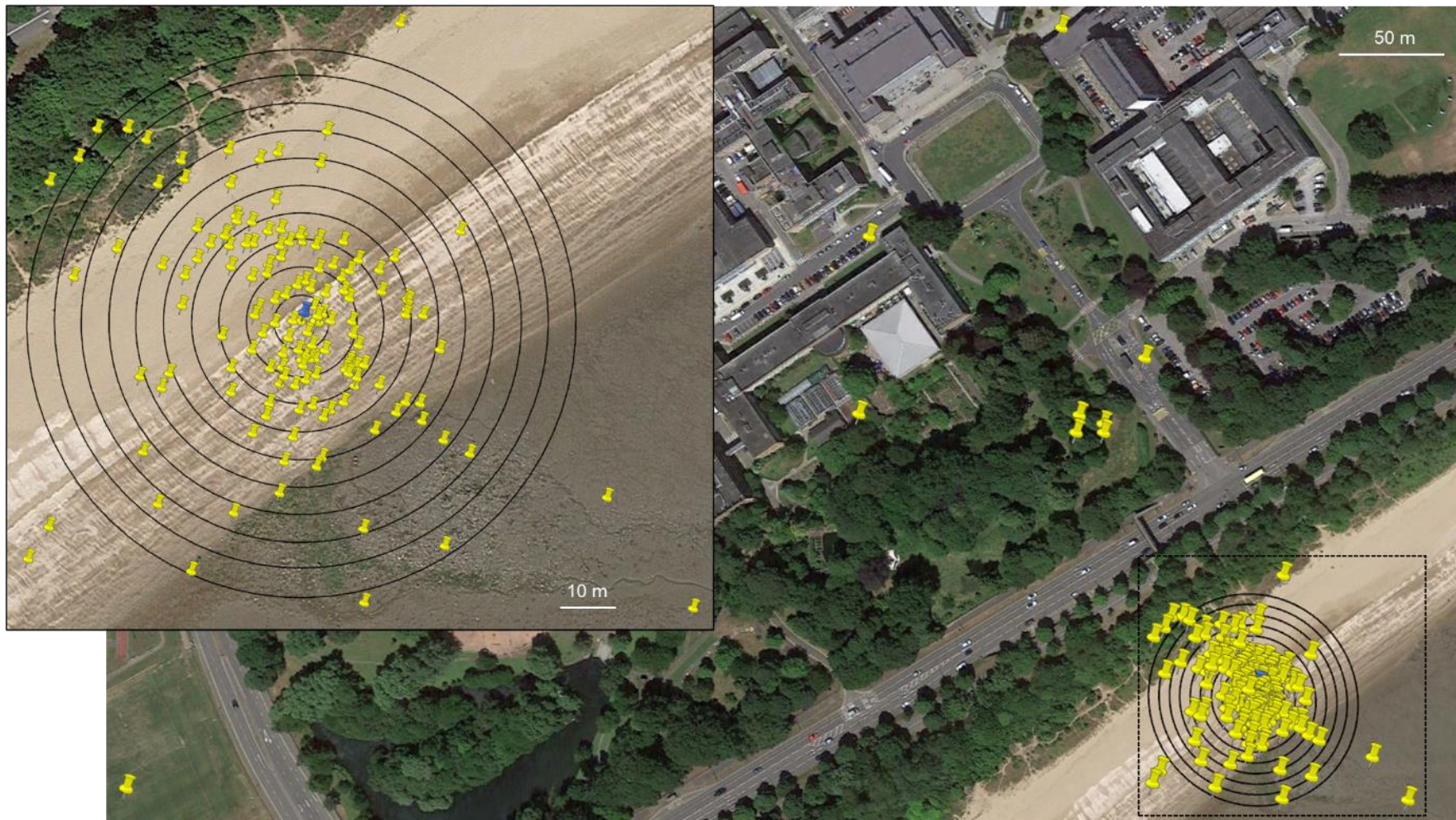


Fig. S5.4. Fastloc-GPS position acquisition accuracy test (2 of 2) at Swansea Bay (see text). Blue marker shows true location of GPS device (51.6067 N, -3.978283 E). Yellow markers show position fixes obtained. Black rings radiating from the GPS position shown for scale (5-50 m radius).



Fig. S5.5. Location of VHF tests undertaken in Swansea and Carmarthen Bay. Blue circles indicate position of the VHF transmitter, squares indicate positions that transmissions were attempted to be received from.

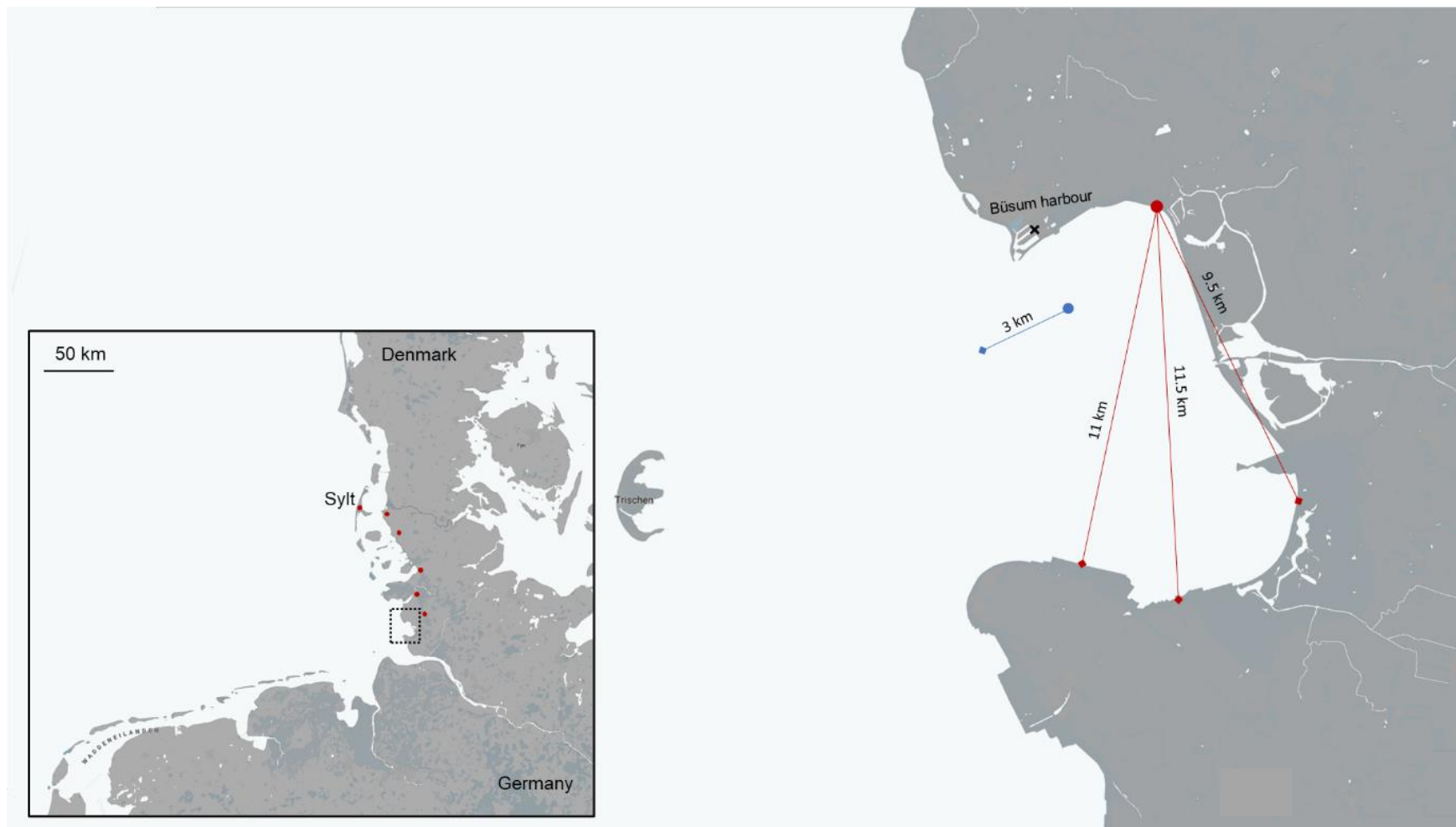


Fig. S5.6. Location of VHF and SPOT tests undertaken in Büsum. Blue circle indicates the position of the VHF transmitter; blue square indicates the position that the VHF transmissions were attempted to be received from on the boat. Red circle indicates position of SPOT transmitter on Büsum dike; red squares show examples of the positions that this SPOT's transmissions were attempted to be received from with the Gonionmeter. Black cross indicates the position of ITAW where a SPOT tag was transmitting from; red dots (inset) show locations *en route* to Sylt that were stopped at to attempt to detect these transmissions.

Housing for Daily Diary and pressure sensor

I developed a bespoke housing for the DD circuit board and pressure sensor. This consisted of a robust, transparent block of polycarbonate (Fig. S5.7; Table 5.1). An internal groove was cut out (9 x 13 mm) to house the DD, battery, and wiring connections. A further section (63 x 23 x 7 mm) was cut in the upper surface to accommodate the Fastloc-GPS which was superglued directly to this housing (Loctite[®] 422 Instant Adhesive). A plug at the rear was used to seal the DD using a silicone-greased o-ring and fixed with two 2 mm stainless steel screws that penetrated into the main housing (Table 5.1; Fig. S5.7-5.8). This plug measured 9 x 30 x 12 mm (including the length of the screw extrusion). The plug's internal section on which the o-ring sat measured 4 x 18 x 9 mm (Table 5.1). This plug also housed the pressure sensor with its own micro o-ring (Table 5.1) in a central 5 mm circular cavity; a 3 mm circular cavity exposed the sensor to the external environment (Fig. S5.7-5.8). The pressure sensor I used is typically circuit-board mounted (Table 5.1). However, I adapted it to be used as an external sensor by potting it in the 5 mm cavity using epoxy glosscoat resin (Vosschemie, Uetersen, Germany) and soldering electrical wiring directly from the component to the main DD circuit board. Prior to potting, I coated the wire connections to the pressure sensor using Plasti Dip (Plastidip UK Ltd., Hampshire, UK) to prevent short circuiting (Fig. S5.8). DD housings were pressure tested to 60 m in a pressure test chamber.

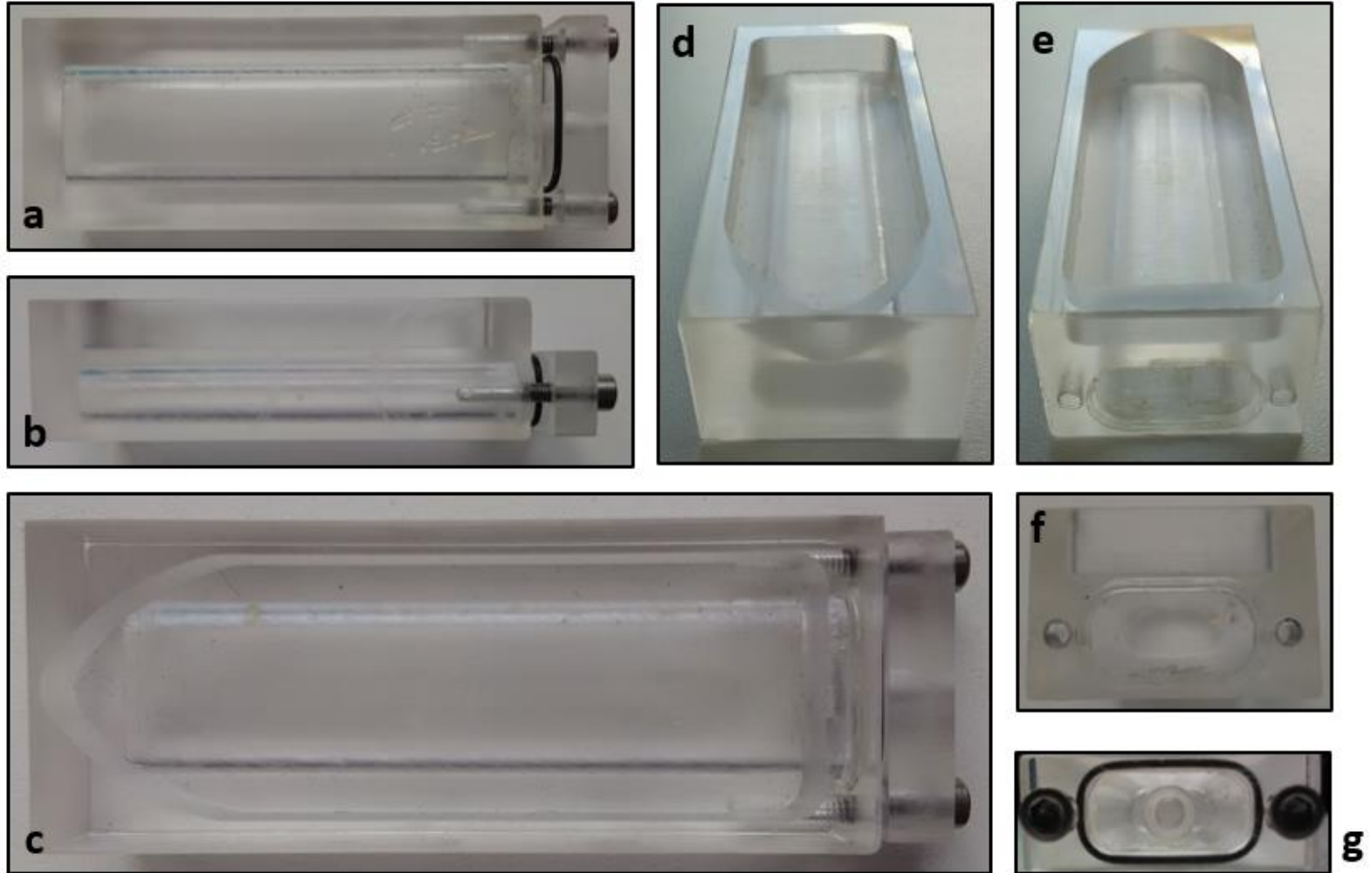


Fig. S5.7. Housing for the Daily Diary (DD) IMU (see also Fig. S5.8): (a) Bottom view with plug and screws in place (not fully closed). O-ring used to seal the housing also observable (see Fig. 8). (b) Side view. (c) Top view highlighting groove for Fastloc-GPS device to sit in (see later). (d) Front view. (e) Rear view. Note the slight groove in the entrance to the cavity for the o-ring to sit. (f) View of opening at rear of tag highlighting two 2 mm holes for screw. (g) View of plug in rear of tag with screws and o-ring seal in place. No pressure sensor is fitted here (refer to Fig. S5.8). Dimensions in text.

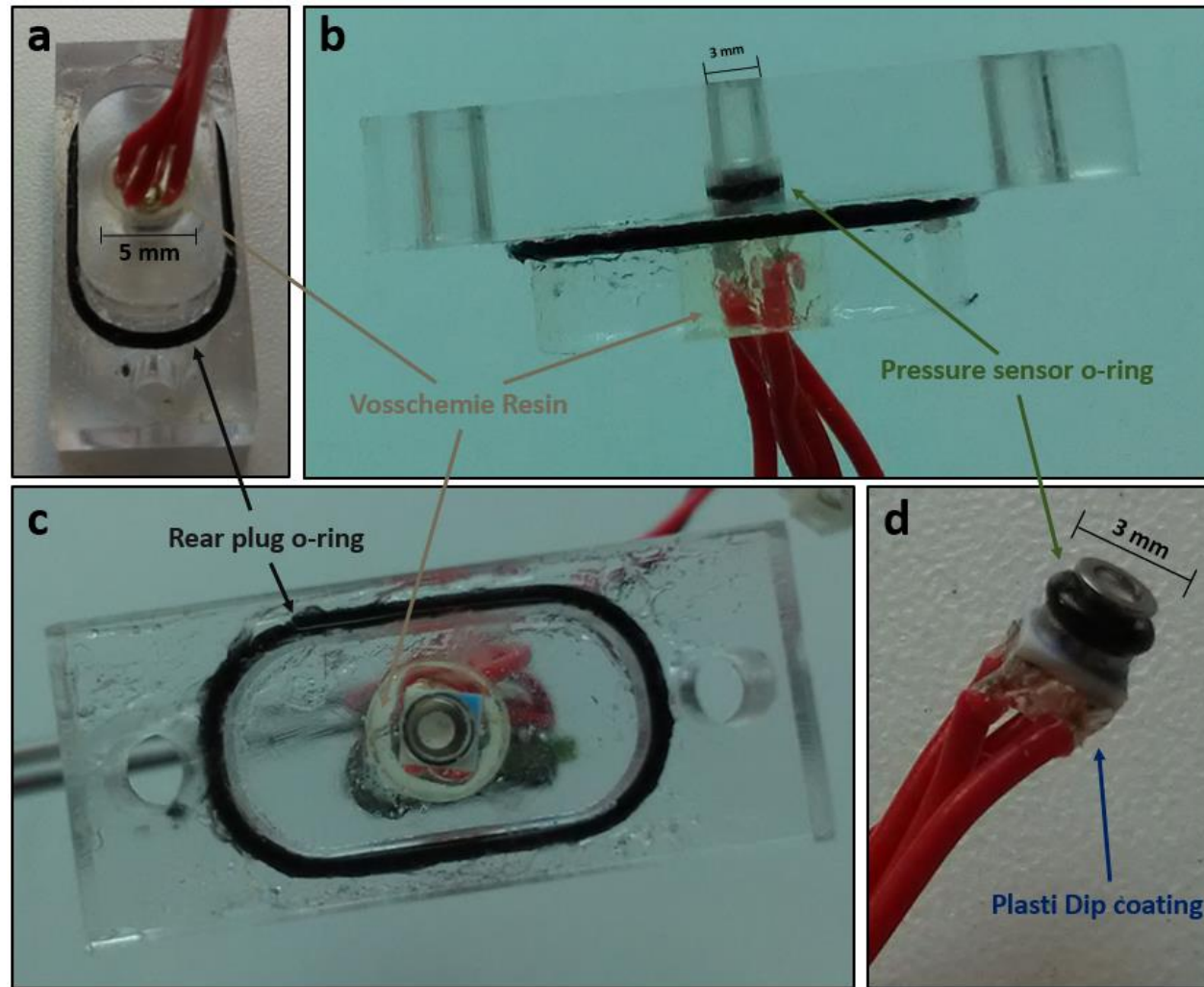


Fig. S5.8. Rear plug for DD housing and with potted pressure sensor. (a) Side view showing wires entering 5 mm cavity where pressure sensor was placed. (b) Top view showing pressure sensor in place with o-ring. Slight discoloration highlights the Vosschemie resin that has filled the cavity. (c) rear view of plug showing pressure sensor in place and exposed to the external environment. (d) Pressure sensor prior to potting with Plasti Dip coating covering wire connections.

GTR corrosion duration tests

9 GTRs (model G7) were tested to ensure that they corroded at their expected rate (7 days at 16 °C, 6.5 days at 19 °C). The GTRs were suspended in a saltwater bath (Fig. S5.14) and were monitored at regular time intervals for a continuous period until they were observed to have fully corroded. The water in the saltwater bath was kept flowing steadily using a submerged air pommel stone and fresh saltwater was added at regular intervals; this ensured that water temperature and salinity were kept constant and that the water did not become stagnant. Water temperature and salinity were monitored using a temperature probe and a refractometer, respectively. 5 of the GTRs were submerged permanently, with the other 4 following a 50/50 wet/dry cycle, being exposed to air for 12 hours, then submerged for 12. At each 6-hourly time check, GTRs were inspected for signs of corrosion or to see if they had fully corroded.

All tested GTRs corroded within ± 12 hours ($\pm 7\%$) of their expected duration. Specifically, 5 of the continuously submerged GTRs had fully corroded and broken into two pieces between 6.5–7.25 days. The 4 GTRs on a 50/50 cycle corroded fully at between 13.5–14.5 days. I note that these results occurred in spite of the temperature being below optimum and salinity below average; the temperature during the test was 14.2 ± 0.77 °C (mean \pm SD) and salinity was 31.1 ± 1.2 ‰. I anticipate that the relatively vigorous, continuous water flow in the tests may have contributed to slightly increased corrosion rates.

Release mechanism tests

I conducted separate tests of the release mechanism using the full tag setup with the tag attached to the baseplate via the GTR. These test were performed to check that the tag released as expected from the baseplate, and to determine if a bungee cord was preferable over heavy duty rubber bands (e.g. Icon Flexpack Ltd, Burnley, UK). Specifically, I submerged the full tag setup in a saltwater bath and left it submerged continuously until the GTR had fully corroded and broke. In contrast to the *GTR corrosion rate tests*, I checked these GTRs every 6-hourly but only after the expected corrosion duration had

elapsed. I undertook four of these tests with various GTR models and elastic cord combinations (Table S5.2).

The GTRs in tests 1 and 2 (Table S5.2) had corroded completely at between 30–36 hours respectively, remaining unbroken for up to ca. 6–12 hours (25–50 %) longer than expected. In test 3 the GTR had broken by 60 hours, up to ca. 12 hours longer than expected (25 %). I anticipate that, in contrast to GTRs being completely exposed to water in the *GTR corrosion duration tests*, the water flow around the GTRs was reduced during these tests by being placed inside the cavity of the tag housing; this may have contributed to a reduced or uneven corrosion rate. In test 4, on checking the GTR at 4 days, I noted that the water was stagnant due to a failure to the air supply and I was unable to determine for how long the water had been static. However, as a result I observed a build-up of salt crystals and corroding GTR material inside the cavity of the tag housing; the lack of water flow had prevented this from being flushed out. On restoring water flow this material steadily dispersed from the cavity. The GTR was still intact and it took an additional 2 days (50 %) to fully corrode. This important serendipitous discovery motivated me to increase the size of the GTR cavity to mitigate build up of corrosive material.

I observed differences in the efficacy of the release mechanism once the GTRs had fully corroded and the elastic cord had retracted. Specifically, in the tags that used heavy duty rubber bands (tests 2 and 4), the eyelets of the GTRs had not retracted successfully from the cavity. In test 1 the eyelets had retracted as expected, and in test 3 only the eyelet on the side using the bungee cord had retracted successfully (Table S5.2). However, a gentle amount of movement successfully dislodged the eyelets stuck in the cavity and I hence would not expect this to be a major issue in wild deployments. In any case, it was clearly preferable to use bungee cord for the release mechanism (Table S5.2).

Finally, I also observed that once the GTRs had corroded and the elastic cord retracted the eyelets from the cavity, the tag housing only came free from the baseplate with some slight forward movement of the tag.

Table S5.2. Details of the GTR models and elastic cord used in release mechanism tests using the full tag setup.

Test	GTR	Expected corrosion duration	Elastic cord
1	A4	24 hr (13 °C); 18 hr (16 °C).	Bungee cord on both sides
2	A4	24 hr (13 °C); 18 hr (16 °C).	Two heavy duty rubber bands on both sides
3	B4	48 hr (8 °C); 36 hr (14 °C).	Bungee cord one side, two heavy duty rubber bands on other side
4	D4	96 hr (13 °C); 84 hr (16 °C).	Single heavy duty rubber band on both sides

Tag calibration

Immediately prior to deployment, all tags required that their DD be calibrated by recording data in each of the tri-axial accelerometry and magnetometry channels. Device calibration must take place at the field site due to regional variations in magnetic field intensity (Williams et al., 2017). To calibrate the accelerometer, tags were moved in repetitive motions up and down, forward and back, and side to side, to record data in their dorso-ventral (heave), anterior-posterior (surge), and lateral (sway) axes, respectively (see Shepard et al., 2008). To calibrate the magnetometer, tags were first rotated through 360° in each of their yaw, pitch, and roll axes (see Williams et al., 2017). Following this, tags were gently rolled over in-hand whilst rotating them through each of their axes; this serves to collect all data required to generate *g*-spheres (acceleration; Wilson et al., 2016), *m*-spheres (magnetometry; Williams et al., 2017) and *o*-spheres (orientation; Wilson et al., 2020) from collected data, which can be used for analysis of animal movement and behaviour. Finally, to ground truth the magnetic compass at the deployment site, the tag is held in its “on-animal” orientation and, via clockwise rotation, is pointed towards each of the cardinal and intercardinal compass directions in turn. All calibrations were commenced facing due North.

Tag fastening

On one occasion, in preparing a tag, I observed that if the cable tie securing the bungee cord was not fastened tightly enough then it was possible for the release mechanism to slip free. I attribute this to human error as opposed to it being a fundamental flaw of the release mechanism design. Indeed, when tags were setup correctly, breaking the release mechanism in this way required considerable force which was not normally expected to occur. Rather, this acted as a failsafe if an animal got the tag stuck. I note however that such force may well be generated if the tag were to become trapped between rocks or a cave wall which could happen with grey seal deployments on Ramsey Island. This may well have been the cause of tag 8’s premature release in its first deployment.

Tag floatation and counterbalance

The general condition of the floats in all the tags that were recovered was very good, with only minor abrasions. The wedge-shaped design of the float gave it good overall stability from wave action when tags had detached. Because the tag needed to lie flat on the seal's back when deployed, only the dorsal side of the float could be raised to provide the required buoyancy. This asymmetry caused a slight imbalance in buoyancy which was corrected for using a counterbalance in the nose of the tag housing to orientate the tag vertically. The wedge shape of the float will have generated some additional hydrodynamic drag, although this was necessary to ensure the tag housing came free from the baseplate. Future designs would be improved by tapering the float to encourage smooth reattachment of water flow; something that I investigated in Chapter 6. Tags floated with approximately 4 mm of float exposed above the surface of the water; the base of the VHF antenna (Tags 1–4) was at the same level as this, whereas the base of the SPOT antenna (Tags 5–9) were a further 10 mm above this (in line with manufacturer's guidelines). Whilst tags were floating, both the VHF and SPOT antennas were exposed fully which was a requirement for their proper functioning.

Transmitters and tag recovery

Test deployments

Transmitters functioned well during the tests. VHF transmitters were detectable at all distances across Swansea Bay (Fig. S5.5) and a strong signal was detected from up to 18 km across Camarthen Bay between Llangennith and Pendine; the signal became weaker at distances greater than this (Fig. S5.5). Detecting transmissions from on board the boat in Büsum bay proved more difficult; I was able to detect the VHF well up to 2 km away, but between 2.5–3 km it was difficult to maintain continuous detection, with the signal being intermittent (receiving transmissions every 10-30 seconds) (Fig. S5.6). On returning to the tag however I observed that tethering to a fixed buoy had

caused it to float poorly at the surface. Specifically, the wind had blown the tag until the tether became taught which then pulled the surface of the tag (and thus a portion of the VHF antenna) underwater; this will have caused any transmission signal to attenuate. When the tether was released and the tag floated freely, continuous detection was re-established. Overall, the detection range of the VHF transmitters was on par with what has been previously reported or estimated (600 m; Andersen, Teilmann, Dietz, Schmidt, & Miller, 2014; 2 km; Lowther et al., 2015; 2–3.5 km; Chilvers, Corkeron, Blanshard, Long, & Martin, 2001; 12 km; Thompson, Hammond, Nicholas, & Fepak, 1991; 20km; Thompson & Miller, 1990).

SPOT tags were detectable at up to 20 km using the Goniometer. This range is considerably less than the maximum range of 100 km advised by manufacturers, however I anticipate that this was due to interference of the signal with buildings around ITAW where the transmitter was positioned. At distances of less than 2–3 km from the transmitter the Goniometer did not receive clear signals. Instead, at these shorter distances, I was able to detect the transmitter well using the UHF receiver.

In line with their expected functioning, neither the VHF nor the SPOT tags transmitted whilst their antenna (and in the case of the latter both saltwater switches) were submerged.

Appendix VI: Supplementary material for Chapter 6

Contents

Appendix S6.1: A review of the use of computational fluid dynamics (CFD) in biologging design

Appendix S6.2: Limitations to be aware of in the use of CFD for biologging tag design and impact quantification studies

Appendix S6.3: Step-by-step guide to modelling the drag impact of biologging tags with CFD simulations using ANSYS FLUENT™

Appendix S6.4: Further technical details for the CFD modelling approach

Appendix S6.5: Tag-induced impact on lift coefficient (Cl)

Appendix S6.6: Example figure of a CFD simulation of tag-induced drag in lateral flow

Appendix S6.1: A review of the use of computational fluid dynamics (CFD) in biologging design

The use of CFD to examine tag design and tag impact has grown within the biologging community since the mid-2000s (Pavlov et al., 2007). Several commercial tag manufacturers are now utilising CFD to assess tags during product development, although results from these studies are generally not published. Indeed, the use of CFD to examine tag-induced drag remains relatively limited in the primary, peer-reviewed literature and its full potential has not yet been realised.

Pavlov et al., (2007), examined tags attached to the dorsal fins of dolphins, but did not consider the position of the tag, or alternative tag attachment options, as optimisation parameters to reduce impact. Later, Pavlov & Rashad (2012) extended their work to use CFD to comprehensively investigate tag impact by modelling drag on a tagged versus an un-tagged dolphin (modifying the speed, pitch and yaw of the dolphin to account for a range of dolphin swimming characteristics); although they did not modify or attempt to optimise the tag *per se*. Similarly, Hazekamp et al., (2010) applied CFD to quantify the effect of a tag on a model grey seal but did not consider any optimisation procedure such as reducing tag size or changing tag design. van der Hoop et al., (2014) used CFD to examine the drag generated by tags on dolphins, comparing both *in vitro* and *in vivo* methods, but did not consider multiple optimisation parameters such as tag size, design or positioning of the tag on the animal to reduce tag-induced drag. Balmer et al., (2014) investigated the drag of a satellite transmitter attached to different positions on a dolphin's dorsal fin but used the same tag form, modifying instead the position of the antenna. Shorter et al., (2014) used CFD to test the hydrodynamic loading of three different tag forms, demonstrating that modifications to tag shape can reduce drag. However, while the tag design features achieved a reduction in drag, they also introduced large lift forces, which are unwanted, and the study did not investigate the additional effect of device positioning on the target animal (which has been shown to be a key issue; Bannasch et al., (1994) and Vandenabeele et al., (2014)). Furthermore, Shorter et al., (2014) assessed only the drag loading of tags in isolation and not of the tags placed on a model

animal. This is important as it is necessary to model the tag and animal together, in order to account for the contours of the animal and thus appropriately model the boundary layer of the flow around the animal associated with the tag (Evans et al., 2011; Kyte et al., 2018).

Fiore et al., (2017) extended the work by Shorter et al., (2014) and used CFD to reduce the net drag loading of suction cup tags. This work investigated changes in drag by modifying tags by adding different “flow control elements”. Although this is elegant in conception, it adds to the complexity of tag design and is not necessarily the most effective way to reduce drag whilst maintaining simplicity for tag manufacturers or ecologists designing tags in-house. Recently, van der Hoop et al., (2018) built on their previous work in 2014 by using CFD to assess the effect of tag size on hydrodynamic drag loading in bottlenose dolphins and investigate the associated kinetic and metabolic impacts of increased drag; however, additional optimisation factors such as tag position and shape were not assessed.

Thus, while there have been several advances in the use of CFD to design tags and quantify their impact, no publication has yet examined an approach which simultaneously considers device size (Vandenabeele et al., 2015), shape (Shorter et al., 2014) and positioning along the animal’s body (Bannasch et al., 1994; Vandenabeele et al., 2014).

Appendix S6.2: Limitations to be aware of in the use of CFD for biologging tag design and impact quantification studies

The use of CFD to assess tag-induced drag is clearly an increasingly popular method and one that boasts several advantages over experimental alternatives (Kyte et al., 2018). However, it is important to note that CFD has some limitations and one of the aims of my work is to help ecologists become aware of these and efficiently deal with them.

Firstly, Kyte et al., (2018) demonstrate that CFD analysis can be sensitive to the choice of turbulence model used. Indeed, many of the studies listed in Appendix S6.1 employ the k - ϵ turbulence model which is likely to underpredict the drag impact of a tag (see Kyte et al., 2018 for details). These assessments could be improved by using the Spalart-Allmaras turbulence model (as used by us here), or a combination of the SST turbulence model with a y -boundary layer transition model (as demonstrated in Kyte et al., 2018). Second, when using CFD it is often required to simplify the geometries of the model animal, as including all external features such as eyes, vibrissae or flippers can be impractical (Kyte et al., 2018). In a real environment these features would affect the measured drag values and hence the analyst must be aware that exclusion of these will affect the results. Furthermore, a standardised model animal geometry will not be able to represent all of the intricate differences between individual animals, nor the size differences between life history stages, or species that are sexually dimorphic. Tag geometries may also be simplified, for example by removing external antennae, and these simplifications will affect the results – for example external antennae have been shown to be important contributors to tag-induced drag (Wilson 2004). It is hence important that users tailor the geometries used to suit their specific research aims and study species used.

Finally, it is worth noting that, since CFD relies on approximate, numerical solutions to the governing fluid dynamic equations, there will always be some discrepancies in absolute force predictions between independent studies. Absolute force predictions will also be a function of the type of numerical scheme used to solve the equations in a particular solver and the resolution of

the CFD mesh (Kyte et al., 2018). Since absolute forces are also sensitive to the square of the freestream flow speed, fluid dynamicists usually use CFD to find relationships between non-dimensionalised input and output parameters, e.g. Reynolds' number as the input, and lift and drag coefficients as the output. This removes the strong dependency of the CFD results on the freestream speed chosen and allows for scaling analysis to take place as a post-processing step, as is the case in this Chapter. Nevertheless, more often than not, CFD is used as a design tool (Evans et al., 2011), whereby simulations are run in order to answer the question of whether a change in design has improved or degraded performance, rather than to determine precise absolute force values.

My aim in this work was to undertake comparative analysis between different shaped and sized tags, in different placement positions. All other conditions, such as the absence of certain external features on the tag and seal geometries, were identical for all simulations, hence keeping such comparative analyses valid. Researchers wanting to use CFD to obtain results that are comparable to real animals in the wild should aim to use a geometry that is as close to the real animal as possible (Kyte et al., 2018). For example, the seal geometry in my study was modelled without external features such as flippers and vibrissae which will have inevitably affected the results (Kyte et al., 2018). That being said, it is necessary that some external features will be simplified as to not do so would make mesh generation impractical (Kyte et al., 2018). Indeed, varying degrees of geometric simplification can be deemed acceptable (and indeed informed) by the aim of the research (Kyte et al., 2018). For further details, see Appendix S6.4.

Appendix S6.3: Step-by-step guide to modelling the drag impact of biologging tags with CFD simulations using ANSYS FLUENT™

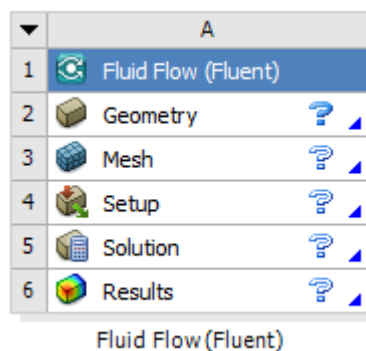
Note this guide assumes that the user has a watertight CAD geometry of the seal/animal to be studied in either STEP (.stp) or IGES (.igs) formats along with a watertight CAD model of the transponder/tag in either STEP (.stp) or IGES (.igs) format.

Part I: Geometry Import and Preparation

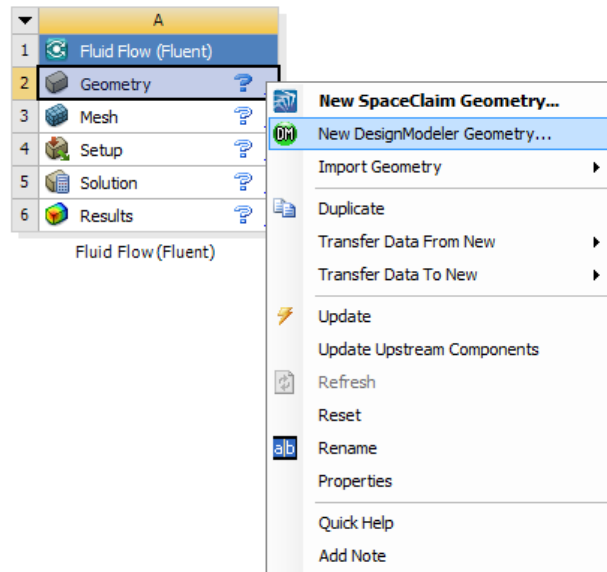
- 1) Open ANSYS Workbench (in this study I used Workbench version 18.2):



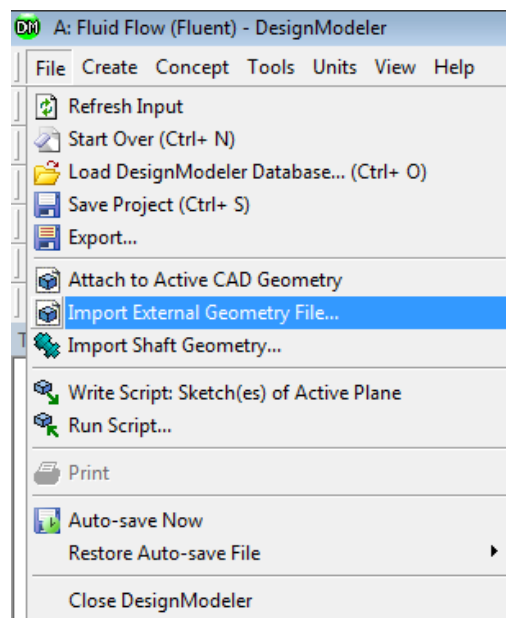
- 2) Open Fluid Flow (Fluent) from the left-hand menu. The following dialogue box should appear:



3) Right click *Geometry* followed by *New DesignModeler Geometry*:

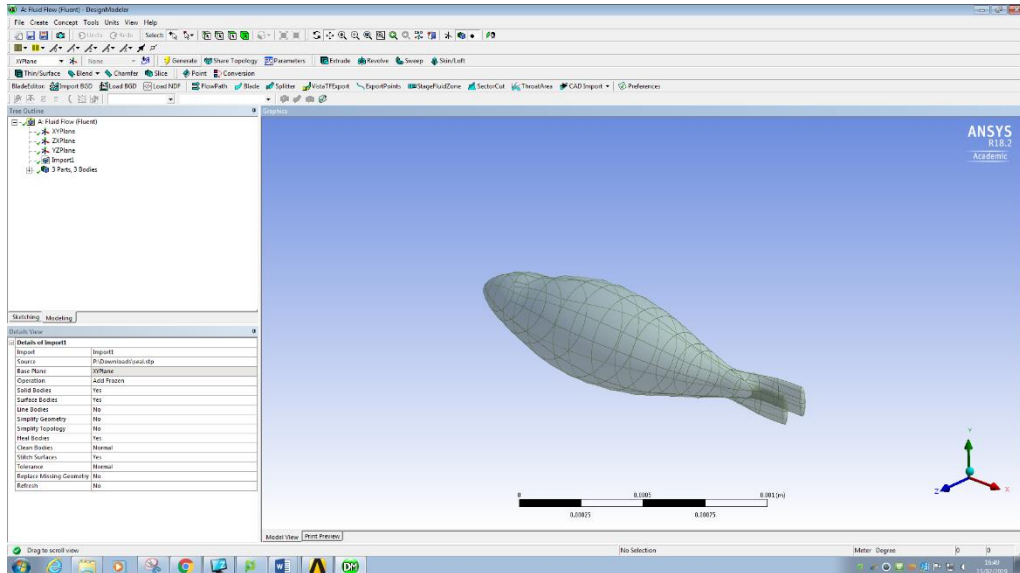


4) In 'DesignModeler', click *File > Import External Geometry File*:



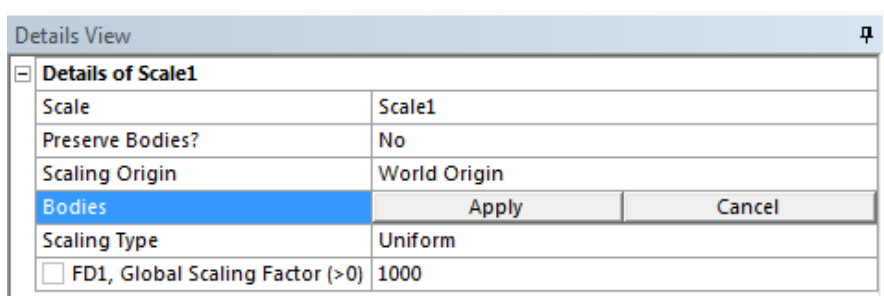
5) Select the seal geometry file (.stp or .igs) from the dialogue that opens.

When the file has been selected, click *Open* followed by *Generate*. The geometry should appear in the main window:



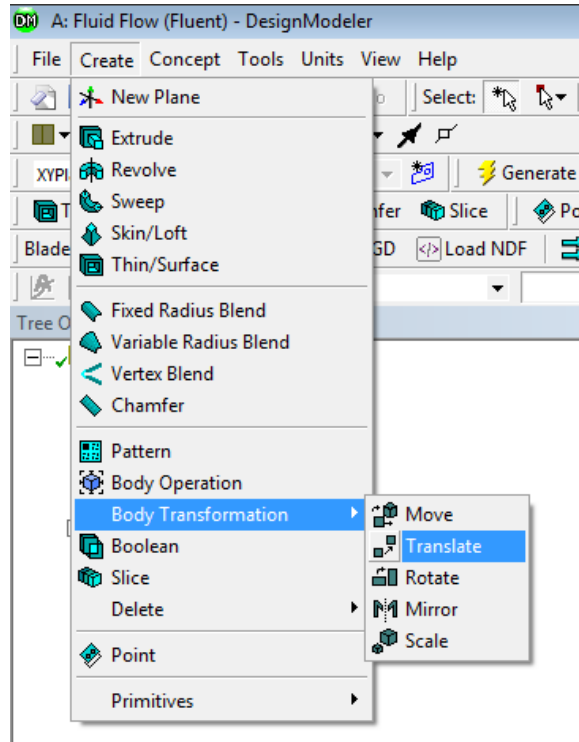
6) Check the scaling of the model using the scale on the bottom of the screen.

If scaling is incorrect (typically the body should be scaled in metres), select *Create > Body Transformation > Scale* from the toolbar at the top of the page. The following dialogue should appear:

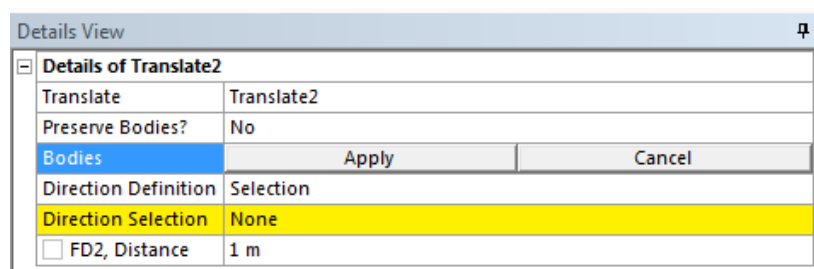


Select *Bodies* followed by the geometry that requires scaling and click *Apply*. Input the scaling factor in the *FD1, Global Scaling Factor (>0)* box and click *Generate* (at the top of the screen).

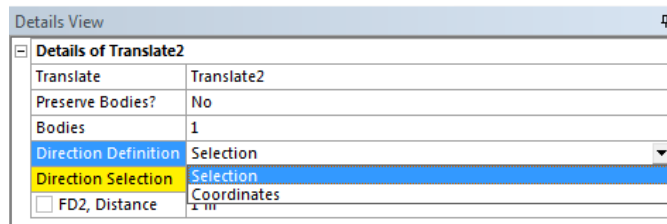
- 7) To add the tag, import the geometry file by repeating steps 4 and 5, and adjust scale as required (using step 6).
- 8) To move the tag into its required location, select *Create > Body Transformation > Translate* from the top toolbar:



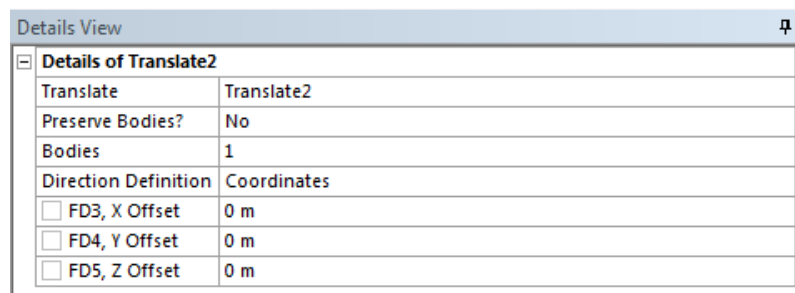
Then select the tag as the body to be translated and click *Apply*:



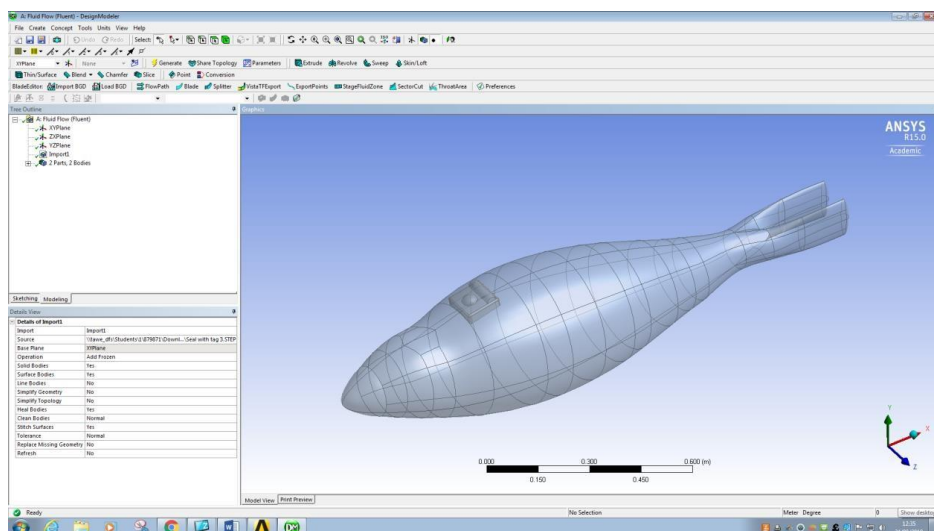
Select *Direction Definition > Co-ordinates*:



Input the required co-ordinates into the *X Offset*, *Y Offset* and *Z Offset* boxes to move the tag to the desired location and click *Generate*. N.B. The co-ordinates can be changed multiple times to position the tag at precise location on the seal. Ensure that no small gaps are left between the seal and tag bodies (geometries) when doing the translation.



The combined seal geometry with positioned tag should now be visible in the main window:



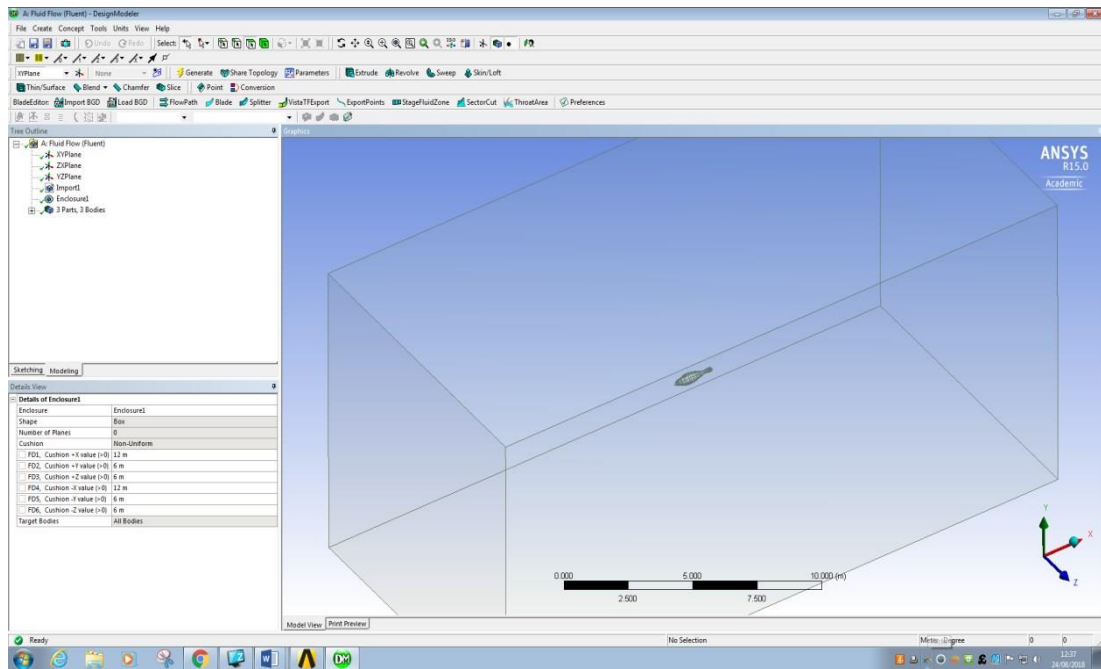
9) Next, you must generate an 'enclosure' (or 'domain') within which the fluid flow will be modelled. Go to the top toolbar and select *Tools > Enclosure*, and the following dialogue should appear:

The image shows a software dialog box titled 'Details View' with a sub-header 'Details of Enclosure1'. It contains a table with the following data:

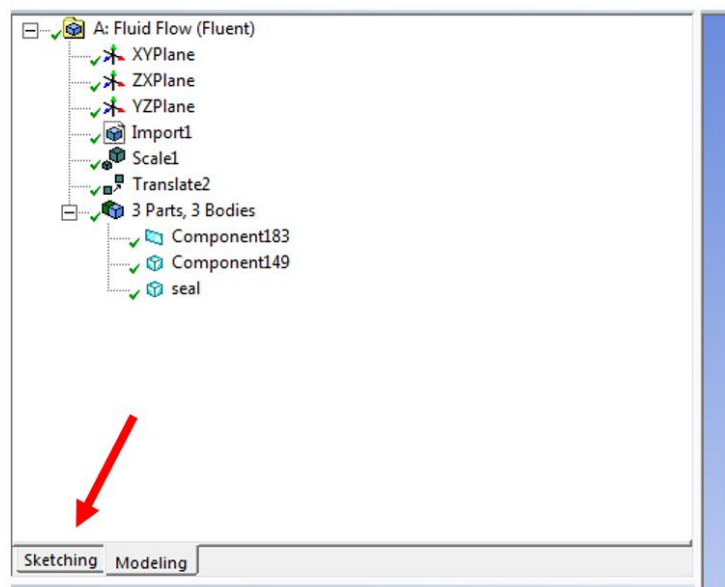
Details of Enclosure1	
Enclosure	Enclosure1
Shape	Box
Number of Planes	0
Cushion	Non-Uniform
<input type="checkbox"/> FD1, Cushion +X value (>0)	12 m
<input type="checkbox"/> FD2, Cushion +Y value (>0)	6 m
<input type="checkbox"/> FD3, Cushion +Z value (>0)	6 m
<input type="checkbox"/> FD4, Cushion -X value (>0)	12 m
<input type="checkbox"/> FD5, Cushion -Y value (>0)	6 m
<input checked="" type="checkbox"/> FD6, Cushion -Z value (>0)	6 m
Target Bodies	All Bodies
Merge Parts?	No

Input the required dimensions of the domain. Typically, the length, width and height of the domain should be several times larger than the length of the body, with the body positioned centrally. For example, in this study the length, width and height dimensions of the domain (in metres) were as follows: $(24 + \text{seal length}) \times (12 + \text{seal width}) \times (12 + \text{seal height})$.

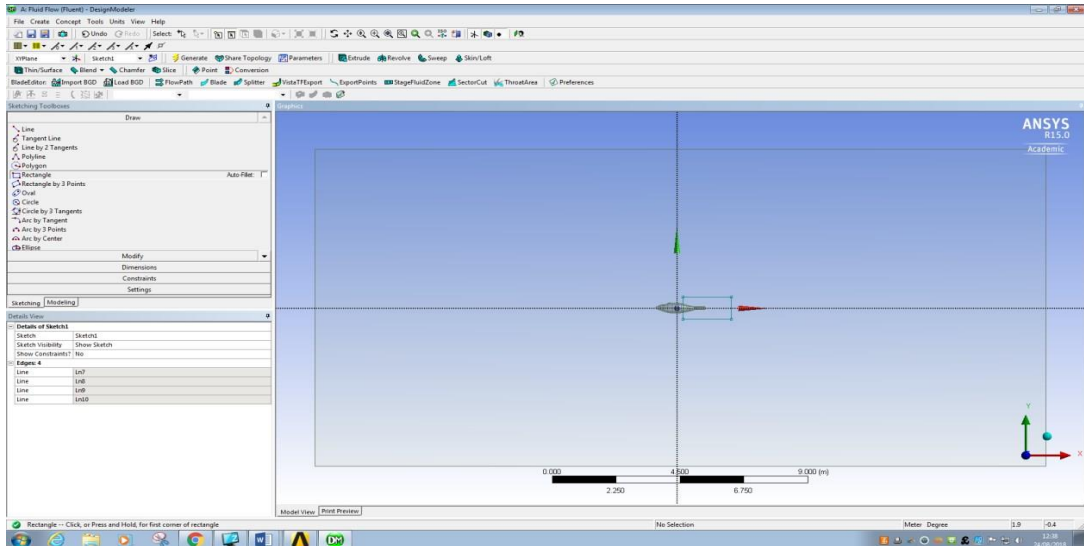
Click *Generate* and the enclosure should appear in the main window:



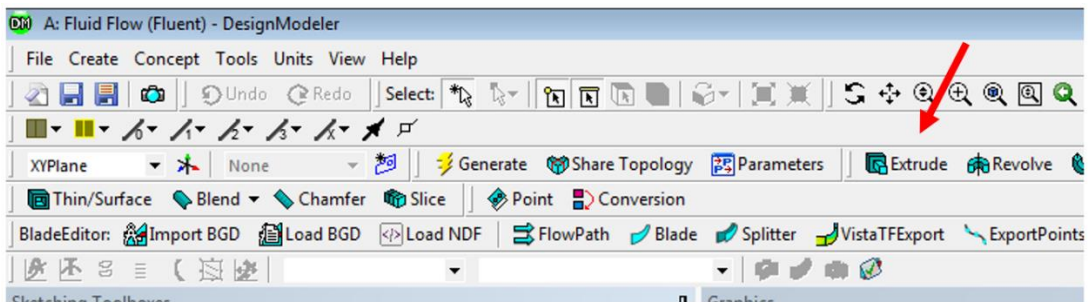
10) To create a zone of mesh refinement around the body, you must create an extruded box to define the area in which it will be required. Switch to the 'Sketching' tab from the 'Modeling' tab as shown below.



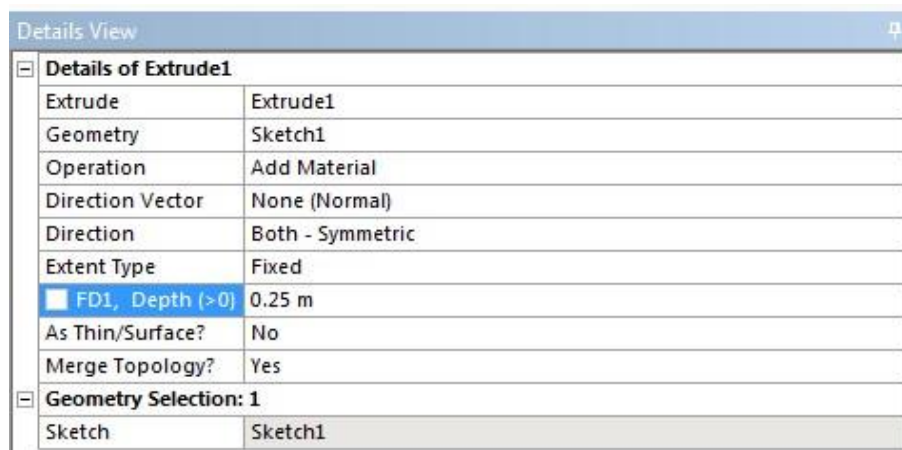
Use the *Rectangle* tool to draw the refinement zone where required. You can dimension it by using the *Dimensions* list and selecting the dimension direction required.



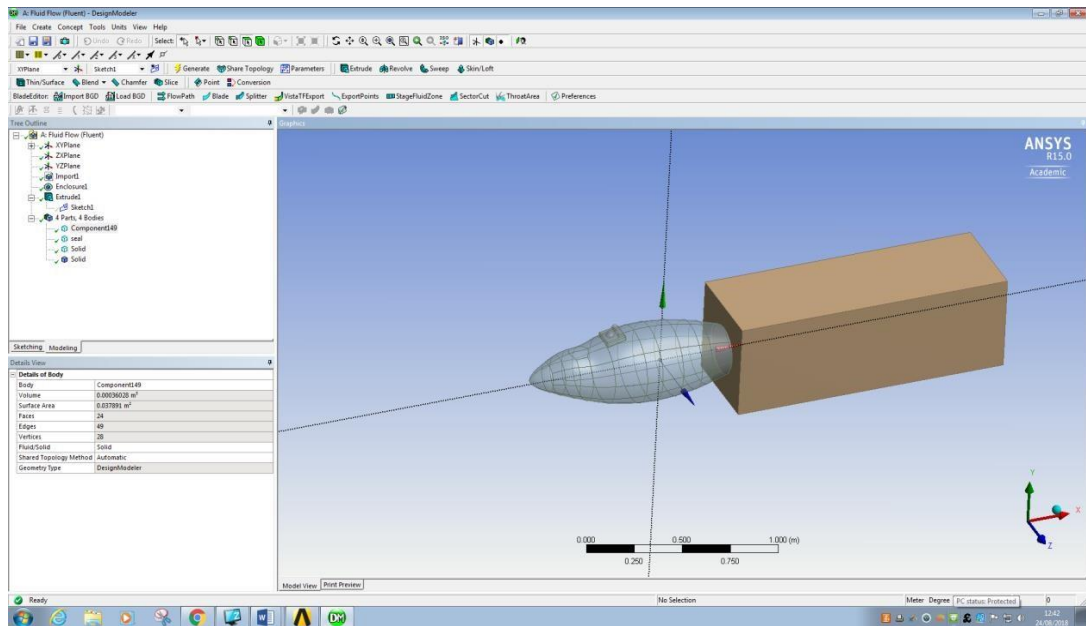
Once the rectangle has been drawn, extrude it by selecting the *Extrude* tool from the top toolbar:



The following dialogue should appear:

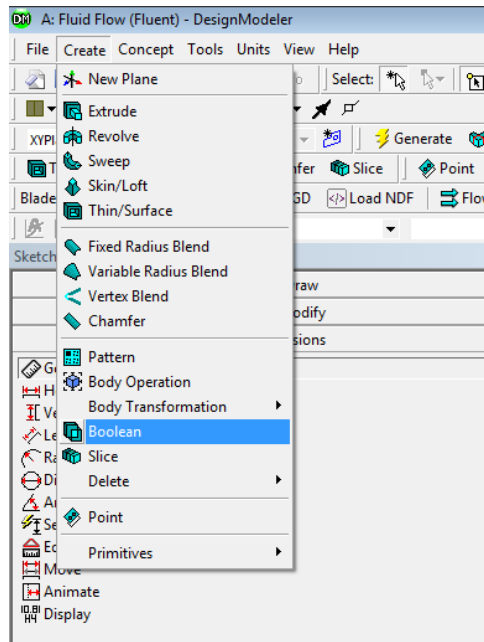


As the rectangle has been drawn at the centre of the geometry, select *Both – Symmetric* as the chosen *Direction*, then choose to *Add Material* in the *Operation* box as shown above. Select a depth (*FD1, Depth (>0)*) for the box to be extruded in both directions and then click *Generate*. The extruded refinement zone box will appear in the main window:

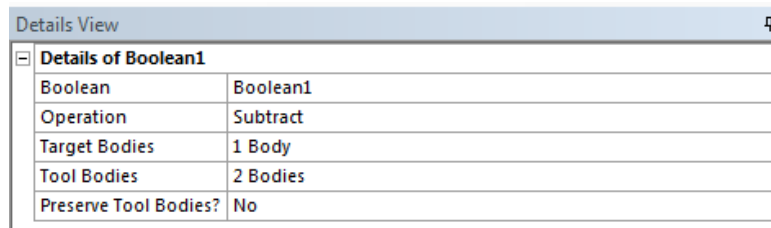


11) Next, a Boolean must be generated to identify the calculation area (the area in which you wish to simulate the fluid flow i.e. outside of the seal geometry but within the enclosure/domain boundary).

Select *Create > Boolean* from the top toolbar:

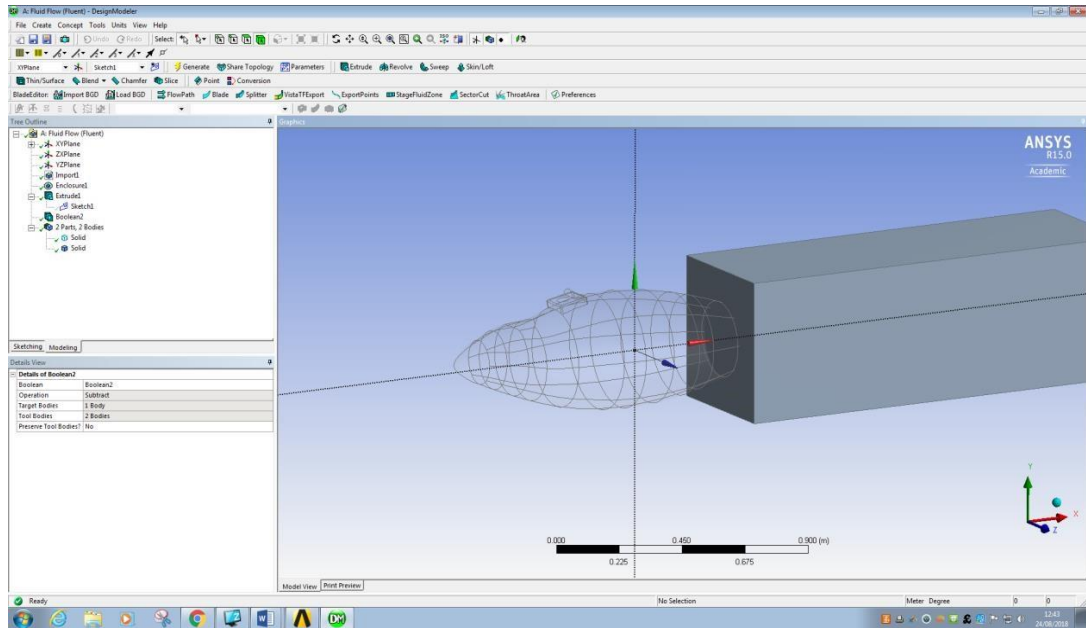



The following dialogue box will appear:



Select *Subtract* as the operation. Select the large enclosure as the *Target Bodies* and click *Apply*. Select the seal and tag as the *Tool Bodies* and click *Apply* followed by *Generate*.

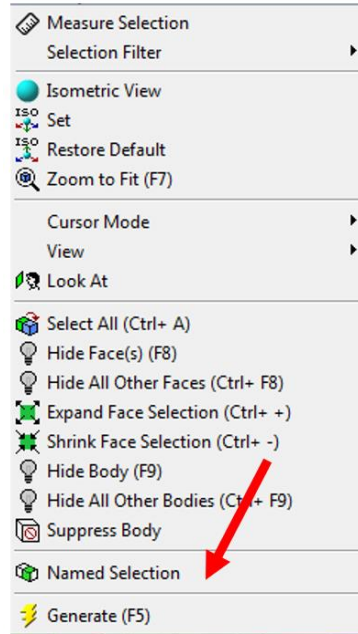
The Boolean should appear in the dialogue on the upper left hand side, and the seal and tag should appear transparent as below. If any errors occur in generating the Boolean, ensure that the seal and tag are in contact without any gaps between them.



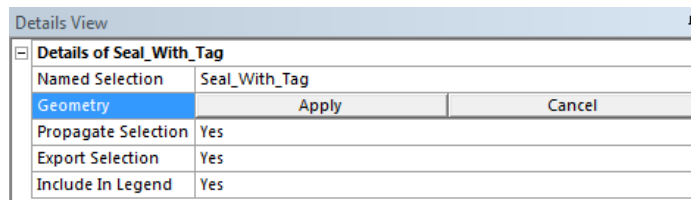
12) Next, each part of the geometry needs to be named. Select the  symbol from the top toolbar and select *Box Selection*. Now, choose to select only faces by choosing the following symbol from the top toolbar:



Use this tool to select all faces of both the animal and transponder by drawing a box around them. When these are highlighted, right click on the highlighted objects and select *Named Selection*.



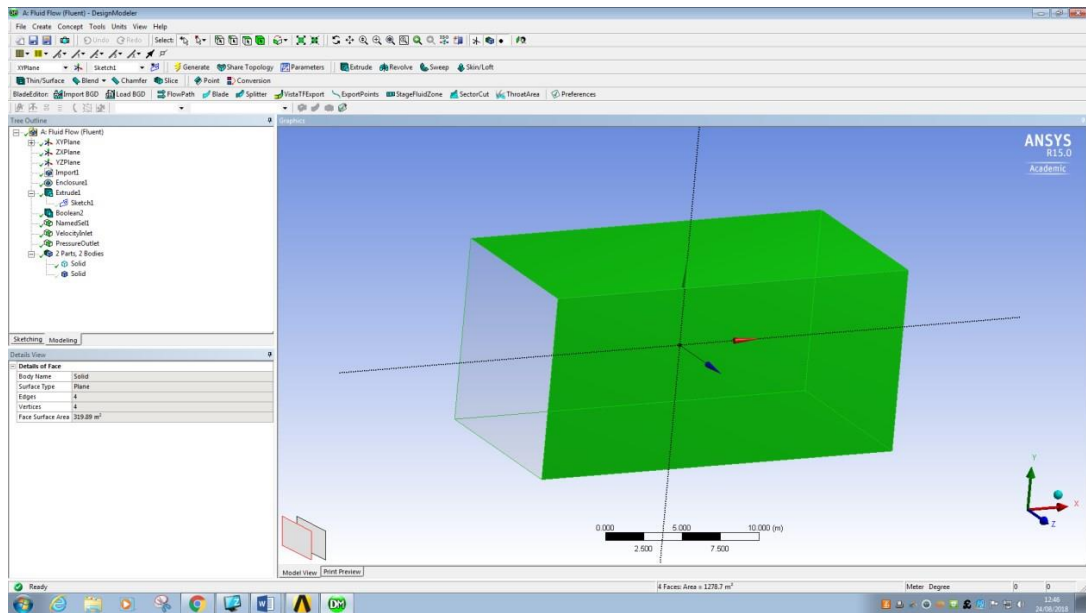
The following dialogue box should appear in the bottom corner:



Click *Apply*, and then input an appropriate name in the *Named Selection* Box. Click *Generate*, and your named selection should appear in the upper left dialogue.

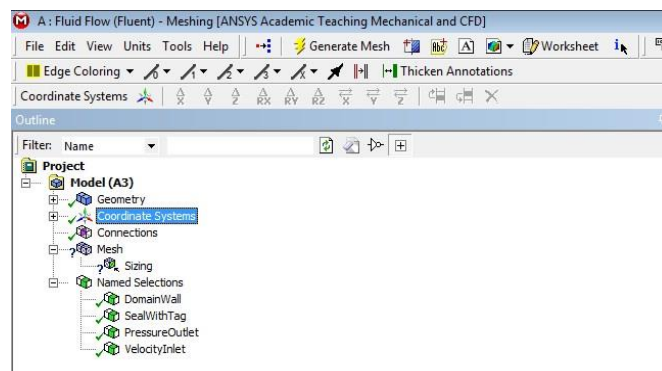
Select the  symbol from the top toolbar to return to *Single Select*.

Select the two side faces and the top and bottom faces of the large enclosure (taking care not to select the front and rear faces). Right click and perform *Named Selection* once again (as above), this time naming the selection *Domain Wall*. Click *Generate*.



Repeat these steps to name the front wall of the large enclosure “*VelocityInlet*”, and the rear wall “*PressureOutlet*”. Using this terminology allows the Fluent CFD solver to recognise which surfaces are being used for which purpose later on.

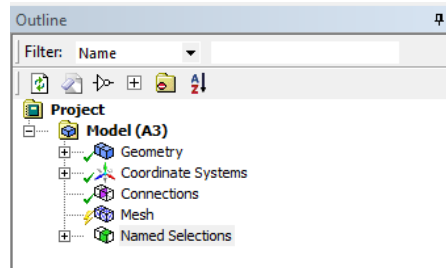
You should be left with a list of named selections on the left hand side as shown:



Part II: Mesh Generation

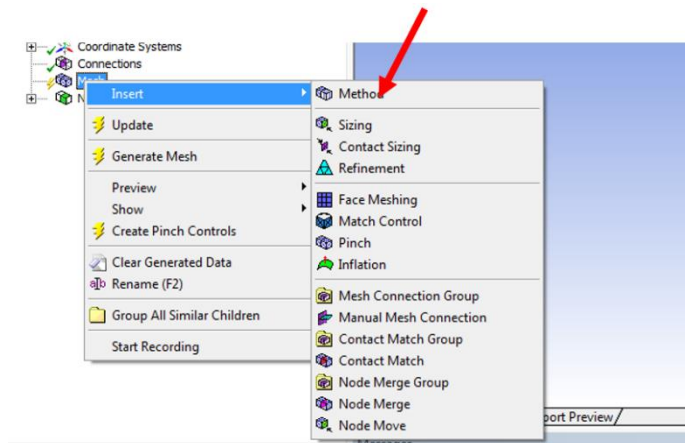
13) Close *DesignModeler* and open *Mesh* from the ANSYS Workbench.

The following menu should be on the left when the window opens:



NB. The following mesh settings were selected after completing a formal mesh convergence study to determine the optimum mesh resolution to achieve accuracy of results at minimal computational cost (refer to Methods section in the paper for details).

14) Right click on *Mesh* and select *Insert > Sizing*:

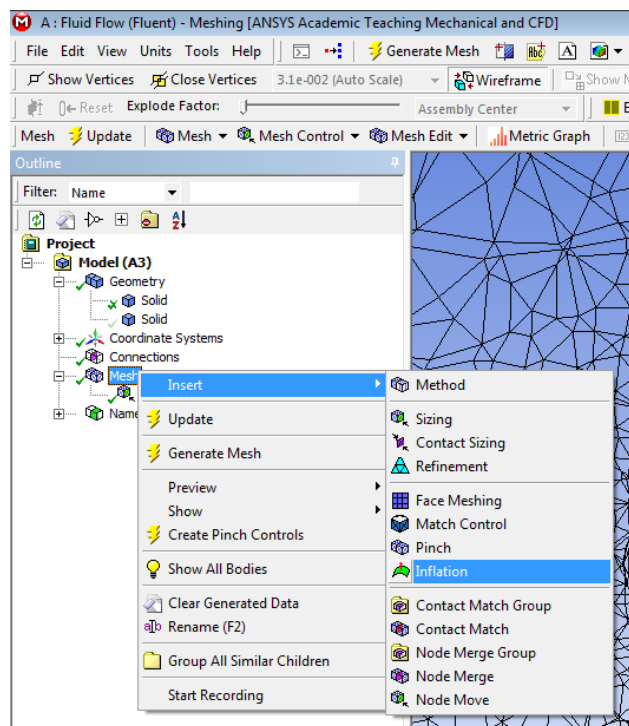


The following dialogue appears:

Details of "Face Sizing" - Sizing	
Scope	
Scoping Method	Named Selection
Named Selection	SealWithTag
Definition	
Suppressed	No
Type	Element Size
<input type="checkbox"/> Element Size	4.5e-003 m
Behavior	Soft
<input type="checkbox"/> Curvature Normal Angle	Default
<input type="checkbox"/> Growth Rate	Default
<input type="checkbox"/> Local Min Size	Default (4.5e-003 m)

For *Scoping Method*, choose *Named Selection*. For *Named Selection*, choose the seal and tag combined. For *Type*, choose *Element Size*. Input the chosen element size as 4.5e-3. Leave all other settings as default.

15) Right click on *Mesh* and select *Insert > Inflation*.

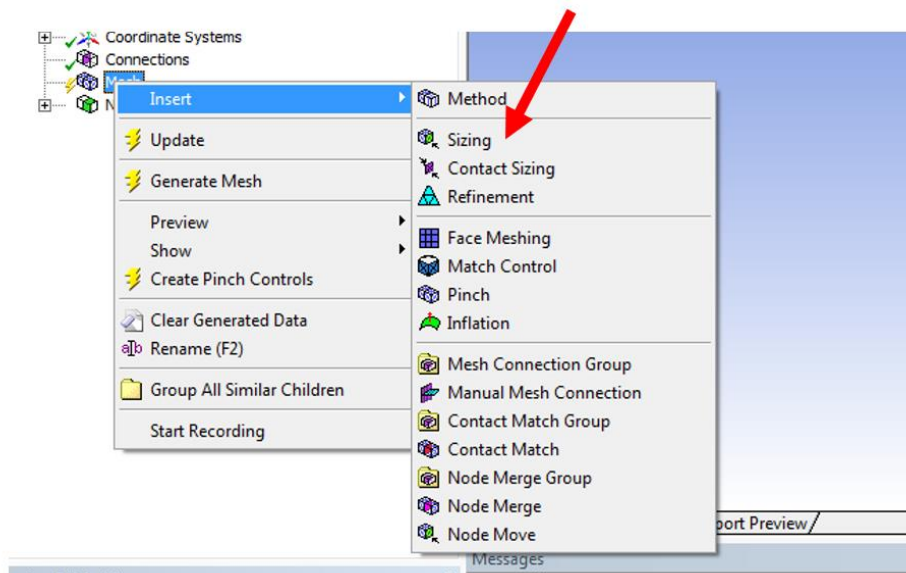


The following dialogue appears:

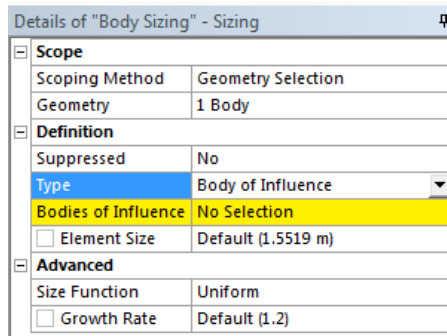
Details of "Inflation" - Inflation	
Scope	
Scoping Method	Geometry Selection
Geometry	1 Body
Definition	
Suppressed	No
Boundary Scoping Method	Named Selections
Boundary	SealWithTag
Inflation Option	First Layer Thickness
<input type="checkbox"/> First Layer Height	5.23e-005 m
<input type="checkbox"/> Maximum Layers	20
<input type="checkbox"/> Growth Rate	1.2
Inflation Algorithm	Pre

For *Scoping Method*, select *Geometry Selection*. For the *Geometry*, select the Boolean on the screen (the large box with the animal within it) and click *apply*. For *Boundary Scoping Method*, choose *Named Selections*. For *Boundary*, select the seal with tag from the menu and click *Apply*.

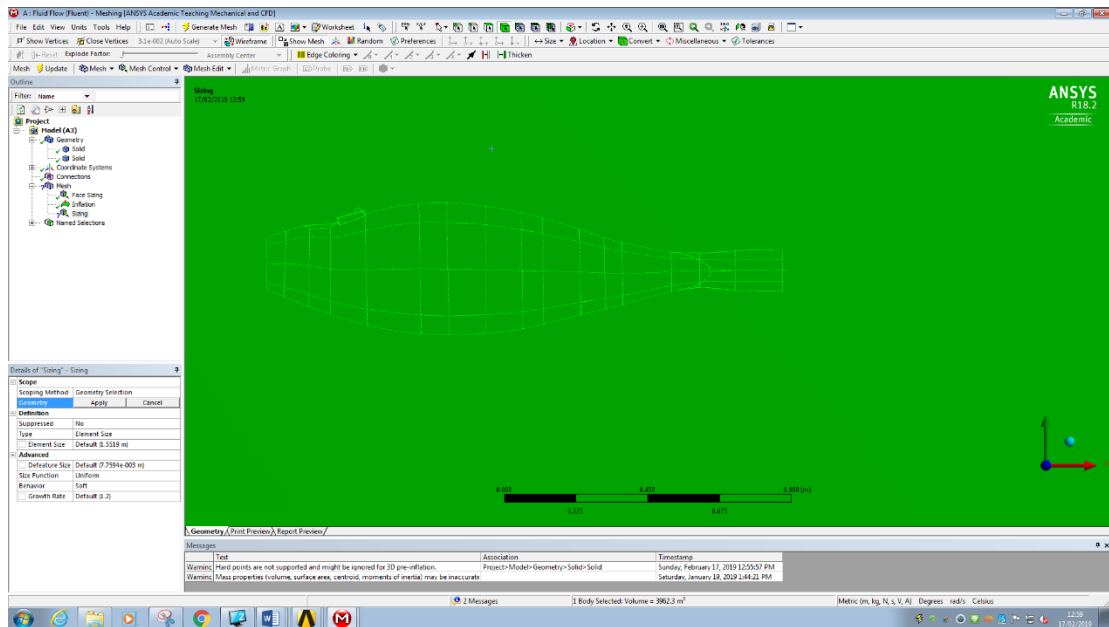
16) Right click on *Mesh* and select *Insert > Sizing*.



The following dialogue should appear:



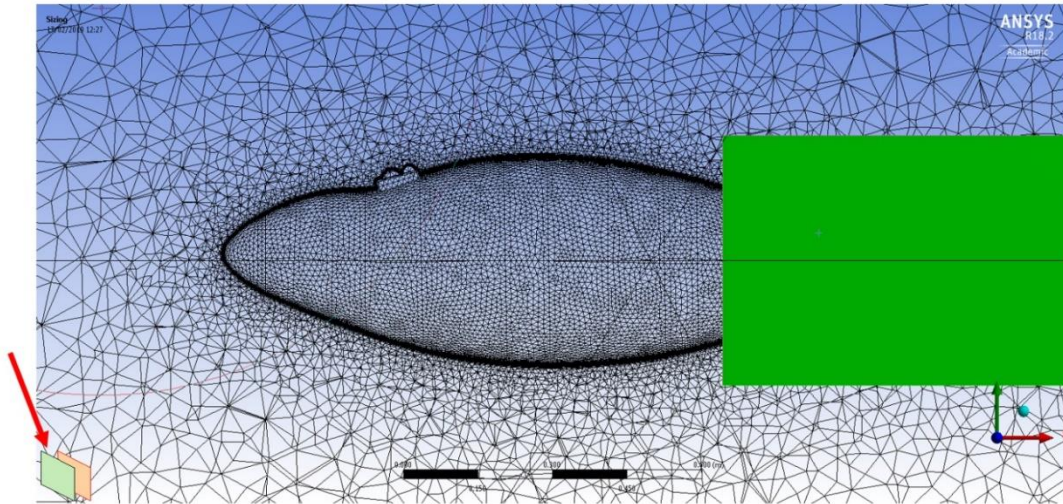
For *Scoping Method*, choose *Geometry Selection*. For the *Geometry*, select the Boolean once again, as shown below.

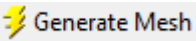


For *Type*, select *Body of Influence*. For the body of influence, select the refinement zone box. Select this by using the following symbol at the



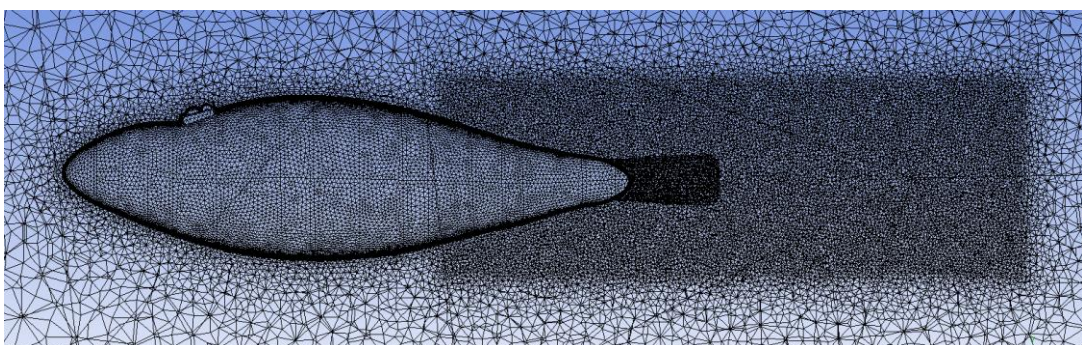
bottom of the page:



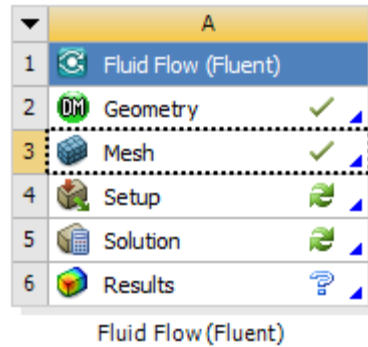
For *Element Size*, input the chosen size – in this case, 0.01 – and click *Generate Mesh* 

- 17) Wait for the mesh to finish generating, and then click *Mesh* on the left-hand panel to examine the mesh created. You may wish to use the section view tool to examine the mesh in more detail, as some parts may not be visible otherwise.

Below is an example of a mesh generated for this study shown using a section view along the length of the seal.

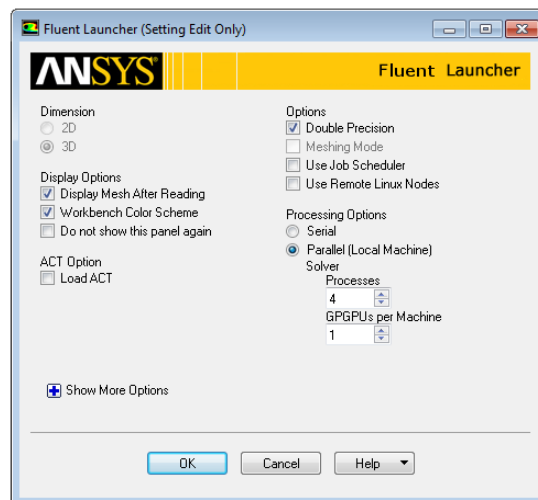


18) Exit the meshing environment and return to the workbench. Before proceeding, ensure that there is a green tick next to the word *Mesh* (as shown below). If there is not, right click on the word *Mesh* and click *Update*. Wait for the project to update before proceeding.

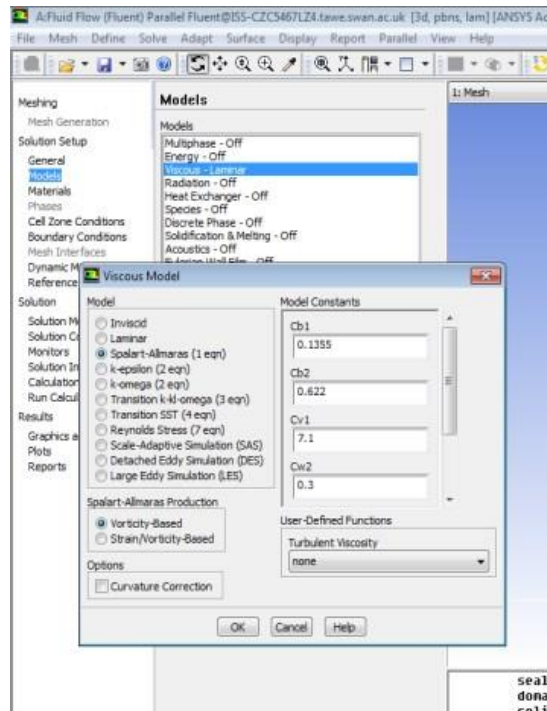


Part III: CFD Simulation

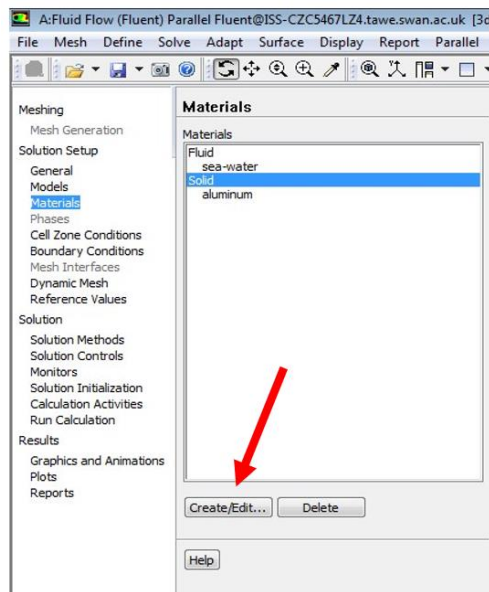
19) Double click *Setup* to open 'Fluent Launcher' and the following window will appear:



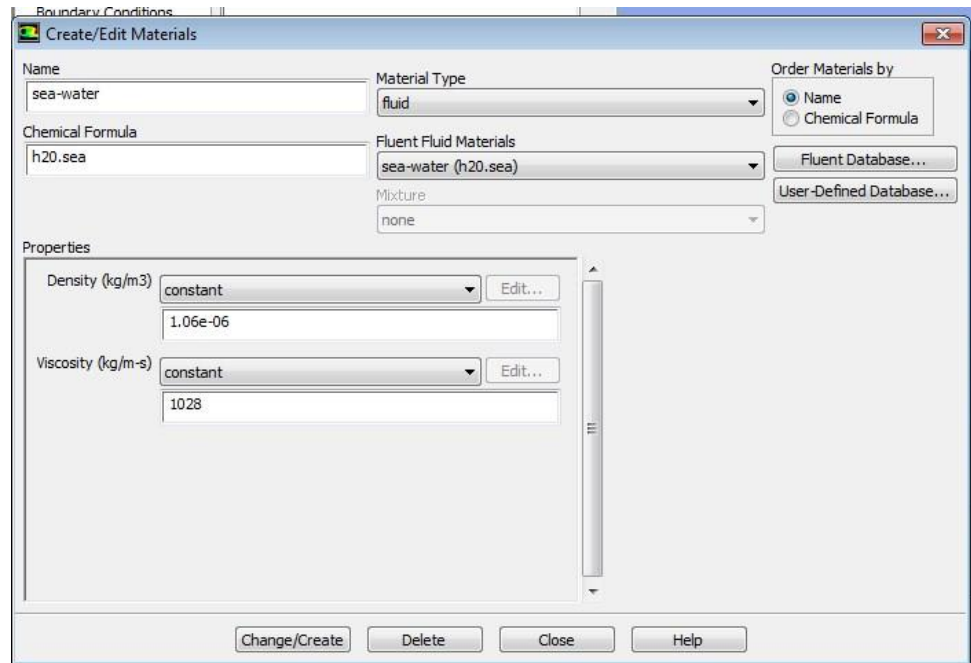
20) Select *Models* from the side pane. Double click *Viscous- Laminar* and choose *Spalart-Allmaras (1 eqn)* from the dialogue that appears as shown below. Click *OK*.



21) Select *Materials* from the side panel and click *Create/Edit*.



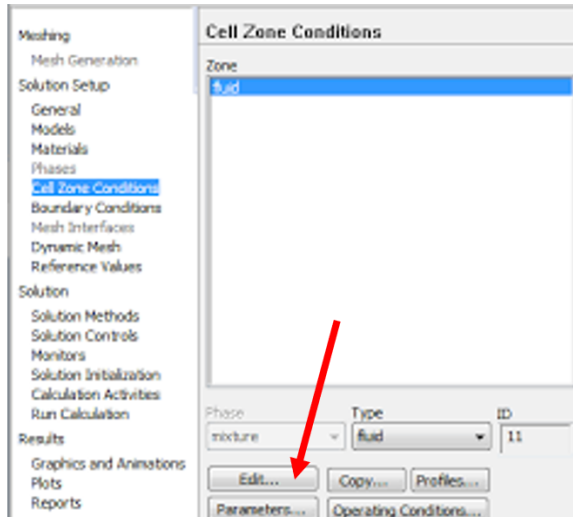
The following dialogue should appear:



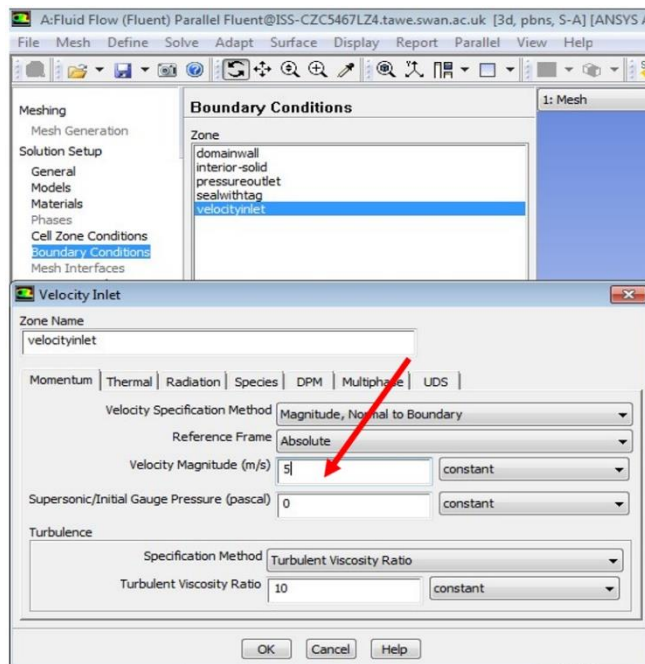
Input the density and viscosity of sea water as 1.06e-06 and 1028 respectively. Allocate *sea-water* as the name, and *h20.sea* as the Chemical Formula (other names/chemical formulas can be used, and different values for density and viscosity can be inputted).

Click *Change/Create*. If asked if you'd like to overwrite another material, select *No*.

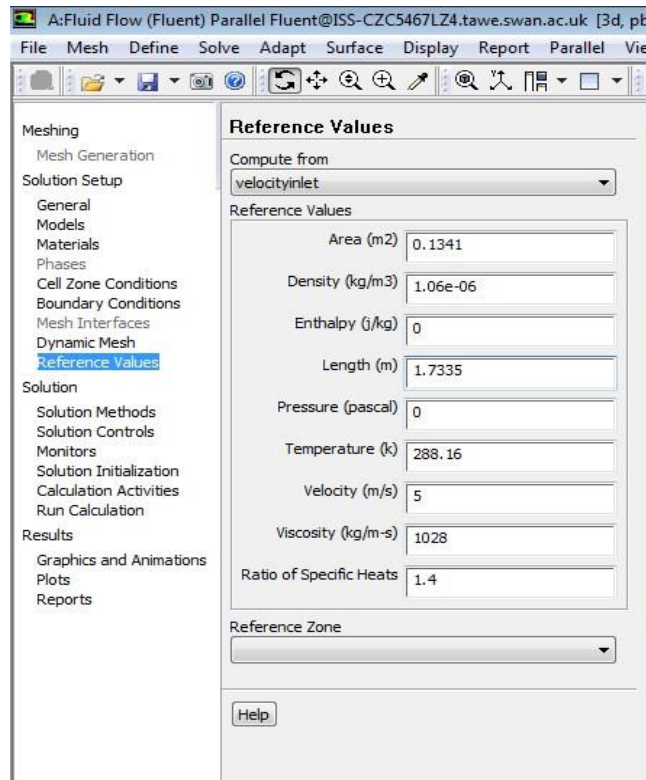
22) Click on *Cell Zone Conditions*. Select the fluid, then *Edit*. Change the *Material name* to sea water and click *OK*. Then return to materials and delete any other materials (other than sea-water) from the fluids list.



23) Select *Boundary Conditions* from the side panel. Double click on *velocityinlet* and set the freestream velocity that you wish to simulate; here “5” (m/s). Click *OK*.

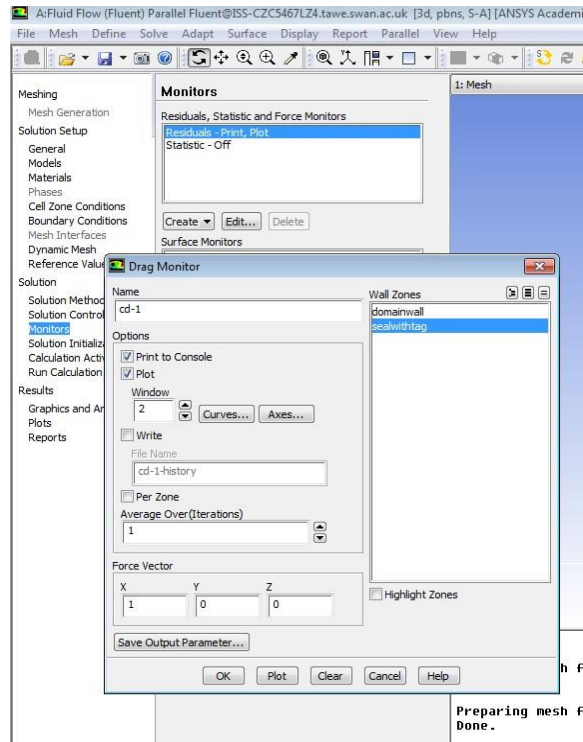


24) Select *Reference Values* from the side panel. In the drop down menu *Compute from*, select *velocityinlet*. For *Area*, input your projected frontal area onto the *velocityinlet* face. The length should be the length of the seal in the flow direction.



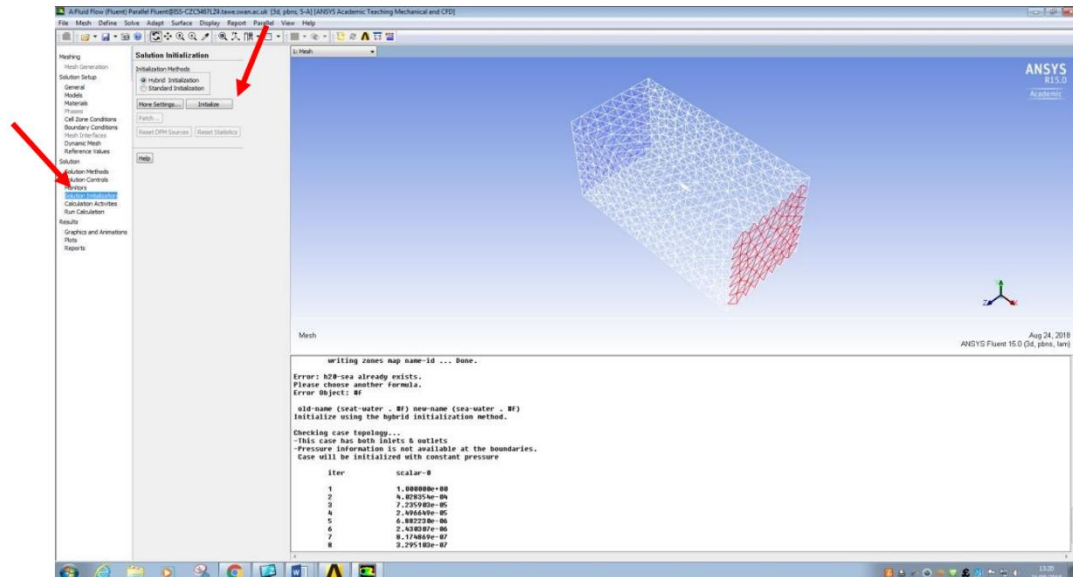
25) Select *Solution Methods* and change the *Turbulent Kinetic Energy* to *Second Order Upwind*.

26) Select *Monitors* from the side panel. Select *Residuals - Print, Plot* then click the *Create* drop down menu. In turn, create a monitor for drag, lift and moment – the following dialogue box should appear each time:



Select the seal with tag in the *Wall Zones* box and check both the *Print to Console* and *Plot* boxes. Click *OK* to create.

27) Select *Solution Initialization* from the side panel and click *initialize*. You will see writing appear in the text box at the bottom of the screen:



28) When the text box tells you that the initialization is complete, select *Run Calculation* from the side panel.

29) As the simulation runs, you can observe graphs generated by the results being calculated by using the drop down menu at the top of the screen. The graphs showing the evolution of lift, drag and moments should converge to steady state values until the solver terminates.

30) Return to the Ansys Workbench and the *Results* tab can be used to create the plots of force coefficients and visualisation of the solution field as required.

Appendix S6.4: Further technical details for the CFD modelling approach

Maintaining simplicity in CFD modelling

For simplicity in the CFD modelling, external tag features such as the tag antennae were removed from the geometries. I note that removal of antennae will inevitably affect absolute measures of tag-induced drag, because external features cause increased turbulence; indeed Wilson et al., (2004) showed considerable effects of antenna length, diameter and rigidity, and Balmer et al., (2014) showed that non-optimum antenna positioning could increase drag by up to 15%. Nevertheless, different degrees of geometric simplification can be deemed acceptable (and indeed informed) by the aim of the research (Kyte et al., 2018). My main aim here was to exemplify the CFD method by assessing effects of size, shape, and position of the main body of tags on induced drag experienced by a tagged seal, by quantifying differences between two different tag designs; thus I made sure that external features, such as antennae, were removed from both geometries compared.

Steady state assumption

In this work the assumption was made that a steady state solution existed for each (non-dynamic) simulation. This allows for local time integration within the CFD solver, as a precise time history of the solution was not necessary.

Mesh convergence study and mesh generation

A mesh convergence study was undertaken to determine the appropriate mesh resolution necessary to generate flowfield solutions with minimal dependency on the underlying mesh. Specifically, the simulation mesh was progressively refined to determine the mesh resolution at which force coefficients were stable (to three significant figures) and, therefore, solutions assumed to be mesh independent. This determined the appropriate mesh resolution for the remainder of the study.

The surface mesh was generated using the Delaunay advancing front method (Löhner & Oñate 2004) and the fine, quasi-structured boundary layer mesh was constructed using an advancing layers method (Wang et al., 2017) with a growth rate of 1.2 (i.e. each mesh layer increasing in size by a factor of 1.2 as

you step away from the body surface) as seen in Fig. 1(a). The unstructured, isotropic, tetrahedral volume mesh for the remainder of the domain surrounding the seal geometry was constructed using a standard Delaunay, point-insertion method directed by a user defined cell size distribution function (Walton et al., 2017). The surrounding domain should be several times the size of the animal geometry with the geometry positioned centrally; my domain extended 12 m in front and behind the seal, and 6 m above, below, left, and right of the seal. The solver used within Fluent was a vertex-centred, finite volume numerical scheme for the incompressible Reynolds-Averaged Navier-Stokes equations (Evans et al., 2011) with the Spalart-Allmaras turbulence model (Spalart & Allmaras 1994). This turbulence model was chosen as it is one of the standard choices used in the aerospace industry and tends to have minimal dependency on the underlying mesh used (Evans et al., 2009). All simulations were run, assuming a steady-state solution existed, using local Runge-Kutta timestepping until a steady solution was achieved, i.e. 3 significant figures of accuracy in output force coefficients.

Flow equations

The Reynolds number, Re , of the flow simulations, defined as

$$Re = \frac{\rho VL}{\mu} \quad (1)$$

where ρ is the fluid density (1028 kg m^{-3}), V is the freestream flow velocity (5 m s^{-1}), L is the seal length (1734 mm) and μ is the dynamic viscosity of salt water ($1.09 \times 10^{-3} \text{ Pa s}$) was 8.2×10^6 .

All non-dimensional drag coefficients, C_d , defined as

$$C_d = \frac{D}{\frac{1}{2}\rho V^2 A} \quad (2)$$

where D is the absolute drag value (in Newtons) of each seal and tag combination, were determined.

Appendix S6.5: Tag-induced impact on lift coefficient (C_i)

Tag A had a considerably larger low pressure region than tag B (Fig. 5.4) which would potentially negatively impact the ease of movement of the animal, by contributing to a lift force trying to pull the tag off the animal (Fiore et al., 2017). This is important because high and low pressure differentials could act to increase shear loading or downforce, which can lead to early detachment of a tag from an animal, or injury at the site of attachment respectively (Fiore et al., 2017).

I note that both tags generated substantial variation in the lift coefficient C_i , when compared to the untagged animal. However, the net magnitude of both the positive or negative lift forces (i.e. a force contributing to pulling the tag off the animal or pushing the tag down on to the animal, respectively) was markedly smaller in comparison to their net drag loading. Specifically, across all positions, the lift forces generated by the tags were an order of magnitude smaller than the drag force generated, with the largest relative magnitude of C_i only 8.5% (tag A mean: 3.46%; tag B mean: 1.14%) (Table 5.2). Whilst these values are very small, I note importantly that tag A generated larger absolute lift values than tag B across all positions except 7 and 9 (Table 5.2). Moreover, the direction of resultant lift force generated by the tags was not consistent across attachment positions, for example in positions 1–7 tag A generated lift ($C_i = 0.00005$ – 0.00614), whereas in positions 8 and 9 it generated downforce ($C_i = -0.0000$ – -0.00257) (Table 2). In the most extreme case there was a -200 % change in lift: from 0.00259 in the untagged animal case to -0.00257 when tag A was placed at position 8. This demonstrates that tag positioning is crucial not only for determining the magnitude of impact, but also for its direction (i.e. up-thrust or downforce).

Appendix S6.6: Example figure of a CFD simulation of tag-induced drag in lateral flow.

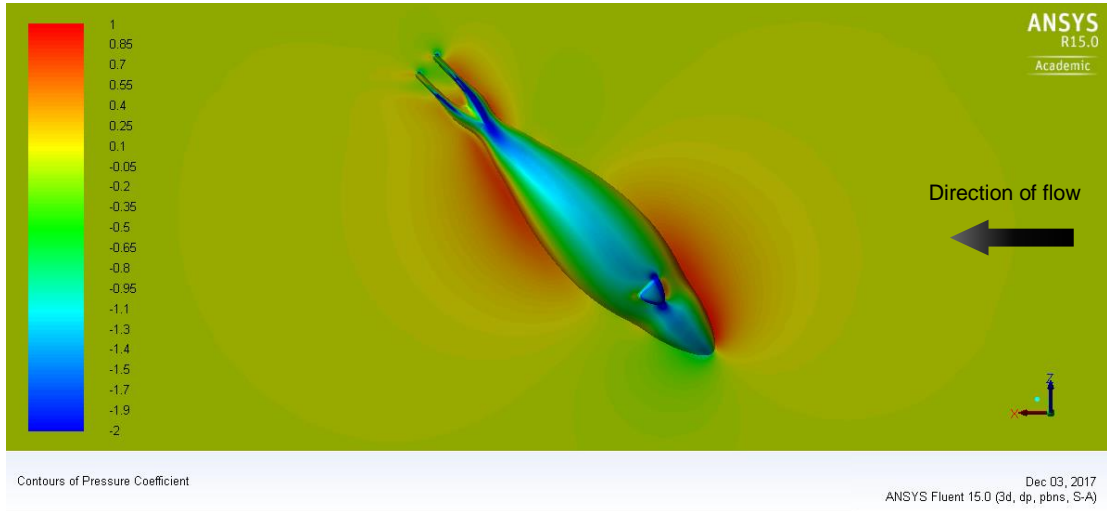


Fig. S6.6. Example figure of a CFD simulation of tag-induced drag in lateral flow. Here the model seal is positioned at 45° to the oncoming flow (black arrow shows direction of flow) with tag B placed at position 2 and flow speed 5 ms⁻¹.

Appendix VII: Supplementary material: Other

Contents

Appendix S7.1: Swansea University ethical approval application

Appendix S7.2: Ethical application approval decision letter

Appendix S7.3: Risk assessment for seal capture and tag deployment

Appendix S7.4: Risk matrix for seal capture and tag deployment

Appendix S7.5: Risk assessment for tag building

Appendix S7.6: R scripts

Appendix S7.1: Swansea University ethical approval application

APPLICATION FOR ETHICAL APPROVAL OF PROJECTS INVOLVING LIVE VERTEBRATES OR CEPHALOPODS THAT DO NOT INVOLVE HANDLING OR CONFINEMENT

RESEARCH CANNOT COMMENCE UNTIL ETHICAL APPROVAL HAS BEEN OBTAINED

Please note form is opened as read-only.

Reference Number:

STU_BIOL_65421_161017164514_1

Status: Approved Proposal : [College Ethics Committee DECISION Details](#)

Submitted By: James Bull

Submitted Date: 11 Jul 2018

1. Title of Research Project/teaching activity involving live animals:

Seal biollogging Wadden Sea (North Sea, Germany)

2. College:

Science

3. Staff/students undertaking research:

William Kay

Dr James C. Bull Professor Luca Börger

4. Primary staff contact detail (Name, E-mail, Phone):

Luca Borger - [REDACTED]

5. A. Proposed start date of project/activity:

01-01-2016

5.B. Duration:

3.5 years

6. Location(s) where the project/activity will take place:

Wadden Sea (North sea,

7. Partner bodies /organisations:

(i) their full, official name(s) / tle(s);

(ii) details of the work to be carried out (a) at the partner(s) and (b) at the University;

(iii) details of the relevant ethical approval(s) from the partner(s), including reference numbers.

As advised by College of Science AWERB, I am submitting my ethics application for the approved project for which I am already nominated to conduct research under, in order for me to obtain my own personal approval number. The approved project for which I am referring to is in the name of Professor Luca Borger - Approval Number: SU-Ethics- Staff-260418/70 - Reference Number: STAFF_BIOL_14156_110418161246_1

8. Please state or tick, as appropriate, the following questions relating to your project:(tick any that apply during the progression of an experiment)

a) species and taxon: Grey seal (*Halichoerus grypus*) and Harbour seal (*Phoca vitulina*)

b) approximate number: Please refer to approved project

life stage:

Juvenile/Adults

Mammal, bird or reptile embryo beyond

halfway through incubation/gestation

period Amphibian, cephalopod or fish

larvae capable of independent feeding

Strictly only gametes/very early developmental stages of embryos

9. A. Does the proposed project/activity involve a Schedule 1 killing method (as defined by ASPA 1986) being carried out by members of this University's staff or by its student?

Yes No

9. B. If yes, please list the individuals involved and provide training details:

10. Provide a **brief** scientific background for the work, and describe any pilot work undertaken:

Please refer to approved project - Approval Number: SU-Ethics-Staff-260418/70 - Reference Number: STAFF_BIOL_14156_110418161246_1

11. Please provide a clear methodology for the work to be undertaken:

Please refer to approved project - Approval Number: SU-Ethics-Staff-260418/70 - Reference Number: STAFF_BIOL_14156_110418161246_1

12. Provide a **brief** statement of how science will advance or people or animals will benefit from this project:

Please refer to approved project - Approval Number: SU-Ethics-Staff-260418/70 - Reference Number: STAFF_BIOL_14156_110418161246_1

13. Why do animals have to be used in this study? Explain your choice of species, and justify the number of subjects to be used with a power analysis where appropriate.

Please refer to approved project - Approval Number: SU-Ethics-Staff-260418/70 - Reference Number: STAFF_BIOL_14156_110418161246_1

14. What effects will your research have on the study organisms, and how suffering will be kept to a minimum?

Please refer to approved project - Approval Number: SU-Ethics-Staff-260418/70 - Reference Number: STAFF_BIOL_14156_110418161246_1

15. How will you dispose of carcasses/animals (tick any that apply):

Landfill

Samped/analysis/other destruction of biomass

Released

Sent live to external organisation

16. Please provide details of any animal-related training required by staff / students as part of this project / activity. How will their competency be assured?

DECLARATION 1

I certify that the answers to the questions given above are true and accurate to the best of my knowledge and belief and I take full responsibility for it. I also confirm that I have read the University's Policy Framework on [Research Ethics & Governance](#) and will abide by its



ethical guidelines, as well as the ethical principles underlying good practice appropriate to my discipline.

DECLARATION 2

I also confirm that I understand that all projects and activities involving live animals shall be undertaken in accordance with relevant external and internal policies, regulations, codes of practice and other requirements, and that further information on these is available from University and College research and teaching support services. (Further information on the college ethics committee is available via

cosethics@swansea.ac.uk).

Appendix S7.2: Ethical application approval decision letter

College Ethics Committee/AWERB Group DECISION on Ethical Review

Application Details

Project Title: Advanced Telemetry and Bio-logging for Investigating Grey Seal Interactions

Applicant Name: William Kay

Submitted by: James Bull

Having examined the information included in the above application with Reference No. STU_BIOL_65421_161017164514_1, this Committee has decided to:

Approve this application

Low Moderate High

Any amendments to approved proposals should be emailed to College Ethics Committee for

Reject this application and allow for resubmission provided the ethical issues raised by the College Ethics Committee/AWERB Group below are addressed Return for minor amendment/clarification (please resubmit using the

Comments:

The CoS Ethics Committee has no ethical concerns and approves this

Last Updated Date: 24 Jul 2018

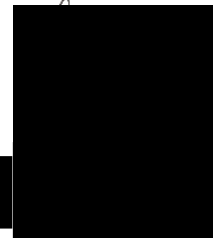
Appendix S7.3: Risk assessment for seal capture and tag deployment

Risk Assessment for Teaching, Administration and Research Activities

Swansea University; College of Science

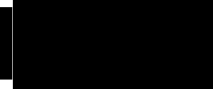
Name William Kay

Signature
date 30/09/16



Supervisor* James Bull

Signature
date 30/09/16



Activity title Capture and handling of grey and harbour seals

Base location (room no.) 147

(* the supervisor for all HEFCW funded academic and non-academic staff is the HOC)

University Activity Serial # (enter Employee No. or STUREC No.....)

Start date of activity (cannot predate signature dates)

End date of activity (or ‘on going’) On going

Level of worker (delete as applicable).....

PG, academic staff

Approval obtained for Gene Manipulation Safety Assessment by SU ?

~~Yes~~/not applicable

Licence(s) obtained under “Animals (Scientific Procedures) Act (1986)” ?

Yes/~~not applicable~~

Approval obtained for use of radioisotopes by COS ?

~~Yes~~/not applicable

Record of specialist training undertaken

Course	date
Wild Mammal and Bird Home Office Course – Animals (Scientific Procedures) Act, 1986 Universities’ Training Group - Animal and Plant Health Agency (APHA) – York, UK	08/02/16-11/02/16
British Divers Marine Life Rescue (BDMLR) Marine Mammal Medic – Swansea Bay, Swansea	21/05/16-22/05/16
Rescue Emergency Care (REC) Remote First Aid – Swansea University	12/09/16-15/09/16
Sea Mammal Research Unit Seal Capture and Handling training – Norfolk, The Wash	10/10/16-12/10/16
Sea Mammal Research Unit Seal Capture and Handling training – Loch Fleet, Scotland, UK	14/02/17-17/02/17
British Ecological Society Remote Fieldwork Training and Outdoor First Aid – Yorkshire Moors, UK	17/03/17-20/03/17
The Institute for Terrestrial and Aquatic Wildlife Seal Capture and Handling training – Lorenzensplate, Germany	09/10/17-11/10/17

The Institute for Terrestrial and Aquatic Wildlife Seal Capture and Handling training – Lorenzensplate, Germany	19/03/18-23/03/18
British Ecological Society Remote Fieldwork Training and Outdoor First Aid – Yorkshire Moors, UK	24/03/18-27/03/18
Sea Mammal Research Unit Seal Capture and Handling Training – Bardsey Island, Wales, UK	10/05/18-13/05/18

Summary of protocols used; protocol sheets to be appended plus COSHH details for chemicals of category A or B with high or medium exposure

Protocol Details						Protocol Details					
#	Assessment					#	Assessment				
	1st date	Frequency of re-assessment	Hazard category	Secondary containment level	Exposure potential		1st date	Frequency of re-assessment	Hazard category	Secondary containment level	Exposure potential
1						11					

See notes in handbook for help in filling in form (Continue on another sheet if necessary)

Bioscience and Geography Protocol Risk Assessment Form
(Expand or contract fields, or append additional sheets as required; insert NA if not applicable)

<p>Protocol # 1 Rush and Grab land based net deployment and Seine and tangle net boat-based technique</p>	<p>Title: “Rush and Grab” technique and “Seine and tangle net technique” for the capture and handling of wild grey and harbour seals for the deployment of animal tracking devices.</p>
<p>Description:</p> <p>“Rush and Grab” While seals are hauled out on land, boats approach the shore and land to deploy people carrying individual hoop nets. Seals are caught using hoop nets before they reach the water. Alternatively, seals are approached from behind on land and caught before they enter the water.</p> <p>“Seine and tangle net” While seals are hauled out on land, boats approach and deploy a net in front of the haul out site. Animals flush into the net and become entangled. Multiple persons exit the boats and haul the large net on to shore. Animals are transferred into hoop nets for processing.</p> <p>Risks for attaching tags: Do not get superglue on skin.</p>	

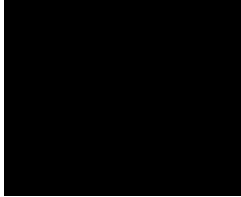
Location:
circle which Bioscience and Geography Local Rules apply –

Boat (Field) ~~Genetic-~~
 ~~Manipulation~~ ~~Laboratory~~ ~~Office/Facility~~ ~~Radioisotope~~

Identify here risks and control measures for work in this environment, additional to Local Rules

- Work is to always be conducted in line with local risk assessments and following protocols from collaborative research teams such as SMRU or ITAW – example attached here. Protocols and local risk assessments to have a signed declaration statement from person undertaking fieldwork
- The boat which is used may change depending on circumstance. Always confirm specific boat risk assessment and health and safety procedures with the coxswain.
- See attached **Seal Capture Risk Assessment Matrix** for further details.

Chemicals	Quantity	Hazards	Category (A,B,C,D)*	Exp.Score
Loctite glue (422)	50 ml	inhalation, eye irritation, stickiness	A	Low
Hazard Category (known or potential) A (e.g. carcinogen/teratogen/mutagen) B (e.g. v.toxic/toxic/explosive/pyrophoric) C (e.g. harmful/irritant/corrosive/high flammable/oxidising) D (e.g. non classified)			Exposure Potential Circle the highest Exposure Score above. Use this to calculate the exposure potential for the <u>entire</u> protocol (see handbook). Indicate this value below. <input checked="" type="radio"/> Low <input type="radio"/> Medium <input type="radio"/> High	
Primary containment (of product) sealed flask/bottle/glass/plastic/other (state) : Plastic sealed container Storage conditions and maximum duration : Room temp until date shown				
Secondary containment (of protocol) open bench/fume hood/special (state) : NA				
Disposal e.g. autoclaving of biohazard, SU chemical disposal: SU chemical disposal				
Identify other control measures (circle or delete) - latex/nitrile/heavy gloves; screens; full face mask; dust mask; protective shoes; spillage tray; ear-defenders; other (state): Latex gloves				
Justification and controls for any work outside normal hours: NA				
Emergency procedures (e.g. spillage clearance; communication methods):				

Follow eye irrigation guidance if in eyes. If inhaled or ingested seek medical assistance and do not induce vomiting. If stuck fingers or similar seek medical assistance and do not attempt to fix.	
Supervision/training for worker (circle)	
<input checked="" type="radio"/> None required <input checked="" type="radio"/> Supervised always	<input type="radio"/> Already trained
<input type="radio"/> Training required	
Declaration I declare that I have assessed the hazards and risks associated with my work and will take appropriate measures to decrease these risks, as far as possible eliminating them, and will monitor the effectiveness of these risk control measures.	
<i>Name & signature of worker:</i> William Kay	
<i>Name & counter-signature of supervisor:</i> James Bull	
<i>Date:</i> 10/01/2016	
Date of first reassessment	Frequency of reassessments
10/01/2016	None

Guidance for Completion of Bioscience and Geography Protocol Risk Assessment Form

Note – you are strongly advised to complete electronic versions of this form, enabling you to readily expand and contract sections as required to ensure clarity and adequate documentation. Do **not** delete any sections! Instead, mark inappropriate sections with NA (not applicable) and contract the section to save space on the final printed form.

Protocol - any self-contained procedure. This could be any activities undertaken, be they lab-work, use of equipment, fieldwork or office work. Your complete research/teaching/administration **activity** (e.g. undergraduate project, PhD study, research grant, other) is therefore made up from separate **protocols**. If the protocol is mainly of low hazard, but with one or more hazardous components, consider making the manipulation of the latter a separate protocol and tie them together by completing the “*Associated Protocol*” box. This is because the entire protocol must be conducted under conditions required for the handling of the most hazardous component.

Title/Description - give sufficient detail to make it obvious what the protocol involves.

Location – identify which local rules apply. More than one rule may apply. Then add any additional risks and control measures peculiar to this protocol (e.g. site-specific fieldwork information; use of autoclaves, sonicators; mechanical, electrical hazards). You may also wish to stress any particularly important risks and controls even if indicated in local rules.

Chemicals etc. - give name, maximum quantity used, list hazards, hazard category (see Table 1) and calculate the **Exposure Score** (see Table 2) for **every** chemical used. Expand the area in the table as required.

Exposure Potential (see Table 3) - complete this section for the chemical which has the **highest** exposure score in your chemical list as this defines the highest risk factor.

Primary containment/Storage - detail how and where, and for how long, the resultant product from the protocol will be stored. The product must be labelled with the

date of synthesis, and disposed of (see below) before the maximum duration time has elapsed.

Secondary containment - detail where the protocol will be performed (refer to Table 5).

Disposal - detail how you will dispose of surplus reagents and the product of the protocol. Final disposal must be undertaken within the period noted in the 'maximum duration' under 'Storage' (above).

Identify other control measures – typically these refer to special protective clothing etc.

Justification and controls for any work outside normal hours – out of hours working is only allowed under special conditions (e.g. 24h sampling, sampling related to tides etc.); convenience is not an acceptable reason.

Emergency procedures - detail how spillages etc. would be handled, including clearance of the laboratory etc. as required. For field work indicate emergency communication and first-aid coverage.

Supervision/training - detail here what special supervision and training is required by the worker named at the bottom of the form. Note that all undergraduates are always considered as research incompetent. First-year PhD students and MSc students are not to be used to supervise the activities of others.

Declaration - both the worker and the supervisor must sign this on the date entered here.

Reassessment - the first reassessment must be undertaken as soon as possible after the first time the protocol has been undertaken in order to identify any unforeseen hazards. After this first reassessment, the protocol should be reassessed every 6-12m, depending on the nature of the chemicals, to take account of changing knowledge concerning the hazardous nature of chemicals. The protocol must be reassessed immediately if new knowledge on the chemical hazards becomes available.

NOTE - standard protocols can be produced for each environment **BUT** each worker must have their own personalised version, signed by them and their supervisor, and dated. These completed personalised protocols must then be appended to the SU risk assessment form for the Teaching/Research activity belonging to the individual.

COSHH Assessment - modified from "COSHH in Laboratories" published by the Royal Society of Chemistry, July 1989

Hazards, Risks and Containment - Definition of terms

Hazard potential for doing harm, *e.g.* toxic, flammable, carcinogenic *etc*

Exposure potential the risk to the user depends very much on the exposure, which depends on the physical properties of the material, the quantity used and for how long.

$$\text{Risk} = \text{"Hazard"} \times \text{"Exposure Potential"}$$

The risk is decreased to a safe level by:

- a) Containment
- b) Personal Protection
- c) Good Laboratory Practice (GLP)

Levels of containment

The containment required for a given activity is of two basic kinds: the primary (or intrinsic) containment provided by the apparatus or equipment in which the substances are handled and the additional (or secondary) containment needed to ensure appropriate control of exposure.

HAZARD CATEGORY

TABLE 1- General Guidelines for determining hazard categories

A	EXTREME HAZARD	Substances of known or suspected exceptional toxicity (e.g. carcinogen, teratogen, potential mutagen)
B	HIGH HAZARD	All substances whose toxicity exceeds that of the medium hazard category, except for those known or believed to be so highly toxic as to merit special precautions (i.e. those in the “extreme” category)
C	MEDIUM HAZARD	Substances meeting criteria for CPL* classification as “Harmful” or ‘Irritant’
D	LOW HAZARD	Substances not matching criteria for CPL* classification as “Harmful” or “Irritant”

CPL = the Classification, Packaging and Labelling Regulations 1984.

NOTE:

1. The toxicity considered should be that of the substance or mixture handled, including any impurities.
2. Substances may have other properties (*e.g.* flammability) which may call for additional precautions.
3. The above general guidance may need to be supplemented by developing additional criteria with the help of expert toxicological advice. (Additional criteria may be developed using, for example, data given in HSE Guidance Notes such as EH40).
4. Time factors, such as frequency and duration of activity should also be considered. Short duration tasks, involving a few seconds exposure at infrequent intervals, should not affect the initial estimate, whereas continuous operations on a daily basis would probably raise the estimate to the next highest category.

EXPOSURE SCORE

TABLE 2 - exposure score to be calculated for all chemicals used in a protocol

EXPOSURE SCORE				
Calculation Value		1	2	3
(i)	Quantity	<1g	1-100g	>100g
(ii)	Properties	Dense solid Non- volatile liquid No skin absorption	Dusty solids Lyophilised solids Volatile liquids (b.p.>80°C)	Gases, Aerosols Highly volatile liquids (b.p.<80° C) Solutions promoting skin absorption
(iii)	Pressure	Normal	Low/Vacuum	>1 atmosphere
(iv)	Temperature	Room temperature	25°C - 100°C	>100°C

Exposure Score calculation = (i) x (ii) x (iii) x (iv)

The Exposure Potential

TABLE 3 - Rough calculation of exposure potential

EXPOSURE SCORE (FROM TABLE 2)			
Total score	<10	10-54	>54
Exposure Potential	L (low)	M (medium)	H (high)

Secondary containment level calculation

Table 5 - use to determine secondary containment

SECONDARY CONTAINMENT LEVEL					
Hazard Category		A	B	C	D
Exposure potential (from table 3)	H	SA	SA	FH	FH
	M	SA	FH	FH	OB
	L	FH	FH	OB	OB

OB = Open Bench;

FH = Fume Hood;

SA = Special Attention (see supervisor)

Appendix S7.4: Risk matrix for seal capture and tag deployment

College of Science Matrix Risk Assessment Form

Completed by:	William Kay
Name of Supervisor if applicable:	James Bull
Date:	30/09/16
Department:	Biosciences
Location:	Wallace Room 145

Type of activity being risk assessed and give brief explanation of overall task:

Rush and Grab: While seals are hauled out on land, boats approach the shore and land to deploy people carrying individual hoop nets. Seals are caught using hoop nets before they reach the water. Alternatively, seals are approached from behind on land and caught before they enter the water.

Seine and tangle nets: Capture and handling of wild grey and harbour seals for the deployment of animal tracking tags. While seals are hauled out on land, boats approach and deploy a net in front of the haul out site. Animals flush into the net and become entangled. Multiple persons exit the boats and haul the net on to shore where animals are transferred into individual nets for processing. As per Jeffries, S. J., Brown, R. F., & Harvey, J. T. (1993). Techniques for capturing, handling and marking harbor seals. *Aquatic mammals*, 19, 21-21.

It is possible to identify the level of risk by carrying out a simple calculation: (L) Likelihood/Frequency of Exposure X (C)

Severity/Consequence

Likelihood / Frequency of Occurrence	L
1 – RARE – Can't believe this will ever happen again	
2 – UNLIKELY – Do not expect it to happen but it is possible	
3 – POSSIBLE – May recur occasionally	
4 – LIKELY – Will probably recur but is not a persistent issue	
5 – ALMOST CERTAIN – Likely to occur on many occasions	

X

Consequence/Severity of outcome	C
1 – NONE – No injury or adverse outcome	
2 – MINOR – Short term harm or damage (Injury that will be resolved in 1 month)	
3 – MODERATE – Semi permanent injury (Injury taking up to 1 Yr to resolve)	
4 – MAJOR – Permanent harm (Loss of body part(s), RIDDOR reportable injury)	
5 – CATASTROPHIC - Death	

Once the level of risk has been identified, Action should be taken as soon as is reasonably practicable. However, the following may provide guidelines for determining the level of risk and the timescale by which action should be taken.

Likelihood	Consequence					TOTAL (R)	LEVEL OF RISK	TIMESCALE
	1 - NONE	2 - MINOR	3 - MODERATE	4 - MAJOR	5 - CATASTROPHIC			
1 - RARE	1	2	3	4	5	12-25	HIGH	IMMEDIATE
2 - UNLIKELY	2	4	6	8	10	6-10	MEDIUM	12 MONTHS
3 - POSSIBLE	3	6	9	12	15	1-5	LOW	NO PRIORITY
4 - LIKELY	4	8	12	16	20			
5 - ALMOST CERTAIN	5	10	15	20				

No:	Hazards and Associated Risks	People at Risk	Risk Factor			Risk Reduction measures	New Risk Factor			Comments
			L	C	R		L	C	R	
1	Remote fieldwork locations mean that other risks and hazards are enhanced.	All	2	2	4	Ensure team take every precaution to mitigate risks and hazards. Have emergency procedures in place.	2	2	4	Team will always have a means of communication with the emergency services – either through mobile phone or VHF radio. Own first aid kit on site and trained first aiders present.
2	Falling on uneven or slippery ground e.g. rocks, wet surfaces (seaweed etc.)	All	3	3	9	All team to wear appropriate footwear and take care when moving across uneven ground.	2	2	4	Appropriate footwear is provided as part of standard PPE.
3	Hot/sunny weather - Hyperthermia, dehydration, exhaustion, sunburn	All	1	3	3	Wear appropriate clothing for the conditions including sunscreen where necessary. Stay hydrated.	1	3	3	
4	Cold conditions particularly on account of windchill – hypothermia	All	1	3	3	Wear appropriate clothing for the conditions. Stay hydrated.	1	3	3	Drysuits or waders plus thermal gloves provided as part of standard PPE.
5	Water bodies – drowning	All	1	5	5	Extreme caution to be taken throughout fieldwork operations particularly with	1	5	5	Lifejackets are provided as part of standard PPE.

No:	Hazards and Associated Risks	People at Risk	Risk Factor			Risk Reduction measures	New Risk Factor			Comments
			L	C	R		L	C	R	
6	Direct handling and manipulation of wild seals – bites and scratches, transmission of zoonotic disease in mucus and/or faeces: <i>Mycoplasma phocacerebrale</i> , <i>Brucella sp.</i> , <i>Salmonella</i> , seal pox, human influenza. Potential transmission of respiratory disease via nasal discharge, coughing, sneezing.	All involved in animal handling	2	5	10	<p>Regards to operating in and around water bodies. Do not exceed waist deep water. Always wear a lifejacket when operating in or near to water. No lone working in water.</p> <p>All persons working directly with animals to take extreme caution and be vigilant at all times. Always adhere to instructions and guidance from experience seal handlers. Always cover seal's head with a damp cloth. Always wear appropriate PPE, particularly gloves and face masks if signs of respiratory disease are present. Unless otherwise required, always keep clear of the head and rear end</p>	1	5	5	Consult doctor immediately if an individual is bitten, scratched or inhales respiratory transmission. <i>M. phocacerebrale</i> does not respond well to broad spectrum antibiotics – except for tetracycline. Insist to medical professionals that tetracycline is administered at the earliest opportunity and casualty to be monitored/checked-in on for a minimum of 48 hours. Further medical guidance in Barnett, J., Knight, A., Stevens, M. (2013). British Divers Marine Life Rescue Marine Mammal Medic Handbook. The Printed Word, Horsham. 7th Ed.

No:	Hazards and Associated Risks	People at Risk	Risk Factor			Risk Reduction measures	New Risk Factor			Comments
			L	C	R		L	C	R	
7	Injury from boat – propeller, knocks and bangs, potential concussion, ejected from fast-moving vessel.	All	1	5	5	of seals. Always work in pairs (minimum) when handling seals. Vigilance to be maintained and caution taken while on board boats. Listen to instruction from coxswain at all times. Hold on tightly when the boat is travelling at speed. Do not approach the rear of vessels for risk of propeller injury. Wear lifejackets at all times.	1	5	5	Full boat familiarisation to be undertaken immediately on boarding.
8	Fire on board boat	All	1	4	4	In case of fire follow emergency procedures – call 999, issue Mayday, fight fire where possible or evacuate to liferaft.	1	4	4	Boat to be coded and inspected as per standard servicing requirements.
9	Entanglement in nets leading to potentially serious injury – drowning, water inhalation leading to secondary drowning, ankle/leg injury, put at	All involved in animal catching.	1	5	5	Extreme caution to be taken at all times when working around lines and nets.	1	5	5	

No:	Hazards and Associated Risks	People at Risk	Risk Factor			Risk Reduction measures	New Risk Factor			Comments
			L	C	R		L	C	R	
10	<p>greater risk of threat of seals.</p> <p>Manual handling injuries when transferring seals and lifting equipment.</p>	All	2	3	6	<p>Particular care to be taken during net deployment and hauling-in. Care also to be taken when transferring seals from large seine net to individual hoop nets – work in pairs and follow instruction from experienced individuals.</p> <p>Always work in pairs (or more) when handling seals and other heavy equipment. Keep back straight while lifting.</p>	1	3	3	Adult seals are generally > 70 kg. Juveniles and weaners are 30 – 70 kg. Always work in pairs for any animal > 20 kg in weight (typically only newly born pups would weigh less than this).

Appendix S7.5: Risk assessment for building tags



COLLEGE OF SCIENCE CONTROL OF SUBSTANCES HAZARDOUS TO HEALTH RISK ASSESSMENT FORM

Before filling in this form, *please read the Notes*, as indicated.

This form **MUST BE COMPLETED** prior to the commencement of any work involving risks to health from a hazardous substance, so that a suitable and sufficient assessment of health risks is made (*see Note 1 at the back of this form*)

PART A	RISK EVALUATION	
A1	Department	BIOSCIENCES
A2	Title of Work Activity*	<div style="border: 1px solid black; padding: 2px;">Tag building (work with resins, silastic, silicone and associated catalysts)</div> <div style="border: 1px solid black; padding: 2px;">Battery duration tests and Galvanic Timed Release (GTR) tests</div>
		<i>*Choose a title or give a serial number so as to facilitate departmental filing and/or retrieval of risk assessments.</i>
A3	Location(s) of Work	<div style="border: 1px solid black; padding: 2px;">SLAM Lab</div> <div style="border: 1px solid black; padding: 2px;">W023A</div>
A4	Hazardous Substance(s) Classification	
	(Note 2) (Tick 1 or more boxes)	
	Very Toxic <input checked="" type="checkbox"/>	Toxic <input checked="" type="checkbox"/> Harmful <input checked="" type="checkbox"/> Corrosive <input checked="" type="checkbox"/> Irritant <input checked="" type="checkbox"/>
	Substance(s) with MEL or OES <input type="checkbox"/>	Dust <input type="checkbox"/> Carcinogen (or suspected carcinogen) <input checked="" type="checkbox"/>
	Micro-organism <input type="checkbox"/>	<i>(See Notes 3 and 4)</i>
	Specify particularly dangerous or hazardous substance(s) (Note4). Also complete classification overleaf.	

Fibreglass and/or Polyester resins, Q-Cel glass microspheres, silastic, silicone and associated catalysts. Batteries and GTRs. See overleaf and individual Health and Safety Data Sheets (HSDS).

Total number of hazardous substances involved in the work activity

8

A4

Hazardous Substances: Classification List of Individual Substances

Refer to MSDS information supplied by manufacturer if necessary

<u>Substance Name</u> *Other information may be included beneath the hazard classification beside each substance e.g. Route see A6	<u>Hazard Classification</u> (tick as appropriate) v. toxic toxic harmful corrosive irritant reactive dust flammable							
1) Fibreglass/Polyester resin	<input type="checkbox"/>	<input checked="" type="checkbox"/>	<input type="checkbox"/>	<input checked="" type="checkbox"/>	<input checked="" type="checkbox"/>	<input type="checkbox"/>	<input type="checkbox"/>	<input checked="" type="checkbox"/>
2) MEKP Catalyst	<input type="checkbox"/>	<input checked="" type="checkbox"/>	<input type="checkbox"/>	<input checked="" type="checkbox"/>	<input checked="" type="checkbox"/>	<input type="checkbox"/>	<input type="checkbox"/>	<input checked="" type="checkbox"/>
3) Acetone	<input type="checkbox"/>	<input checked="" type="checkbox"/>	<input type="checkbox"/>	<input checked="" type="checkbox"/>	<input checked="" type="checkbox"/>	<input type="checkbox"/>	<input type="checkbox"/>	<input checked="" type="checkbox"/>
4) Q-Cel glass microspheres	<input type="checkbox"/>	<input type="checkbox"/>	<input type="checkbox"/>	<input checked="" type="checkbox"/>	<input checked="" type="checkbox"/>	<input type="checkbox"/>	<input checked="" type="checkbox"/>	<input type="checkbox"/>
5) Silicone and silastic	<input type="checkbox"/>	<input checked="" type="checkbox"/>	<input type="checkbox"/>	<input type="checkbox"/>	<input type="checkbox"/>	<input type="checkbox"/>	<input type="checkbox"/>	<input type="checkbox"/>
6) Curing agent (for use with silastic)	<input type="checkbox"/>	<input checked="" type="checkbox"/>	<input type="checkbox"/>	<input checked="" type="checkbox"/>	<input checked="" type="checkbox"/>	<input type="checkbox"/>	<input type="checkbox"/>	<input checked="" type="checkbox"/>
7) Magnesium (GTRs)	<input type="checkbox"/>	<input type="checkbox"/>	<input type="checkbox"/>	<input type="checkbox"/>	<input checked="" type="checkbox"/>	<input type="checkbox"/>	<input type="checkbox"/>	<input type="checkbox"/>
8) Batteries	<input checked="" type="checkbox"/>	<input checked="" type="checkbox"/>	<input type="checkbox"/>	<input checked="" type="checkbox"/>	<input checked="" type="checkbox"/>	<input type="checkbox"/>	<input type="checkbox"/>	<input checked="" type="checkbox"/>
9)	<input type="checkbox"/>	<input type="checkbox"/>	<input type="checkbox"/>	<input type="checkbox"/>	<input type="checkbox"/>	<input type="checkbox"/>	<input type="checkbox"/>	<input type="checkbox"/>
10)	<input type="checkbox"/>	<input type="checkbox"/>	<input type="checkbox"/>	<input type="checkbox"/>	<input type="checkbox"/>	<input type="checkbox"/>	<input type="checkbox"/>	<input type="checkbox"/>
11)	<input type="checkbox"/>	<input type="checkbox"/>	<input type="checkbox"/>	<input type="checkbox"/>	<input type="checkbox"/>	<input type="checkbox"/>	<input type="checkbox"/>	<input type="checkbox"/>
12)	<input type="checkbox"/>	<input type="checkbox"/>	<input type="checkbox"/>	<input type="checkbox"/>	<input type="checkbox"/>	<input type="checkbox"/>	<input type="checkbox"/>	<input type="checkbox"/>
13)	<input type="checkbox"/>	<input type="checkbox"/>	<input type="checkbox"/>	<input type="checkbox"/>	<input type="checkbox"/>	<input type="checkbox"/>	<input type="checkbox"/>	<input type="checkbox"/>
14)	<input type="checkbox"/>	<input type="checkbox"/>	<input type="checkbox"/>	<input type="checkbox"/>	<input type="checkbox"/>	<input type="checkbox"/>	<input type="checkbox"/>	<input type="checkbox"/>

A
5

Grounds for Concluding Exposure is not a Risk to Health

Quantities or rate of use of substance(s) are too small to constitute any risk to health under foreseeable circumstances of use, even if control measures broke down*.

**If there are reasonable grounds for reaching the conclusion that risks are insignificant, finish this assessment now by signing page 8 (N.B. in most instances this will not apply i.e the vast majority of laboratory procedures have some form of inherent risk in them(e.g. hazardous chemicals) and completion of the form is usually the normal procedure)*

A6

Route by which the Substances are Hazardous to Health

(Tick 1 or more boxes)

Inhalation Ingestion Skin Absorption by Direct Contact, Skin or Eyes
Injection via sharps

A7

What could be the Effect of Exposure to the above Hazardous Substances?

(Tick 1 or more boxes)

Single Acute Exposure: Serious Not Serious Not Known
Repeated Low Exposure: Serious Not Serious Not Known
Adverse Effect Could be: Long Term Short Term Not Known
Effects could be harmful to the Human Reproductive System: Yes No Not Known
The micro-organism could infect an individual and an infected person could infect others

A8

Engineering Control Measures:

(Tick 1 or more boxes)

The work will be carried out on the open bench The work will be carried out in a fume cupboard(s)
Specify the location of fume cupboards*
**Fume cupboards must be used in accordance with University local guidance or codes of practice*
The work will require some other local exhaust ventilation Specify below

A8

The work will be carried out in a glove box or other sealed system

Specify:

The work will be carried out in a laboratory at the required biological containment level
and in a biological safety cabinet, class insert number where relevant
ACDP Category Genetic Manipulation Category*

**Individuals performing this category of work must be registered with and seek permission from the Genetic Modification Safety Committee (GMSC) prior to beginning work. A separate risk assessment must also be completed and approved by the GMSC.*

A9

Personal Protective Equipment Requirements

(Tick 1 or more boxes)

The following personal protective equipment may be necessary for a part or all of the work.

Eye Protection

Face Protection

Hand Protection

Foot Protection

Respiratory Protection

Other (e.g. protective clothing)

Specify:

Eye protection: Goggles
Face protection: Face mask
Hand protection: Rubber/latex gloves
Respiratory Protection: Face mask
Other (e.g. protective clothing): Lab coat

PART B

DESCRIPTION OF THE WORKING PRACTICE

NB: Part B2 of this form must always be completed for work by postgraduate research students and for final year undergraduates carrying out similar research work.

B1 Instructions for the Work Activity

(Tick 1 box only)

The work activity consists of well documented routine procedures carried out frequently in a controlled environment and requiring only simple and easily understandable verbal instructions. (Note 5)

The work activity consists of procedures requiring a specific scheme of work*

**A Part B2 "Scheme of Work" must be completed for this type of work activity*

B2 Scheme of Work (Continue on a separate sheet, if necessary)

See Note 6: State how the work activity is going to be carried out safely. Specify handling precautions of hazardous substances. Give sufficient details to identify the precautions necessary to control potential risks. Identify all potential hazards i.e. biological, chemical, physical, mechanical.

All work to be undertaken in fume cupboard. Full PPE to be worn at all times. Care taken when handling all substances. Tell supervisor when undertaking work. Do not work when tired.

B3 Training for the Work Activity

Specific training will be required: Yes No

Any special training required to ensure that persons involved in the work activity can operate safely should be described here. This is particularly important so that persons can understand and comply effectively with the scheme of work (B2), where this had been formulated

Specific training needed from academic supervisor: Professor Rory P. Wilson. To be assessed by Dr Jim C. Bull.

B4 Supervision

(Tick 1 or more boxes)

See Note 7.

- The supervisor will approve straightforward routine work in progress.
- The supervisor will specifically approve the scheme of work, **B2**.
- The supervisor will provide supervision personally to control the work

B5 Monitoring

(Tick 2 boxes)

See Note 8.

- Monitor for airborne contaminant will be required Yes No
- Biological monitoring of workers will be required Yes No

B5 Contingency Planning*

(Tick 1 or more boxes)

**Contingency planning is required to limit the extent of the risk arising from an uncontrolled release of a hazardous substance and for regaining control as quickly as possible.*

Written emergency instructions will be provided for workers and others who might be affected, on site:

Yes No

Biological monitoring of workers will be required Yes No

Provision of the following may be required in an emergency:

Spill Neutralization Chemicals

Eye Irrigation Point	<input checked="" type="checkbox"/>	Body Shower	<input type="checkbox"/>	Other First Aid Provisions	<input checked="" type="checkbox"/>
Breathing Apparatus (with trained operator)	<input type="checkbox"/>	External Emergency Services	<input checked="" type="checkbox"/>		

B7 Disposal of Waste Residues
(Tick 1 or more boxes)

In-house to District Council Waste Collection, after rendering safe

In-house to drain, after rendering safe In-house to incinerator, after rendering safe if appropriate

To specialist licensed Waste Disposal Contractor Other (e.g. inter-departmental)

Specify:


Swansea University Hazardous Waste

B8 Implications for other Persons
(Tick 1 or more boxes)

The following persons may need to be told, in part or in full, about the information contained in this risk assessment. Such persons may be named in **B9** (ii).
Written emergency instructions will be provided for workers and others who might be affected, on site:

Academic Staff	<input type="checkbox"/>	Postgraduate Staff	<input type="checkbox"/>	Postgraduate Students	<input checked="" type="checkbox"/>
Undergraduate Students	<input type="checkbox"/>	Technical Staff	<input type="checkbox"/>	Cleaning Staff	<input type="checkbox"/>
Visitors	<input type="checkbox"/>	Others	<input type="checkbox"/>	Specify	<input type="checkbox"/>

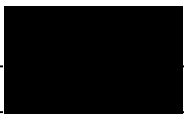
B9 Accreditation

(1) **Signature of Assessor**  **Name** Dr James C. Bull **Date** 10/01/2016
and/or **Signature of Supervisor** **Name** **Date**

(ii) **Signature of All Persons receiving a copy of this Risk Assessment***

A copy of this assessment must be given to each postgraduate research student and/or to each final year undergraduate doing like work, and he/she must sign a receipt, at **B9(ii).*

I/We have received a copy of Parts A and B of this Risk Assessment.

Signature		Name	William P. Kay	Date	10/01/16
_____	_____	_____	_____	_____	_____

(iii) **Date of Next Assessment (see Note 9)**

1).....NA..... 2) 3)

A COPY OF THIS ASSESSMENT MUST BE RETAINED BY THE HEAD OF DEPARTMENT, OR HIS/HER REPRESENTATIVE, FOR AS LONG AS IT IS RELEVANT.

Notes On Completion of the COSHH Form

Note 1: Persons completing this form should make themselves aware of the Health and Safety Commission Approved Codes of Practice "Control of Substances Hazardous to Health", and "Control of Carcinogenic Substances", the HSE booklet "COSHH Assessments"

Note 2: The COSHH Regulations do **NOT** apply where either the Control of Asbestos at Work or the Control of Lead at Work Regulations apply or where the risk to health is solely from radiation, noise, pressure, explosive or flammable properties, heat or cold, nor to medicines administered to patients.

A substance should be regarded as hazardous to health if it is hazardous in the form in which it occurs in the work activity, including by-products and waste residues.

(a) Any substance which is listed as "very Toxic", "toxic", "corrosive", "harmful", or "irritant" in Part

IA of the Approved List for the Classification, Packaging and Labelling of Dangerous Substances Regulations, 1984, (2nd edition onwards) is a substance hazardous to health.

Exposure (b) Any substance which has an MEL (Maximum Exposure Limit) or OES (Occupational Standard) given in the HSE Guidance Note EH.40 (current year date) is a substance hazardous to health.

(c) Micro-organisms which create a hazard to the health of any person, where the hazard arises out of or in connection with a work activity. Hazard classification of pathogens is given in the booklet "Categorisation of Pathogens etc.", Advisory Committee on Dangerous Pathogens. See also the relevant Advisory Committee on Genetic Manipulation/Health and Safety Executive Notes.

(d) A dust of any kind is a substance hazardous to health when present in a "substantial" concentration. See the Approved Code of Practice, paragraph 2(1) and HSE Guidance Note EH.40.

(e) Any other substance is hazardous if it creates a risk to health comparable to any of the above.

Note 3: Refer to the HSC Approved Code of Practice. "Control of Carcinogenic Substances".

Note 4: A Part **B2** "Scheme of Work" **must** be completed for this type of work activity (i.e. part B of this COSHH form)

Note 5: Where an assessment of risk is simple and obvious and where the work activity is straightforward and clear verbal instructions can be given easily, a written scheme of work (Part **B2**) is unnecessary. Complete the other sections of Part B.

Note 6: The scheme of work is a statement of how the work activity is going to be carried out safely. It should specify the ways in which the hazardous substances are to be used or handled, and should give sufficient details to identify the precautions necessary to control the risks that arise from working with the hazardous substances. Remember that potential hazards are not restricted to toxic substances and also include: chemical (e.g. corrosive acids etc.), biological (e.g. human tissue or pathogens etc.), physical (electricity, temperature, radiation etc.), mechanical (centrifuges, high-pressure equipment etc). Step by step details of the technique are not necessarily required, although this can be appended to the COSHH form for future reference if desired.

Note 7: The level of supervision must always be appropriate to the competence of the individuals involved in the work activity.

Note 8: For the majority of work, atmospheric monitoring should not be necessary for protecting health, providing sufficient thought has gone into ensuring the adequacy of control measures in relation to risks, and the control measures are properly used and maintained. For further information on monitoring and health surveillance see the Approved Code of Practice.

Note 9: This assessment should be reviewed immediately if there is any reason to suppose that the original assessment is no longer valid due to significant changes in the work activity, arising for example, from the introduction of new hazardous substances, new personnel, changes in procedures or reported ill-health. Otherwise, the assessment should be reviewed annually.

Appendix S7.6: R scripts

To obtain R codes for analyses undertaken in this thesis, please visit my github:
<https://github.com/willpkay>